The Dissertation Committee for Lance Thomas Lepovitz Certifies that this is the approved version of the following Dissertation:

Synthesis and Evaluation of Novel Anti-Trypanosomal Compounds, Diversity-Oriented Synthesis of Spirocyclic β-Phenethylamines, and the Total Synthesis of Exotines A and B

Committee:

Stephen F. Martin, Supervisor

Adrian Keatinge-Clay

Hung-Wen Liu

Michael J. Krische

Eric V. Anslyn

Synthesis and Evaluation of Novel Anti-Trypanosomal Compounds, Diversity-Oriented Synthesis of Spirocyclic β-Phenethylamines, and the Total Synthesis of Exotines A and B

by

Lance Thomas Lepovitz

Dissertation

Presented to the Faculty of the Graduate School of

The University of Texas at Austin

in Partial Fulfillment

of the Requirements

for the Degree of

Doctor of Philosophy

The University of Texas at Austin

May 2019

Dedication

To my mother and father for a lifetime of guidance, support, love, and encouragement, and to my wife Lauren for her unwavering love and support throughout.

Acknowledgements

First and foremost, I would like to acknowledge Dr. Stephen F. Martin for his invaluable mentorship, training, and support. I would also like to acknowledge all of the past and present members of the Martin lab who've helped me along the way, in particular Dr. Daniel Klowsowski, Alex Goodnough, Zachary White, Dr. Timothy Hodges, Dr. J. Caleb Hethcox, Dr. James Sahn, Dr. Rachel Wypych, Dr. Shawn Blumberg, Zhipeng Wang, and Michael Wood. Finally, I would like to acknowledge Steve Sorey, Angela Spangenberg, Dr. Vincent Lynch, and Dr. Ian Riddington for their assistance with NMR, X-ray, and mass spectrometry analysis.

Abstract

Synthesis and Evaluation of Novel Anti-Trypanosomal Compounds, Diversity-Oriented Synthesis of Spirocyclic β-Phenethylamines, and the Total Synthesis of Exotines A and B

Lance Thomas Lepovitz, Ph.D.

The University of Texas at Austin, 2019

Supervisor: Stephen F. Martin

First, collections of conformationally flexible δ-lactam and piperidine analogs were designed and synthesized following the discovery of a rigid indoloquinolizidine scaffold whose derivatives inhibit the growth of *Trypanosoma brucei*, the protozoan parasite that causes human African trypanosomiasis, via the inhibition of methionyl-tRNA synthetase (*Tb*MetRS). Many of δ-lactam and piperidine analogs were found to be superior *T. brucei* growth inhibitors relative to the initial indoloquinolizidine compounds; however, it was also found that these flexible compound sets displayed greatly diminished activity against *Tb*MetRS. Then, a diversity-oriented synthesis (DOS) of spirocyclic β-phenethylamines was realized via the development of an intramolecular aza-Hosomi-Sakurai reaction. Facile elaboration of these aza-spirocyclic scaffolds was demonstrated through a variety of means, and several derivatives were identified as potent Sigma-1 receptor (σ1R) ligands in a biochemical screen. Finally, a one-step biomimetic total synthesis of the cyclohepta[*b*]indole-coumarin natural products exotines

A and B was achieved via the development of an acid-catalyzed three-component cyclization reaction between indole, prenal, and *trans*-dehydoosthol. Some mechanistic aspects of this process are investigated, and evidence is obtained which supports the mechanism of a [4 + 2] cycloaddition followed by a 1,2-migration, in accordance with the original biosynthetic proposal of Jiang.

Table of Contents

List of Tables

List of Figures

List of Schemes

SYNTHESIS AND EVALUATION OF NOVEL ANTI-TRYPANOSOMAL COMPOUNDS

Chapter 1. Human African Trypanosomiasis: Etiology, Current and Prospective Treatments

1.1. HUMAN AFRICAN TRYPANOSOMIASIS

Human African Trypanosomiasis (HAT)—also known as African sleeping sickness—is a deadly disease caused by the protozoan parasite *Trypanosoma brucei* (*T. brucei*). The disease has an at-risk population of 60 million people throughout sub-Saharan Africa, and is transmitted to humans via the tsetse fly, which resides over roughly 10 million kilometers of the African landmass.[1] HAT is classified as a neglected tropical disease (NTD) by the World Health Organization (WHO) because it predominantly affects impoverished populations in developing (sub)tropical nations.[2–4] There have been several incidences of HAT epidemics during the 20th century, the first around the turn of the century, another in 1920, and the most recent HAT epidemic lasted from 1970 until the late 1990s.[2,4] These epidemics were brought under control initially via culling animal reservoirs of the disease and deforestation and later via management of the insect vector and proactive surveillance of populations for disease presence.[1,2] As a result of these practices, the number of new cases of HAT dropped below 10,000 in 2009 for the first time in 50 years, and in 2015 there were only 2804 new cases reported, leading the WHO to project that elimination of the disease as a public health concern may be achievable in the near future.[4] However, caution is warranted as HAT incidences are chronically under-reported due to its occurrence predominantly in rural communities and in regions lacking adequate health infrastructure.[1,2] For instance, a study estimated that in 2007 there were 18,592 people in the Democratic Republic of Congo (DRC)—the country with the greatest incidence of the disease in modern times—with HAT, which is more than twice the amount reported to the WHO that year.[1] Indeed, examining of the history of HAT outbreaks shows that they often coincide with periods of war, famine, and economic instability that hamper or prevent adequate surveillance, diagnosis,

and treatment.[1,2,4] These societal vagaries, along with the difficult treatment regimens required by current HAT chemotherapeutics and the emergence of drug-resistant strains of *T. brucei,* provide the impetus for continued research and the development of better methods for preventing, containing, and treating this deadly disease.[1,2,5,6]

There are three subspecies of *T. brucei: T b gambiense,* which is responsible for approximately 97% of HAT cases, *T b rhodesiense,* a more virulent strain which is responsible for the remaining 3% of cases, and *T b brucei,* which infects animals and is used to study the parasite *in vitro*.[1,2] The subspecies *gambiense* and *rhodesiense* occupy separate geographic regions in Africa, except for Uganda where both have been observed.[1,2] Humans are the main reservoir of *T b gambiense,* while animals such as cattle act as the main reservoir for *T b rhodesiense*.[1] After the blood-sucking tsetse fly bites a *T. brucei* reservoir, the parasite enters the midgut and undergoes morphological and biochemical changes to reach its mature, infective state upon migrating to the salivary glands of the tsetse fly.[1] From here, the mature parasite can be spread to new human and animal hosts.

Upon entering a human host, the progression of the disease is divided into two distinct stages, the haemolymphatic "early" stage and the meningo-encephalitic "late" stage. During the haemolymphatic stage the parasite resides in the bloodstream of the host, and the effects of the infection at this stage are diffuse. The spleen or liver may become enlarged, cardiac disorders may be observed, and various dysfunctions of the endocrine system may occur.[1] Intermittent fever is common during the first stage as the body of the host mounts an immune response to the invading parasite. *T. brucei* has evolved sophisticated mechanisms for evading these immune responses. Roughly 10% of the *T. brucei* genome encodes for variant surface glycoproteins (VSGs) which are expressed on the parasite's outer surface.[1] The parasite achieves a high degree of antigenic variation by rapidly switching the expressed VSG, and only a single VSG is present on the cell surface at a given time; because of this, it is unlikely that we will see development of a vaccine for HAT.[1,2] Having successfully evaded the immune response of the host, the parasite is free to proliferate and spread throughout the host, eventually crossing the blood-brain barrier

(BBB) and taking up residence in the central nervous system (CNS) in the late, meningo-encephalitic stage of infection.[1,2] During the late stage various neurological effects are present, with one of the most common being profound disturbances in the sleep/wake cycle of the host—hence the disease's common namesake of "sleeping sickness".[1,2] Psychiatric symptoms are frequently observed, along with motor disturbances, neuropathy, and meningoencephalitis or brain inflammation.[1,2] The course of the disease varies with the infecting subspecies. With *T b gambiense* disease onset is slow and progression to the second stage usually occurs after several months. On the other hand, in *T b rhodesiense* infections progression to the second stage occurs rapidly, usually in a matter of weeks.[1] Both forms of the disease are usually fatal if left untreated, although cases of spontaneous remission in *T b gambiense* infection have been observed.[1]

1.1.1. Current Treatments for HAT

There are five medicines currently used to treat HAT, and their use varies with the disease stage and with the *T brucei* subspecies responsible for the infection. Pentamidine (**1.1**) and suramin (**1.2**) are the first-line treatments for early-stage *T b gambiense* and *T b rhodesiense* infections, respectively (Figure 1.1). Late-stage disease treatment requires that the medicine cross the BBB, which the polyionic compounds **1.1** and **1.2** are unable to do. For late-stage treatment, eflornithine (**1.3**)—alone or in combination with nifurtimox (**1.4**)—and melarsoprol (**1.5**) are used against *T b gambiense* and *T b rhodesiense* infections, respectively (Figure 1.1). The currently available treatments are broadly considered to be unsatisfactory owing to their (severe) toxicity, difficult and sometimes painful dosage regimens, and incidences of drug resistance.[1,2,6]

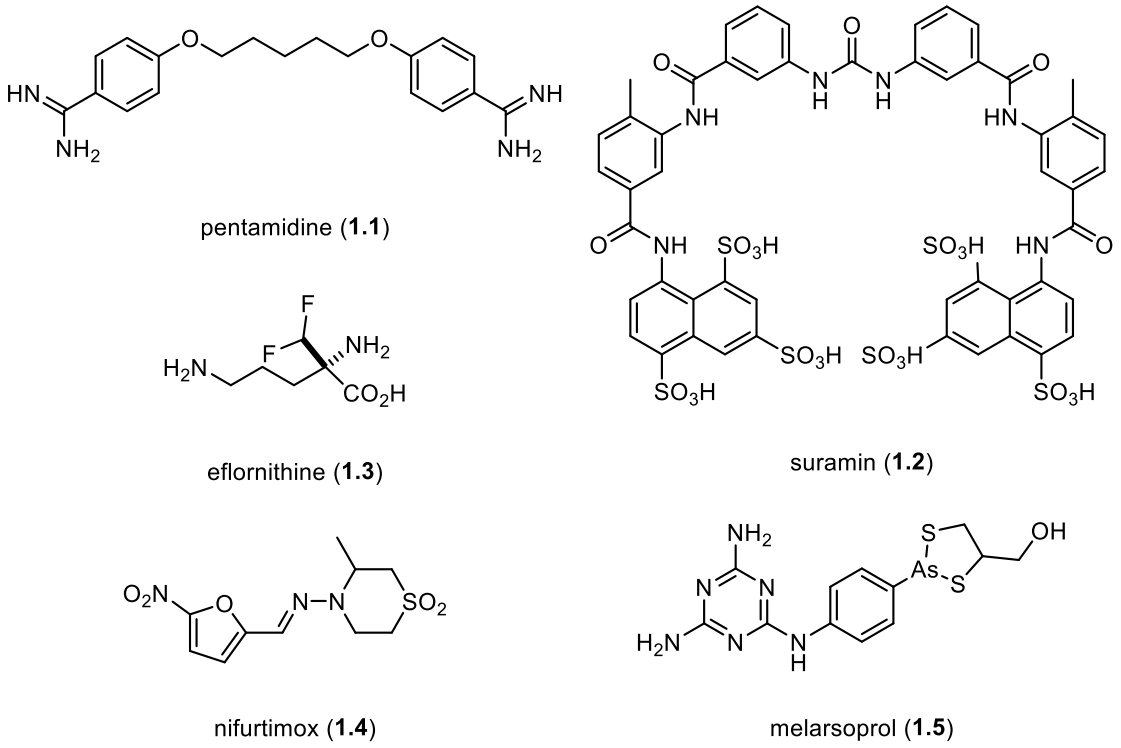

Figure 1.1. Medicines currently used to treat HAT

Pentamidine (**1.1**), developed in the 1930's, is the first-line treatment for early-stage *T b gambiense* infections.[6] It is a diaryl diamidine that exists as a di-cation at physiological pH, thereby preventing pentamidine from being absorbed by the intestine. Hence, it is most commonly administered via intramuscular injetion.[6] The drug is administered at a 4 mg/kg dosage in 24 h intervals for 7 days.[2,5,6] Pentamidine is taken up into trypanosomes via the P2 aminopurine permease transporter and the high-affinity pentamidine transporter 1 (HAPT1), leading to millimolar intra-trypanosomoal concentrations of pentamidine when the parasite is exposed to micromolar extracellular concentrations.[5,6] The exact mechanism by which pentamidine kills trypanosomes remains unknown; however, it has been shown that pentamidine binds to DNA via ionic interactions with the phosphate backbone, and it appears that the mitochondrion is an important site of activity for the drug.[5–7] In *Leishmania tropica*, a protozoan parasite closely related to trypanosomes, pentamidine was found to accumulate in the mitochondrion and bring about a disintegration of mitochondrial kinetoplast DNA.[8] The most

common side effects of pentamidine treatment are pain at the site of injection, gastrointestinal (GI) distress and hypoglycemia.[2] Pentamidine resistance has been induced in trypanosomes *in vitro* but is not a significant concern in the field, as resistance comes at the cost of greatly reduced virulence.[5,6] Pentamidine is ineffective for the treatment of *T b rhodesiense* infections.[6]

Suramin (**1.2**) is a polysulfonated naphthalene that is the first-line treatment against early-stage *T b rhodesiense* infections.[1,2] It has been used to treat *T. brucei* infections since 1922, giving it the distinction of being one of the oldest antimicrobial drugs still in use.[5] Suramin is administered via slow intravenous injection in 20mg/kg dosage five times over the course of four weeks.[2,6] Like pentamidine, the mechanism of action of suramin is not well understood.[5,6] It is thought to enter the trypanosome via endocytosis, and it can bind to many different proteins via electrostatic interactions with its six sulfonate moieties. Its high affinity for serum proteins lead to a long half-life of 41–78 days.[5,6] Some evidence points to glycolysis as being a likely site of activity as suramin has been shown to inhibit several glycolytic enzymes, and it is a hundred-fold less active against procyclic trypanosomes than against bloodstream trypanosomes that require glycolysis to survive.[6] The most common side effects of suramin treatment are renal failure, peripheral neuropathy, and hypersensitivity reactions.[1,2] Resistance to suramin in the field is rare but has been reported.[6]

Nifurtimox/eflornithine combination therapy (NECT), which was approved in 2009, is the first-line treatment for late-stage *T b gambiense* infections.[1,9] Eflornithine (**1.3**), a fluorinated ornithine analog, is an ornithine decarboxylase (ODC) inhibitor developed in the 1970s. Before the advent of NCET, eflornithine monotherapy was the first-line treatment for late-stage *T b gambiense* infections.[2,6] The ODC enzyme is an essential component of polyamine biosynthesis, and ODC turnover happens more slowly in trypanosomes than in mammalian cells making eflornithine less toxic to host cells than trypanosomes.[5,6] While safer and more effective than melarsoprol (*vide infra*), eflornithine monotherapy also suffers from severe liabilities. Eflornithine has a half-life of only three hours, mid-micromolar GI_{50} values, and is not orally available. These combined factors result in an incredibly difficult dosage regimen of 100 mg/kg

intravenous injections every six hours for 14 days, roughly half of a kilogram of the drug in total for an average-sized individual.[5,6] The main advantage of NCET is that it allows for a reduction in eflornithine dosage to a more manageable, but still severe, regimen of 200 mg/kg every 12 hours for 7 days when nifurtimox (**1.4**)—a drug used to treat the related trypanosomal infection Chagas disease—is co-administered orally once per day.[5,9] Eflornithine and NCET can have serious side effects including bone marrow toxicity, convulsions, alopecia, and GI disorders.[2,6] Resistance to eflornithine via loss of the *Tb*AAT6 transporter has been demonstrated in *vitro* and observed in isolated incidences in the field; however, it is hoped that use of NCET will mitigate the threat of eflornithine-resistant trypanosomes.[1,9] Eflornithine and NCET are ineffective against *T b rhodesiense*.[1,9]

Melarsoprol (**1.5**), an organic arsenical introduced in 1949, is the only available treatment for late-stage *T b rhodesiense* infection, and is still used to treat *T b gambiense* infections in resource-poor and isolated settings where eflornithine and NCET are not accessible.[1,2] It is administered intravenously, at 2.2 mg/kg dosage in 24 hour intervals for 10 days.[2] Like pentamidine, melarsoprol is taken up in trypanosomes via the P2 transporter, whereupon it causes rapid lysing of trypanosomes, but the mechanism by which this happens is poorly understood.[6] It is thought that the arsenic in melarsoprol interacts with the thiol group of trypanothiol, a small molecule that maintains the reducing environment in trypanosomes, thus rendering the trypanosome more sensitive to oxidative stress.[6] Melarsoprol is highly toxic and has severe side effects, the most alarming of which is reactive encephalopathy or swelling of the brain, which results in death for 5.9% of patients undergoing melarsoprol treatment.[1] Other side effects include agranulocytosis, peripheral neuropathy, cardiac arrythmias, rashes, and inflammation.[1] Resistance to melarsoprol in the field has been documented, and treatment failures are increasingly common; however, it is not clear to what extent these failures are due to drug resistance.[1,5]

1.1.2. Emerging HAT Treatments

There are currently two drug candidates in clinical trials for the treatment of HAT: the nitro-imidazole fexinidazole (**1.6**) and the oxaborole SCYX-7158 (**1.7**) (Figure 1.2).[5] First synthesized in the 1970s and developed as a broad-spectrum antimicrobial agent that was never advanced beyond preclinical research, fexinidazole (**1.6**) was rediscovered via compound mining of >700 nitro-heterocycles as part of the Drugs for Neglected Diseases *initiative* (DND*i*).[10] Fexinidazole and its sulfoxide and sulfone metabolites are active against both *T b rhodesiense* and *T b gambiense in vitro*, with IC_{50} values of 0.7–3.3 μM, values comparable to eflornithine (**1.3**) and nifurtimox (**1.4**) but significantly less potent than melarsoprol (**1.5**).[10,11] Its mechanism of action has yet to be determined, but it is thought to involve reductive bio-activation of the drug via nitroreductase activity.[10] Fexinidazole displays negligible cytotoxicity at its effective dosage, good oral bioavailability, and it was found to cure mouse models of both *T b rhodesiense* and *T b gambiense* infections.[10,11] It has been advanced through phase 3 clinical trials, and in late 2018 fexinidazole was recommended by the European Medicines Agency for treatment of late-stage *T b gambiense* infections, with distribution of the drug in endemic countries expected to begin in 2019.[12,13]

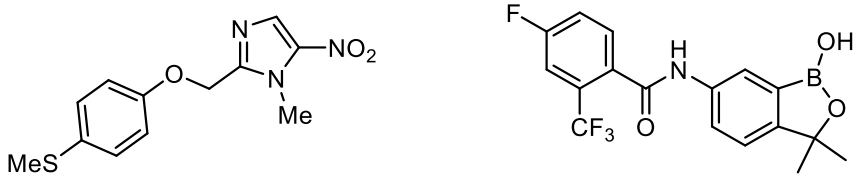

fexinidazole (**1.6**) SCYX-7158 (**1.7**)

Figure 1.2. HAT drug candidates currently in clinical trials

SCYX-7158 (**1.7**) is a unique benzoxaborole compound that is currently in phase II/III clinical trials for the treatment of late-stage *T b gambiense* infection. It was developed after screening of a library of boron-based compounds at Anacor Pharmaceuticles identified several benzoxaboroles with promising anti-trypanosomal activity.[5,14] SCYX-7158 displays good pharmacokinetic properties, oral bioavailability, and it was successful in curing murine models

of *T b brucei* infection.[5,14] Its mechanism of action is unknown, but a proteomic study found that SCYX-7158 interacts with 13 different trypanosome proteins that do not share any common cellular function, suggesting that SCYX-7158 displays polypharmacological activity, a property that may render it less susceptible to the emergence of drug resistance.[15] The phase II/III clinical trial assessing the efficacy of SCYX-7158 for treatment of late-stage *T b gambiense* HAT is estimated to be completed in June 2020.

1.2. AMINOACYL-TRNA SYNTHETASE INHIBITORS

Aminoacyl-tRNA synthetases (AARS) are integral components of the cellular protein translation machinery, and they are responsible for charging tRNA molecules with their cognate amino acid via a two-step process.[16,17] In the first step (Equation 1.1) the AARS catalyzes the esterification of its cognate amino acid (AA) with adenosine triphosphate (ATP) to form an aminoacyl-adenylate (AA-AMP) intermediate and pyrophosphate (PPi).[16,17] In the second step (Equation 1.2), the AA-AMP intermediate is transesterified with its cognate tRNA to form an aminoacylated tRNA (AA-tRNA) and adenosine monophosphate (AMP).[16,17] Thus charged, the AA-tRNA can participate in polypeptide and protein synthesis at the ribosome.[16,17] In addition to this essential function, eukaryotic AARSs often serve as proofreaders ensuring translational fidelity via their editing domain, and they can be involved in transcription regulation, immune responses, and other cellular signaling pathways.[17]

$$\mathrm{AA + ATP + AARS \rightarrow AA\text{-}AMP{\cdot}AARS + PPi} \qquad (1.1)$$

$$\mathrm{AARS{\cdot}AA\text{-}AMP + tRNA \rightarrow AA\text{-}tRNA + AMP + AARS} \qquad (1.2)$$

AARSs are attractive targets for chemotherapeutic development for several reasons. The inhibition of AARSs causes an interruption of chain elongation at the ribosome thus halting protein synthesis, leading to a downregulation of RNA and DNA polymerase activity and ultimately the inhibition of cellular growth and proliferation.[16] Many parasites including *T. brucei* undergo continuous proliferation inside a host organism, making AARSs and other protein synthesis machinery good targets for chemotherapeutics because even in the absence of selectivity for parasite versus host enzymes, the chemotherapy will be more damaging to

parasites than host cells due to their higher rate of growth and proliferation.[17] However, selectivity for parasite AARSs is often achievable in both microbial and eukaryotic targets, as there is often a high degree of evolutionary divergence between mammalian AARSs and their bacterial or protozoan counterparts that result in substantial differences in their active site structures.[16,17] The utility of AARS inhibitors as anti-infective agents is borne out by the success of the topical antibiotic mupirocin (**1.8**, Figure 1.3), a selective bacterial isoleucyl-tRNA synthetase (IleRS) inhibitor commonly prescribed for the treatment of methicillin-resistant *Staphylococcus aureus* (MRSA) infections.[16]

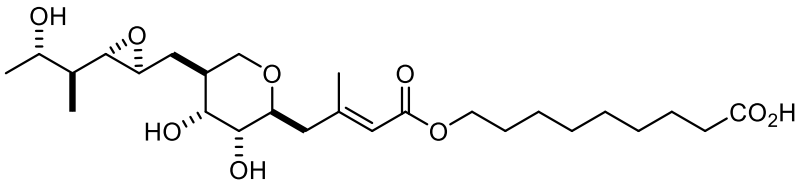

mupirocin (**1.8**)

Figure 1.3. Mupirocin (**1.8**), an isoleucyl-tRNA synthetase inhibitor used for the treatment of MRSA

1.2.1. *T. brucei* Leucyl-and-Isoleucyl-tRNA Synthetase Inhibitors

Several classes of AARS inhibitors have been developed targeting *T. brucei* isoleucyl tRNA synthetase (*Tb*IleRS) and leucyl-tRNA synthetase (*Tb*LeuRS).[17] Cestari and Stuart identified and screened a series of putative *Tb*IleRS inhibitors obtained from the National Cancer Institute These compounds were identified based on their structural homology with the isoleucyl-adenylate (Ile-AMP) intermediate, which is known to bind tightly ($K_d = 10^{-9}$ M) to IleRS.[18] From this screen, adenosine diastereomer **1.9** (Figure 1.4) was identified as a promising lead displaying potent *in vitro* activity and ≈900-fold parasite selectivity, and it was successful in curing a murine model of *T brucei* infection.[18] Ding and co-workers developed a series of *Tb*LeuRS inhibitors inspired by the antifungal benzoxaborole tavaborole (**1.10**, Figure 1.4), which inhibits LeuRS by trapping $tRNA^{Leu}$ in its editing site via the formation of a borate adduct with the 3'

terminal ribose of $tRNA^{Leu}$.[19,20] They built a homology model of the *Tb*LeuRS editing site and used this structure to guide the design of a series of substituted benzoxaboroles. They thus identified C(6) as the optimal site of substitution and prepared analogs such as **1.11** (Figure 1.4), which displayed a *Tb*LeuRS IC_{50} of 5 μM, *T. brucei* GI_{50} of 0.4 μM, and >100-fold parasite selectivity.[20] Zhao and co-workers also developed *Tb*LeuRS inhibitors using homology modeling of the *Tb*LeuRS active site to screen compounds from the Specs database *in silico*.[21] In this way, they identified several potential inhibitors with a 2-pyrrolidinone scaffold, and they subsequently synthesized and assayed a series of analogs, the best of which (**1.12**, Figure 1.4) displayed moderate (IC_{50} = 32 μM) activity against *Tb*LeuRS.[21] Finally, Zhang and co-workers developed a series of thiourea compounds designed to inhibit *Tb*LeuRS by mimicking the Leu-AMP intermediate, the most potent of which (**1.13**, Figure 1.4) displayed an IC_{50} of 1.1 μM.[22] Unfortunately, none of the compounds were active against *T. brucei* cell cultures at concentrations up to 100 μM, which the authors attribute to the poor membrane permeability of the compounds.[22]

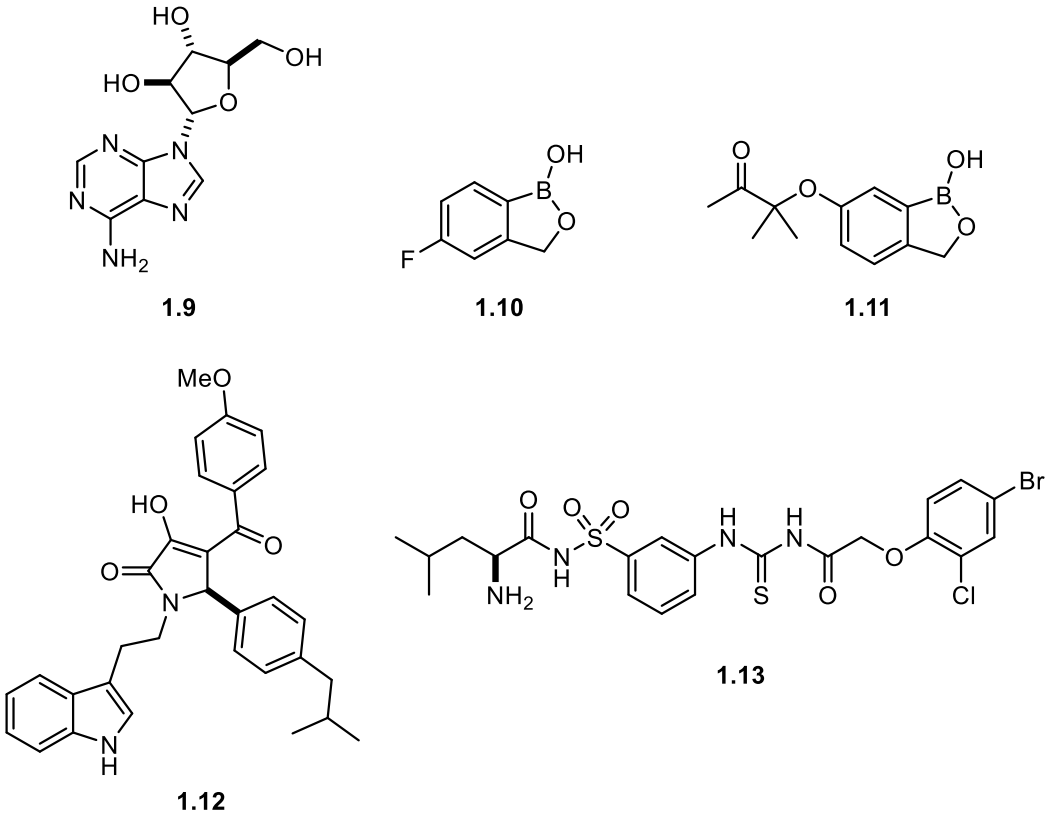

Figure 1.4. Adenosine-like *Tb*IleRS inhibitor **1.9**, fungal LeuRS inhibitor tavaborole (**1.10**), benzoxaborole *Tb*LeuRS inhibitor **1.11**, pyrrolidinone *Tb*LeuRS inhibitor **1.12**, thiourea *Tb*LeuRS inhibitor **1.13**

1.2.2. *T. brucei* Methionyl-tRNA Synthetase Inhibitors

The evolutionary and biochemical properties of *T. brucei* methionyl-tRNA synthetase (MetRS) make it an attractive target for chemotherapeutic development. Specifically, *Tb*MetRS is a type 1 MetRS, a distinction based on sequence similarity and susceptibility to various inhibitors. Type 1 MetRSs are found in Gram-positive bacteria including *S. aureus*, whereas type 2 MetRSs are usually found in archaea and eukaryotes, as well as some Gram-negative bacteria.[23] Mammalian cells contain both types of MetRSs, with type 2 MetRS present in the cytoplasm and type 1 MetRS present in the mitochondria.[23] Comparison of the sequence of *Tb*MetRS with human cytoplasmic MetRS reveals substantial differences in active site residues.[23,24] Selective type 1 MetRS inhibitors have been developed in the pharmaceutical industry as broad-spectrum antibiotics, culminating in the discovery of REP8839 (**1.14**, Figure

1.5), a diaryl diamine MetRS inhibitor that is currently in clinical trials for the treatment of *S. aureus* skin and wound infections.[25,26] In addition to validating type 1 MetRSs as druggable targets, the development of REP8839 provided a chemotype that has served as the basis for development of *Tb*MetRS inhibitors.

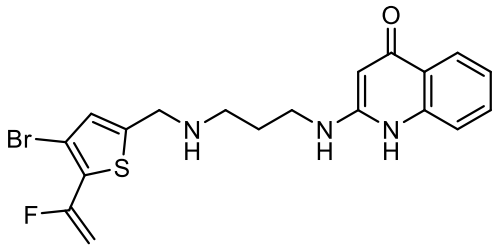

REP8839 (**1.14**)

Figure 1.5. The structure of REP8839 (**1.14**), a diaryl diamine MetRS inhibitor in clinical trials for treatment of topical *S. aureus* infections

Seminal work on the development of selective and potent *T. brucei* methionyl-tRNA synthetase (*Tb*MetRS) inhibitors was done by the research groups of Buckner, Fan, Verlinde, and Hol at the University of Washington—Seattle. In their preliminary studies they demonstrated via RNAi knockdown that *Tb*MetRS is essential for *T. brucei* growth. They then prepared a series of aminoquinolone diaryl diamines inspired by REP8839 (**1.14**, Figure 1.5), from which *meta*-dichlorinated analog **1.15** (Figure 1.6) emerged as their lead compound with a *T. brucei* 50% growth inhibition (GI_{50}) value of 4 nM and >5000-fold parasite selectivity.[23] However the compounds displayed several liabilities, including poor oral bioavailability and membrane permeability, a plasma half-life of only 1 hour, and in a mouse model of *T. brucei* infection **1.15** was only able to suppress parasitemia for 7-8 days.[23,27] These undesirable properties were attributed to the aminoquinolone moiety, which was known from antibacterial drug development to have poor bioavailability.[27]

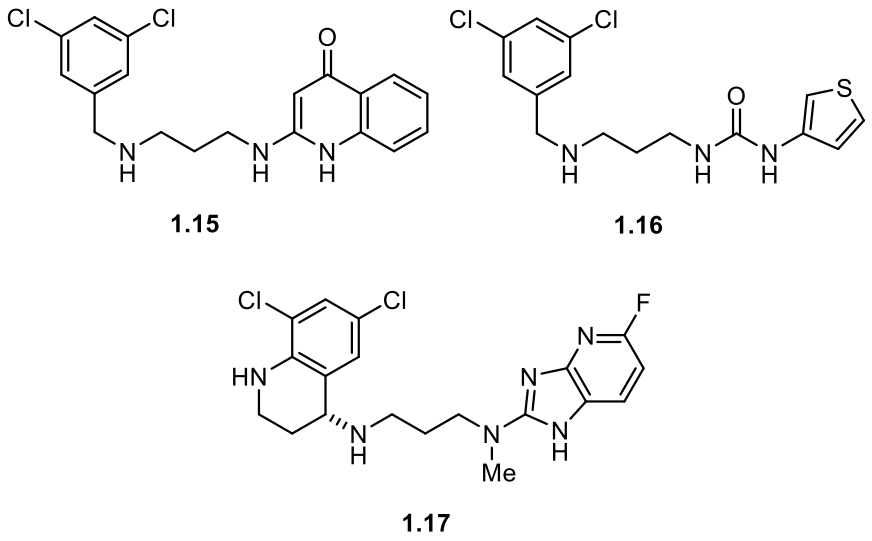

Figure 1.6. *Tb*MetRS inhibitors **1.15–1.17** developed by the Fan, Buckner, Verlinde, and Hol labs

A second series of urea-based diaryl diamines (*e.g.* **1.16**, Figure 1.6) was then designed, based on the rationale that the aryl-urea moiety should be able to participate in the same hydrogen-bonding and π-stacking interactions (*vide infra*) as the aminoquinoline moiety while imparting more desirable pharmacological properties.[27] Their lead compound **1.16** displayed 28 nM *Tb*MetRS IC_{50} and 220 nM *T. brucei* GI_{50} values, >50-fold parasite selectivity, and oral bioavailability and brain permeability in mice.[27] However, **1.16** was found to be just as metabolically labile as **1.15** with a plasma half-life of roughly 1 hour, and ultimately it was not able to rescue a mouse model of *T. brucei* infection.[27] Subsequent work found that incorporation of a halogenated aza-benzimidizole moiety (*e.g.* **1.17**, Figure 1.6) resulted in improved potency (**1.17** *T. brucei* GI_{50} = 0.4 nM), oral bioavailability and brain penetration, and **1.17** reproducibly cured a mouse model of early-stage *T. brucei* infection.[28]

The development of the *Tb*MetRS inhibitors exemplified by **1.15–1.17** was aided by extensive X-ray crystal structures of the inhibitors complexed with *Tb*MetRS.[24,29,30] These structures revealed the binding mode of the inhibitors, allowed for the identification of key interactions between the inhibitor and *Tb*MetRS, and provided fundamental insights into the structural biochemistry of *Tb*MetRS. Specifically, it was found that the *N*-benzyl moieties

occupy an enlarged methionine-binding pocket, with the chlorine atom of *m*-chlorinated analogs such as **1.15–1.17** occupying the same position as the sulfur atom of methionine.[24,29,30] The heteroaromatic moieties of **1.15–1.17** occupy a mostly hydrophobic pocket that is occluded in the methionine-bound *Tb*MetRS structure, dubbed the auxiliary pocket.[24,29,30] Binding in the auxiliary pocket is facilitated by a key hydrogen-bonding interaction between the carboxylate group of Asp_{287} and the various heteroaromatic *N*-H groups and π-stacking interactions with $Tyr_{250.}$[24,29,30] They also found that TbMetRS undergoes dramatic conformational changes upon binding with various substrates, as grossly different enzyme structures were observed in the methionine-bound, methionyl-AMP-bound, and inhibitor-bound complexes.[24] Analysis of the various *Tb*MetRS-substrate binding modes led the authors to conclude that their inhibitors bind to *Tb*MetRS via a conformational selection mechanism, as opposed to an induced-fit mechanism.[24] The insights gained from these studies informed the design of our *Tb*MetRS inhibitors, which will be described further in Chapter 2.

1.3. Previous Work in the Martin Lab

The Martin lab has a long-standing history in the twin fields of natural products synthesis and diversity-oriented synthesis (DOS) of targeted compound libraries via multi-component assembly processes (MCAPs).[31] These two research arenas are frequently symbiotic, as new targets and strategies for total synthesis often inspire and inform the development of new MCAP methodologies and DOS applications.[31] This relationship is nicely illustrated by the previous work in our lab, which led us to the discovery and development of novel *Tb*MetRS inhibitors.

1.3.1 Development of a Multi-Component Vinylogous Mannich Reaction for Indole Alkaloid Synthesis

As part of an ongoing program in the synthesis of indole alkaloids, the Martin lab sought to develop a concise synthesis of the *heteroyohimbinoid* and *coryantheoid* alkaloids tetrahydroalstonine (**1.18**), cathenamine (**1.19**), and geissoschizine (**1.20**, Scheme 1.1) utilizing a

hetero-Diels-Alder reaction.[32] To enable this strategy they sought an expeditious route for the synthesis of the hetero-Diels-Alder substrate **1.24**. To that end, dihydro-*β*-carboline **1.21**, which was prepared in two steps from tryptamine, was treated with *trans*-crotonyl chloride (**1.22**) in the presence of silyl dienol ether **1.23** at –78 ˚C, and upon warming the *N*-acyl-iminium intermediate underwent a vinylogous Mannich reaction to deliver **1.24** in 78% yield. Heating **1.24** in refluxing mesitylene brought about the desired hetero-Diels-Alder reaction to generate adduct **1.25** in 89% yield as a 9:1 mixture of diastereomers. Subsequent introduction of the E-ring carbomethoxy group was achieved via acylation with trichloroacetyl chloride followed by methanolysis to give key intermediate **1.26**. Full reduction of the amide moiety of **1.26** with alane and sodium cyanoborohydride delivered tetrahydroalstonine (**1.18**) in 90% yield, while partial reduction with lithium diethoxyaluminum hydride furnished cathenamine (**1.19**) in 70% yield. Finally, opening of the dihydropyran ring of **1.26** followed by a challenging 1,2-reduction of the *α,β*-unsaturated amide completed the synthesis of geissoschizine (**1.20**) in 35% yield over two steps.[32]

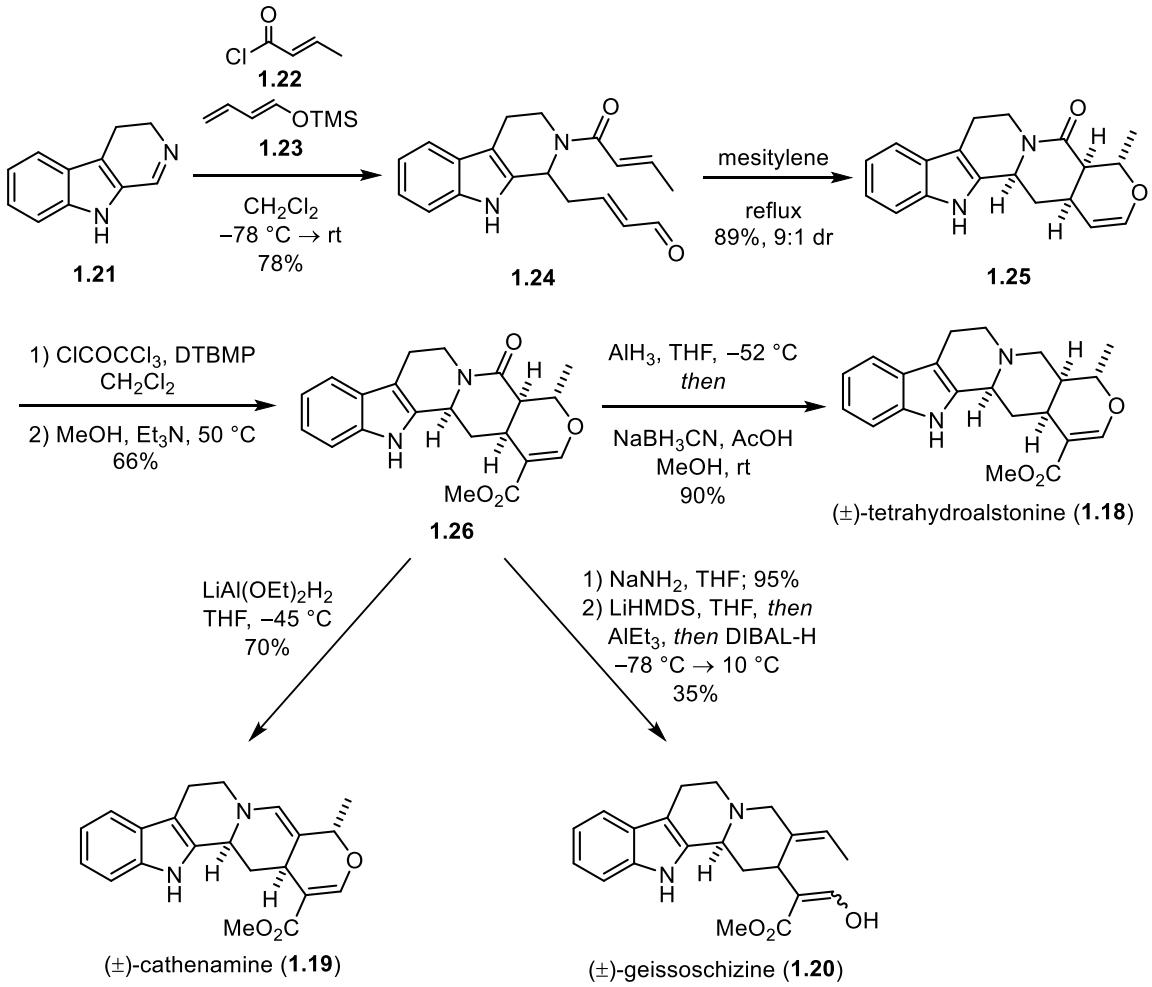

Scheme 1.1. Martin lab synthesis of tetrahydroalstonine (**1.18**), cathenamine (**1.19**), and geissoschizine (**1.20**)

The synthesis of **1.18–1.20** is remarkable for the brevity with which the A-E rings of the *heteroyohimbinoid* natural products were constructed, a mere two steps from known compound **1.21**. The obvious advantages of this approach led the Martin lab to apply the *β*-carboline vinylogous Mannich/(hetero)Diels-Alder reaction manifold to the synthesis of other indole alkaloids including oxogambirtanine (**1.27**), pteropodine (**1.28**), akuammicine (**1.29**), and strychnine (**1.30**, Figure 1.7).[33–36] In addition to the dihydro-*β*-carboline-derived natural products **1.27–1.30**, the VMR was also utilized in the synthesis of rugulovasines A & B (**1.31a,b**), setoclavine (**1.32**), pumiliotoxin 251D (**1.33**) and croomine (**1.34**, Figure 1.7).[37–39] These syntheses expanded the scope of the VMR by pioneering the use of siloxyfurans as the dienic

component to form *β*-amino butenolides, which in the syntheses of setoclavine **1.32** and pumiliotoxin **1.33** underwent subsequent lactone-lactam rearrangements. [37–39] These and other studies demonstrated that the VMR was quite generalizable, tolerating a wide variety of imino groups, acylating agents, and π-nucleophiles.[31,33] This generalizability enabled the development of a multi-component assembly process (MCAP), which was utilized to rapidly prepare diverse libraries of compounds inspired by bioactive natural products and medicines (*see Chapter 3 for further discussion*).[31]

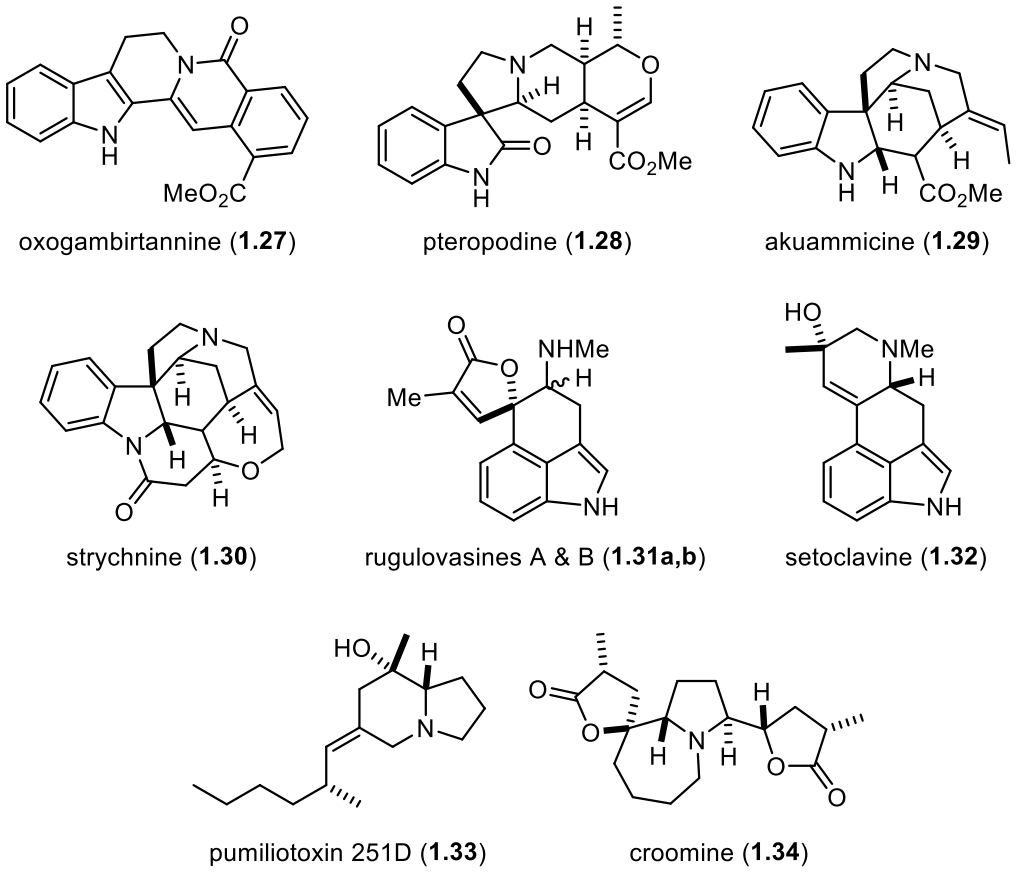

Figure 1.7. Other alkaloids synthesized in the Martin lab via the vinylogous Mannich reaction

1.3.2. Synthesis of *Yohimbine* and *Corynanthe* Alkaloid Analogs via a Multi-Component Assembly Process

Alkaloids from the *yohimbine* and *corynanthe* families (*e.g.* **1.18**, **1.20**, Scheme 1.1) are known to display an array of useful biological activities, often mediated by action at the α-adrenergic receptor.[40,41] Accordingly, these natural product scaffolds make attractive templates for a diversity-oriented synthesis (DOS), which the Martin lab developed using a Mannich-type MCAP as a key diversity-introducing step. Dihydro-β-carbolines **1.21**, **1.31**, and **1.32** were treated with **1.22** in the presence of silyl enol ether **1.33** to generate aldehydes **1.34–1.36**. Condensation of these aldehydes with *N*-methyl hydroxylamine in the presence of base lead to the formation of a nitrone *in situ*, which underwent a [3 + 2] dipolar cycloaddition upon heating with the pendant olefin to deliver isoxazolidines **1.37–1.39** in 38–60% yield over two steps (Scheme 1.2).[41]

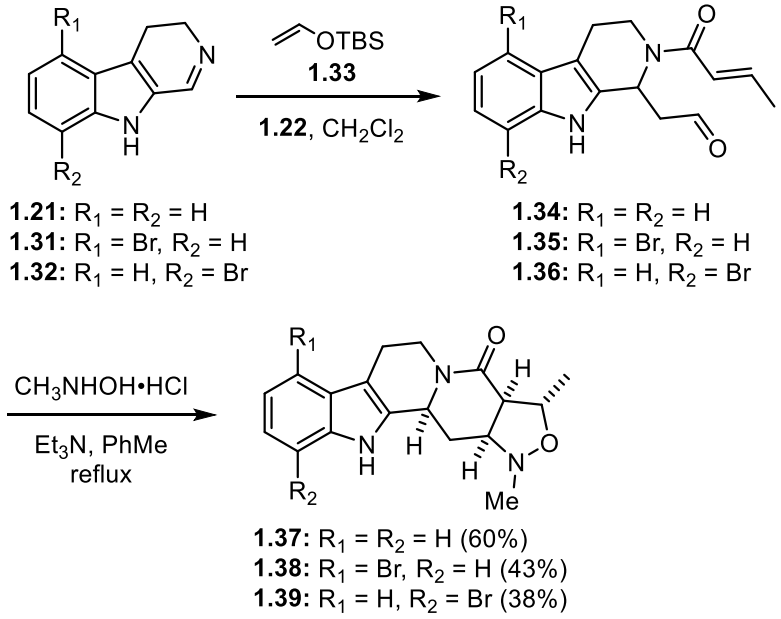

Scheme 1.2. Synthesis of isoxazolidines **1.37–1.39**

Intermediates **1.37–1.39** were subsequently carried through divergent synthetic sequences to deliver libraries of functionalized analogs with diverse chemotypes. Nor-bromo isoxazolidine **1.37** was reduced with $LiAlH_4$ to the amine **1.40**, and both **1.37** and **1.40** underwent reductive

ring opening to deliver amino alcohols **1.41** and **1.42** (Scheme 1.3). The secondary amino group of **1.41** and **1.42** was then functionalized with an array of reagents to generate the tertiary amines, (sulfon)amides, (thio)ureas, and carbamates that comprise analog sets **1.43** and **1.44** (Scheme 1.3).[41] Brominated isoxazolidines **1.38** and **1.39** underwent Suzuki coupling with a range of electron-rich, neutral, and deficient boronic acids, furnishing biaryl lactams **1.45** and **1.47** that were reduced with alane and lithium aluminum hydride, respectively, to deliver amino-isoxazolidines **1.46** and **1.48** (Scheme 1.4). Reductive ring-opening of **1.45–1.48** followed by *N*-functionalization delivered biaryl analog sets **1.53–1.56** (Scheme 1.4)**.** In total, 180 analogs with diverse steric and electronic functionality were prepared via these synthetic sequences, enabling exploration of the structure-activity relationships (SAR) for any target biological receptor.[41]

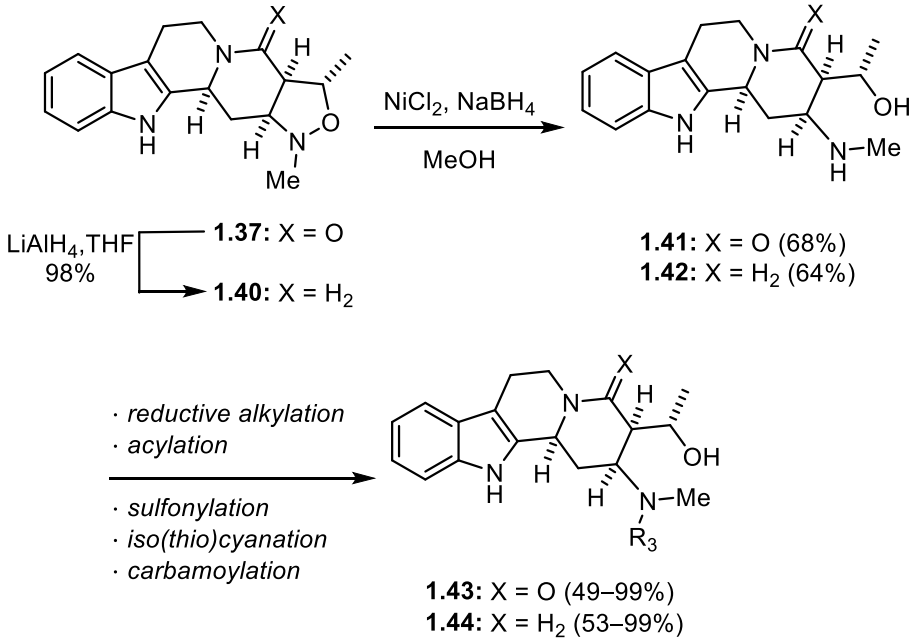

Scheme 1.3. Synthesis of amino- and amido- analog sets **1.43** and **1.44**

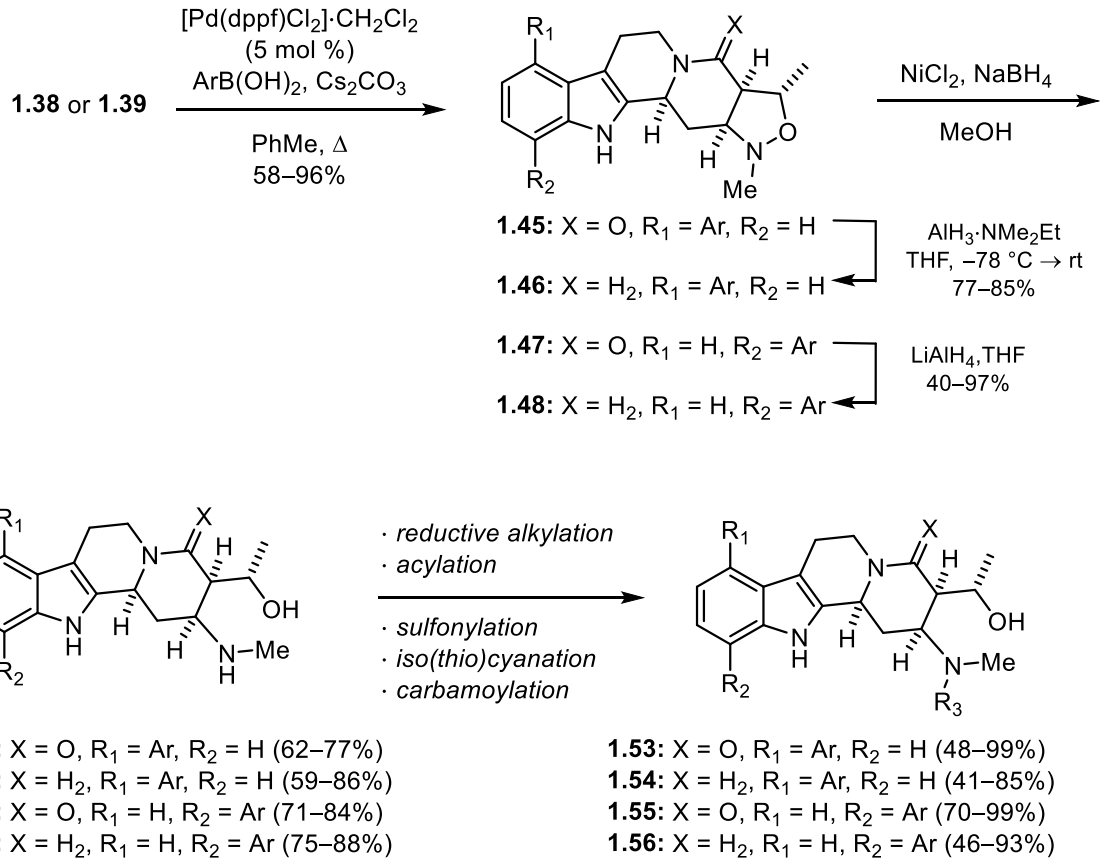

Scheme 1.4. Synthesis of biaryl analog sets **1.53–1.56**

Screening of analog sets **1.43–1.44** and **1.53–1.56** was carried out by the National Institute of Health's (NIH) Molecular Library Probe Production Center Network (MLPCN) and the National Institute of Mental Health's Psychoactive Drug Screening Program (PDSP).[41,42] The Molecular Libraries Initiative (MLI)—a component of the 2004 NIH Roadmap for Medical Research—was a far-reaching program that sought to leverage the then-recently-completed sequencing of the human genome and facilitate public-sector research into the development of new classes of biological tool compounds and therapeutic leads.[42,43] These screening efforts identified several analogs in our molecular libraries as having promising biological activity, including several compounds that inhibited *Tb*MetRS and *T. brucei* growth *in vitro*.[41] These initial hits formed the basis of our efforts to develop novel HAT therapeutic leads, which will be discussed further in Chapter 2.

Chapter 2. Development of Novel Anti-Trypanosomal Compounds

2.1 Initial Hits & Design of Target Scaffolds

Our work on the development of novel anti-trypanosomal compounds from the initial hits **2.1–2.3** (Figure 2.1) identified by the NIH MLI began with an analysis of their SAR and a comparison of their structural features with the *Tb*MetRS inhibitors developed by the the Buckner, Fan, Verlinde, and Hol labs (*see section* **1.2.2**).[23,24,27–30]

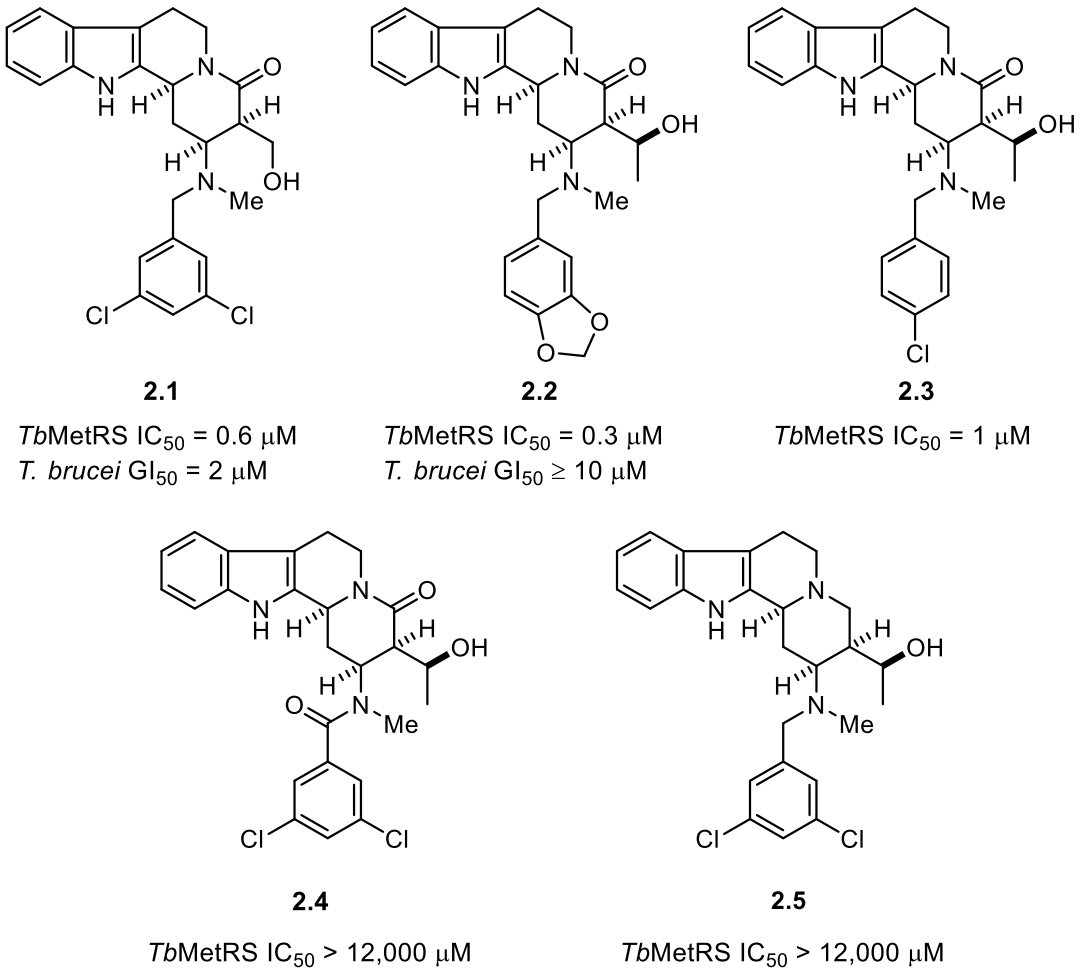

Figure 2.1. *Tb*MetRS initial hits **2.1–2.3** and inactive analogs **2.4–2.5**

Comparison of our initial hits with the *Tb*MetRS inhibitors synthesized by Fan and co-workers revealed notable similarities and differences (*see* Figure 1.6). Both feature *N*-benzyl and

heteroaromatic moieties, but in our compounds these substituents are connected via a rigid quinolizinone core, whereas in the majority of the Fan compounds they are joined by a flexible diaminopropane linker.[23,27,28,30] Our initial hits displayed the following *Tb*MetRS IC_{50} values: **2.1** IC_{50} = 0.6 μM**,** **2.2** IC_{50} = 0.3 μM, and **2.3** IC_{50} = 1 μM (Figure 2.1). Benzamide **2.4** and diamine **2.5** were both inactive against *Tb*MetRS; this finding will prove to be significant during the later stages of our studies (*vide infra*). This limited SAR was in accordance with that observed by Fan and co-workers. Namely, the increased activity of *m*-dichloro analogs relative to *p*-chloro analogs.[23,27] While none of their compounds featured a *N*-piperonyl moiety, they did find that *m*-methoxy substitution seemed to improve activity, while *p*-methoxy substitution did not.[27] These similarities lead us to hypothesize that our compounds might interact with *Tb*MetRS in a similar fashion, with the *N*-benzyl moiety occupying the methionine-binding pocket and the heteroaromatic moiety occupying the auxiliary pocket (*see* Figure 2.2).

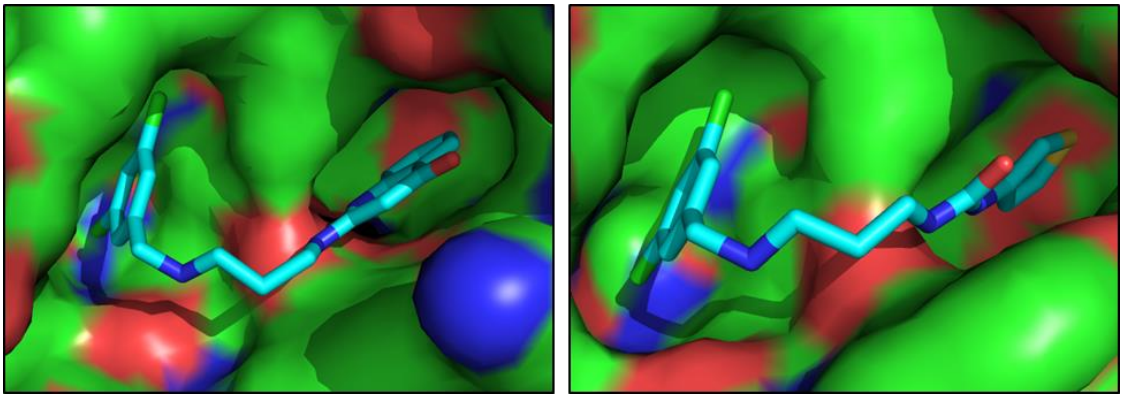

Figure 2.2. Crystal structures of aminoquinoline and urea inhibitors **1.15** (left) and **1.16** (right) bound to *Tb*MetRS (*see* Figure 1.6). PDB: 4EG5, 4MVW

Analysis of the X-ray structures of compounds such as **1.15** and **1.16** in complex with *Tb*MetRS lead us to a rationale for the design of analogs of **2.1–2.3**. The crystal structures of **1.15** and **1.16** bound *Tb*MetRS show that the inhibitors must adopt a bent conformation in order for the *N*-benzyl and heteroaromatic moieties to access their respective binding pockets while

avoiding the central ridge formed by Val_{473} (Figure 2.2).[23,27] Based on this observation, we reasoned that increasing the conformational flexibility of our analogs might enable them to adopt an optimal orientation while mitigating any steric clash with Val_{473}, thus improving their binding affinity and anti-trypanosomal activity. To test this hypothesis, we envisioned severing the C(2)–C(3) bond of our scaffold **2.6** to give a scaffold with the general structure **2.7** (Figure 2.3). In addition to increasing the flexibility of the scaffold, we reasoned that this would allow for a more modular synthesis with late-stage diversification of either the indole or *N*-benzyl substituents and variation of the linker connecting the heteroaromatic (indole) substituent to the scaffold core. At the outset of the project, we planned to prepare two distinct series of compounds, differentiated by the presence or absence of a R_2 alkoxy motif on the lactam core of **2.7**. The alkoxy-lactam compounds (X = O, R_2 = $CH(CH_3)OH$, CH_2OH) were prepared by Dr. Alan R. Meis, and their synthesis will not be discussed here.[44] A third series of compounds with a piperidine core was also prepared, following the discovery of a piperidine analog that displayed potent *T. brucei* growth inhibition (*vide infra*).

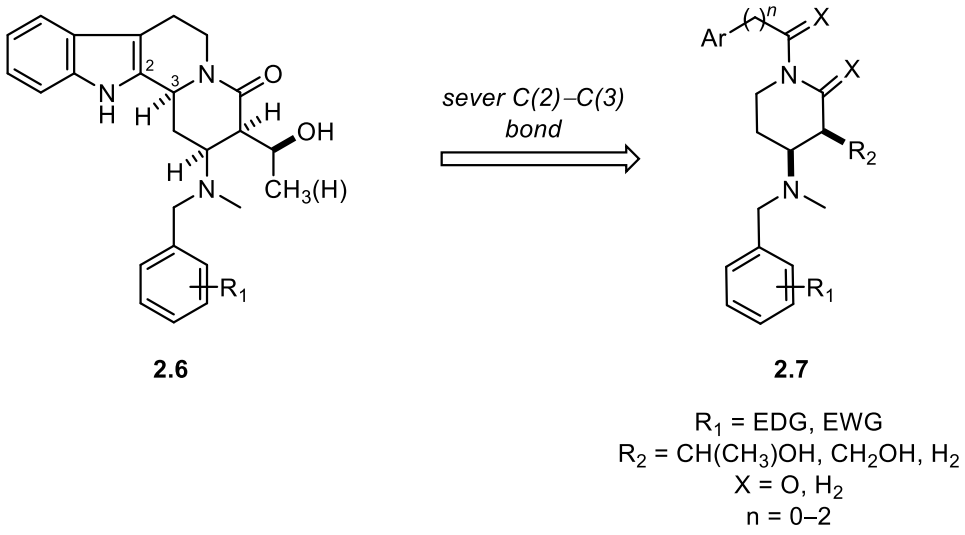

Figure 2.3. Design of conformationally flexible scaffold **2.7** from initial hit scaffold **2.6**

2.2 Synthesis of Lactam & Piperidine Analog Sets

2.2.1. Synthesis of *δ*-Lactam Analogs

Our initial plan for the synthesis of *δ*-lactam analogs was to introduce the heteroaromatic moiety and alkyl linker in the final step via *N*-alkylation of a fully functionalized lactam ring (*e.g.* **2.14** → **2.16**, Scheme 2.1). This route was attractive to us because it would enable late-stage introduction of both the *N*-benzyl and heteroaromatic moieties. The synthesis of **2.16** began with the partial hydrolysis of malonate **2.8** to generate carboxy-acid **2.9**, which was then converted to an acyl chloride and treated with amine **2.10** in the presence of catalytic iodine to generate cyclization precursor **2.11** in 45% yield**.** Sodium hydride-promoted Dieckmann cyclization, followed by saponification and decarboxylation delivered keto-lactam **2.12** in 50% yield. Subsequent reductive amination with benzylamine **2.13** followed by deprotection with CF_3CO_2H (TFA) gave amino-lactam alkylation substrate **2.14**. Unfortunately, attempts effect the alkylation of **2.14** with **2.15** using sodium hydride or sodium hexamethyldisilazide as the base in a variety of solvent and temperature regimes only resulted in the hydrolysis or elimination of alkyl bromide **2.15** to generate tryptophol or 3-vinylindole, respectively.

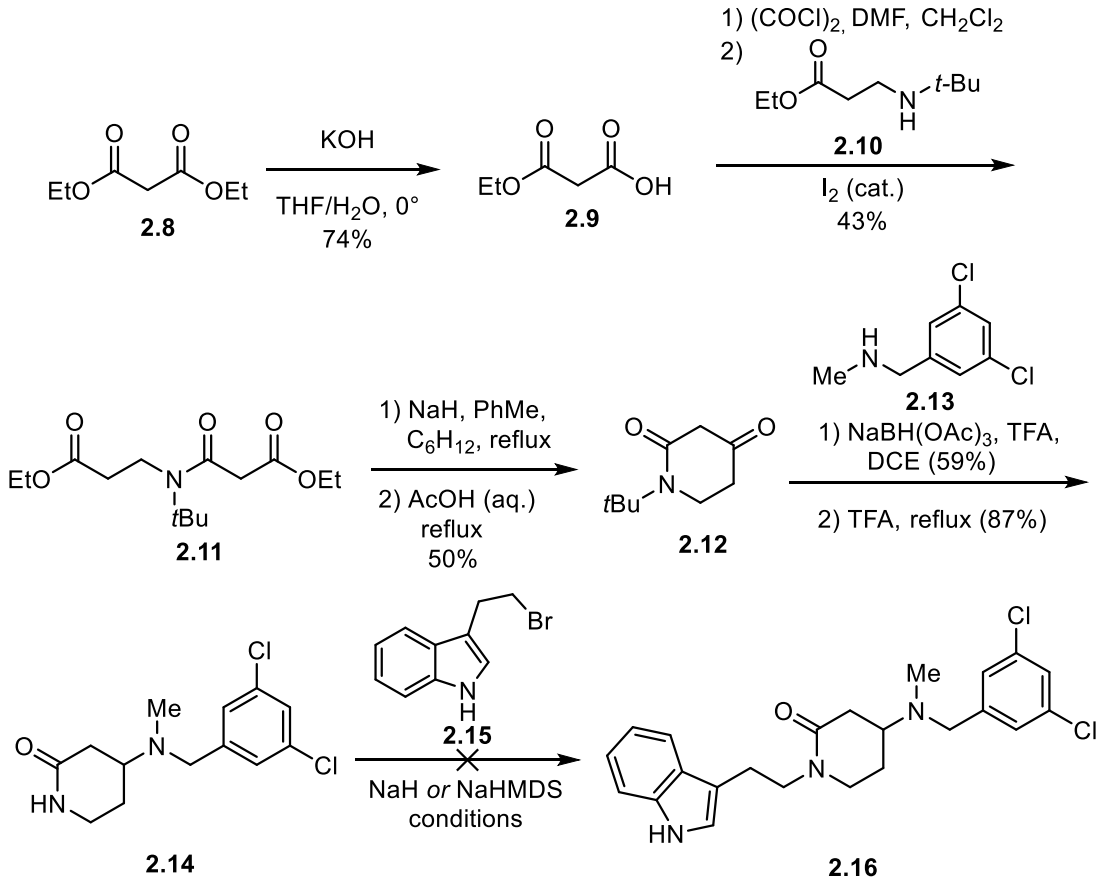

Scheme 2.1. Failed synthesis of lactam analog **2.16** via amide *N*-alkylation

For our revised synthesis of **2.16**, we decided to include indole-ethyl moiety from the outset and thus avoid the problematic lactam alkylation. While this approach would not enable facile variation of the linker-heteroaromatic moiety, it would still allow us to readily introduce various *N*-benzyl groups. In the event, conjugate addition of tryptamine (**2.17**) into ethyl acrylate gave intermediate **2.18**, which underwent *N*-(3-dimethylaminopropyl)-*N'*-ethylcarbodiimide (EDCI)-mediated acylation with **2.9** to generate **2.19** (Scheme 2.2). Cyclization and saponification/decarboxylation gave keto-lactam **2.20**, which was reductively aminated with **2.13** to deliver *N*-dichlorobenzyl lactam analog **2.16** in 10% yield, along with significant quantities of vinylogous urea **2.21**, which proved resistant to reduction.

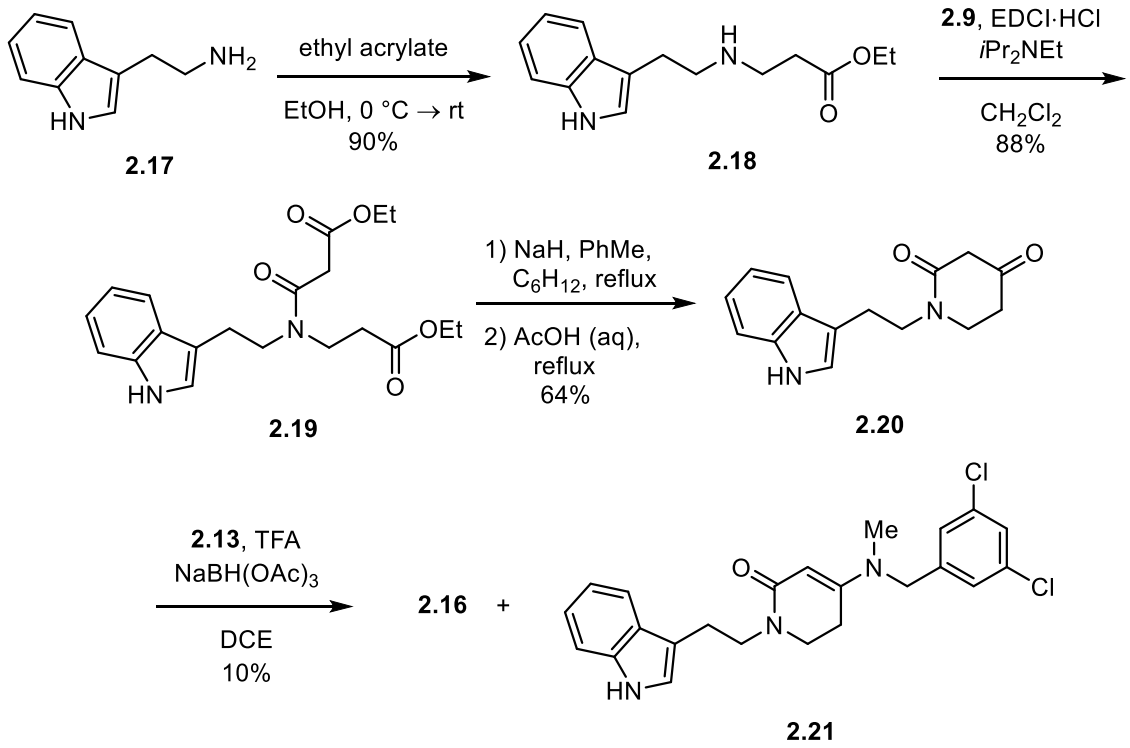

Scheme 2.2. Synthesis of *δ*-lactam analog **2.16** via a revised route

Attempts were made to optimize the reductive amination of **2.20** with secondary benzylamines such as **2.13**, but we invariably observed large quantities of vinylogous urea side-products and thus concluded that an alternate approach was needed. We reasoned that the use of a primary amine instead of a secondary amine for the reductive amination of **2.20** might mitigate enamine (vinylogous urea) formation, and after some experimentation, we found that **2.20** readily underwent reductive amination with methylamine to generate methylamino-lactam **2.22** in 71% yield, with no trace of any vinylogous urea byproducts. Reductive alkylation of **2.22** with various substituted benzaldehydes **2.23** furnished *δ*-lactam analog set **2.24 – 2.31** in 58–81% yield.

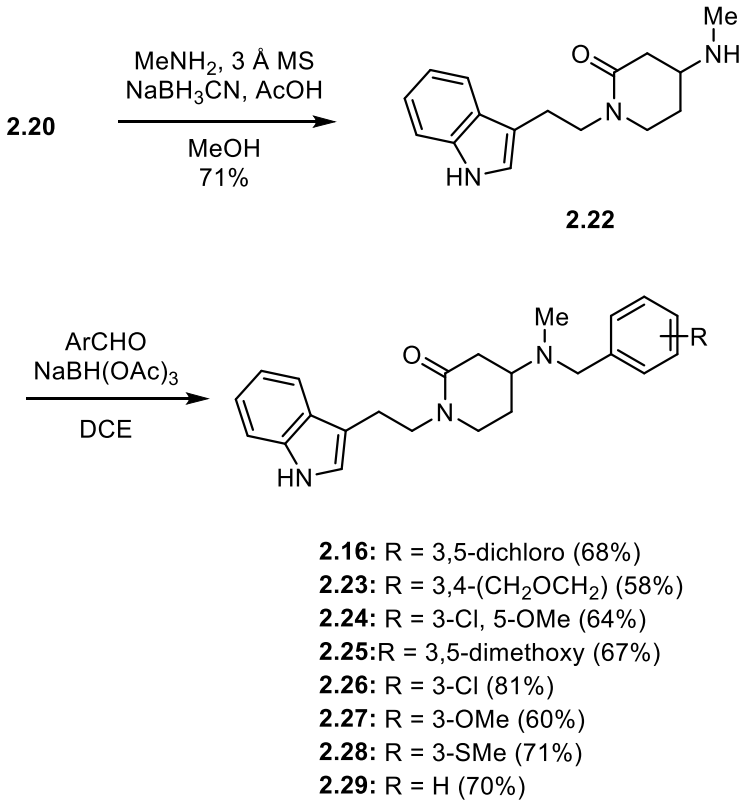

Scheme 2.3. Synthesis of *δ*-lactam analogs **2.16** and **2.23–2.29** via amino-lactam **2.22**

Drawing inspiration from the compounds prepared by Fan and co-workers (*see* Figure 1.6), we also sought to prepare analogs with a secondary *N*-benzyl moiety. This was achieved via the treatment of keto-lactam **2.20** with excess ammonium acetate and sodium cyanoborohydride to generate primary amine **2.30** (Scheme 2.4). Subsequent imine formation followed by reduction delivered *N*-H analogs **2.31** and **2.32**.

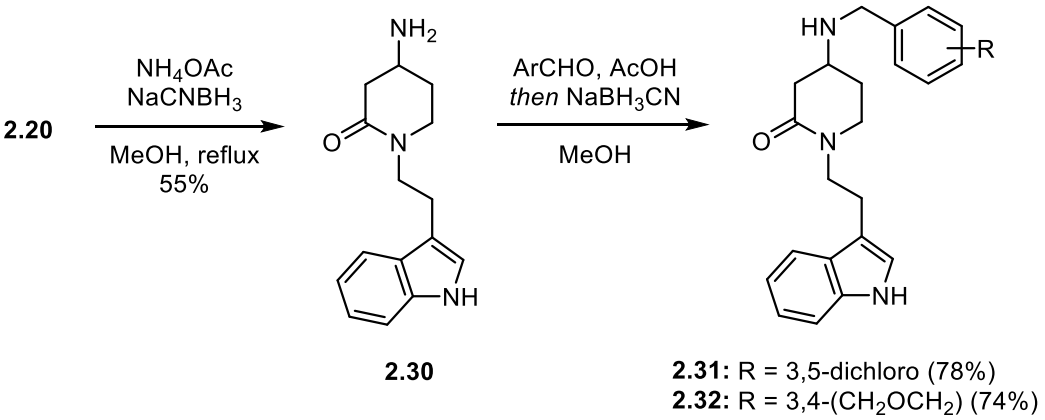

Scheme 2.4. Synthesis of *N*-H analogs **2.31** and **2.32**

Having thus secured an initial series of *δ*-lactam analogs designed to probe the SAR of the *N*-benzyl moiety and finding that several of these compounds did indeed inhibit *T. brucei* growth *in vitro*, we returned our attention to securing a route for the late-stage introduction of the heteroaromatic-linker moiety. During the course of these investigations we developed an improved synthesis of alkylation substrate **2.14**, summarized in Equation 2.1.

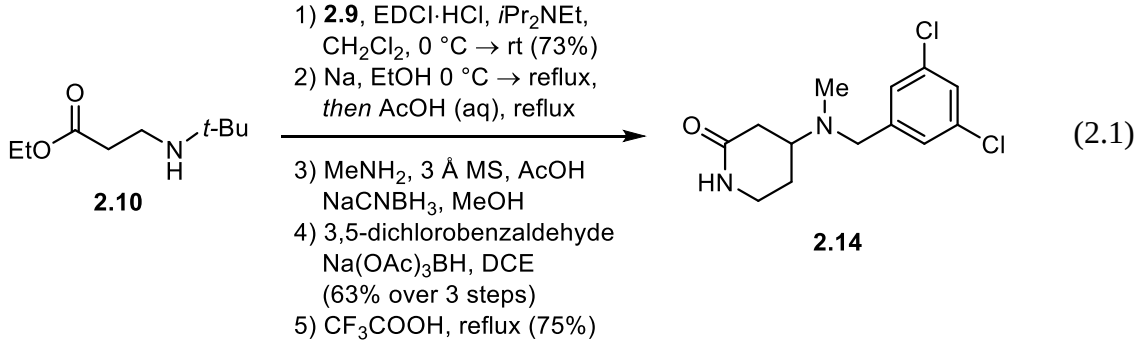

(2.1)

After discovering precedent for the use of potassium hydroxide in DMSO to effect *N*-alkylation of a *δ*-lactam, we successfully utilized these conditions to alkylate **2.14** with bromo-ethers **2.33** and **2.34**, which was prepared in three steps from *o*-allylphenol, to generate phenyl-ether and phenol analogs **2.36** and **2.37** in 44% and 33% yield, respectively.[45] However, when we attempted to use these conditions to prepare 7-aza-indole analog **2.38** via alkylation with **2.35**, only returned starting material and uncharacterized degradation products were obtained.[46]

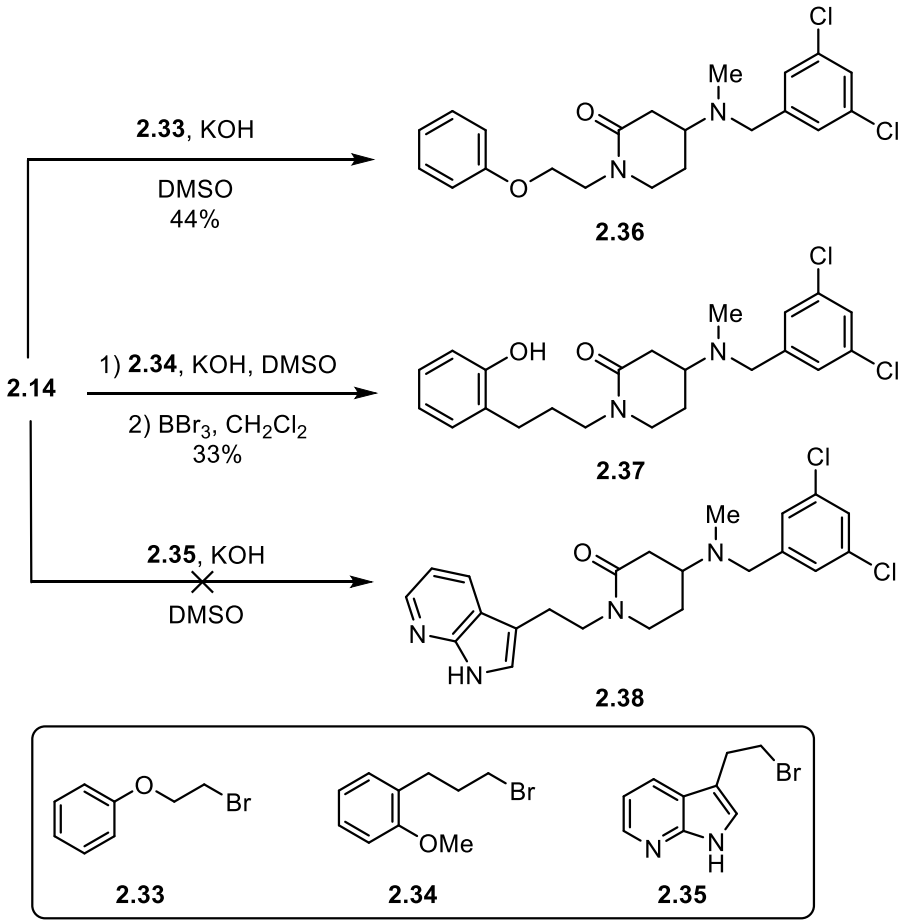

Scheme 2.5. Alkylation of **2.14** with **2.33–2.35** using KOH/DMSO conditions

The low yields and limited substrate scope of these *δ*-lactam *N*-alkylation reactions prompted us to explore an alternate strategy for introducing the heteroaromatic moiety. We envisioned that incorporation of a pendant *N*-acetonitrile group on our *δ*-lactam core might allow for facile derivatization via Buchwald-Hartwig or Chan-Lam cross-coupling reactions of the masked amino moiety. To pursue this idea, we prepared **2.41** from *β*-alanine (**2.39**) via a three-step esterification, *N*-alkylation, and *N*-acylation sequence. Unfortunately, subjecting **2.41** to our optimized Dieckmann conditions generated an intractable mixture of byproducts, and this strategy was not pursued further.

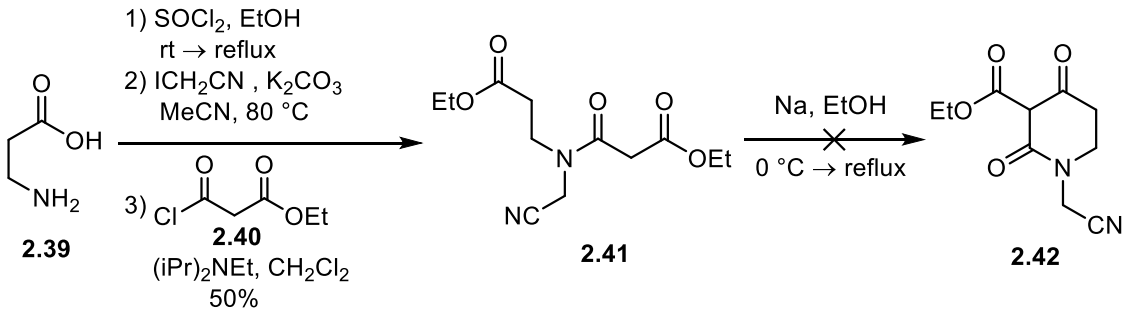

Scheme 2.6. Attempted synthesis of *δ*-lactams with an *N*-CH_2CN functional handle

2.2.2. Synthesis of Piperidine Analogs

We initially set out to prepare acyl-piperidines with the general structure **2.43** (Figure 2.4) to test the effects of restricting a rotor on our heteroaromatic linker. In addition to this SAR insight, the piperidine scaffold **2.43** was attractive to us for its ease of derivatization at both the *N*-benzyl and heteroaromatic sites.

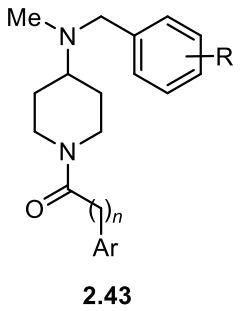

2.43

Figure 2.4. Acyl-piperidine scaffold **2.43**

Preparation of acyl-piperidine analogs began with reductive amination of Boc-piperidone **2.44** with methylamine to generate **2.45**, which was then reductively alkylated and Boc-deprotected to deliver diamines **2.46** and **2.47** (Scheme 2.7). The free *N*-H of **2.46** and **2.47** was then acylated with a series of indole carboxylic acids to deliver acyl-piperidine analogs **2.51–2.54**. Analogs **2.51** and **2.52** were designed for direct comparison with *δ*-lactam analogs **2.16** and **2.24**, while 5'MeO- derivative **2.53** was prepared because we had found that other 5'-MeO-analogs had shown increased potency in a *T. brucei* growth inhibition assay (*vide infra*). When

2.51–2.53 were found to be inactive against *T. brucei*, we prepared the indole-propionic acid derivative **2.54** to see if increasing the linker length would improve activity, but **2.54** likewise proved to be inactive.

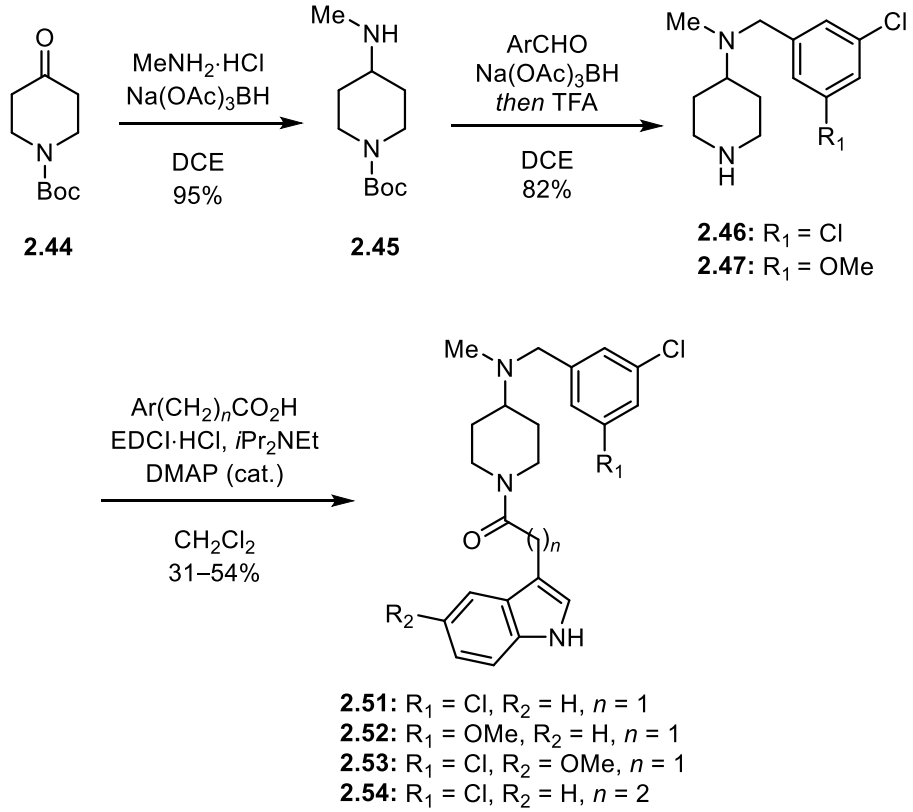

Scheme 2.7. Synthesis of acyl piperidines **2.51–2.54**.

Hoping to gain a new lead from our failed series of acyl-piperidines, we reduced **2.51** with lithium aluminum hydride to generate piperidine analog **2.55** (Equation 2.2).

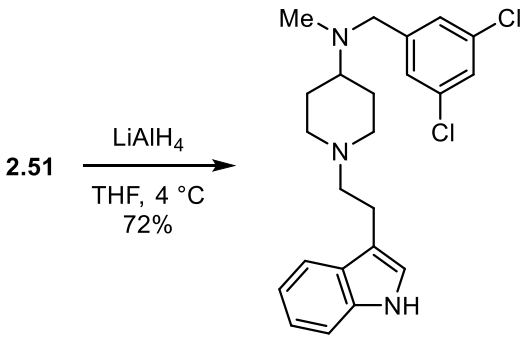

2.55

(2.2)

We were initially hesitant to prepare piperidine diamines such as **2.55**, due to finding such compounds to be inactive in the context of our initial tetracyclic scaffold (*e.g.* **2.5**, Figure 2.1). Contrary to our expectations, **2.55** was an excellent *T. brucei* growth inhibitor, so we pivoted to the preparation of a small library of analogs built around a piperidine core.

For our piperidine library, we sought to vary both the *N*-benzyl and heteroaromatic substituents. Thus, a series of *N*-benzyl variants **2.56–2.59** were prepared from **2.45**, and **2.46** was re-synthesized following this new procedure (Equation 2.3). While the reductive alkylation/Boc-deprotection sequence had previously been telescoped for the synthesis of **2.46** and **2.47** (*see* Scheme 2.7), we found that this procedure suffered from reproducibility issues, and we thus opted for the two-step sequence shown in Equation 2.3.

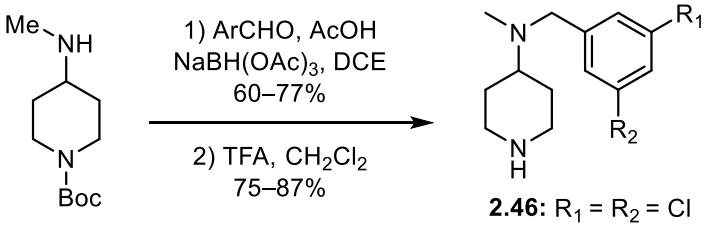

2.45

2.46: $R_1 = R_2 = Cl$
2.56: $R_1 = Cl$, $R_2 = H$
2.57: $R_1 = MeO$, $R_2 = H$
2.58: $R_1 = MeS$, $R_2 = H$
2.59: $R_1 = R_2 = H$

(2.3)

Derivatization of **2.46** and **2.56–2.59** via the introduction of heteroaromatic-linker moieties was achieved via divergent synthetic sequences dictated by the availability of the various *N*-functionalizing reagents and the compatibility of the amide (or keto-amide) reducing agents with the functional groups present on the molecule. For amido- compounds with aryl chloride substituents such as **2.51** and **2.60–2.62**, we found that using the Lewis-acidic reducing

agents alane and borane mitigated competitive dehalogenation during the preparation of **2.55** and **2.63–2.65** (Scheme 2.8). Fluorinated derivative **2.67** required extra consideration, as we found that the use of acid during workup of the borane-mediated ketoamide reduction resulted in facile reduction of the electron-deficient indole ring to form a difficult-to-separate indoline byproduct. Thankfully, we were able to find conditions to lyse the diamine-borane adducts—cesium fluoride and sodium carbonate in refluxing ethanol—which did not result in any indoline formation, thus generating fluorinated analog **2.67**. [47] The synthesis of **2.67** was developed in collaboration my undergraduate mentee Alexandra Pham.

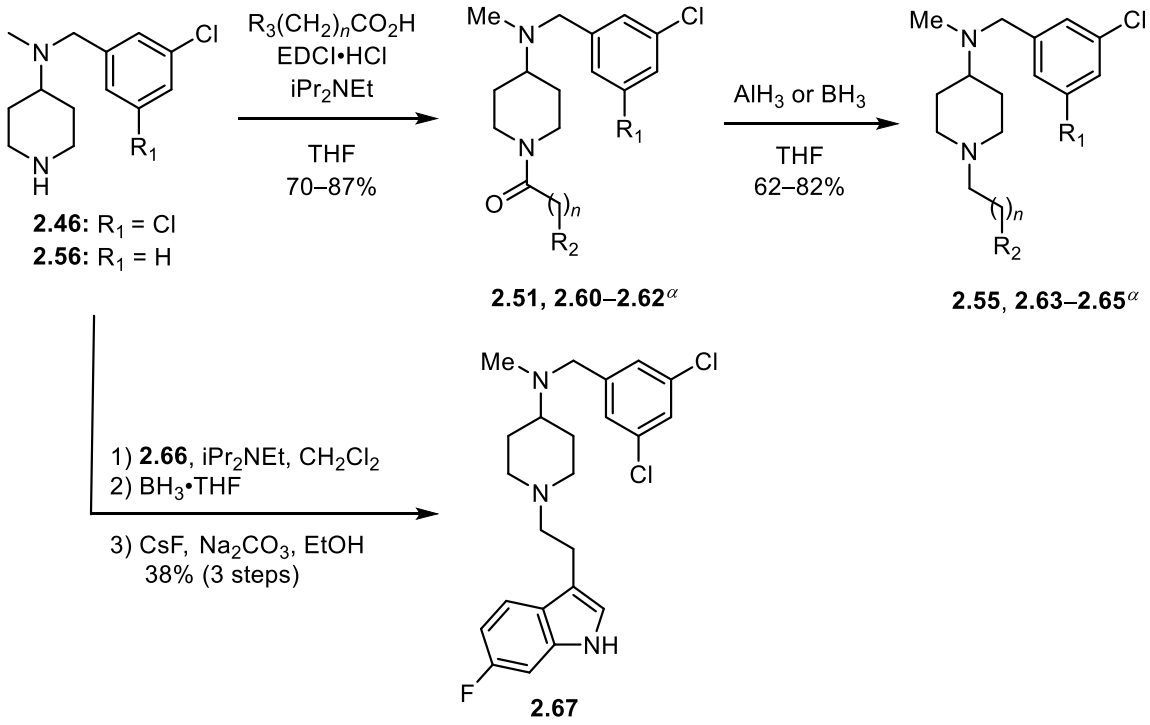

Scheme 2.8. Synthesis of piperidine analogs **2.55**, **2.63–2.65**, and **2.67**.

To enable comparison of the *N*-benzyl substituent SAR on the piperidine scaffold with our other scaffolds, three additional 5'-MeO-indole analogs were prepared for direct comparison with **2.63** and **2.65** (*see* Scheme 2.8). Piperidine intermediates **2.57–2.59** (*see* Equation 2.3) were treated with ketoacyl chloride **2.68**, and the resultant ketoamide was reduced with lithium aluminum hydride to deliver analogs **2.69 – 2.71** (Scheme 2.9).

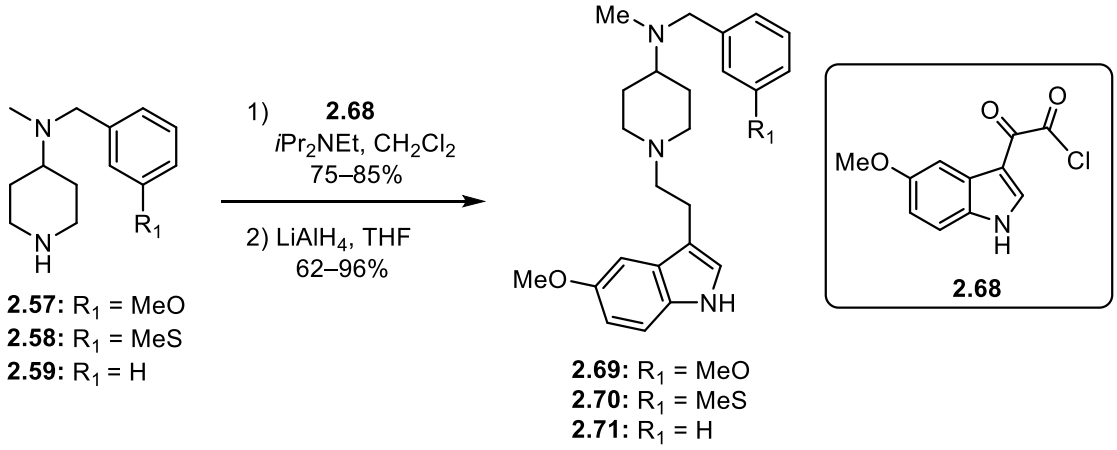

Scheme 2.9. Synthesis of piperidine analogs **2.69 – 2.71**

Aza-indole analog **2.72** and phenyl-urea analog **2.73** were prepared via alkylation or acylation of **2.46** with **2.35** (*see* Scheme 2.5) or phenyl isocyanate, respectively (Scheme 2.10).

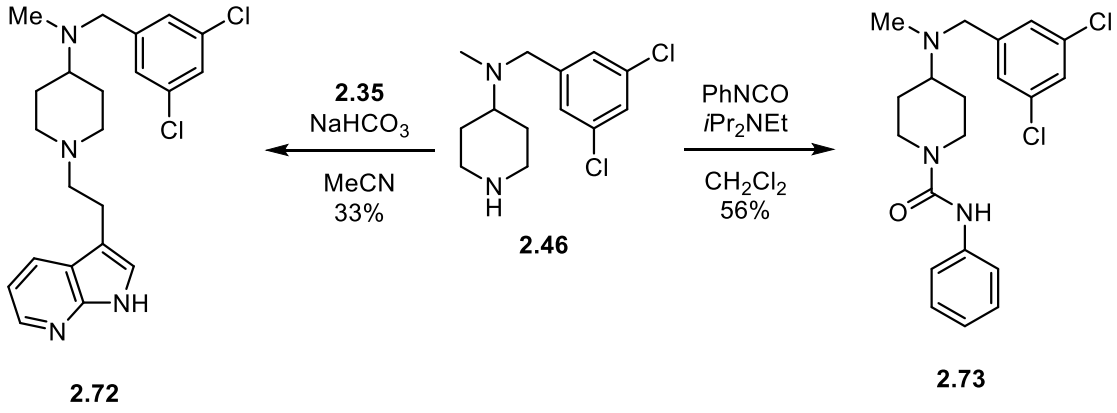

Scheme 2.10. Synthesis of piperidine analogs **2.72** and **2.73**

Finally, analog **2.76** was prepared to assess the effect of a benzamide moiety on the piperidine scaffold. To this end, *N*-methylamino intermediate **2.45** (*see* Scheme 2.7) was acylated with mixed anhydride **2.74**; Boc-deprotection and alkylation with **2.75** delivered benzamide analog **2.76**. This synthetic sequence was developed and carried out by Alexandra Pham.

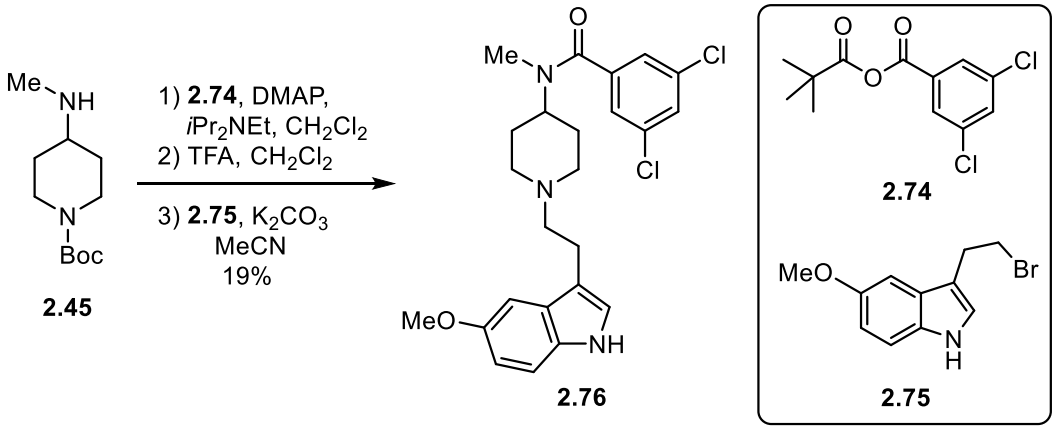

Scheme 2.11. Synthesis of piperidine benzamide analog **2.76**

2.3 BIOLOGICAL EVALUATION OF INHIBITORS

To assess the viability of our analogs as anti-trypanosomal compounds, we assayed their inhibition of *T. brucei* growth *in vitro,* their inhibition of recombinant *Tb*MetRS in an aminoacylation assay, and their ability to stabilize *Tb*MetRS via complexation in a thermal shift assay. The *T. brucei* growth inhibition assay was performed by our collaborators in the Mensa-Wilmot Lab at The University of Georgia, whereas the aminoacylation and thermal shift assays were performed in our lab and will be discussed further in Section 2.3.2.

2.3.1. *T. brucei* Growth Inhibition

Our initial series of lactam (**2.16**, **2.23–2.29**) and hydroxylactam (**2.77–2.84**) analogs, shown in Table 2.1, were designed to probe the SAR around the *N*-benzyl substituent and to make direct comparisons between the two scaffold types. Analysis of their GI_{50} values appears to support our central hypothesis that scaffolds with increased flexibility would display improved anti-trypanosomal activity, as both **2.77** and **2.16** were five-fold more active against *T. brucei* than initial hit **2.1**, which displayed a GI_{50} of 25.3 μM in this assay (Figure 2.5). We found the hydroxylactam scaffold to be superior to the lactam scaffold, as **2.77–2.84** were better growth inhibitors than their counterparts **2.16** and **2.23–2.29**. This trend may be explained by the difference in solubility between the two scaffolds, as we found many lactam analogs were sparingly soluble in aqueous media, while the hydroxy-lactam analogs readily went into solution. Finally, our SAR trends appeared to be broadly in agreement with those observed by Fan and co-workers. For example, the *m*-chloro analogs **2.16, 2.24, 2.26, 2.77, 2.79,** and **2.81** were relatively potent while the *m*-diMeO analogs **2.25** and **2.80** and unsubstituted analogs **2.29** and **2.84** were considerably less potent.[23,27]

Table 2.1. Growth inhibition (GI_{50}) of *T. brucei* with hydroxylactam analogs **2.77–2.84** and lactam analogs **2.16** and **2.23 – 2.29**

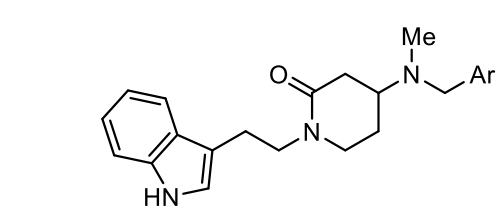

2.16, **2.23–2.29**

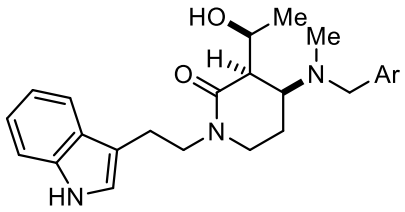

2.77–2.84

Ar =

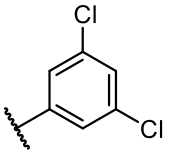

2.16: 7.1 μM[α]
2.77: 4.3 μM

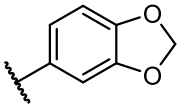

2.23: ≥ 10 μM
2.78: 3.9 μM

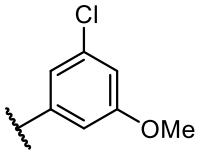

2.24: 6.2 μM
2.79: 4.8 μM

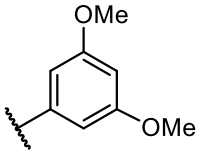

2.25 ≥ 10 μM
2.80: ≥ 10 μM

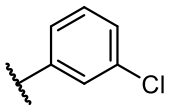

2.26: 9.0 μM
2.81: 2.1 μM

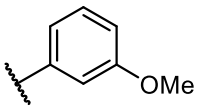

2.27: ≥ 10 μM
2.82: 5.7 μM

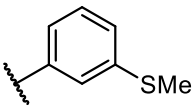

2.28: ≥ 10 μM
2.83: 2.3 μM

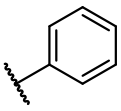

2.29: ≥ 10 μM
2.84: ≥ 10 μM

[α] error values were consistently <10% with the exception of **2.78** (18%) and **2.83** (26%)

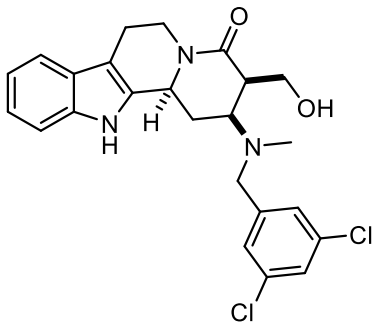

2.1
T. brucei GI_{50} = 25.3 μM

Figure 2.5. *T. brucei* GI_{50} of initial hit **2.1**, as determined by UGa collaborators

Lactam *N*-H analogs **2.31** and **2.32** and phenyl ether/phenol analogs **2.36** and **2.37** were all found to have *T. brucei* GI_{50} values ≥ 10 μM (Table 2.2). Because 8 of the 12 lactam analogs had GI_{50} values ≥ 10 μM, and so derivatives of this scaffold were not pursued any further.

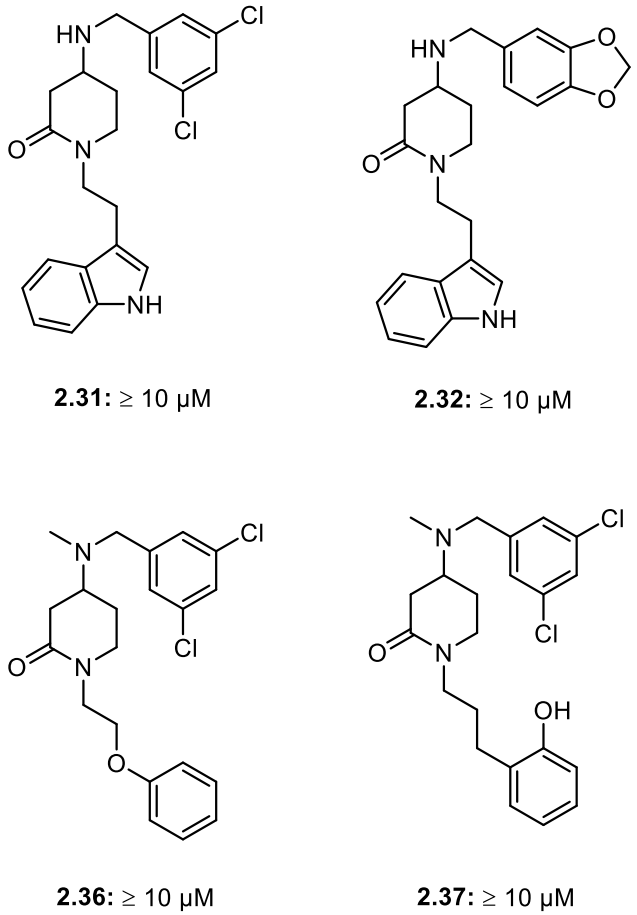

2.31: ≥ 10 μM **2.32:** ≥ 10 μM

2.36: ≥ 10 μM **2.37:** ≥ 10 μM

Figure 2.6. Growth inhibition (GI_{50}) of *T. brucei* with lactam *N*-H analogs **2.31, 2.32** and phenyl ether/phenol analogs **2.36, 2.37**.

In the interest of further elucidating the SAR of our hydroxylactam scaffold, Dr. Alan Meis prepared analogs **2.85–2.91** (Table 2). These analogs were designed to probe the SAR of the indole-lactam linker length (**2.85, 2.86**), of substituents on the indole ring (**2.87–2.90**), and of the pendant hydroxyethyl moiety (**2.91**). Considering our hypothesized binding mode in which the heteroaromatic and *N*-benzyl moieties occupy two binding pockets separated in space, we were surprised to find that one-carbon and three-carbon analogs **2.85** and **2.86** were equipotent

with each other and with two-carbon analog **2.77** (GI_{50} = 4.3 μM, *see* Table 2.1). However, the introduction of substituents on the indole ring did have a substantial effect on the activity against *T. brucei*. The addition of a methoxy substituent at the 5'-position as in **2.87** resulted in a five-fold increase in activity, making this our most potent analog to date; addition of a benzyloxy substituent at the 5'- or the 4'-positions as in **2.88** and **2.89** resulted in a two-fold increase in activity. This potentiating effect was not observed with the addition of a hydroxyl substituent, as 5'-hydoxy analog **2.90** was equipotent with unsubstituted analog **2.77**. We also wanted to determine what effect, if any, the methyl group of the pendant hydroxyethyl substituent has, because it was absent in initial hit **2.1**, but present in **2.2** (*see* Figure 2.1). Comparing the nor-methyl analog **2.91** with **2.77**, we found the presence or absence of the methyl group had little effect *T. brucei* growth inhibition.

Table 2.2. Growth inhibition (GI_{50}) of *T. brucei* with hydroxylactam analogs **2.85–2.91**

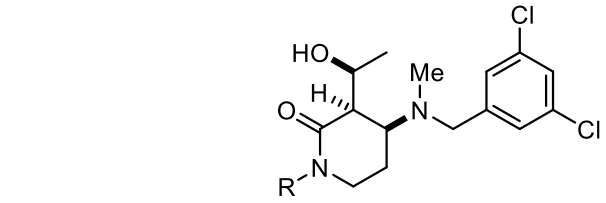

2.85–2.90

R =

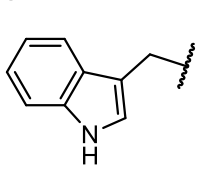

2.85: 4.1 μM[α]

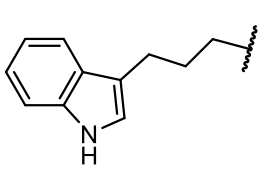

2.86: 5.5 μM

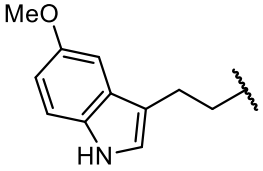

2.87: 0.95 μM

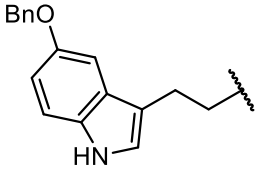

2.88: 2.1 μM

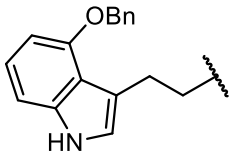

2.89: 2.0 μM

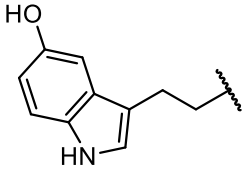

2.90: 5.5 μM

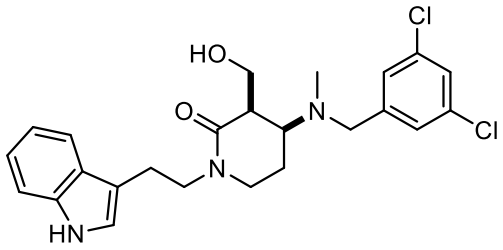

2.91: 5.5 μM

[α] error values were consistently <10% with the exception of **2.85** (15%), **2.88** (19%) and **2.90** (11%)

The piperidine analog series was notable for producing several potent *T. brucei* growth inhibitors and for demonstrating SAR trends that caused us to question the hypothesized binding mode of our compounds with *Tb*MetRS. As mentioned previously, acyl-piperidines **2.51–2.54** (*see* Scheme 2.7) have GI_{50} values ≥ 10 μM. However, *N*-alkyl piperidine **2.55** displayed a GI_{50} value of 1.7 μM (Table 2.4), making it one of our most potent compounds, second only to the 5'-MeO-indolyl hydroxylactam derivative **2.87** (*see* Table 2.3) at this stage of the project. Several

N-dichlorobenzyl piperidine derivatives were prepared to assess SAR of the heteroaromatic substituent on the piperidine nitrogen, the results of which are summarized in Table 2.4. Analysis of 5'-methoxyindolyl analog **2.63** was complicated by a discrepancy in results. In an initial screen **2.63** displayed a GI_{50} in the range of 1–5 μM, but in a follow-up assay the GI_{50} was 25 μM. We tentatively suspect that this discrepancy is due to degradation of the compound and believe the initial measurement to be indicative of the correct GI_{50} value, based on the observed potency of other *N*-dichlorobenzyl and 5'-methoxyindolyl piperidine analogs. Despite this ambiguity, we can conclude that incorporation of a 5'-methoxyindolyl substituent on the piperidine scaffold did not have the same potentiating effect that was observed with the hydroxylactam scaffold, as **2.55** and **2.63** appear to be roughly equipotent. The introduction of an electron-deficient 6'-fluoroindolyl moiety in analog **2.67** likewise had little effect on activity. Replacement of the indolyl group of **2.55** with a benzimidazole moiety in analog **2.64** proved inconsequential, while introduction of a 7-azaindole moiety in **2.72** resulted in a four-fold reduction in activity. Finally, phenyl-urea analog **2.73** was found to have a GI_{50} value $\geq$ 10 μM, which was in accord with the poor activity observed with acyl-piperidine derivatives **2.51–2.54**.

Table 2.3. Growth inhibition (GI_{50}) of *T. brucei* with piperidine analogs **2.55, 2.63, 2.64, 2.67, 2.72,** and **2.73**

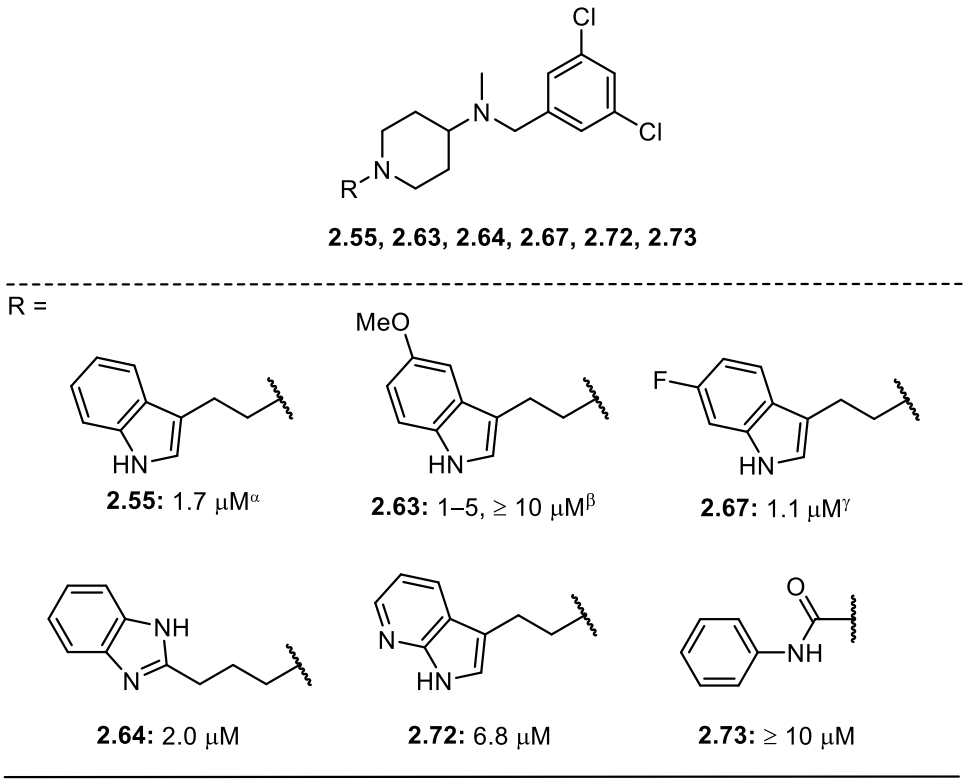

α error values were consistently <10% with the exception of **2.64** (30%). β initial screen showed GI_{50} to be in the range of 1–5 μM, follow-up screen gave $GI_{50} \geq 10$ μM. γ error not determined.

We also prepared a series of 5'-MeO-indolyl piperidine derivatives to probe the SAR of *N*-benzyl substituents, the results of which are summarized in Table 2.5. These SAR trends diverged considerably from those which were observed in the lactam and hydroxylactam analog series (*see* Table 2.1). Thioanisole derivative **2.70** was one of the most potent piperidine analogs with a GI_{50} of 1.6 μM, consistent with the observed potency of thioanisole hydroxylactam analog **2.83** (Table 2.1). However, *m*-chloro and *m*-MeO-benzyl piperidine analogs **2.65** and **2.69** were equipotent (GI_{50} = 3.5–3.6 μM), which was inconsistent with the previous observation that *m*-chloro analogs were consistently more potent than *m*-methoxy analogs in the lactam and hydroxylactam analog series (*c.f.* **2.26** and **2.81**, **2.27** and **2.82**, Table 2.1). Inconsistent SAR was also observed with unsubstituted *N*-benzyl analog **2.71**, which displayed a GI_{50} value of 6.1 μM, wherease the unsubstituted *N*-benzyl lactam and hydroxylactam analogs **2.29** and **2.84** both had

GI_{50} values ≥ 10 μM. Finally, *m*-dichloro benzamide analog **2.76** displayed a GI_{50} value of 2.9 μM, while in the initial tetracyclic series of compounds benzamide analogs (*e.g.* **2.4**, Figure 2.1) were found to have GI_{50} values ≥ 10 μM.

Table 2.4. Growth inhibition (GI_{50}) of *T. brucei* with piperidine analogs **2.65, 2.69–2.71, 2.76**: *N*-benzyl substituent SAR.

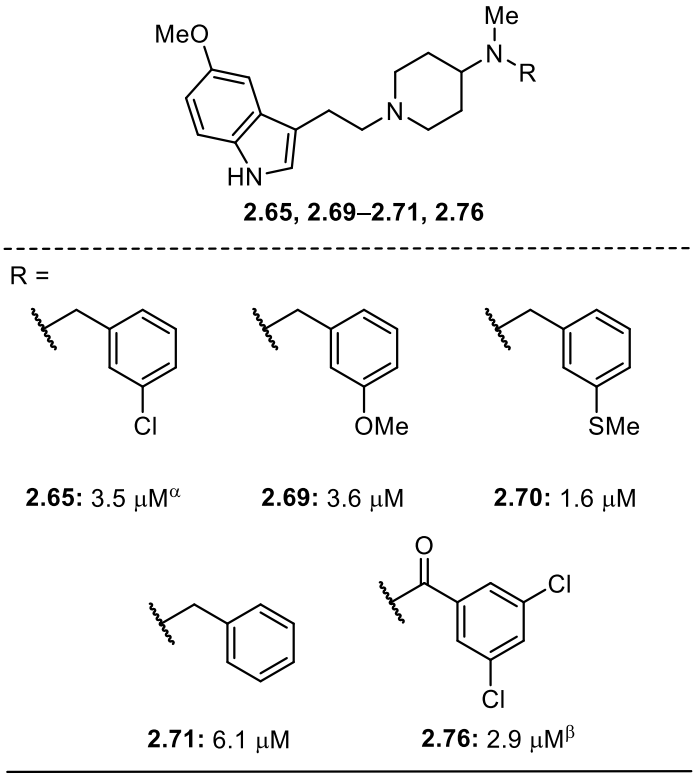

α error values were consistently <10% with the exception of **2.71** (11%).
β error not determined

While the inconsistencies in SAR observed between scaffolds could be rationalized as the result of subtle stereoelectronic effects, the paucity of observable SAR within analogs of the same scaffold—most noticeable in the piperidine analog series—raised concerns regarding the hypothesized binding mode of our compounds to *Tb*MetRS and the presumption that the observed inhibition of *T. brucei* growth was occurring via the inhibition of *Tb*MetRS. To address these concerns, we decided to evaluate our compounds as inhibitors of *Tb*MetRS *in vitro.*

2.3.2. Inhibition of *T. brucei* MetRS

At the inception of our program to develop potent analogs of initial hits **2.1** and **2.2**, we had intended to determine their ability to inhibit *T. brucei* growth, and to determine their binding energetics with *Tb*MetRS using isothermal titration calorimetry (ITC). We also planned structural studies of selected complexes using X-ray crystallography. However, our efforts toward the latter were thwarted by low yields of recombinant *Tb*MetRS obtained from expression in *E. coli*. Unfortunately, we were also not able to use the radiolabeled methionine *Tb*MetRS aminoacylation inhibition assay developed by Buckner and co-workers, as our lab was not equipped or authorized to use radioactive materials.[27] Ultimately we settled on the use of a colorimetric pyrophosphatase-coupled *Tb*MetRS aminoacylation inhibition assay, adapted from the procedure developed by Cestari and Stuart for the analysis of *Tb*IleRS inhibitors (*see* Section 1.2.1).[18,48] In this assay, the pyrophosphate (PP_i) byproduct generated from aminoacyl-adenylate formation is converted to phosphate (P_i) by the enzyme pyrophosphatase. P_i concentration is then measured via its complexation with the malachite green reagent using visible-light spectrophotometry.[49] To calibrate our assay we tested our initial hit **2.1**, which we found to have an IC_{50} value of 4.9 ± 1.5 μM, as well as **2.92**, a representative phenyl-urea inhibitor developed by Fan, which was found to have an IC_{50} value of 1.6 ± 0.3 μM (Figure 2.5). The discrepancy between the IC_{50} values determined by us for **2.1** and **2.92** and those determined by the MLPCN or the Buckner lab is not surprising, as IC_{50} values are assay-specific and vary with enzyme and substrate concentration. We were by necessity using higher concentrations of *Tb*MetRS, ATP, methionine, and tRNA in our colorimetric assay than was used in their radiolabeled methionine assay, which led to higher IC_{50} values.[50]

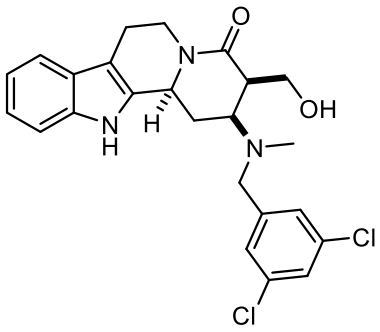

2.1
*Tb*MetRS IC_{50} = 4.9 ± 1.5 μM,
R^2 = 0.98
T. brucei GI_{50} = 25.3 μM

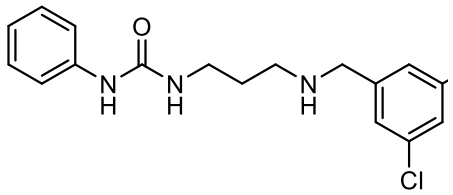

2.92
*Tb*MetRS IC_{50} = 1.6 ± 0.3 μM,
R^2 = 0.96
T. brucei GI_{50} = 0.3 μM

Figure 2.7. *Tb*MetRS IC_{50} and *T. brucei* GI_{50} values for positive controls **2.1** and **2.92**.

What was surprising, however, was the discovery that most of our analogs are inactive against *Tb*MetRS at concentrations up to 200 μM. The handful of compounds that displayed >15% inhibition at 200 μM are shown in Table 2.5. Hydroxy-lactam analogs **2.77, 2.79, 2.84**, and **2.90** were all weakly active. It is interesting that *N*-dichlorobenzyl analog **2.77** was active, but the *N*-piperonyl analog **2.78** and the nor-methyl *N*-dichlorobenzyl analog **2.87** were inactive, because these two compounds were the most direct analogs of our initial hits **2.1** and **2.2** (*see* Table 2.1 and 2.3). It is also noteworthy that the 5'-hydroxyindolyl analog **2.90** was one of the most potent *Tb*MetRS inhibitors, while 5'-hydroxyindolyl analog **2.87**, our most potent *T. brucei* growth inhibitor, was completely inactive against *Tb*MetRS. The lactam series fared worse, with only the *N*-dichlorobenzyl analog **2.16** and *N*-H dichlorobenzyl analog **2.31** displaying any activity. Acyl-piperidine analog **2.52** was weakly active, and none of the piperidine analogs displayed any activity against *Tb*MetRS. These results were corroborated via a thermal shift assay, in which all of our "flexible" analogs displayed negligible ΔT_m values, but **2.1** showed a ΔT_m of 2.4 ˚C.[51] Collectively, the results of our *Tb*MetRS assays show that our strategy for improving our initial hits by increasing their conformational flexibility paradoxically abolished their activity against *Tb*MetRS, while maintaining, and in many cases improving, their activity as *T. brucei* growth inhibitors.

Table 2.5. Percent inhibition (> 15%) of *Tb*MetRS at 200 μM inhibitor concentration.

Inhibitor (200 μM)	% Inhibition of *Tb*MetRS ± SEM
2.77	28 ± 7
2.79	17 ± 5
2.84	17 ± 2
2.90	27 ± 3
2.16	17 ± 11
2.31	31 ± 2
2.52	17 ± 8

2.3 INDOLOQUINOLIZIDINE ANALOG SYNTHESIS AND ANALYSIS

For the final phase of the project, we set to apply the insights gained from our flexible analog sets to the indoloquinolizidine scaffold of our initial hits. Specifically, we targeted analogs with 5' substituents on the indole ring, because 5'-methoxy analog **2.87** was our most potent *T. brucei* growth inhibitor, and 5'-hydroxy analog **2.90** displayed relatively potent anti-*Tb*MetRS activity (*see* Tables 2.3 and 2.5).

Synthesis of the 5'-methoxyindolyl analog **2.98** and the 5'-hydroxyindolyl analog **2.99** was realized via the synthetic sequence developed by Granger and co-workers using 5-methoxytryptamine **2.94**, which was readily prepared from 5-methoxyindole (**2.93**), as our starting material (Scheme 2.12). A boron tribromide (BBr_3)-mediated demethylation converted **2.98** to **2.99**.

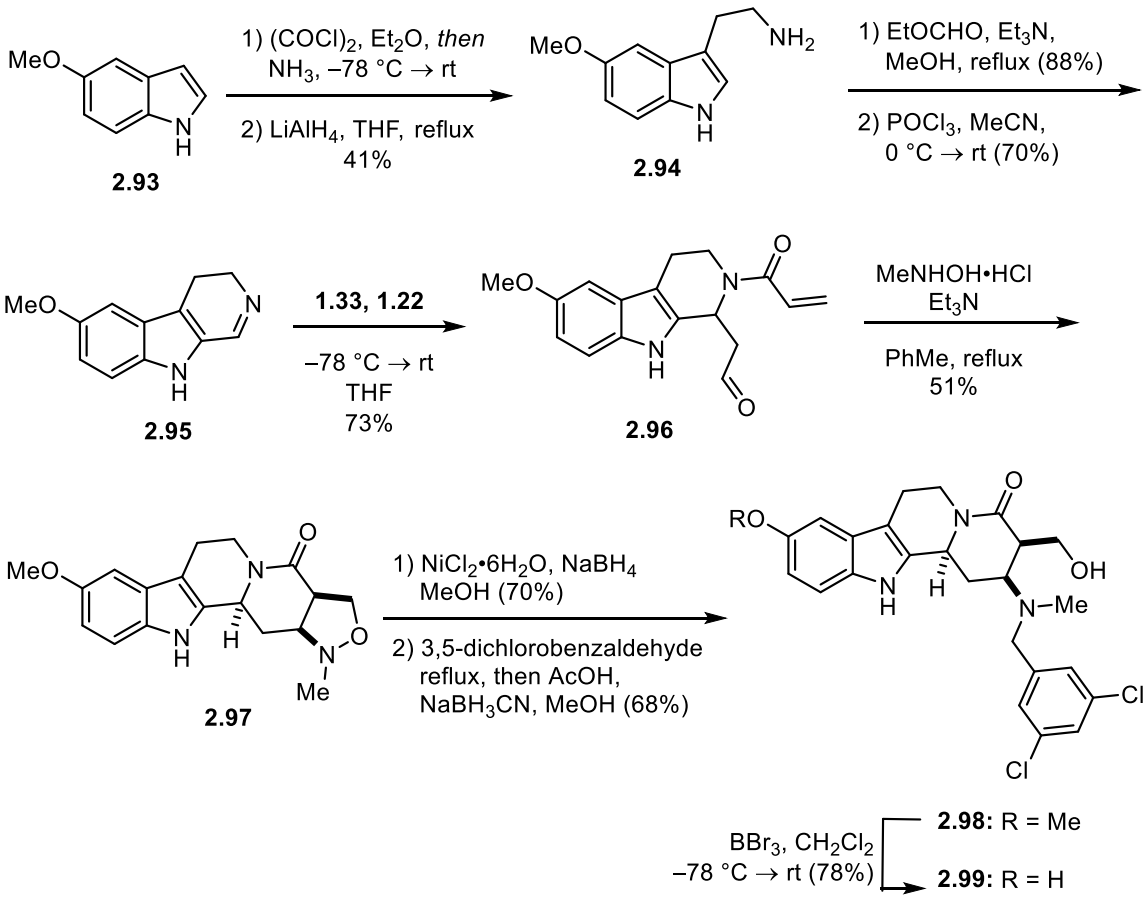

Scheme 2.12. Synthesis of indoloquinolizidine analogs **2.98** and **2.99**

Comparing the biological activity of **2.98** and **2.99** with **2.1** revealed that addition of the 5'-indolyl substituents resulted in a decrease in *Tb*MetRS inhibition that was 2–3-fold for **2.99** and >20-fold for **2.98**. Interestingly, both **2.98** and **2.99** showed a 2-to-3-fold increase in *T. brucei* growth inhibition relative to **2.1**. This discrepancy suggests that the indoloquinolizidine analogs act on other cellular targets in addition to *Tb*MetRS to inhibit *T. brucei* growth. However even with this increase in potency, the indoloquinolizidine analogs were still inferior to most of our flexible analogs in terms of *T. brucei* growth inhibiton.

Table 2.6. GI_{50} and IC_{50} values of indoloquinolizidine analogs

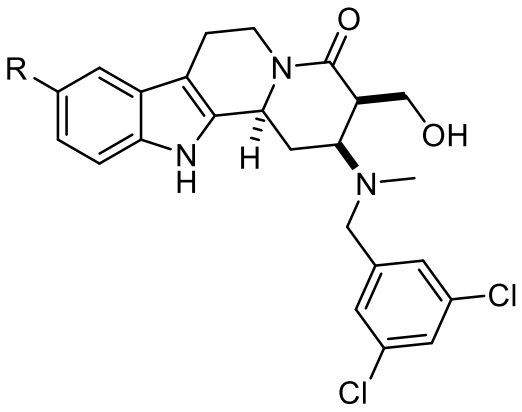

Compound	R =	IC_{50} (μM) ± SEM	GI_{50} (μM)
2.1	H	4.9 ± 1.5	25.3
2.98	OMe	>100	11. 7
2.99	OH	12.5 ± 1.8	8.4

2.4. SUMMARY & CONCLUSIONS

In the endeavor to synthesize and biochemically analyze novel leads for the treatment of HAT, we developed robust protocols for the synthesis of a library of hydroxylactam, lactam, and piperidine analogs of our initial hits **2.1** and **2.2**. These analogs were assayed for inhibition of *T. brucei* growth *in vitro* by our collaborators at the University of Georgia, and we found that many of these compounds have GI_{50} values that are lower than our initial hit **2.1**, with our most potent growth inhibitor **2.69** displaying a 25x increase in activity relative to **2.1**. However, when we queried the ability of our analogs to inhibit *Tb*MetRS in an aminoacylation assay, we found that they were all essentially inactive at biologically relevant concentrations. Finally, we prepared indoloquinolizidine analogs **2.98** and **2.99** to leverage the results of our SAR studies on a scaffold known to inhibit *Tb*MetRS, and found that they were superior *T. brucei* growth inhibitors but inferior *Tb*MetRS inhibitors relative to **2.1**.

A clue as to why our flexible analogs do not inhibit *Tb*MetRS may be found in the work of Fan and co-workers, which was published subsequent to our work, in which they prepared 1,3-disubstituted piperidine **2.100** and its acyclic analog **2.101** and found them to be roughly equipotent in their binding and inhibition of *Tb*MetRS (Figure 2.6).[30] Furthermore, examination of the crystal structures of **2.100** and **2.101** bound to *Tb*MetRS reveals that the orientation and position of the two molecules is nearly identical.[30] This result suggests that the 1,3-disubstituted piperidine core preorganizes the two aromatic substituents into a bent orientation optimal for binding with *Tb*MetRS, in contrast with our 1,4-disubstituted piperidine and lactam scaffolds which would disfavor such an orientation. Re-examining our initial hits **2.1** and **2.2** (*see* Figure 2.1), we can see that the indoloquinolizidine motif likewise enforces a bent orientation between the two aromatic substituents, leading to the conclusion that severing the C(2)–C(3) bond of **2.1** and **2.2** removed a key conformational constraint that preorganized the ligands into a favorable orientation for binding with *Tb*MetRS.

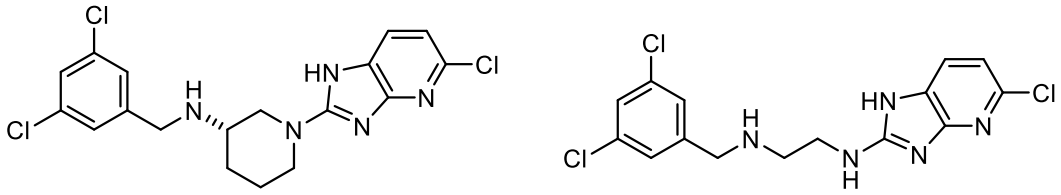

2.100
*Tb*MetRS ΔT_m = 19.0 °C
*Tb*MetRS IC_{50} < 50 nM

2.101
*Tb*MetRS ΔT_m = 18.4 °C
*Tb*MetRS IC_{50} < 50 nM

Figure 2.8. *Tb*MetRS inhibitors **2.100** and **2.101** developed by Fan and co-workers

DIVERSITY-ORIENTED SYNTHESIS OF SPIROCYCLIC *BETA*-PHENETHYLAMINES

Chapter 3. Multi-Component Assembly Processes for Diversity-Oriented Synthesis, Privileged Scaffolds, Aza-Spirocycles, and Intramolecular Aza-Hosomi-Sakurai Reactions

3.1 Multi-Component Assembly Processes for Diversity-Oriented Synthesis

The utility of vinylogous Mannich reaction (VMR) as a generalizable tool for the rapid construction of *N*-heterocycles was first demonstrated by the expedient syntheses of structurally diverse alkaloid natural products (*see* Section 1.3.1).[32,33,36–39,52] Generalization of this process led lead to the development and application of a VMR-based multi-component assembly process (MCAP) to the diversity-oriented synthesis (DOS) of novel compound libraries, many of which displayed useful biological activity.[31]

3.1.1. Diversity-Oriented Synthesis

Diversity-oriented synthesis (DOS) is concerned with the development of synthetic methods and strategies to prepare libraries of small molecules with high degrees of diversity and complexity.[53–55] The main impetus for preparing such libraries is to identify new bioactive compounds for use in chemical genetics or drug discovery and to explore under-represented or unknown areas of chemical space.[53–55] New bioactive compounds may be identified either by their activity toward a specific protein target or via a phenotypic screen.[53,54] From this perspective, it is obvious why a high degree of structural diversity is desirable, as a more diverse set of molecules will have a greater probability of eliciting a desired biological responses than a more "focused" set of molecules, provided little is known in advance about the target pharmacophore.[54] As a corollary, a structurally diverse compound library would be expected to elicit a broader range of biological activities than a focused library, and would thus be of greater utility in a chemical genetics sense, where chemical probes are used to explore biological systems and characterize the functional activity of proteins via their perturbation with small

molecules.[53,54] Structural complexity is also an important feature of a DOS compound library, as it has been postulated that increasing molecular complexity engenders specificity for a given protein target and correlates with the likelihood of success of a molecule as a drug candidate, although the generality of these observations have been called into question.[54–59]

The development of DOS strategies and tactics can be thought of as an extension or evolution of combinatorial chemistry strategies.[53] Combinatorial chemistry techniques emerged from the development of solid-phase synthesis of peptides and small molecules.[60] These techniques often utilize solid-phase synthesis in a "split-pool" or "one bead, one compound" regime to rapidly generate a large library of compounds—differing primarily in their functional appendages—often in a highly automatable fashion.[53,54,60] However, these libraries often display low degrees of scaffold diversity and thus are of limited utility for the identification of new therapeutic leads or in chemical genetics endeavors, where scaffold diversity is of paramount importance.[53,54] It is this emphasis on scaffold diversity, in addition to stereochemical and functional group/appendage diversity, that distinguishes DOS methods from traditional combinatorial chemistry methods.[53,54]

While there are many different approaches that may be utilized in the development of a DOS method, there are some general features and strategies that warrant discussion. In contrast with target-oriented synthesis, DOS sequences are not evaluated in a retrosynthetic fashion, but instead are developed in a forward synthetic fashion to generate branched, divergent synthesis pathways.[55,61,62] DOS sequences often incorporate multi-component reactions (MCRs) or tandem reactions as a means of simultaneously introducing multiple functional handles that can subsequently serve as branch points for functionalization and cyclization reactions.[53,55,61,63,64] Cycloaddition reactions such as the Diels-Alder reaction and [3+2] dipolar cycloadditions are also frequently used in DOS due to their ability to generate multiple bonds and stereocenters in the course of a single reaction.[31,53,61] For the introduction of appendage and functional group diversity, cross-coupling and heteroatom-functionalization reactions are often utilized, as is the case in classical combinatorial chemistry.[53,54,61] A general strategy for DOS known as the "build-

couple-pair" strategy described by Nielsen and Schreiber is illustrated in Scheme 3.2.[62] Synthons with diverse stereochemical and functional motifs **3.2** are built from simple starting materials **3.1** and then coupled to prepare functionalized templates **3.3**, which are subsequently paired in an intramolecular fashion to generate a set of structurally diverse scaffolds (**3.4**, Scheme 3.2).[54,62] This general strategy has been used by numerous research groups to prepare libraries of structurally diverse, stereochemically rich compounds for a variety of applications, and is analogous to the strategies utilized in the Martin Lab's application of the MCAP to DOS endeavors.[54,62]

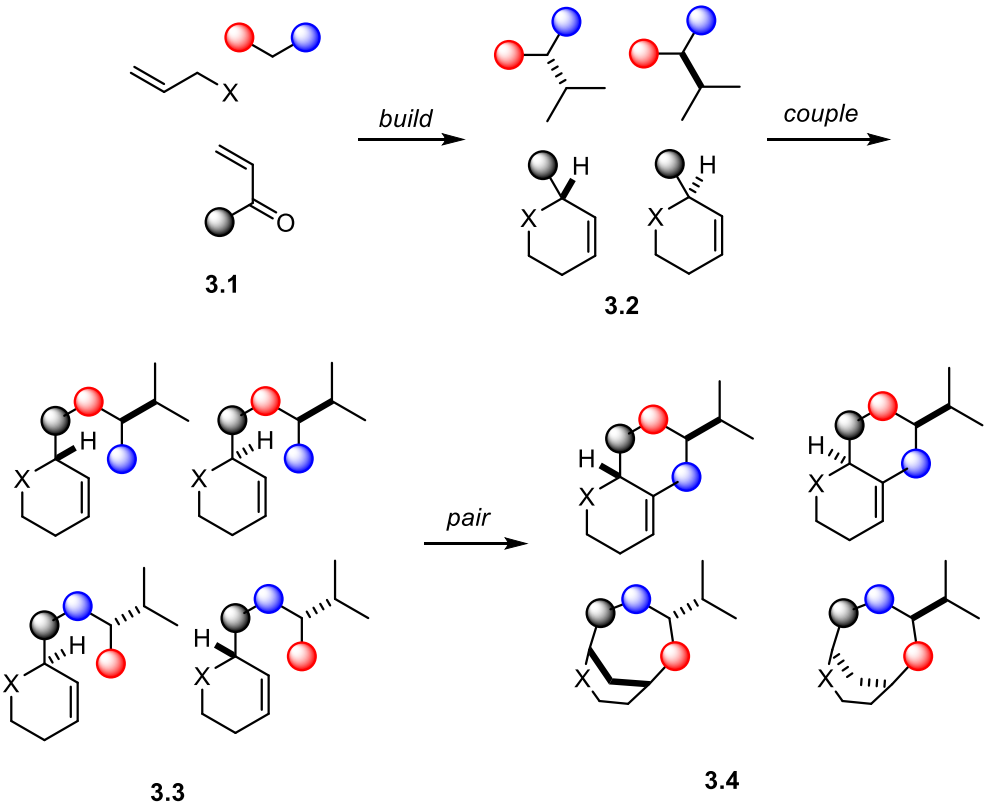

Scheme 3.1. An example of the "build-couple-pair" DOS strategy described by Nielsen and Schreiber[62]

3.1.2. Development and Applications of the Martin Lab MCAP

The general features of the Martin MCAP approach to preparing diverse collections of small molecules are outlined in Scheme 3.2: an aryl aldehyde **3.5** and a primary amine **3.6** are

condensed to form an imine **3.7** which is subsequently activated via treatment with an acylating agent **3.8** to undergo electrophilic addition with a nucleophile **3.9** to form amides with the general structure **3.10**. Incorporation of appropriate functional groups in the reaction inputs **3.5–3.8** allows for subsequent ring-forming and functionalization reactions of **3.10** to generate polycyclic scaffolds such as **3.11** with diverse skeletal structures and functionalities. The MCAP is conceptually similar to an MCR, in which three or more "building block" substrates are combined to form a single product; however, the MCAP often requires a sequential addition of reactants to avoid undesired side-reactions.[31,63]

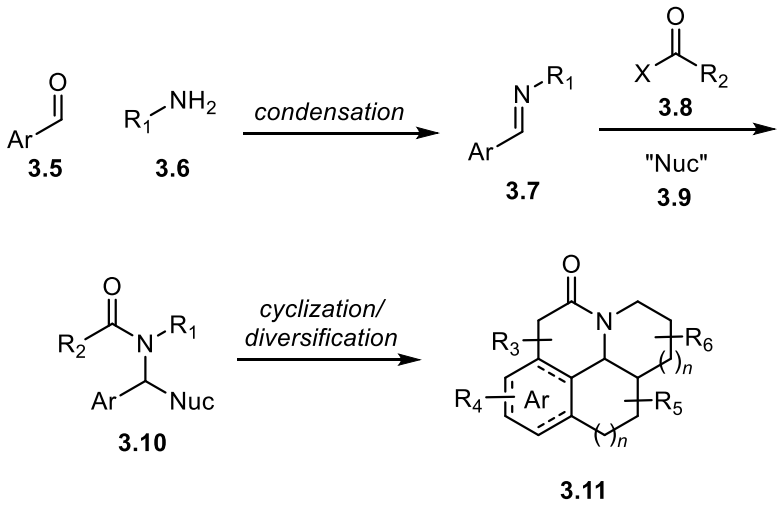

Scheme 3.2. General outline of the Martin Lab MCAP

In pioneering studies carried out by Sunderhaus, Dockendorf, and Martin, various facets of the MCAP were explored.[65,66] A key finding of these exploratory studies was the realization that the experimental procedure for the MCAP reaction could be altered to accommodate the differing reactivity of various substrates. For instance, the imine formed from condensation of the amine **3.6** and aldehyde **3.5** inputs could be isolated in a discreet step, or directly reacted with an acyl chloride **3.8** and nucleophile **3.9**.[65,66] The character of the nucleophile **3.9** has a significant influence on the experimental condition required to achieve the desired reactivity. For example, when **3.9** is a weak π-nucleophile such as a silyl enol ether, the imine must first be

activated via acylation with **3.8** before electrophilic addition can occur. Conversely, when **3.9** is a strong nucleophile such as a Grignard reagent, addition to the imine can be carried out in the absence of **3.8**, and the resultant amine may be isolated or subjected to subsequent acylation with **3.8** in a one-pot fashion.[65,66] This procedural flexibility enabled the utilization of the MCAP with a variety of substrates, and some noteworthy and illustrative examples of which will be described in the following section.

One key strategy for scaffold preparation that was developed in these exploratory studies was the combination of the MCAP with subsequent ring-closing metathesis (RCM) and intramolecular Heck cyclization reactions. An early example of this strategy is shown in Scheme 3.3, in which indolic aldehyde **3.12** underwent a two-step MCAP where it was first condensed with allylamine, and then sequentially treated with allylmagnesium bromide and benzyl chloroformate to furnish **3.13**.[65,66] RCM of **3.13** in the presence Grubbs catalyst **3.14** formed the tetrahydropyridine ring, which was subjected to an intramolecular Heck cyclization to deliver the novel ergoline-like scaffold **3.15**. While **3.15** itself was not found to display any noteworthy biological activity, the development of the MCAP/RCM/Heck reaction manifold and its attendant application to DOS compound libraries would result in the discovery of a family of compounds with potent biological activity and exciting therapeutic potential (*vide infra*).

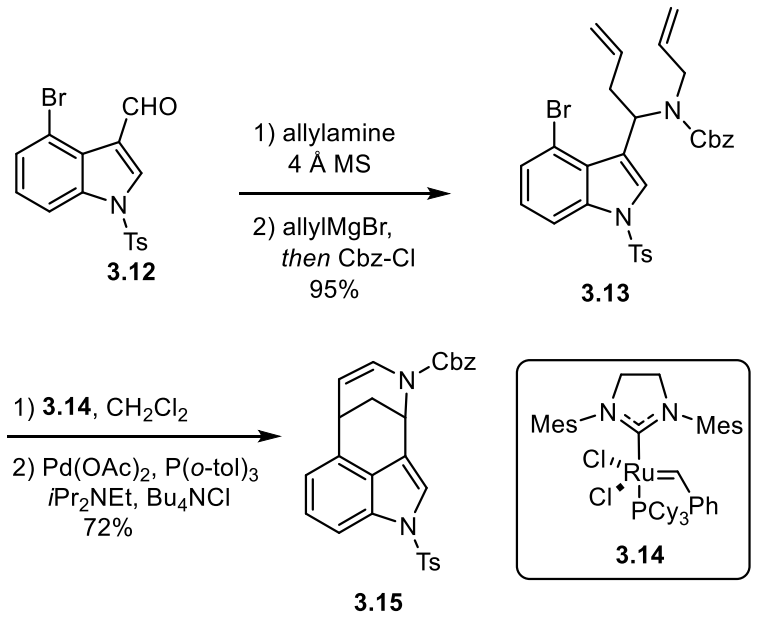

Scheme 3.3. Synthesis of **3.15** via a MCAP/RCM/Heck reaction sequence

Another key tactic that emerged from these exploratory studies was the combination of the MCAP and a [3 + 2] dipolar cycloaddition with an azomethine ylide, nitrone, or azide dipole, and this general strategy was extended to the synthesis of a variety of scaffolds (*see also* Section 1.3.2).[40,41,65–71] In the work of Hardy and Martin, this strategy was leveraged to prepare pyrrolidine and isoxazolidine-fused 2-arylpiperidine scaffolds, an example of which shown in Scheme 3.4.[67] Cycloaddition precursor **3.16** was prepared via a two-step MCAP involving condensation of **3.17** with allylamine, followed by treatment with **3.18** and **3.19**.[67] Treatment of **3.16** with sarcosine derivative **3.20** and heating generated an azomethine ylide that underwent a [3+2] dipolar cycloaddition to furnish **3.21**. Removal of the *N*-pentenoyl group of **3.21** with molecular iodine and HCl revealed pyrrolidine-fused piperidine **3.22**. The *N*-H and aryl bromide moieties of **3.22** were exploited for subsequent diversification via *N*-functionalization, cross-coupling, and intramolecular cyclization reactions. Additionally, MCAP products such as **3.16** were also made to undergo nitrone [3 + 2] dipolar cycloadditions to furnish isoxazolidine-fused piperidines that were elaborated in an analogous fashion.[67] In screening efforts undertaken by the NIH Molecular Library Probe Production Center Network (MLPCN) (*see* Section 1.3.2), **3.22**

was found to inhibit RAD52 (IC_{50} = 4.6 μM), a therapeutic target for BRCA2-mediated breast cancer.[31]

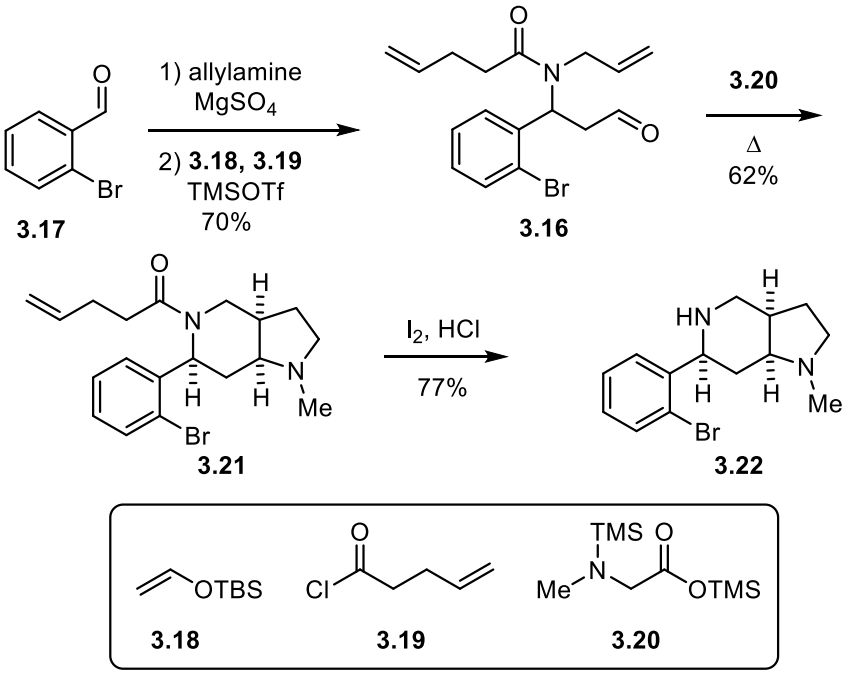

Scheme 3.4. Synthesis of pyrrolidine-fused 2-arylpiperidine **3.17** via a MCAP/azomethine ylide [3 + 2] dipolar cycloaddition sequence

A fruitful application of the MCAP/dipolar cycloaddition reaction manifold was developed by Donald, Wood, and Martin in the synthesis of triazole-fused benzodiazepines via a Huisgen-type azide-alkyne [3 + 2] cycloaddition.[68,70] An example of this strategy is shown in Scheme 3.5, in which azo-benzaldehyde **3.23** undergoes condensation with propargylamine to generate **3.24**, which was activated with acetyl chloride to undergo Huisgen [3 + 2] cycloaddition to furnish *N*-acetyl benzodiazepine **3.25**. Alternatively, **3.24** underwent a Huisgen [3 + 2] cycloaddition when heated, and the resultant *N*-H benzodiazepine scaffold could be *N*-functionalized in a subsequent step to generate derivatives such as the *p*-methoxy benzamide **3.26**. The pendant nitrile group of **3.25** and **3.26** could be exploited for further elaboration. For example, deprotonation of the amino nitrile **3.25** with sodium hydride and subsequent capture of the anion with benzyl bromide furnished the alkylated derivative **3.27**. Alternatively, treatment

of **3.26** with Schweizer's reagent generated the pyrrole-fused analog **3.28**. Screening of this compound set by the MLPCN identified several analogs with notable biological activity. For instance, **3.27** was found to inhibit 5-methyl-CpG-binding domain protein 2 (29% inh. at 4.4 μM), which is involved in the epigenetic gene silencing that occurs as a result of DNA hyper-methylation in cancerous cells, and **3.28** was found to inhibit the SWI/SNF chromatin remodeling complex (AC_{40} = 4.6 μM), which plays an essential role in the induction of pluripotency in stem cells and in tumor suppression.[31,72,73]

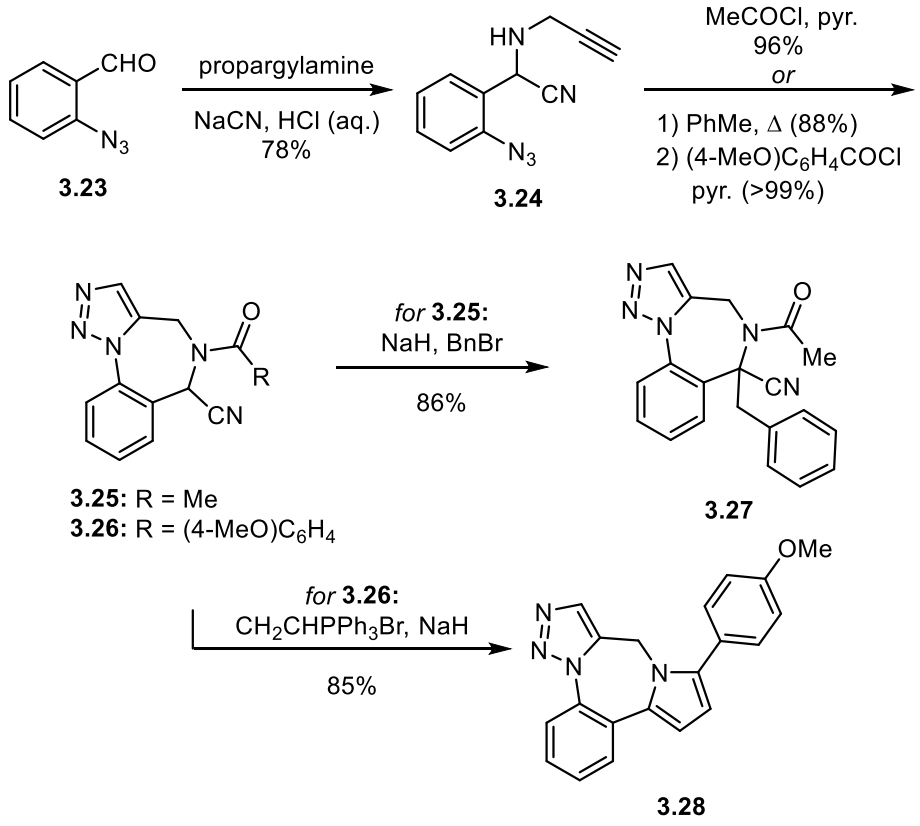

Scheme 3.5. Synthesis of triazole-fused [1,4]-benzodiazepines **3.22** and **3.23** via a MCAP/Huisgen [3 + 2] dipolar cycloaddition sequence

The MCAP/[3 + 2] dipolar cycloaddition reaction manifold was further extended by the work of Granger, Kaneda and Martin, in which they explored the use of bromo-dihydroisoquinoline **3.29** as an MCAP input (Scheme 3.6).[69,71] They found that **3.29** underwent a

one-pot MCAP/Huisgen [3 + 2] cycloaddition cascade vial sequential treatment with a metal acetylide and then with azido-benzoyl chloride **3.30** to furnish the fused tetrahydroisoquinoline-benzodiazepines **3.31** and **3.32**, which were subsequently derivatized via cross-coupling reactions with the aryl bromide moiety. Alternatively, **3.29** was treated with **3.18** and **3.33** to effect an *N*-acyl-iminium MCAP reaction, and the resultant aldehyde underwent condensation and nitrone [3 + 2] dipolar cycloaddition to furnish isoxazolidine **3.34**, which was elaborated via a three-step cross coupling/ring opening/*N*-functionalization reaction sequence to furnish analogs such as **3.35** (*see* Section 1.3.2). MLPCN screening of this compound set identified **3.32** as an inhibitor of transactive response DNA-binding protein 43 (TDP-43) (AC_{50} = 35.5 μM). Aggregation of mutated TDP-43 in nerve cells is a marker for neurodegenerative diseases such as amylotrophic lateral sclerosis (ALS) and frontotemporal lobar degeneration, and compounds that inhibit TDP-43 may be useful tool compounds for studying these diseases.[31,74] Urea derivative **3.35** was also found to display useful biological activity as an inhibitor of the hepatitis C virus (AC_{50} = 2.0 μM).[31]

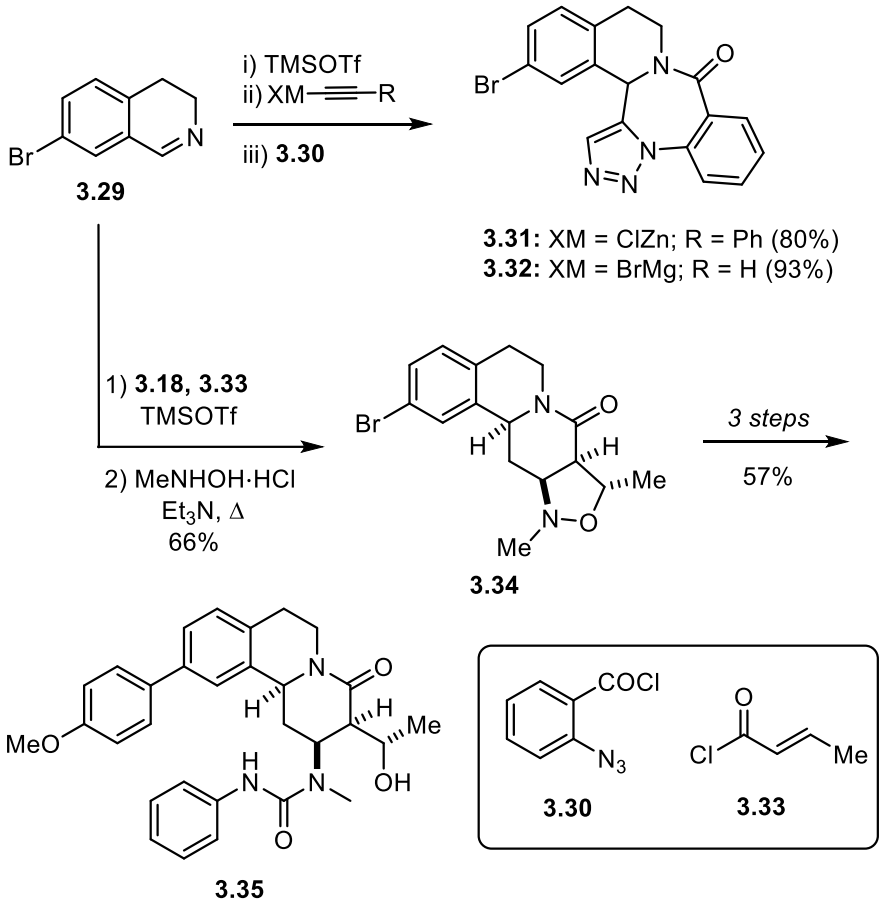

Scheme 3.6. Synthesis of tetrahydroisoquinoline derivatives **3.26, 3.27,** and **3.30** via MCAP/[3 + 2] dipolar cycloaddition sequences

As mentioned previously, the MCAP/RCM/Heck reaction manifold proved to be one of the most fruitful extensions of the MCAP to DOS library generation. This strategy was developed by Sahn and Martin for the preparation of norbenzomorphans via reaction sequences such as the one depicted in Scheme 3.7.[75–78] Benzaldehydes **3.36** and **3.37** underwent an *N*-acyl-iminium-type MCAP to deliver **3.38** and **3.39**, which were then cyclized via RCM and intramolecular Heck reactions to furnish norbenzomorphan scaffolds **3.40** and **3.41**.[76] Subsequent ionic reduction of **3.40** and **3.41** gave **3.42** and **3.43**, which were functionalized via a Buchwald-Hartwig amination with piperazine and reductive alkylation with propionaldehyde to deliver norbenzomorphan analogs **3.44** and **3.45**.[78] In this fashion, libraries of norbenzomorphan

derivatives were prepared and screened for their activity at various central nervous system (CNS) receptors by the Psychoactive Drug Screening Program (PDSP) at UNC Chapel Hill.

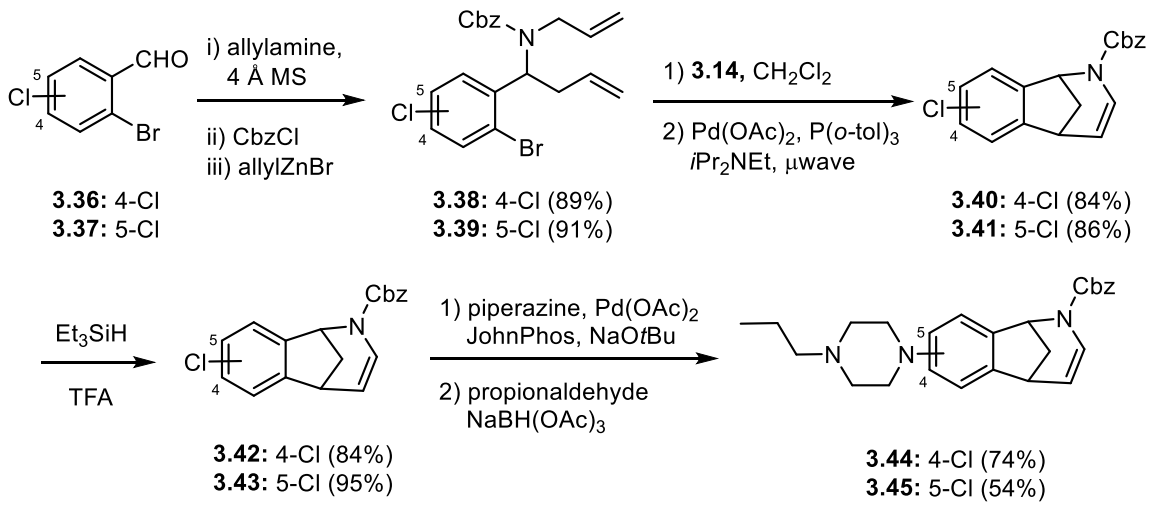

Scheme 3.7. Synthesis of norbenzomorphans **3.44** and **3.45** via an MCAP/RCM/Heck reaction sequence

Screening of **3.44**, **3.45**, and many other norbenzomorphan analogs by the PDSP revealed that these scaffolds display remarkable activity at the sigma 1 (σ1) and sigma 2 (σ2) receptors.[78] Sigma receptors are transmembrane proteins that reside primarily on the endoplasmic reticulum and are distributed throughout the central and peripheral nervous system.[78,79] Broadly speaking, they are known to be involved in intracellular calcium regulation and neuronal survival or apoptosis.[78,79] The σ1 receptor is well studied, having been cloned, sequenced and structurally characterized via X-ray crystallography, and compounds that target the σ1 receptor are currently in clinical trials for the treatment of Alzheimer's disease, epilepsy and pain.[78] The σ2 receptor is less well-studied, primarily due to the fact that, prior to our work in this field, it had never been cloned. However, σ2 ligands were known in the literature, and the σ2 receptor shows promise as a chemotherapeutic and diagnostic target for cancer as it is overexpressed in proliferating tumor cells.[78] Our research found **3.44** and **3.45** to be potent and selective ligands for the σ1r and σ2r, respectively: **3.44** σ1 K_i = 8.7 nM, σ2 K_i = 29.3 nM; **3.45** σ1 K_i = 230 nM, σ2 K_i = 5.1 nM.[78] This

relationship between aryl substitution and σ receptor subtype selectivity appears to be general, with 4-substituted ligands preferring σ1 and 5-substituted ligands preferring σ2.[78] This discovery of a new class of potent, selective σ2 receptor ligands has spurred a great deal of research in our group, including the investigation of norbenzomorphan σ2 ligands for the treatment of Alzheimer's disease,[80] neuropathic pain,[81] traumatic brain injury,[82] and alcohol use withdrawal.[83] We have also discovered other chemical scaffolds capable of potently inhibiting the σ2 receptor such as isoindolines[84] and aminotetralins, and the latter was used in work which led to the isolation and cloning of the σ2 receptor and its identification as transmembrane protein (TMEM) 97.[85]

Taken together, these examples illustrate the utility and generalizability of the MCAP procedure for the rapid synthesis of compound libraries built around unique, diverse scaffolds. Furthermore, many of these compounds were found to display promising biological activities, which lead to fruitful medicinal chemistry and chemical biology research programs focused on human African trypanosomiasis (*see* Chapter 2) and the σ2 receptor. Thus, we expect that future endeavors to expand the MCAP and apply it to DOS will likewise pay dividends in the arenas of chemical biology and drug discovery.

3.2 Privileged Structures

One of the most important considerations in developing a useful DOS procedure is the design of molecular scaffolds to be prepared and elaborated via the DOS method.[86] This process can be daunting, as it is estimated that there are over 10^{60} possible configurations of carbon-based small (< 500 daltons) molecules.[87] DOS scaffold design may be driven by the desire to explore new or under-represented areas of this vast chemical space.[55,61] However, it is often desirable to design DOS scaffolds that populate areas of chemical space that have been pre-validated as biologically relevant.[86] In this case, the scaffold design process is informed by the

structures (or substructures) of natural products or drugs with desirable (bio)chemical properties, which are commonly referred to as "privileged structures".[55,86]

3.2.1. Definition, History, and Examples of Privileged Structures

The concept of a privileged structure was first introduced by Evans in 1988, which he defined as "a single molecular framework able to provide high-affinity ligands for more than one type of receptor."[88] This concept emerged from his work on the development of cholecystokinin (CCK) antagonists such as **3.46** (Figure 5) that contained a 1,4-benzodiazepine nucleus.[88,89] The 1,4-benzodiazepine scaffold forms the core of benzodiazepine class of drugs, of which diazepam (**3.47**, Figure 5)—trade name Valium—is a noteworthy example.[90] Benzodiazepines are commonly prescribed for their anxiolytic and sleep-inducing effects, which are primarily induced via action at γ-amino butyric acid (GABA) and receptors in the CNS.[90] By modifying substituents around the 1,4-benzodiazepine core, Evans and co-workers were able to produce compounds such as **3.46** that were potent CCK receptor antagonists (**3.46** IC_{50} = 3.4 μM), but did not display any activity at benzodiazepine receptors.[88,89] This ability of the benzodiazepine nucleus to produce ligands that bind with high affinity to different biological receptors lead Evans to designate it as a "privileged" scaffold.

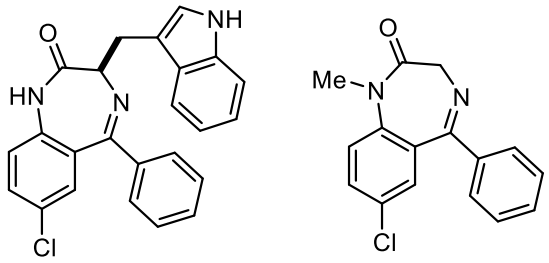

CCK antagonist **3.46** diazepam (**3.47**)

Figure 3.1. 1,4-benzodiazepines **3.46** and **3.47** which display divergent biological activities

Since its initial conception, the designation of a privileged structure has been broadened to include scaffolds or substructures whose derivatives frequently display biological activity,

without the criterion that these activities must be mediated by different biological receptors.[91,92] Natural products provide numerous examples of privileged structures, which is not surprising given that the enzymatic machinery that produces natural products does so for a specific biochemical purpose.[86,91,93] Natural product scaffolds and the enzymatic machinery that produce them are highly conserved throughout nature, and there are many examples of natural product classes whose individual family members display diverse biological activity.[93] Analysis and hierarchical classification of the substructures found within and across natural product families, and the relationship between these substructures and the attendant biological activities of their derivatives (natural and unnatural) is one of the principal components of biology-oriented synthesis (BIOS), which seeks to use these analyses to guide the synthesis of compound libraries enriched in bioactivity.[93]

Many medicines are either natural products themselves or are derived from natural products. So there are numerous examples of privileged scaffolds that are found in both natural products and drugs, some examples of which are shown in Figure 3.2.[91,93] The steroid skeleton **3.48** is ubiquitous in the worlds of natural products and medicinal chemistry, and its derivatives display widely divergent bioactivity. For instance, the aminosterol squalamine (**3.49**), isolated from the tissue of the spiny dogfish shark *Squalaus acanthias*, has both antimicrobial and antiangiogenic activity, while the synthetic testosterone derivative quinbolone (**3.50**) is an anabolic and androgenic steroid.[94,95]

Many nitrogenous heterocycles are classified as privileged structures, of which tetrahydroisoquinoline (THIQ, **3.51**) and tetrahydro-*β*-carboline (THBC, **3.54**) are two noteworthy examples (Figure 3.2, *see also* Section 1.3.1 *for additional examples of THBC natural products*).[96,97] The THIQ natural product erythravine (**3.52**), which is isolated from the Brazilian ornamental tree *Erythrina mulungu* and belongs to the large *Erythrina* family of alkaloids whose members frequently display CNS activity, is a potent nicotinic acetylcholine receptor antagonist with demonstrated anxiolytic and anticonvulsive activity.[98–100] Apomorphine (**3.53**) is a semi-synthetic THIQ morphine derivative and dopamine receptor agonist.[101]

Apomorphine (**3.48**) is used for the relief of symptoms associated with Parkinson's disease.[101,102] It is also a potent emetic and sedative, and it has been used historically for the treatment of a multitude of conditions including alcoholism, poisoning, and respiratory disorders.[101,102] The THBC natural product reserpine (**3.55**), isolated from the Indian snake root *Rauvolfia serpentina*, likewise has a long, storied history of medical use.[52] Reserpine exhibits sympatholytic activity via the depletion of catecholamine and serotonin neurotransmitters, and was one of the first antipsychotic drugs.[103,104] While today reserpine is rarely used as an antipsychotic, owing to its serious and sometimes irreversible side effects, it still finds use in the treatment of hypertension.[103,104] Finally, tadalafil (**3.56**) is a synthetic THBC phosphodiesterase 5 inhibitor commonly prescribed for the treatment of erectile dysfunction.[105]

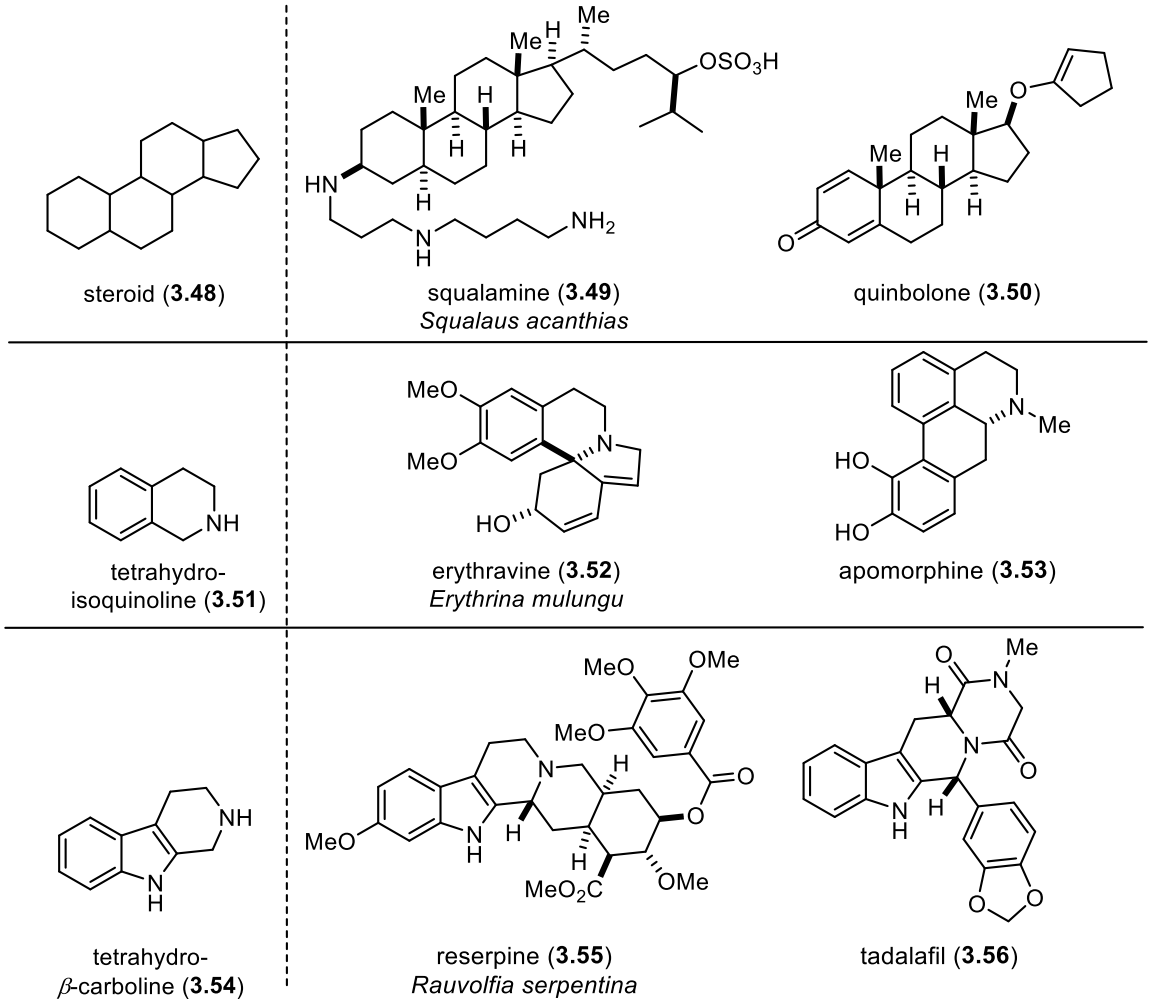

Figure 3.2. Privileged structures (left) and representative natural products (center) and synthetic medicines (right)

3.2.2. *β*-Phenethylamine (PEA) as a Privileged Structure

An especially well-known, occasionally notorious privileged structure is *β*-phenethylamine (**3.57**, Figure 3.3). Unsubstituted *β*-phenethylamine (PEA, **3.57**), which is formed from the decarboxylation of phenylalanine, is widely distributed throughout nature, having been identified in algae, fungi, bacteria, and numerous plant species, as well as in the brains of humans and other mammals.[106] PEA is classified as a trace amine neurotransmitter because it is present in the nervous system at much lower concentrations than the biogenic amine neurotransmitters serotonin, dopamine, (nor)epinephrine, and histamine owing to its rapid

metabolism by monoamine oxidase B (MAO-B).[106] The neurochemical effects of PEA are mediated by its activation of the G protein coupled-receptor (GPCR) trace amine-associated receptor 1 (TAAR1), which results in a downstream inhibition of serotonin, dopamine, and norepinephrine reuptake.[107] This monoamine reuptake inhibition may confer the stimulatory and amphetamine(**3.58**)-like subjective and physiological effects of PEA that have led to its popularity as a nutritional supplement.[106,107]

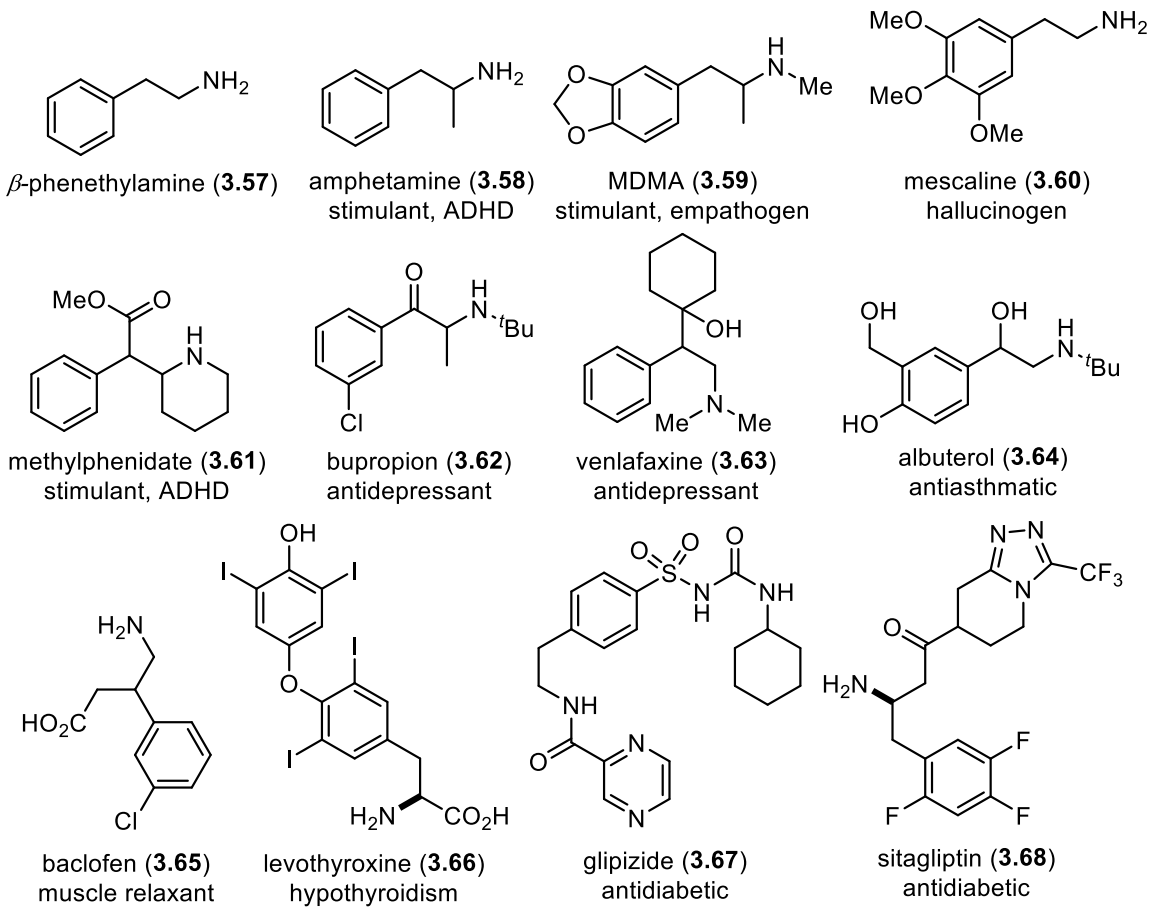

Figure 3.3. *β*-phenethylamine (PEA, **3.52**) and noteworthy derivatives

As mentioned previously, PEA is a somewhat notorious privileged structure, as it is found in psychostimulants such as amphetamine (**3.58**, Figure 3.3), which is used therapeutically for the treatment of attention deficit hyperactivity disorder (ADHD) and obesity, but it has a high potential for abuse and addiction.[108] Substituted amphetamines such as *N*-methylamphetamine

(meth) and 3,4-methylenedioxymethamphetamine (MDMA, **3.59**) are also well-known drugs of abuse, although in recent years there has been renewed clinical interest in the use of MDMA (**3.59**) as a psychotherapeutic tool, especially in the treatment of post-traumatic stress disorder (PTSD).[109,110] The PEA scaffold can also be found in hallucinogenic drugs such as mescaline (**3.60**), the active ingredient in preparations of the peyote cactus that have been used by indigenous Americans for over 5700 years.[110,111]

However, there are also many licit members of the PEA family of drugs. In fact, 25 of the 200 most-prescribed medications in 2016 were phenethylamines.[112] Many of these medicines act on the same monoamine neurotransmitter systems as PEA itself, such as the aforementioned amphetamine and methylphenidate (**3.61**), which both stimulate noradrenergic and dopaminergic neurotransmission and are primarily used for the treatment of ADHD.[108] The antidepressants bupropion (**3.62**) and venlafaxine (**3.63**) likewise stimulate monoamine neurotransmission. Bupropion is a norepinephrine and dopamine reuptake inhibitor while venlafaxine is a serotonin and norepinephrine reuptake inhibitor.[113] Albuterol (**3.64**) is a β-adrenergic (epinephrine) receptor agonist and bronchodilator used for the treatment of asthma symptoms.[114] There are also examples of medicines containing the phenethylamine structure whose biological activity and therapeutic indication deviates considerably from that of "traditional" β-phenethylamines. For instance, the phenethylamino-acid baclofen (**3.65**) is a skeletal muscle relaxant and GABA receptor agonist, and levothyroxine (**3.66**) is a thyroid hormone used in the treatment of hypothyroidism.[115,116] It is also found in the antidiabetic medications glipizide (**3.67**) and sitagliptin (**3.68**). Glipizide (**3.67**) stimulates the release of insulin from pancreatic β cells, while sitagliptin (**3.68**) helps to regulate blood glucose levels via the inhibition of dipeptidyl peptidase 4.[117,118] In conclusion, the PEA scaffold is a highly validated privileged structure with numerous examples of derivatives that display powerful and useful biological activity.

3.3 AZA-SPIROCYCLES

Spirocyclic scaffolds having two ring systems are fused via a single carbon atom are found in numerous natural products, and these frameworks are increasingly being investigated for their use in drug discovery.[119–122] Spirocyclic ring systems display several properties that make them attractive molecular scaffolds: They are inherently rigid and often contain multiple sp^3-hybridized carbon atoms and chiral centers.[56,57,122] Molecules with rigid scaffolds tend to be more selective for a given biological target than their flexible analogs, and a common tactic in drug development is the incorporation of rigidifying elements such as spirocyclic ring systems into a scaffold to impart greater selectivity and binding affinity. However the application of this tactic is not always straightforward, as shown by Martin's research into the effects of conformational constraints on protein-ligand interactions.[121,123] Three-dimensionality is an important feature for drug scaffolds because it enables them to better occupy protein binding sites and make multiple contacts with binding site residues.[120–122] Spirocyclic scaffolds are often globular or capsule-shaped and can bear substituents that project with well-defined geometry into all three dimensions, making them attractive platforms for optimizing interactions within a target binding site.[122] Attendant to this three-dimensionality is the degree of molecular complexity often found in spirocyclic molecules. Complexity, quantified via the fraction of sp^3-hybridized carbon atoms and the number of chiral centers in a molecule, has been shown to correlate with target specificity, aqueous solubility, metabolic stability, and ultimately with success in the drug development process.[56,57]

3.2.1. Aza-Spirocycles in Drug Discovery

Aza-spirocycles are especially interesting scaffolds from a drug discovery perspective, as nitrogenous heterocycles are among the most common structural motifs found in pharmaceuticals.[96] An elegant demonstration of the potential utility of aza-spirocyclic scaffolds can be found in the work of Burkhard and co-workers, who synthesized a series of 2,6-

diazaspiro[3.3]heptanes **3.69** and compared their physiochemical and biochemical properties with an analogous series of piperazines **3.70** (Figure 3.4).[124] They found that in most cases the spirocyclic compounds **3.69** displayed decreased lipophilicity, increased solubility in aqueous buffer, and were less susceptible to oxidative degradation by human liver microsomes than their non-spirocyclic analogs **3.70**.[124]

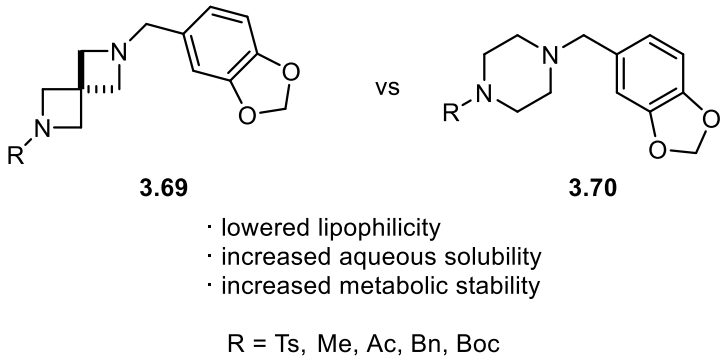

Figure 3.4. Comparison of 2,6-diazaspiro[3.3]heptane scaffold **3.69** with piperazine scaffold **3.70**

A more medically relevant example of aza-spirocycle incorporation can be found in the work of Johansson and coworkers during lead optimization of melanin concentrating hormone receptor 1 (MCHr1) antagonists for the treatment of obesity.[125] They found that substitution of the amino-oxetane moiety in analogs such as **3.71** with an 2-oxa-6-azaspiro[3.3]heptane moiety in their lead compound **3.72** dramatically slowed the metabolism of the molecule in a human liver microsome (HLM) assay and also resulted in diminished human ether-a-go-go (HERG) channel affinity without affecting potency of the compound at MCHr1.

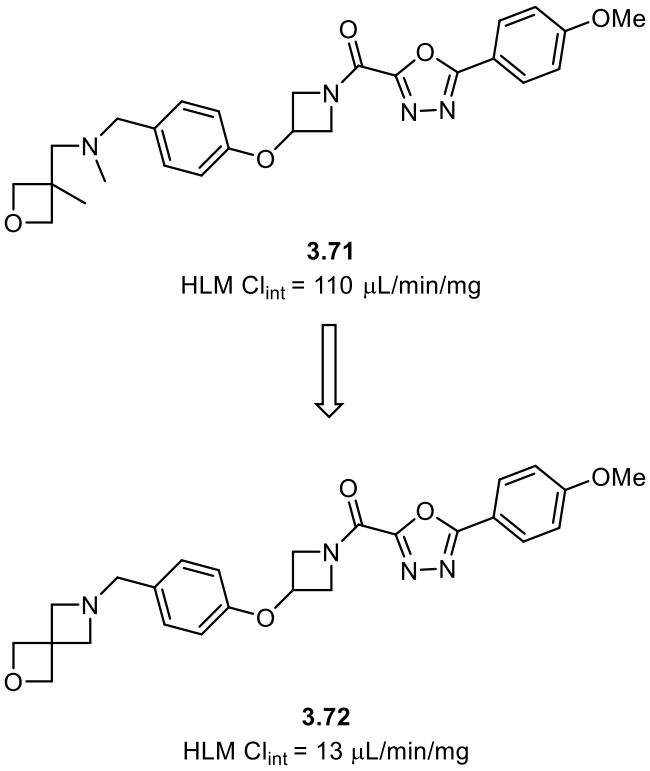

Figure 3.5. Incorporation of an aza-spirocycle slows degradation by human liver microsomes (HLMs)

Some examples of aza-spirocycles that are currently in clinical trials or are approved for medical use are shown in Figure 3.6. The spiro-piperidine **3.73** is an acetyl-CoA carboxylase inhibitor that has progressed through phase 1 clinical trials for the treatment of metabolic syndrome.[122] Spiro-oxindole **3.74** is an antagonist of the calcitonin gene-related peptide which has completed phase 2 clinical trials for the treatment of migraine.[122] Sigma-1 receptor agonist **3.75** is used as a radioligand for cancer diagnostic positron emission tomography (PET) imaging.[122] Finally, rolapitant (**3.76**) is a neurokinin 1 antagonist that was approved in 2015 for the treatment of chemotherapy-induced nausea.[122] Interestingly, the molecular targets of **3.72** and **3.74**–**3.76** are all GPCRs, and it has been suggested that spirocycles may be privileged scaffolds for GPCR ligands.[122]

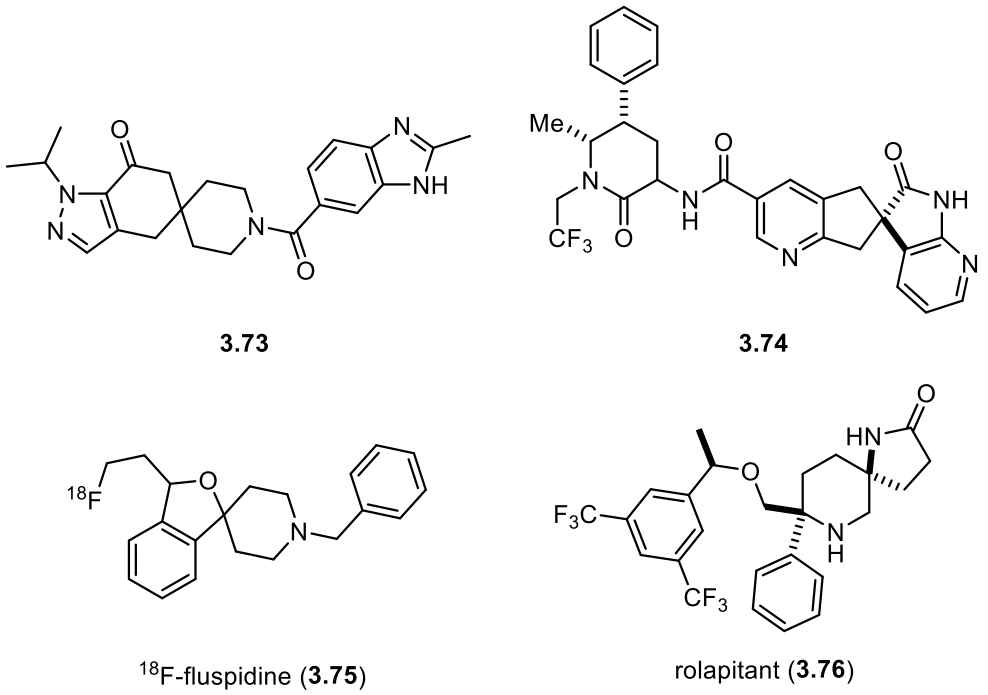

Figure 3.6. Aza-spirocycles currently in clinical trials, approved diagnostic tools and medicines

3.2.2. Aza-Spirocycles in Natural Products

Aza-spirocycles can also be found in the skeletons of numerous bioactive natural products.[126] Here we will limit our discussion to natural products containing a 1-azaspiro[5.5]undecane (**3.76**) or 1-azaspiro[4.5]decane (**3.77**) core, as these motifs will be the focus of our DOS methodology (Figure 3.7, *see* Chapter 4). However, it is worth mentioning that there are many examples of other aza-spirocyclic motifs in the spiro-oxindole and spiro-indoline classes of natural products, which display diverse bioactivity and have been the subject of numerous total syntheses and DOS methodologies.[127–131]

The aza-undecane scaffold **3.76** is found throughout the *Erythrina* family of alkaloids (*e.g.* erythravine, **3.52**), which are known for being potent NAChR inhibitors (Figure 3.7, *see also* Section 3.2.1).[98–100] It is also present in histrionicotoxin (**3.78**) and its partially-to-fully saturated congeners, which are isolated from the skin of the Colombian poison arrow frog *Dendrobates histrionicus* and exhibit potent and highly subtype-selective NAChR inhibition, making them useful tool compounds for the study of neurophysiology.[132] Many members of the

Lycopodium family of alkaloids contain the **3.76** motif, including the prototypical member lycopodine (**3.79**).[133] Extracts of *Lycopodium* clubmosses have a long history of use in Chinese folk medicine, and members of this alkaloid family display wide-ranging bioactivity and are under continual investigation for the treatment of various cardiovascular, neuromuscular, and neurodegenerative diseases. Lycopodine (**3.79**) itself is cytotoxic and has shown promise as a chemotherapeutic agent.[133,134] Finally the **3.76** subunit is present in the protoberberine alkaloid karachine (**3.80**), that was isolated from the root bark of *Berberis aristate*.[135,136] Preparations of *Berberis aristate* are used in Unani medicine for the treatment of jaundice and other skin conditions, although it is unclear if karachine itself contributes to this therapeutic activity.[135,136] While not as frequently observed as **3.76**, 1-azaspiro[4.5]decane (**3.77**) ring system can also be found in several natural products, including the *Lycopodium* alkaloid annotine (**3.81**), which has been shown to effect the maturation of dendritic cells, and methyl homodaphniphyllate (**3.82**), which is isolated from the Yuzuriha tree but does not have any known biological activity.[137–139] Many of these alkaloids and their congeners have been the subject of total synthesis, including erythravine (**3.52**),[100,140] histrionicotoxin (**3.78**),[132,141] lycopodine (**3.79**, *see ref. 143 for additional references*),[142–145] karachine (**3.80**),[136] and methyl homodaphniphyllate (**3.82**).[137,146–148]

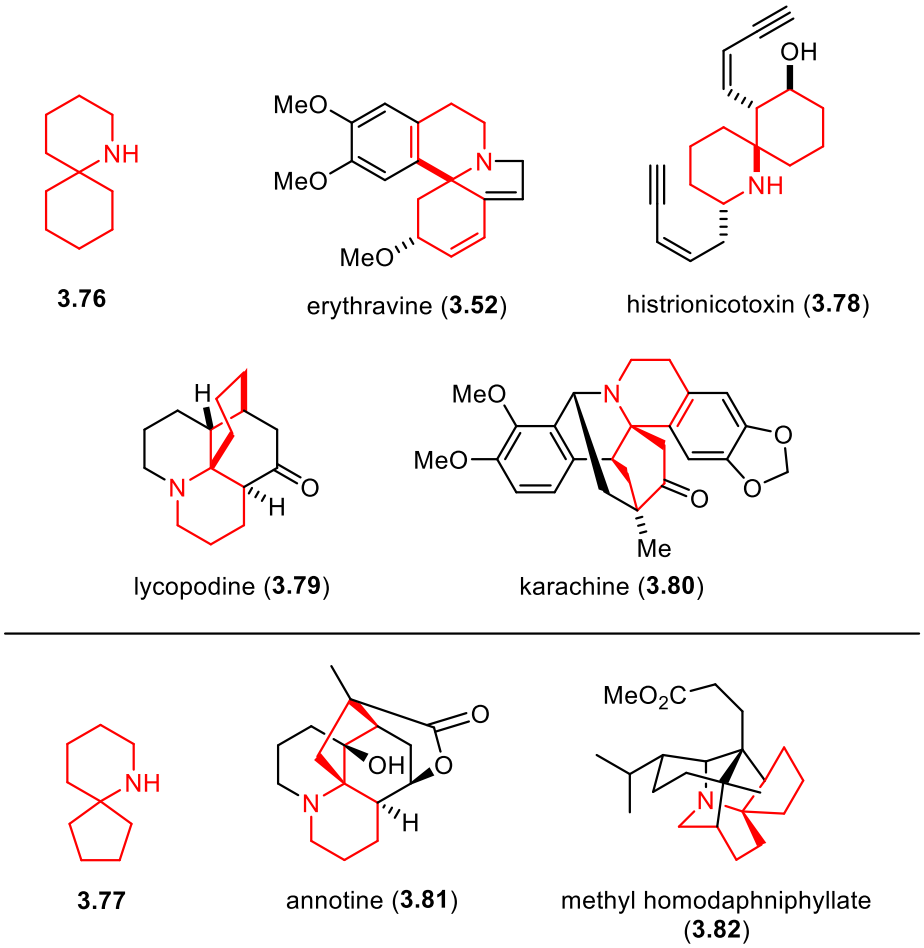

Figure 3.7. Representative natural products containing 1-azaspiro[5.5]undecane (**3.76**) and 1-azaspiro[4.5]decane (**3.77**) ring systems

3.4. The Intramolecular Aza-Hosomi-Sakurai Reaction

The Hosomi-Sakurai reaction, developed by Akira Hosomi and Hideki Sakurai, is a Lewis acid-catalyzed allylation of a carbonyl derivative **3.83** with an allylsilane (**3.84**) to generate homoallylic alcohols such as **3.85** (Equation 3.1).[149,150] The observed reactivity is due to the *β*-effect of the silyl group, which stabilizes the intermediate carbocation **3.86** via $\sigma \rightarrow \pi$ donation from the σ(Si-C) bond to the vacant p orbital on the adjacent carbon atom.[150] As a result, the reaction is highly regioselective for electrophilic attack at the terminal allylic carbon atom, and when optically active allylsilanes are used, the reaction proceeds with varying degrees of stereoselectivity to give predominantly *anti*-$S_E`$ products.[150] In their initial work, Homosi and

Sakurai treated aliphatic and benzylic aldehydes and ketones with substituted allylsilanes in the presence of titanium (IV) chloride to provide homoallylic alcohols in good yields and stereoselectivities.[149] Subsequent studies expanded the scope of the reaction to include acetals, α,β-unsaturated carbonyl compounds, acid halides, epoxides, allyl and alkyl halides, and iminium ions as electrophilic components in the reaction.[150–156]

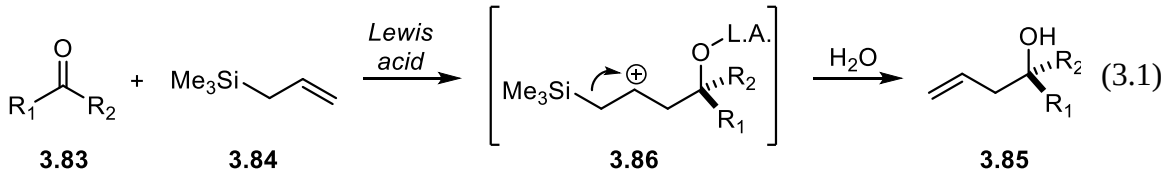

3.83 **3.84** **3.86** **3.85** (3.1)

Seminal work on the use of iminium ions in the Hosomi-Sakurai reaction was performed by Grieco, Fobare and Larsen (Figure 3.8).[157,158] They found that treatment of allylsilanes **3.87** with benzylamine-TFA salt and formaldehyde in water triggered a domino reaction sequence in which electrophilic addition of **3.87** to *N*-benzylmethanimine leads to the formation of an intermediate homoallylamine, which subsequently undergoes a condensation/intramolecular aza-Prins cascade to deliver 4-hydroxypiperidines with the general structure **3.88** (Figure 3.8a).[158] Substitution at the R_1 and R_2 positions of **3.87** is tolerated, and when R_1=R_2=cycloalkyl they obtained cis-fused bicycles, while incorporation of a pendant alkoxy group at the R_2 position resulted in the formation of spirocyclic oxacycles. In most instances, competitive protodesilylation of **3.87** was not observed.

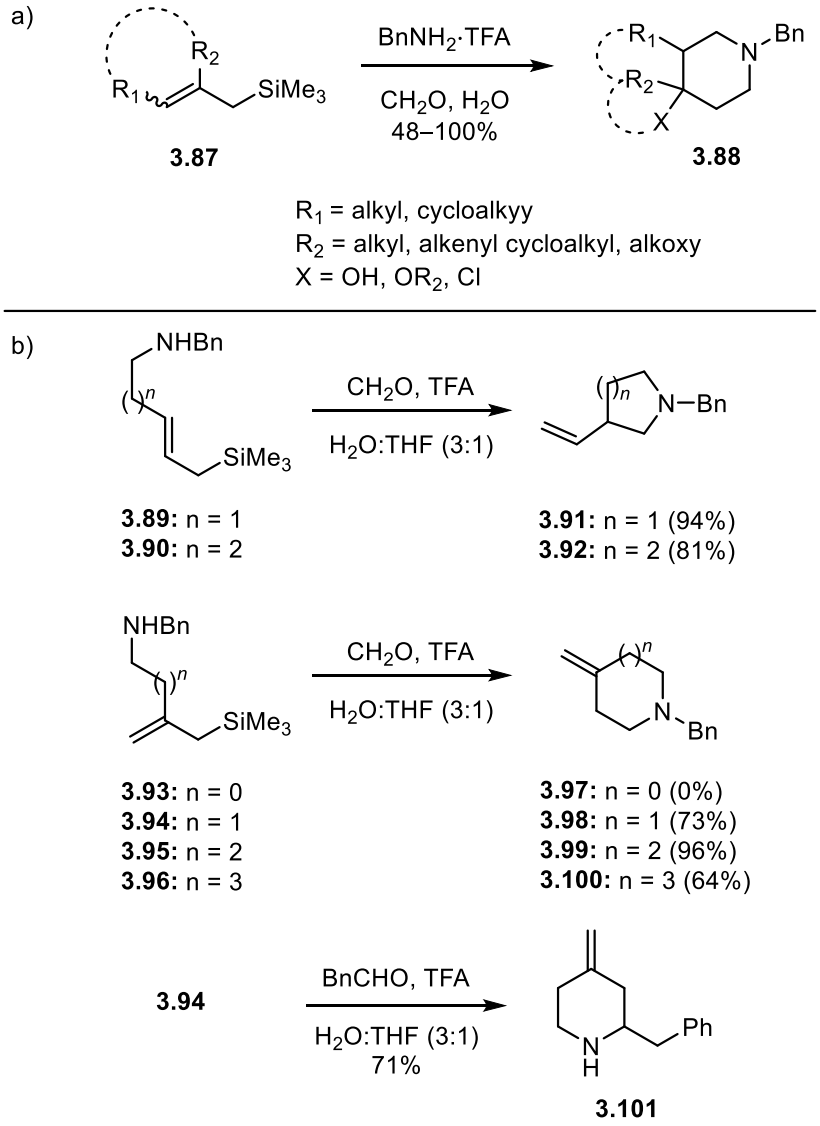

Figure 3.8. Aza-Hosomi-Sakurai reactions for *N*-heterocycle synthesis developed by Grieco, Fobare, and Larsen. a) intermolecular reactions b) intramolecular reactions

Grieco and Fobare later extended their methodology to intramolecular cyclizations with amino-allylsilanes, as shown in Figure 3.8b.[157] *Trans*-disubstituted amino-allylsilanes **3.89** and **3.90** participated in the reaction to deliver pyrrolidine and piperidine products **3.91** and **3.92** with pendant olefin groups. Use of gem-disubstituted amino-allylsilanes **3.93–3.96** was also investigated, and while **3.93** did not cyclize to give pyrrolidine **3.97**, **3.94–3.96** readily underwent cyclization to generate piperidine, azepane and azocine products **3.98–3.100**. Finally,

they found that substituted aldehydes could serve as substrates in the reaction, as **3.94** underwent condensation and cyclization with phenylacetaldehyde to form phenethylamino- piperidine **3.101**. This general strategy for the synthesis of *N*-heterocycles has since seen widespread application in natural products synthesis, and many methodological variants and extensions have been reported.[159–167]

3.4.1. Cascade Aza-Hosomi-Sakurai Reactions for the Synthesis of Quinolizidines and Indolizidines

The Martin Lab recently developed a cascade aza-Hosomi-Sakurai reaction sequence for the one-pot synthesis of natural products and derivatives of the quinolizidine and indolizidine scaffolds.[168,169] The general features of the cascade sequence developed by Amorde and co-workers are shown in Scheme 3.8. Briefly, an amino-allylsilane **3.102** and an acetal-aldehyde **3.103** are condensed to form an imine **3.104** that is poised to undergo sequential acid-catalyzed cyclizations to form a hemiaminal species **3.105**, which can then be intercepted with a nucleophile to deliver functionalized *N*-bicycles with the general structure **3.106**.

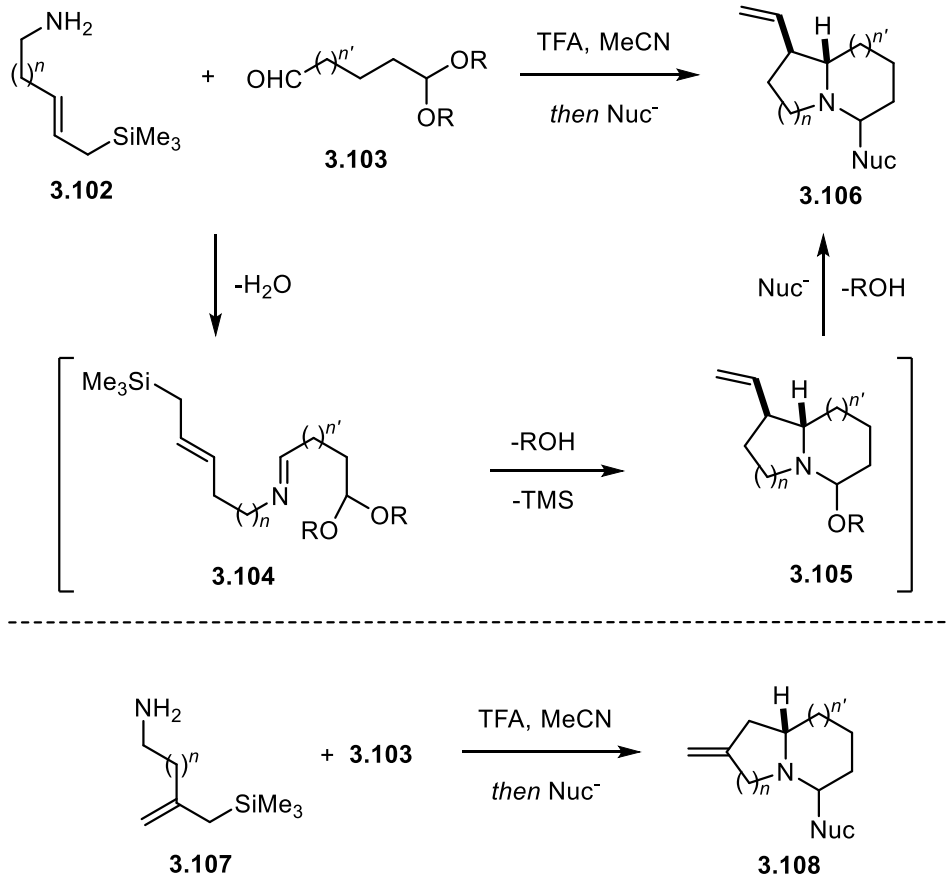

Scheme 3.8. Cascade Aza-Hosomi-Sakurai reactions for the synthesis of amino-bicycles **3.106** and **3.108**

The general applicability of this strategy was demonstrated by the reaction sequences shown in Scheme 3.9.[168,169] Reaction of the amino-allylsilanes **3.102a** (n = 0) or **3.102b** (n = 1) with acetal-aldehydes **3.103a** (n = 0) or **3.103b** (n = 1) furnished amino-bicycles **3.109–3.111** as single diastereomers. The reaction proved to be most efficient for the synthesis of quinolizidines, as **3.109** was formed in 75% yield, whereas the indolizidines **3.110** and **3.111** were formed in 36% and 45% yield, respectively. Ozonolysis of **3.109–3.111**, followed by hydride reduction delivered the natural products (±)-epilupinine (**3.112**) and (±)-tashiromine (**3.113**) in 88% and 56% yield, respectively, as well as indolizidine analog **3.114** in 56% yield.

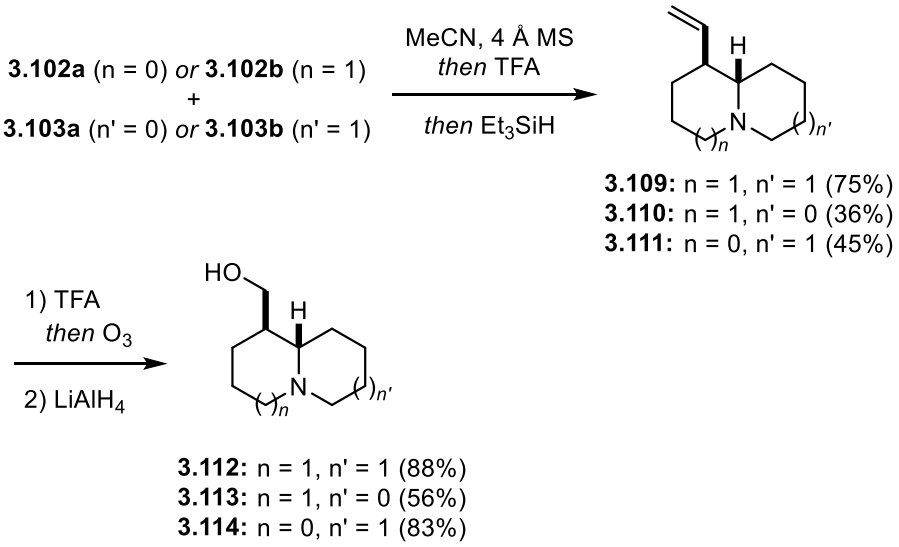

Scheme 3.9. Synthesis of (±)-epilupinine (**3.107**), (±)-tashiromine (**3.108**), and indolizidine **3.109**

The use of chiral amino-allylsilane **3.115** enabled the enantioselective synthesis of the quinolizidine natural product (–)-epimyrtrine (**3.117**).[168,169] Treatment of **3.115** with **3.103b** under standard cyclization conditions furnished intermediate **3.116** as an inconsequential mixture of diastereomers following interception of the quinolizidine iminium ion with sodium cyanide. Reduction of the α-aminonitrile moiety of **3.116** followed by ozonolysis delivered an inseparable mixture (95:5) of (–)-epimyrtrine (**3.117**) and (+)-myrtrine (**3.118**) in 52% yield over two steps.

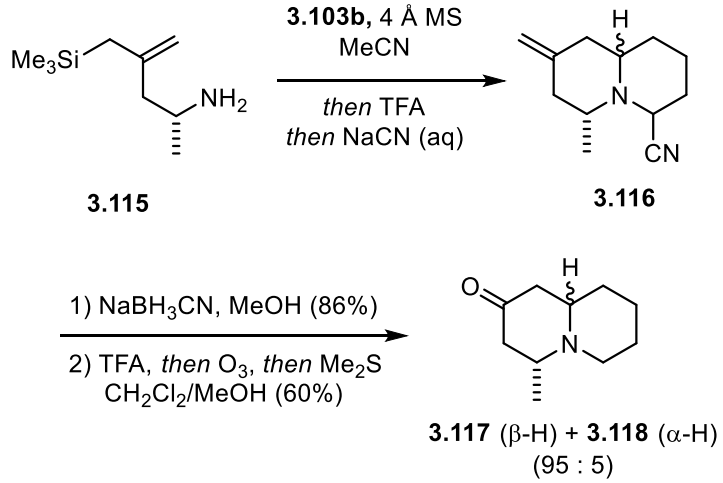

Scheme 3.10. Synthesis of (–)-epimyrtrine (**3.117**) and (+)-myrtrine (**3.118**)

Further studies were directed toward the synthesis of novel scaffolds via the cascade aza-Hosomi-Sakurai reaction manifold.[168,169] For instance, reaction of amino-allylsilane **3.119** with **3.103b** and sodium cyanide produced α-aminonitrile **3.120**, which underwent α-alkylation with sulfonate **3.121** to generate **3.122** (Scheme 3.11, top). The pendant allylsilane moiety of **3.122** underwent Lewis-acid-mediated cyclization to deliver the spiro-quinolizidine scaffold **3.123** in 81% yield. The use of cyclohexanone acetal **3.124** as a cyclization substrate with **3.119** resulted in a diastereomeric mixture of spirocyclic tricycles (**3.125**) which were then reduced with sodium borohydride to deliver **3.126** and **3.127** as an inseparable mixture (1.1:1) in 60% yield. These studies laid the groundwork for our use of an intramolecular aza-Hosomi-Sakurai cyclization in the DOS of aza-spirocyclic compounds, which will be discussed further in Chapter 4.

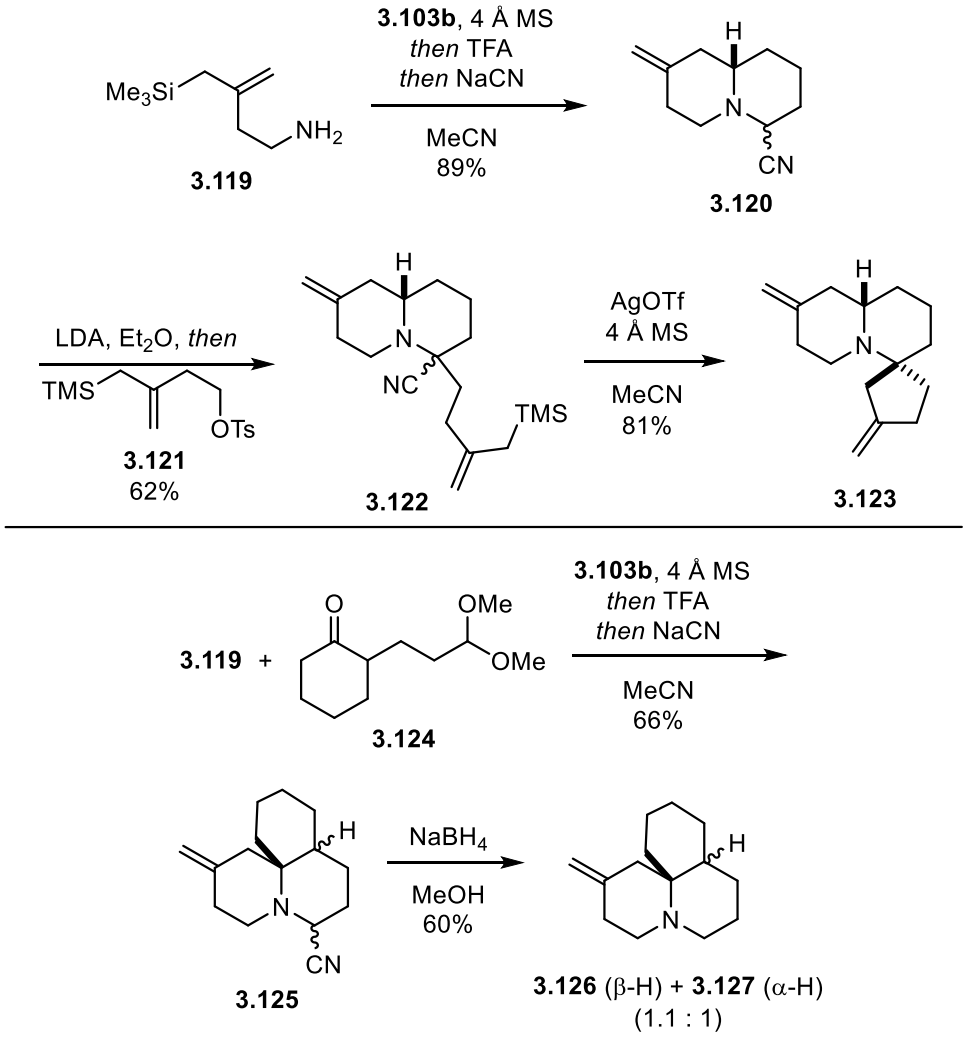

Scheme 3.11. Synthesis of spiro- tricycles **3.118, 3.121,** and **3.122**

Chapter 4. Diversity-Oriented Synthesis of Spirocyclic *β*-Phenethylamines

Building on the Martin lab's prior work in the development of diversity-oriented syntheses (DOSs) using multi-component assembly processes (MCAPs, *see* Section 3.1.2) and our use of intramolecular aza-Hosomi-Sakurai reactions for the synthesis of *N*-heterocycles (*see* Section 3.4.1), we endeavored to develop a new DOS methodology for the synthesis of aza-spirocyclic scaffolds with the general structure **4.1** (Scheme 4.1). We anticipated that derivatives of **4.1** would display a high degree of biological relevance, as **4.1** combines the *β*-phenethylamine motif discussed in Section 3.2.2 with the [6.6] and [6.5] aza-spirocyclic scaffolds discussed in Section 3.3.2, both of which appear in numerous CNS-active molecules. From a DOS standpoint, **4.1** possesses several functional handles that can serve as branch points for subsequent elaboration and diversification.

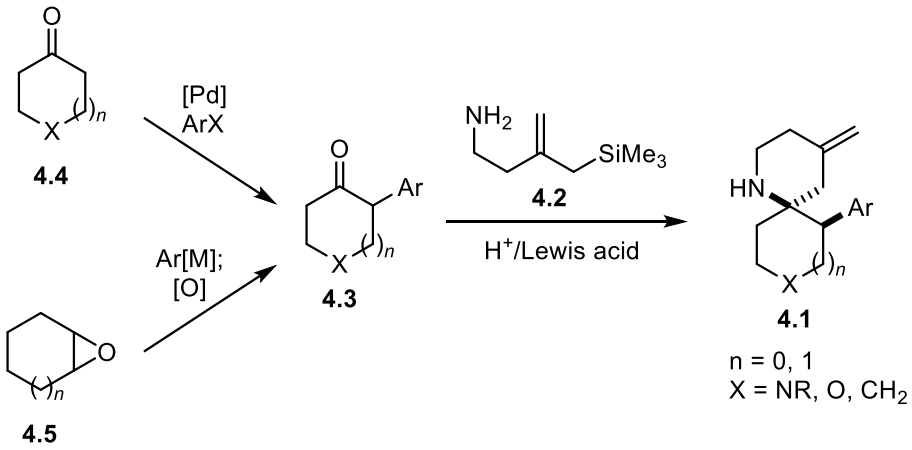

Scheme 4.1. Synthesis of *β*-phenethylamine spirocyclic scaffold **4.1**

We envisioned synthesizing **4.1** via a tandem imine condensation/aza-Hosomi-Sakurai cyclization sequence between the known amino-allylsilane **4.2**[166] and β-aryl ketones with the general structure **4.3** (Scheme 4.1). We expected that the reaction would deliver **4.1** with a *syn*

stereochemical relationship between the amino and aryl groups due to a 1,2-stereoinduction effect from the *β*-aryl group during addition of the pendant allylsilane to the iminium ion. Preparation of the β-aryl ketone substrate **4.3** could be accomplished via the use of Hartwig's [Pd]-catalyzed enolate arylation reaction between an aryl halide and cyclic ketone **4.4**. Alternately, **4.3** could be prepared from cyclic epoxide **4.5** via a two-step nucleophilic addition, oxidation sequence (Scheme 4.1).[170]

Elaboration of **4.1** could also be achieved through a variety of approaches. For instance, the piperidine nitrogen atoms could be alkylated or acylated to generate *N*-functionalized scaffolds such as **4.6**, or the exocyclic olefin could be hydrated or ozonolyzed to introduce alcohol or ketone moieties as in **4.7** and **4.8**, respectively. An appropriately substituted aryl group on **4.1** could participate in cross-coupling reactions to generate biaryl scaffolds such as **4.9**, and finally, **4.1** could undergo an intramolecular Pictet-Spengler reaction to generate spirocyclic tetrahydro- isoquinoline and *β*-carboline scaffolds **4.10** and **4.11** (Scheme 4.2).

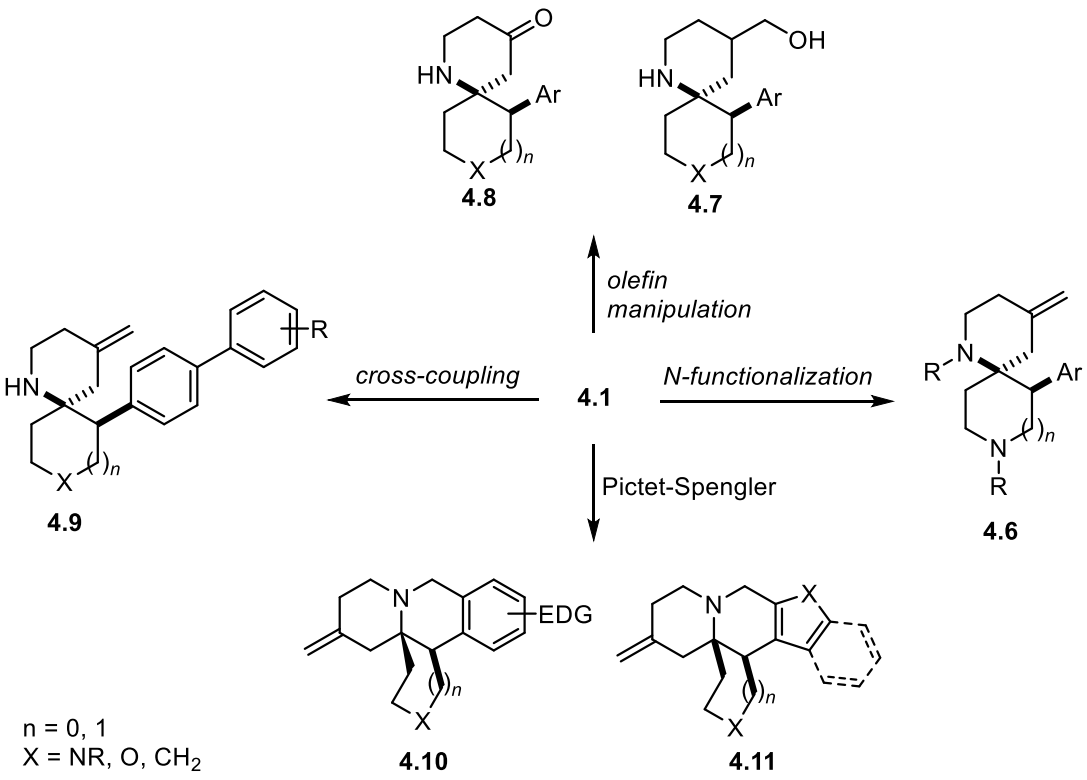

Scheme 4.2. Elaboration and diversification of **4.1** to generate functionalized scaffolds **4.6–4.11**

4.1 Synthesis of Cyclic Beta-Aryl Ketone Substrates

The first challenge to be met in reducing our new DOS method to practice was securing a robust, high-yielding protocol for the synthesis of the requisite cyclic β-aryl ketone substrates **4.3** (*see* Scheme 1). To this end, we attempted to reproduce Kawatsura and Hartwig's [Pd]-catalyzed enolate arylation protocol for the synthesis of phenyl cyclohexanone **4.13**, which they obtained in 73% yield using condition set 1 in Figure 4.1a.[170] Initial attempts gave **4.13** in <30% yield, along with large quantities of an arylation-aldol byproduct, which is tentatively assigned the structure of **4.14**. We hypothesized that trace moisture present in the reaction may have been responsible for the unexpected low yield, but rigorous exclusion of water from the reactants and solvent provided only a modest increase in the yield of **4.13** to 44% (Entry 1, Figure 4.1a). Another marginal increase in yield was achieved through increasing the catalyst loading and switching to the more active [Pd^0] catalyst $Pd(^tBu_3P)_2$, which delivered **4.13** in 52% yield, along

with 22% of the difficult-to-separate byproduct **4.14** (Entry 2, Figure 4.1a). We reasoned that lowering the reaction temperature might suppress the aldol side reaction; however, we found that at room temperature the proportion of **4.14** formed relative to **4.13** was increased, although the overall conversion was very low (Entry 3, Figure 4.1a). We also evaluated other substrates in the reaction such as *m*-chloroanisole (**4.15**) and Boc-piperidone **4.17**, and we found that these substrates likewise delivered their products **4.16** and **4.18** in low yields of 25% and 35% respectively, along with substantial quantities of uncharacterized byproducts.

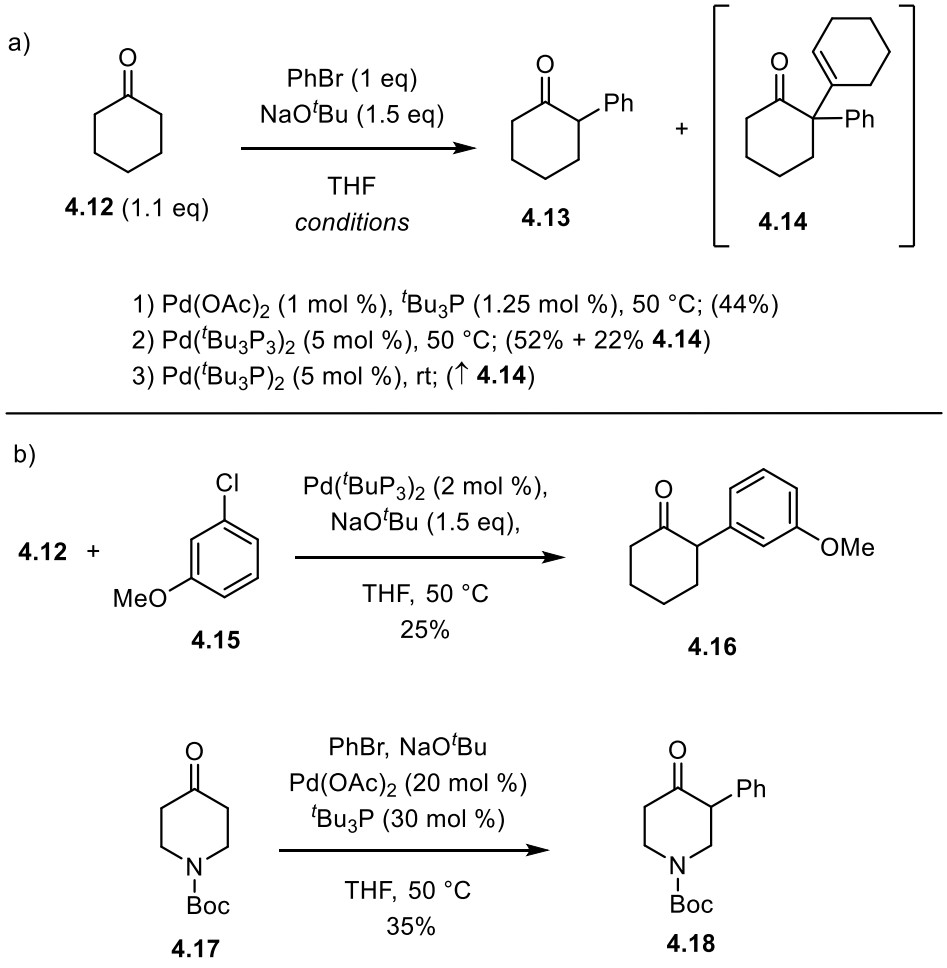

Figure 4.1. Synthesis of *β*-aryl ketones via [Pd] catalyzed enolate arylation. a) attempts to optimize reaction conditions. b) additional reaction substrates **4.15** and **4.17**.

The persistent problems encountered in our attempts to use a [Pd]-catalyzed enolate arylation led us to pursue the epoxide **4.5** addition-oxidation strategy that we had conceived as a

backup plan for the synthesis of β-aryl ketones **4.3** (*see* Scheme 4.1). This strategic pivot is analogous to the strategies used by Yang and co-workers in their work on the asymmetric fluorination of cyclic *β*-aryl ketones.[171] They prepared their *β*-aryl ketone substrates primarily via a two-step procedure comprised of a $BF_3 \cdot OEt_2$-mediated reaction of an aryllithium reagent with cyclohexene oxide, followed by alcohol oxidation with Dess-Martin or Swern reagents (*see* Scheme 4.1).[171,172] Only when this approach was not practical, such as in the synthesis of piperidone **4.18** (Figure 4.1) did they utilize [Pd]-enolate arylation chemistry, suggesting that they found the addition-oxidation sequence to be preferable, despite requiring an additional step.[171]

In the event, we found that the addition of aryllithium reagents into cyclohexene or cyclopentene oxide (**4.19, 4.20**) in the presence of $BF_3 \cdot OEt_2$ readily delivered *trans*-*β*-aryl alcohols **4.21**–**4.27** (Figure 4.2a). The aryllithium reagents were generated from the corresponding aryl bromide and *n*-butyllithium (*n*-BuLi), although 2-lithiofuran (for **4.25**) was prepared via C-H lithiation of furan with *n*-BuLi. We also investigated a modified procedure for lithium-halogen exchange to prepare **4.27** and found that the use of *tert*-BuLi instead of *n*-BuLi resulted in a marginally improved yield of **4.27** (54% → 64%). Finally, *β*-indolyl alcohol **4.28** was prepared according to a literature procedure from indole (**4.29**) and cyclohexene oxide (**4.19**) via the generation of the indolyl-Grignard reagent (Figure 4.2b).[173]

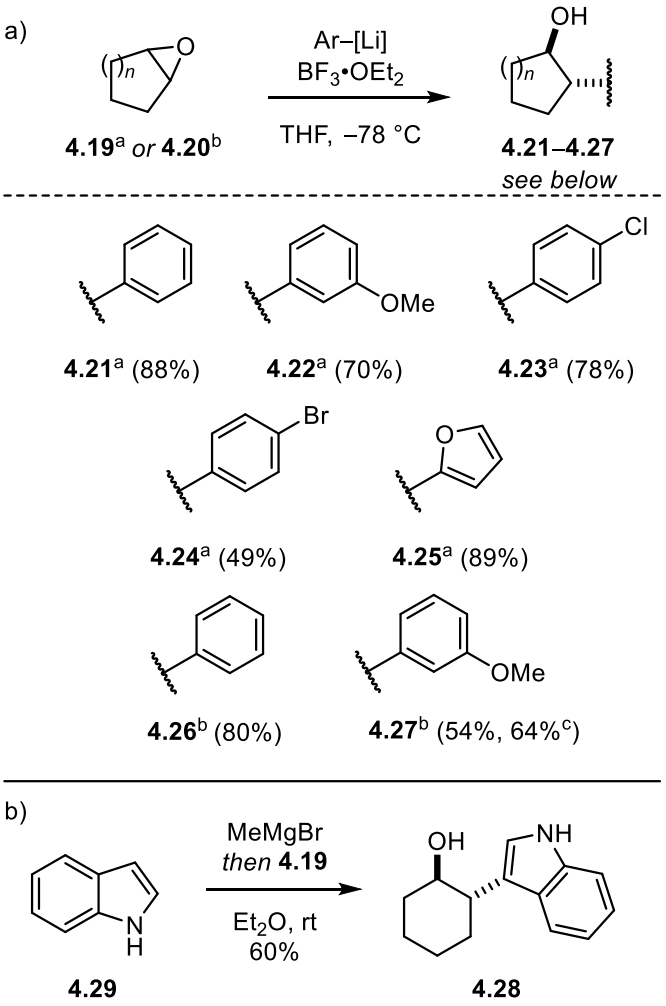

Figure 4.2. Synthesis of *β*-aryl cyclohexanols and cyclopentanols; a) addition of Ar-[Li] reagents with $BF_3 \cdot OEt_2$;[172] b) addition of an indolyl-Grignard reagent;[173] [a]) n = 2. [b]) n = 1; [c]) *t*-BuLi used for lithium-halogen exchange instead of *n*-BuLi

With *β*-aryl alcohols **4.21**–**4.28** in hand, we turned our attention to the necessary oxidation (Figure 4.3). Pyridinium chlorochromate (PCC) reliably oxidized alcohols **4.21**–**4.23** to their respective ketones; however, the oxidation of heteroaromatic substrates **4.25** and **4.28** produced complex mixtures containing degradation products, even when the reaction was cooled to 0 ˚C (Figure 4.3a). We next investigated the use of Dess-Martin periodinane for the oxidation of **4.25** and **4.28** and found that it delivered furyl- ketone **4.33** in 66% yield; however, indolyl-ketone **4.34** proved elusive because **4.28** rapidly degraded upon exposure to the reaction conditions (Figure 4.3b). Swern oxidation of **4.28** provided **4.34** in variable yields ranging from

20–70%, and this procedure was further complicated by the formation of α-oxidation byproduct **4.35**, which proved difficult to separate from **4.34** (Figure 4.3c).[173] Gratifyingly, we found that treatment of **4.28** with 2-iodoxybenzoic acid (IBX) in refluxing ethyl acetate delivered **4.34** in >95% yield (Figure 4.3d).[174] Additionally, these conditions proved to be effective for a variety of other substrates and, in this fashion, ketones **4.30–4.33** and **4.37–4.38** were prepared in >95% yield, while *p*-bromophenyl ketone **4.36** was generated in 87% yield (Figure 4.3d).

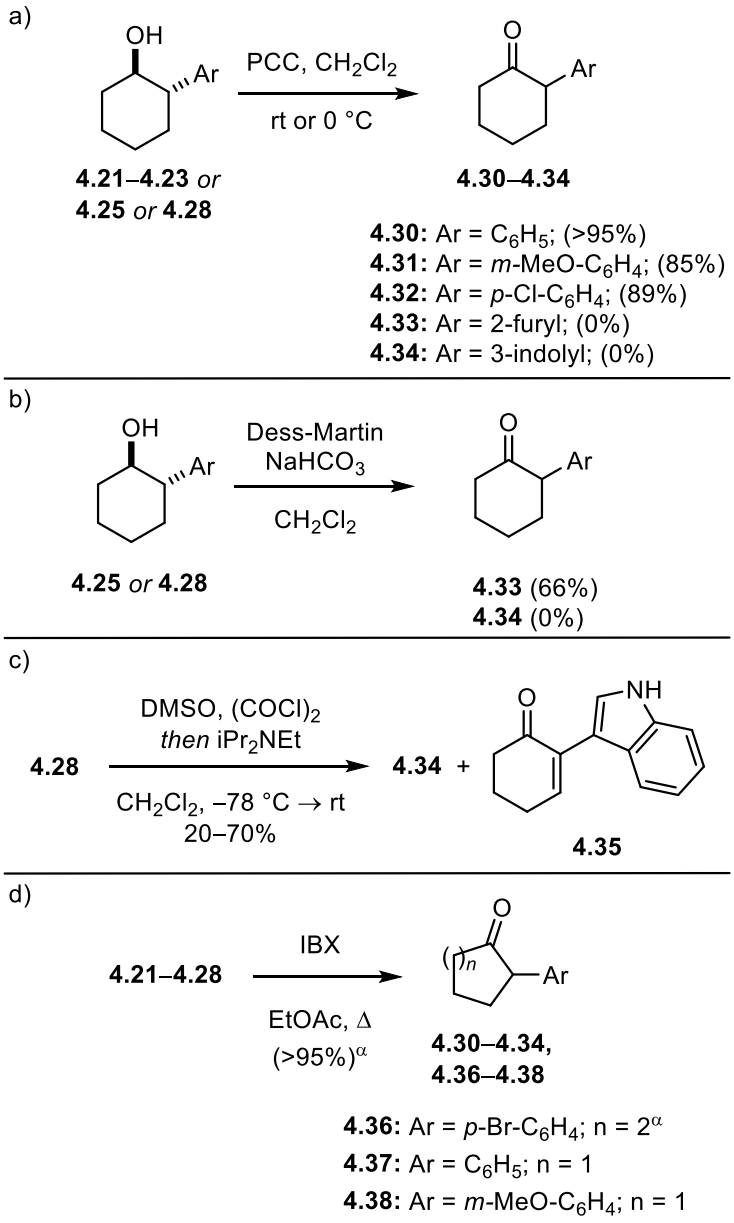

Figure 4.3. Oxidation of alcohols **4.21**–**4.28**; a) oxidations with PCC; b) oxidations with DMP; c) Swern oxidation of **4.28**; d) oxidations with IBX; $^{\alpha}$) yield of **4.36** = 87%

4.2 Development of the Aza-Hosomi-Sakurai Spirocyclization Reaction

Our initial effort to develop the cascade condensation/aza-Hosomi-Sakurai cyclization used conditions inspired by those used by Amorde and co-workers for their cascade cyclization reactions (Table 4.1, *see* Section 3.4.1).[168,169] While we were pleased to find that the reaction of ketone **4.30** and amino-allylsilane **4.2** in the presence of trifluoroacetice acid (TFA) delivered

the desired aza-spirocycle **4.39** as a single diastereomer (Entry 1, Table 4.1), the reaction was sluggish, taking roughly three days to go to completion gave only 50% yield. We reasoned that the addition of molecular sieves may accelerate the reaction by driving imine formation via the removal of water, but we found that they had only a modest effect on the reaction rate and yield (Entry 2). However, we found that heating to 50 °C substantially increased the reaction rate, leading to formation of **4.39** in 54–58% yield after 18–22 hours, along with significant quantities of protodesilylated **4.2** (Entries 3 and 4). In accord with our expectations that the formation of an iminium ion was necessary for cyclization to occur, we found that the reaction did not proceed in the absence of acid, even with heating over the course of four days (Entry 5). Finally, a promising result was obtained when we used acetic acid instead of TFA to promote the reaction: Compound **4.39** was obtained in 63% yield after only 24 hours (Entry 6). We also explored reaction conditions analogous to those used by Grieco and Fobare for intramolecular aza-Hosomi-Sakurai cyclizations, but found that the reaction barely proceeded at room temperature, and upon heating generated a complex mixture of products from which no **4.39** was obtained (Entry 7).[157]

Table 4.1. Optimization of aza-Hosomi-Sakurai cyclization: conditions in MeCN

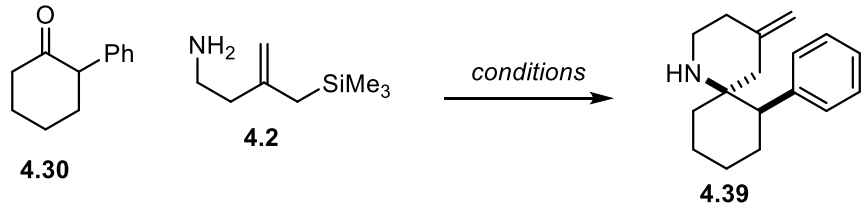

4.30 **4.2** **4.39**

Entry	Conditions	Yield (%)
1	TFA, MeCN, rt, 72 h	50
2	TFA, MeCN, 3Å MS, rt, 66 h	58
3	TFA, MeCN, 3Å MS, 50 °C, 22 h	54
4	TFA, MeCN, 50 °C, 18 h	58
5	MeCN, 3Å MS, 50 °C, 96 h	0
6	AcOH, MeCN, 3Å MS, rt, 24 h	63
7	TFA, H_2O:THF (1:3), reflux	0

To better understand and improve our cascade imine formation/cyclization reaction, we elected to optimize the individual steps separately, so we set out to identify conditions that would allow us to quantitatively form imine **4.40** (Table 4.2). Unfortunately, both magnesium sulfate in CH_2Cl_2 (Entry 1, Table 4.2) and molecular sieves in MeCN (Entry 2) produced marginal amounts of **4.40** relative to starting ketone **4.30** after extended reaction times, while the use of molecular sieves in a Soxhlet extractor with refluxing toluene (Entry 3) resulted in the formation of a complex mixture. To our surprise, the use of molecular sieves in methanol resulted in formation of cyclized product **4.39** and only trace amounts of **4.40** (Entry 4, *c.f.* Entry 5, Table 4.1), as did use of the Lewis acid titanium (IV) isopropoxide ($Ti(O\textit{i}Pr)_4$) in methanol (Entry 5). The results in Entries 4 and 5 suggest that quantitative imine formation may not be readily achieved, as it appears that while formation of the imine is sluggish, the subsequent attack of the pendant amino-allylsilane occurs rapidly under favorable conditions.

Table 4.2. Attempts to quantitatively form imine **4.40**

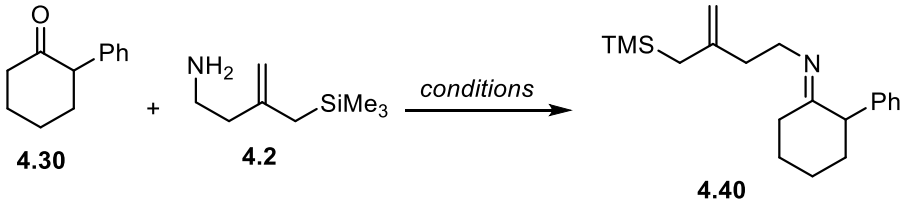

4.30 + **4.2** → **4.40**

Entry	Conditions	Results
1	$MgSO_4$, CH_2Cl_2, rt, 96 h	5 : 1 **4.30** : **4.40**
2	3Å MS, MeCN, 40 °C, 24 h	10 : 1 **4.30** : **4.40**
3	3Å MS, PhMe, reflux (Soxhlet extractor)	Decomposition
4	3Å MS, MeOH, 18 h	**4.39** observed
5	AcOH, 3Å MS, rt, 24 h	**4.39** observed

The results in Tables 4.1 and 4.2 led us to our optimized conditions for the condensation/aza-Hosomi-Sakurai reaction: Namely, use of acetic acid in methanol with or without molecular sieves delivered **4.39** in a reproducible 67% yield and dr ≥ 20:1 after 24 hours (Table 4.3, entry 1). While titanium (IV) isopropoxide also gave promising results, we found the yields obtained from these reactions to be highly variable (Entry 2). Another titanium Lewis acid, $TiCl_4$—which was used by Hosomi and Sakurai in their initial studies—resulted in a complex mixture with large quantities of protodesilylated **2** (Entry 3).[149] We investigated other protic acids and again found that weak acids such as benzoic acid (Entry 4) catalyzed the reaction effectively, delivering the product **4.39** in 50% yield, whereas the strong acid *p*-toluenesulfonic acid (*p*-TsOH) produced only trace amounts of **4.39** after 24 hours. Building on the realization that weak acids are effective promoters of the reaction, we investigated the use of pyridinium salts and found that pyridinium hydrochloride (Entry 6) likewise generated **4.39** in 50% yield, while HF·pyridine resulted in the formation of a complex mixture.

Table 4.3. Optimized aza-Hosomi-Sakurai conditions, and additional screening; [a]) dr ≥ 20:1 in all instances where **4.39** was isolated [b]) comparable yields were obtained in the presence of 3 Å mol sieves

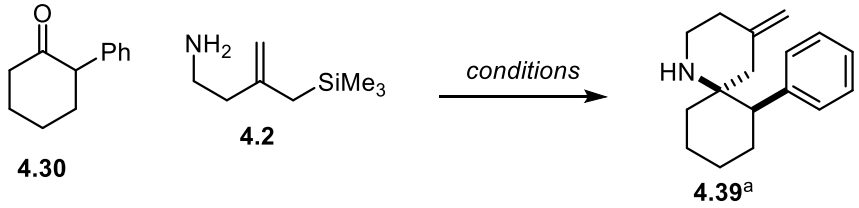

4.30 **4.2** **4.39**[a]

Entry	**Conditions**	**Yield of 4.39**[a]
1	AcOH, MeOH	67%[b]
2	$Ti(OiPr)_4$, MeOH	21–71%
3	$TiCl_4$, CH_2Cl_2, –78 ˚C	decomposition
4	BzOH, 3Å MS, MeOH	50%
5	*p*TsOH, 3Å MS, MeOH	trace
6	Pyr·HCl, MeOH	50%
7	HF·Pyr, MeCN	decomposition

With optimized conditions for the condendsation/aza-Hosomi-Sakurai reaction in hand, we set to applying them to β-aryl ketone substrates **4.18, 4.31–4.34,** and **4.36–4.38**. We found that the reaction worked well with cyclohexanone and piperidone substrates, delivering [5.5] spirocycles **4.41–4.46** in 65–82% yield and ≥ 20:1 dr (Table 4.4).

Table 4.4. Synthesis of aza-spirocycles **4.41–4.46**; [a]) dr ≥ 20:1

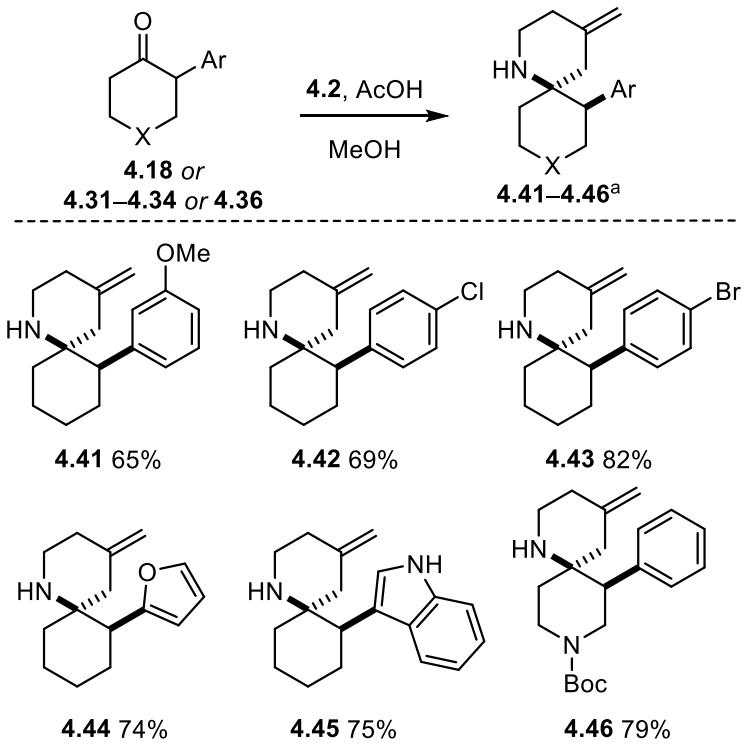

When cyclopentanone substrates **4.37** and **4.38** were subjected to our optimized conditions, we found that the reaction proceeded slowly, requiring 3-4 days to generate products **4.47** and **4.48** in 59% and 45% yield, respectively (Figure 4.4a and 4.4b, entry 1). This decrease in reaction rate relative to cyclohexanone substrates may be explained by unfavorable torsional interactions generated during hemiaminal formation, and is consistent with general trends in which the rate of electrophilic addition to cyclopentanone substrates is slower than that of cyclohexanone substrates.[175] The addition of molecular sieves did not appreciably increase the reaction rate (Figure 4.4a, entry 2); however, heating the reaction (Figure 4.4a, entries 3 and 4; Figure 4.4b, entry 2) resulted in reduced reaction times with comparable yields. While cyclizations with β-aryl cyclohexanones produced the *cis* isomer in diastereomeric ratios > 20:1, the aryl cyclopentanones tested gave diastereomeric ratios in the range of 2:1–3:1 (Figure 2b, entry 2). A similar erosion in diastereoselectivity has been observed in the proline-catalyzed aldol reactions of cyclopentanone and cyclohexanone.[176]

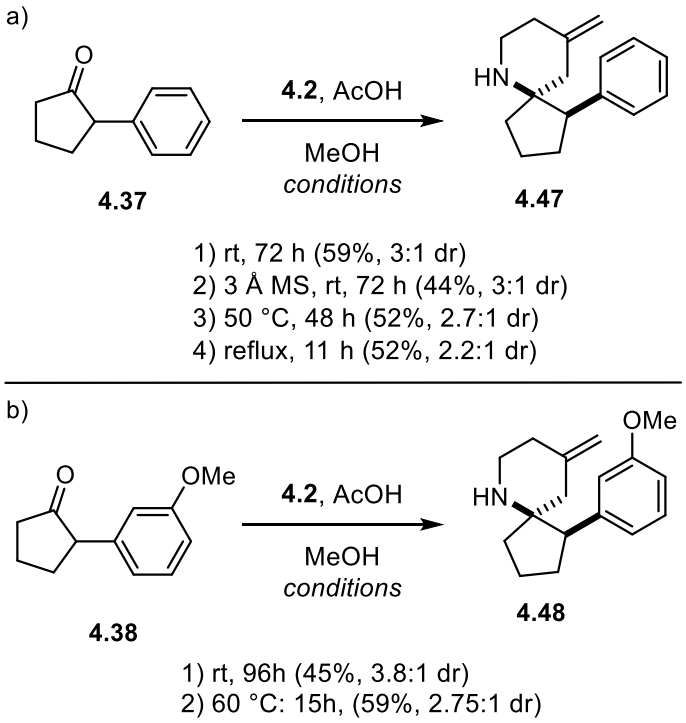

Figure 4.4. Condensation/aza-Hosomi-Sakurai cyclization conditions for cyclopentanone substrates **4.37** (a) and **4.38** (b)

Finally, we briefly investigated the use of the aza-Hosomi-Sakurai cyclization on the nor-aryl ketone substrates cyclohexanone (**4.12**) and Boc-piperidone **4.17** (Scheme 4.3). In both instances we found that the reaction worked well, delivering spirocyclic piperidine **4.49** and bis-piperidine **4.50** in 75% and 87% yield, respectively**.**

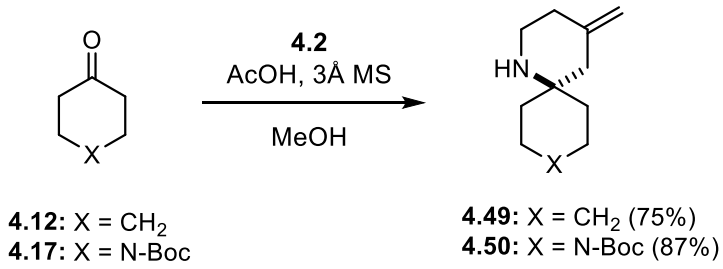

Scheme 4.3. Synthesis of nor-aryl aza-spirocycles **4.49** and **4.50**

4.3 Elaboration and Diversification of Spirocyclic Scaffolds

4.3.1. Diversification Through *N*-Functionalizations

The piperidine *N*-H of aza-spirocycles **4.39** and **4.41–4.48** provides a convenient functional handle for additional scaffold elaboration. Despite being a neopentyl center, we found that the *N*-H of prototypical scaffold **4.39** readily underwent *N*-acetylation, reductive *N*-methylation, and *N*-carbamoylation reactions to deliver *N*-functionalized derivatives **4.49**, **4.50**, and **4.51** respectively (Scheme 4.3). These reactions with **4.39** serve as examples for *N*-functionalization reactions that could be potentially performed on any of our spirocyclic scaffolds for the synthesis of a whole library of *N*-functionalized aza-spirocycle derivatives.

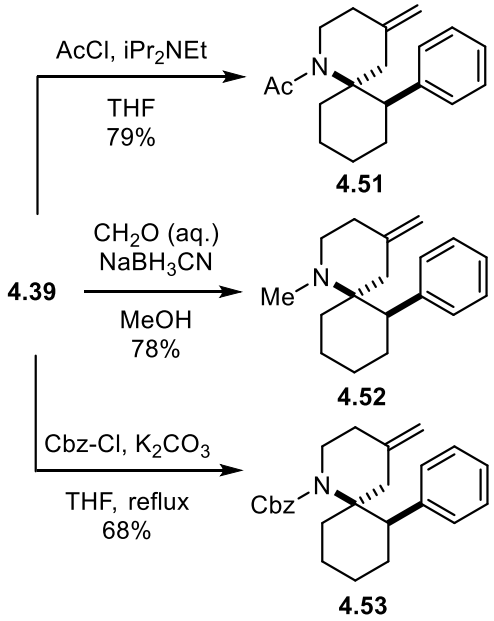

Scheme 4.4. *N*-Functionalization of spirocyclic scaffold **4.39**

We also performed sequential *N*-functionalization reactions on our bis-piperidine scaffold **4.46** via the sequence shown in Scheme 4.5. Alkylation of the neopentyl *N*-H with benzyl bromide proceeded in 69% yield, followed by a quantitative Boc-deprotection to deliver diamine **4.54**. Reductive methylation of **4.54** with formaldehyde and sodium cyanoborohydride furnished the *N*-*di*alkylated bis-piperidine derivative **4.55** in 79% yield.

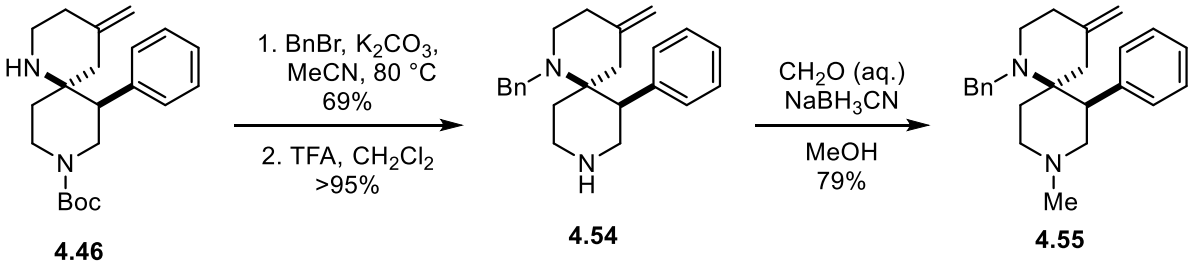

Scheme 4.5. *N*-functionalization reactions of bis-piperidine scaffold **4.46**

Finally, we investigated *N*-functionalization reactions on the nor-aryl scaffolds **4.49** and **4.50.** Conversion of **4.49** to its *N*-acetyl derivative **4.56** proceeded in 78% yield; a one-pot method for preparing **4.56** from cyclohexanone (**4.12**), amino-allylsilane **4.2**, and acetyl chloride was also achieved, albeit in only 29% yield (Scheme 4.6). We also attempted to elaborate bis-piperidine scaffold **4.50** to the caged compound **4.58** by bridging the two amines through alkylation of **4.57** with 1,2-dibromoethane, but these reactions only resulted in returned starting material and uncharacterized degradation products (Scheme 4.7).

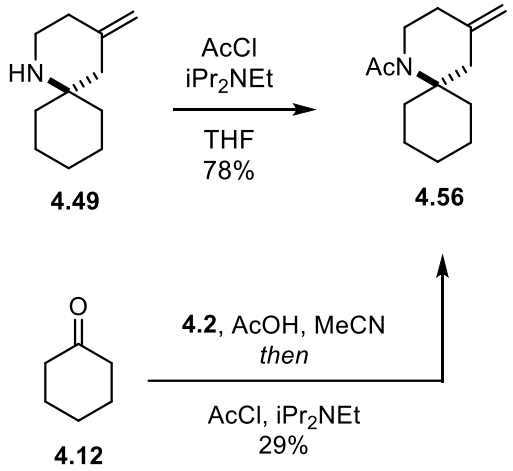

Scheme 4.6. Synthesis of *N*-acetyl nor-aryl derivative **4.56**

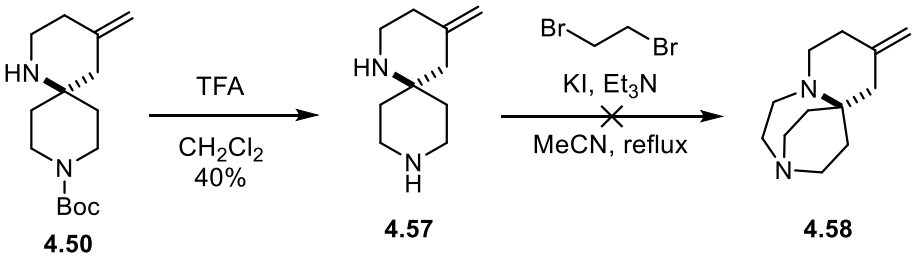

Scheme 4.7. Attempted synthesis of caged tricycle **4.58**

4.3.2. Diversification Through Suzuki Couplings

Cross-coupling reactions are robust methods to generate diversity from a common intermediate by utilizing different coupling partners. Accordingly, we investigated the feasibility of using halo-phenyl scaffold **4.42** and later **4.43** as substrates for Suzuki coupling reactions. In the event, aryl chloride **4.42** underwent coupling with boronic acid **4.59** in the presence of $Pd(^tBu_3P)_2$ to deliver the desired product **4.60** in 26% yield, along with 52% yield of a Suzuki/Buchwald-Hartwig coupling product with the tentative structure **4.61** (Scheme 4.8). We attempted to minimize the formation of this side product through screening catalysts and solvents, but invariably obtained either returned starting material or a mixture of **4.60** and **4.61**.

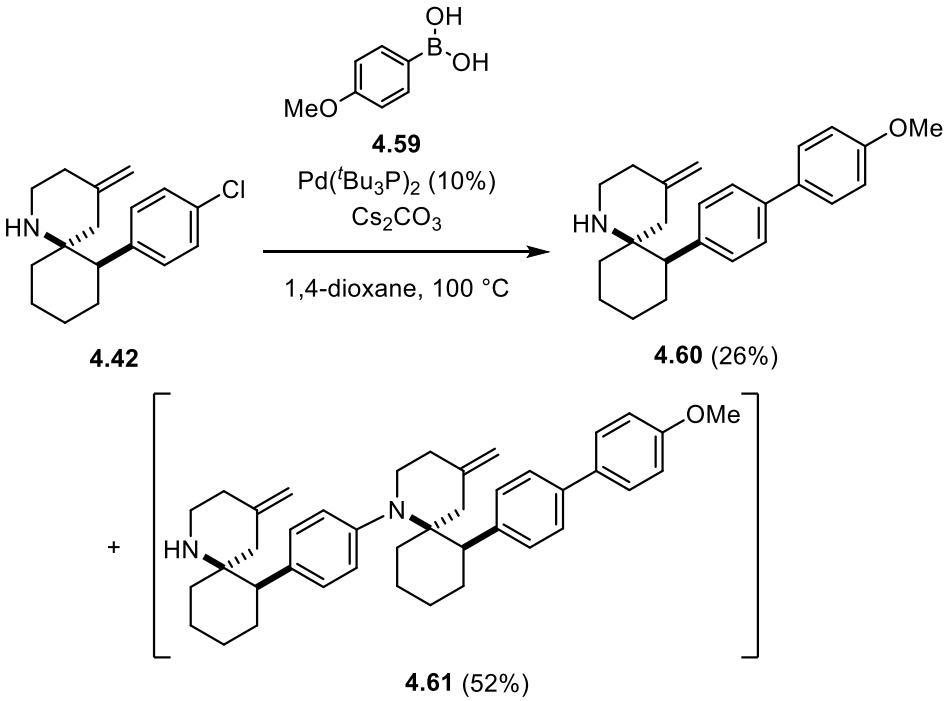

Scheme 4.8. Troublesome Suzuki coupling of aryl chloride scaffold **4.42**

We sought to obviate this side reaction through protection of the piperidine nitrogen of **4.42**. Accordingly, Cbz-protection of **4.42** gave **4.62**, which underwent Suzuki coupling with **4.59** to deliver biaryl derivative **4.63** in 58% yield (Scheme 4.9). Unfortunately, the removal of the Cbz protecting group of **4.63** proved to be problematic. We anticipated that traditional methods of Cbz-deprotection, such as metal-catalyzed hydrogenolysis conditions, would be incompatible with the olefinic group of **4.63**, so we attempted to apply Coleman and Shah's conditions for chemoselective carbamate cleavage using triethylsilane and a palladium catalyst.[177] After some optimization, we were able to obtain **4.60** in 59% yield (82% BRSM) after 72 hours.

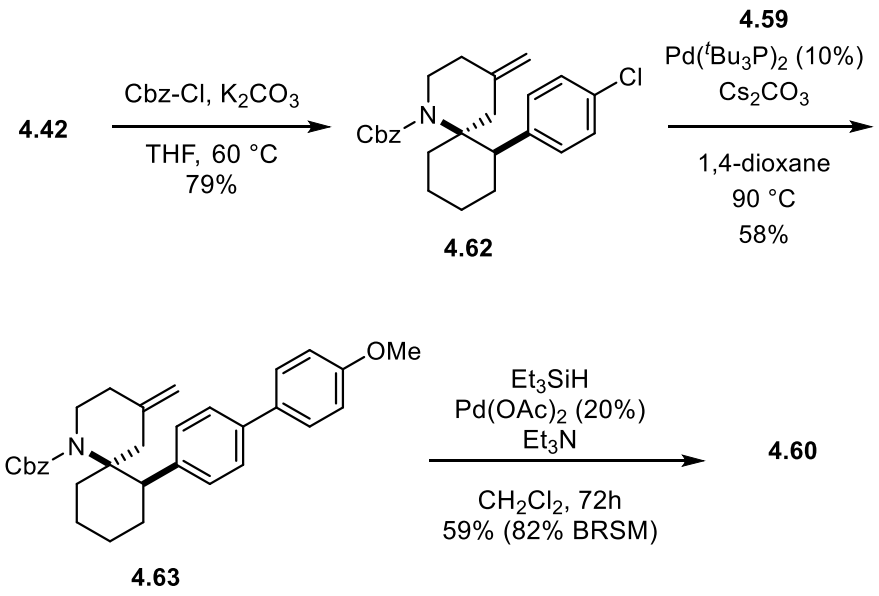

Scheme 4.9. Protection, Suzuki coupling, and deprotection of **4.42**

The long reaction times, mediocre yields, and the need for discreet protection and deprotection steps all greatly diminished the utility of a Suzuki coupling reaction with aryl chloride **4.42**. Accordingly, we prepared aryl bromide **4.43** to evaluate its performance as a Suzuki coupling partner. In retrospect, we should have investigated **4.43** sooner, but we were hesitant to pursue this strategy due to anticipated problems with the initial organolithium formation and epoxide addition (*see* Figure 4.2). In the event, we found that **4.43** readily underwent Suzuki coupling with **4.59** to deliver *p*-methoxy biphenyl **4.60** in 71% yield with no Buchwald-Hartwig side-products observed, and could also be coupled with **4.65** to prepare *p*-fluoro derivative **4.65** in >95% yield.[178]

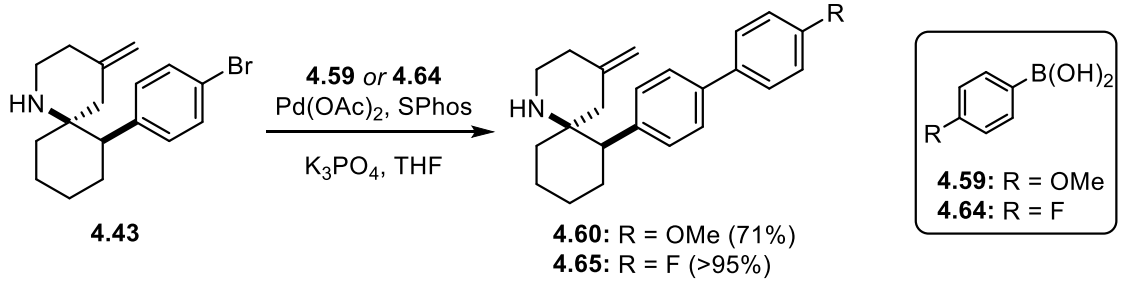

Scheme 4.10. Suzuki coupling of aryl bromide scaffold **4.43**

4.3.3. Hydroboration-Oxidation and Ozonolysis

In dreaming up new ways to diversify our central scaffold, we realized that protocols for the addition of polar functional groups would be desirable as our core scaffold is relatively nonpolar. The polarity of a molecule has a large impact on its behavior in biological systems, especially with regard to membrane permeability, and the ability to readily modulate the polarity of a given set of analogs is highly desirable for the medicinal chemist.[179] To this end, we developed protocols for the hydroboration-oxidation and ozonolysis of the olefin functionality on our scaffold.

Our work on the hydroboration-oxidation of prototypical scaffold **4.39** is summarized in Scheme 4.10. Using conditions that were adapted from the work of Rejzek and co-workers, we found that treatment of **4.39** with borane-dimethyl sulfide at –78 ˚C followed by the addition of sodium hydroxide and hydrogen peroxide delivered **4.66** as a single diastereomer in 62% yield.[180] Notably, Rejzek found that running the reaction at –78 ˚C resulted in a highly diastereoselective hydroboration, which was attributed to an initial coordination of the borane reagent to the piperidine nitrogen atom followed by an intramolecular hydroboration. We also investigated the use of the bulky borane reagent 9-BBN to see what effect, if any, it would have on the diastereoselectivity of the hydroboration. Interestingly, we found that using 9-BBN resulted in exclusive formation of the other diastereomer **4.67**. Unfortunately, we were not able to satisfactorily purify **4.67** due to persistent contamination with cyclooctane diol byproduct **4.68**.

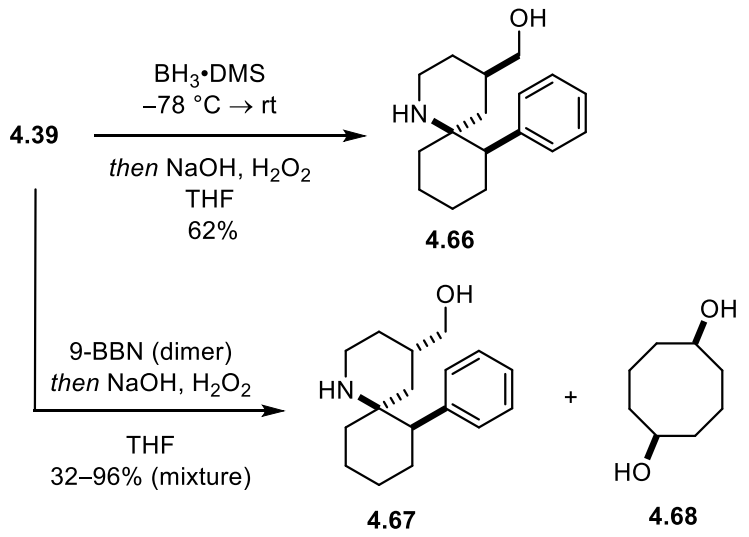

Scheme 4.11. Hydroboration-oxidation of **4.39**

Finally, we secured conditions for selective ozonolysis of the olefin moiety. To obviate concerns regarding amine oxidation, we used *N*-acetyl derivative **4.51**, which readily underwent ozonolysis to deliver spiro-piperidone **4.69** in 69% yield.

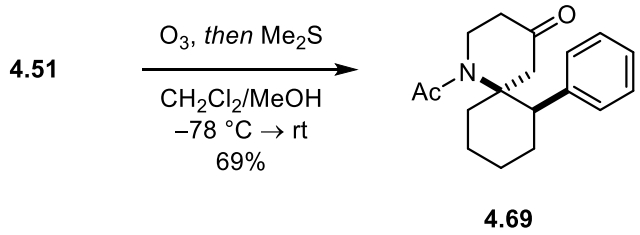

Scheme 4.12. Ozonolysis of **4.51**

4.3.4. Pictet-Spengler Cyclizations

The reactions discussed in Sections 4.3.1–4.3.3 are all robust methods for introducing diverse substituents to the central spirocyclic scaffold; however, the only method for introducing scaffold diversity has been the use of different β-aryl ketone substrates in the aza-Hosomi-Sakurai cyclization. Thus, we were interested in developing a method for late-stage scaffold diversification, analogous to the "pair" stage of the "build-couple-pair" strategy (*see* Section 3.1.1). We noticed that the piperidine *N*-H and arene moieties of **4.39** and **4.41**–**4.48** are spatially

oriented such that the incorporation of a bridging methylene unit between the two groups appeared to be a reasonable strategy for scaffold diversification. We envisioned that we could achieve this transformation via the use of an intramolecular Pictet-Spengler cyclization.

Our initial work in this area interrogated the use of phenyl scaffold **4.39** as a cyclization substrate. We explored several conditions adapted from literature reports on Pictet-Spengler cyclizations of pheylalanine derivatives, such as aqueous formaldehyde in formic acid or acetic acid/ethanol mixtures. We invariably obtained either returned starting material **4.39** or a complex mixture of degradation products with no trace of the desired tetracycle **4.70** (Equation 4.1).[181] However, we found that the use of the more electron-rich *m*-anisole derivative **4.41** as a substrate for the Pictet-Spengler reaction resulted in clean conversion to tetrahydroisoquinoline (THIQ) scaffold **4.71** in 73% yield (Equation 4.2). Furan substrate **4.44** likewise underwent cyclization under similar conditions to deliver the tetrahydrofuropyridine scaffold **4.72** in 75% yield (Equation 4.3).

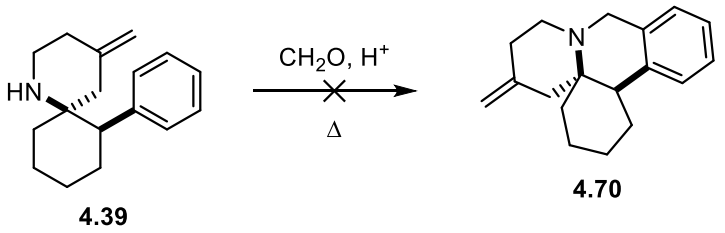

4.39 4.70 (4.1)

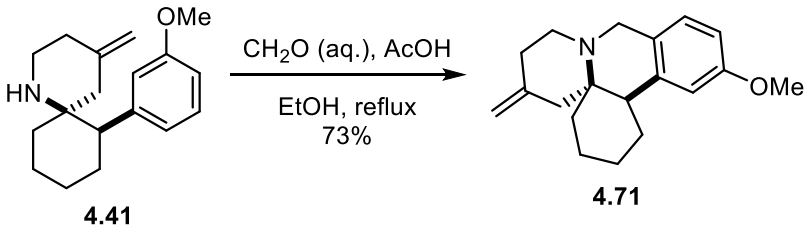

4.41 4.71 (4.2)

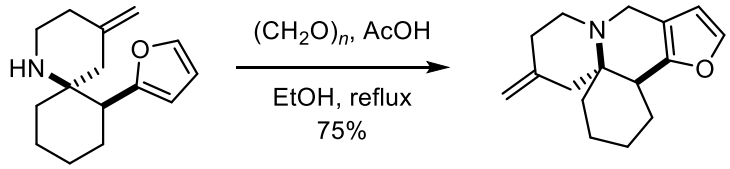

4.44 4.72 (4.3)

Identification of reliable conditions for cyclization of the [4.5] spirocycle **4.48** to THIQ **4.73** required some experimentation, as shown in Table 4.5. Subjecting **4.48** to the same conditions (10 eq CH_2O, 2 eq AcOH, EtOH, reflux) identified for the synthesis of **4.71** and **4.72** resulted in an inseparable mixture (3:1) of *o*- and *p*- cyclization products **4.73** and **4.74** in 76% combined yield (Table 4.5, Entry 1). On the other hand, use of Cook's neutral aprotic Pictet-Spengler conditions delivered only returned starting material (Entry 2).[182] However, the use of formic acid as a solvent resulted in exclusive formation of the *p*- product **4.73** (Entry 3), which after some optimization was produced in 92% yield (Entry 4). Interestingly, a similar trend was observed in the Pictet-Spengler cyclization of dopamine and acetaldehyde to form salsolinol, the product of *p*- cyclization, and isosalsolinol, the product of *o*- cyclization. In strongly acidic media salsolinol was formed exclusively, while in weakly acidic and neutral media a mixture of salsolinol and isosalsolinol was produced.[183] This phenomenon was studied computationally by Almodovar and co-workers, who concluded that the increase in *ortho*-selectivity as neutral pH is approached may be due to the formation of a iminium/phenolate zwitterion prior to

cyclization.[183] While the formation of such a species is not possible in our system, the parallel trend is intriguing.

Table 4.5. Optimization of Pictet Spengler cyclization to form **4.70**

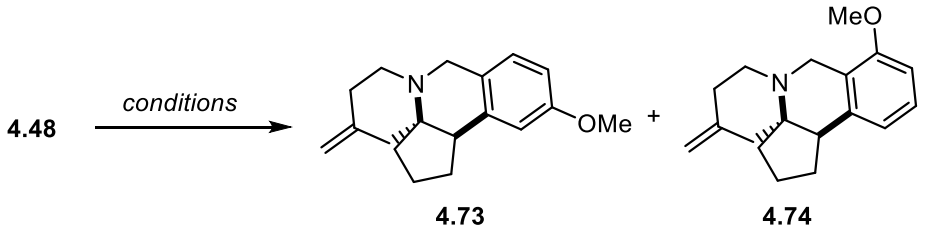

4.73 **4.74**

Entry	Conditions	Yield
1	CH_2O (aq), AcOH, EtOH, reflux	76% (3:1, **4.73:4.74**)
2	$(CH_2O)_n$, PhMe, reflux	RSM
3	CH_2O (aq), HCO_2H, 90 ˚C	55% (**4.73**)
4	CH_2O (aq), HCO_2H, 50 ˚C	92% (**4.73**)

Finally, we identified conditions for the Pictet-Spengler cyclization of indolic spirocycle **4.45** to prepare tetrahydro-β-carboline scaffold **4.73** (Scheme 4.13). Subjecting **4.45** to our "standard" conditions with aqueous formaldehyde resulted in the formation of **4.75** in 23% yield, along with 14% of a compound that has been tentatively assigned the structure **4.76** on the basis of ^{1}H NMR (Scheme 4.13, top). The use of paraformaldehyde in ths reaction delivered **4.75** in 45% yield, along with a different hydroxy-methylene adduct with the tentative structure of **4.77** in 19% yield (Scheme 4.13, middle). However, by using Cook's neutral aprotic Pictet-Spengler conditions, we were able to obtain **4.75** in 69% yield, with no trace of any hydroxy-methylene byproducts.[182]

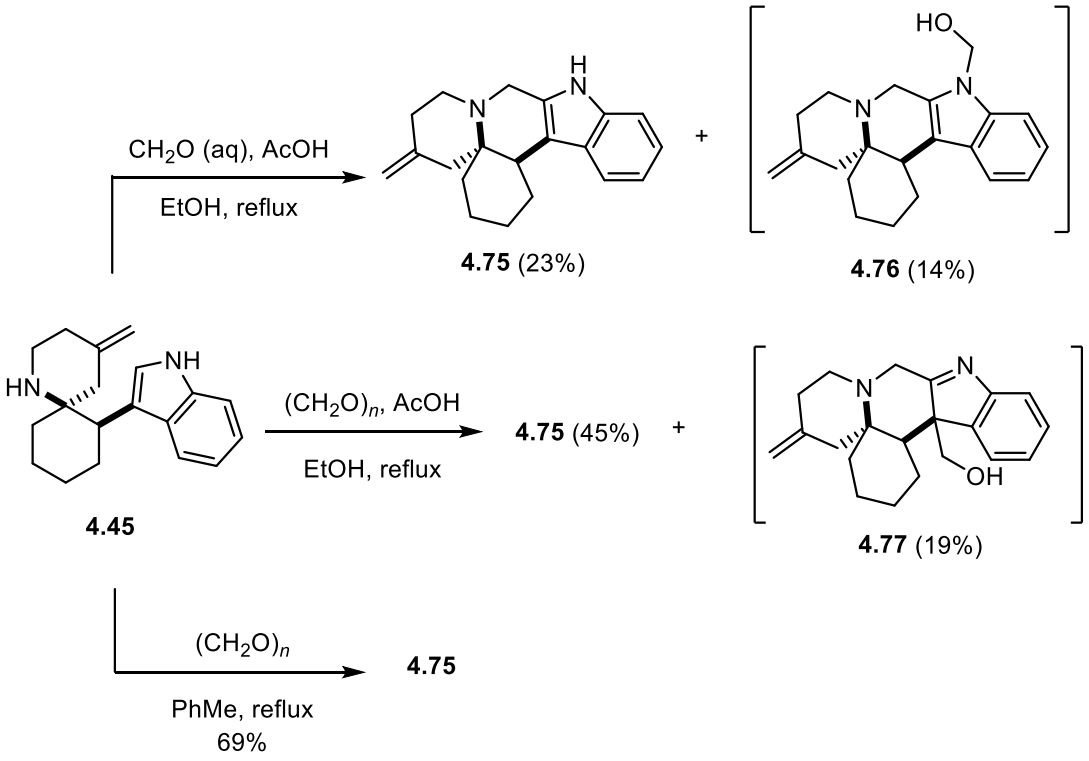

Scheme 4.13. Synthesis of tetrahydro-β-carboline scaffold **4.75**

4.4. BIOLOGICAL TESTING

To query the potential biological relevance of our spirocyclic β-phenethylamine compound set, we submitted select compounds to the Psychoactive Drug Screening Program for a broad screen against common CNS receptors. All of the compounds were found to be potent inhibitors of the Sigma 1 (Sig1R) and/or Sigma 2 (Sig2R)/TMEM97 receptors, especially Pictet-Spengler products **4.71** and **4.75**, which displayed 8 nM and 45 nM Sig1R K_i values (Table 4.6). The amino alcohol **4.66** was found to be selective for the (Sig2R)/TMEM97 receptor, displaying a 452 nM K_i value and 5-fold selectivity for Sig2R/TMEM97 over Sig1R. Aza-bicyclic derivatives **4.45, 4.54,** and **4.66** appear to be selective for the sigma receptors, as these were the only receptors which they inhibited with sub-micromolar potency, while THIQ **4.71** also inhibited the alpha-2A adrenergic receptor (K_i=531 nM), and tetrahydro-β-carboline **4.75** proved to be a promiscuous binder, exhibiting mid-nanomolar (100 – 500 nM) inhibition of the

dopamine transporter, the histamine H1 receptor, and several serotonin and adrenergic receptor subtypes.

Table 4.6. Activity of select compounds at the Sigma 1 (Sig1R) and Sigma 2 (Sig2R)/TMEM97 receptors

Compound	**Sig1R K_i (nM)**	**Sig2R/TMEM97 K_i (nM)**
4.45	1446	463
4.54	542	502
4.66	2257	452
4.71	8	152
4.75	45	308

Unfortunately, we later identified a contaminant that may have skewed the results of the PDSP screen for compound **4.71**. Specifically, we found that over the course of its storage at 4 ˚C, roughly 50% of **4.71** had been oxidized to benzamide **4.78** (Scheme 4.14). In deuterochloroform this oxidation process was more rapid, with approximately 50% conversion to **4.78** occurring when **4.71** was left overnight in $CDCl_3$ at room temperature. We found that we could inhibit this oxidation via the addition of triethylamine to the solution of **4.71** in $CDCl_3$, suggesting that the oxidation is acid-catalyzed. Interestingly, no oxidation products were observed for the analogous cyclopentyl-THIQ **4.73** or tetrahydro-β-carboline **4.75** after prolonged storage, while trace amounts may have been observed in ^{1}H NMR spectra of furan derivative **4.72**. Unfortunately, the PDSP screen of **4.71** occurred after it had been in storage for several months, and we do not know the extent to which **4.78** was present at the time of the assay. While this certainly calls the PDSP results for **4.71** into question, a favorable interpretation would be that **4.71** is probably a *more* potent Sig1R inhibitor than indicated, as the

proposed pharmacophore model for the Sigma 1 receptor requires the presence of a basic amine group, so it seems likely that any **4.78** present in the assay probably did not contribute significantly to Sig1R inhibition.[79]

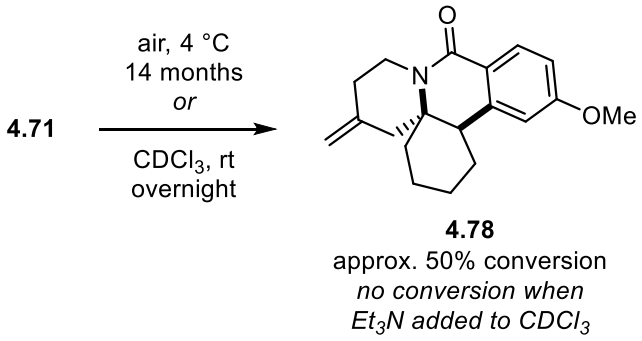

Scheme 4.14. Spontaneous oxidation of **4.71** to benzamide **4.78**

4.5. CONCLUDING REMARKS

In summary, we have developed a DOS methodology for the preparation and diversification of spirocyclic β-phenethylamines, THIQs and tetrahydro-β-carbolines. Key to this development was the optimization of a tandem condensation/aza-Hosomi-Sakurai spiro-cyclization process that proceeds in good yield and excellent diastereoselectivity with cyclohexyl substrates under exceedingly mild conditions. We found that cyclopentyl substrates could also participate in this process to generate [4.5]-spirocyclic scaffolds, albeit in decreased yield and diastereoselectivity. We also demonstrated several strategies for subsequent elaboration of our spirocyclic β-phenethylamine scaffolds via *N*-functionalization, Suzuki coupling, olefin manipulation, and Pictet-Spengler cyclization. Finally, we submitted several compounds for a CNS receptor screen, and found them to be potent inhibitors of the Sigma 1 and Sigma 2/TMEM97 receptors. It is our hope that this work may lead to the development of new drug leads or biochemical tool compounds built around or inspired by our novel, bioactive chemical scaffolds.

THE TOTAL SYNTHESIS OF EXOTINES A & B

Chapter 5. The Isolation and Biosynthesis of Exotines A & B, the Trauner Synthesis of Exotine B, and [4 + 3] Cycloaddition Reactions for the Synthesis of Cyclohepta[*b*]indoles

5.1 Isolation and Characterization of Exotines A & B

Exotine A (**5.1**) and B (**5.2**) were isolated from the roots of *Murraya exotica* by the Jiang and coworkers in 2015 (Figure 5.1).[184] The core structure of these novel alkaloids is comprised of isopentenyl-substituted indole (atoms no. 1–14, Liu *et al.* numbering system) and coumarin (atoms no. 1'–14') units, which combine to form the unique coumarin-cyclohepta[*b*]indole ring system of exotine A and B, heretofore unobserved among known natural products.[184,185] The structures of **5.1** and **5.2** were elucidated via 2D-NMR experiments and their absolute stereochemistry was confirmed by single-crystal X ray diffraction using anomalous dispersion.[184]

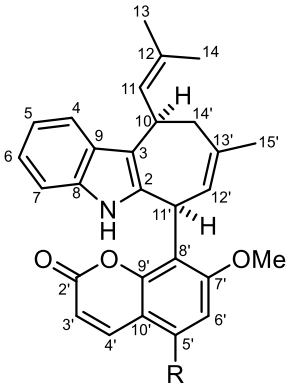

Figure 5.1. Structures of exotines A (**5.1**) and B (**5.2**) isolated from *Murraya exotica* (Jiang *et al.* numbering system)[184]

Plants of the genus *Murraya* are known for being rich sources of bioactive coumarin,[186,187] carbazole,[188–190] and polyphenol[191] natural products, some of which have shown promise as anti-inflammatory[186,192], anti-microbial,[193,194] anti-diabetic,[188] and hepatoprotective[191]

agents. *M. exotica*, commonly known as the orange jasmine or Chinese box plant, is an ornamental shrub that grows widely throughout southern China. The extracts of the roots and leaves of *M. exotica* have a long history of use by people in this region for the treatment of rheumatism, cough, fever, and as anti-infective and anti-nociceptive agents.[184,186,192] Accordingly, exotine A (**5.1**) and B (**5.2**) were assayed for biological activity and were found to inhibit lipopolysaccharide-induced nitric oxide (NO) production in BV2 microglial cells (IC_{50} = 9.2 and 39.9 μM, respectively).[184] NO is a prolific signaling molecule that plays a role in many physiological processes, and aberrant NO production has been linked to pathologies such as migraine, shock, dermatitis, necrosis, and tumor growth and metastasis.[195–197] Thus, compounds that inhibit NO production such as **5.1** and **5.2** represent potential new leads for the treatment of the aforementioned disease states.[195–197]

5.1.1. Jiang's Proposed Biosynthesis of Exotines A and B

Jiang *et al.* proposed a biosynthesis of exotine A (**5.1**) and B (**5.2**), which can be seen in Scheme 5.1.[184] They proposed that 3-prenylindole (**5.3**) is oxidized to the conjugated indolenine **5.4**, which then undergoes a Diels-Alder cycloaddition with coumarin-dienes *trans*-dehydroosthol (**5.5**) or gleinadiene (**5.6**), both of which have been isolated from *M. exotica* extracts, to generate *spiro*-indolenine adduct **5.7**.[186] Subsequent 1,2-alkyl migration furnishes the natural products **5.1** and **5.2**.

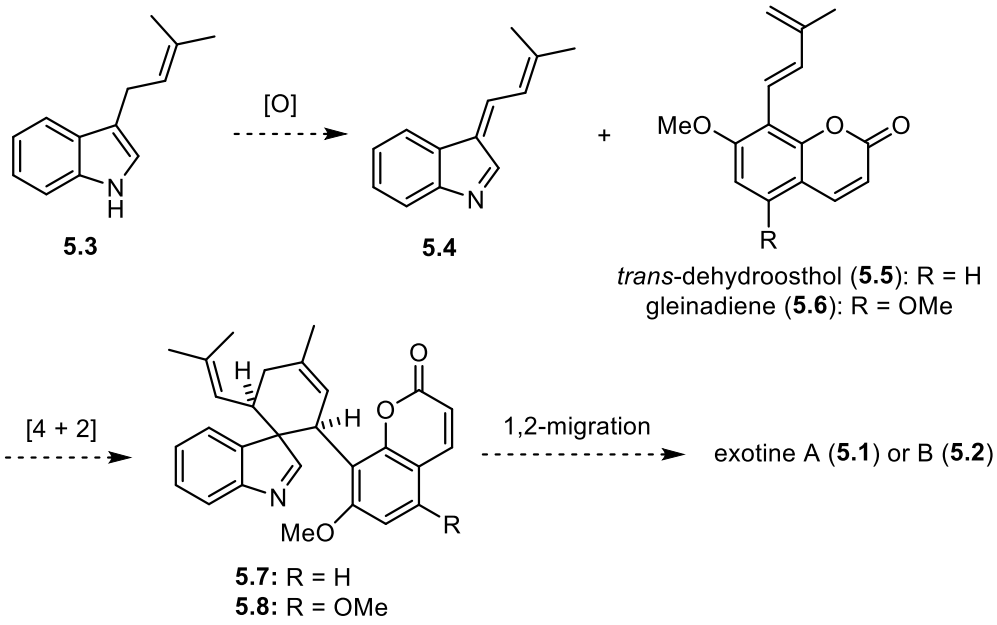

Scheme 5.1. Jiang's proposed biosynthesis of exotine A (**5.1**) and B (**5.2**)[184]

Jiang's biosynthetic hypothesis is analogous to the proposed biosynthesis of the natural products murrapanine (**5.9**) and yuehchukene (**5.10**, Scheme 5.2).[198,199] The cytotoxic indole-napthoquinone alkaloid murrapanine (**5.9**), which was isolated from *M. paniculata* by Wu and co-workers, may arise biosynthetically from a Diels-Alder cycloaddition between oxidized 3-prenylindole tautomer **5.11** and quinone **5.12**. Indeed, Wu demonstrated the feasibility of such a transformation in their concise synthesis of **5.9** (Scheme 5.2, top).[198]

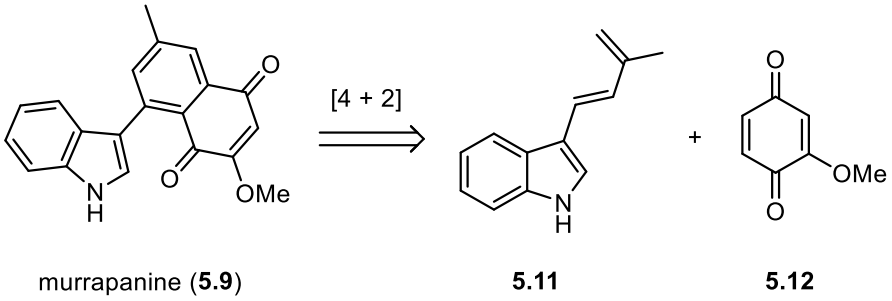

Scheme 5.2. Putative biosynthesis of murrapanine (**5.9**)

The dimeric prenyl-indole alkaloid yuehchukene (**5.10**) was isolated as a racemic mixture from *M. paniculata* by Kong and co-workers, who found that it exhibited potent anti-

implantation activity.[199] A biosynthetic proposal and concomitant biomimetic synthesis of yuehchukene (**5.10**) was advanced by Cheng and co-workers, who reasoned that **5.10** could arise from a Diels-Alder cycloaddition of **5.11** with its protonated form **5.13** to generate an intermediate **5.14** that could then undergo electrophilic addition at indole C(2) to form the cyclopentyl ring and thus furnish the natural product **5.10**.[200] In their synthesis of yuehchukene (**5.10**) Cheng *et al*. found that when **5.11** was heated in benzene containing trace amounts of trifluoroacetic acid (TFA), it underwent the desired [4+2]/cyclization cascade to deliver **5.10** in 10% yield.[200] The subsequent work of Wenkert[201,202] and Sheu[203,204] further refined and elaborated upon the biomimetic synthesis of yuehchukene (**5.10**) developed by Cheng.[200]

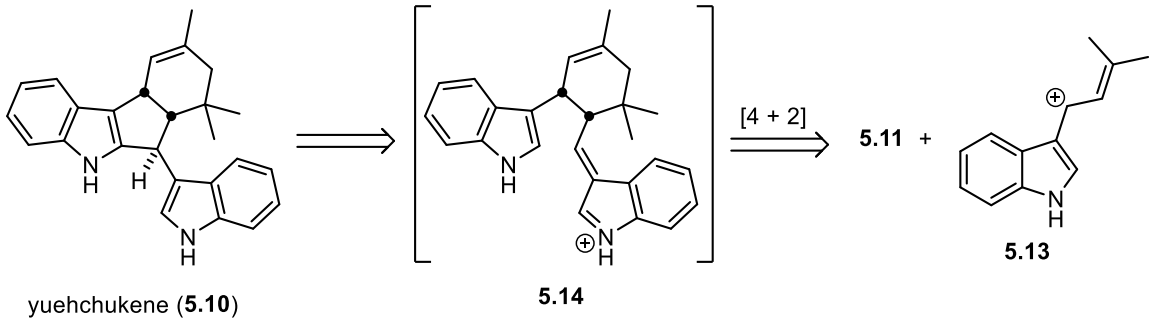

Scheme 5.3. Proposed biosynthesis of yuehchukene (**5.10**)

5.2. THE TRAUNER SYNTHESIS OF EXOTINE B

In 2018, Trauner and coworkers reported the first total synthesis of (±)-exotine B (**5.2**, Scheme 5.4).[205] The researchers initially undertook exploratory studies to investigate the feasibility of a biomimetic synthesis of **5.2** via a Diels-Alder reaction between **5.4** and gleinadiene (**5.6**, *see* Scheme 5.1). However, this approach was not successful. Their subsequent retrosynthetic analysis hinged on a late-stage Fischer indole synthesis/ring expansion sequence to convert aldehyde **5.15** to the natural product **5.2** (Scheme 5.3). They envisioned arriving at **5.15** via a Diels-Alder reaction between gleinadiene (**5.6**) and enal **5.16**, where R is a group which can be elaborated to the isobutenyl moiety of the natural product.

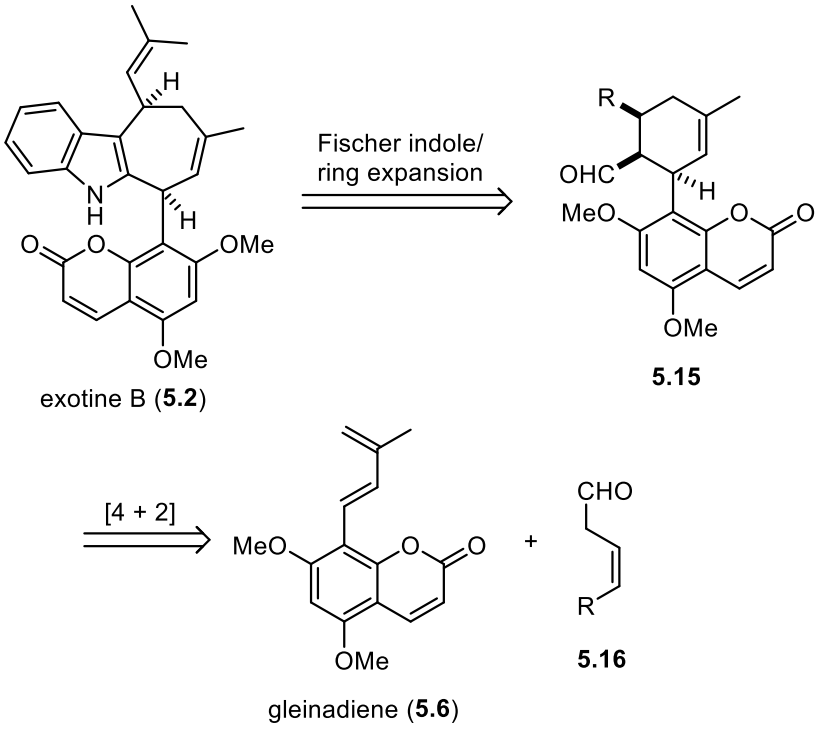

Scheme 5.4. Trauner's retrosynthetic analysis of exotine B (**5.2**)

In order to investigate the feasibility of this route, Trauner and co-workers first accessed gleinadiene (**5.6**), which had previously been prepared by Reisch and co-workers from 5-methoxy-7-hydroxycoumarin in four steps and 19% yield.[206] In the event, they found that 5,7-dimethoxycoumarin (**5.17**) readily underwent regioselective iodination with *N*-iodosuccinimide in the presence of catalytic TFA to furnish iodocoumarin **5.18** in 94% yield (Scheme 5.5).[205] Subsequent Suzuki coupling of **5.18** with boronic ester **5.19** using Buchwald's conditions delivered gleinadiene (**5.6**) in 94% yield. Thus, **5.6** was accessed in two steps and 88% overall yield, a notable improvement on the synthesis of **5.6** reported by Reisch.[206]

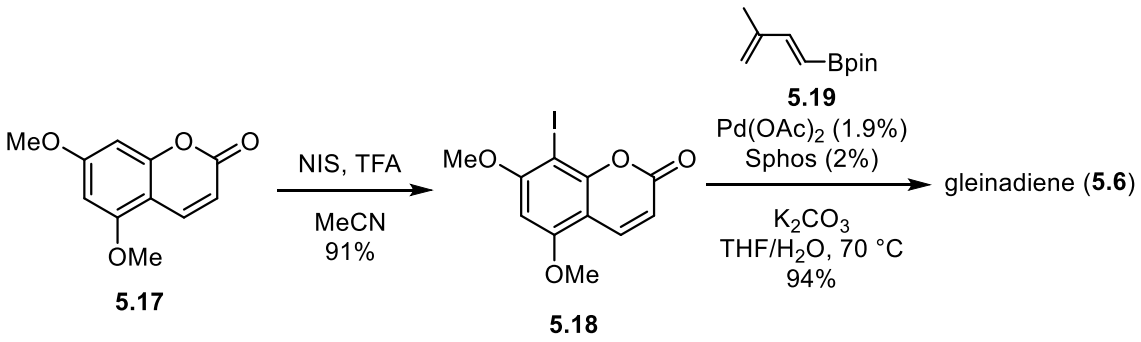

Scheme 5.5. Synthesis of gleinadiene (**5.6**)

With gleinadiene (**5.6)** in hand, Trauner and co-workers investigated its participation in Diels-Alder reactions, initially with maleic anhydride (Scheme 5.6).[205] Treatment of **5.6** with maleic anhydride and phenyldiethylamine in dichloromethane delivered **5.20** as a single diastereomer in 75% isolated yield, although the authors found that greater overall yields were obtained when they carried this product forward without purification. Regioselective ring-opening (>10:1) of the anhydride **5.20** was achieved via the use of isopropylamine in DMF, followed by methylation of the carboxylate to deliver amido-ester **5.21** in 78% yield over three steps. Unfortunately, attempts to perform a chemoselective reduction of the ester or amide groups of **5.21** met with failure, and this route was not pursued further.

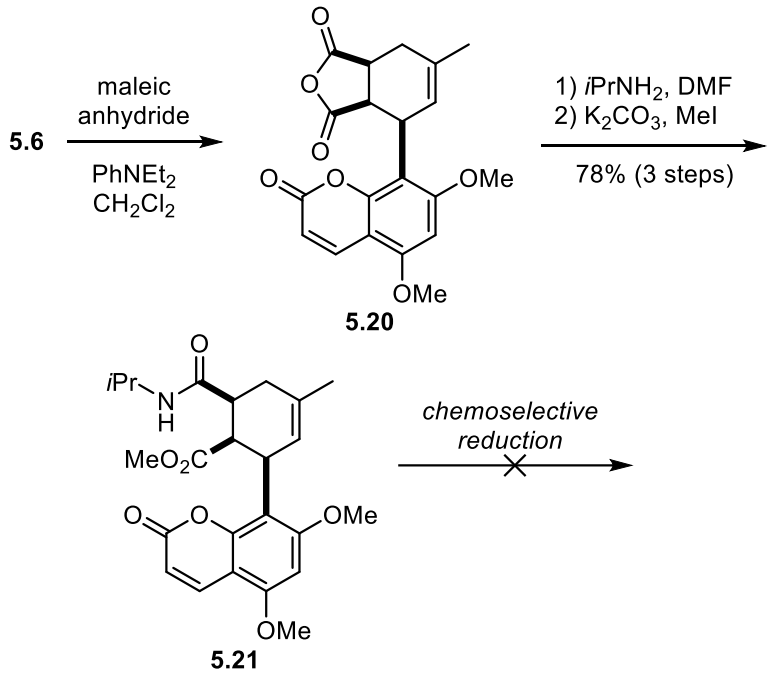

Scheme 5.6. Diels-Alder reaction of **5.6** with maleic anhydride, and attempted reduction of amido-ester **5.21**

Anxious to query the feasibility of a Fischer indole/ring expansion strategy for the synthesis of the exotine scaffold, they then pursued studies with model substrate **5.22** which they prepared via a Diels-Alder reaction of **5.6** with acrolein (Scheme 5.7).[205] They found that **5.22** underwent the desired Fischer indole/ring expansion reaction upon treatment with phenyhydrazine and trifluoroacetic acid; however, these conditions also promoted an olefin isomerization to furnish the conjugated cyclohepta[*b*]indole **5.23**. In an attempt to mask the olefin of **5.22** the authors converted it to the epoxide **5.24**. Unfortunately, **5.24** was not stable to Fischer indolization conditions, and a complex mixture of decomposition products was obtained. From these studies the authors concluded that their Fischer indolization/ring expansion strategy was not feasible, due to the high propensity for the olefin to isomerize under the acidic conditions required for this transformation.

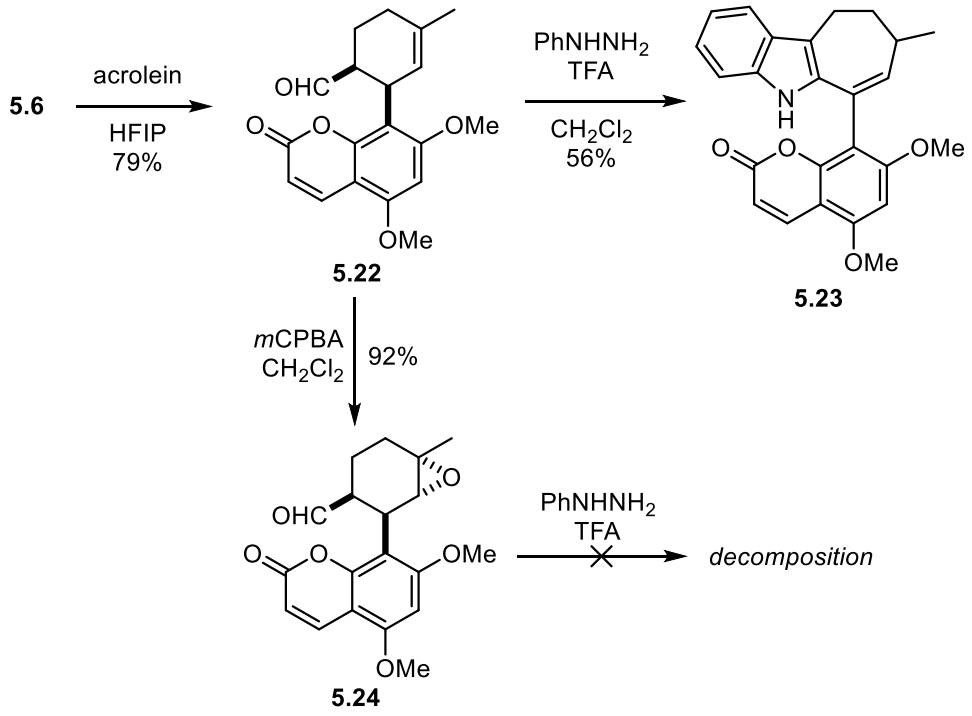

Scheme 5.7. Fischer indole syntheses with model substrate **5.22**

Thus thwarted, Trauner and co-workers turned their attention to a new strategy for the synthesis of exotine B (**5.2**), one which utilized Wu's gallium(III) Lewis acid-catalyzed three-component (3C) cyclohepta[*b*]indole synthesis (*see* Section 5.3 *for further discussion*) to construct the carbon framework of **5.2**.[207] This strategy was realized via the union of gleinadiene (**5.6**), indole (**5.25**), and thioether-aldehyde **5.26** in the presence of catalytic $Ga^{(III)}$ triflate to produce coumarin-cyclohepta[b]indole scaffold **5.27** and *epi*-**5.27** as a mixture (2:1) of diastereomers in 35% combined yield, which could be separated via recrystallization (Scheme 5.8).[205] The decision to use the masked enal **5.26** followed unsuccessful attempts to use prenal as a substrate for the 3C reaction, which would have resulted in the direct formation of their target **5.2** (*see* Chapter 6 *for further discussion*). Thus, all that remained in their synthesis of **5.2** was the conversion of the pendant thioether moiety in **5.27** to the requisite isobutenyl group. This was accomplished via a two-step sequence of oxidation and elimination to generate terminal olefin **5.28** (Scheme 5.8). Isomerization of the pentant olefin in **5.28** to exotine B (**5.2**) proved to be

challenging, due to competing isomerization of the cycloheptane olefin. After some experimentation, they found that pre-activation of Crabtree's catalyst with hydrogen gas followed by purging the system with argon and subsequent addition of **5.22** delivered a mixture (1:1) of exotine B (**5.2**) and isomer **5.23**, which were separated via high-performance liquid chromatography (HPLC) to furnish analytically pure **5.2** in 39% isolated yield.

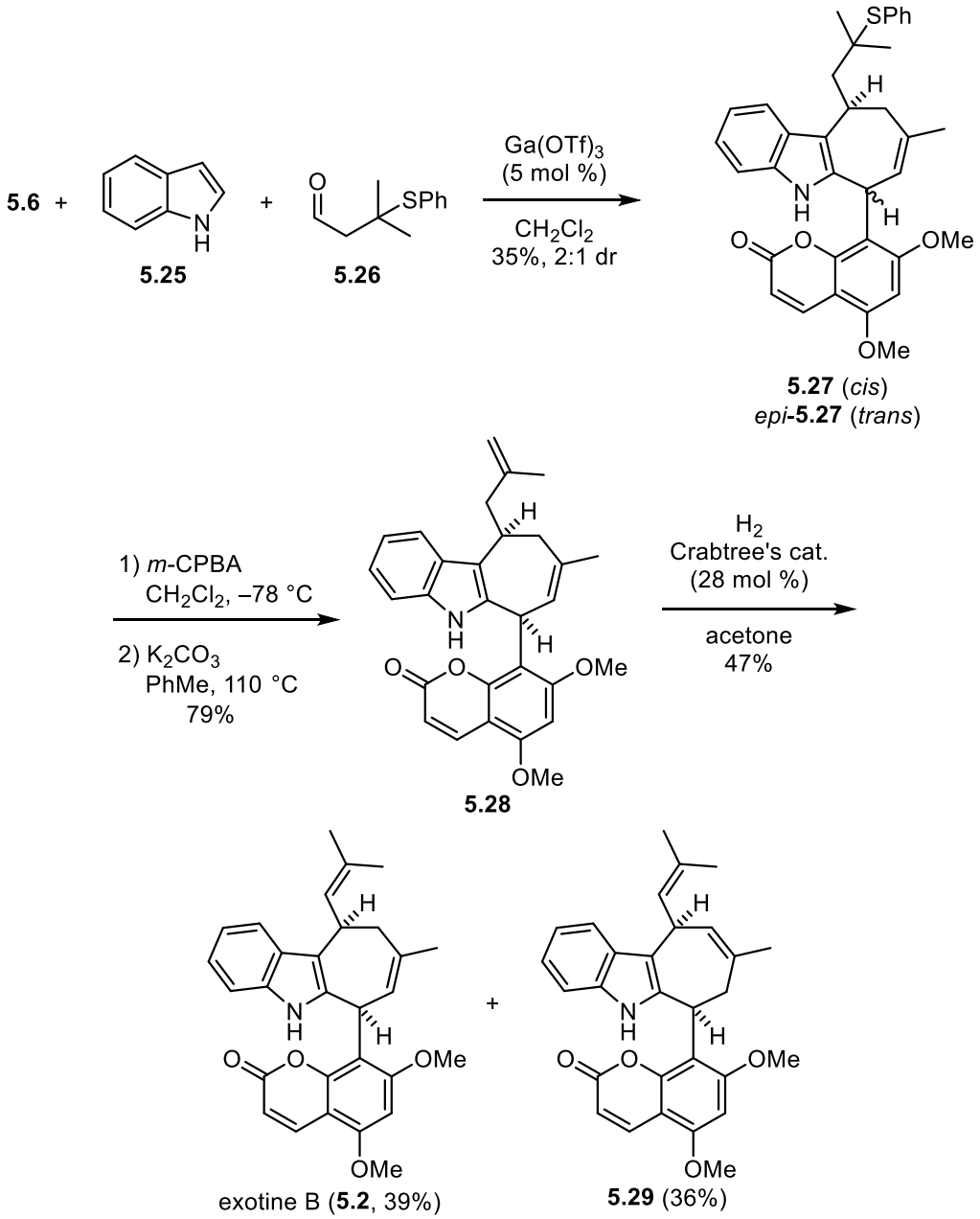

Scheme 5.8. Completion of the synthesis of exotine B (**5.2**) using Wu's $Ga^{(III)}$ cyclohepta[*b*]indole synthesis

Having thus completed their synthesis of **5.2** in six steps LLS (8 total) and 6% overall yield, Trauner and co-workers also offered an alternate biosynthetic proposal for the formation of exotines A (**5.1**) and B (**5.2**) (Scheme 5.9, *c.f.* Scheme 5.1).[205] Namely, they proposed that **5.1** and **5.2** arise from a [4 + 3] cycloaddition reaction between allylindolyl cation **5.13** and

coumarin-diene **5.5** or **5.6**. This alternate biosynthetic hypothesis is based on the proposed mechanism for the $Ga^{(III)}$ 3C cyclohepta[b]indole synthesis which, according to DFT calculations performed by Wu and co-workers, likely proceeds via a concerted [4 + 3] cycloaddition reaction (*see* Section 5.3).[207]

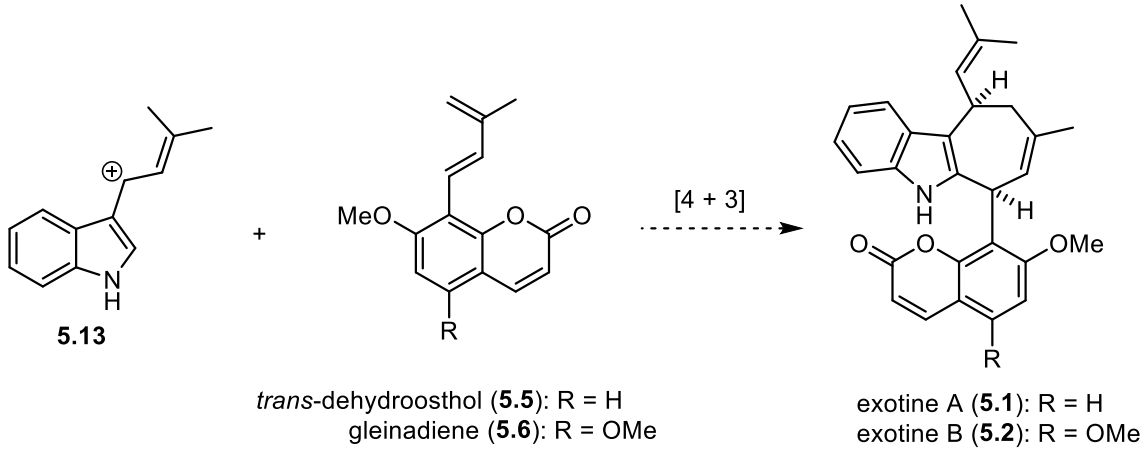

Scheme 5.9. Alternate biosynthetic proposal advanced by Trauner

5.3. [4 + 3] CYCLOADDITION REACTIONS FOR THE SYNTHESIS OF CYCLOHEPTA[*b*]INDOLES

The cyclohepta[*b*]indole ring system (Figure 5.2, in red) can be found in numerous natural products (Figure 5.2a) and pharmaceutical research compounds (Figure 5.2b) that display potent and diverse bioactivity.[185] For instance, the natural product actinophyllic acid (**5.29**), isolated from *Alstonia actinophylla*, is a potent carboxypeptidase U (CPU) inhibitor which has been the subject of total synthesis by the Martin lab (*see* Section 5.3.2) as well as the Overman lab.[208,209] The bis-indole pigment arcyriacyanin A (**5.30**), isolated from *Arcyria nutans*, is a protein kinase C and protein tyrosine kinase inhibitor and has been prepared twice via total synthesis.[185] Ambiguine D isonitrile (**5.31**) is a representative member of the large ambiguine (ambiguines A–Q) family of natural products, many of which (ambiguines D–G and I–Q) contain a cyclohepta[b]indole ring system.[183,208] The ambiguines are isolated from the algae *Fischerella ambigua* and display diverse antifungal and antimicrobial activity, and in early 2019

the first total synthesis of an ambiguine alkaloid (ambiguine P) was reported by the Sarpong group.[210,211] Ervatamine (**5.32**) is the prototypical member of another large family of alkaloids known as the ervitsines and ervatamines, which contain many members having a cyloheptaindole skeleton.[185] Ervatamine (**5.32**) itself is a sodium channel blocker, and other members of this family display anti-cholinergic and anti-inflammatory activity; several ervatamines have been prepared via total synthesis by the Bosch lab.[185,212–214] Turning from natural products to pharmaceutical ligands, SIRT1-inhibitor IV (**5.33**) is a cyclohepta[b]indole-carboxamide sirtuin histone deacetylase (HDAC) SIRT1 inhibitor developed by Napper and co-workers.[215] HDAC inhibitors are a relatively new class of drugs which have shown great promise as chemotherapeutic agents for the treatment of various forms of cancer.[216] Finally, the homomorphinan-cyclohepta[*b*]indole **5.34** is an opioid receptor ligand developed by Fujii and co-workers that displays potent and selective inhibition of the δ-opioid receptor.[217]

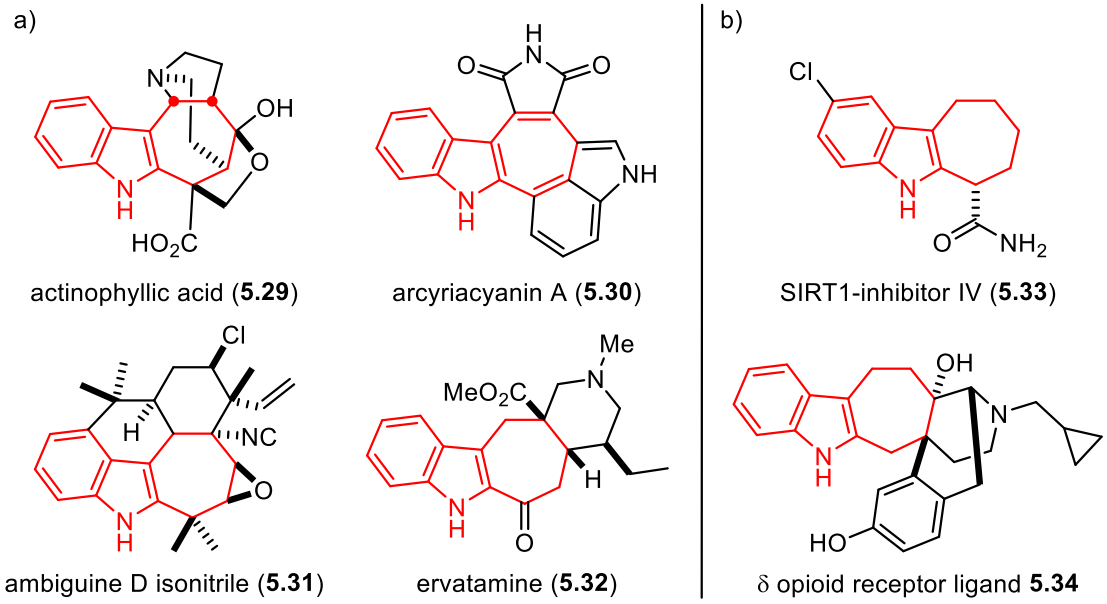

Figure 5.2. Representative natural products (a) and pharmaceutical compounds (b) with a cyclohepta[*b*]indole motif (in red)

Owing their interesting structures and biological activities, many methods have been developed for the synthesis of cyclohepta[*b*]indole derivatives. Classical approaches to cyclohepta[b]indoles have often utilized the venerable Fischer indole synthesis; however, this

approach has the limitation of not working well for cyclohepta[b]indoles with unsymmetrical functionalization of the cycloheptane ring, because regioisomeric product mixtures are often obtained.[185] Accordingly, there have been many recent reports in the literature of methods for preparing the cyclohepta[b]indole ring system, several of which utilize (formal) [4 + 3] cycloaddition reactions (Figure 5.3, *see* ref. 183 *for additional examples of recent cyclohepta[b]indole synthesis methods*).[185] In 2013 Tang and coworkers developed a one-pot platinum-catalyzed formal [4 + 3] cycloaddition for the synthesis of bridged cyclohepta[*b*]indoles **5.37** from alkynyl anilines **5.35** and siloxy-dienes **5.36** via the formation of a vinyl Fisher carbene (Figure 5.3a). A nearly identical method was published by the Iwasawa lab in the same year.[218,219] Li and coworkers developed a multi-step, one-pot hydroamination/cycloaddition cascade sequence in which *N*-tosylaniline **5.38** undergoes a silver triflate-promoted hydroamination to form **5.39**, which is subsequently treated with zinc chloride and a diene **5.40** to form disubstituted cyclohepta[*b*]indoles with the general structure **5.41** (Figure 5.3b).[220] Finally, Hsung and coworkers developed a multi-step sequence for the synthesis of dihydrofuran-bridged cyclohepta[*b*]indoles **5.44** via a putative [4 + 3] cycloaddition between furan and an oxyallyl cation **5.43** generated from allenamide **5.42** (Figure 5.3c).[221] The resultant cycloadduct **5.44** then underwent an intramolecular Grignard addition/dehydration sequence to form the indole moiety of **5.45** (Figure 5.3c).[221] The use of oxyallyl cations such as **5.43** generated from allenamides—pioneered by Hsung in earlier studies—as 3-pi components in [4 + 3] cycloaddition reactions is one of the few examples of nitrogen-stabilized allyl cations being used in such reactions, and provides important precedent for the development of Wu's cyclohepta[*b*]indole methodology (*see* Section 5.3.1).[222–224] Clearly, the use of (formal) [4 + 3] cycloaddition reactions is a powerful strategy for the synthesis of substituted cyclohepta[*b*]indoles, as demonstrated by the examples in Figure 5.3 as well as by the $Ga^{(III)}$ methodology developed by Wu, which will be discussed in detail in the following section.

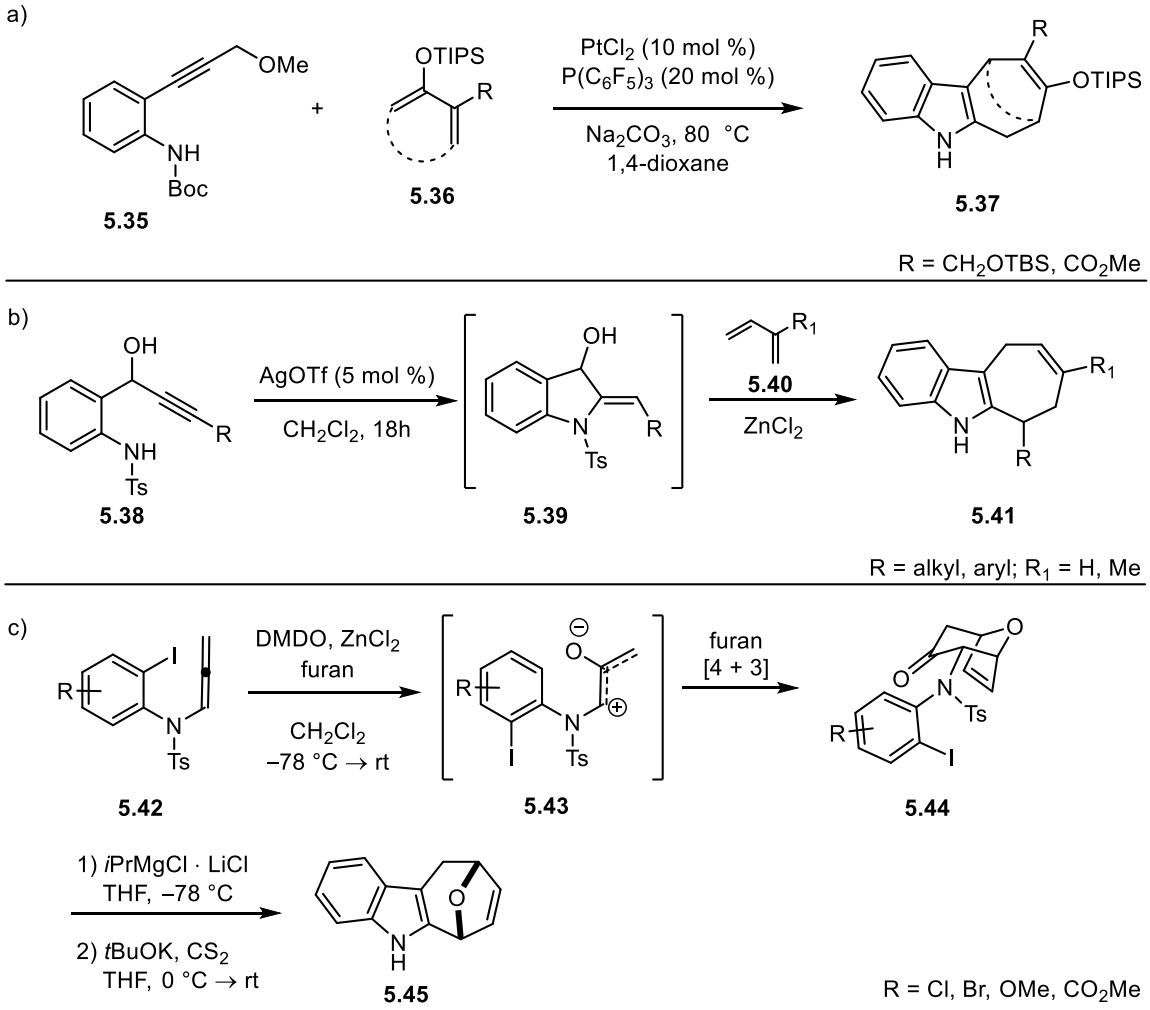

Figure 5.3. Methods for synthesizing cylcohepta[*b*]indoles via [4 + 3] cycloaddition reactions: a) vinyl Fischer carbene approach developed by Tang.[218] b) hydroamination approach developed by Li.[220] c) allenamide approach developed by Hsung.[221]

5.3.1. Wu's Gallium(III)-Catalyzed Three-Component [4 + 3] Cyclohepta[*b*]indole Synthesis

In 2012, the Wu group published a landmark study on the use of a [4 + 3] cycloaddition reaction for the synthesis of cyclohepta[*b*]indoles. This was the first reported instance of a [4 + 3] reaction being used to prepare the cyclohepta[*b*]indole skeleton, a strategy which was subsequently utilized by numerous groups (*see preceding section*).[207] The general features of the reaction can be seen in Scheme 5.10: An indole **5.46**, and a ketone or aldehyde **5.47** are condensed in the presence of a diene **5.48** and an acid catalyst, such as a $Ga^{(III)}$ Lewis acid to

form an indolyl cation **5.49**, which subsequently undergoes [4 + 3] cycloaddition with diene **5.48** to generate the substituted cycloheptaindole scaffold **5.50**.

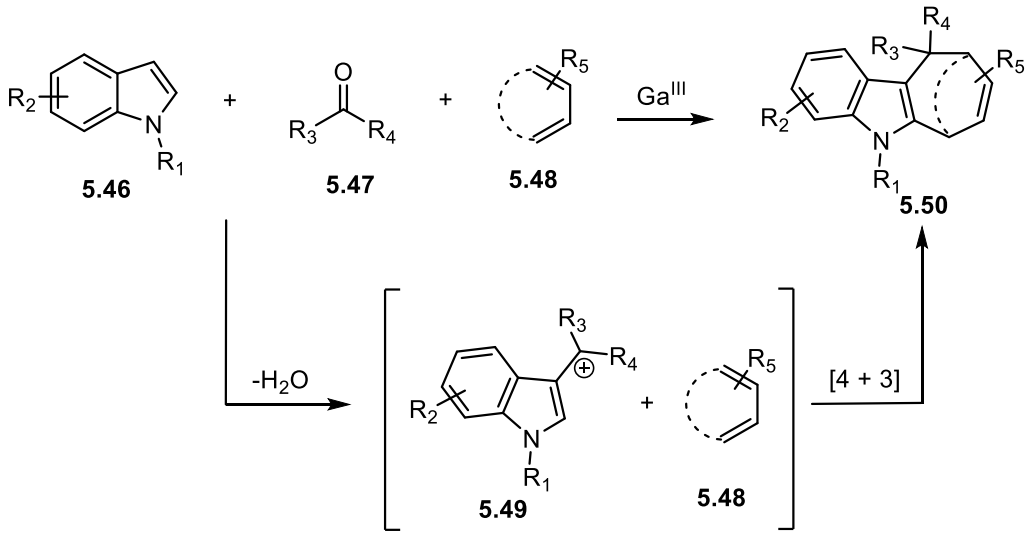

Scheme 5.10. General features of Wu's three-component [4 + 3] cyclohepta[*b*]indole synthesis

In addition to the precedent provided by the work of Hsung and co-workers (*see* Figure 5.3c), a key inspiration for Wu's methodology comes from the work of Winne and Pattenden, who discovered in their approach to the diterpene natural product rameswaralide an acid-promoted intramolecular [4 + 3] cycloaddition of furan **5.50** to generate tetracyclic compound **5.51** as a single diastereomer in quantitative yield (Equation 5.1).[225] Winne and co-workers went on to develop an intermolecular variant of this reaction, in which 2-furyl alcohols **5.53** are reacted with dienic components **5.54** in the presence of titanium(IV)chloride ($TiCl_4$) to generate cycloheptyl-furans with the general structure **5.55** (Equation 5.2).[226] The reaction is thought to proceed via the initial ionization of the 2-furyl alcohol to generate a stabilized 2-oxyallyl cation, which subsequently undergoes a [4 + 3] cycloaddition with the pendant vinyl butanolide group, based on DFT calculations performed by Winne and co-workers.[226] Their calculations indicate that both stepwise and concerted [4 + 3] processes are viable, but the stepwise [4 + 3] pathway was consistently found to be more energetically favorable pathway.

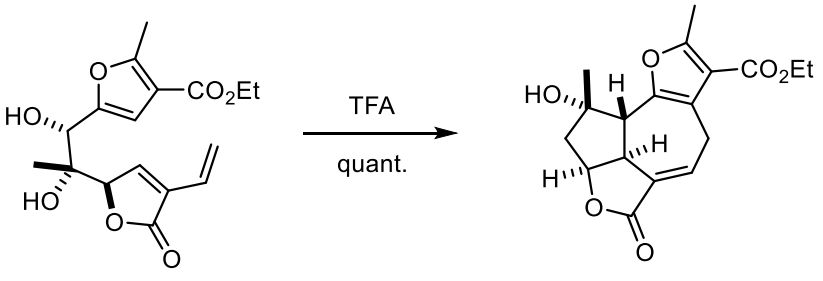

5.51 **5.52** (5.1)

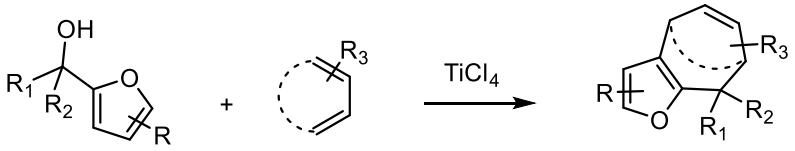

5.53 **5.54** **5.55** (5.2)

To identify conditions for their three-component [4 + 3] cycloaddition Wu and co-workers screened a variety of Lewis and Brønsted acids with model substrates **5.56, 5.57,** and **5.58**, selected examples of which are shown in Table 5.1. They found that the gallium(III) salts gallium(III)bromide ($GaBr_3$) and gallium(III)triflate ($Ga(OTf)_3$) were excellent promoters of the reaction, delivering cyclohepta[*b*]indole **5.59** in 94% and 91% yield, respectively (Table 5.1, entries 1 and 2). Another group 13 Lewis acid, indium(III)bromide ($InBr_3$) likewise catalyzed the reaction, delivering **5.59** in 92% yield; however, the use of indium(III)triflate resulted in only 54% yield of **5.59**, which the authors note was accompanied by substantial quantities of degradation products (Table 5.1, entries 3 and 4). Gallium(III)chloride and indium(III)chloride were not effective catalysts for this process, delivering only the addition product of **5.56** and **5.57** with no trace of cyclohepta[*b*]indole **5.59**. They also briefly explored the use of Brønsted acids *p*-toluenesulfonic acid (*p*-TsOH) and trifluoromethanesulfonic acid (TfOH) and found that *p*-TsOH resulted in the slow formation of **5.59,** delivering only 52% yield after two hours, while TfOH gave **5.59** in 83% yield after 2 hours (Table 5.1, entries 5 and 6). Under all of the conditions tested, **5.59** and its *trans*- isomer were formed as a mixture (3:1–5:1) of diastereomers. From these studies, the authors concluded that the reaction was most effectively

promoted by the $Ga^{(III)}$ salts in Entries 1 and 2 (Table 5.1), and so they embarked on an exploration of the substrate scope of their newly developed reaction with these catalysts.

Table 5.1. Screening of acid catalysts for the synthesis of cyclohepta[*b*]indole **5.59**

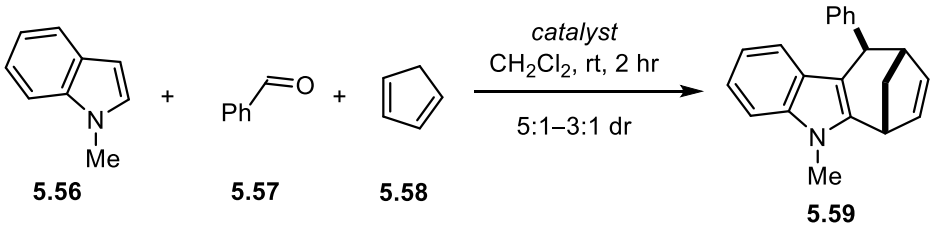

5.56 **5.57** **5.58** **5.59**

Entry	Catalyst (10 mol %)	Yield
1	$GaBr_3$	94%
2	$Ga(OTf)_3$	91%
3	$InBr_3$	92%
4	$In(OTf)_3$	54%
5	*p*-TsOH	52%
6	TfOH	83%

The incorporation of electron-donating and electron-withdrawing indolic substituents in substrate **5.60** was found to be well-tolerated in its reaction with acetone (**5.61**) and cyclopentadiene (**5.62**) to deliver 5'-substituted cyclohepta[*b*]indoles **5.63** in 73–87% yield (Figure 5.4a). The scope of the carbonyl component was also also investigated, and it was found that (hetero)aromatic and aliphatic aldehydes **5.64** participated in the reaction with indole (**5.64**) and **5.62** to furnish **5.66** as a mixture of diastereomers in 75–91% yield (Figure 5.4b). The diastereoselectivity of the reaction was highly dependent on the nature of the aldehyde component **5.64**, with electron-rich *p*-methoxybenzyl, 2-furyl, and 2-thiophenyl groups leading to ≥10:1 selectivity for the *syn* product **5.66**, while an electron-deficient *p*-trifluoromethylbenzyl substituent resulted in only 2:1 *syn* selectivity; an ethyl substituent delivered a mixture (1:1) of **5.66** and its *anti*- diastereomer (Figure 5.4b). Cyclic ketones such as cyclobutanone,

cyclopentanone, and cyclohexanone were also found to participate in the reaction with indole (**5.65**) and cyclopentadiene (**5.62**), delivering their respective products in 81–91% yield (not shown).

They also investigated various dienic components and found that, in general, the yield of the reaction suffered when dienes other than cyclopentadiene (**5.62**) were used, and the use of the more active $Ga(OTf)_3$ catalyst at a higher catalyst loading (20 mol %) was necessary to achieve satisfactory conversion. For instance, hexadiene **5.67a** reacted with *N*-methylindole (**5.56**) and benzaldehyde (**5.57**) to deliver **5.68a** in only 54% yield, but with a high degree of diastereoselectivity (> 10:1 dr) for the all-*syn* isomer. The use of isoprene (**5.67b**) resulted in formation **5.68b** in only 48% yield; however, they did not observe any regioisomeric products, suggesting that a high degree of regioselectivity can be expected when unsymmetrical dienes are used. Finally, the authors noted that the use of more electron-rich dienic components such as Danishefsky's diene or heteroaromatic dienes such as pyrrole, furan, or thiophene only resulted in the formation of addition products with the general structure **5.69**, although no experimental details were provided (Figure 5.4d).

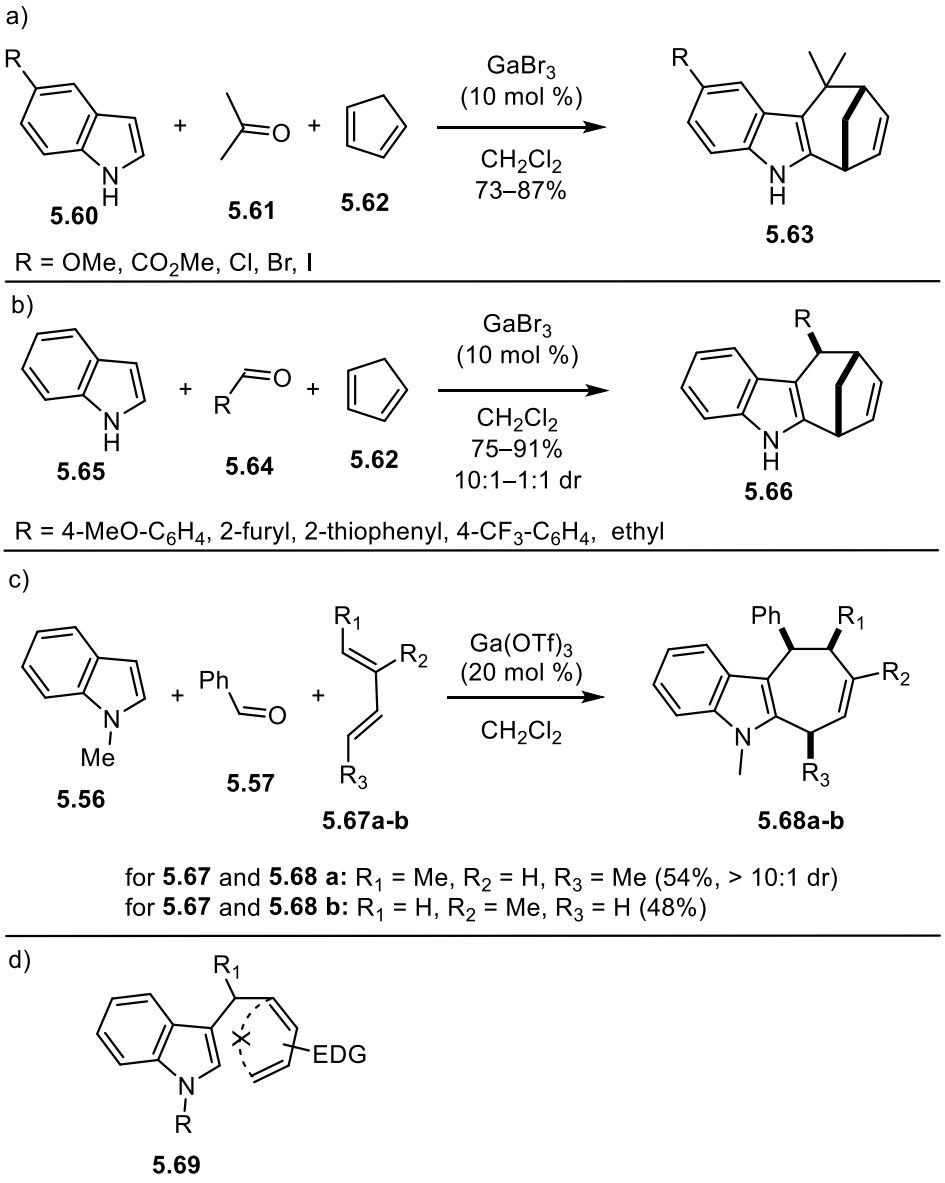

Figure 5.4. Exploration of the substrate scope of Wu's three-component [4 + 3] cycloaddition reaction. a) 5'-substituted indole substrates **5.60.** b) aldehyde substrates **5.64.** c) diene substrates **5.67a-b.** d) addition product **5.69** formed when electron-rich dienes were used

Finally, Wu and co-workers used DFT calculations to probe the mechanism of their three-component cyclohepta[*b*]indole synthesis.[207] They found that the lowest-energy pathway for the reaction of indole (**5.65**), dimethyl ketal **5.70**, and cyclopentadiene (**5.62**) is a stepwise [4 + 3] pathway, in which indolyl cation **5.71** undergoes nucleophilic addition with **5.62** to form

allyl cation intermediate **5.72** which subsequently undergoes ring closure at the C(2) position of indole, followed by rearomatization to furnish the cyclohepta[*b*]indole product **5.73**. Their calculations suggest that the formation of **5.73** via a concerted [4 + 3] cycloaddition pathway is disfavored, in agreement with the calculations performed by Winne and co-workers (*vide supra*).[226] Their calculations also suggest that the reaction pathway in which **5.73** is formed via a concerted or stepwise [4 + 2] cycloaddition followed by a 1,2-alkyl migration is disfavored, although results obtained in our studies toward the total synthesis of exotines A and B will call this suggestion into question (*see* Section 6.3).

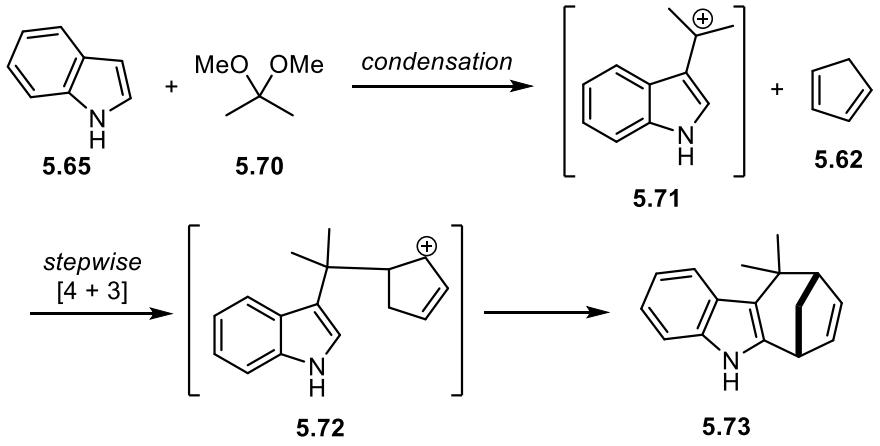

Scheme 5.11. Proposed mechanism for the formation of cyclohepta[*b*]indole **5.73** based on DFT calculations performed by Wu and co-workers

5.3.2. The Martin Lab Synthesis of Actinophyllic Acid & Related Work

In 2013, the Martin lab reported the total synthesis of the cyclohepta[*b*]indole natural product (±)-actinophyllic acid (**5.29**, Scheme 5.11; *see also* Figure 5.2 *and attendant discussion*).[209,227] Their retrosynthetic analysis (Scheme 5.12) hinged on the preparation of functionalized cyclohepta[*b*]indole **5.74** via a formal [4 + 3] cycloaddition reaction between 2-indolyl cation precursor **5.76** and dihydroazepine derivative **5.77**.

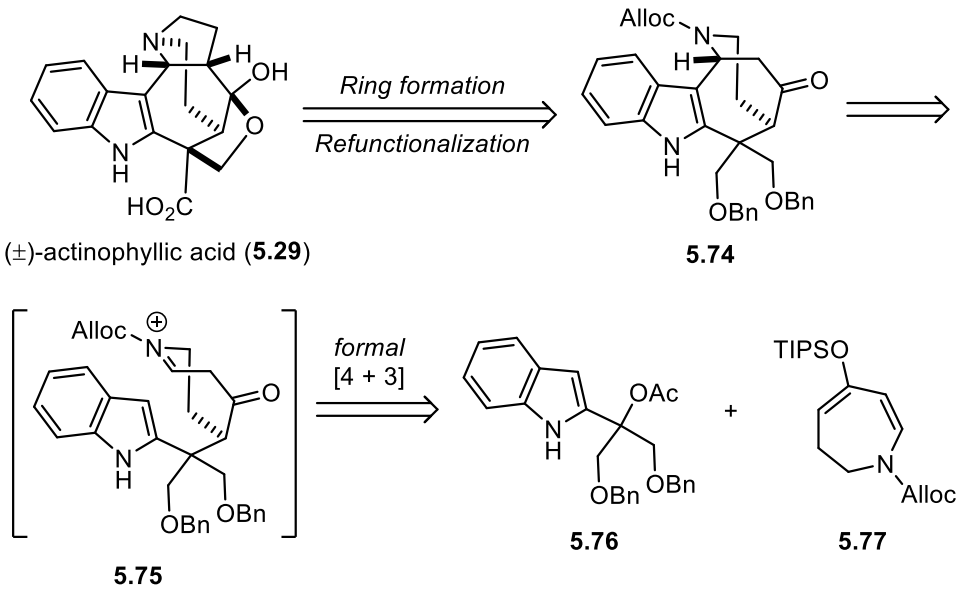

Scheme 5.12. The Martin lab retrosynthesis of (±)-actinophyllic acid (**5.29**)

The interception of β-indolyl cations with π-nucleophiles was previously investigated by the Martin lab for the formal synthesis of several members of the *N*-methylwelwitindolinone family of natural products (**5.78**, Figure 5.12a).[228,229] For instance, when the unstable indole-3-carbinol **5.79**, which was generated from **5.80** via addition of methyl Grignard, was treated with silyl ketene acetal **5.81** in the presence of trimethylsilyl trifluoromethanesulfonate (TMSOTf), the substitution product **5.82** was formed and subsequently elaborated to **5.78** (Figure 5.12a). This strategy was also found to be applicable generally for the synthesis of β-heteroaryl propionates **5.83** from heteroaromatic carbinols with the general structure **5.84** and silyl ketene acetal **5.85** (Figure 5.12b).[230]

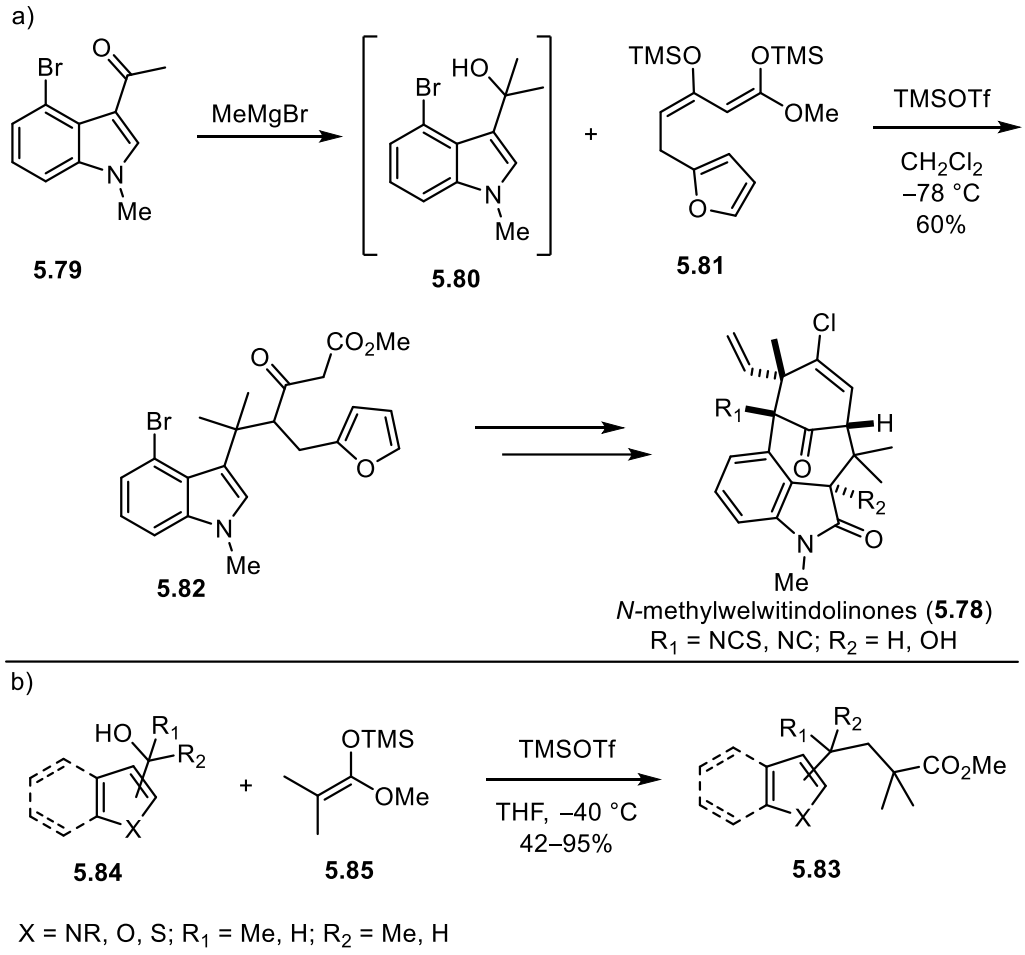

Figure 5.5. Interception of β-aryl cations with π-nucleophiles. a) formal synthesis of *N*-methylwelwitindolinones (**5.78**). b) synthesis of β-heteroaryl propionates **5.83**

The details of Martin's synthesis of (±)-actinophyllic acid (**5.29**) is shown in Scheme 5.13.[209,227] Preparation of cyclization precursor **5.76** was accomplished via a one-pot sequence in which indole (**5.65**) was converted to indolyl acetate **5.76** in 85% yield via reaction of a C(2)-lithiated indole *N*-carboxylate dianion with ketone **5.86** followed by acetylation of the resultant alkoxide. The dienic substrate **5.77** was prepared from dihydroazepinone **5.87** via a straightforward sequence of *N*-alloc protection and silyl enol ether formation. The cascade ionization/formal [4 + 3] cycloaddition reaction of **5.76** and **5.77** proceeded in the presence of TMSOTf and 2,6-di-*tert*-butylpyridine to deliver cyclohepta[*b*]indole **5.74** in 92% yield. The indole nitrogen atom of **5.74** was then Boc-protected to mitigate gramine-type fragmentation,

and *N*-alloc deprotection then furnished amine **5.88** in 76% yield. Construction of the pyrrolidine ring was accomplished via reductive alkylation of **5.88** with chloroacetaldehyde, followed by treatment with sodium *tert*-butoxide to generate **5.89** in 83% yield. Indole Boc-deprotection and hydrogenolysis of the O-benzyl groups generated an intermediate diol that spontaneously cyclized to form tetrahydrofuranyl diol **5.90**. Oxidation of the pendant hydoxymethylene group to the requisite carboxylic acid proved challenging, but sequential treatment with excess IBX and *N*-hydroxysuccinimide, followed by saponification of the resultant succinimidate ester delivered (±)-actinophyllic acid (**5.29**) in 31% yield as its hydrochloride salt. The remarkable efficiency with which (±)-actinophyllic acid (**5.29**) was prepared, in only 10 steps from known materials, is a testament to the utility of (formal) [4 + 3] cycloaddition reactions for the synthesis of cyclohepta[*b*]indole natural products, which will be further demonstrated in our synthesis of exotines A (**5.1**) and B (**5.2**, *see* Chapter 6).

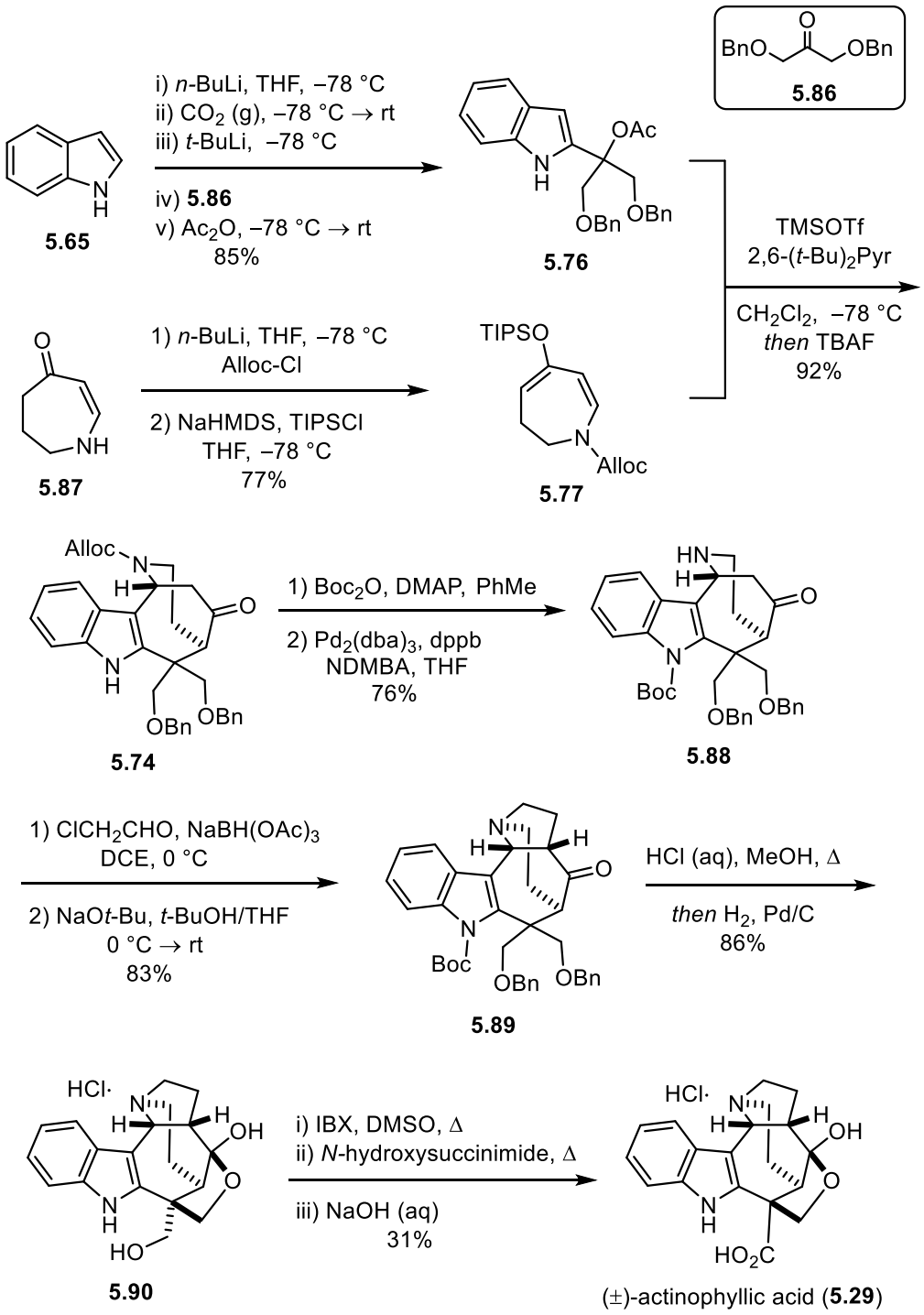

Scheme 5.13. The Martin lab synthesis of (±)-actinophyllic acid (**5.29**)

Chapter 6. The Total Synthesis of Exotines A and B

Owing to their unique coumarin-cyclohepta[*b*]indole skeletons and intriguing biological activity (*see* Section 5.1), the Martin lab sought to develop a concise synthesis of exotines A (**6.1**) and B (**6.2**, Scheme 6.1).[184]

6.1. First-Generation Synthetic Strategy

In our initial strategy for the preparation of **6.1** and **6.2**, we envisioned introducing the requisite methoxycoumarin moiety via palladium-catalyzed cross-coupling of **6.3** with the known halo-coumarins **6.4** (Scheme 6.1).[206,231] An advantage of this approach would be that the nature of the functional groups participating in the cross coupling (R_1 on **6.3**, X on **6.4**) could be varied to optimally achieve the desired transformation and *syn*-stereochemical outcome.[232] For instance, **6.4** (X = Br, I) could be converted to an organometallic species and coupled with **6.3** when it bears a suitable R_1 group (*e.g.* R_1 = OAc) for the generation of a π-allylpalladium species.[232,233] Alternately, if $R_1 = B(OR)_2$, **6.3** could undergo Suzuki-type coupling with **6.4** (X = Br, I).[234] We envisioned using Wu's $Ga^{(III)}$ [4 + 3] cycloaddition methodology (*see* Section 5.3.1) or an acid-catalyzed variant thereof to prepare **6.3** from indole (**6.6**), prenal (**6.7**) and diene **6.8** in a three-component, one-pot fashion.[207] While the precedent in Wu's work suggested that we might expect the isobutenyl and R_1 groups in **6.3** to display a *syn*-steroechemical relationship (*see* **5.68a**, Figure 5.4c), we were unsure how relevant this precedent would be to our proposed reaction with prenal (**6.7**) and diene **6.8**, which are notably different from the substrates used by Wu and co-workers.[207] Here it is important to note that Trauner and co-workers did not publish their synthesis of exotine B (**6.2**, *see* Section 5.2) until after we had already prepared exotine A (**2.1**, *vide infra*), so our decision to utilize a variant of Wu's methodology in our synthesis of the exotines was not in any way informed by the work of Trauner, but rather was inspired by Wu's method.[205]

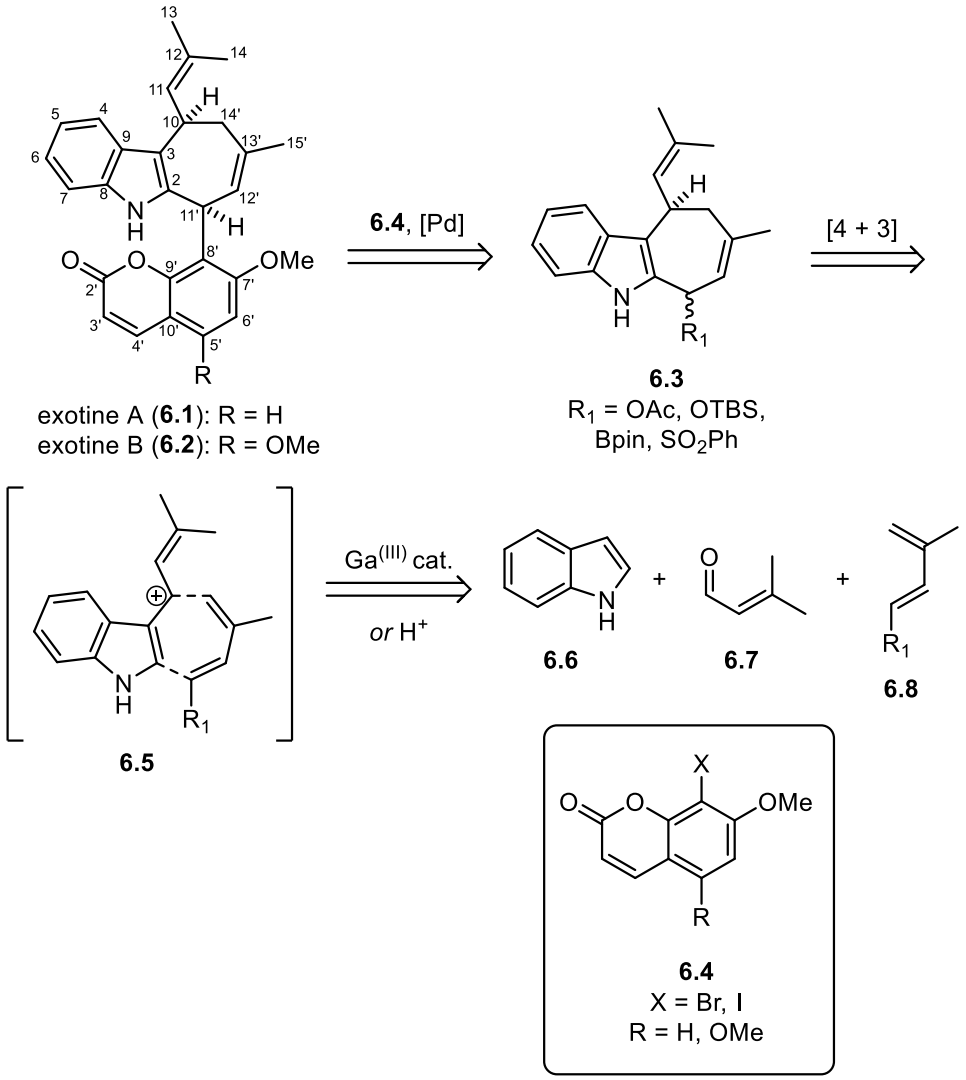

Scheme 6.1. First-generation retrosynthetic analysis of exotines A (**6.1**) and B (**6.2**, Jiang *et al.* numbering system)[184]

Prior to our investigation of the synthetic sequence depicted in Scheme 6.1, we performed two brief model studies. First, we invesigated the viability of prenal (**6.7**) as a cyclization substrate in a three-component reaction with indole (**6.6**) and cyclopentadiene (**6.9**, Equation 6.1). We found that in the presence of catalytic gallium(III)triflate ($Ga(OTf)_3$), the reactants were converted to cyclohepta[*b*]indole **6.10** in 41% yield and 10:1 dr. The stereochemistry **6.10** was not determined conclusively, but it appears that the dominant diastereomer of **6.10** displays a *syn*- stereochemical relationship between the isobutenyl group

and the bridging methylene group based on comparison of its ^{1}H NMR spectra with the products prepared by Wu and co-workers.[207] We also investigated the reaction of indole (**6.6**) and prenal (**6.7**) with isoprene (**6.11**) and found that while it appears the desired cyclohepta[*b*]indole **6.12** was formed, again based on comparison of the ^{1}H NMR spectrum with an analogous compound prepared by Wu, it readily degraded under ambient conditions to produce a complex mixture.

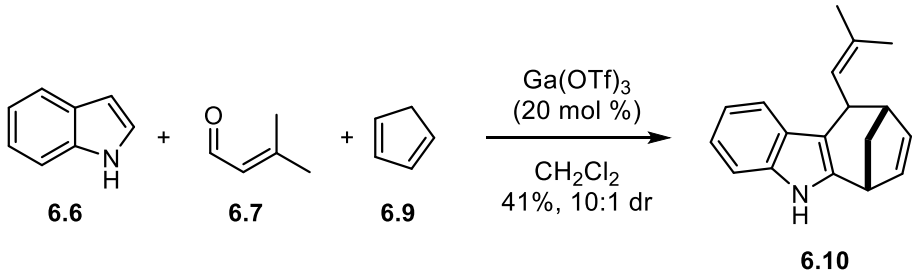

(6.1)

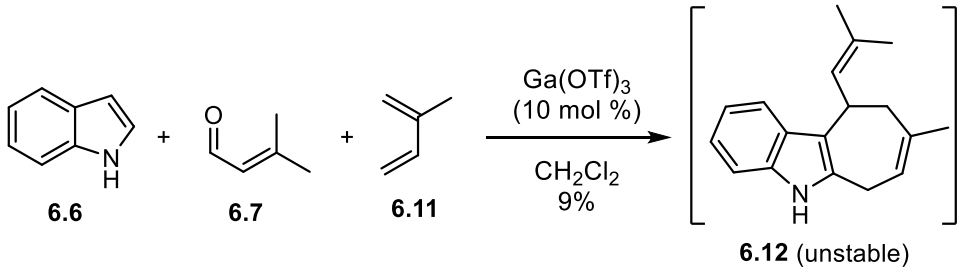

(6.2)

Having established the viability of prenal (**6.7**) as a cyclization substrate, we turned our attention to the synthesis and analysis of the dienic component **6.8** (*see* Scheme 6.1). We first investigated reactions with the acetoxy-diene **6.13**, which was prepared from prenal (**6.7**) according to a literature procedure.[235] In the event, treatment of **6.13** with indole (**6.6**), prenal (**6.7**), and gallium(III)triflate in several different aprotic solvents resulted in the formation of a complex mixture from which no trace of the desired product **6.14** was observed (Equation 6.3). We did, however, observe and partially isolate a compound to which we have tentatively assigned the structure of triene **6.15** (8–24% yield) , which presumably arises from **6.14** via the elimination of acetic acid, as well as indole-indolenine addition product **6.16** (5–20% yield). We also found that the presence of of the hindered base 2,6-di-*tert*-butyl pyridine completely shut down the reaction, delivering only returned starting material. We were encouraged by the

formation of **6.14** in these studies, because it demonstrated that the three-component cyclization was viable with dienes bearing weakly electron-donating functionalities such as the acetoxy group in **6.13**. We had been concerned about the viability of using dienes with electron-donating groups, owing to the observation of Wu and co-workers that electron-rich dienes failed to cyclize (*see* Section 5.3.1).[207] However, these studies also made clear to us that **6.13** was not a good choice for a cyclization substrate, as it appears that the acetoxy group in the product **6.14** is, unsurprisingly, labile under the reaction conditions.

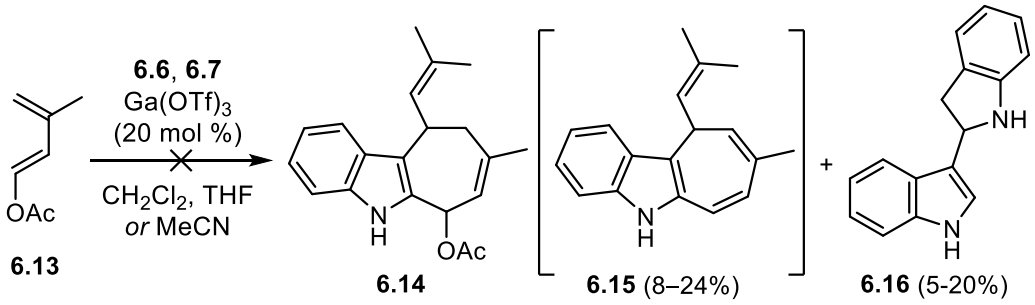

(6.2)

Boronyl and sulfonyl dienes **6.17** and **6.18**, each of which was prepared according to literature procedures, [236–238] were also investigated as cyclization substrates (Equation 6.3). Subjecting **6.17** to our standard reaction conditions with **6.6** and **6.7** at 0 ˚C or room temperature resulted in a complex mixture from which no trace of **6.19** or its elimination product was observed; however, we did observe isoprenyl-indole byproduct **6.20**, as well as the indole-indoline byproduct **6.16** (*see* Equation 6.2), returned starting material prenal (**6.7**) and trace quantities of **6.17**. Reactions of sulfonyl diene **6.18** with **6.6** and **6.7** likewise failed to produce the desired product **6.21**, delivering only returned **6.7** and **6.18** and uncharacterized side products (Equation 6.3). The absence of any signal corresponding to a cyclization product in reactions involving **6.17** or **6.18**, as well as the fact that in both cases the dienes were not completely consumed during the course of their reactions with **6.6** and **6.7** suggests that **6.17** and **6.18** are too unreactive to participate in the cyclization, perhaps due to the electron-withdrawing nature of their boronyl and sulfonyl substituents.[239]

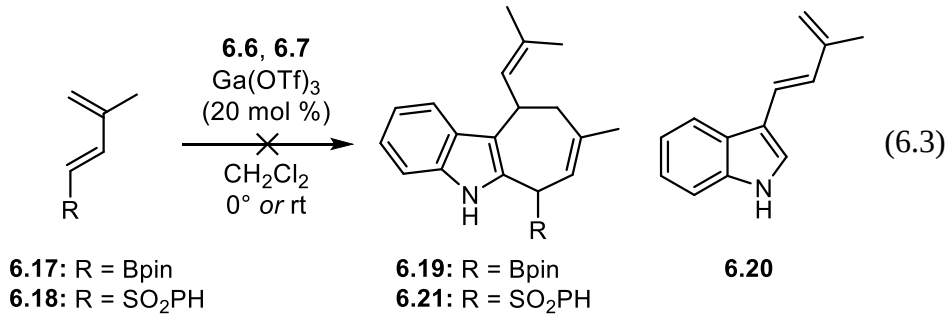

(6.3)

6.17: R = Bpin
6.18: R = SO_2PH

6.19: R = Bpin
6.21: R = SO_2PH

6.20

Finally, we investigated the use of siloxy-dienes as cyclization substrates starting with *tert*-butyldimethylsiloxy (OTBS) diene **6.22**, which was prepared according to literature procedure.[235] Although no trace of product **6.23** was observed when the reaction of **6.22** with **6.6** and **6.7** was performed at room temperature, trace quantities of a compound with an *m/z* corresponding to **6.23** (382.3, $m + H^+$) were observed in the LCMS spectra when the reaction was carried out at 0 ˚C, as well as the *m/z* of cyclization-elimination product **6.15** (250.2, $m + H^+$) (*see* Equation 6.2). However, the presence of a trace of the *m/z* corresponding to **6.23** could also be the uncyclized isomer **6.24**, which is likely present in the reaction mixture. Indeed, we were able to partially isolate a compound that appears to be protonolysis product of **6.24**, the uncyclized enal **6.25**. Mixed oligomeric species in which two or more units of the diene have been incorporated into a cyclized or uncyclized product such as **6.26** were also observed, and **6.26** was partially isolated in 12% yield. The apparent Mukaiyama aldol product **6.27** was also isolated in 5% yield, and higher-order oligomers of this type were also observed in the LCMS spectra of the mixture.

Collectively, these results indicate that **6.22** can participate in the three-component cyclization to form **6.23**, but, just as with acetoxy-diene **6.13** and its cyclization product **6.14**, the -OTBS moiety of the product is not stable to the reaction conditions and either undergoes elimination to form triene **6.15** or substitution with an additional unit of diene **6.22** to form species such as the cyclic form **6.26**. The use of triisopropylsiloxy (OTIPS) diene **6.28** gave similar results, delivering a complex mixture of products from which a trace quantities of a

compound with the *m/z* (424.3, *m* + H^+) corresponding to product **6.29** was observed, along with substantial quantities of **6.20** and various oligomeric species.[240]

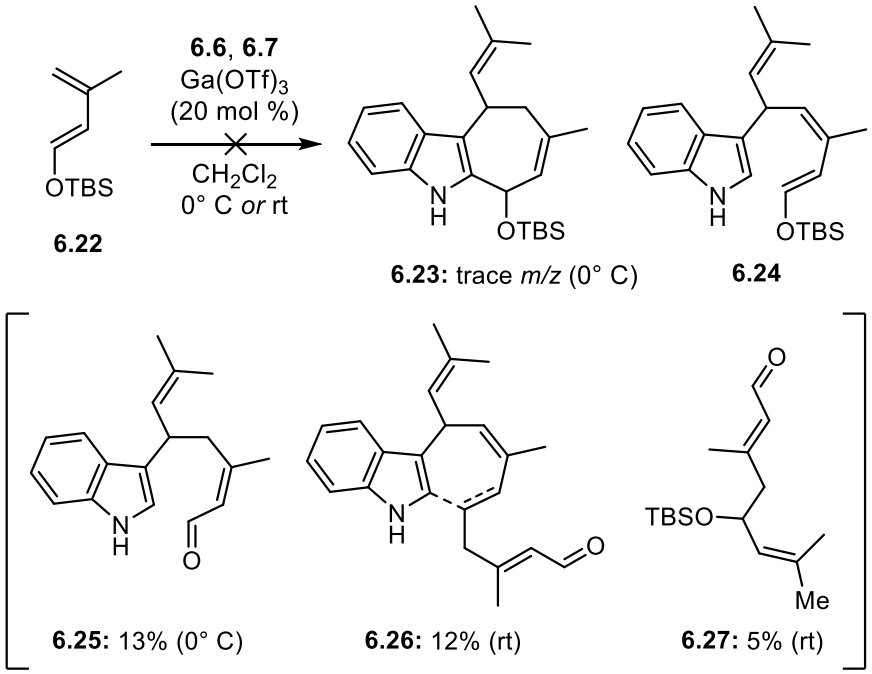

Figure 6.1. Three-component reactions with OTBS diene **6.22**

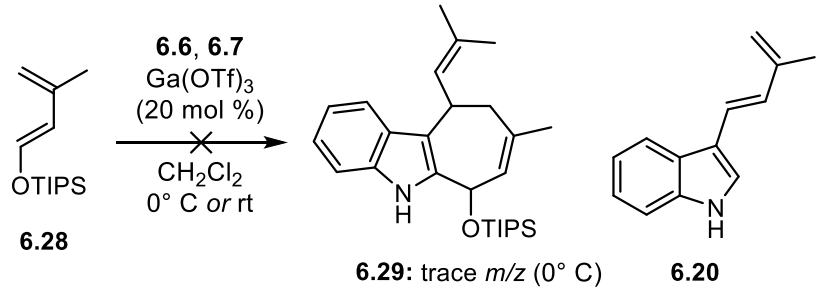

(6.3)

In the above studies, the reactant stoichiometry was similar to that of Wu and co-workers, with a slight excess of prenal (**6.7**) and a larger excess of the diene (2 – 4 equivalents) relative to indole (**6.6**). Noting that the formation of diene oligomers such as **6.26** and **6.27** appeared to be a major problem in the reactions with siloxy-dienes **6.22** and **6.28**, we reasoned that reducing the stoichiometry of the dienic component and preventing it from engaging in side-reactions with prenal (**6.7**) might encourage the formation of our desired product. To this end, we prepared

indolyl allyl alcohol **6.30** (Figure 6.2) according to the procedure of Sheu and coworkers, who used **6.30** as an allyl cation precursor in their biomimetic synthesis of yuehchukuene (**5.10**, *see* Scheme 5.3).[203] In the event, treatment of **6.30** with siloxy-diene **6.28** and gallium(III)triflate generated no trace of the desired cyclization product **6.29**; however, a product which we believe to be aldehyde **6.25** was isolated in 28% yield when the reaction was run at 0 ˚C. Running the reaction at room temperature produced significant quantities of a species with an *m/z* corresponding to the dimer **6.31** (499.3, $m + H^+$).

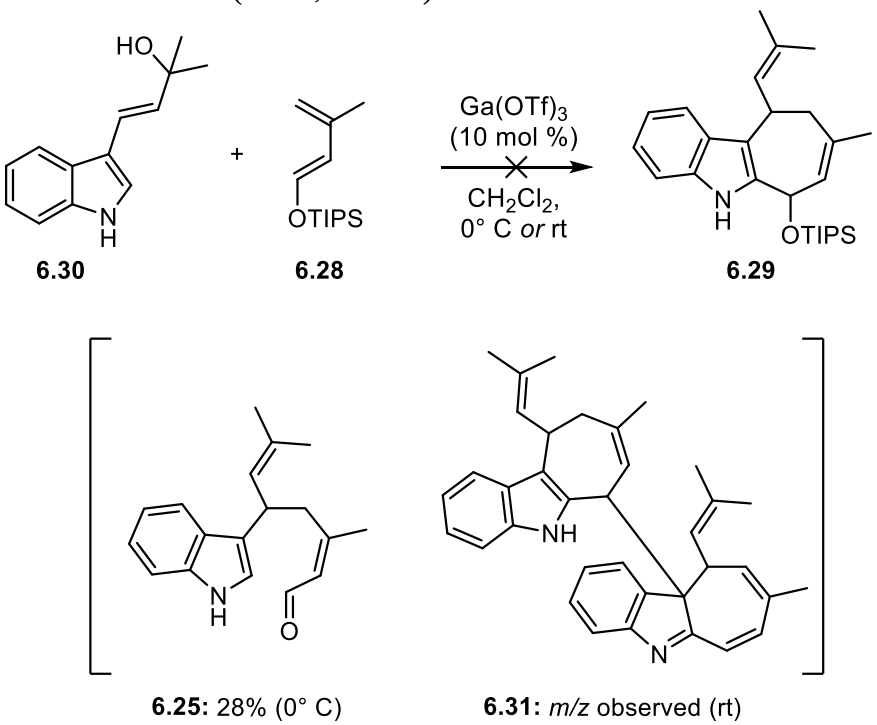

Figure 6.2. Reactions with indolyl allyl alcohol **6.30**

In conclusion, our studies of three-component cyclization reactions with the functionalized dienes **6.13, 6.17, 6.18, 6.27**, and **6.28** suggested that the presence of an ionizable functional group at C(11') of the exotine scaffold (*see* Scheme 6.1) would likely lead to degradation of the desired cyclohepta[*b*]indole product. With this in mind, we set out to devise an alternate strategy for the preparation of exotines A (**6.1**) and B (**6.2**, *see* Scheme 6.1).

6.2 Second-Generation Synthetic Strategy

Our failure to prepare cyclohepta[*b*]indoles related to **6.3** led us to re-evaluate our strategy for the synthesis of exotines A (**6.1**) and B (**6.2**, *see* Scheme 6.1). Since the presence of a suitable functional group for cross-coupling reactions seems to cause problems with the three-component cyclization to form **6.3**, we reasoned that it might be advantageous to form the isopentenyl-coumarin unit C(2'–15') prior to cyclization (Scheme 6.2). Specifically, we wondered if the coumarin-dienes *trans*-dehydroosthol (**6.32**) and gleinadiene (**6.33**) would participate in a three-component cyclization with indole (**6.6**) and prenal (**6.7**) to prepare exotines A (**6.1**) and B (**6.2**) in a single chemical transformation. In addition to potentially enabling a more efficient synthesis of our targets **6.1** and **6.2**, this approach was attractive to us because it mirrors, in a general sense, the biosynthetic proposal advanced by Jiang (*see* Section 5.1.1) and our attendant studies could shed light on the feasibility of Jiang's proposed biosynthesis (*vide infra*).[184]

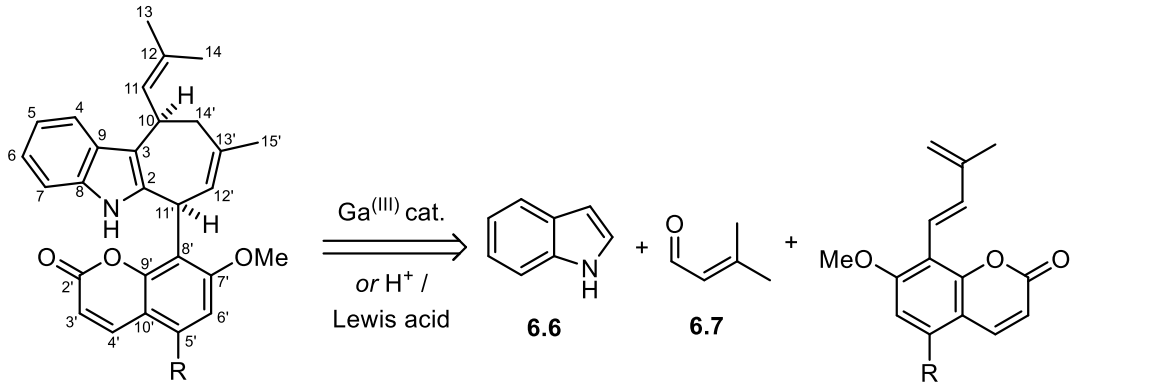

exotine A (**6.1**): R = H
exotine B (**6.2**): R = OMe

trans-dehydroosthol (**6.32**): R = H
gleinadiene (**6.33**): R = OMe

Scheme 6.2. Second-generation retrosynthetic analysis of exotines A (**6.1**) and B (**6.2**, Jiang *et al.* numbering system)[184]

To query the potential feasibility of this approach, we first performed a model study with phenyl diene **6.34**, which was prepared from propargyl alcohol **6.35** using Kimber's Suzuki

coupling/allene isomerization methodology (Scheme 6.3).[241] Gratifyingly, we found that incubation of **6.34** with indole (**6.6**) and prenal (**6.7**) in the presence of gallium(III)triflate resulted in the formation of a mixture (2:1) of phenyl cyclohepta[*b*]indoles **6.36**, albeit in only 23% yield.

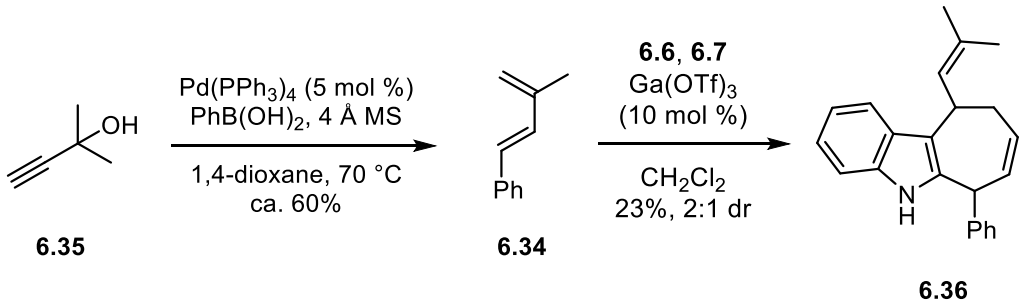

Scheme 6.3. Model study of three-component cyclization with phenyl diene **6.34**

Encouraged by the results of this model study, we set out to investigate a three-component cyclization with *trans*-dehydroosthol (**6.32**) as the dienic component. The synthesis of **6.32** proceeded from 7-hydroxycoumarin (**6.37**), which was iodinated and methylated to give **6.38** in 44% yield according to the procedure of Lauret.[242] Heck coupling of **6.38** with allyl alcohol **6.39** proceeded in 81% yield according to the procedure of Murray,[243] and elimination of the tertiary alcohol to produce **6.32** was accomplished via a modified version of the procedure used by Reisch.[244] In particular, we found that using pyridine as both a base and solvent instead of Hünig's base in chloroform resulted in improved yields of **6.32**. After Trauner and co-workers published their synthesis of exotine B (**6.2**), we investigated the use of their regioselective 5,7-dimethoxycoumarin iodination conditions (*see* Scheme 5.4) on 7-methoxycoumarin (**6.40**, Equation 6.4).[205] Unfortunately, we found that **6.40** preferentially undergoes iodination at C(2) instead of C(8) to generate the undesired iodocoumarin **6.41**.

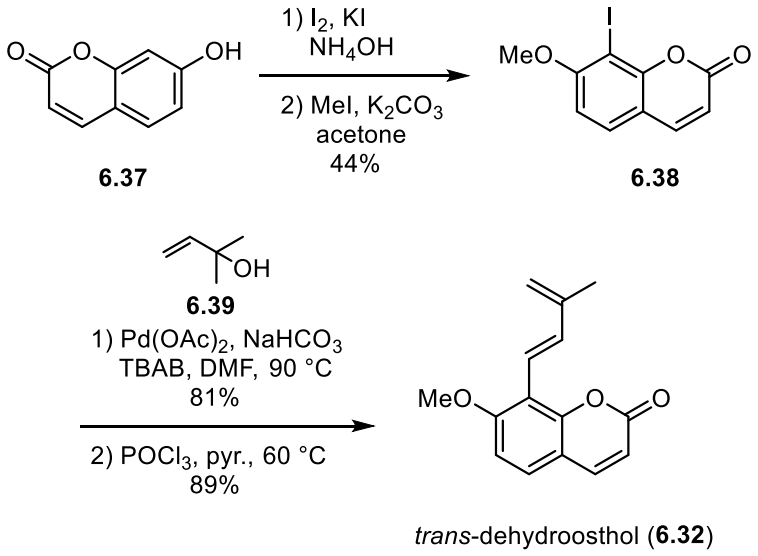

Scheme 6.4. Synthesis of *trans*-dehydroosthol (**6.32**)

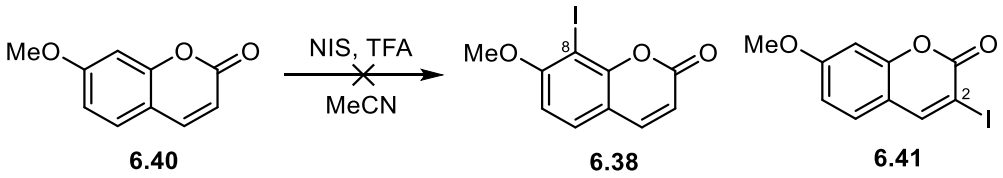

(6.4)

With **6.32** in hand, we began our investigation of the three-component cyclization with indole (**6.6**) and prenal (**6.7**) (Table 6.1). To our delight, we found that the reaction of **6.32**, **6.6**, and **6.7** in the presence of catalytic gallium(III)triflate delivered a mixture (4:1) of exotine a (**6.1**) and *epi*-exotine A (**6.42**) in 17% combined yield (Table 6.1, Entry 1). The use of other group 13 Lewis acid catalysts such as gallium(III) bromide ($GaBr_3$) and indium(III) bromide ($InBr_3$) delivered similar yields and diastereomeric ratios (Entries 2 and 3), which was in accordance with the results observed by Wu and co-workers in their optimization studies (*see* Table 5.1).[207] A major improvement in the diasteromeric ratio was obtained when the reaction was run at 0 ˚C in the presence of catalytic gallium(III) triflate, delivering **6.1** in 14% yield and >20:1 dr; however, this also extended the reaction time to 120 hours (Entry 4). Thankfully, we found when we used stoichiometric *p*-toluenesulfonic acid (*p*-TsOH) instead of catalytic gallium(III) triflate

at 0 ˚C the reaction time was reduced to 24 hours while maintaining a comparable yield (13%) and dr (>20:1) of **6.1** (Entry 5). At room temperature the reaction was complete within one hour and delivered a mixture (2:1) of **6.1** and **6.42** in 26% yield (Entry 6).

Table 6.1. Initial screening of conditions for the preparation of exotine A (**6.1**)

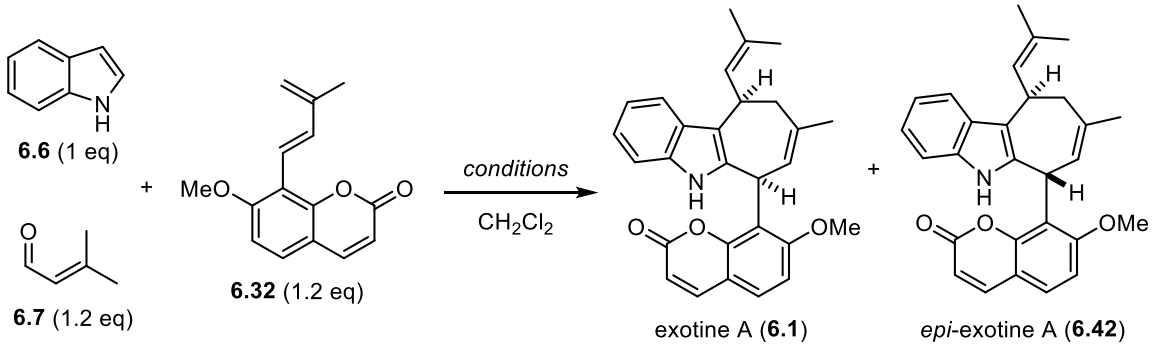

Entry	Acid	temp. (°C)	Time (h)	Result[a,b]
1	$Ga(OTf)_3$ (20 mol %)	rt	5	17%, 4:1 dr
2	$GaBr_3$ (0.2 eq)	rt	20	15%, 3.5:1 dr
3	$InBr_3$ (0.2 eq)	rt	5	14%, 4:1 dr
4	$Ga(OTf)_3$ (0.2 eq)	0	120	14%, >20:1 dr
5	*p*-TsOH (1 eq)	0	24	13%, >20:1 dr
5	*p*-TsOH (1 eq)	rt	1	26%, 2:1 dr

[a]) Combined yield of a mixture of **6.1** and **6.42** after purification by column chromatography; [b]) Diastereomeric ratios calculated from ^1H NMR integrations of the purified mixture of **6.1** and **6.42**

While we were pleased to have prepared exotine A (**6.1**) and optimized the diastereoselectivity of the three-component cyclization, the persistently low yields of **6.1** indicated that the reaction required further optimization. Thus, we undertook a broad screen of reaction conditions, systematically varying the acid catalyst, temperature, solvent, and stoichiometry of the reactants (Table 6.2). By adjusting the stoichiometry to make *trans*-dehydroosthol (**6.32**) the limiting reagent while using excess indole (**6.6**, 4 eq) and prenal (**6.7**, 3 eq), we observed a large increase (17% → 39–45%) in the yield of **6.1** and **6.43** while

maintaining a high (16:1–>20:1) level of diastereoselectivity for **6.1** (Table 6.2, Entry 1). We then screened various solvents including diethyl ether, tetrahydrofuran, toluene, acetonitrile, nitromethane, dimethylformamide, trifluoroethanol, and hexafluoroisopropanol; toluene and acetonitrile (MeCN, Entry 2) both gave encouraging results, but neither was better than dichloromethane (CH_2Cl_2, Entry 1). We were curious as to how the gallium(III) triflate catalyst would perform in a reaction where **6.43** is the limiting reagent. Unfortunately, after 120 hours only 50% conversion of **6.43** to **6.1** was observed, and we did not pursue further studies with this catalyst (Entry 3).

Table 6.2. Further screening of conditions for the preparation of exotine A (**6.1**)

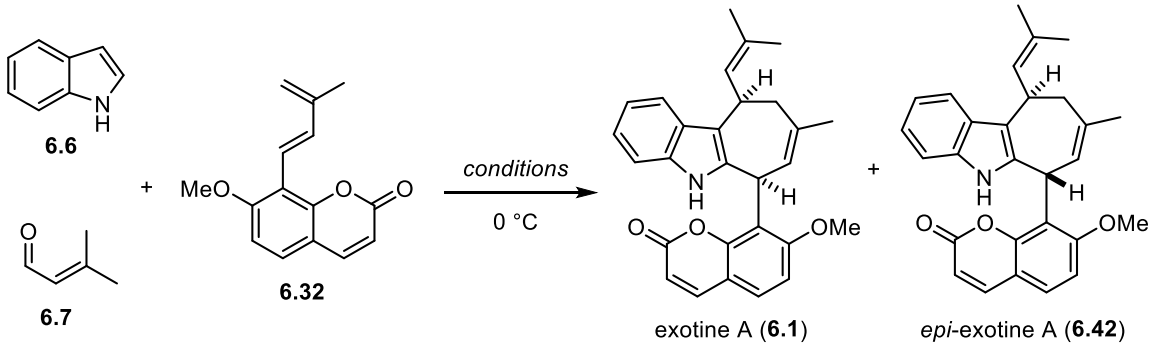

Entry	Acid	Solvent	Time (h)	Stoichiometry	Result[a,b]
1	*p*-TsOH (1 eq)	CH_2Cl_2	24	**6.6** (4 eq), **6.7** (3 eq), **6.32** (1 eq)	39–45%, 16:1–>20:1 dr
2	*p*-TsOH (1 eq)	MeCN	24	**6.6** (4 eq), **6.7** (3 eq), **6.32** (1 eq)	30%, >20:1 dr
3	$Ga(OTf)_3$ (0.2 eq)	CH_2Cl_2	120	**6.6** (2 eq), **6.7** (2 eq), **6.32** (1 eq)	1:1 **6.32:6.1** (120 h)
4	TFA (1 eq)	CH_2Cl_2	24	**6.6** (4 eq), **6.7** (3 eq), **6.32** (1 eq)	43%, 10:1 dr
5	Tf_2NH (1 eq)	CH_2Cl_2	24	**6.6** (4 eq), **6.7** (3 eq), **6.32** (1 eq)	41%, 6:1 dr
6	TfOH (1 eq)	CH_2Cl_2	16–24	**6.6** (4 eq), **6.7** (3 eq), **6.32** (1 eq)	33–42 %, 10:1–>20:1 dr
7	TfOH (1 eq)	CH_2Cl_2	8 or 24	**6.6** (2 eq), **6.7** (2 eq), **6.32** (1 eq)	0%
8	TMSOTf (1 eq)	CH_2Cl_2	24	**6.6** (4 eq), **6.7** (3 eq), **6.32** (1 eq)	0–56%, 10:1–>20:1 dr

[a]) Combined yield of a mixture of **6.1** and **6.42** after purification by column chromatography; [b]) Diastereomeric ratios calculated from ^{1}H NMR integrations of the purified mixture of **6.1** and **6.42**

We did, however, examine other protic and Lewis acid catalysts. For instance, trifluoroacetic acid (TFA) was found to be a competent acid catalyst, furnishing **6.1** and **6.43** in yields comparable to those observed with *p*-toluenesulfonic acid, albeit with slightly reduced diastereoselectivity (Table 2, Entry 3). *β*-Camphorsulfonic acid gave similar results, but required additional equivalents of indole (**6.6**) to be added over the course of reaction for complete consumption of **6.32** to be observed. Acetic acid failed to catalyze the reaction at all, even in

refluxing dichloromethane, suggesting that a stronger protic (or Lewis) acid is necessary for the reaction to occur. Thus, we turned our investigation to two of the strongest protic acids, trifluoromethanesulfonic acid (triflic acid, TfOH) and bistriflimide (Tf_2NH).[245] The use of bistriflimide resulted in a 41% combined yield of **6.1** and **6.43**, but the dr of 6:1 was disappointing, and this catalyst was not explored further (Entry 4). Triflic acid delivered promising but variable results (*vide infra*), generating **6.1** and **6.43** in 33 – 42% yield, and 10:1–>20:1 dr, over the course of 16–24 hours using our standard reaction conditions (Entry 5). We undertook studies to optimize the reaction with triflic acid, screening solvents (toluene, acetonitrile, nitromethane), reaction time (8 – 48 h), and temperature (0 ˚C, -20 ˚C), but were not able to improve upon the results obtained in Entry 5. Interestingly, when the stoichiometry of the reaction was adjusted to two equivalents of indole (**6.6**) and prenal (**6.7**) relative to **6.32** and triflic acid, we did not observe or isolate any exotine A (**6.1**, *see* Section 6.3 *for further discussion*). Finally, we investigated the Lewis acid trimethylsilyl trifluoromethanesulfonate (TMS triflate, TMSOTf), which had been previously used in the Martin lab for the generation of indolyl carbocations that were subsequently trapped by π-nucleophiles (*see* Section 5.3.2).[209,227,230] We found that the use of TMS triflate gave highly variable results (Entry 8). In one trial we obtained **6.1** and **6.43** in 56% yield and 13:1 dr, while in another trial we obtained **6.1** and **6.43** in a 29% yield and 10:1 dr. In one instance we did notisolate any **6.1**! While we cannot offer a definitive explanation for this high degree of variability, we suspect that it is due to an interplay between the sparing solubility of triflic acid, which is generated during the course of the reaction, in dichloromethane, and experimental details such as stir rate, reaction vessel (conical vial vs. round-bottomed flask), and the physical distribution of insoluble precipitate that forms during the course of the reaction. Ultimately, we concluded that the use of *p*-toluenesulfonic acid as our acid catalyst under the conditions described in Entry 1 delivered the best and most consistent yields of exotine A (**6.1**).

Having thus secured optimized conditions for the synthesis of exotine A (**6.1**), we wondered if these same conditions could be used to prepare exotine B (**6.2**) in a one-pot fashion

from gleinadiene (**6.33**), indole (**6.6**) and prenal (**6.7**, *see* Scheme 6.2). At this point in our studies, Trauner and co-workers had published their synthesis of exotine B (**6.2**), and we were both concerned and intrigued by their inability to use prenal (**6.7**) in their gallium(III) triflate-catalyzed three-component cyclization with indole (**6.6**) and gleinadiene (**6.33**, *see* Scheme 5.8 and attendant discussion).[205] In the event, we found that gleinadiene (**6.33**), prepared according to the method of Trauner, readily participated in the *p*-toluenesulfonic acid-catalyzed three-component cyclization with **6.6** and **6.7**, delivering a mixture (4:1) of exotine B (**6.2**) and its epimer (**6.43**) in 50% combined yield (Equation 6.5).[205] Thus, it seems that the use of *p*-toluenesulfonic acid as an acid catalyst for these types of three-component cyclization reactions offers some advantages over gallium(III) triflate, as its use resulted in improved yields and reaction times in our synthesis of exotine A (**6.1**) and enabled a more direct synthesis of exotine B (**6.2**) that did not require the use of a masked isobutenyl group.

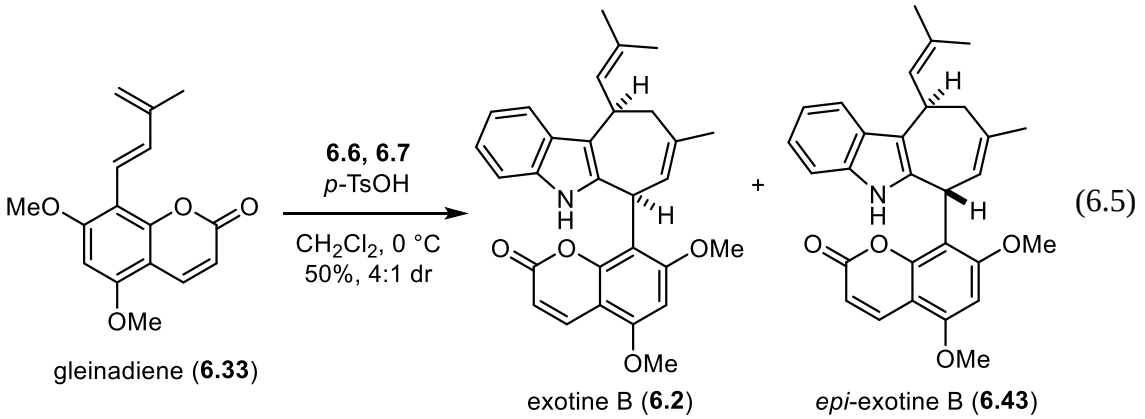

(6.5)

6.3 MECHANISTIC STUDIES

6.3.1. Acid-Catalyzed Epimerization of Exotine A to *epi*-Exotine A

During the course of our efforts to optimize the acid-catalyzed three-component cyclization for the synthesis of exotine A (**6.1**, *see* Tables 6.1 *and* 6.2), we observed several interesting results, side products, and general trends that warranted additional investigation. For

instance, there was a high degree of variability in the observed diastereomeric ratios of **6.1** and **6.42** when several different acid catalysts, especially triflic acid and TMS triflate, were used. This observation led us to wonder if exotine A (**6.1**) might be epimerizing to *epi*-exotine A (**6.42**) under the reaction conditions. To query this hypothesis, we incubated a mixture of **6.1** and **6.42** (30:1) with one equivalent of *p*-toluenesulfonic acid in deutero-methylene chloride and monitored the course of the reaction by ^{1}H NMR spectroscopy (Equation 6.6). We observed a swift equilibration of the mixture to an apparent equilibrium of 1.8 to 1 exotine A (**6.1**) to *epi*-exotine A (**6.42**) over the course of five hours. This diastereomeric ratio is roughly equivalent to what was observed when we performed the three-component cyclization with *p*-toluenesulfonic acid at room temperature (*see* Table 6.1, Entry 6), or with gallium(III) triflate in refluxing dichloromethane (not shown).

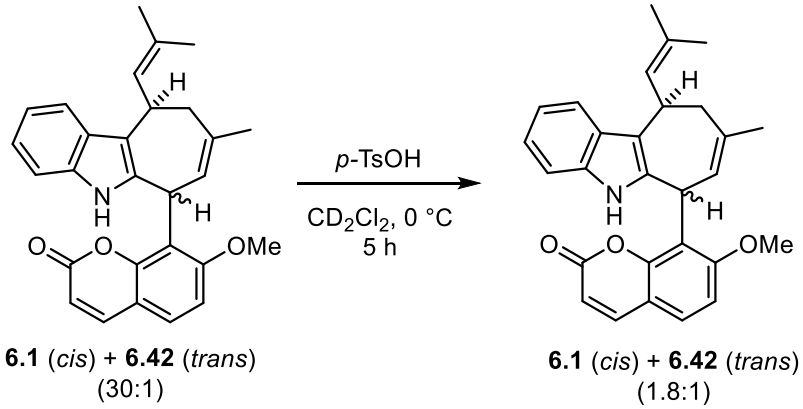

6.1 (*cis*) + **6.42** (*trans*) (30:1) → **6.1** (*cis*) + **6.42** (*trans*) (1.8:1) (6.6)

The equilibration of **6.1** to a mixture of **6.1** and **6.42** in the presence of *p*-toluenesulfonic acid provides some insight into the variable diastereomeric ratios observed in Table 6.2, but it raises other questions. Namely, if this equilibration occurs within five hours at 0 ˚C, how were we ever able to attain high (>20:1) diastereomeric ratios of **6.1** when the reaction is performed over the course of 24 hours in the presence of strong acids such as *p*-toluenesulfonic acid? We believe that the answer to this question may involve the indole-indoline side product **6.16** observed in our early studies toward the synthesis of exotine A (*see* Equation 6.2). We reasoned that the weakly basic aniline nitrogen atom of **6.16** could exert a buffering effect on the three-

component cyclization and slow the conversion of **6.1** to **6.42**. We had observed trace quantities of **6.16** throughout our optimization studies (*see* Section 6.2), but we were unsure of the extent of its formation under our optimized reaction conditions. Thus, we first subjected indole (**6.6**) to 0.25 equivalents of *p*-toluenesulfonic acid in CH_2Cl_2 at 0˚C and obtained a 38% yield of **6.16** (with respect to **6.6**) after 22 hours (Equation 6.7). We did not expect greater than a 50% yield of **6.16**, because once 50% of indole (**6.6**) is converted to **6.16**, there would be equal quantities of **6.16** and *p*-toluensulfonic acid in the reaction mixture, which we assumed would slow or shut down the formation of additional **6.16**. With **6.16** in hand, we incubated it with mixture of **6.1** and **6.42** (25:1) and *p*-toluenesulfonic acid (Equation 6.8). While we did observe some conversion of **6.1** to **6.42**, the rate was substantially slower than what was observed in the absence of **6.16** (*see* Equation 6.6), and after 20 hours at 0˚C the original mixture (25:1) of **6.1** and **6.42** had been transformed into a 15:1 mixture (Equation 6.7). While these studies do not offer definitive proof that **6.16** is exerting a buffering effect in our three-component cyclization reactions, they do offer a plausible explanation for the discrepancy between the results obtained in Equation 6.6 and the generally high levels of diastereoselectivity observed in our three-component cyclization reactions (*see* Table 6.2).

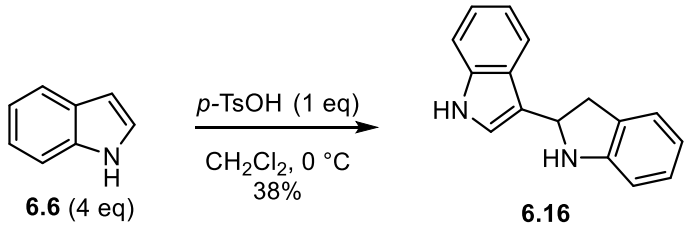

6.6 (4 eq) **6.16** (6.7)

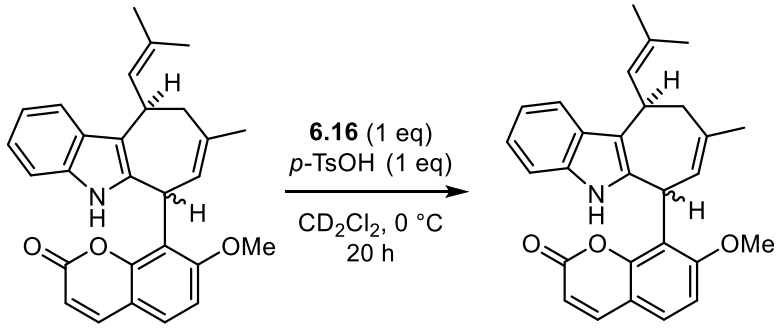

6.1 (*cis*) + **6.42** (*trans*) (25:1) **6.1** (*cis*) + **6.42** (*trans*) (15:1) (6.8)

Another question that emerged from the preceding studies was the nature of the mechanism by which **6.1** is converted to **6.42**. To probe this question, we treated a mixture of **6.1** and **6.42** (10:1) with d_1-trifluoroacetic acid (F_3CCO_2D) and observed the formation of a mixture (2:1) of **6.44** and **6.45** with deuterium incorporated exclusively at C11' (Scheme 6.5). Based on this result, we believe that epimerization of **6.1** occurs via an initial deuteration at C3, followed by deprotonation at C11' to generate the enamine **6.46**, which is then deuterated at C11' and dedeuterated at C3 to regenerate the indole ring system of **6.44** and **6.45**. A similar experiment was performed with exotine B (**6.2**) and its epimer **6.43** (*see* Equation 6.5), and exclusive incorporation of deuterium at C11' was again observed. Epimerization of the indole C(2) α-position (C11' in **6.1** and **6.2**) is well-precedented in the literature. For example, such a process was utilized for one of the final steps of Woodward's synthesis of reserpine.[246]

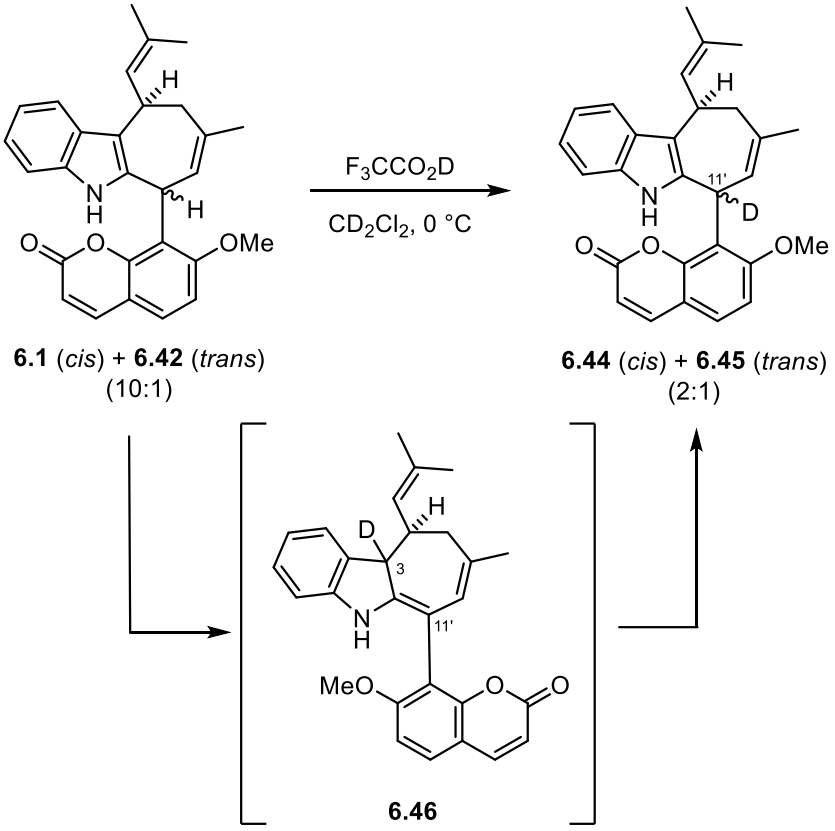

Scheme 6.5. Deuterium incorporation experiment to probe the mechanism of acid-catalyzed epimerization of **6.1**

6.3.2. Side-Products and Proposed Intermediates of the Three-Component Cyclization

During our optimization studies we also observed the persistent presence of large quantities of various compounds that appeared to be isomeric with exotine A (**6.1**) based on low-resolution mass spectrometry analysis. The yield of one group of these byproducts increased when the reactions were run at lower temperatures. For example, when the reaction was run at –20 ˚C we isolated a mixture (10:1) of **6.1** and **6.42** in 19% yield. An inseparable mixture of isomeric compounds was also produced in 58% yield, and we hypothesized that these compounds might be uncyclized intermediates such as **6.47** or spirocyclic indolenine intermediates/byproducts **6.48** (Equation 6.9).

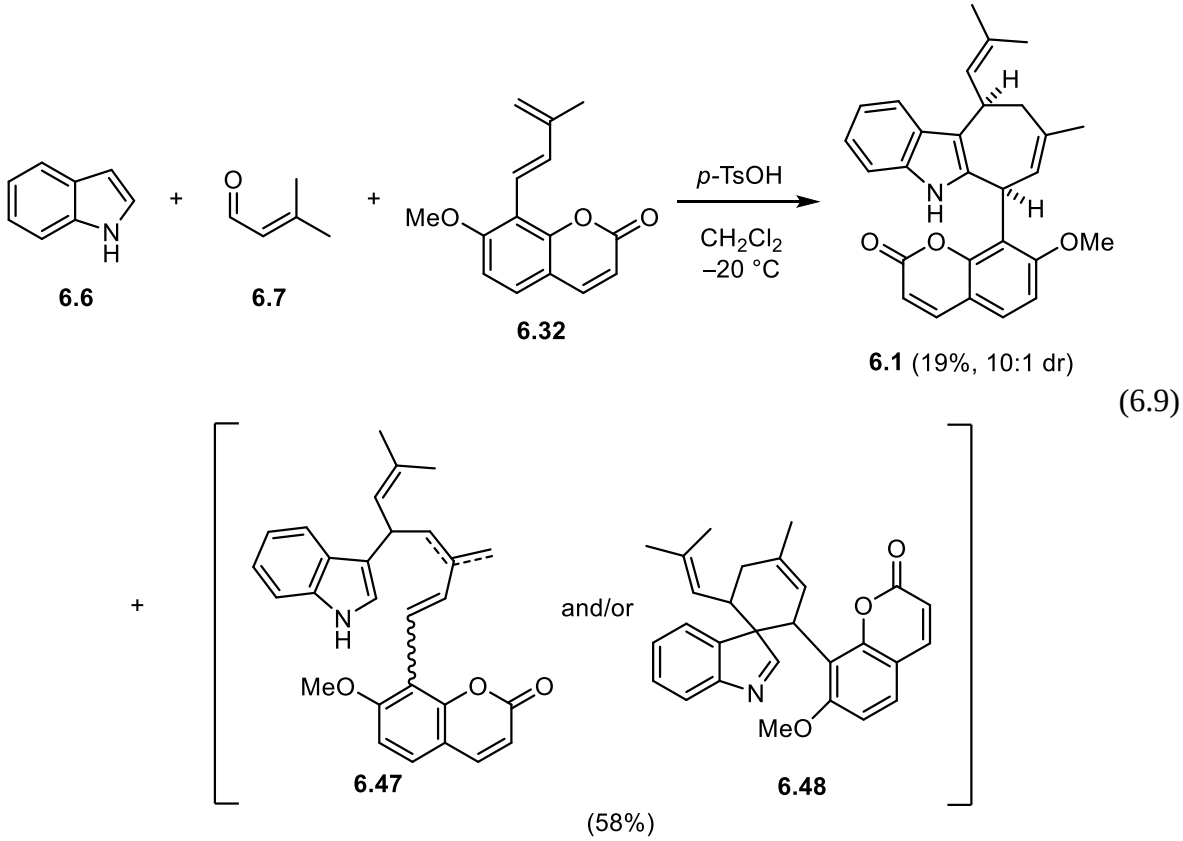

(6.9)

Intrigued by the possibility that we had isolated intermediates of the three-component cyclization, we subjected the mixture, which we believed comprised **6.47** and/or **6.48**, to additional treatment with *p*-toluenesulfonic acid in dichlormethane, and we observed the formation of additional quantities of exotine A (**6.1**) and *epi*-exotine A (**6.42**). We also isolated

another inseparable mixture of isomeric compounds that we referred to as nonpolar isomers, as they were less polar than **6.1**. These same nonpolar isomers were also observed and isolated as a mixture from various three-component reaction experiments.

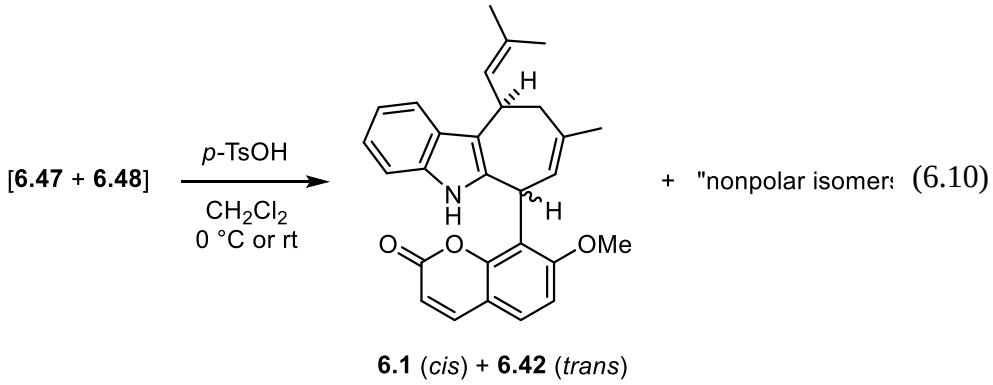

(6.10)

6.1 (*cis*) + **6.42** (*trans*)

We made extensive efforts to purify this mixture of [**6.47 + 6.48**] via HPLC, but invariably obtained a mixture of compounds even when the HPLC trace suggested a clean separation. This observation suggested to us that at least some of the compounds that comprise the mixture are unstable. Analysis of the major components of the [**6.47 + 6.48**] mixture by ^{1}H, ^{13}C, and 2D (HSQC) NMR revealed characteristic signals that suggest the major components diastereomeric are 3,3'-spiroindolenines **6.48**. We observed singlets at δ 8.65 and 8.34 ppm in the ^{1}H NMR spectrum that correlate (HSQC) to peaks at δ 175.1 and 174.5 ppm in the ^{13}C NMR spectrum. We also observed peaks at δ 65.6 and 65.5 ppm in the ^{13}C NMR spectrum which do not correlate (HSQC) with any ^{1}H NMR signals. These signals are consistent with the known chemical shifts of N=**C**-**H** groups and spiro- carbon atoms of other 3,3'-spiroindolenine compounds.[247,248]

Thankfully, we were eventually able to isolate the major component of the "nonpolar isomers" mixture via HPLC, which was unambiguously assigned as the rearranged isomer **6.49** via 2D-NMR and X-ray crystallography (Figure 6.3). While we were not able to isolate and fully characterize the minor isomer of the "nonpolar isomer" mixture, we strongly suspect that it is the *cis*-epimer of **6.49**, **6.50** based on analysis of the ^{1}H NMR spectra (Figure 6.4). The structure of the rearranged isomer **6.49** lends further support to our hypothesis that the [**6.47 + 6.48**] mixture

is (primarily) 3,3'-spiroindolenine diastereomers **6.48** (*see* Equation 6.9), as **6.49** is formed from the [**6.47 + 6.48**] mixture, and there is no plausible mechanism by which **6.49** could arise during the course of our three-component cyclization reactions *except* via the intermediacy of **6.48**.

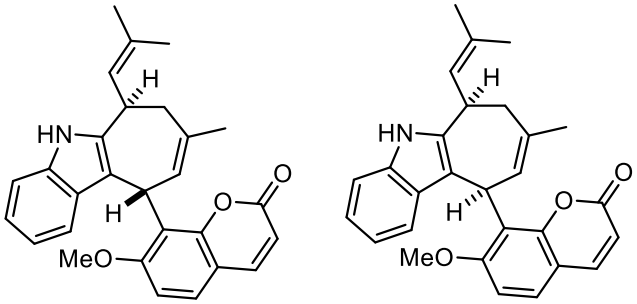

6.49 **6.50**

Figure 6.3. Rearranged isomer **6.49** and its epimer **6.50**

Having partially elucidated the nature of these intermediates and byproducts, we desired a more rigorous accounting of the relative proportions of (*epi*-)exotine A (**6.1, 6.43**), **6.48**, and **6.49** formed under our optimized three-component cyclization conditions. To address this, we performed another reaction of **6.6**, **6.7**, and **6.32** with *p*-toluenesulfonic acid and obtained a mixture (10:1) of exotine A (**6.1**) and its epimer (**6.42**) in 45% combined yield, and a mixture (1.7:1) of **6.49** and its putative epimer **6.51** in 31% combined yield, and **6.48** in 28% yield. This accounts for nearly 100% of the mass balance of our limiting reagent **6.32** (Scheme 6.6).

When **6.48** was treated with *p*-toluenesulfonic acid in dichloromethane, we isolated an additional 5% of a mixture (2:1) of exotine A (**6.1**) and *epi*-exotine A (**6.43**) (Scheme 6.6). This result suggests that our "optimized" conditions are in fact close to optimal, at least with respect to conversion of the productive diastereomer of the **6.48** mixture to exotine A (**6.1**).

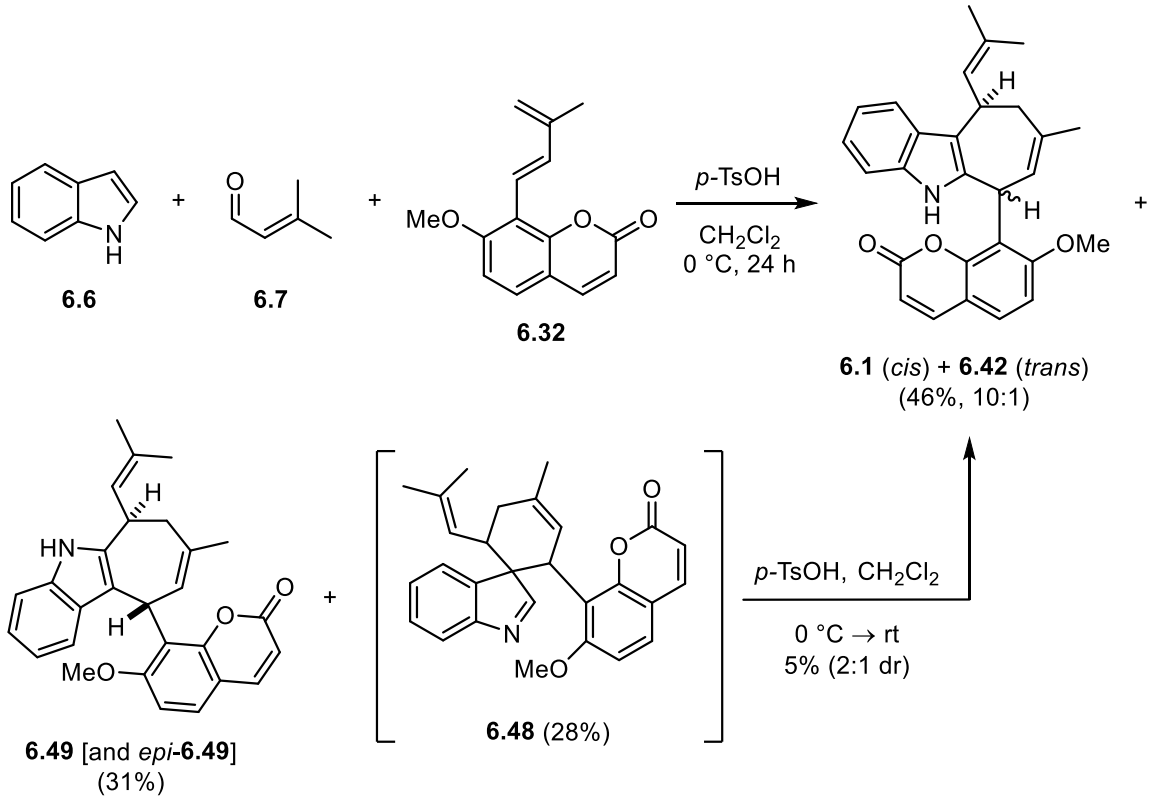

Scheme 6.6. Quantitation and analysis of the byproducts of the three-component cyclization of **6.6**, **6.7,** and **6.32**

6.4 CONCLUDING REMARKS

In conclusion, we have developed extraordinarily concise syntheses of the cyclohepta[*b*]indole-coumarin natural products exotines A (**6.1**) and B (**6.2**), by a process that features a single chemical transformation from the known compounds *trans*-dehydroosthol (**6.32**) and gleinadiene (**6.33**) (*see* Table 6.2 *and* Equation 6.5). The synthesis of exotine A (**6.1**) proceeds in 43% yield and 17:1 dr, whereas the synthesis of exotine B (**6.2**) proceeds in 50% yield and 4:1 dr. To achieve these syntheses, we undertook extensive studies toward optimizing an acid-catalyzed three-component cyclization reaction between indole (**6.6**), prenal (**6.7**), and *trans*-dehydroosthol (**6.32**), using *p*-toluenesulfonic acid in dichloromethane at 0 ˚C.[207] We found that exotine A (**6.1**) is partially epimerized in the presence of strong acids such as *p*-toluensulfonic acid and d_1-trifluoroacetic acid, and provided a plausible mechanism for this

epimerization based on our deuterium incorporation experiments (*see* Scheme 6.5). Finally, we isolated and characterized a byproduct of the three-component cyclization, the rearranged cyclohepta[*b*]indole-coumarin isomer **6.49** that, along with our partial characterization and attendant studies of the 3,3'-spiroindolenine mixture **6.48**, lends support to Jiang's biosynthetic proposal of a [4+2] cycloaddition followed by ring expansion (*see* Scheme 6.6, *see also* Section 5.1.1).[184] It is our hope this work may inform and enable future studies on the biological activities of the exotines or synthetic analogs thereof, as well as the use of acid-catalyzed three-component cyclization reactions for the synthesis of indole alkaloids.

Chapter 7. Experimental Procedures

General. Tetrahydrofuran and diethyl ether were dried by filtration through two columns of activated, neutral alumina prior to use. Methanol, acetonitrile and dimethylformamide were dried by filtration through two columns of activated molecular sieves, and toluene was dried by filtration through one column of activated, neutral alumina followed by one column of Q5 reactant. Benzene was distilled from sodium and benzophenone. Methylene chloride, diisopropylamine, triethylamine, and diisopropylethylamine were distilled from calcium hydride immediately prior to use. Pyridine was distilled from potassium hydroxide (KOH) and calcium hydride and stored over KOH. Dioxane was distilled from sodium metal and benzophenone prior to use. All solvents were determined to have less than 50 ppm H_2O by Karl Fischer coulometric moisture analysis. All reagents were reagent grade and used without purification unless otherwise noted. All reactions involving air or moisture sensitive reagents or intermediates were performed under an inert atmosphere of nitrogen or argon in glassware that was flame dried. Solutions were degassed using three freeze-thaw cycles under vacuum. Reaction temperatures refer to the temperature of the cooling/heating bath. Volatile solvents were removed under reduced pressure using a Büchi rotary evaporator at 25–30 °C. Thin layer chromatography performed using run on pre-coated plates of silica gel with a 0.25 mm thickness containing 60F-254 indicator (Merck). Chromatography was performed using forced flow (flash chromatography) and the indicated solvent system on 230-400 mesh silica gel (E. Merck reagent silica gel 60) according to the method of Still,[249] unless otherwise noted.

Infrared (IR) spectra were obtained either neat on sodium chloride or as solutions in the solvent indicated and reported as wavenumbers (cm^{-1}). Proton nuclear magnetic resonance (^1H NMR) and carbon nuclear magnetic resonance (^{13}C NMR) spectra were obtained at the indicated field as solutions in $CDCl_3$ unless otherwise indicated. Chemical shifts are referenced to the deuterated solvent and are reported in parts per million (ppm, δ) downfield from tetramethylsilane (TMS, δ = 0.00 ppm). Coupling constants (*J*) are reported in Hz and the

splitting abbreviations used are: s, singlet; d, doublet; t, triplet; q, quartet; m, multiplet; comp, overlapping multiplets of magnetically nonequivalent protons; br, broad; app, apparent.

7.1 Synthesis and Evaluation of Novel Anti-Trypanosomal Compounds

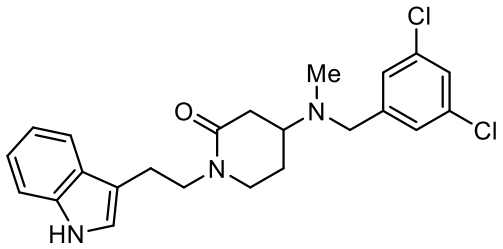

1-(2-(1H-Indol-3-yl)ethyl)-4-((3,5-dichlorobenzyl)(methyl)amino)piperidin-2-one (2.16) (LTL-IV-084). To a stirred solution of amine **2.22** (16 mg, 0.11 mmol) and 3,5-dichlorobenzaldehyde (25 mg, 0.314 mmol) in 1,2-dichloroethane (1.4 mL) was added sodium triacetoxyborohydride (45 mg, 0.21 mmol). The reaction was stirred for 4 h, whereupon it was diluted with CH_2Cl_2 (50 mL) and washed with sat. $NaHCO_3$ (50 mL) and brine (50 mL). The organic layer was dried (Na_2SO_4) and concentrated under reduced pressure to afford crude **2.16**. The crude material was purified via flash column chromatography, eluting with hexanes:EtOAc:TEA (40:60:1) to furnish 17 mg (68%) of **2.16** as a yellow solid. ^{1}H NMR (400 MHz, $CDCl_3$) δ 8.10 (s, 1 H), 7.66 (d, *J* = 7.9 Hz, 1 H), 7.37 (d, *J* = 8.1 Hz, 1 H), 7.24 (s, 1 H), 7.31 – 7.25 (comp, 3 H), 7.18 (td, *J* = 8.1, 7.0 Hz, 1 H), 7.10 (td, *J* = 7.9, 7.0 Hz, 1 H), 7.05 (d, *J* = 2.3 Hz, 1 H), 3.74 – 3.50 (comp, 4 H), 3.17 – 3.00 (comp, 4 H), 2.94 – 2.81 (m, 1 H), 2.65 (dd, *J* = 17.2, 5.2 Hz, 1 H), 2.51 – 2.41 (m, 1 H), 2.16 (s, 3 H), 2.05 – 1.91 (m, 1 H), 1.60 (qd, *J* = 11.5, 6.0 Hz, 1 H); ^{13}C NMR (100 MHz, $CDCl_3$) δ 144.0, 137.0, 135.6, 128.2, 127.9, 127.4, 122.7, 122.5, 120.0, 119.4, 113.9, 111.8, 57.31, 57.29, 48.4, 46.9, 37.6, 35.0, 26.6, 23.7; IR (NaCl, film) 3624, 2509, 2929, 2855, 2793, 2242, 1623, 1569, 1499, 1456, 1433, 1345, 1303, 1231, 1209, 1158, 1125, 1098, 1074, 1036 cm^{-1}; HRMS (ESI) *m/z* calc'd for $C_{23}H_{25}Cl_2N_3O$ (M+H)+ 430.1447; found 430.1448.

NMR assignment. ^{1}H NMR (400 MHz, $CDCl_3$) δ 8.10 (s, 1 H, H1), 7.66 (d, *J* = 7.9 Hz, 1 H, H5), 7.37 (d, *J* = 8.1 Hz, 1 H, H8), 7.24 (s, 1 H, H22), 7.31 – 7.25 (comp, 3 H, H20, H22), 7.13 (t, *J* = 7 Hz, 1 H, H7), 7.05 (d, *J* = 2.3 Hz, 1 H, H2), 3.74 – 3.50 (comp, 4 H, H10, H18), 3.17 – 3.00 (comp, 4 H, H12, H11), 2.94 – 2.81 (m, 1 H, H14), 2.65 (dd, *J* = 3 Hz, 17 Hz, 1 H, H15), 2.51 – 2.41 (m, 1 H, H15), 2.16 (s, 3 H, H17), 2.05 – 1.91 (m, 1 H, H13), 1.60 (qd, *J* = 11.5, 6.0 Hz, 1 H, H13); ^{13}C NMR (100 MHz, $CDCl_3$) δ 170.0 (C16), 144.0 (C19), 137.0 (C9), 135.6 (C22), 128.2 (C4), 127.9 (C21), 127.4 (C20), 122.7 (C6), 122.5 (C2), 120.0 (C7), 119.4 (C5), 113.9 (C3), 111.8 (C8), 57.31 (C18), 57.29 (C14), 48.4 (C10), 46.9 (C12), 37.6 (C15), 35.0 (C17), 26.6 (C13), 23.7 (C11).

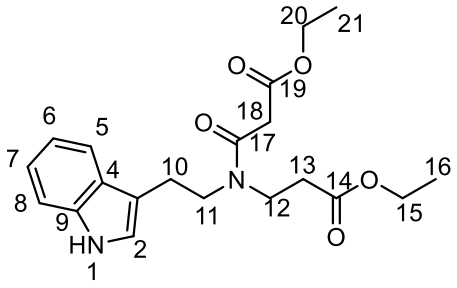

2.19

Ethyl 3-((2-(1H-indol-3-yl)ethyl)(3-ethoxy-3-oxopropyl)amino)-3-oxopropanoate (2.19) (LTL-II-150). Amine **2.18** (3.00 g, 11.5 mmol) and malonic acid **2.9** (1.68 g, 12.6 mmol) were dissolved in CH_2Cl_2 (250 mL) and the solution was cooled to 0 °C, whereupon EDCI•HCl (2.43 g, 12.6 mmol) and *i*-Pr_2NEt (3.30 g, 25.2 mmol, 4.38 mL) were added. The reaction was warmed to room temperature and stirred for 40 h, whereupon the reaction was diluted with CH_2Cl_2 (250 mL) and washed with 1 M HCl (500 mL). The aqueous layer was then extracted with an additional portion of CH_2Cl_2 (250 mL). The combined organic layers were washed with brine (500 mL), dried (Na_2SO_4) and concentrated under reduced pressure to yield 4.3g (99%) of crude **2.19** as an amber oil (4.3g 99%) which was judged to be >90% pure by ^{1}H NMR and carried forward without further purification. For characterization, a portion of the crude product was purified via column chromatography, eluting with hexanes/EtOAc (3:1 → 1:1) to provide

2.18 as an off-white solid. ^{1}H NMR (3:2 rotamer mixture) (400 MHz, $CDCl_3$) δ 8.24 (s, 0.5 H), 8.15 (s, 0.3 H), 7.71 (d, *J* = 7.8 Hz, 0.3 H), 7.59 (d, *J* = 7.8 Hz, 0.6 H), 7.40 (t, *J* = 8.7 Hz, 0.9 H), 7.25 – 7.18 (m, 1 H), 7.18 – 7.11 (m, 0.9 H), 7.06 (d, *J* = 2.3 Hz, 0.3 H), 7.00 (d, *J* = 2.4 Hz, 0.6 H), 4.26 (q, *J* = 7.1 Hz, 0.7 H), 4.18 – 4.11 (comp, 3 H), 3.70 (t, *J* = 7.0 Hz, 1.2 H), 3.65 – 3.59 (comp, 1.9 H), 3.58 (s, 0.7 H), 3.55 (t, *J* = 7.1 Hz, 0.7 H), 3.16 (s, 1.2 H), 3.08 – 3.01 (comp, 1.9 H), 2.69 (t, *J* = 7.0 Hz, 1.2 H), 2.57 (t, *J* = 7.1 Hz, 0.7 H), 1.32 (t, *J* = 7.1 Hz, 1.2 H), 1.28 – 1.22 (comp, 4.7 H); ^{13}C NMR (100 MHz, $CDCl_3$) (3:2 rotamer mixture) δ 172.1, 170.1, 167.8, 167.6, 166.4, 166.1, 136.3, 127.3, 126.9, 122.4, 122.3, 122.1, 122.0, 119.7, 119.4, 118.8, 118.1, 112.9, 111.7, 111.4, 111.1, 61.4, 61.3, 61.0, 60.6, 49.9, 46,9, 44.5, 42.4, 41.2, 40.9, 36.6, 32.6, 29.7, 24.8, 23.2, 14.2, 14.1, 14.0; IR (NaCl, film) 3417, 2983, 2920, 2361, 2255, 2128, 1731, 1642, 1458, 1370, 1319, 1260, 1190, 1159, 1097, 1027, 1007, 824, 746, 618 cm^{-1}; HRMS (ESI) *m/z* calcd for $C_{20}H_{26}N_2O_5$ (M+Na)+ 397.1734; found 397.1733.

NMR Assignment. ^{1}H NMR (3:2 rotamer mixture) (400 MHz, $CDCl_3$ δ 8.24 (s, 0.5 H, H1), 8.15 (s, 0.3 H, H1), 7.71 (d, *J* = 7.8 Hz, 0.3 H, H5), 7.59 (d, *J* = 7.8 Hz, 0.6 H, H5), 7.40 (t, *J* = 8.7 Hz, 0.9 H, H8), 7.25 – 7.18 (m, 1 H, H6), 7.18 – 7.11 (m, 0.9 H, H7), 7.06 (d, *J* = 2.3 Hz, 0.3 H, H2), 7.00 (d, *J* = 2.4 Hz, 0.6 H, H2), 4.26 (q, *J* = 7.1 Hz, 0.7 H, H15, H20), 4.18 – 4.11 (comp, 3 H, H15, H20), 3.70 (t, *J* = 7.0 Hz, 1.2 H, H12), 3.65 – 3.59 (comp, 1.9 H, H11), 3.58 (s, 0.7 H, H18), 3.55 (t, *J* = 7.1 Hz, 0.7 H, H12), 3.16 (s, 1.2 H, H18), 3.08 – 3.01 (comp, 1.9 H, H10), 2.69 (t, *J* = 7.0 Hz, 1.2 H, H13), 2.57 (t, *J* = 7.1 Hz, 0.7 H, H13), 1.32 (t, *J* = 7.1 Hz, 1.2 H, H16, H21), 1.28 – 1.22 (comp, 4.7 H, H16, H21); ^{13}C NMR (100 MHz, $CDCl_3$) (3:2 rotamer mixture) δ 172.1 (C19), 170.1 (C19), 167.8 (C14), 167.6 (C14), 166.4 (C17), 166.1 (C17), 136.28 (C9), 136.26 (C9), 127.3 (C4), 126.9 (C4), 122.4 (C6), 122.3 (C2), 122.1 (C6), 122.0 (C2), 119.7 (C7), 119.4 (C7), 118.8 (C5), 118.1 (C5), 112.9 (C3), 111.7 (C3), 111.4 (C8), 111.1 (C8), 61.4 (C15/C20), 61.3 (C15/C20), 61.0 (C15/C20), 60.6 (C15/C20), 49.9 (C11), 46.9 (C11), 44.5 (C12), 42.4 (C12), 41.2 (C18), 40.9 (C18), 36.6 (C13), 32.6 (C13), 24.8 (C10), 23.2 (C10), 14.2 (C16/C21) , 14.1 (C16/C21), 14.0 (C16/C21).

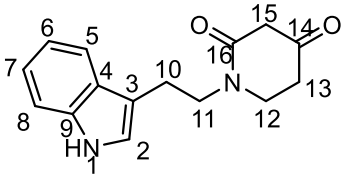

2.20

1-(2-(1H-Indol-3-yl)ethyl)piperidine-2,4-dione (2.20) (LTL-II-139). A suspension of NaH (60% w/w in mineral oil, 135 mg, 3.80 mmol) in cyclohexane (20 mL) was heated under reflux, and a solution of **13** (700 mg, 1.90 mmol) in toluene (3 mL) was added dropwise. The reaction was stirred under reflux for 6 h during which time a tan precipitate formed. The reaction was then cooled to room temperature, and the solvent was removed under reduced pressure. The flask was then cooled to 0 °C, EtOH (20 mL) was added, and the reaction was stirred for an additional 2 h. The solution was then diluted with H_2O (200 mL) and 1 M HCl was added until pH = 1, and the aqueous solution was extracted with CH_2Cl_2 (3x 100 mL). The combined organic layers were washed with brine (100 mL), dried ($MgSO_4$) and concentrated under reduced pressure to afford a tan solid which was then resuspended in AcOH (2 mL) and H_2O (18 ml). The solution was heated under reflux until all starting material was consumed, as judged by LC-MS. The solution was cooled to room temperature, neutralized with sat. $NaHCO_3$ (100 mL), and extracted with CH_2Cl_2 (3x 100 mL). The combined organic extracts were then washed with brine (200 mL), dried ($MgSO_4$) and concentrated under reduced pressure to afford crude **2.20**. The crude material was purified via flash column chromatography, eluting with hexanes:EtOAc (75:25 → 40:60) to furnish 313 mg (64%) of **2.20** as an off-white solid. ^{1}H NMR (400 MHz, $CDCl_3$) δ 8.04 (bs, 0.5 H), 7.65 (d, *J* = 7.8 Hz, 0.99 H), 7.39 (d, *J* = 8.0 Hz, 1.05 H), 7.23 (t, *J* = 7.2 Hz, 1.18 H), 7.16 (t, *J* = 7.2, 1.08 H), 7.07 (s, 0.96 H), 3.85 (t, *J* = 6.9 Hz, 2.00 H), 3.34 (t,s overlapping, 3.90 H), 3.11 (t, *J* = 7 Hz, 2.05 H), 2.34 (t, *J* = 6.1 Hz, 1.91 H); ^{13}C NMR (100 MHz, $CDCl_3$) δ 203.8, 168.1, 136.3, 127.3, 122.3, 122.1, 119.6, 118.5, 112.9, 111.4, 49.0, 44.4, 38.5, 23.7; IR (NaCl, film) 3283, 2924, 2854, 2362, 1726, 1644, 1489, 1644, 1489, 1457, 1350, 1227, 1095, 1011, 745 cm^{-1}; HRMS (ESI) *m/z* calcd for $C_{15}H_{16}N_2O_2$ (M+Na)+ 279.1104; found 279.1100.

NMR Assignment. ^{1}H NMR (400 MHz, $CDCl_3$) δ 8.04 (bs, 0.5 H, H1), 7.65 (d, *J* = 7.8 Hz, 0.99 H, H5), 7.39 (d, *J* = 8 Hz, 1.05 H, H8), 7.23 (t, *J* = 7.2 Hz, 1.18 H, H6), 7.16 (t, *J* = 7.2, 1.08 H, H7), 7.07 (s, 0.96 H, H2), 3.85 (t, *J* = 6.9 Hz, 2.00 H, H10), 3.34 (t,s overlapping, 3.90 H, H12, H15), 3.11 (t, *J* = 7 Hz, 2.05 H, H11), 2.34 (t, *J* = 6.1 Hz, 1.91 H, H13); ^{13}C NMR (100 MHz, $CDCl_3$) δ 203.8 (C14), 168.1 (C16), 136.3 (C9), 127.3 (C4), 122.3 (C6), 122.1 (C2), 119.6 (C7), 118.5 (C5), 112.9 (C3), 111.4 (C8), 49.0 (C10), 48.6 (C13), 44.4 (C12), 38.5 (C13), 23.7 (C11).

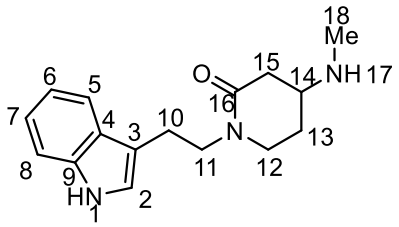

2.22

1-(2-(1H-Indol-3-yl)ethyl)-4-(methylamino)piperidin-2-one (2.22) (LTL-IV-080). To a solution of ketone **2.20** (65 mg, 0.25 mmol) in methanol (2.5 mL) was added methylamine (78 mg, 2.5 mmol, 33% wt. soln. in EtOH), AcOH (150 mg, 2.5 mmol), and $NaBH_3CN$ (31 mg, 0.5 mmol) and the resulting mixture was stirred for 16 hours at room temperature, whereupon an additional portion of $NaBH_3CN$ (31 mg, 0.5 mmol) was added. After stirring for an additional 3 h, the reaction was diluted in 1 M HCl (50 mL) and washed with Et_2O (50 mL). The aqueous layer was treated with 1 M NaOH until the solution turned cloudy and pH > 10, and the resulting mixture was diluted with brine (20 mL) and extracted with CH_2Cl_2 (3 x 50 mL). The combined organic layers were dried (Na_2SO_4) and concentrated under reduced pressure. The crude material was purified via column chromatography, eluting with CH_2Cl_2:MeOH:Et_3N (95 : 5 : 1) to yield 45 mg (66%) of **2.22** as a white foam. ^{1}H NMR (400 MHz, $CDCl_3$) δ 8.02 (s, 1 H), 7.66 (d, *J* = 7.9 Hz, 1 H), 7.37 (dt, *J* = 8.1, 1.0 Hz, 1 H), 7.20 (ddd, *J* = 8.1, 7.0, 1.3 Hz, 1 H), 7.13 (ddd, *J* = 7.9, 7.0, 1.1 Hz, 1 H), 7.06 (d, *J* = 2.3 Hz, 1 H), 3.66 (td, *J* = 7.1, 2.9 Hz, 2 H), 3.25 – 3.18 (m, 1

H), 3.16 – 3.08 (m, 1 H), 3.07 – 3.02 (comp, 2 H), 2.86 – 2.78 (m, 1 H), 2.68 (ddd, *J* = 17.1, 5.3, 1.8 Hz, 1 H), 2.41 (s, 3 H), 2.22 (dd, *J* = 17.1, 8.6 Hz, 1 H), 1.90 (dt, *J* = 8.1, 5.0 Hz, 1 H), 1.58 – 1.46 (m, 1 H); ^{13}C NMR (500 MHz, $CDCl_3$) δ 168.3, 136.3, 127.5, 122.001, 121.968, 119.3, 118.7, 113.1, 111.2, 53.2, 48.12, 45.7, 43.42, 38.8, 33.3, 28.4, 22.9; IR (NaCl, film) 3252, 3053, 2926, 2856, 2799, 2361, 1624, 1498, 1456, 1344, 1302, 1264, 1233, 1158, 1102, 1011 cm^{-1}; HRMS (ESI) *m/z* calcd for $C_{16}H_{21}N_3O$ (M+Na)+ 294.1577; found 294.1574.

NMR Assignment. ^{1}H NMR (400 MHz, $CDCl_3$) δ 8.02 (s, 1 H, H1), 7.66 (d, *J* = 7.9 Hz, 1 H, H5), 7.37 (dt, *J* = 8.1, 1.0 Hz, 1 H, H8), 7.20 (ddd, *J* = 8.1, 7.0, 1.3 Hz, 1 H, H6), 7.13 (ddd, *J* = 7.9, 7.0, 1.1 Hz, 1 H, H7), 7.06 (d, *J* = 2.3 Hz, 1 H, H2), 3.66 (td, *J* = 7.1, 2.9 Hz, 2 H, H10), 3.25 – 3.18 (m, 1 H, H12), 3.16 – 3.08 (m, 1 H, H12), 3.07 – 3.02 (comp, 2 H, H11), 2.86 – 2.78 (m, 1 H, H14), 2.68 (ddd, *J* = 17.1, 5.3, 1.8 Hz, 1 H, H15), 2.41 (s, 3 H, H18), 2.22 (dd, *J* = 17.1, 8.6 Hz, 1 H, H15), 1.90 (dt, *J* = 8.1, 5.0 Hz, 1 H, H13), 1.58 – 1.46 (m, 1 H, H13); ^{13}C NMR (500 MHz, $CDCl_3$) δ 168.3 (C16), 136.3 (C9), 127.5 (C4), 122.001(C6), 121.968 (C2), 119.3 (C7), 118.7 (C5), 113.1 (C3), 111.2 (C8), 53.2 (C14), 48.12 (C10), 45.7 (C12), 38.8 (C15), 33.3 (C18), 28.4 (C13), 22.9 (C11).

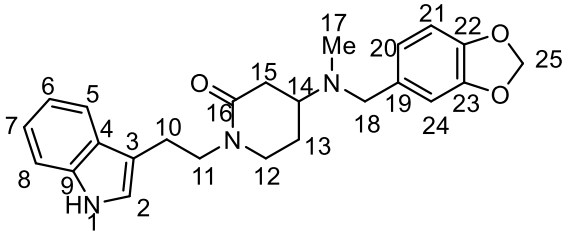

2.23

1-(2-(1H-Indol-3-yl)ethyl)-4-((benzo[d][1,3]dioxol-5-ylmethyl)(methyl)amino)piperidin-2-one (2.23) (LTL-IV-087). The title compound was prepared following the general procedure of **2.16**. The crude material was purified by flash column chromatography, eluting with hexanes:EtOAc:Et_3N (33:66:1) to furnish 14 mg (58%) of **2.23** as a white solid. ^{1}H NMR (400 MHz, $CDCl_3$) δ 8.16 (s, 1 H), 7.65 (d, *J* = 7.8 Hz, 1 H), 7.36 (d, J = 8.2 Hz, 1 H), 7.19 (ddd, *J* = 8.2, 7.0, 1.3 Hz, 1 H), 7.11 (ddd, *J* = 7.8, 7.0, 1.1 Hz, 1 H),

7.03 (d, *J* = 2.3 Hz, 1 H), 6.82 (d, *J* = 1.5 Hz, 1 H), 6.77 – 6.69 (comp, 2 H), 5.94 (s, 2 H), 3.74 – 3.58 (comp, 2 H), 3.45 (s, 2 H), 3.21 – 3.09 (comp, 2 H), 3.09 – 2.99 (comp, 2 H), 2.80 (dtd, *J* = 11.0, 5.8, 5.2, 3.5 Hz, 1 H), 2.62 (ddd, *J* = 16.9, 5.2, 2.2 Hz, 1 H), 2.44 (dd, *J* = 17.0, 10.8 Hz, 1 H), 2.16 (s, 3 H), 1.91 (d, *J* = 12.7 Hz, 1 H), 1.61 (dtd, *J* = 12.8, 11.1, 5.7 Hz, 1 H); ^{13}C NMR (100 MHz, $CDCl_3$) δ 169.4, 148.0, 146.9, 136.5, 127.8, 122.3, 122.2, 122.0, 119.6, 119.0, 113.5, 111.5, 109.3, 108.2, 101.2, 58.0, 56.7, 48.4, 47.0, 37.4, 35.1, 26.6, 23.3; IR (film, NaCl) 3260, 2927, 1625, 1489, 1442, 1343, 1302, 1240, 1096, 1038, 929, 807, 741 cm^{-1}; HRMS (ESI) *m/z* calc'd for $C_{24}H_{27}N_3O_3$ (M+Na)+ 428.1945; found 428.1939.

NMR Assignment. ^{1}H NMR (400 MHz, $CDCl_3$) δ 8.16 (s, 1 H, H1), 7.65 (d, *J* = 7.8 Hz, 1 H, H5), 7.36 (d, J = 8.2 Hz, 1 H, H8), 7.19 (ddd, *J* = 8.2, 7.0, 1.3 Hz, 1 H, H6), 7.11 (ddd, *J* = 7.8, 7.0, 1.1 Hz, 1 H, H7), 7.03 (d, *J* = 2.3 Hz, 1 H, H2), 6.82 (d, *J* = 1.5 Hz, 1 H, H24), 6.77 – 6.69 (comp, 2 H, H20, H21), 5.94 (s, 2 H, H25), 3.74 – 3.58 (comp, 2 H, H10), 3.45 (s, 2 H, H18), 3.21 – 3.09 (comp, 2 H, H12, H11), 3.09 – 2.99 (comp, 2 H, H12, H11), 2.80 (dtd, *J* = 11.0, 5.8, 5.2, 3.5 Hz, 1 H, H14), 2.62 (ddd, *J* = 16.9, 5.2, 2.2 Hz, 1 H, H15), 2.44 (dd, *J* = 17.0, 10.8 Hz, 1 H, H15), 2.16 (s, 3 H, H17), 1.91 (d, *J* = 12.7 Hz, 1 H, H13), 1.61 (dtd, *J* = 12.8, 11.1, 5.7 Hz, 1 H, H13); ^{13}C NMR (100 MHz, $CDCl_3$) δ 169.4 (C2), 148.0 (C23), 146.9 (C22), 136.5 (C9), 127.8 (C4), 122.3 (C6), 122.2 (C2), 122.0 (C20), 119.6 (C7), 119.0 (C5), 113.5 (C3), 111.5 (C8), 109.3 (C21), 108.2 (C24), 101.2 (C25), 58.0 (C18), 56.7 (C14), 48.4 (C10), 47.0 (C12), 37.4 (C15), 35.1 (C17), 26.6 (C13), 23.3 (C11).

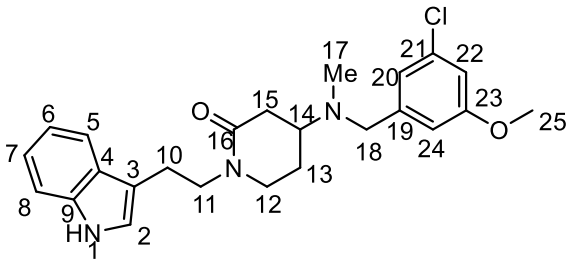

2.24

1-(2-(1H-Indol-3-yl)ethyl)-4-((3-chloro-5-methoxybenzyl)(methyl)amino)piperidin-2-one (2.24) (LTL-II-185). The title compound was prepared following the general procedure of

2.16. The crude material was purified via flash column chromatography, eluting with EtOAc:Et_3N (99:1) to furnish 19 mg (64%) of **2.24** as a pale yellow solid. ^{1}H NMR (400 MHz, $CDCl_3$) δ 8.16 (s, 1 H), 7.65 (d, *J* = 7.8 Hz, 1 H), 7.36 (dt, *J* = 8.1, 0.9 Hz, 1 H), 7.19 (ddd, *J* = 8.1, 7.0, 1.2 Hz, 1 H), 7.11 (ddd, *J* = 7.8, 7.0, 1.1 Hz, 1 H), 7.03 (d, *J* = 2.4 Hz, 1 H), 6.90 (app s, 1 H), 6.79 (t, *J* = 2.1 Hz, 1 H), 6.75 (app s, 1 H), 3.79 (s, 3 H), 3.73 – 3.59 (comp, 2 H), 3.47 (s, 2 H), 3.22 – 2.99 (comp, 4 H), 2.79 (tdd, *J* = 11.0, 5.2, 3.1 Hz, 1 H), 2.62 (ddd, *J* = 17.0, 5.2, 2.2 Hz, 1 H), 2.43 (dd, *J* = 17.0, 10.8 Hz, 1 H), 2.17 (s, 3 H), 1.90 (dt, *J* = 9.8, 3.6 Hz, 1 H), 1.60 (dtd, *J* = 12.8, 11.1, 5.7 Hz, 1 H); ^{13}C NMR (100 MHz, $CDCl_3$) δ 169.1, 160.3, 142.6, 136.2, 134.7, 127.5, 122.03, 121.94 120.8, 119.3, 118.8, 113.2, 112.73, 112.69, 111.2, 57.6, 56.7, 55.5, 48.1, 46.7, 37.4, 34.9, 26.3, 23.0; IR (NaCl, film) 3262, 3056, 2933, 2853, 2361, 1623, 1576, 1498, 1459, 1431, 1344, 1312, 1271, 1233, 1150, 1097, 1053, 980, 845, 743, 679, 621 cm^{-1}; HRMS (ESI) *m/z* calc'd for $C_{24}H_{28}ClN_3O_2$ (M+Na)+ 448.1762; found, 448.1758.

NMR Assignment. ^{1}H NMR (400 MHz, $CDCl_3$) δ 8.16 (s, 1 H, H1), 7.65 (d, *J* = 7.8 Hz, 1 H, H5), 7.36 (dt, *J* = 8.1, 0.9 Hz, 1 H, H8), 7.19 (ddd, *J* = 8.1, 7.0, 1.2 Hz, 1 H, H7), 7.11 (ddd, *J* = 7.8, 7.0, 1.1 Hz, 1 H, H6), 7.03 (d, *J* = 2.4 Hz, 1 H, H2), 6.90 (app s, 1 H, H22), 6.79 (t, *J* = 2.1 Hz, 1 H, H20), 6.75 (app s, 1 H, H24), 3.79 (s, 3 H, H25), 3.73 – 3.59 (comp, 2 H, H10), 3.47 (s, 2 H, H18), 3.22 – 2.99 (comp, 4 H, H12, H11), 2.79 (tdd, *J* = 11.0, 5.2, 3.1 Hz, 1 H, H14), 2.62 (ddd, *J* = 17.0, 5.2, 2.2 Hz, 1 H, H15), 2.43 (dd, *J* = 17.0, 10.8 Hz, 1 H, H15), 2.17 (s, 3 H, H17), 1.90 (dt, *J* = 9.8, 3.6 Hz, 1 H, H13), 1.60 (dtd, *J* = 12.8, 11.1, 5.7 Hz, 1 H, H13); ^{13}C NMR (100 MHz, $CDCl_3$) δ 169.1 (C16), 160.3 (C23), 142.6 (C19), 136.2 (C9), 134.7 (C21), 127.5 (C4), 122.03 (C6), 121.94 (C2), 120.8 (C20), 119.3 (C5), 118.8 (C7), 113.2 (C3), 112.73 (C22), 112.69 (C24), 111.2 (C8), 57.6 (C18), 56.7 (C14), 55.5 (C25), 48.1 (C10), 46.7 (C12), 37.4 (C15), 34.9 (C17), 26.3 (C13), 23.0 (C11).

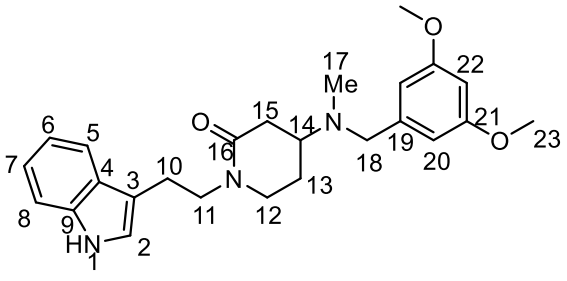

2.25

1-(2-(1H-Indol-3-yl)ethyl)-4-((3,5-dimethoxybenzyl)(methyl)amino)piperidin-2-one (2.25) (LTL-II-154). The title compound was prepared following the general procedure of **2.16**. The crude material was purified via flash column chromatography, eluting with hexanes:EtOAc:Et_3N (50:50:1 → 0:99:1) to furnish 31 mg (67%) of **2.25** as a white solid. ^{1}H NMR (400 MHz, $CDCl_3$) δ 8.31 (s, 1 H), 7.64 (d, *J* = 7.9 Hz, 1 H), 7.35 (dt, *J* = 8.1, 1.0 Hz, 1 H), 7.18 (ddd, *J* = 8.2, 7.0, 1.2 Hz, 1 H), 7.11 (ddd, *J* = 8.0, 7.0, 1.1 Hz, 1 H), 6.99 (d, *J* = 2.4 Hz, 1 H), 6.49 (d, *J* = 2.3 Hz, 2 H), 6.37 (t, *J* = 2.3 Hz, 1 H), 3.79 (s, 6 H), 3.73 – 3.57 (comp, 2 H), 3.49 (s, 2 H), 3.16 (ddd, *J* = 12.1, 5.5, 3.1 Hz, 1 H), 3.11 – 2.95 (comp, 3 H), 2.81 (tdd, *J* = 10.9, 5.0, 3.0 Hz, 1 H), 2.62 (ddd, *J* = 17.0, 5.2, 2.2 Hz, 1 H), 2.45 (dd, *J* = 17.0, 10.8 Hz, 1 H), 2.20 (s, 3 H), 1.94 – 1.86 (m, 1 H), 1.61 (dtd, *J* = 12.8, 11.2, 5.6 Hz, 1 H); ^{13}C NMR (100 MHz, $CDCl_3$) δ 170.1, 161.6, 137.0, 128.1, 122.64, 122.58, 119.9, 119.3, 113.7, 111.8, 107.0, 99.5, 58.5, 56.7, 55.6, 48.3, 46.9, 37.6, 35.1, 26.2, 23.1; IR (NaCl, film) 3261, 3057, 2936, 2840, 2792, 2243, 1613, 1498, 1457, 1430, 1344, 1299, 1234, 1204, 1154, 1101, 1065, 983, 910, 836, 739 cm^{-1}; HRMS (ESI) *m/z* calcd for $C_{25}H_{31}N_3O_3$ (M+Na)+ 444.2258; found 444.2252.

NMR Assignment. ^{1}H NMR (400 MHz, $CDCl_3$) δ 8.31 (s, 1 H, H1), 7.64 (d, *J* = 7.9 Hz, 1 H, H5), 7.35 (dt, *J* = 8.1, 1.0 Hz, 1 H, H8), 7.18 (ddd, *J* = 8.2, 7.0, 1.2 Hz, 1 H, H6), 7.11 (ddd, *J* = 8.0, 7.0, 1.1 Hz, 1 H, H7), 6.99 (d, *J* = 2.4 Hz, 1 H, H2), 6.49 (d, *J* = 2.3 Hz, 2 H, H20), 6.37 (t, *J* = 2.3 Hz, 1 H, H22), 3.79 (s, 6 H, H23), 3.73 – 3.57 (comp, 2 H, H10), 3.49 (s, 2 H, H18), 3.16 (ddd, *J* = 12.1, 5.5, 3.1 Hz, 1 H, H12), 3.11 – 2.95 (comp, 3 H, H12, H11), 2.81 (tdd, *J* = 10.9, 5.0, 3.0 Hz, 1 H, H14), 2.62 (ddd, *J* = 17.0, 5.2, 2.2 Hz, 1 H, H15), 2.45 (dd, *J* = 17.0, 10.8 Hz, 1 H, H15), 2.20 (s, 3 H, H17), 1.94 – 1.86 (m, 1 H, H13), 1.61 (dtd, *J* = 12.8, 11.2, 5.6 Hz, 1

H, H13); ^{13}C NMR (100 MHz, $CDCl_3$) δ 170.1 (C16), 161.6 (C21), 140.9 (C19), 137.0 (C9), 128.1 (C4), 122.64 (C6), 122.58 (C2), 119.9 (C5), 119.3 (C7), 113.7 (C3), 111.8 (C8), 107.0 (C20), 99.5 (C22), 58.5 (C18), 56.7 (C14), 55.6 (C23), 48.3 (C10), 46.9 (C12), 37.6 (C17), 35.1 (C15), 26.2 (C13), 23.1 (C11).

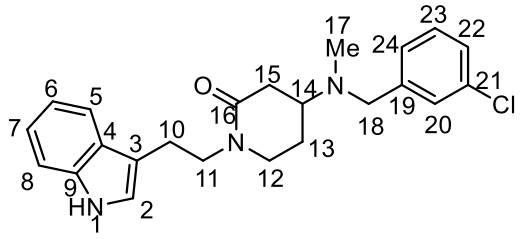

2.26

1-(2-(1H-Indol-3-yl)ethyl)-4-((3-chlorobenzyl)(methyl)amino)piperidin-2-one (2.26) (LTL-IV-013). The title compound was prepared following the general procedure of **2.16**. The crude material was purified via flash column chromatography, eluting with hexanes:EtOAc:Et_3N (50:50:1) to furnish 29 mg (81%) **2.26** as a pale yellow solid. ^{1}H NMR (400 MHz, $CDCl_3$) δ 8.15 (s, 0.89 H), 7.65 (d, *J* = 8 Hz, 1.24 H), 7.27 (m, 4.76 H), 7.21 (t, *J* = 7 Hz, 1.59 H), 7.13 (t, *J* = 7 Hz, 1.37 H), 7.05 (d, *J* = 2 Hz, 1.31 H), 3.74 (comp, 3.96 H), 3.12 (comp, 5.07 H), 2.69 (d, *J* = 18 Hz, 0.99 H), 2.53 (m, 0.83 H), 2.25 (s, 2.93 H), 2.10 (m, 1.21 H), 1.69 (m, 1.49 H); ^{13}C NMR (100 MHz, $CDCl_3$) δ 135.2, 133.3, 128.6, 127.6, 126.4, 123.8, 121.0, 120.9, 118.3, 117.7, 112.2, 110.2, 56.4, 55.8, 47.1, 45.6, 36.2, 33.7, 25.3, 22.0; IR (NaCl, film) 3251, 3055, 2925, 2853, 1742, 1626, 1575, 1497, 1456, 1433, 1344, 1303, 1260, 1231, 1161, 1097, 1075, 1030, 784, 742, 684 cm^{-1}; HRMS (ESI) *m/z* calcd for $C_{23}H_{26}ClN_3O$ (M+Na)+ 418.1657; found 418.1649.

NMR Assignment. ^{1}H NMR (400 MHz, $CDCl_3$) δ 8.15 (s, 0.89 H, H1), 7.65 (d, *J* = 8 Hz, 1.24 H, H5), 7.38 (d, *J* = 8 Hz, 2.80 H, H8) 7.27 (m, 4.76 H, H20, H22, H23, H24), 7.21 (t, *J* = 7 Hz, 1.59 H, H6), 7.13 (t, *J* = 7 Hz, 1.37 H, H7), 7.05 (d, *J* = 2 Hz, 1.31 H, H2), 3.74 (comp, 3.96 H, H10, H18), 3.12 (comp, 5.07 H, H12, H11, H14), 2.69 (d, *J* = 18 Hz, 0.99 H, H15), 2.53 (m, 0.83 H, H15), 2.25 (s, 2.93 H, H17), 2.10 (m, 1.21 H, H13), 1.69 (m, 1.49 H, H13); ^{13}C

NMR (100 MHz, $CDCl_3$) δ 135.2 (C9), 133.3 (C21), 128.6 (C23), 127.6 (C4), 126.6 (C22), 126.4 (C20), 123.8 (C24), 121.0 (C6), 120.9 (C2), 118.3 (C7), 117.7 (C5), 112.2 (C3), 110.2 (C8), 56.4 (C18), 55.8 (C14), 47.1 (C10), 45.6 (C12), 36.2 (C15), 33.7 (C17), 25.3 (C13), 22.0 (C11).

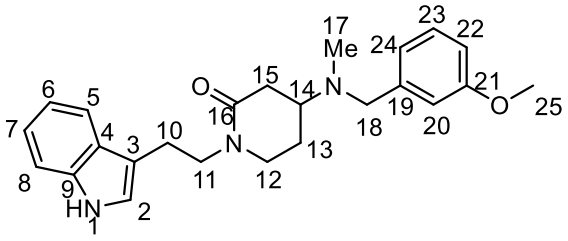

2.27

1-(2-(1H-Indol-3-yl)ethyl)-4-((3-methoxybenzyl)(methyl)amino)piperidin-2-one (2.27) (LTL-II-153). The title compound was prepared following the general procedure of **2.16**. The crude material was purified via flash column chromatography, eluting with EtOAc:Et_3N (99:1) to furnish 26 mg (60%) of **2.27** as a white solid. ^{1}H NMR (400 MHz, $CDCl_3$) δ 8.28 (s, 1 H), 7.64 (d, *J* = 7.6 Hz, 1 H), 7.35 (dt, *J* = 8.1, 0.9 Hz, 1 H), 7.23 (t, *J* = 8.0 Hz, 1 H), 7.18 (ddd, *J* = 8.1, 7.0, 1.3 Hz, 1 H), 7.11 (ddd, *J* = 8.0, 7.0, 1.1 Hz, 1 H), 7.00 (d, *J* = 2.4 Hz, 1 H), 6.92 – 6.84 (comp, 2 H), 6.81 (ddd, *J* = 8.2, 2.6, 1.1 Hz, 1 H), 3.81 (s, 3 H), 3.72 – 3.58 (comp, 2 H), 3.53 (s, 2 H), 3.16 (ddd, *J* = 12.1, 5.6, 3.1 Hz, 1 H), 3.13 – 2.95 (comp, 3 H), 2.81 (tdd, *J* = 11.0, 5.1, 3.1 Hz, 1 H), 2.64 (ddd, *J* = 16.9, 5.2, 2.2 Hz, 1 H), 2.46 (dd, *J* = 16.9, 10.8 Hz, 1 H), 2.19 (s, 3 H), 1.92 (d, *J* = 12.7 Hz, 1 H), 1.62 (dtd, *J* = 12.8, 11.2, 5.6 Hz, 1 H); ^{13}C NMR (100 MHz, $CDCl_3$) δ 169.2, 159.7, 136.3, 129.3, 127.5, 122.02, 121.97, 121.0, 119.3, 118.7, 114.2, 113.1, 112.5, 111.2, 58.0, 56.5, 55.2, 48.1, 46.7, 37.3, 34.9, 26.2, 23.0; IR (NaCl, film) 3261, 3055, 2935, 2852, 2791, 2360, 2242, 1624, 1491, 1456, 1344, 1304, 1268, 1152, 1011, 1043, 978, 910, 784, 743, 695 cm^{-1}; HRMS (ESI) *m/z* calcd for $C_{24}H_{29}N_3O_2$ (M+H)+ 392.2333; found 392.2329.

NMR assignment. ^{1}H NMR (400 MHz, $CDCl_3$) δ 8.28 (s, 1 H, H1), 7.64 (d, *J* = 7.6 Hz, 1 H, H5), 7.35 (dt, *J* = 8.1, 0.9 Hz, 1 H, H8), 7.23 (t, *J* = 8.0 Hz, 1 H, H23), 7.18 (ddd, *J* = 8.1, 7.0, 1.3 Hz, 1 H, H6), 7.11 (ddd, *J* = 8.0, 7.0, 1.1 Hz, 1 H, H7), 7.00 (d, *J* = 2.4 Hz, 1 H, H2),

6.92 – 6.84 (comp, 2 H, H20, H24), 6.81 (ddd, *J* = 8.2, 2.6, 1.1 Hz, 1 H, H22), 3.81 (s, 3 H, H25), 3.72 – 3.58 (comp, 2 H, H10), 3.53 (s, 2 H, H18), 3.16 (ddd, *J* = 12.1, 5.6, 3.1 Hz, 1 H, H12), 3.13 – 2.95 (comp, 3 H, H12, H11), 2.81 (tdd, *J* = 11.0, 5.1, 3.1 Hz, 1 H, H14), 2.64 (ddd, *J* = 16.9, 5.2, 2.2 Hz, 1 H, H15), 2.46 (dd, *J* = 16.9, 10.8 Hz, 1 H, H15), 2.19 (s, 3 H, H17), 1.92 (d, *J* = 12.7 Hz, 1 H, H13), 1.62 (dtd, *J* = 12.8, 11.2, 5.6 Hz, 1 H, H13); ^{13}C NMR (100 MHz, $CDCl_3$) δ 169.2 (C16), 159.7 (C21), 136.3 (C9), 129.3 (C24), 127.5 (C4), 122.02 (C6), 121.97 (C2), 121.0 (C23), 119.3 (C5), 118.7 (C7), 114.2 (C20), 113.1 (C3), 112.5 (C22), 111.2 (C8), 58.0 (C18), 56.5 (C14), 55.2 (C25), 48.1 (C10), 46.7 (C12), 37.3 (C15), 34.9 (C17), 26.2 (C13), 23.0 (C11).

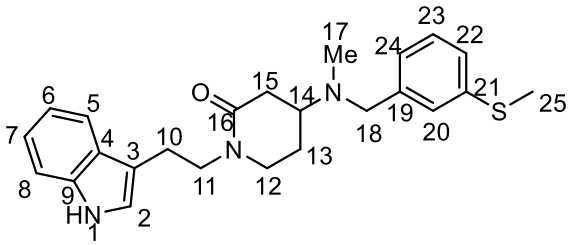

2.28

1-(2-(1H-Indol-3-yl)ethyl)-4-(methyl(3-(methylthio)benzyl)amino)piperidin-2-one (2.28) (LTL-II-157). The title compound was prepared following the general procedure of **2.16**. The crude material was purified via flash column chromatography, eluting with EtOAc:Et_3N (99:1) to furnish 32 mg (71%) of **2.28** as an off-white solid. ^{1}H NMR (400 MHz, $CDCl_3$) δ 8.28 (s, 1 H), 7.64 (d, *J* = 7.8 Hz, 1 H), 7.35 (dt, *J* = 8.1, 1.0 Hz, 1 H), 7.26 – 7.08 (comp, 5 H), 7.06 (dt, *J* = 7.5, 1.4 Hz, 1 H), 6.99 (d, *J* = 2.4 Hz, 1 H), 3.66 (t, *J* = 7.5 Hz, 2 H), 3.51 (s, 2 H), 3.16 (ddd, *J* = 12.1, 5.5, 3.1 Hz, 1 H), 3.12 – 2.96 (comp, 3 H), 2.80 (tdd, *J* = 11.0, 5.1, 3.1 Hz, 1 H), 2.63 (ddd, *J* = 16.9, 5.2, 2.2 Hz, 1 H), 2.48 (comp, 4 H), 2.18 (s, 3 H), 1.90 (dt, *J* = 12.8, 3.4 Hz, 1 H), 1.61 (dtd, *J* = 12.8, 11.2, 5.6 Hz, 1 H); ^{13}C NMR (100 MHz, $CDCl_3$) δ 169.2, 140.0, 138.4, 136.3, 128.8, 127.4, 126.6, 125.4, 125.1, 121.96, 119.26, 118.7, 113.1, 111.2, 57.8, 56.5, 48.1, 46.7, 37.3, 34.9, 26.3, 23.0, 15.8; IR (NaCl, film) 3261, 3054, 2922, 2854, 1622, 1498, 1456,

1344, 1303, 1232, 1158, 1100, 1030, 780, 743, 686 cm^{-1}; HRMS (ESI) *m/z* calcd for $C_{24}H_{29}N_3OS$ (M+Na)+ 430.1924; found 430.1920.

NMR assignment. ^{1}H NMR (400 MHz, $CDCl_3$) δ 8.28 (s, 1 H, H1), 7.64 (d, *J* = 7.8 Hz, 1 H, H5), 7.35 (dt, *J* = 8.1, 1.0 Hz, 1 H, H8), 7.26 – 7.08 (comp, 5 H, H24, H23, H20, H7, H6), 7.06 (dt, *J* = 7.5, 1.4 Hz, 1 H, H22), 6.99 (d, *J* = 2.4 Hz, 1 H, H2), 3.66 (t, *J* = 7.5 Hz, 2 H, H10), 3.51 (s, 2 H, H18), 3.16 (ddd, *J* = 12.1, 5.5, 3.1 Hz, 1 H, H12), 3.12 – 2.96 (comp, 3 H, H12, H11), 2.80 (tdd, *J* = 11.0, 5.1, 3.1 Hz, 1 H, H14), 2.63 (ddd, *J* = 16.9, 5.2, 2.2 Hz, 1 H, H15), 2.48 (comp, 4 H, H25, H15), 2.18 (s, 3 H, H17), 1.90 (dt, *J* = 12.8, 3.4 Hz, 1 H, H13), 1.61 (dtd, *J* = 12.8, 11.2, 5.6 Hz, 1 H, H13); ^{13}C NMR (100 MHz, $CDCl_3$) δ 169.2 (C16), 140.0 (C19), 138.4 (C21), 136.3 (C9), 128.8 (24), 127.4 (C4), 126.6 (C23), 125.4 (C20), 125.1 (C21), 122.0 (C6, C2), 119.3 (C7), 118.7 (C5), 113.1 (C3), 111.2 (C8), 57.8 (C18), 56.5 (C14), 48.1 (C10), 46.7 (C12), 37.3 (C15), 34.9 (C17), 26.3 (C13), 23.0 (C11), 15.8 (C15).

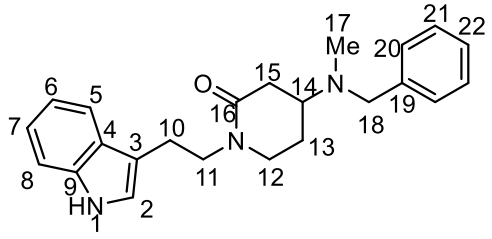

2.29

1-(2-(1H-Indol-3-yl)ethyl)-4-(benzyl(methyl)amino)piperidin-2-one (2.29) (LTL-IV-012). The title compound was prepared following the general procedure of **2.16**. The crude material was purified via flash column chromatography, eluting with EtOAc:Et_3N (99:1) to furnish 23 mg (70%) of **2.29** as a white solid. ^{1}H NMR (400 MHz, $CDCl_3$) δ 8.03 (s, 1 H), 7.65 (d, *J* = 7.8 Hz, 1 H), 7.36 (d, *J* = 8.2 Hz, 1 H), 7.34 – 7.26 (comp, 5 H), 7.19 (ddd, *J* = 8.2, 7.0, 1.2 Hz, 1 H), 7.12 (ddd, *J* = 8.0, 7.0, 1.1 Hz, 1 H), 7.03 (d, *J* = 2.3 Hz, 1 H), 3.66 (hept, *J* = 6.8, 6.1 Hz, 2 H), 3.56 (s, 2 H), 3.21 – 2.99 (comp, 4 H), 2.87 – 2.77 (m, 1 H), 2.69 – 2.61 (m, 1 H), 2.47 (dd, *J* = 17.0, 10.8 Hz, 1 H), 2.19 (s, 3 H), 1.98 – 1.89 (m, 1 H), 1.63 (qd, *J* = 11.5, 5.6 Hz, 1 H); ^{13}C NMR (100 MHz, $CDCl_3$) δ 136.2, 128.9, 128.4, 127.5, 122.05, 121.91, 119.4, 118.8,

113.2, 111.2, 57.9, 56.6, 48.1, 46.7, 26.3, 23.0; IR (NaCl, film) 2923, 2851, 2793, 2242, 1625, 1496, 1456, 1343, 1302, 1260, 1233, 1159, 1101, 1074, 1025, 909, 813, 741, 700 cm^{-1}; HRMS (ESI) *m/z* calcd for $C_{23}H_{27}N_3O$ (M+Na)+ 384.2046; found 384.2039.

NMR Assignment. ^{1}H NMR (400 MHz, $CDCl_3$) δ 8.03 (s, 1 H, H1), 7.65 (d, *J* = 7.8 Hz, 1 H, H5), 7.36 (d, *J* = 8.2 Hz, 1 H, H8), 7.34 – 7.26 (comp, 5 H, H22, H21, H20), 7.19 (ddd, *J* = 8.2, 7.0, 1.2 Hz, 1 H, H6), 7.12 (ddd, *J* = 8.0, 7.0, 1.1 Hz, 1 H, H7), 7.03 (d, *J* = 2.3 Hz, 1 H, H2), 3.66 (hept, *J* = 6.8, 6.1 Hz, 2 H, H10), 3.56 (s, 2 H, H18), 3.21 – 2.99 (comp, 4 H, H12, H11), 2.87 – 2.77 (m, 1 H, H14), 2.69 – 2.61 (m, 1 H, H15), 2.47 (dd, *J* = 17.0, 10.8 Hz, 1 H, H15), 2.19 (s, 3 H, H17), 1.98 – 1.89 (m, 1 H, H13), 1.63 (qd, *J* = 11.5, 5.6 Hz, 1 H, H13); ^{13}C NMR (100 MHz, $CDCl_3$) δ 136.2 (C9), 128.9 (C21), 128.4 (C20), 127.5 (C4), 122.05 (C6), 121.91 (C2), 119.4 (C7), 118.8 (C5), 113.2 (C3), 111.2 (C8), 57.9 (C18), 56.6 (C14), 48.1 (C10), 46.7 (C12), 26.3 (C13), 23.0 (C11).

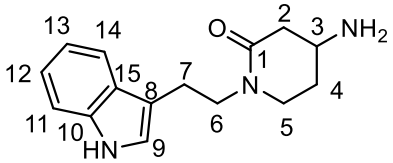

2.30

1-(2-(1H-Indol-3-yl)ethyl)-4-aminopiperidin-2-one (LTL-IV-011). A solution of **2.20** (26 mg, 0.1 mmol), NH_4OAc (144 mg, 2 mmol), and $NaBH_3CN$ (32 mg, 0.5 mmol) in MeOH (2 mL) was stirred while heating under reflux for 3 h, whereupon the solution was cooled to rt and diluted with 1 M aq NaOH. The aqueous layer was extracted with CH_2Cl_2 (3 x 20 mL), dried (Na_2SO_4) and concentrated via rotary evaporation. The crude material was purified by flash chromatography eluting with CH_2Cl_2:MeOH:Et_3N (97:3:1 → 95:5:1) to give 14 mg (54%) of **2.30** as a white solid. ^{1}H NMR (400 MHz, CD_3CN) δ 9.20 (s, 1 H), 7.64 (ddt, J = 7.8, 1.4, 0.8 Hz, 1 H), 7.40 (dt, J = 8.1, 1.0 Hz, 1 H), 7.15 (ddd, *J* = 8.2, 7.0, 1.3 Hz, 1H), 7.11 (d, *J* = 2.2 Hz, 1H), 7.07 (ddd, *J* = 8.0, 7.0, 1.1 Hz, 1H), 3.64 – 3.49 (comp, 2 H), 3.29 (dt, J = 12.1, 5.3 Hz, 1 H), 3.22 – 3.06 (comp, 2 H), 2.96 (dddd, J = 8.0, 7.2, 1.8, 0.9 Hz, 2 H), 2.47 (ddd, J = 17.0, 5.1,

1.8 Hz, 1 H), 2.05 – 1.98 (m, 1 H), 1.82 (dtdd, J = 13.2, 5.1, 3.2, 1.8 Hz, 1 H), 1.47 (dtdd, J = 13.0, 9.2, 5.4, 0.6 Hz, 1 H), 1.30 – 1.20 (m, 2 H); ^{13}C NMR (101 MHz, CD_3OD) δ 168.1, 136.7, 127.4, 122.1, 121.0, 118.3, 117.8, 111.6, 110.9, 48.6, 48.2, 45.6, 44.8, 38.0, 28.7, 22.4; IR (film, NaCl) 3728, 2926, 1617, 1500, 1456, 1343, 1304, 1261, 1232, 1158, 1103, 1016 cm $^{-1}$; HRMS (ESI) *m/z* calcd for $C_{15}H_{19}N_3O$ (M+Na)+ 280.1420; found 280.1427.

NMR Assignment. ^{1}H NMR (400 MHz, CD_3CN) δ 9.20 (s, 1 H, *N*-H), 7.64 (ddt, J = 7.8, 1.4, 0.8 Hz, 1 H, H14), 7.40 (dt, J = 8.1, 1.0 Hz, 1 H, H11), 7.15 (ddd, *J* = 8.2, 7.0, 1.3 Hz, 1H, H12), 7.11 (d, *J* = 2.2 Hz, 1H, H9), 7.07 (ddd, *J* = 8.0, 7.0, 1.1 Hz, 1H, H13), 3.64 – 3.49 (comp, 2 H, H6), 3.29 (dt, J = 12.1, 5.3 Hz, 1 H, H5), 3.22 – 3.06 (comp, 2 H, H5, H3), 2.96 (dddd, J = 8.0, 7.2, 1.8, 0.9 Hz, 2 H, H7), 2.47 (ddd, J = 17.0, 5.1, 1.8 Hz, 1 H, H2), 2.05 – 1.98 (m, 1 H, H2), 1.82 (dtdd, J = 13.2, 5.1, 3.2, 1.8 Hz, 1 H, H4), 1.47 (dtdd, J = 13.0, 9.2, 5.4, 0.6 Hz, 1 H, H4), 1.30 – 1.20 (m, 2 H, *N*-H_2)

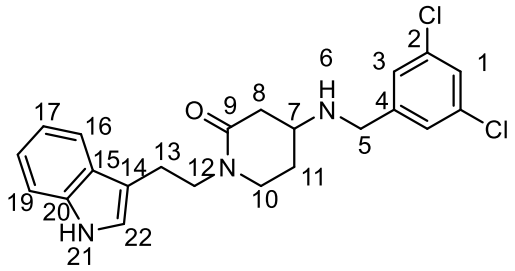

2.31

1-(2-(1H-Indol-3-yl)ethyl)-4-((3,5-dichlorobenzyl)amino)piperidin-2-one (2.31) (LTL-IV-006). A solution of **2.30** (20 mg, 0.08 mmol), 3,5-dichlorobenzaldehyde (15 mg, 0.09 mmol), and AcOH (0.08 mL, 0.08 mmol) in MeOH (1.5 mL) was stirred at room temperature for 3 h. Then, $NaBH_3CN$ (10 mg, 0.16 mmol) was added and the reaction was stirred for an additional 14 h, whereupon the reaction was diluted with saturated $NaHCO_3$ (20 mL) and extracted with CH_2Cl_2 (3 x 20 mL). The combined organic layers were dried (Na_2SO_4) and concentrated via rotary evaporation. The crude material was purified by flash column

chromatography, eluting with hexanes:EtOAc:Et_3N (50:50:1 → 0:100:1) to give 25 mg (78%) of **2.31** (25 mg, 78%) as a white foam. ^{1}H NMR (400 MHz, $CDCl_3$) δ 8.14 (s, 1 H), 7.68 – 7.62 (d, *J* = 8.1 Hz 1 H), 7.35 (d, *J* = 8.1 Hz, 1 H), 7.25 (t, *J* = 1.9 Hz, 1 H), 7.22 – 7.16 (comp, 3 H), 7.11 (m, 1 H), 7.04 (d, *J* = 2.3 Hz, 1 H), 3.78 – 3.59 (comp, 4 H), 3.21 (dt, *J* = 11.3, 5.4 Hz, 1 H), 3.15 – 3.01 (comp, 3 H), 2.92 (tdd, *J* = 8.4, 5.1, 3.1 Hz, 1 H), 2.67 (dd, *J* = 17.1, 5.2 Hz, 1 H), 2.24 (dd, *J* = 17.1, 8.2 Hz, 1 H), 1.93 – 1.81 (m, 1 H), 1.54 (m, 1 H). ^{13}C NMR (101 MHz, CDCl3) δ 168.2, 143.7, 136.2, 134.9, 127.5, 127.2, 126.3, 122.0, 121.9, 119.3, 118.7, 113.3, 111.2, 50.9, 49.9, 48.2, 45.6, 39.4, 29.0, 23.0; IR (NaCl, film) 3263, 3058, 2926, 2855, 1624, 1568, 1456, 1431, 1343, 1301, 1229, 1100 cm^{-1}. HRMS (ESI) *m/z* calcd for C_{22} $H_{23}Cl_2N_3O$ (M+H)+ 438.1112; found 438.1110.

NMR Assignment. ^{1}H NMR (400 MHz, $CDCl_3$) δ 8.14 (s, 1 H, H21), 7.68 – 7.62 (d, *J* = 8.1 Hz, 1 H, H16), 7.35 (d, *J* = 8.1 Hz, 1 H, H19), 7.25 (t, *J* = 1.9 Hz, 1 H, H1), 7.22 – 7.16 (comp, 3 H, H3, H18), 7.11 (m, 1 H, H17), 7.04 (d, *J* = 2.3 Hz, 1 H, H22), 3.78 – 3.59 (comp, 4 H, H5, H13), 3.21 (dt, *J* = 11.3, 5.4 Hz, 1 H, H10), 3.15 – 3.01 (comp, 3 H, H12, H10), 2.92 (tdd, *J* = 8.4, 5.1, 3.1 Hz, 1 H, H7), 2.67 (dd, *J* = 17.1, 5.2 Hz, 1 H, H8), 2.24 (dd, *J* = 17.1, 8.2 Hz, 1 H, H8), 1.93 – 1.81 (m, 1 H, H11), 1.54 (m, 1 H, H11). ^{13}C NMR (101 MHz, CDCl3) δ 168.20 (C9), 143.74 (C4), 136.23 (C20), 134.93 (C1), 127.47 (C15), 127.23 (C2), 126.32 (C3), 122.03 (C17), 121.93 (C22), 119.34 (C18), 118.73 (C16), 113.25 (C14), 111.18 (C19), 50.86 (C5), 49.90 (C7), 48.20 (C13), 45.64 (C10), 39.35 (C8), 28.97 (C11), 22.97 (C12).

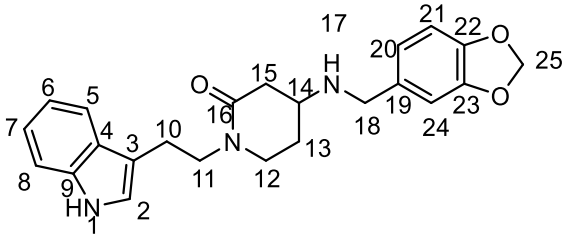

2.32

1-(2-(1H-Indol-3-yl)ethyl)-4-((benzo[d][1,3]dioxol-5-ylmethyl)amino)piperidin-2-one (2.32) (LTL-IV-007). The title compound was prepared following the general procedure of **2.31**.

The crude material was purified by flash column chromatography, eluting with hexanes:EtOAc:Et_3N (50:50:1 → 0:100:1) to give 23 mg (74%) of **2.32** (25 mg, 78%) as a white solid. ^{1}H NMR (400 MHz, $CDCl_3$) δ 8.24 (s, 0.78 H), 7.65 (d, *J* = 8 Hz, 0.88 H), 7.37 (d, *J* = 8 Hz, 0.96 H), 7.21 (t, *J* = 7 Hz, 1.00 H), 7.13 (t, *J* = 7 Hz, 0.97 H), 7.04 (d, *J* = 2 Hz, 0.92 H), 6.87 (s, 0.88 H), 6.80 (t, *J* = 8 Hz, 1.99 H), 5.95 (s, 2.15 H), 3.26 (comp, 4.10 H), 3.19 (comp, 4.18 H), 3.00 (m, 1.05 H), 2.74 (dd, *J* = 3 Hz, 17 Hz, 0.95 H), 2.39 (m, 0.96 H), 1.94 (m, 0.86 H), 1.68 (m, 1.03 H), 0.89 (m, 1.11 H); ^{13}C NMR (100 MHz, $CDCl_3$) δ 186.1, 147.8, 146.9, 136.2, 127.4, 122.0, 122.0, 121.5, 119.3, 118.7, 113.1, 111.2, 108.8, 108.2, 101.0, 50.4, 50.3, 48.1, 45.7, 38.8, 28.5, 23.0; IR (NaCl, film) 3264, 2925, 1622, 1502, 1490, 1444, 1244, 1302, 1249, 1100, 1038, 928, 810, 743 cm^{-1}; HRMS (ESI) *m/z* calcd for $C_{23}H_{25}N_3O_3$ (M+H)+ 392.1969; found 392.1969.

NMR assignment. ^{1}H NMR (400 MHz, $CDCl_3$) δ 8.24 (s, 0.78 H, H1), 7.65 (d, *J* = 8 Hz, 0.88 H, H5), 7.37 (d, *J* = 8 Hz, 0.96 H, H8), 7.21 (t, *J* = 7 Hz, 1.00 H, H6), 7.13 (t, *J* = 7 Hz, 0.97 H, H7), 7.04 (d, *J* = 2 Hz, 0.92 H, H2), 6.87 (s, 0.88 H, H20), 6.80 (t, *J* = 8 Hz, 1.99 H, H21, H24), 5.95 (s, 2.15 H, H25), 3.26 (comp, 4.10 H, H10, H18), 3.19 (comp, 4.18 H, H12, H11), 3.00 (m, 1.05 H, H14), 2.74 (dd, *J* = 3 Hz, 17 Hz, 0.95 H, H15), 2.39 (m, 0.96 H, H15), 1.94 (m, 0.86 H, H13), 1.68 (m, 1.03 H, H13), 0.89 (m, 1.11 H, H17); ^{13}C NMR (100 MHz, $CDCl_3$) δ 168.1 (C16), 147.8 (C23), 146.9 (C22), 136.2 (C9), 127.4 (C4), 122.0 (C6), 122.0 (C2), 121.5 (C20), 119.3 (C4), 118.7 (C5), 113.1 (C3), 111.2 (C8), 108.8 (C21), 108.2 (C24), 101.0 (C25), 50.4 (C18), 50.3 (C14), 48.1 (C10), 45.7 (C12), 38.8 (C15), 28.5 (C13), 23.0 (C11).

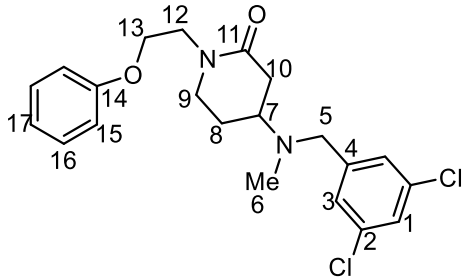

2.36

4-((3,5-Dichlorobenzyl)(methyl)amino)-1-(2-phenoxyethyl)piperidin-2-one (LTL-II-202). Powdered KOH (22.4 mg, 0.4 mmol) and **2.14** (30 mg, 0.1 mmol) were dissolved in DMSO (1 mL). Then *β*-bromophenetole (40.2 mg, 0.2 mmol) was added, and the reaction was stirred at room temperature for 2 h, whereupon it was poured into 1 M HCl (50 mL) and the aqueous layer was washed with hexanes (50 mL). 1 M NaOH was then added to the aqueous layer until the solution became opaque. The aqueous layer was then extracted with CH_2Cl_2 (3 x 50 mL). The combined organic layers were then dried (Na_2SO_4) and concentrated via rotary evaporation. The crude material was then purified by flash column chromatography, eluting with hexanes:EtOAc (2:1) to give 18 mg (44%) of **2.36** as a white solid. ^{1}H NMR (400 MHz, $CDCl_3$) δ 7.33 – 7.17 (comp, 5 H), 6.95 (tt, *J* = 7.3, 1.1 Hz, 1 H), 6.92 – 6.84 (comp, 2 H), 4.17 (t, *J* = 5.1 Hz, 2 H), 3.83 – 3.66 (comp, 2 H), 3.58 (ddd, *J* = 12.3, 5.5, 3.1 Hz, 1 H), 3.49 (d, *J* = 12.1 Hz, 3 H), 2.89 (tdd, *J* = 11.0, 5.2, 3.2 Hz, 1 H), 2.61 (ddd, *J* = 17.0, 5.3, 2.2 Hz, 1 H), 2.41 (dd, *J* = 17.0, 10.8 Hz, 1 H), 2.18 (s, 3 H), 2.05 (dq, *J* = 6.6, 3.4 Hz, 1 H), 1.75 (dtd, *J* = 12.9, 11.3, 5.5 Hz, 1 H) ppm; ^{13}C NMR (101 MHz, $CDCl_3$) δ 169.4, 158.5, 143.2, 134.9, 129.5, 127.2, 126.7, 121.0, 114.4, 66.4, 57.0, 48.1, 47.1, 37.4, 34.8, 26.6 ppm. IR (NaCl, film) 3064, 2938, 2872, 2791, 1644, 1599, 1568, 1496, 1456, 1433, 1341, 1301, 1242, 1172, 1153, 1125, 1098, 1079, 1046 cm^{-1}; HRMS (ESI) *m/z* calcd for $C_{21}H_{24}Cl_2N_2O_2$ (M+H)+ 407.1288; found 407.1291.

NMR Assignment. ^{1}H NMR (400 MHz, $CDCl_3$) δ 7.33 – 7.17 (m, 5 H, H1, H3, H14), 6.95 (tt, *J* = 7.3, 1.1 Hz, 1 H, H16), 6.92 – 6.84 (m, 2 H, H15), 4.17 (t, *J* = 5.1 Hz, 2 H, H13), 3.83 – 3.66 (m, 2 H, H12), 3.58 (ddd, *J* = 12.3, 5.5, 3.1 Hz, 1 H, H9), 3.49 (d, *J* = 12.1 Hz, 3 H, H9, H5), 2.89 (tdd, *J* = 11.0, 5.2, 3.2 Hz, 1 H, H7), 2.61 (ddd, *J* = 17.0, 5.3, 2.2 Hz, 1 H, H10), 2.41 (dd, *J* = 17.0, 10.8 Hz, 1 H, H10), 2.18 (s, 3 H, H6), 2.05 (dq, *J* = 6.6, 3.4 Hz, 1 H, H8), 1.75 (dtd, *J* = 12.9, 11.3, 5.5 Hz, 1 H, H8); ^{13}C NMR (101 MHz, $CDCl_3$) δ 169.38 (C11), 158.48 (C14), 143.21 (C4), 134.88 (C1), 129.51 (C16), 127.22 (C2), 126.71 (C3), 120.96 (C17), 114.36 (C15), 66.35 (C13), 57.02 (C7), 48.09 (C12), 47.13 (C9), 37.40 (C10), 34.77 (C6), 26.61 (C8).

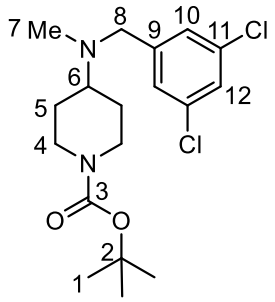

7.1

Tert-butyl 4-((3,5-dichlorobenzyl)(methyl)amino)piperidine-1-carboxylate (7.1) (LTL-IV-026). A solution of tert-butyl 4-(methylamino)piperidine-1-carboxylate (44 mg, 0.2 mmol), 3,5-dichlorobenzaldehyde (53 mg, 0.3 mmol), acetic acid (12 mg, 0.2 mmol), and sodium triacetoxyborohydride (85 mg, 0.4 mmol) in 1,2-dichloroethane (2 mL) was stirred at room temperature for 18 h, whereupon the solution was diluted with 1 M NaOH (15 mL) and extracted with Et_2O (3 x 15 mL). The combined organic extracts were dried (Na_2SO_4) and concentrated via rotary evaporation. The crude material was purified by flash chromatography eluting with hexane:EtOAc:Et_3N (95:5:1) to give 48 mg (64%) of **7.1** as an opaque white oil. ^{1}H NMR (400 MHz, $CDCl_3$ δ 7.23 – 7.19 (comp, 3 H), 4.16 (s, 2 H), 3.50 (s, 2 H), 2.75 – 2.61 (comp, 2 H), 2.55 (tt, J = 11.5, 3.6 Hz, 1 H), 2.17 (s, 3 H), 1.83 – 1.70 (comp, 2 H), 1.45 (comp, 11 H). ^{13}C NMR (101 MHz, $CDCl_3$) δ 154.7, 143.9, 134.7, 126.9, 126.7, 79.4, 61.1, 57.0, 43.1, 37.7, 28.4, 27.9; IR (NaCl, film) 2975, 2940, 2854, 2788, 1694, 1590, 1569, 1451, 1425, 1365, 1330, 1275, 1244, 1159, 1111, 1046, 1004 cm^{-1}. HRMS (ESI) *m/z* calcd for C_{18} $H_{26}Cl_2N_2O_2$ (M+H)+ 373.1444; found 373.1454.

NMR Assignment. ^{1}H NMR (400 MHz, $CDCl_3$ δ 7.23 – 7.19 (comp, 3 H, H12, H10), 4.16 (s, 2 H, H4), 3.50 (s, 2 H, H8), 2.75 – 2.61 (comp, 2 H, H4), 2.55 (tt, J = 11.5, 3.6 Hz, 1 H, H6), 2.17 (s, 3 H, H7), 1.83 – 1.70 (comp, 2 H, H5), 1.45 (comp, 11 H, H5, H1). ^{13}C NMR (101 MHz, $CDCl_3$) δ 154.7 (C3), 143.9 (C9), 134.7 (C12), 126.9 (C11), 126.7 (C10), 79.4 (C2), 61.1 (C6), 57.0 (C8), 43.1 (C4), 37.7 9C7), 28.4 (C1), 27.9 (C5).

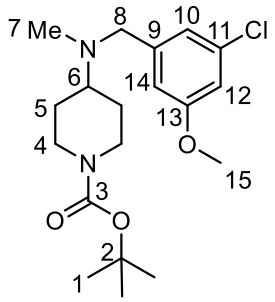

7.2

Tert-butyl 4-((3-chloro-5-methoxybenzyl)(methyl)amino)piperidine-1-carboxylate (7.2) (LTL-IV-027). The title compound was prepared following the general procedure of **7.1**. The crude material was purified via flash column chromatography, eluting with hexane:EtOAc:Et_3N (95:5:1) to give 57 mg (77%) of **7.2** as a clear oil. ^{1}H NMR (400 MHz, $CDCl_3$) δ 6.91 (t, J = 1.6 Hz, 1 H), 6.76 (d, J = 1.7 Hz, 2 H), 4.15 (s, 2 H), 3.78 (s, 3 H), 3.49 (s, 2 H), 2.68 (s, 2 H), 2.54 (tt, J = 11.4, 3.6 Hz, 1 H), 2.18 (s, 3 H), 1.77 (d, J = 12.8 Hz, 2 H), 1.45 (comp, 11 H). ^{13}C NMR (101 MHz, $CDCl_3$) δ 160.2, 154.7, 143.2, 134.6, 120.8, 112.6, 112.5, 79.4, 60.8, 57.5, 55.4, 43.1, 37.7, 28.4, 27.9; IR (NaCl, film) 2939, 2853, 2789, 1694, 1599, 1578, 1460, 1425, 1365, 1315, 1272, 1244, 1159, 1111, 1053 cm^{-1}. HRMS (ESI) *m/z* calcd for $C_{19}H_{29}ClN_2O_3$ (M+H)+ 369.1939; found 369.1944.

NMR Assignment. ^{1}H NMR (400 MHz, $CDCl_3$) δ 6.91 (t, J = 1.6 Hz, 1 H, H12), 6.76 (d, J = 1.7 Hz, 2 H, H10, H14), 4.15 (s, 2 H, H4), 3.78 (s, 3 H, H15), 3.49 (s, 2 H, H8), 2.68 (s, 2 H, H4), 2.54 (tt, J = 11.4, 3.6 Hz, 1 H, H6), 2.18 (s, 3 H, H7), 1.77 (d, J = 12.8 Hz, 2 H, H5), 1.45 (comp, 11 H, H5, H1). ^{13}C NMR (101 MHz, $CDCl_3$) δ 160.2 (C13), 154.7 (C3), 143.2 (C9), 134.6 (C11), 120.8 (C10), 112.6 (C12), 112.5 (C14), 79.4 (C2), 60.8 (C6), 57.5 (C8), 55.4 (C15), 43.1 (C4), 37.7 (C7), 28.4 (C1), 27.9 (C5).

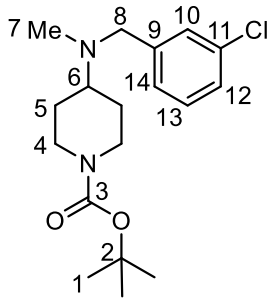

7.3

Tert-butyl 4-((3-chlorobenzyl)(methyl)amino)piperidine-1-carboxylate (7.3) (LTL-IV-028). The title compound was prepared following the general procedure of **7.1**. The crude material was dissolved in hexanes and a solution of HCl in 1,4-dioxane was added until the HCl salt of **7.3** precipitated out of solution. The suspension was decanted and washed with additional hexanes (2 x 10 mL), and the resultant residue was resuspended in 1M aq. NaOH (20 mL). The aqueous layer was extracted with Et_2O (3 x 15 mL), dried (Na_2SO_4) and concentrated via rotary evaporation to give 48 mg (71%) of **7.3** as a clear oil. ^{1}H NMR (300 MHz, $CDCl_3$) δ 7.33 (s, 1 H), 7.25 – 7.16 (comp, 3 H), 4.17 (s, 2 H), 3.54 (s, 2 H), 2.82 – 2.45 (comp, 3 H), 2.19 (s, 3 H), 1.79 (d, *J* = 12.6 Hz, 2 H), 1.46 (comp, 11 H); ^{13}C NMR (101 MHz, $CDCl_3$) δ 154.7, 142.2, 134.1, 129.4, 128.5, 127.0, 126.6, 79.4, 60.9, 57.4, 43.4 37.6, 28.4, 28.0; IR (NaCl, film) 2937, 2853, 2788, 1694, 1598, 1574, 1475, 1452, 1424, 1365, 1330, 1275, 1243, 1158, 1111, 1075, 1043, 1001 cm^{-1}. HRMS (ESI) *m/z* calcd for $C_{18}H_{27}ClN_2O_2$ (M+H)+ 339.1834; found 339.1842.

NMR Assignment. ^{1}H NMR (300 MHz, $CDCl_3$) δ 7.33 (s, 1 H, H10), 7.25 – 7.16 (comp, 3 H, H12, H13, H14), 4.17 (s, 2 H, H4), 3.54 (s, 2 H, H8), 2.82 – 2.45 (comp, 3 H, H4, H6), 2.19 (s, 3 H, H7), 1.79 (d, J = 12.6 Hz, 2 H, H5), 1.46 (comp, 11 H, H5, H1). ^{13}C NMR (101 MHz, $CDCl_3$) δ 154.7 (C3), 142.2 (C9), 134.1 (C11), 129.4 (C13), 128.5 (C10), 127.0 (C14), 126.6 (C12), 79.4 (C2), 60.9 (C6), 57.4 (C8), 43.4 (C4), 37.6 (C7), 28.4 (C1), 28.0 (C5).

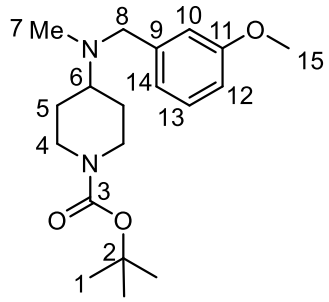

7.4

Tert-butyl 4-((3-methoxybenzyl)(methyl)amino)piperidine-1-carboxylate (7.4) (LTL-IV-016). The title compound was prepared following the general procedure of **7.1**. The crude material was purified by flash chromatography eluting with hexane/EtOAc/Et_3N (90:10:1) to give 44 mg (69%) of **7.4** as a clear oil. ^{1}H NMR (400 MHz, $CDCl_3$) δ 7.22 (t, J = 8.0 Hz, 1 H), 6.89 (dt, J = 3.6, 1.5 Hz, 2 H), 6.78 (ddd, J = 8.1, 2.6, 1.0 Hz, 1 H), 4.15 (s, 2 H), 3.80 (s, 3 H), 3.55 (s, 2 H), 2.67 (d, J = 13.4 Hz, 2 H), 2.62 – 2.51 (m, 1 H), 2.20 (s, 3 H), 1.79 (d, *J* = 12.6 Hz, 2H), 1.46 (s, 11 H); ^{13}C NMR (101 MHz, $CDCl_3$) δ 159.6, 154.7, 141.6, 129.1, 120.9, 114.0, 112.2, 79.3, 60.6, 57.9, 55.1, 43.4, 37.6, 28.4, 27.9; IR (NaCl, film) 2940, 2853, 2787, 1695, 1601, 1587, 1488, 1454, 1425, 1365, 1330, 1274, 1243, 1158, 1110, 1046, 1003 cm^{-1}. HRMS (ESI) *m/z* calcd for $C_{19}H_{30}N_2O_3$ (M+H)+ 335.2329; found 335.2324.

NMR Assignment. ^{1}H NMR (400 MHz, $CDCl_3$) δ 7.22 (t, J = 8.0 Hz, 1 H, H13), 6.89 (comp, 2 H, H12, H10), 6.78 (ddd, J = 8.1, 2.6, 1.0 Hz, 1 H, H14), 4.15 (s, 2 H, H4), 3.80 (s, 3 H, H15), 3.55 (s, 2 H, H8), 2.67 (d, J = 13.4 Hz, 2 H, H4), 2.62 – 2.51 (m, 1 H, H6), 2.20 (s, 3 H, H7), 1.79 (d, *J* = 12.6 Hz, 2H, H5), 1.46 (s, 11 H H5, H1); ^{13}C NMR (101 MHz, $CDCl_3$) δ 159.6 (C11), 154.7 (C3), 141.6 (C9), 129.1 (C13), 120.9 (C14), 114.0 (C10), 112.2 (C12), 79.3 (C2), 60.6 (C6), 57.9 (C8), 55.1 (C15), 43.4 (C4), 37.6 (C7), 28.4 (C1), 27.9 (C5);

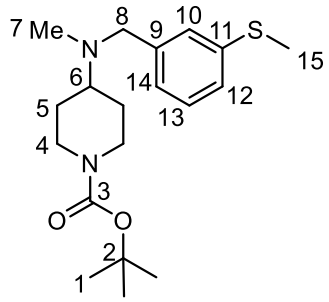

7.5

Tert-butyl 4-(methyl(3-(methylthio)benzyl)amino)piperidine-1-carboxylate (7.5) (LTL-IV-020). The title compound was prepared following the general procedure of **7.1**. The crude material was purified by flash chromatography eluting with hexane/EtOAc/Et_3N (90:10:1) to give 45 mg 967%) of **7.5** as an off-white oil. ^{1}H NMR (400 MHz, $CDCl_3$) δ 7.22 (s, 2 H), 7.12 (dt, J = 7.9, 1.3 Hz, 1 H), 7.10 – 7.05 (m, 1 H), 4.16 (s, 2 H), 3.53 (s, 2 H), 2.68 (t, J = 12.5 Hz, 2 H), 2.56 (tt, J = 11.3, 3.6 Hz, 1 H), 2.48 (s, 3 H), 2.19 (s, 3 H), 1.79 (d, J = 12.8 Hz, 2 H) 1.46 (comp, 11 H). ^{13}C NMR (101 MHz, $CDCl_3$) δ 154.7, 140.7, 138.2, 128.6, 126.7, 125.4, 124.9, 79.3, 60.8, 57.8, 43.4, 37.6, 28.4, 27.9, 15.8. IR (NaCl, film) 2975, 2929, 2854, 2787, 1695, 1592, 1574, 1474, 1425, 1365, 1330, 1275, 1243, 1159, 1110, 1082, 1043, 1001 cm^{-1}. HRMS (ESI) *m/z* calcd for $C_{19}H_{30}N_2O_2S$ (M+Na)+ 373.1920; found 373.1934.

NMR Assignment. ^{1}H NMR (400 MHz, $CDCl_3$) δ 7.22 (s, 2 H, H10, H12), 7.12 (dt, J = 7.9, 1.3 Hz, 1 H, H13), 7.10 – 7.05 (m, 1 H, H14), 4.16 (s, 2 H, H4), 3.53 (s, 2 H, H8), 2.68 (t, J = 12.5 Hz, 2 H, H4), 2.56 (tt, J = 11.3, 3.6 Hz, 1 H, H6), 2.48 (s, 3 H, H15), 2.19 (s, 3 H, H7), 1.79 (d, J = 12.8 Hz, 2 H, H5) 1.46 (comp, 11 H, H5, H1). ^{13}C NMR (101 MHz, $CDCl_3$) δ 154.7 (C3), 140.7 (C9), 138.2 (C11), 128.6 (C10), 126.7 (C13), 125.4 (C12), 124.9 (C14), 79.3 (C2), 60.8 (C6), 57.8 (C8), 43.4 (C4), 37.6 (C7), 28.4 (C1), 27.9 (C5), 15.8 (C15);

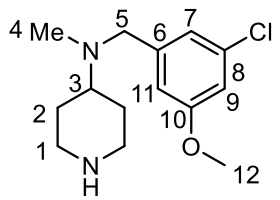

2.47

N-(3-Chloro-5-methoxybenzyl)-N-methylpiperidin-4-amine (2.47) (LTL-IV-033). A solution of tert-butyl 4-((3-chloro-5-methoxybenzyl)(methyl)amino)piperidine-1-carboxylate (52 mg, 0.14 mmol) and trifluoroacetic acid (160 mg, 1.4 mmol) in CH_2Cl_2 (2.8 mL) was stirred at room temperature for 24 h, whereupon the solvent was removed by rotary evaporation. The resulting solid was resuspended in 1 M HCl (20 mL) and washed with Et_2O (20 mL). 3 M NaOH was added to the aqueous layer until the solution became cloudy, whereupon it was extracted with CH_2Cl_2 (3 x 20 mL), dried (Na_2SO_4) and concentrated via rotary evaporation to give 33 mg, (87%) of **2.47** as a clear oil. ^{1}H NMR (400 MHz, $CDCl_3$) δ 6.92 (ddd, J = 1.9, 1.3, 0.6 Hz, 1 H), 6.79 – 6.74 (comp, 2 H), 3.78 (d, J = 0.5 Hz, 3 H), 3.51 (s, 2 H), 3.24 – 3.11 (comp, 2 H), 2.64 – 2.47 (comp, 3 H), 2.20 (s, 3 H), 1.80 (s, 2 H), 1.58 – 1.44 (comp, 2 H). ^{13}C NMR (101 MHz, $CDCl_3$) δ 160.2, 143.4, 134.5, 120.9, 112.7, 112.5, 60.9, 57.3, 55.4, 46.1, 37.6, 29.0. IR (NaCl, film) 3303, 2940, 2849, 2791, 1599, 1578, 1461, 1430, 1356, 1316, 1271, 1148, 1094, 1053, 1006 cm^{-1}. HRMS (ESI) *m/z* calcd for $C_{14}H_{21}ClN_2O$ (M+H)+ 269.1415; found 269.1418.

NMR Assignment. ^{1}H NMR (400 MHz, $CDCl_3$) δ 6.92 (ddd, J = 1.9, 1.3, 0.6 Hz, 1 H, H9), 6.79 – 6.74 (comp, 2 H, H7, H11), 3.78 (d, J = 0.5 Hz, 3 H, H12), 3.51 (s, 2 H, H5), 3.24 – 3.11 (comp, 2 H, H1), 2.64 – 2.47 (comp, 3 H, H1, H3), 2.20 (s, 3 H, H4), 1.80 (s, 2 H, H2), 1.58 – 1.44 (comp, 2 H, H2). ^{13}C NMR (101 MHz, $CDCl_3$) δ 160.2 (C10), 143.4 (C6), 134.5 (C8), 120.9 (C9), 112.7 (C7), 112.5 (C11), 60.9 (C3), 57.3 (C5), 55.4 (C12), 46.1 (C1), 37.6 (C4), 29.0 (C2).

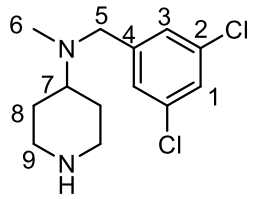

2.46

N-(3,5-Dichlorobenzyl)-N-methylpiperidin-4-amine (2.46) (LTL-IV-032). The title compound was prepared following the general procedure of **2.47** to give 25 mg (76%) of **2.46** as a yellow paste. ^{1}H NMR (400 MHz, $CDCl_3$) δ 7.22 (t, *J* = 0.6 Hz, 3 H), 3.52 (s, 2 H), 3.18 (d, *J* =

12.2 Hz, 2 H), 2.66 – 2.46 (m, 4 H), 2.19 (s, 3 H), 1.51 (qd, *J* = 12.1, 4.1 Hz, 3 H); ^{13}C NMR (100 MHz, $CDCl_3$) δ 144.1, 134.7, 126.9, 126.8, 61.1, 56.9, 46.1, 37.7, 29.0; IR (NaCl, film) 2941, 2851, 2791, 1589, 1568, 1449, 1432, 1384, 1353, 1273, 1208, 1045 cm^{-1}; HRMS (ESI) *m/z* calcd for $C_{13}H_{18}Cl_2N_2$ (M+H)+ 273.0920; found 273.0923.

NMR Assignments. ^{1}H NMR (400 MHz, $CDCl_3$) δ 7.22 (t, *J* = 0.6 Hz, 3 H, H1, H3), 3.52 (s, 2 H, H5), 3.18 (d, *J* = 12.2 Hz, 2 H, H9), 2.66 – 2.46 (m, 3 H, H9, H7), 2.19 (s, 3 H, H6), 1.81 (d, *J* = 12.2 Hz, 2 H, H8) 1.51 (qd, *J* = 12.1, 4.1 Hz, 2 H, H8); ^{13}C NMR (100 MHz, $CDCl_3$) δ 144.13 (C4), 134.71 (C1), 126.93 (C2), 126.78 (C3), 61.14 (C7), 56.86 (C5), 46.11 (C9), 37.72 (C6), 28.99 (C8).

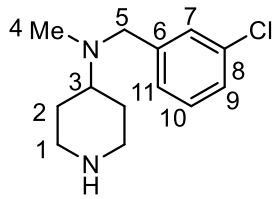

2.56

N-(3-Chlorobenzyl)-N-methylpiperidin-4-amine (2.56) (LTL-IV-031). The title compound was prepared following the general procedure of **2.47** to give 15 mg (79%) of **2.56** as a yellow oil. ^{1}H NMR (400 MHz, $CDCl_3$) δ 7.34 – 7.31 (m, 1 H), 7.25 – 7.16 (comp, 3 H), 3.54 (s, 2 H), 3.15 (dt, J = 12.7, 3.4 Hz, 2 H), 2.64 – 2.46 (comp, 3 H), 2.19 (s, 3 H), 1.82 (dt, J = 12.7, 2.7 Hz, 2 H), 1.49 (qd, J = 12.3, 4.3 Hz, 2 H). ^{13}C NMR (101 MHz, $CDCl_3$) δ 142.5, 134.1, 129.4, 128.6, 126.9, 126.6, 61.2, 57.2, 46.3, 37.6, 29.3. IR (NaCl, film) 3291, 3061, 2939, 2850, 2789, 1597, 1574, 1472, 1451, 1429, 1356, 1324, 1260, 1209, 1147, 1075, 1043, 1003 cm^{-1}. HRMS (ESI) *m/z* calcd for $C_{13}H_{19}ClN_2$ (M+H)+ 239.1310; found 239.1313.

NMR Assignment. ^{1}H NMR (400 MHz, $CDCl_3$) δ 7.34 – 7.31 (m, 1 H, H7), 7.25 – 7.16 (comp, 3 H, H9, H10, H11), 3.54 (s, 2 H, H5), 3.15 (dt, J = 12.7, 3.4 Hz, 2 H, H1), 2.64 – 2.46 (comp, 3 H, H1, H3), 2.19 (s, 3 H, H4), 1.82 (dt, J = 12.7, 2.7 Hz, 2 H, H2), 1.49 (qd, J = 12.3,

4.3 Hz, 2 H, H2). ^{13}C NMR (101 MHz, $CDCl_3$) δ 142.5 (C6), 134.1 (C8), 129.4 (C10), 128.6 (C7), 126.9 (C11), 126.6 (C9), 61.2 (C3), 57.2 (C5), 46.3 (C1), 37.6 (C4), 29.3 (C2).

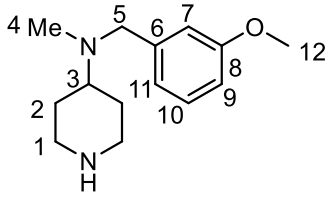

2.57

N-(3-Methoxybenzyl)-N-methylpiperidin-4-amine (2.57) (LTL-IV-029). The title compound was prepared following the general procedure of **2.47** to give 15 mg (79%) of **2.57** as a yellow oil. ^{1}H NMR (400 MHz,$CDCl_3$) δ 7.21 (t, J = 8.0 Hz, 1 H), 6.92 – 6.87 (comp, 2 H), 6.78 (ddd, J = 8.3, 2.6, 1.0 Hz, 1 H), 3.80 (s, 3 H), 3.55 (s, 2 H), 3.19 – 3.09 (d, J = 12.3 Hz, 2 H), 2.62 – 2.47 (comp, 3 H), 2.21 (s, 3 H), 1.87 – 1.79 (br, 2 H), 1.51 (td, J = 12.1, 4.0 Hz, 2 H). ^{13}C NMR (101 MHz, $CDCl_3$) δ 159.6, 141.8, 129.1, 121.0, 114.1, 112.2, 61.0, 57.7, 55.1, 46.4, 37.6, 29.3. IR (NaCl, film) 3306, 2939, 2839, 2788, 1691, 1600, 1488, 1454, 1361, 1318, 1269, 1150, 1046 cm^{-1}. HRMS (ESI) *m/z* calcd for $C_{14}H_{22}N_2O$ (M+H)+ 235.1805; found 235.1805.

NMR Assignment. ^{1}H NMR (400 MHz,$CDCl_3$) δ 7.21 (t, J = 8.0 Hz, 1 H, H10), 6.92 – 6.87 (comp, 2 H, H7, H9), 6.78 (ddd, J = 8.3, 2.6, 1.0 Hz, 1 H, H11), 3.80 (s, 3 H, H12), 3.55 (s, 2 H, H5), 3.19 – 3.09 (d, J = 12.3 Hz, 2 H, H1), 2.62 – 2.47 (comp, 3 H, H1, H3), 2.21 (s, 3 H, H4), 1.87 – 1.79 (comp, 2 H, H2), 1.51 (td, J = 12.1, 4.0 Hz, 2 H, H2). ^{13}C NMR (101 MHz, $CDCl_3$) δ 159.6 (C8), 141.8 (C6), 129.1 (C10), 121.0 (C11), 114.1 (C7), 112.2 (C9), 61.0 (C3), 57.7 (C5), 55.1 (C12), 46.4 (C1), 37.6 (C4), 29.3 (C2).

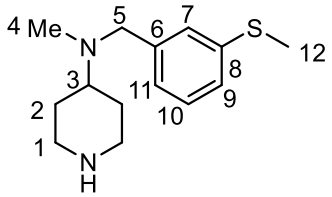

2.58

N-Methyl-N-(3-(methylthio)benzyl)piperidin-4-amine (2.58) (LTL-IV-034). The title compound was prepared following the general procedure of **2.47** to give 23 mg (84%) of **2.58** as a pale yellow oil. ^{1}H NMR (400 MHz, $CDCl_3$) δ 7.25 – 7.19 (comp, 2 H), 7.12 (ddd, J = 7.8, 2.0, 1.2 Hz, 1 H), 7.10 – 7.06 (m, 1 H), 3.54 (s, 2 H), 3.19 – 3.08 (comp, 2 H), 2.62 – 2.45 (comp, 6 H), 2.19 (s, 3 H), 1.85 (d, J = 8.8 Hz, 2 H), 1.56 – 1.42 (comp, 2 H); ^{13}C NMR (101 MHz, $CDCl_3$) δ 140.9, 138.1, 128.6, 126.8, 125.5, 124.9, 61.0, 57.6, 46.4, 37.6, 29.3, 15.8; IR (NaCl, film) 3292, 2938, 2850, 2790, 1591, 1572, 1471, 1422, 1356, 1325, 1273, 1213, 1147, 1084, 1042 cm^{-1}. HRMS (ESI) *m/z* calcd for $C_{14}H_{22}N_2S$ (M+H)+ 251.1576; found 251.1584.

NMR Assignment. ^{1}H NMR (400 MHz, $CDCl_3$) δ 7.25 – 7.19 (comp, 2 H, H7, H9), 7.12 (ddd, J = 7.8, 2.0, 1.2 Hz, 1 H, H10), 7.10 – 7.06 (m, 1 H, H11), 3.54 (s, 2 H, H5), 3.19 – 3.08 (comp, 2 H, H1), 2.62 – 2.45 (comp, 6 H, H1, H3, H12), 2.19 (s, 3 H, H4), 1.85 (d, J = 8.8 Hz, 2 H, H2), 1.56 – 1.42 (comp, 2 H, H2); ^{13}C NMR (101 MHz, $CDCl_3$) δ 140.9 (C6), 138.1 (C8), 128.6 (C7), 126.8 (C10), 125.5 (C9), 124.9 (C11), 61.0 (C3), 57.6 (C5), 46.4 (C1), 37.6 (C4), 29.3 (C2), 15.8 (C12).

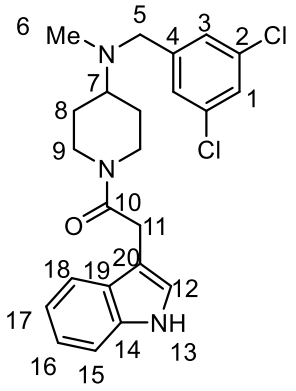

2.51

1-(4-((3,5-Dichlorobenzyl)(methyl)amino)piperidin-1-yl)-2-(1H-indol-3-yl)ethan-1-one (2.51) (LTL-II-269). Indole-3-acetic acid (72 mg, 0.41 mmol) was suspended in CH_2Cl_2 (4 mL), then EDCI-HCl (79 mg, 0.41 mmol) and iPr_2NEt (0.14 mL, 0.82 mmol) were added. **2.46** dissolved in CH_2Cl_2 (1 mL) was then added, followed by DMAP (5 mg, 0.04 mmol). The

reaction was stirred at room temperature for 24 hours whereupon it was diluted with CH_2Cl_2 (25 mL) and washed with 1 M aq. NaOH (50 mL). The aqueous layer was then extracted with an additional volume of CH_2Cl_2 (25 mL). The organic layers were combined and dried (Na_2SO_4) and concentrated *in vacuo* to give a yellow oil. Purification via flash column chromatography, eluting with 50 : 50 : 1 hexanes : ethyl acetate : TEA gave 67 mg (42%) of **2.51** as a white solid. ^{1}H NMR (400 MHz, $CDCl_3$) δ 8.17 (s, 1 H), 7.65 (dq, *J* = 7.9, 0.9 Hz, 1 H), 7.35 (dt, *J* = 8.1, 1.0 Hz, 1 H), 7.22 (t, *J* = 2.0 Hz, 1 H), 7.19 (ddd, *J* = 8.2, 7.0, 1.2 Hz, 1 H), 7.16 - 7.14 (m, 2 H), 7.13 (ddd, *J* = 8.0, 7.1, 1.1 Hz, 1 H), 7.09 (dd, *J* = 2.3, 1.1 Hz, 1 H), 4.74 (d, *J* = 13.7 Hz, 1 H), 4.05 – 3.93 (m, 1 H), 3.86 (dd, *J* = 4.4, 1.0 Hz, 2 H), 3.37 (s, 2 H), 2.93 (td, *J* = 12.9, 2.7 Hz, 1 H), 2.55 (td, *J* = 11.2, 10.6, 3.0 Hz, 2 H), 2.07 (s, 3 H), 1.80 (d, *J* = 13.0 Hz, 1 H), 1.58 (d, *J* = 13.0 Hz, 1 H), 1.40 (qd, *J* = 12.3, 4.4 Hz, 1 H), 1.12 (qd, *J* = 12.3, 4.3 Hz, 1 H) ppm; ^{13}C NMR (126 MHz, $CDCl_3$) δ 170.1, 144.0, 136.4, 135.0, 127.3, 127.3, 126.9, 122.6, 122.5, 119.9, 119.1, 111.4, 109.8, 61.1, 57.1, 46.1, 41.8, 37.9, 31.9, 28.7, 27.7 ppm; IR (NaCl, film) 3058, 2926, 2857, 2790, 1624, 1568, 1454, 1434, 1353, 1268, 1227, 1149, 1125, 1098, 1047 cm^{-1}; HRMS (ESI) *m/z* calcd for $C_{23}H_{25}Cl_2N_3O$ (M+Na)+ 452.1267; found, 452.1268.

NMR Assignment. ^{1}H NMR (400 MHz, $CDCl_3$) δ 8.17 (s, 1 H, H13), 7.65 (dq, *J* = 7.9, 0.9 Hz, 1 H, H18), 7.35 (dt, *J* = 8.1, 1.0 Hz, 1 H, H15), 7.22 (t, *J* = 2.0 Hz, 1 H, H1), 7.19 (ddd, *J* = 8.2, 7.0, 1.2 Hz, 1 H, H16), 7.16 - 7.14 (m, 2 H, H3), 7.13 (ddd, *J* = 8.0, 7.1, 1.1 Hz, 1 H, H17), 7.09 (dd, *J* = 2.3, 1.1 Hz, 1 H, H12), 4.74 (d, *J* = 13.7 Hz, 1 H, H9), 3.99 (d, *J* = 13.7 Hz, 1 H, H9), 3.86 (dd, *J* = 4.4, 1.0 Hz, 2 H, H11), 3.37 (s, 2 H, H5), 2.93 (td, *J* = 12.9, 2.7 Hz, 1 H, H9), 2.55 (td, *J* = 11.2, 10.6, 3.0 Hz, 2 H, H9), 2.07 (s, 3 H, H6), 1.80 (d, *J* = 13.0 Hz, 1 H, H8), 1.58 (d, *J* = 13.0 Hz, 1 H, H8) 1.40 (qd, *J* = 12.3, 4.4 Hz, 1 H, H8), 1.12 (qd, *J* = 12.3, 4.3 Hz, 1 H, H8) ppm; ^{13}C NMR (126 MHz, $CDCl_3$) δ 170.1 (C10), 144.0 (C4), 136.4 (C14), 135.0 (C1), 127.3 (C2), 127.3 (C3), 126.9 (C19), 122.6 (C17), 122.5 (C12), 120.0 (C16), 119.1 (C18), 111.4 (C20), 109.9 (C15), 61.1 (C7), 57.1 (C5), 46.1 (C9), 41.8 (C11), 37.9 (C6), 28.7 (C8).

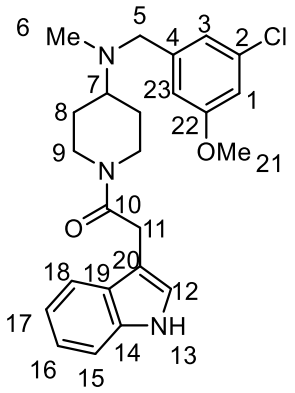

2.52

1-(4-((3-Chloro-5-methoxybenzyl)(methyl)amino)piperidin-1-yl)-2-(1H-indol-3-yl)ethan-1-one (2.52) (LTL-II-259). Following the general procedure described for **2.51**, 30 mg (31%) of **2.52** was obtained as a white solid. ^{1}H NMR (400 MHz, $CDCl_3$) δ 8.16 (s, 1 H), 7.65 (ddt, *J* = 7.8, 1.5, 0.8 Hz, 1 H), 7.36 (dt, *J* = 8.1, 1.0 Hz, 1 H), 7.20 (ddd, *J* = 8.2, 7.0, 1.3 Hz, 1 H), 7.13 (ddd, *J* = 8.0, 7.0, 1.1 Hz, 1 H), 7.09 (dt, *J* = 2.3, 1.0 Hz, 1 H), 6.86 (dd, *J* = 2.0, 1.3 Hz, 1 H), 6.76 (t, *J* = 2.2 Hz, 1 H), 6.72 (dd, *J* = 2.5, 1.3 Hz, 1 H), 4.79 – 4.68 (m, 1 H), 4.05 – 3.92 (m, 1 H), 3.90 – 3.84 (comp, 2 H), 3.78 (s, 3 H), 3.39 (s, 2 H), 2.98 – 2.87 (m, 1 H), 2.63 – 2.49 (comp, 2 H), 2.09 (s, 3 H), 1.81 (d, *J* = 12.9 Hz, 1 H), 1.63 (d, *J* = 12.9 Hz, 1 H), 1.49 – 1.32 (comp, 3 H), 1.22 – 1.10 (comp, 2 H); ^{13}C NMR (101 MHz, $CDCl_3$) δ 169.8, 160.7, 143.1, 136.1, 134.6, 127.1, 122.3, 122.2, 120.8, 119.7, 118.8, 112.7, 112.5, 111.2, 109.6, 60.4, 57.4, 55.5, 45.9, 41.6, 37.7, 31.6, 28.4, 27.5; IR (NaCl, film) 3057, 2933, 2862, 2791, 1624, 1576, 1458, 1355, 1315, 1228, 1150, 1097, 1052 cm^{-1}; HRMS (ESI) *m/z* calcd for $C_{24}H_{28}ClN_3O_2$ (M+Na)+ 448.1762; found 448.1764.

NMR Assignment. ^{1}H NMR (400 MHz, $CDCl_3$) δ 8.16 (s, 1 H, H13), 7.65 (ddt, *J* = 7.8, 1.5, 0.8 Hz, 1 H, H18), 7.36 (dt, *J* = 8.1, 1.0 Hz, 1 H, H15), 7.20 (ddd, *J* = 8.2, 7.0, 1.3 Hz, 1 H, H16), 7.13 (ddd, *J* = 8.0, 7.0, 1.1 Hz, 1 H, H17), 7.09 (dt, *J* = 2.3, 1.0 Hz, 1 H, H12), 6.86 (dd, *J* = 2.0, 1.3 Hz, 1 H, H1), 6.76 (t, *J* = 2.2 Hz, 1 H, H3), 6.72 (dd, *J* = 2.5, 1.3 Hz, 1 H, H22), 4.79 – 4.68 (m, 1 H, H9), 4.05 – 3.92 (m, 1 H, H9), 3.90 – 3.84 (m, 2 H, H11), 3.78 (s, 3 H, H21), 3.39 (s, 2 H, H5), 2.98 – 2.87 (m, 1 H, H9), 2.63 – 2.49 (m, 2 H, H9, H7), 2.09 (s, 3 H, H6), 1.81 (d, *J*

= 12.9 Hz, 1 H, H8), 1.63 (d, *J* = 12.9 Hz, 1 H, H8), 1.49 – 1.32 (m, 3 H, H8), 1.22 – 1.10 (m, 2 H, H8); ^{13}C NMR (101 MHz, $CDCl_3$) δ 169.8 (C10), 160.7 (C23), 143.1 (C4), 136.1 (C14), 134.6 (C2), 127.1 (C19), 122.3 (C13), 122.2 (C12), 120.8 (C3), 119.7 (C18), 118.8 (C16), 112.7 (C1), 112.5 (C22), 111.2 (C20), 109.6 (C15), 60.4 (C7), 57.4 (C5), 55.5 (C21), 45.9 (C9), 41.6 (C11), 37.7 (C6), 31.6 (C8);

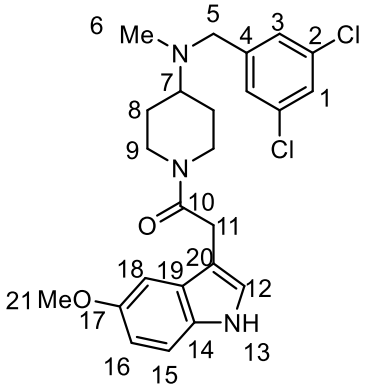

2.53

1-(4-((3,5-Dichlorobenzyl)(methyl)amino)piperidin-1-yl)-2-(5-methoxy-1H-indol-3-yl)ethan-1-one (2.53) (LTL-II-278). Following the genearl procedure described for **2.51**, 45 mg (54%) of **2.53** was obtained as a white solid. ^{1}H NMR (400 MHz, $CDCl_3$) δ 8.31 (s, 1 H), 7.23 – 7.20 (comp, 2 H), 7.16 – 7.14 (comp, 2 H), 7.10 – 7.08 (m, 1 H), 7.03 – 7.01 (m, 1 H), 6.84 (ddd, *J* = 8.8, 2.5, 0.4 Hz, 1 H), 4.74 (dt, *J* = 13.3, 2.2 Hz, 1 H), 4.04 – 3.93 (m, 1 H), 3.88 – 3.77 (comp, 5 H), 3.36 (s, 2 H), 2.92 (ddd, *J* = 13.5, 12.3, 2.7 Hz, 1 H), 2.55 (tt, *J* = 12.5, 3.1 Hz, 2 H), 2.06 (s, 3 H), 1.85 – 1.75 (m, 1 H), 1.67 – 1.55 (m, 1 H), 1.46 – 1.33 (m, 1 H), 1.21 – 1.03 (m, 1 H); ^{13}C NMR (101 MHz, $CDCl_3$) δ 169.8, 154.1, 143.7, 134.7, 131.3, 127.4, 127.0, 126.6, 123.0, 112.4, 111.9, 109.0, 100.5, 77.3, 77.2, 77.0, 76.7, 60.7, 57.0, 56.8, 55.9, 45.8, 41.5, 37.6, 31.9, 31.8, 29.7, 29.6, 29.3, 29.2, 28.4, 27.8, 27.4, 26.1, 22.5, 14.0; IR (NaCl, film) 2926, 2855, 1623, 1588, 1568, 1487, 1452, 1354, 1270, 1216, 1170, 1098, 1056 cm^{-1}; HRMS (ESI) *m/z* calcd for $C_{24}H_{27}Cl_2N_3O_2$ (M+H)+ 460.1553; found 460.1560.

NMR Assignment. ^{1}H NMR (400 MHz, $CDCl_3$) δ 8.31 (s, 1 H, H13), 7.23 – 7.20 (m, 2 H, H1, H15), 7.16 – 7.14 (m, 2 H, H3), 7.10 – 7.08 (m, 1 H, H18), 7.03 – 7.01 (m, 1 H, H12), 6.84 (ddd, *J* = 8.8, 2.5, 0.4 Hz, 1 H, H16), 4.74 (dt, *J* = 13.3, 2.2 Hz, 1 H, H9), 4.04 – 3.93 (m, 1 H, H9), 3.88 – 3.77 (m, 5 H, H21, H11), 3.36 (s, 2 H, H5), 2.92 (ddd, *J* = 13.5, 12.3, 2.7 Hz, 1 H, H9), 2.55 (m, 2 H, H9, H7), 2.06 (s, 3 H, H6), 1.85 – 1.75 (m, 1 H, H8), 1.67 – 1.55 (m, 1 H, H8), 1.46 – 1.33 (m, 1 H, H8), 1.21 – 1.03 (m, 1 H, H8); ^{13}C NMR (101 MHz, $CDCl_3$) δ 169.9 (C10), 154.1 (C17), 143.8 (C4), 134.7 (C1), 131.3 (C14), 127.4 (C2), 127.0 (C3), 126.7 (C19), 123.1 (C12), 112.5 (C16), 112.0 (C15), 109.1 (C20), 100.5 (C18), 60.8 (C7), 56.8 (C5), 55.9 (C21), 45.9 (C9), 41.6 (C11), 37.6 (C6), 28.4 (C8);

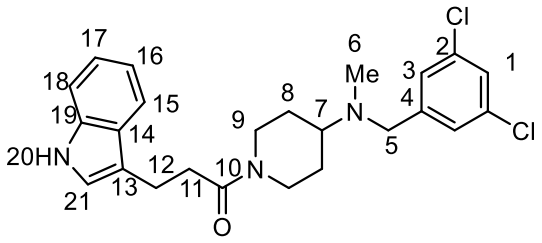

2.54

1-(4-((3,5-Dichlorobenzyl)(methyl)amino)piperidin-1-yl)-3-(1H-indol-3-yl)propan-1-one (2.54) (LTL-III-012). A solution of indole-3-propionic acid (62 mg, 0.33 mmol), 1-ethyl-3-(3-dimethylaminopropyl)carbodiimide hydrochloride (EDCI-HCl) (59 mg, 0.31 mmol), 4-dimethylaminopyridine (2 mg, 0.02 mmol), N,N-diisopropylethylamine (0.15 mL, 0.88 mmol), and amine **2.46** (60 mg, 0.22 mmol) in CH_2Cl_2 (5 mL) was stirred at room temperature for 24 h. The reaction was diluted with additional CH_2Cl_2 (20 mL), and the solution was washed with sat. $NaHCO_3$ (50 mL). The aqueous layer was extracted with an additional portion of CH_2Cl_2 (25 mL). The combined organic layers were dried (Na_2SO_4) and concentrated via rotary evaporation. The crude material was purified by flash chromatography eluting with EtOAc/hexane/Et_3N (50:50:1) to give 48 mg (50 %) of the **2.54** as a white foam. ^{1}H NMR (400 MHz, $CDCl_3$) δ 8.26 (s, 1 H), 7.61 (dd, *J* = 8.0, 1.1 Hz, 1 H), 7.33 (dt, *J* = 8.1, 0.9 Hz, 1 H), 7.23 (t, *J* = 2.0 Hz, 1 H), 7.20 – 7.15 (comp, 3 H), 7.12 (m, 1 H), 7.03 (d, *J* = 2.3 Hz, 1 H, H), 4.71 (d, *J* = 13.2 Hz, 1 H),

3.88 – 3.74 (m, 1 H), 3.40 (s, 2 H), 3.21 – 3.05 (comp, 2 H), 2.92 – 2.64 (comp, 3 H), 2.60 – 2.43 (comp, 2 H), 2.10 (s, 3 H), 1.77 (d, *J* = 12.8 Hz 1 H), 1.63 (d, *J* = 12.8 Hz, 1 H), 1.32 (qd, *J* = 12.2, 4.2 Hz, 1 H), 1.08 (qd, *J* = 12.2, 4.2 Hz, 1 H). ^{13}C NMR (101 MHz, CDCl3) δ 171.1, 143.8, 136.3, 134.7, 127.2, 127.0, 126.7, 121.9, 121.7, 119.2, 118.7, 115.3, 111.2, 60.9, 56.9, 45.2, 41.2, 37.6, 33.9, 28.5. IR (film, NaCl) 3266, 3058, 2926, 2856, 2791, 2243, 1622, 1568, 1454, 1434, 1354, 1267, 1228, 1148, 1124, 1098, 1047 cm^{-1}. HRMS (ESI) *m/z* calcd for $C_{24}H_{27}Cl_2N_3O$ (M+H)+ 444.1604; found 444.1610

NMR Assignment. ^{1}H NMR (400 MHz, $CDCl_3$) δ 8.26 (s, 1 H, H20), 7.61 (dd, *J* = 8.0, 1.1 Hz, 1 H, H15), 7.33 (dt, *J* = 8.1, 0.9 Hz, 1 H, H18), 7.23 (t, *J* = 2.0 Hz, 1 H, H1), 7.20 – 7.15 (comp, 3 H, H3, H17), 7.12 (m, 1 H, H16) 7.03 (d, *J* = 2.3 Hz, 1 H, H21), 4.71 (d, *J* = 13.2 Hz, 1 H, H9), 3.88 – 3.74 (m, 1 H, H9), 3.40 (s, 2 H H5), 3.21 – 3.05 (comp, 2 H, H12), 2.92 – 2.64 (comp, 3 H, H11, H9), 2.60 – 2.43 (comp, 2 H, H9, H7), 2.10 (s, 3 H, H6), 1.77 (d, *J* = 12.8 Hz 1 H, H8), 1.63 (d, *J* = 12.8 Hz, 1 H, H8), 1.32 (qd, *J* = 12.2, 4.2 Hz, 1 H, H8), 1.08 (qd, *J* = 12.2, 4.2 Hz, 1 H, H8); ^{13}C NMR (101 MHz, $CDCl_3$) δ 171.1 (C10), 143.8 (C4), 136.3 (C19), 134.7 (C1), 127.2 (C2), 127.0 (C3), 126.7 (C14), 121.9 (C21), 121.7 (C15), 119.2 (C17), 118.7 (C16), 115.3 (C13), 111.2 (C18), 60.9 (C7), 56.9 (C5), 45.2 (C9), 41.2 (C12), 37.6 (C6), 33.9 (C11), 28.5 (C9).

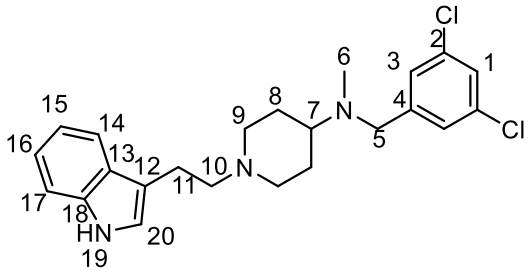

2.55

1-(2-(1H-Indol-3-yl)ethyl)-N-(3,5-dichlorobenzyl)-N-methylpiperidin-4-amine (LTL-III-048). A solution of **2.51** (50 mg, 0.12 mmol) in THF (0.6 mL) was added to a suspension of $LiAlH_4$ (20 mg, 0.50 mmol) in THF (0.6 mL) at 0 °C. The mixture was then warmed to room temperature and stirred for 4 h. The reaction was then cooled to 0 °C and sat. aq. NH_4Cl (5 mL)

was added. A precipitate formed, which was removed by vacuum filtration. The filtrate was then made basic by the addition of sat. aq. $NaHCO_3$ and extracted with CH_2Cl_2 (3 x 20 mL). The combined organic layers were dried (Na_2SO_4) and concentrated via rotary evaporation. The crude material was purified via flash chromatography eluting with EtOAc/hexane/Et_3N (50:50:1) to give 36 mg (72%) of **2.55** as a white paste. ^{1}H NMR (400 MHz, $CDCl_3$) δ 8.13 – 8.05 (s, 1 H), 7.61 (d, *J* = 7.8 Hz, 1 H), 7.34 (dt, *J* = 8.0, 0.9 Hz, 1 H), 7.23 (s, 3 H), 7.21 – 7.16 (m, 1 H), 7.15 – 7.09 (m, 1 H), 7.01 (d, *J* = 2.2 Hz, 1 H), 3.80 – 3.71 (m, 1 H), 3.53 (s, 2 H), 3.21 – 3.11 (comp, 2 H), 3.02 – 2.93 (comp, 2 H), 2.75 – 2.65 (comp, 2 H), 2.46 (tt, *J* = 11.5, 3.8 Hz, 1 H), 2.21 (s, 3 H), 2.05 (td, *J* = 11.8, 2.4 Hz, 2 H), 1.85 (comp, 3 H), 1.70 (qd, *J* = 12.0, 3.8 Hz, 2 H). ^{13}C NMR (101 MHz, $CDCl_3$) δ 144.2, 136.2, 134.7, 127.4, 126.9, 126.8, 122.0, 121.4, 119.2, 118.8, 114.5, 111.1, 61.3, 59.3, 57.0, 53.4, 37.9, 27.9, 23.2. IR (NaCl, film) 3412, 3179, 3057, 2943, 2853, 2808, 2360, 1620, 1589, 1568, 1455, 1433, 1376, 1353, 1303, 1228, 1145, 1097, 1049, 1014 cm^{-1}. HRMS (ESI) *m/z* calcd for $C_{23}H_{27}Cl_2N_3$ (M+H)+ 416.1655; found 416.1656.

NMR Assignment. ^{1}H NMR (400 MHz, $CDCl_3$) δ 8.13 – 8.05 (s, 1 H, H19), 7.61 (d, J = 7.8 Hz, 1 H, H14), 7.34 (d, J = 8.0 Hz, 1 H, H17), 7.23 (comp, 3 H, H1, H3), 7.21 – 7.16 (m, 1 H, H16), 7.15 – 7.09 (m, 1 H, H15), 7.01 (d, J = 2.2 Hz, 1 H, H20), 3.53 (s, 2 H, H5), 3.21 – 3.11 (m, 2 H, H9), 3.02 – 2.93 (comp, 2 H, H10), 2.75 – 2.65 (comp, 2 H, H11), 2.46 (tt, J = 11.5, 3.8 Hz, 1 H, H7), 2.21 (s, 3 H, H6), 2.05 (td, J = 11.8, 2.4 Hz, 2 H, H9), 1.85 (comp, 2 H, H8), 1.70 (qd, J = 12.0, 3.8 Hz, 2 H, H8). ^{13}C NMR (101 MHz, $CDCl_3$) δ 144.2 (C4), 136.2 (C18), 134.7 (C1), 127.4 (C13), 126.9 (C2), 126.8 (C3), 122.0 (C15), 121.4 (C20), 119.2 (C16), 118.8 (C14), 114.5 (C12), 111.1 (C17), 61.3 (C7), 59.3 (C9), 57.0 (C5), 53.4 (C10), 37.9 (C6), 27.9 (C8), 23.2 (C11).

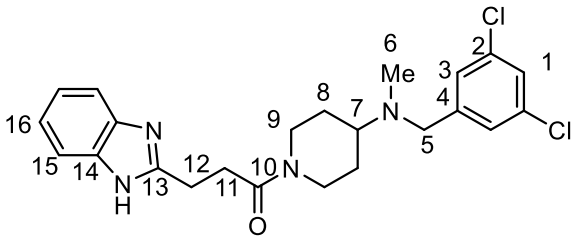

2.61

3-(1H-Benzo[d]imidazol-2-yl)-1-(4-((3,5-dichlorobenzyl)(methyl)amino)piperidin-1-yl)propan-1-one (2.61) (LTL-III-163). The title compound was prepared following a procedure analogous to that of **2.54**. The crude material was purified by flash chromatography eluting with EtOAc/Et_3N (100:1) to give 82 mg (61%) of **2.61** as a ____. ^{1}H NMR (400 MHz, $CDCl_3$) δ 10.31 (s, 1 H), 7.74 – 7.38 (m, 2 H), 7.24 – 7.17 (comp, 5 H), 4.71 (d, *J* = 13.1 Hz, 1 H), 3.90 (d, *J* = 13.6 Hz, 1 H), 3.48 (s, 2 H), 3.32 – 3.23 (comp, 2 H), 3.06 – 2.94 (m, 1 H), 2.84 (dd, *J* = 7.3, 4.2 Hz, 2 H), 2.70 – 2.57 (comp, 2 H), 2.15 (s, 3 H), 1.91 – 1.81 (comp, 2 H), 1.45 (qd, *J* = 14.2, 12.9, 6.2 Hz, 2 H). ^{13}C NMR (101 MHz, $CDCl_3$) δ 170.6, 154.6, 143.6, 134.8, 127.1, 126.7, 122.0, 60.7, 57.0, 45.0, 41.6, 37.6, 31.6, 28.4, 27.7, 24.5; IR (NaCl, film) 3200, 3057, 2945, 2857, 2789, 2360, 2344, 1631, 1568, 1538, 1450, 1353, 1271, 1226, 1152, 1098, 1046 cm^{-1}. HRMS (ESI) *m/z* calcd for $C_{23}H_{26}Cl_2N_4O$ (M+Na)+ 467.1376; found 467.1385.

NMR Assignment. ^{1}H NMR (400 MHz, $CDCl_3$) δ 10.31 (s, 1 H, N-H), 7.74 – 7.38 (m, 2 H, H15), 7.24 – 7.17 (comp, 5 H, H16, H13, H1), 4.71 (d, *J* = 13.1 Hz, 1 H, H9), 3.90 (d, *J* = 13.6 Hz, 1 H, H9), 3.48 (s, 2 H, H5), 3.32 – 3.23 (comp, 2 H, H12), 3.06 – 2.94 (m, 1 H, H7), 2.84 (dd, *J* = 7.3, 4.2 Hz, 2 H, H11), 2.70 – 2.57 (comp, 2 H, H9), 2.15 (s, 3 H, H6), 1.91 – 1.81 (comp, 2 H, H8), 1.45 (qd, *J* = 14.2, 12.9, 6.2 Hz, 2 H, H8). ^{13}C NMR (101 MHz, $CDCl_3$) δ 170.6 (C10), 154.6 (C13), 143.6 (C4), 134.8 (C1), 127.1 (C2), 126.7 (C3), 122.0 (C16), 60.7 (C7), 57.0 (C5), 45.0 (C9), 41.6 (C12), 37.6 (C6), 31.6 (C11), 28.4 (C8).

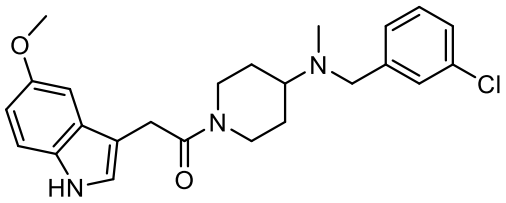

2.62

1-(4-((2-Chlorobenzyl)(methyl)amino)piperidin-1-yl)-2-(5-methoxy-1H-indol-3-yl)ethan-1-one (2.62) (LTL-IV-070). A solution **2.56** (28 mg, 0.12 mmol), 2-(5-methoxy-1H-indol-3-yl)acetic acid (37 mg, 0.18 mmol), EDCI·HCl (35 mg, 0.18 mmol), and iPr_2NEt (0.8 mL, 0.48 mmol) in THF (1.2 mL) was stirred at rt for 2 h. The reaction was then diluted with 1 M aq. NaOH (20 mL) and extracted with CH_2Cl_2 (3 x 15 mL). The combined organic extracts were dried (Na_2SO_4) and concentrated via rotary evaporation. The crude material was purified by flash chromatography, eluting with hexanes:EtOAc:Et_3N (40:60:1) to give the title compound (40 mg, 78%) as an amber solid. ^{1}H NMR (400 MHz, $CDCl_3$) δ 8.00 (s, 1 H), 7.29 – 7.27 (m, 1 H), 7.24 (dd, J = 8.8, 0.6 Hz, 1 H), 7.22 – 7.19 (m, 2 H), 7.15 – 7.11 (m, 1 H), 7.10 (d, J = 2.5 Hz, 1 H), 7.07 (d, J = 2.2 Hz, 1 H), 6.89 – 6.82 (m, 1 H), 4.73 (d, J = 13.5 Hz, 1 H), 4.02 (d, J = 16.7 Hz, 1 H), 3.86 (s, 3 H), 3.83 (dd, J = 2.9, 1.0 Hz, 2 H), 3.42 (s, 2 H), 2.93 (s, 1 H), 2.63 – 2.50 (m, 2 H), 2.08 (s, 3 H), 1.82 (d, J = 13.1 Hz, 1 H), 1.64 (d, J = 12.8 Hz, 1 H), 1.43 (qd, J = 12.1, 4.3 Hz, 1 H), 1.22 – 1.10 (m, 1 H). ^{13}C NMR (101 MHz, $CDCl_3$) δ 169.8, 154.1, 142.1, 134.2, 131.3, 129.5, 128.5, 127.4, 127.0, 126.6, 123.0, 112.5, 111.9, 109.2, 100.5, 60.6, 57.3, 55.9, 45.9, 41.6, 37.6, 31.8, 28.5, 27.4. IR (NaCl, flim) 3267, 3056, 2941, 2858, 2244, 2127, 1625, 1486, 1451, 1357, 1332, 1302, 1267, 1216, 1171, 1097, 1055 cm^{-1}. HRMS (ESI) *m/z* calcd for $C_{24}H_{28}ClN_3O_2$ (M+Na)+ 448.1762; found 448.1774.

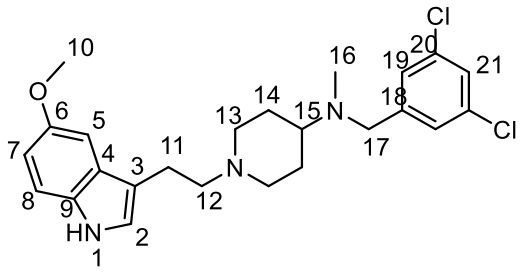

2.63

N-(3,5-Dichlorobenzyl)-1-(2-(5-methoxy-1H-indol-3-yl)ethyl)-N-methylpiperidin-4-amine (2.63) (LTL-IV-068). The title compound was prepared following a procedure analogous to that of **2.65**. The crude material was purified by flash chromatography eluting with hexanes/EtOAc/Et_3N (50:50:1) to give 18 mg (82%) of **2.63** as a white solid. ^{1}H NMR (400 MHz, $CDCl_3$) δ 7.92 (s, 1 H), 7.23 (s, 4 H), 7.05 (d, *J* = 2.4 Hz, 1 H), 7.00 (d, *J* = 2.4 Hz, 1 H), 6.85 (dd, *J* = 8.8, 2.4 Hz, 1 H), 3.86 (s, 3 H), 3.54 (s, 2 H), 3.17 (d, *J* = 11.3 Hz, 2 H), 3.00 – 2.89 (comp, 2 H), 2.74 – 2.65 (comp, 2 H), 2.47 (tt, *J* = 11.4, 3.8 Hz, 1 H), 2.21 (s, 3 H), 2.06 (t, *J* = 11.4 Hz, 2 H), 1.84 (d, *J* = 12.2 Hz, 2 H), 1.72 (td, *J* = 12.1, 3.7 Hz, 2 H); ^{13}C NMR (101 MHz, $CDCl_3$) δ 154.1, 144.5, 135.0, 131.6, 128.1, 127.2, 127.0, 122.5, 114.4, 112.4, 112.0, 101.0, 61.5, 59.5, 57.5, 56.2, 53.7, 38.2, 28.2, 23.5; IR (NaCl, film) 3412, 3143, 2927, 2854, 2808, 1625, 1588, 1568, 1486, 1454, 1435, 1377, 1354, 1281, 1263, 1217, 1173, 1144, 1119, 1098, 1064 cm^{-1}; HRMS (ESI) *m/z* calcd for $C_{24}H_{29}Cl_2N_3O$ (M+H)+ 446.1760; found 446.1770.

NMR Assignment. ^{1}H NMR (400 MHz, $CDCl_3$) δ 7.92 (s, 1 H, H1), 7.23 (comp, 4 H, H8, H19, H21), 7.05 (d, *J* = 2.4 Hz, 1 H, H5), 7.00 (d, *J* = 2.4 Hz, 1 H, H2), 6.85 (dd, *J* = 8.8, 2.4 Hz, 1 H, H7), 3.86 (s, 3 H, H10), 3.54 (s, 2 H, H17), 3.17 (d, *J* = 11.3 Hz, 2 H, H13 eq), 3.00 – 2.89 (comp, 2 H, H12), 2.74 – 2.65 (comp, 2 H, H11), 2.47 (tt, *J* = 11.4, 3.8 Hz, 1 H, H15), 2.21 (s, 3 H, H16), 2.06 (t, *J* = 11.4 Hz, 2 H, H13 ax), 1.84 (d, *J* = 12.2 Hz, 2 H, H14 eq), 1.72 (td, *J* = 12.1, 3.7 Hz, 2 H, H14 ax); ^{13}C NMR (101 MHz, $CDCl_3$) δ 154.1 (C10), 144.5 (C18), 135.0 (C21), 131.6 (C9), 128.1 (C20), 127.2 (C19), 127.0 (C4), 122.5 (C2), 114.4 (C3), 112.4 (C8), 112.0 (C7), 101.0 (C5), 61.5 (C15), 59.5 (C13), 57.5 (C17), 56.2 (C10), 53.7 (C12), 38.2 (C16), 28.2 (C14), 23.5 (C11).

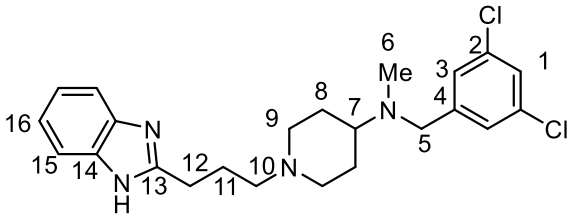

2.64

1-(3-(1H-Benzo[d]imidazol-2-yl)propyl)-N-(3,5-dichlorobenzyl)-N-methylpiperidin-4-amine (2.64) (LTL-III-165). To a stirred suspension of $NaBH_4$ (32 mg, 0.85 mmol) in THF (0.7 mL) was added a solution of I_2 (99 mg, 0.39 mmol) in THF (0.7 mL) while cooling at 0 ˚C. Once the solution turned clear, **2.61** (40 mg, 0.09 mmol) was added, and the solution was warmed to room temperature and stirred overnight, whereupon the reaction was quenched via the slow addition of MeOH (1 mL). The mixture was concentrated via rotary evaporation, resuspended in 3 M HCl (3 mL), and heated under reflux for an additional 6 h. The reaction was then cooled to room temperature, 1 M NaOH (20 mL) was added, and the aqueous solution was extracted with CH_2Cl_2 (3 x 15 mL. The combined organic layers were dried (Na_2SO_4) and concentrated via rotary evaporation, and the crude material was purified via column chromatography, eluting with EtOAc:MeOH:Et_3N (100:0:1 → 95:5:1) to give the title compound (32 mg, 82%) as a white solid. ^{1}H NMR (400 MHz, $CDCl_3$) δ 7.52 (dd, *J* = 6.0, 3.2 Hz, 2 H), 7.26 – 7.24 (comp, 3 H), 7.19 (dd, *J* = 6.0, 3.2 Hz, 2 H), 3.57 (s, 2 H), 3.17 – 3.04 (comp, 4 H), 2.61 – 2.54 (comp, 2 H), 2.50 (ddt, *J* = 11.4, 7.6, 3.8 Hz, 1 H), 2.27 (s, 3 H), 2.07 (td, *J* = 12.0, 2.4 Hz, 2 H), 2.02 – 1.95 (comp, 2 H), 1.91 (d, *J* = 13.0, 2.8 Hz, 2 H), 1.81 – 1.68 (comp, 2 H); ^{13}C NMR (101 MHz, $CDCl_3$) δ 155.7, 143.9, 134.8, 127.1, 126.8, 121.7, 114.6, 60.7, 59.0, 57.4, 53.3, 37.8, 29.5, 28.2, 23.7; IR (NaCl, film) 3056, 2944, 2785, 2248, 2192, 1622, 1590, 1568, 1541, 1451, 1431, 1379, 1352, 1304, 1272, 1211, 1123, 1098, 1051, 1026 cm^{-1}; HRMS (ESI) *m/z* calcd for $C_{23}H_{28}Cl_2N_4$ (M+H)+ 431.1764; found 431.1785.

NMR Assignment. ^{1}H NMR (400 MHz, $CDCl_3$) δ 7.52 (dd, *J* = 6.0, 3.2 Hz, 2 H, H15), 7.26 – 7.24 (comp, 3 H, H3, H1), 7.19 (dd, *J* = 6.0, 3.2 Hz, 2 H, H16), 3.57 (s, 2 H, H5), 3.17 – 3.04 (comp, 4 H, H12, H9), 2.61 – 2.54 (comp, 2 H, H10), 2.50 (ddt, *J* = 11.4, 7.6, 3.8 Hz, 1 H, H7), 2.27 (s, 3 H, H6), 2.07 (td, *J* = 12.0, 2.4 Hz, 2 H, H9), 2.02 – 1.95 (comp, 2 H, H11), 1.91 (d, *J* = 13.0, 2.8 Hz, 2 H, H8), 1.81 – 1.68 (comp, 2 H, H8); ^{13}C NMR (101 MHz, $CDCl_3$) δ 155.7 (C13), 143.9 (C4), 134.8 (C1), 127.1 (C2), 126.8 (C3), 121.7 (C16), 114.6 (C15), 60.7 (C7), 59.0 (C9), 57.4 (C5), 53.3 (C10), 37.8 (C6), 29.5 (C12), 28.2 (C8), 23.7 (C11);

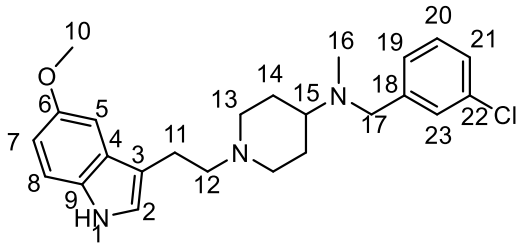

2.65

N-(3-Chlorobenzyl)-1-(2-(5-methoxy-1H-indol-3-yl)ethyl)-N-methylpiperidin-4-amine (2.65) (LTL-IV-071). To a solution of **2.62** (22 mg, 0.05 mmol) in THF (1 mL) was added a 0.5 M solution of alane in toluene (0.15 mmol, 0.3 mL) and stirred for 3 h at rt. The reaction was then diluted with 1 M NaOH (20 mL) and extracted with CH_2Cl_2 (3 x 15 mL). The combined organic extracts were dried (Na_2SO_4) and concentrated via rotary evaporation. The crude material purified by flash chromatography eluting with hexanes/EtOAc/Et_3N (40:60:1) to give 13 mg (62%) of **2.65** as a yellow paste. ^{1}H NMR (400 MHz, $CDCl_3$) δ 7.97 (s, 1 H), 7.34 (t, *J* = 1.8 Hz, 1 H), 7.25 – 7.17 (comp, 4 H), 7.05 (d, *J* = 2.4 Hz, 1 H), 6.99 (d, *J* = 2.2 Hz, 1 H), 6.84 (dt, *J* = 8.9, 2.3 Hz, 1 H), 3.85 (s, 3 H), 3.56 (s, 2 H), 3.18 (d, *J* = 11.3 Hz, 2 H), 2.99 – 2.90 (comp, 2 H), 2.74 – 2.65 (comp, 2 H), 2.56 – 2.40 (m, 1 H), 2.21 (s, 3 H), 2.12 – 2.02 (comp, 2 H), 1.85 (d, *J* = 12.5 Hz, 2 H), 1.80 – 1.66 (comp, 2 H). ^{13}C NMR (101 MHz, $CDCl_3$) δ 153.9, 142.5, 134.1, 131.3, 129.4, 128.6, 127.8, 126.9, 126.7, 122.3, 114.1, 112.1, 111.8, 100.7, 61.0,

59.2, 57.4, 56.0, 53.4, 37.8, 27.8, 23.2. IR (NaCl, film) 3156, 3049, 2939, 2853, 2808, 2249, 1625, 1581, 1484, 1453, 1356, 1301, 1261, 1216, 1172, 1144, 1119, 1068, 1040 cm^{-1}. HRMS (ESI) *m/z* calcd for $C_{24}H_{30}ClN_3O$ (M+Na)+ 434.1970; found 434.1977.

NMR Assignment. ^1H NMR (400 MHz, $CDCl_3$) δ 7.97 (s, 1 H, H1), 7.34 (t, *J* = 1.8 Hz, 1 H, H21), 7.25 – 7.17 (comp, 4 H, H19, H20, H23, H8), 7.05 (d, *J* = 2.4 Hz, 1 H, H5), 6.99 (d, *J* = 2.2 Hz, 1 H, H2), 6.84 (dt, *J* = 8.9, 2.3 Hz, 1 H, H7), 3.85 (s, 3 H, H10), 3.56 (s, 2 H, H17), 3.18 (d, *J* = 11.3 Hz, 2 H, H13), 2.99 – 2.90 (comp, 2 H, H12), 2.74 – 2.65 (comp, 2 H, H11), 2.56 – 2.40 (m, 1 H, H15), 2.21 (s, 3 H, H16), 2.12 – 2.02 (comp, 2 H, H13), 1.85 (d, *J* = 12.5 Hz, 2 H, H14), 1.80 – 1.66 (comp, 2 H, H14).

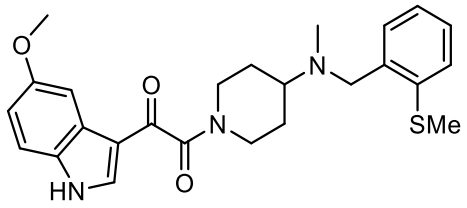

7.6

1-(5-Methoxy-1H-indol-3-yl)-2-(4-(methyl(3-(methylthio)benzyl)amino)piperidin-1-yl)ethane-1,2-dione (7.6) (LTL-III-147). To a solution of **2.58** (23 mg, 0.09 mmol) and iPr_2NEt (0.03 mL, 0.18 mmol) in CH_2Cl_2 (1 mL) was added 2-(5-methoxy-1H-indol-3-yl)-2-oxoacetyl chloride (32 mg, 0.13 mmol) , and the reaction was stirred at rt for 48 h. The reaction was then diluted with 1 M aq. NaOH (20 mL) and extracted with CH_2Cl_2 (3 x 15 mL). The combined organic extracts were dried (Na_2SO_4) and concentrated via rotary evaporation. The crude material was purified by flash chromatography, eluting with hexanes:EtOAc:Et_3N (20:80:1) to give 32 mg (79%) of **7.6** as a light tan foam. ^1H NMR (400 MHz, $CDCl_3$) δ 8.99 (s, 1 H), 7.85 (d, J = 3.0 Hz, 2 H), 7.14 (d, J = 7.5 Hz, 1 H), 7.08 (d, J = 7.6 Hz, 1 H), 6.95 (dd, J = 8.9, 2.5 Hz, 1 H), 4.71 (d, J = 13.4 Hz, 1 H), 3.91 (d, J = 1.8 Hz, 4 H), 3.56 (s, 2 H), 3.06 (t, J = 11.7 Hz, 1 H), 2.84 – 2.67 (comp, 2 H), 2.49 (d, J = 0.6 Hz, 3 H), 2.21 (s, 3 H), 2.01 – 1.94 (m, 1 H), 1.84

(d, J = 13.0 Hz, 1 H), 1.68-1.52 (comp, 2 H). ^{13}C NMR (101 MHz, $CDCl_3$) δ 186.1, 166.3, 156.8, 140.3, 138.4, 131.4, 128.8, 126.6, 126.1, 125.4, 125.0, 114.7, 114.3, 112.8, 103.2, 60.4, 57.8, 55.8, 45.9, 41.1, 37.7, 28.6, 27.8, 15.8. IR (NaCl, film) 3225, 2947, 2248, 1627, 1518, 1474, 1439, 1367, 1298, 1268, 1243, 1211, 1179, 1128, 1088, 1033 cm^{-1}. HRMS (ESI) *m/z* calcd for $C_{25}H_{29}N_3O_3S$ (M+H)+ 452.2002; found 452.2019.

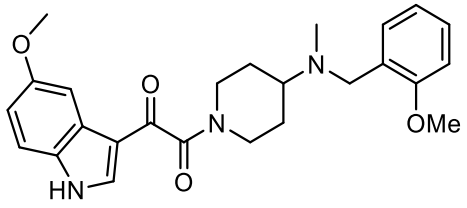

7.7

1-(5-Methoxy-1H-indol-3-yl)-2-(4-((2-methoxybenzyl)(methyl)amino)piperidin-1-yl)ethane-1,2-dione (7.7) (LTL-III-152). The title compound was prepared following a procedure analogous to that of **7.6**. The crude material was purified by flash chromatography eluting with EtOAc/Et_3N (100:1) to give 82 mg (75%) of **7.7** as a white foam. ^{1}H NMR (400 MHz, $CDCl_3$) δ 10.12 (s, 1 H), 7.78 (d, J = 2.5 Hz, 1 H), 7.65 (s, 1 H), 7.22 (t, J = 8.3 Hz, 2 H), 6.91 – 6.85 (comp, 3 H), 6.78 (ddd, J = 8.2, 2.5, 1.1 Hz, 1 H), 4.66 (d, J = 13.4 Hz, 1 H), 3.87 (comp, 4 H), 3.79 (s, 3 H), 3.55 (s, 2 H), 3.02 (td, J = 13.8, 13.0, 2.7 Hz, 1 H), 2.83 – 2.64 (comp, 2 H), 2.20 (s, 3 H), 1.97 (dd, J = 10.1, 5.7 Hz, 1 H), 1.81 (d, J = 12.7 Hz, 1 H), 1.61 (dtd, J = 16.1, 12.3, 4.2 Hz, 2 H). ^{13}C NMR (101 MHz, $CDCl_3$) δ 186.1, 166.4, 159.7, 156.7, 141.2, 135.5, 131.4, 129.3, 126.1, 121.0, 114.7, 114.3, 114.1, 112.9, 112.3, 103.1, 60.2, 58.0, 55.8, 55.2, 45.88, 41.1, 37.7, 28.6, 27.8. IR (NaCl, film) 3231, 2949, 2362, 2249, 1628, 1519, 1487, 1439, 1364, 1299, 1211, 1179, 1149, 1089, 1042 cm^{-1}. HRMS (ESI) *m/z* calcd $C_{25}H_{29}N_3O_4$ (M+H)+ 436.2231; found 436.2232.

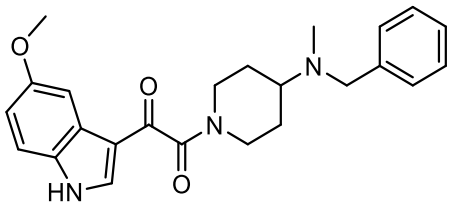

7.8

1-(4-(Benzyl(methyl)amino)piperidin-1-yl)-2-(5-methoxy-1H-indol-3-yl)ethane-1,2-dione (7.8) (LTL-III-150). The title compound was prepared following a procedure analogous to that of **7.6**. The crude material was purified by flash chromatography eluting with EtOAc/Et_3N (100:1) to give 80 mg (80%) of **7.8** as a white foam. ^{1}H NMR (400 MHz, $CDCl_3$) δ 9.85 (s, 1 H), 7.80 (d, J = 2.5 Hz, 1 H), 7.70 (d, J = 1.9 Hz, 1 H), 7.33 – 7.27 (comp, 4 H), 7.26 – 7.21 (comp, 2 H), 6.89 (ddd, J = 8.9, 2.5, 0.3 Hz, 1 H), 3.88 (comp, 4 H), 3.57 (s, 2 H), 3.03 (ddd, J = 13.8, 12.1, 2.8 Hz, 1 H), 2.83 – 2.65 (comp, 2 H), 2.20 (s, 3 H), 2.03 – 1.93 (m, 1 H), 1.83 (d, J = 12.7 Hz, 1 H), 1.71 – 1.53 (comp, 2 H). ^{13}C NMR (101 MHz, $CDCl_3$) δ 186.08, 166.27, 156.77, 139.46, 135.33, 131.34, 128.64, 128.30, 126.96, 126.11, 114.72, 114.44, 112.73, 103.24, 60.33, 58.04, 55.76, 45.84, 41.06, 37.58, 28.67, 27.83. IR (NaCl, film) 3216, 2948, 1627, 1518, 1487, 1442, 1365, 1299, 1268, 1243, 1211, 1179, 1129, 1089, 1030, 958 cm^{-1}. HRMS (ESI) *m/z* calcd $C_{24}H_{27}N_3O_3$ (M+Na)+ 428.1945; found 428.1960.

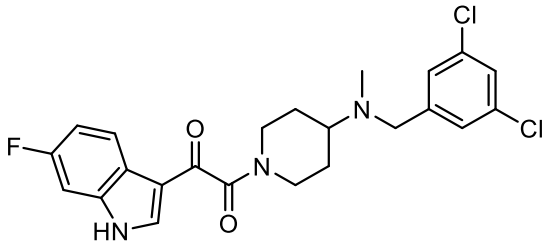

7.9

1-(4-((3,5-Dichlorobenzyl)(methyl)amino)piperidin-1-yl)-2-(6-fluoro-1H-indol-3-yl)ethane-1,2-dione (7.9) (LTL-III-170). The title compound was prepared following a procedure analogous to that of **7.6**. The crude material was purified by flash chromatography eluting with hexanes:EtOAc:Et_3N (50:50:1) to give 160 mg (86%) of **7.9** as a white paste. ^{1}H

NMR (500 MHz, $CDCl_3$) δ 10.14 (s, 1 H), 8.24 (dd, *J* = 8.5, 5.3 Hz, 1 H), 7.76 (s, 1 H), 7.25 – 7.18 (comp, 3 H), 7.09 – 6.96 (comp, 2 H), 4.69 (ddt, *J* = 13.3, 4.7, 2.5 Hz, 1 H), 3.91 (ddt, *J* = 13.6, 5.0, 2.6 Hz, 1 H), 3.52 (s, 2 H), 3.10 – 2.99 (m, 1 H), 2.84 – 2.75 (m, 1 H), 2.70 (tt, *J* = 11.4, 3.6 Hz, 1 H), 2.18 (s, 3 H), 1.97 – 1.93 (m, 1 H), 1.85 – 1.78 (m, 1 H), 1.59 (pd, *J* = 12.5, 4.3 Hz, 2 H); ^{13}C NMR (126 MHz, $CDCl_3$) δ 185.9, 166.1, 161.6, 159.7, 143.6, 136.9, 136.8, 135.8, 135.8, 134.8, 127.2, 126.7, 125.5, 123.0, 123.0, 121.6, 114.5, 111.9, 111.7, 98.7, 98.5, 60.8, 57.1, 56.0, 45.8, 45.6, 41.1, 37.7, 34.6, 34.2, 30.3, 29.7, 28.6, 27.9, 23.4, 22.7, 21.2, 14.8, 14.2, 14.1; IR (NaCl, film) 2926, 2855, 1623, 1595, 1568, 1525, 1504, 1446, 1432, 1372, 1268, 1232, 1150, 1091, 1046 cm^{-1}; HRMS (ESI) *m/z* calcd $C_{23}H_{22}Cl_2FN_3O_2$ (M+H)+ 462.1146; found 462.1156.

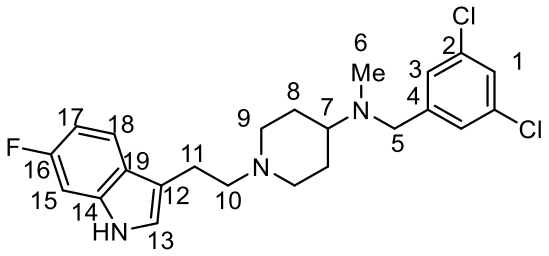

2.67

N-(3,5-Dichlorobenzyl)-1-(2-(6-fluoro-1H-indol-3-yl)ethyl)-N-methylpiperidin-4-amine (2.67) (LTL-III-186). To a stirred suspension of $NaBH_4$ (20 mg, 0.53 mmol) in THF (2 mL) was added I_2 (63 mg, 0.25 mmol) while cooling at 0 ˚C. Once the solution turned clear, 1-(4-((3,5-dichlorobenzyl)(methyl)amino)piperidin-1-yl)-2-(6-fluoro-1H-indol-3-yl)ethane-1,2-dione (46 mg, 0.10 mmol) was added at 0 ˚C, and the solution was then heated under reflux overnight, whereupon saturated aq. $NaHCO_3$ (10 mL) was added and the solution was extracted with CH_2Cl_2 (3 x 15 mL). The combined organic layers were dried (Na_2SO_4) to give a white paste which was then dissolved in EtOH (5 mL) and treated with CsF (60 mg, 0.39 mmol) and Na_2CO_3 (60 mg, 0.57 mmol), and the resulting solution was heated under reflux for 24 h,

whereupon it was cooled to room temperature and filtered over celite, rinsing with EtOAc. The solution was concentrated via rotary evaporation and the resultant crude material was purified via column chromatography, eluting with hexanes:EtOAc:Et_3N (20:80:1) to give 19 mg (44%) of the title compound as a clear paste. ^{1}H NMR (500 MHz, $CDCl_3$) δ 8.02 (s, 1 H), 7.50 (dd, *J* = 8.7, 5.3 Hz, 1 H), 7.23 (s, 3 H), 7.06 – 6.98 (comp, 2 H), 6.88 (td, *J* = 9.2, 2.2 Hz, 1 H), 3.53 (s, 2 H), 3.15 (d, *J* = 10.8 Hz, 2 H), 2.98 – 2.92 (comp, 2 H), 2.69 (dd, *J* = 9.8, 6.6 Hz, 2 H), 2.47 (tt, *J* = 11.4, 3.7 Hz, 1 H), 2.21 (s, 3 H), 2.07 (t, *J* = 11.6 Hz, 2 H), 1.87 – 1.80 (comp, 2 H), 1.71 (qd, *J* = 12.2, 3.6 Hz, 2 H); ^{13}C NMR (126 MHz, $CDCl_3$) δ 161.0, 159.1, 144.2, 136.2, 136.1, 134.7, 127.0, 126.8, 124.1, 121.7, 121.6, 119.6, 119.5, 114.6, 108.1, 107.9, 97.5, 97.3, 61.2, 59.2, 57.0, 53.4, 37.9, 27.9, 23.1; IR (NaCl, film) 2918, 2849, 1567, 1457, 1432, 1245, 1140 cm $^{-1}$ HRMS (ESI) *m/z* calcd $C_{23}H_{26}Cl_2FN_3$ (M+H)+ 434.1561; found 434.1571.

NMR Assignment. ^{1}H NMR (500 MHz, $CDCl_3$) δ 8.02 (s, 1 H, N-H), 7.50 (dd, *J* = 8.7, 5.3 Hz, 1 H, H15), 7.23 (s, 3 H, H1, H3), 7.06 – 6.98 (comp, 2 H, H18, H13), 6.88 (td, *J* = 9.2, 2.2 Hz, 1 H, H17), 3.53 (s, 2 H, H5), 3.15 (d, *J* = 10.8 Hz, 2 H, H9), 2.98 – 2.92 (comp, 2 H, H10), 2.69 (dd, *J* = 9.8, 6.6 Hz, 2 H, H11), 2.47 (tt, *J* = 11.4, 3.7 Hz, 1 H, H7), 2.21 (s, 3 H, H6), 2.07 (t, *J* = 11.6 Hz, 2 H, H9), 1.87 – 1.80 (comp, 2 H, H8), 1.71 (qd, *J* = 12.2, 3.6 Hz, 2 H, H8); ^{13}C NMR (126 MHz, $CDCl_3$) δ 161.0 (C16), 159.1 (C16), 144.2 (C4), 136.2 (C19), 136.1 (C19), 134.7 (C1), 127.0 (C2), 126.8 (C3), 124.1 (C14), 121.7 (C13), 121.6 (C13), 119.6 (C15), 119.5 (C15), 114.6 (C12), 108.1 (C17), 107.9 (C17), 97.5 (C18), 97.3 (C18), 61.2 (C7), 59.2 (C11), 57.0 (C5), 53.4 (C9), 37.9 (C6), 27.9 (C8), 23.1 (C10);

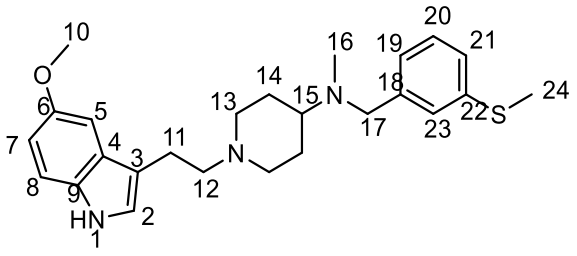

2.70

1-(2-(5-Methoxy-1H-indol-3-yl)ethyl)-N-methyl-N-(3-(methylthio)benzyl)piperidin-4-amine (2.70) (LTL-III-151). A solution of **7.6** (68 mg, 0.15 mmol) in THF (0.5 mL) was added to a stirred suspension of $LiAlH_4$ (57 mg, 1.5 mmol) in THF (1.0 mL) while cooling at 0 ˚C. The reaction vessel was removed from the ice bath and stirred while heating under reflux for 19 hours. The reaction vessel was then cooled to 0 ˚C, whereupon H_2O (0.06 mL) was carefully added, followed by 3M NaOH (0.06 mL) and H_2O (0.18 mL). The mixture was stirred at room temperature for 30 min, during which time the visible precipitate turned from grey to white. $MgSO_4$ was added, and the mixture was stirred for an additional 30 minutes, and then filtered over a pad of celite, washing with EtOAc. The solution was concentrated via rotary evaporation, and the crude material was purified by flash chromatography eluting with hexanes/EtOAc/Et_3N (25:75:1 → 0:100:1) to give 42 mg (66%) of **2.70** as an off-white solid. ^{1}H NMR (400 MHz, $CDCl_3$) δ 7.87 (s, 1 H), 7.25 – 7.20 (comp, 2 H), 7.11 (comp, 2 H), 7.05 (d, *J* = 2.4 Hz, 1 H), 7.00 (d, *J* = 2.4 Hz, 1 H), 6.85 (dd, *J* = 8.8, 2.4 Hz, 1 H), 3.86 (d, *J* = 0.6 Hz, 3 H), 3.56 (s, 2 H), 3.15 (d, *J* = 11.3 Hz, 2 H), 2.98 – 2.90 (comp, 2 H), 2.71 – 2.63 (comp, 2 H), 2.49 (comp, 4 H), 2.25 – 2.19 (s, 3 H), 2.04 (t, *J* = 11.2 Hz, 2 H), 1.85 (d, *J* = 12.1 Hz, 2 H), 1.74 (td, *J* = 12.0, 3.9 Hz, 2 H). ^{13}C NMR (101 MHz, $CDCl_3$) δ 153.9, 140.9, 138.2, 131.3, 128.7, 127.8, 126.8, 125.5, 124.9, 122.3, 114.2, 112.1, 111.8, 110.0, 100.7, 59.2, 57.8, 56.0, 53.5, 37.8, 27.8, 23.2, 15.8. IR (NaCl, film) 3415, 3163, 3047, 2926, 2854, 2807, 1624, 1587, 1484, 1452, 1356, 1301, 1261, 1216, 1172, 1144, 1099, 1037 cm^{-1}. LRMS (ESI) *m/z* calcd for $C_{25}H_{33}N_3OS$ (M+Na)+ 446.2237; found 446.2249.

NMR Assignment. ^{1}H NMR (400 MHz, $CDCl_3$) δ 7.87 (s, 1 H, H1), 7.25 – 7.20 (comp, 2 H, H19, H20), 7.11 (comp, 2 H, H21, H23), 7.05 (d, *J* = 2.4 Hz, 1 H, H5), 7.00 (d, *J* = 2.4 Hz, 1 H, H2), 6.85 (dd, *J* = 8.8, 2.4 Hz, 1 H, H7), 3.86 (d, *J* = 0.6 Hz, 3 H, H10), 3.56 (s, 2 H, H17), 3.15 (d, *J* = 11.3 Hz, 2 H, H13), 2.98 – 2.90 (comp, 2 H, H12), 2.71 – 2.63 (comp, 2 H, H11), 2.49 (comp, 4 H, H24, H15), 2.25 – 2.19 (s, 3 H, H16), 2.04 (t, *J* = 11.2 Hz, 2 H, H13), 1.85 (d, *J* = 12.1 Hz, 2 H, H14), 1.74 (td, *J* = 12.0, 3.9 Hz, 2 H, H14).

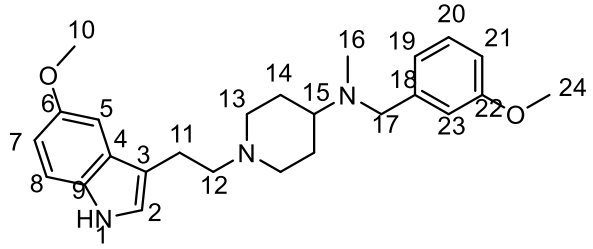

2.69

1-(2-(5-Methoxy-1H-indol-3-yl)ethyl)-N-(3-methoxybenzyl)-N-methylpiperidin-4-amine (2.69) (LTL-III-155). The title compound was prepared following the procedure described for **2.70**. The crude material purified by flash chromatography eluting with hexanes/EtOAc/Et_3N (25:75:1 → 0:100:1) to give 23 mg (62%) of **2.69** as a yellow paste. ^{1}H NMR (400 MHz, $CDCl_3$) δ 7.85 (s, 1 H), 7.25 – 7.20 (comp, 2 H), 7.05 (d, *J* = 2.4 Hz, 1 H), 7.01 (d, *J* = 2.3 Hz, 1 H), 6.94 – 6.89 (comp, 2 H), 6.85 (dd, *J* = 8.8, 2.5 Hz, 1 H), 6.79 (dd, *J* = 8.1, 2.6 Hz, 1 H), 3.86 (s, 3 H), 3.81 (s, 3 H), 3.58 (s, 2 H), 3.16 (d, *J* = 11.2 Hz, 2 H), 2.98 – 2.91 (comp, 2 H), 2.72 – 2.63 (comp, 2 H), 2.56-2.44 (m, 1 H), 2.24 (s, 3 H), 2.10 – 2.00 (comp, 2 H), 1.86 (d, *J* = 12.6 Hz, 2 H), 1.80 – 1.68 (comp, 2 H). ^{13}C NMR (101 MHz, $CDCl_3$) δ 159.7, 153.9, 141.9, 131.4, 129.1, 127.9, 122.3, 121.1, 114.1, 112.3, 112.1, 111.8, 100.7, 60.8, 59.2, 57.9, 56.0, 55.2, 53.5, 37.8, 27.8, 23.2. IR (NaCl, film) 3415, 3154, 3046, 2941, 2831, 1587, 1487, 1455, 1357, 1308, 1267, 1216, 1170, 1147, 1120, 1045 cm^{-1}. LRMS (ESI) *m/z* calcd for $C_{25}H_{33}N_3O_2$ (M+H)+ 408.2646; found 408.2643.

NMR Assignment. ^{1}H NMR (400 MHz, $CDCl_3$) δ 7.85 (s, 1 H, H1), 7.25 – 7.20 (comp, 2 H, H8, H23), 7.05 (d, *J* = 2.4 Hz, 1 H, H5), 7.01 (d, *J* = 2.3 Hz, 1 H, H2), 6.94 – 6.89 (comp, 2

H, H, H23, H24), 6.85 (dd, *J* = 8.8, 2.5 Hz, 1 H, H22), 6.79 (dd, *J* = 8.1, 2.6 Hz, 1 H, H7), 3.86 (s, 3 H, H24), 3.81 (s, 3 H, H10), 3.58 (s, 2 H, H17), 3.16 (d, *J* = 11.2 Hz, 2 H, H13 eq), 2.98 – 2.91 (comp, 2 H, H12), 2.72 – 2.63 (comp, 2 H, H11), 2.56-2.44 (m, 1 H, H15), 2.24 (s, 3 H, H24), 2.10 – 2.00 (comp, 2 H, H13), 1.86 (d, *J* = 12.6 Hz, 2 H, H14), 1.80 – 1.68 (comp, 2 H, H14).

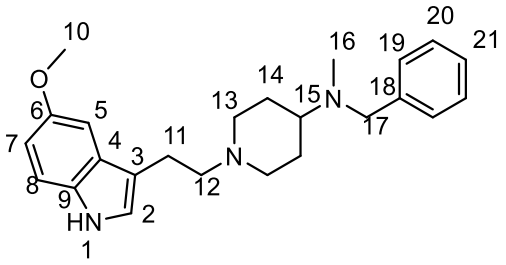

2.71

N-Benzyl-1-(2-(5-methoxy-1H-indol-3-yl)ethyl)-N-methylpiperidin-4-amine (2.71) (LTL-III-154). The title compound was prepared following the procedure described for **2.70**. The crude material purified by flash chromatography eluting with hexanes/EtOAc/Et_3N (25:75:1 → 0:100:1) to give 43 mg (96%) of **2.70** as a yellow paste. ^{1}H NMR (400 MHz, $CDCl_3$) δ 7.85 (s, 1 H), 7.35 – 7.29 (comp, 5 H), 7.24 – 7.21 (m, 1 H), 7.05 (d, *J* = 2.5 Hz, 1 H), 7.00 (d, *J* = 2.4 Hz, 1 H), 6.85 (dd, *J* = 8.8, 2.4 Hz, 1 H), 3.86 (s, 3 H), 3.60 (s, 2 H), 3.16 (d, *J* = 11.2 Hz, 2 H), 2.98 – 2.90 (comp, 2 H), 2.71 – 2.63 (comp, 2 H), 2.55-2.45 (m, 1 H), 2.22 (s, 3 H), 2.09 – 2.00 (comp, 2 H), 1.86 (d, *J* = 12.6 Hz, 2 H), 1.79 – 1.73 (comp, 2 H). ^{13}C NMR (101 MHz, $CDCl_3$) δ 153.9, 140.0, 131.4, 128.8, 128.2, 127.9, 126.8, 122.3, 114.1, 112.1, 111.8, 100.7, 60.8, 59.2, 57.9, 56.0, 53.5, 37.8, 27.8, 23.2. IR (NaCl, film 3416, 3155, 3030, 2942, 2801, 1625, 1584, 1487, 1452, 1360, 1305, 1261, 1216, 1173, 1143, 1118, 1035 cm^{-1}. HRMS (ESI) *m/z* calcd for $C_{24}H_{31}N_3O$ (M+H)+ 378.2540; found 378.2550.

NMR Assignment. ^{1}H NMR (400 MHz, $CDCl_3$) δ 7.85 (s, 1 H, H1), 7.35 – 7.29 (comp, 5 H, H19-21), 7.24 – 7.21 (m, 1 H, H8), 7.05 (d, *J* = 2.5 Hz, 1 H, H5), 7.00 (d, *J* = 2.4 Hz, 1 H, H2), 6.85 (dd, *J* = 8.8, 2.4 Hz, 1 H, H7), 3.86 (s 3 H, H10), 3.60 (s, 2 H, H17), 3.16 (d, *J* = 11.2 Hz, 2 H, H13), 2.98 – 2.90 (comp, 2 H, H12), 2.71 – 2.63 (comp, 2 H, H11), 2.55-2.45 (m, 1 H,

H15), 2.22 (s, 3 H, H16), 2.09 – 2.00 (comp, 2 H, H13), 1.86 (d, *J* = 12.6 Hz, 2 H, H14), 1.79 – 1.73 (comp, 2 H, H14).

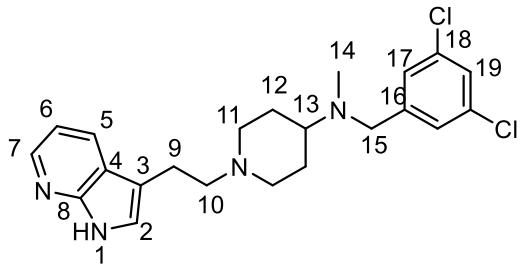

2.72

1-(2-(1H-Pyrrolo[2,3-b]pyridin-3-yl)ethyl)-N-(3,5-dichlorobenzyl)-N-methylpiperidin-4-amine (2.72) (LTL-III-128). A solution of amine **2.46** (50 mg, 0.18 mmol) and alkyl bromide **2.35** (25 mg, 0.11 mmol) in MeCN (1 mL) was stirred under reflux and stirred for 8 h, whereupon the reaction was cooled to room temperature and stirred for an additional 72 h. The reaction mixture was concentrated via rotary evaporation, and the crude material was purified by flash chromatography eluting with $Et_2O/CH_2Cl_2/Et_3N$ (100:0:1 → 66:33:1) to give 15 mg (33%) of **2.72** as a white solid. ^{1}H NMR (400 MHz, CD_3OD) δ 8.20 (d, *J* = 4.3 Hz, 1 H), 8.09 (dd, *J* = 7.9, 1.5 Hz, 1 H), 7.35 (comp, 4 H), 7.14 (dd, *J* = 7.9, 4.8 Hz, 1 H), 4.60 (s, 3 H), 3.65 (s, 3 H), 3.38 (s, 1 H), 3.27 – 3.18 (comp, 4 H), 3.06 (s, 2 H), 2.80 (s, 1 H), 2.25 (s, 3 H), 2.12 (d, *J* = 13.2 Hz, 2 H), 1.88 (s, 2 H). ^{13}C NMR (101 MHz, $(CD_3)_2SO$) δ 198.2, 170.8, 148.9, 143.0, 134.3, 127.3, 127.0, 126.8, 123.9, 119.5, 115.3, 60.2, 56.4, 52.4, 37.8, 21.2, 14.5, 7.6. IR (NaCl, film) 3144, 3096, 3036, 2928, 2856, 2477, 2632, 1570, 1459, 1422,1344, 1288, 1203, 1126, 1103, 1044 cm^{-1}. HRMS (ESI) *m/z* calcd for $C_{22}H_{26}Cl_2N_4$ (M+H)+ 417.1607; found 417.1623.

NMR Assignment. ^{1}H NMR (400 MHz, CD_3OD) δ 8.20 (d, *J* = 4.3 Hz, 1 H, H7), 8.09 (dd, *J* = 7.9, 1.5 Hz, 1 H, H5), 7.35 (comp, 4 H, H17, H19, H2), 7.14 (dd, *J* = 7.9, 4.8 Hz, 1 H, H6), 4.60 (s, 3 H), 3.65 (s, 3 H), 3.38 (s, 1 H), 3.27 – 3.18 (comp, 4 H), 3.06 (s, 2 H), 2.80 (s, 1 H, H13), 2.25 (s, 3 H, H14), 2.12 (d, *J* = 13.2 Hz, 2 H, H12), 1.88 (s, 2 H, H12);

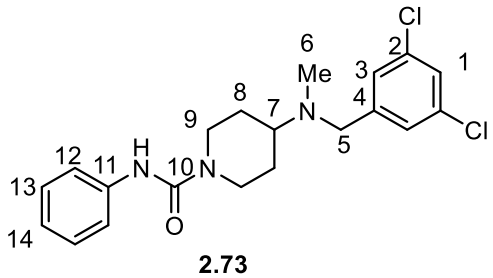

2.73

4-((3,5-dichlorobenzyl)(methyl)amino)-N-phenylpiperidine-1-carboxamide (2.73) (LTL-III-172). A solution of **2.46** (28 mg, 0.1 mmol), phenyl isocyanate (24 mg, 0.2 mmol) and (*i*-Pr)$_2$NEt (13 mg, 0.1 mmol) in CH_2Cl_2 was stirred overnight at room temperature, and the solvent was removed via rotary evaporation. The crude material was resuspended in 1 M aq. HCl (10 mL) and washed with Et_2O (2 x 20 mL). The aqueous layer was then made basic via the addition of 3 M aq. NaOH (10 mL) and extracted with CH_2Cl_2 (5 x 15 mL). The combined organic layers were dried (Na_2SO_4) and concentrated via rotary evaporation to give 22 mg (56%) of the title compound as a white solid. ^{1}H NMR (400 MHz, CD_3OD) δ 7.37 – 7.29 (comp, 5 H), 7.29 – 7.20 (comp, 2 H), 7.04 – 6.97 (m, 1 H), 4.24 (d, *J* = 13.2 Hz, 2 H), 3.61 (s, 2 H), 2.87 (td, *J* = 13.7, 2.5 Hz, 2 H), 2.69 (tt, *J* = 11.5, 3.7 Hz, 1 H), 2.21 (s, 3 H), 1.90 (d, *J* = 12.9 Hz, 2 H), 1.57 (qd, *J* = 12.4, 4.2 Hz, 2 H); ^{13}C NMR (101 MHz, CD_3OD) δ 156.4, 144.0, 139.6, 134.6, 128.1, 126.9, 126.5, 122.6, 120.8, 60.9, 56.5, 43.5, 36.6, 27.7; IR (NaCl, film) 3625, 3127, 3054, 2944, 2855, 2796, 2360, 1636, 1595, 1569, 1536, 1501, 1447, 1353, 1329, 1306, 1243, 1160, 1100, 1041 cm^{-1}. HRMS (ESI) *m/z* calcd for $C_{20}H_{23}Cl_2N_3O$ (M+Na)+ 414.1110; found 414.1121.

NMR Assignment. ^{1}H NMR (400 MHz, CD_3OD) δ 7.37 – 7.29 (comp, 5 H, H12, H3, H1), 7.29 – 7.20 (comp, 2 H, H13), 7.04 – 6.97 (m, 1 H, H14), 4.24 (d, *J* = 13.2 Hz, 2 H, H9), 3.61 (s, 2 H, H5), 2.87 (td, *J* = 13.7, 2.5 Hz, 2 H, H9), 2.69 (tt, *J* = 11.5, 3.7 Hz, 1 H, H7), 2.21 (s, 3 H, H6), 1.90 (d, *J* = 12.9 Hz, 2 H, H8), 1.57 (qd, *J* = 12.4, 4.2 Hz, 2 H, H8);

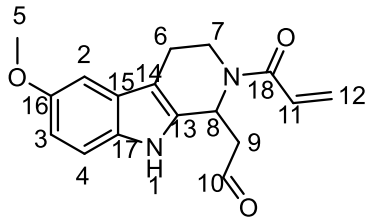

2.96

2-(2-Acryloyl-6-methoxy-2,3,4,9-tetrahydro-1H-pyrido[3,4-b]indol-1-yl)acetaldehyde (LTL-III-312). Dihydro-*β*-carboline **2.95** (20 mg, 0.1 mmol) was dissolved in 1 mL THF and cooled to −78 °C. Silyl enol ether **1.33** (63 mg, 0.4 mmol) and acryloyl chloride **1.22** in THF (0.13 mL, 0.13 mmol, 1M) were added sequentially, and the solution was stirred at −78 °C for 15 min, during which time a tan precipitate formed. The flask was then removed from the ice bath and stirred for an additional 90 min at room temperature. A solution of saturated $NaHCO_3$ (10 mL) was added, and the solution was extracted with CH_2Cl_2 (3 x 15 mL). The combined organic layers were dried (Na_2SO_4) and concentrated via rotary evaporation. The crude material was purified by flash chromatography, eluting with EtOAc:hexane (1:1) to give 22 mg (73%) of the title compound as a yellow foam. ^{1}H NMR (400 MHz, $CDCl_3$) δ 9.92 (d, *J* = 7.4 Hz, 1 H), 8.54 (s, 1 H), 7.23 (d, *J* = 8.7 Hz, 1 H), 6.90 (d, *J* = 2.5 Hz, 1 H), 6.84 (dd, *J* = 8.8, 2.4 Hz, 1 H), 6.66 (dd, *J* = 16.8, 10.6 Hz, 1 H), 6.33 (dd, *J* = 16.8, 1.7 Hz, 1 H), 6.10 (dd, *J* = 9.1, 3.9 Hz, 1 H), 5.77 (dd, *J* = 10.6, 1.7 Hz, 1 H), 4.25 (dd, *J* = 13.8, 4.9 Hz, 1 H), 3.84 (d, *J* = 0.6 Hz, 3 H), 3.48 – 3.36 (m, 1 H), 3.22 – 3.05 (m, 2 H), 2.92 – 2.69 (m, 2 H); ^{13}C NMR (101 MHz, $CDCl_3$) δ 201.6, 165.8, 154.1, 133.4, 131.0, 128.5, 127.8, 126.6, 112.0, 111.9, 107.5, 100.4, 56.0, 48.9, 44.8, 41.4, 22.2; IR (film, NaCl) 3284, 2935, 2847, 1717, 1643, 1592, 1485, 1436, 1293, 1258, 1218, 1139, 1114, 1037 cm^{-1}; HRMS (ESI) *m/z* calcd for $C_{17}H_{18}N_2O_3$ (M+Na)+, 321.1210; found, 321.1220;

NMR Assignments. ^{1}H NMR (400 MHz, $CDCl_3$) δ 9.92 (d, *J* = 7.4 Hz, 1 H, H10), 8.54 (s, 1 H, H1), 7.23 (d, *J* = 8.7 Hz, 1 H, H4), 6.90 (d, *J* = 2.5 Hz, 1 H, H2), 6.84 (dd, *J* = 8.8, 2.4 Hz, 1 H, H3), 6.66 (dd, *J* = 16.8, 10.6 Hz, 1 H, H11), 6.33 (dd, *J* = 16.8, 1.7 Hz, 1 H, H12a), 6.10 (dd, *J* = 9.1, 3.9 Hz, 1 H, H8), 5.77 (dd, *J* = 10.6, 1.7 Hz, 1 H, H12b), 4.25 (dd, *J* = 13.8, 4.9 Hz,

1 H, H7ax), 3.84 (d, *J* = 0.6 Hz, 3 H, H5), 3.48 – 3.36 (m, 1 H, H7eq), 3.22 – 3.05 (comp, 2 H, H9), 2.92 – 2.69 (comp, 2 H, H6); ^{13}C NMR (101 MHz, $CDCl_3$) δ 201.6 (C10), 165.8 (C18), 154.1 (C16), 133.4 (C17), 131.0 (C15), 128.5 (C12), 127.8 (C11), 126.6 (C13), 112.0 (C3), 111.9 (C4), 107.5 (C14), 100.4 (C2), 56.0 (C5), 48.9 (C9), 44.8 (C8), 41.4 (C7), 22.2 (C6);

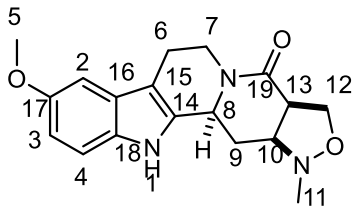

2.97

(3aR,12bS,13aS)-9-Methoxy-1-methyl-3,3a,6,7,12,12b,13,13a-octahydro-1H,4H-indolo[2,3-a]isoxazolo[4,3-g]quinolizin-4-one (2.97) (LTL-IV-001). A solution of aldehyde **2.96** (74 mg, 0.25 mmol), N-methylhydroxylamine hydrochloride (25 mg, 0.3 mmol), and triethylamine (0.08 mL, 0.6 mmol) in toluene (5 mL) was heated under reflux for 2.5 h. The reaction was then cooled to room temperature and concentrated via rotary evaporation. The crude material was purified by flash chromatography eluting with EtOAc:MeOH:Et_3N (99:0:1 → 97:2:1) to give 42 mg (51%) of the title compound as a yellow solid. ^{1}H NMR (400 MHz, DMSO-d_6) δ 10.76 (s, 1 H), 7.19 (dd, *J* = 8.7, 0.5 Hz, 1 H), 6.91 (d, *J* = 2.4 Hz, 1 H), 6.69 (dd, *J* = 8.7, 2.5 Hz, 1 H), 4.89 – 4.72 (comp, 2 H), 4.24 (t, *J* = 9.3 Hz, 1 H), 3.80 (dd, *J* = 8.2, 6.4 Hz, 1 H), 3.73 (s, 3 H), 3.58 (q, *J* = 8.3 Hz, 1 H), 3.32 (s, 1 H), 2.82 (td, *J* = 12.3, 3.8 Hz, 1 H), 2.72 (ddd, *J* = 13.6, 4.1, 2.2 Hz, 1 H), 2.67 – 2.51 (comp, 5 H), 1.30 (q, *J* = 11.9 Hz, 1 H); ^{13}C NMR (101 MHz, DMSO-d_6) δ 169.4, 153.5, 134.5, 131.5, 126.8, 112.0, 111.2, 107.4, 100.3, 67.9, 62.7, 55.6, 55.2, 50.6, 47.2, 43.2, 39.3, 33.8, 21.0, 20.9 ppm; IR (film, NaCl) 3263, 2890, 1600, 1484, 1436, 1324, 1272, 1234, 1173, 1137, 1098, 1044 cm^{-1}; HRMS (ESI) *m/z* calcd for $C_{18}H_{21}N_3O_3$ (M+H)+, 328.16560; found, 328.16640;

NMR Assignment. ^{1}H NMR (400 MHz, DMSO-d_6) δ 10.76 (s, 1 H, H1), 7.19 (dd, *J* = 8.7, 0.5 Hz, 1 H, H4), 6.91 (d, *J* = 2.4 Hz, 1 H, H2), 6.69 (dd, *J* = 8.7, 2.5 Hz, 1 H, H3), 4.89 – 4.72 (comp, 2 H, H7, H8), 4.24 (t, *J* = 9.3 Hz, 1 H, H12), 3.80 (dd, *J* = 8.2, 6.4 Hz, 1 H, H12), 3.73 (s, 3 H, H5), 3.58 (q, *J* = 8.3 Hz, 1 H, H13), 3.32 (s, 1 H, H10), 2.82 (td, *J* = 12.3, 3.8 Hz, 1 H, H7), 2.72 (ddd, *J* = 13.6, 4.1, 2.2 Hz, 1 H, H6), 2.67 – 2.51 (comp, 5 H, H9, H6, H11), 1.30 (q, *J* = 11.9 Hz, 1 H, H9); ^{13}C NMR (101 MHz, DMSO-d_6) δ 169.4 (C19), 153.5 (C17), 134.5 (C18), 131.5 (C16), 126.8 (C14), 112.0 (C4), 111.2 (C3), 107.4 (C15), 100.3 (C2), 67.9 (C12), 62.7 (C10), 55.6 (C5), 50.6 (C8), 47.2 (C13), 43.2 (C11), 39.3 (C7), 33.8 (C9), 20.9 (C6);

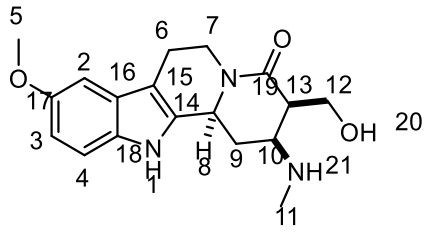

7.9

(2S,3R,12bS)-3-(Hydroxymethyl)-9-methoxy-2-(methylamino)-2,3,6,7,12,12b-hexahydroindolo[2,3-a]quinolizin-4(1H)-one (7.9) (LTL-III-284). Oxazolidinone **2.97** (70 mg, 0.23 mmol) and nickel (II) chloride hexahydrate (109 mg, 0.46 mmol) were dissolved in MeOH (4.5 mL). The solution was cooled to 0 °C, and sodium borohydride (52 mg, 1.38 mmol) was added slowly. The flask was then removed from the ice bath and stirred for 2h at room temperature whereupon the solvent was removed via rotary evaporation. The residue was dissolved in CH_2Cl_2 (2 mL), and 30% aqueous NH_4OH (2 mL) was added. The mixture was stirred for 1.5 h, and the layers were separated. The aqueous layer was extracted with CH_2Cl_2 (3 × 15 mL), and the combined organic layers were dried (Na_2SO_4) and concentrated via rotary evaporation. The crude material was purified by flash chromatography, eluting with CH_2Cl_2MeOH:Et_3N (94:5:1) to give 53 mg (70%) of the title compound as a tan solid. ^{1}H NMR (400 MHz, DMSO-d_6) δ 10.74 (s, 1 H), 7.18 (d, *J* = 8.7 Hz, 1 H), 6.87 (d, *J* = 2.6 Hz, 1 H), 6.67

(dd, *J* = 8.7, 2.5 Hz, 1 H), 4.91 – 4.81 (m, 1 H), 4.79 – 4.71 (m, 1 H), 3.81 – 3.67 (comp, 5 H), 3.12 – 2.99 (m, 1 H), 2.78 (td, *J* = 12.2, 4.1 Hz, 1 H), 2.69 – 2.52 (comp, 4 H), 2.33 (s, 3 H), 1.85 (q, *J* = 11.7 Hz, 1 H). ^{13}C NMR (126 MHz, DMSO-d_6) δ 169.6, 153.6, 135.7, 131.6, 127.1, 112.2, 111.1, 107.2, 100.4, 60.2, 55.8, 54.9, 52.8, 47.5, 34.1, 31.1, 21.3 ppm; IR (film, NaCl) 3247, 2963, 1627,1561, 1435, 1262, 1216, 1091, 1022 cm^{-1}; HRMS (ESI) *m/z* calcd for $C_{18}H_{23}N_3O_3$ (M+Na)+, 352.1632; found, 352.1641.

NMR Assignment. ^{1}H NMR (400 MHz, DMSO-d_6) δ 10.74 (s, 1 H, H1), 7.18 (d, *J* = 8.7 Hz, 1 H, H4), 6.87 (d, *J* = 2.6 Hz, 1 H, H2), 6.67 (dd, *J* = 8.7, 2.5 Hz, 1 H, H3), 4.91 – 4.81 (m, 1 H, H7), 4.79 – 4.71 (m, 1 H, H8), 3.81 – 3.67 (comp, 5 H, H5, H12), 3.12 – 2.99 (m, 1 H, H13), 2.78 (td, *J* = 12.2, 4.1 Hz, 1 H, H7), 2.69 – 2.52 (comp, 4 H, H6, H9, H10), 2.33 (s, 3 H, H11), 1.85 (q, *J* = 11.7 Hz, 1 H, H9). ^{13}C NMR (126 MHz, DMSO-d_6) δ 169.6 (C19), 153.6 (C17), 135.7 (C18), 131.6 (C16), 127.1 (C14), 112.2 (C4), 111.1 (C3), 107.2 (C15), 100.4 (C2), 60.2 (C12), 55.8 (C5), 54.9 (C10), 52.8 (C8), 47.5 (C13), 34.1 (C11), 31.1 (C9), 21.3 (C6);

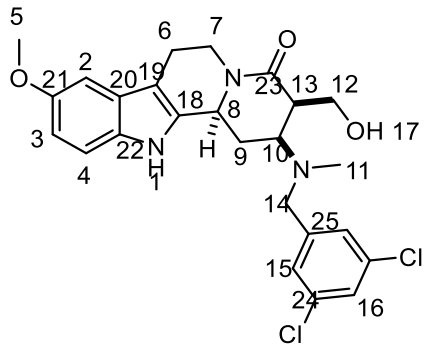

2.98

(2S,3R,12bS)-2-((3,5-Dichlorobenzyl)(methyl)amino)-3-(hydroxymethyl)-9-methoxy-2,3,6,7,12,12b-hexahydroindolo[2,3-a]quinolizin-4(1H)-one (2.98) (LTL-IV-003). A solution of amine **7.9** (20 mg, 0.06 mmol) and 3,5-dichlorobenzaldehyde (21 mg, 0.12 mmol) in MeOH (1.2 mL) was stirred under reflux for 2h. The reaction was cooled to room temperature, acetic acid (0.02 mL, 0.3 mmol) and sodium cyanoborohydride (7.5 mg, 0.12 mmol) were added. The reaction was stirred for 14 h, whereupon additional benzaldehyde **32** (21mg, 0.12 mmol) and

sodium cyanoborohydride (7.5 mg, 0.12 mmol) were added. The reaction was stirred for an additional 24 h, whereupon saturated aqueous $NaHCO_3$ (10 mL) was added, and the resulting mixture was extracted with CH_2Cl_2 (3 x 15 mL). The combined organic layers were dried (Na_2SO_4) and concentrated via rotary evaporation, and the crude material was purified by flash chromatography, eluting with hexanes:EtOAc:Et_3N (75:25:1 → 50:50:1) to give 20 mg (68%) of the title compound as a white solid. ^{1}H NMR (400 MHz, $CDCl_3$) δ 7.65 (s, 1 H), 7.23 (s, 1 H), 7.18 (d, *J* = 2.0 Hz, 2 H), 6.96 (d, *J* = 2.5 Hz, 1 H), 6.86 (dd, *J* = 8.8, 2.5 Hz, 1 H), 5.01 (dd, *J* = 14.0, 2.2 Hz, 1 H), 4.76 (d, *J* = 12.3 Hz, 1 H), 4.02 (d, *J* = 6.8 Hz, 2 H), 3.86 (s, 4 H), 3.60 (d, *J* = 13.8 Hz, 1 H), 3.49 (d, *J* = 13.7 Hz, 1 H), 3.25 (dt, *J* = 11.2, 5.9 Hz, 1 H), 3.06 – 2.93 (m, 2 H), 2.82 (s, 2 H), 2.58 – 2.46 (m, 1 H), 2.20 (s, 3 H), 1.98 – 1.87 (m, 1 H); ^{13}C NMR (101 MHz, DMSO) δ 170.5, 153.6, 145.0, 135.5, 134.4, 131.6, 127.4, 127.0, 126.9, 112.2, 111.2, 107.3, 100.4, 60.2, 59.9, 57.8, 57.0, 55.8, 52.2, 47.6, 38.8, 29.2, 21.2; IR (film, NaCl) 3271, 2921, 2849, 2357, 1616, 1567, 1455, 1433, 1361, 1319, 1285, 1263, 1215, 1175, 1137, 1033 cm^{-1}; HRMS (ESI) *m/z* calcd for $C_{25}H_{27}Cl_2N_3O_3$ (M+H)+, 488.1502; found, 488.1514;

NMR Assignment. ^{1}H NMR (400 MHz, $CDCl_3$) δ 7.65 (s, 1 H, H1), 7.18 (d, *J* = 2.0 Hz, 2 H, H15), 6.96 (d, *J* = 2.5 Hz, 1 H, H2), 6.86 (dd, *J* = 8.8, 2.5 Hz, 1 H, H3), 5.01 (dd, *J* = 14.0, 2.2 Hz, 1 H, H7), 4.76 (d, *J* = 12.3 Hz, 1 H, H8), 4.02 (d, *J* = 6.8 Hz, 2 H, H12), 3.86 (comp, 4 H, H5, H17), 3.60 (d, *J* = 13.8 Hz, 1 H, H14), 3.49 (d, *J* = 13.7 Hz, 1 H, H14), 3.25 (dt, *J* = 11.2, 5.9 Hz, 1 H, H10), 3.06 – 2.93 (comp, 2 H, H7, H13), 2.82 (comp, 2 H, H9, H6), 2.58 – 2.46 (m, 1 H, H6), 2.20 (s, 3 H, H11), 1.98 – 1.87 (m, 1 H, H9); ^{13}C NMR (101 MHz, DMSO) δ 170.5 (C23), 153.6 (C21), 145.0 (C25), 135.5 (C22), 134.4 (C20), 131.6 (C18), 127.4 (C15), 127.0 (C24), 126.9 (C16), 112.2 (C4), 111.2 (C3), 107.3 (C19), 100.4 (C2), 60.2, 59.9 (C12), 57.8 (C10), 57.0 (C14), 55.8 (C5), 52.2 (C8), 47.6 (C13), 38.8 (C11), 29.2 (C9), 21.2 (C6);

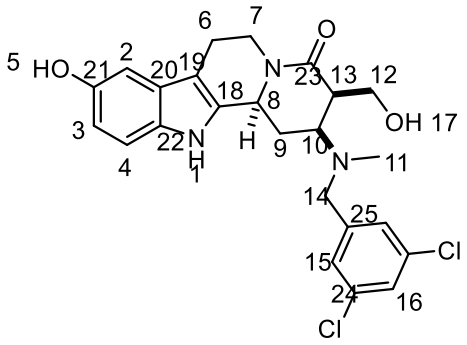

2.99

(2S,3R,12bS)-2-((3,5-Dichlorobenzyl)(methyl)amino)-9-hydroxy-3-(hydroxymethyl)-2,3,6,7,12,12b-hexahydroindolo[2,3-a]quinolizin-4(1H)-one (LTL-IV-004). A 1 M solution of BBr_3 in CH_2Cl_2 (0.06 mmol, 0.06 mL) was added to a stirred solution of **2.98** (10 mg, 0.02 mmol) in CH_2Cl_2 (0.4 mL) at −78 °C, and stirring was continued for 2 h. The flask was then removed from the dry ice/acetone bath and stirred for an additional 3 h at room temperature, whereupon the solvent was removed via rotary evaporation. The residue was resuspended in saturated aqueous $NaHCO_3$ (0.5 mL) and MeOH (0.5 mL), and the mixture was stirred for 1 h. The reaction was then diluted with additional saturated aqueous $NaHCO_3$ (10 mL) and extracted with CH_2Cl_2 (3 x 10 mL). The combined organic layers were dried (Na_2SO_4) and concentrated via rotary evaporation. The crude material was purified by flash chromatography, eluting with hexanes:EtOAc:Et_3N (50:50:1 → 100:0:1) to give 7 mg (78%) of the title compound as a white solid. ^{1}H NMR (400 MHz, CD_3OD) δ 7.35 (d, *J* = 1.9 Hz, 2 H), 7.32 (t, *J* = 1.9 Hz, 1 H), 7.13 (dd, *J* = 8.6, 0.6 Hz, 1 H), 6.80 (dd, *J* = 2.4, 0.6 Hz, 1 H), 6.64 (dd, *J* = 8.6, 2.4 Hz, 1 H), 4.97 – 4.90 (m, 1 H), 4.84 – 4.77 (m, 1 H), 4.10 – 3.98 (comp, 2 H), 3.65 (q, *J* = 14.1 Hz, 2 H), 3.24 – 3.15 (m, 1 H), 3.03 – 2.94 (m, 1 H), 2.94 – 2.86 (m, 1 H), 2.83 – 2.66 (comp, 3 H), 2.23 (s, 3 H), 2.12 – 2.01 (m, 1 H); ^{13}C NMR (101 MHz, CD_3OD) δ 171.5, 150.1, 143.7, 134.7, 133.8, 131.6, 127.2, 126.7, 126.6, 111.1, 110.8, 106.9, 101.9, 60.0, 58.1, 57.2, 52.6, 40.1, 37.6, 28.8, 20.5; IR (film, NaCl) 2923, 2851, 2361, 1614, 1569, 1433, 1358, 1261, 1195, 1036 cm $^{-1}$; HRMS (ESI) *m/z* calcd for $C_{24}H_{25}Cl_2N_3O_3$ $(M+H)^+$, 474.1350; found, 474.1346.

NMR Assignment. ^{1}H NMR (400 MHz, CD_3OD) δ 7.35 (d, *J* = 1.9 Hz, 2 H, H15), 7.32 (t, *J* = 1.9 Hz, 1 H, H16), 7.13 (dd, *J* = 8.6, 0.6 Hz, 1 H, H4), 6.80 (dd, *J* = 2.4, 0.6 Hz, 1 H, H2), 6.64 (dd, *J* = 8.6, 2.4 Hz, 1 H, H3), 4.97 – 4.90 (m, 1 H, H7), 4.84 – 4.77 (m, 1 H, H8), 4.10 – 3.98 (comp, 2 H, H12), 3.65 (q, *J* = 14.1 Hz, 2 H, H14), 3.24 – 3.15 (m, 1 H, H10), 3.03 – 2.94 (m, 1 H, H7), 2.94 – 2.86 (m, 1 H, H13), 2.83 – 2.66 (comp, 3 H, H9, H6), 2.23 (s, 3 H, H11), 2.12 – 2.01 (m, 1 H, H9). ^{13}C NMR (101 MHz, CD_3OD) δ 171.5 (C23), 150.1 (C21), 143.7 (C25), 134.7 (C20), 133.8 (C22), 131.6 (C18), 127.2 (C24), 126.7 (C15), 126.6 (C16), 111.1 (C4), 110.8 (C3), 106.9 (C19), 101.9 (C2), 60.0 (C12), 58.1 (C10), 57.2 (C14), 52.6 (C8), 40.1 (C7), 37.6 (C11), 28.8 (C9), 20.5 (C6).

Expression of full-length *Tb*MetRS and truncated *Tb*MetRS

A 30 ml solution of LB-ampicillin (100 mg / L) was inoculated with one colony of BL21 (de3) transformed with MetRS or truncated MetRS plasmid (plasmids were a generous gift from Wim J. G. Hol). The inoculated solution was cultured overnight at 30 °C, 150 RPM in a shaking incubator. The saturated culture was then diluted 100 x (10 ml : 1000 ml) in 3 x 1 L sterile LB and cultured at 37 °C, 200 RPM until an OD_{600} of 0.6 was reached. At this time, IPTG was added to a final concentration of 0.5 mM, and the temperature of the incubator was reduced to 15 °C. Expression continued for 24 hours, at which time the cells were harvested via centrifugation (15 min, 4000 x g) and the resulting cell pellet was stored at -80 °C until further use.

Purification of full-length *Tb*MetRS

-Thawed frozen cell pellets from 3L of culture and re-suspended in 30 mL of lysis buffer (25 mM HEPES pH 7.0, 500 mM NaCl, 5% glycerol, 10 mM imidazole, 10 mM $MgCl_2$, 10 mM L-Met, 0.025% NaN_3).

-Added 240 uL of DNAse I (40 uL/pellet) and 4 mg PMSF

-Lysed 2x via cell press at 1 drop/sec, 1200 psi

-Spun down lysate 45 min, 12000 RPM, 4 deg C

-Ran FPLC NiNTA column with step gradient. (10 – 30 - 250 mM imidazole)

-Pooled peak fractions and dialyzed into anion exchange buffer A (25 mM HEPES pH 7.0, 5% glycerol, 10 mM L-Met, 0.025% NaN_3).

-Ran FPLC SP/HP column (gradient: 0 – 1 M NaCl)

-Analyzed peak fractions via SDS PAGE, pooled fractions and concentrated with Pall centrifugal concentrator.

-Added glycerol to a final concentration of 50% and stored at -80 ˚C.

Purification of truncated *Tb*MetRS

-Thawed frozen cell pellets from 3L of culture and re-suspended in 30 mL of lysis buffer (25 mM HEPES pH 7.0, 500 mM NaCl, 5% glycerol, 10 mM imidazole, 10 mM $MgCl_2$, 10 mM L-Met, 0.025% NaN_3).

-Added 240 uL of DNAse I (40 uL/pellet) and 4 mg PMSF

-Lysed 2x via cell press at 1 drop/sec, 1200 psi

-Spun down lysate 45 min, 12000 RPM, 4 deg C

-Ran FPLC NiNTA column with step gradient. (10 – 30 - 250 mM imidazole)

-Pooled peak fractions and dialyzed into anion exchange buffer A (25 mM HEPES pH 7.0, 5% glycerol, 10 mM L-Met, 0.025% NaN_3).

-Ran FPLC Q column (gradient: 0 – 1 M NaCl)

-Analyzed peak fractions via SDS PAGE, pooled fractions and concentrated with Pall centrifugal concentrator.

-Added glycerol to a final concentration of 50% and stored at -80 ˚C.

***Tb*MetRS aminoacylation assay**

Protocol was adapted from the procedure of Cestari and Stuart.[48] Reactions were performed in 25 mM HEPES pH 9, 100 mM NaCl, 10 mM MgCl, 50 mM KCl, 1 mM DTT and

3% glycerol with 0.8 mg/mL yeast tRNA (Sigma), 0.2 mM L-methionine, 0.2 mM ATP, 0.1 μM recombinant *Tb*MetRS, and 2 U/mL pyrophosphatase (Sigma) in 50 μL total volume. The reactions were performed in clear, flat-bottom 96-well plates and incubated for 2 hours at room temperature, whereupon 75 μL of a 2:1 mixture of H_2O and freshly prepared malachite green reagent[49] was added, and the mixture was incubated for an additional 20 minutes. Absorbances were then measured at 620 nM using a plate reader. Reactions were performed in triplicate with median values used, and the reported results are the average of two runs. For IC_{50} determination inhibitors were added to the reaction as a solution in DMSO, and the values were calculated in Origin 2016 for Mac using 4-parameter logistic nonlinear regression.

7.2 DIVERSITY-ORIENTED SYNTHESIS OF SPIROCYCLIC B-PHENETHYLAMINES

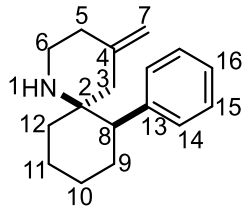

4.39

(6S,7R)-4-Methylene-7-phenyl-1-azaspiro[5.5]undecane (4.39) (LTL-IV-271). A solution of **4.30** (17 mg, 0.1 mmol), **4.2** (19 mg, 0.12 mmol) and AcOH (6 mg, 0.1 mmol) in MeOH (1 mL) was stirred at room temperature for 24 h, whereupon the mixture was diluted with aqueous Na_2CO_3 (1.4 M) and extracted with CH_2Cl_2 (3 x 15 mL). The combined organic extracts were dried (Na_2SO_4) and concentrated via rotary evaporation. The crude material was purified by flash column chromatography, eluting with hexanes:Et_3N (99 : 1) to give 16 mg (67%) of the title compound as a white solid, mp 63–66 ˚C. ^{1}H NMR (500 MHz, $CDCl_3$) δ 7.23 (t, *J* = 7.5 Hz, 2 H), 7.18 – 7.13 (comp, 3 H), 4.60 (s, 1 H), 4.50 (s, 1 H), 2.82 (dd, *J* = 13.5, 6.2 Hz, 1 H), 2.62 (td, *J* = 12.9, 3.6 Hz, 1 H), 2.48 (dd, *J* = 12.8, 3.4 Hz, 1 H), 2.22 – 2.08 (comp, 2 H), 1.99 (dd, *J* = 13.2, 3.4 Hz, 1 H), 1.84 – 1.72 (comp, 3 H), 1.62 – 1.52 (m, 1 H), 1.52 – 1.37 (comp, 3 H), 1.30 (qt, *J* = 13.0, 4.1 Hz, 1 H), 1.12 (s, 1 H), 0.88 (td, *J* = 13.7, 3.8 Hz, 1 H); ^{13}C NMR (126 MHz, $CDCl_3$) δ 145.5, 142.3, 129.6, 128.0, 126.5, 108.6, 55.2, 53.9, 47.2, 41.3, 36.2, 31.8, 27.7, 26.9, 21.0; IR (film, NaCl) 3731, 3632, 3065, 2928, 2853, 2361, 2338, 1651, 1456 cm^{-1}; HRMS (ESI) *m/z* calcd for $C_{17}H_{23}N$ (M+H)+, 242.1903; found 242.1906

NMR Assignment. ^{1}H NMR (500 MHz, $CDCl_3$) δ 7.23 (t, *J* = 7.5 Hz, 2 H, H15), 7.18 – 7.13 (comp, 3 H, H14, H16), 4.60 (s, 1 H, H7), 4.50 (s, 1 H, H7), 2.82 (dd, *J* = 13.5, 6.2 Hz, 1 H, H6), 2.62 (td, *J* = 12.9, 3.6 Hz, 1 H, H6), 2.48 (dd, *J* = 12.8, 3.4 Hz, 1 H, H8), 2.22 – 2.08 (comp, 2 H, H9, H12), 1.99 (dd, *J* = 13.2, 3.4 Hz, 1 H, H5), 1.84 – 1.72 (comp, 3 H, H3, H9), 1.62 – 1.52 (m, 1 H, H5), 1.52 – 1.37 (comp, 3 H, H9, H8), 1.30 (qt, *J* = 13.0, 4.1 Hz, 1 H, H10), 1.12 (s, 1 H, H1), 0.88 (td, *J* = 13.7, 3.8 Hz, 1 H, H7). ^{13}C NMR (126 MHz, $CDCl_3$) δ 145.5

(C4), 142.3 (C13), 129.6 (C16), 128.0 (C15), 126.5 (C14), 108.6 (C7), 55.2 (C2), 53.9 (C8), 47.2 (C3), 41.3 (C6), 36.2 (C5), 31.8 (C12), 27.7 (C9), 26.9 (C10), 21.0 (C11).

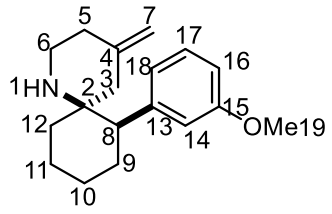

4.41

(6S,7R)-7-(3-Methoxyphenyl)-4-methylene-1-azaspiro[5.5]undecane (4.41) (LTL-IV-291). The title compound was prepared following the general procedure of **4.39**. The crude material was purified by flash column chromatography, eluting with hexanes:Et_3N (99 : 1) to give 55 mg (65%) of the title compound as a white paste. ^{1}H NMR (500 MHz, $CDCl_3$) δ 7.22 (t, *J* = 7.8 Hz, 1 H), 6.86 – 6.75 (comp, 3 H), 4.68 (s, 1 H), 4.57 (s, 1 H), 3.81 (s, 3 H), 2.90 (dd, *J* = 13.6, 6.2 Hz, 1 H), 2.69 (td, *J* = 13.0, 3.6 Hz, 1 H), 2.53 (dd, *J* = 12.8, 3.4 Hz, 1 H), 2.29 – 2.15 (comp, 2 H), 2.12 – 2.02 (d, *J* = 13.6 Hz, 1 H), 1.89 (comp, 3 H), 1.68 (td, *J* = 12.8, 5.6 Hz, 1 H), 1.56 (comp, 2 H), 1.48 (m, 1 H), 1.36 (comp, 2 H), 0.94 (td, *J* = 13.8, 3.8 Hz, 1 H); ^{13}C NMR (126 MHz, $CDCl_3$) δ 159.3, 145.5, 143.9, 128.9, 122.1, 115.5, 111.6, 108.6, 55.2, 55.2, 54.0, 47.3, 41.3, 36.2, 31.8, 27.7, 26.9, 20.9; HRMS (ESI) *m/z* calcd for $C_{18}H_{25}NO$ (M+H)+, 272.2009; found 272.2008.

NMR Assignment. ^{1}H NMR (499 MHz, $CDCl_3$) δ 7.22 (t, *J* = 7.8 Hz, 1 H, H17), 6.86 – 6.75 (comp, 3 H, H14, H16, H18), 4.68 (s, 1 H, H7), 4.57 (s, 1 H, H7), 3.81 (s, 3 H, H19), 2.90 (dd, *J* = 13.6, 6.2 Hz, 1 H, H6), 2.69 (td, *J* = 13.0, 3.6 Hz, 1 H, H6), 2.53 (dd, *J* = 12.8, 3.4 Hz, 1 H, H8), 2.29 – 2.15 (comp, 2 H, H9, H12), 2.07 (d, *J* = 13.6 Hz, 1 H, H5), 1.89 (comp, 3 H, H3, H10), 1.68 (td, *J* = 12.8, 5.6 Hz, 1 H, H5), 1.56 (comp, 2 H, H9, H11), 1.48 (m, 1 H, H11), 1.36 (comp, 2 H, H10, H1), 0.94 (td, *J* = 13.8, 3.8 Hz, 1 H, H12); ^{13}C NMR (126 MHz, $CDCl_3$) δ 159.3 (C15), 145.5 (C4), 143.9 (C13), 128.9 (C17), 122.1 (C18), 115.5 (C14), 111.6 (C16),

108.6 (C7), 55.2 (C2), 55.2 (C19), 54.0 (C8), 47.3 (C3), 41.3 (C6), 36.2 (C5), 31.8 (C12), 27.7 (C9), 26.9 (C10), 20.9 (C11).

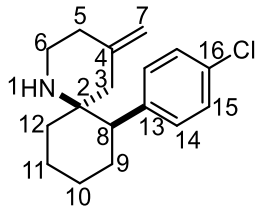

4.42

(6S,7R)-7-(4-Chlorophenyl)-4-methylene-1-azaspiro[5.5]undecane (4.42) (LTL-IV-288). The title compound was prepared following the general procedure of **4.39**. The crude material was purified by flash column chromatography, eluting with hexanes:Et_3N (100 : 1) to give 65 mg (69 %) of the title compound as a yellow oil. ^{1}H NMR (500 MHz, $CDCl_3$) δ 7.28 (d, *J* = 8.5 Hz, 2 H), 7.19 (d, *J* = 8.5 Hz, 2 H), 4.70 (s, 1 H), 4.59 (s, 1 H), 2.95 – 2.83 (m, 1 H), 2.70 (td, *J* = 12.8, 3.5 Hz, 1 H), 2.54 (dd, *J* = 12.8, 3.4 Hz, 1 H), 2.26 – 2.04 (comp, 3 H), 1.90 – 1.80 (comp, 3 H), 1.70 (td, *J* = 12.8, 5.7 Hz, 1 H), 1.54 (comp, 3 H), 1.37 (qt, *J* = 12.6, 4.2 Hz, 1 H), 1.29 – 1.17 (m, 1 H), 0.95 (ddd, *J* = 14.5, 12.4, 4.3 Hz, 1 H); ^{13}C NMR (126 MHz, $CDCl_3$) δ 145.1, 140.8, 132.2, 130.9, 128.1, 108.9, 55.1, 53.3, 47.0, 41.2, 36.0, 31.6, 27.8, 26.8, 20.8. HRMS (ESI) *m/z* calcd for $C_{17}H_{22}ClN$ (M+H)+, 276.1514; found 276.1517.

NMR Assignment. ^{1}H NMR (500 MHz, $CDCl_3$) δ 7.28 (d, *J* = 8.5 Hz, 2 H, H15), 7.19 (d, *J* = 8.5 Hz, 2 H, H14), 4.70 (s, 1 H, H7), 4.59 (s, 1 H, H7), 2.95 – 2.83 (m, 1 H, H6), 2.70 (td, *J* = 12.8, 3.5 Hz, 1 H, H6), 2.54 (dd, *J* = 12.8, 3.4 Hz, 1 H, H8), 2.26 – 2.04 (comp, 3 H, H9, H12, H5), 1.90 – 1.80 (comp, 3 H, H3, H10), 1.70 (td, *J* = 12.8, 5.7 Hz, 1 H, H5), 1.54 (comp, 3 H, H9, H11), 1.37 (qt, *J* = 12.6, 4.2 Hz, 1 H, H10), 1.29 – 1.17 (m, 1 H, H1), 0.95 (ddd, *J* = 14.5, 12.4, 4.3 Hz, 1 H, H12); ^{13}C NMR (126 MHz, $CDCl_3$) δ 145.1 (C4), 140.8 (C13), 132.2 (C16), 130.9 (C14), 128.1 (C15), 108.9 (C7), 55.1 (C2), 53.3 (C8), 47.0 (C3), 41.2 (C6), 36.0 (C5), 31.6 (C12), 27.8 (C9), 26.8 (C10), 20.8 (C11).

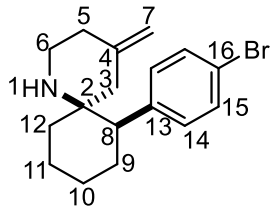

4.43

(6S,7R)-7-(4-Bromophenyl)-4-methylene-1-azaspiro[5.5]undecane (4.43) (LTL-V-038). The title compound was prepared following the general procedure of **4.39**. The crude material was purified by flash column chromatography, eluting with hexanes:Et_3N (100 : 1) to give 105 mg (82%) of the title compound as a white solid. ^{1}H NMR (400 MHz, $CDCl_3$) δ 7.45 – 7.40 (d, *J* = 8.4 Hz, 2 H), 7.15 – 7.09 (d, *J* = 8.4 Hz, 2 H), 4.68 (s, 1 H), 4.57 (s, 1 H), 2.88 (ddd, *J* = 13.2, 6.1, 1.6 Hz, 1 H), 2.68 (td, *J* = 12.8, 3.6 Hz, 1 H), 2.51 (dd, *J* = 12.8, 3.4 Hz, 1 H), 2.25 – 2.03 (comp, 3 H), 1.84 (s, 3 H), 1.69 (td, *J* = 12.7, 6.1 Hz, 1 H), 1.52 (ddt, *J* = 12.7, 8.2, 3.1 Hz, 3 H), 1.36 (qq, *J* = 12.7, 4.7, 4.2 Hz, 1 H), 0.99 – 0.87 (m, 1 H); ^{13}C NMR (126 MHz, $CDCl_3$) δ 145.2, 141.3, 131.3, 131.0, 120.3, 108.9, 55.0, 53.4, 47.0, 41.2, 36.0, 31.6, 27.8, 26.8, 20.8; HRMS (ESI) *m/z* calcd for $C_{17}H_{22}BrN$ (M+H)+ 320.1008; found 320.1000.

NMR Assignment. ^{1}H NMR (400 MHz, $CDCl_3$) δ 7.45 – 7.40 (d, *J* = 8.4 Hz, 2 H, H15), 7.15 – 7.09 (d, *J* = 8.4 Hz, 2 H, H14), 4.68 (s, 1 H, H7), 4.57 (s, 1 H, H7), 2.88 (ddd, *J* = 13.2, 6.1, 1.6 Hz, 1 H, H6), 2.68 (td, *J* = 12.8, 3.6 Hz, 1 H, H6), 2.51 (dd, *J* = 12.8, 3.4 Hz, 1 H, H8), 2.25 – 2.03 (comp, 3 H, H9, H12, H5), 1.84 (s, 3 H, H3, H6), 1.69 (td, *J* = 12.7, 6.1 Hz, 1 H, H5), 1.52 (comp, 3 H, H9, H11), 1.36 (qq, *J* = 12.7, 4.7, 4.2 Hz, 1 H, H10), 0.99 – 0.87 (m, 1 H, H12); ^{13}C NMR (126 MHz, $CDCl_3$) δ 145.2 (C4), 141.3 (C13), 131.3 (C15), 131.0 (C14), 120.3 (C16), 108.9 (C7), 55.0 (C2), 53.4 (C8), 47.0 (C3), 41.2 (C6), 36.0 (C5), 31.6 (C12), 27.8 (C9), 26.8 (C10), 20.8 (C11).

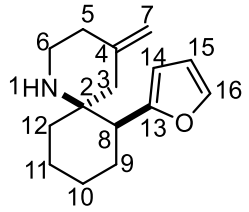

4.44

(6S,7S)-7-(Furan-2-yl)-4-methylene-1-azaspiro[5.5]undecane (4.44) (LTL-IV-281). The title compound was prepared following the general procedure of **4.39**. The crude material was purified by flash column chromatography, eluting with hexanes:Et_3N (100 : 1) to give 34 mg (74 %) of the title compound as a yellow oil. ^{1}H NMR (400 MHz, $CDCl_3$) δ 7.34 (dd, *J* = 1.9, 0.8 Hz, 1 H), 6.33 (dd, *J* = 3.2, 1.9 Hz, 1 H), 6.11 (dd, *J* = 3.2, 0.8 Hz, 1 H), 4.71 (m, 1 H), 4.61 (m, 1 H), 2.91 (ddd, *J* = 13.3, 5.8, 2.6 Hz, 1 H), 2.74 (dd, *J* = 11.5, 3.8 Hz, 1 H), 2.67 (ddd, *J* = 13.3, 11.5, 3.8 Hz, 1 H), 2.16 – 1.93 (comp, 5 H), 1.87 – 1.75 (comp, 2 H), 1.66 – 1.50 (comp, 2 H), 1.49 – 1.40 (m, 1 H), 1.40 – 1.25 (comp, 2 H), 0.99 (ddd, *J* = 14.1, 11.8, 3.7 Hz, 1 H).^{13}C NMR (126 MHz, $CDCl_3$) δ 157.2, 145.3, 141.0, 110.1, 108.8, 106.8, 55.2, 46.6, 46.2, 41.4, 36.2, 31.7, 26.8, 25.8, 20.7. HRMS (ESI) *m/z* calcd for $C_{15}H_{21}NO$ (M+H)+, 232.1696; found 232.1695.

NMR Assignment. ^{1}H NMR (400 MHz, $CDCl_3$) δ 7.34 (dd, *J* = 1.9, 0.8 Hz, 1 H, H16), 6.33 (dd, *J* = 3.2, 1.9 Hz, 1 H, H15), 6.11 (dd, *J* = 3.2, 0.8 Hz, 1 H, H14), 4.71 (m, 1 H, H7), 4.61 (m, 1 H, H7), 2.91 (ddd, *J* = 13.3, 5.8, 2.6 Hz, 1 H, H6), 2.74 (dd, *J* = 11.5, 3.8 Hz, 1 H, H8), 2.67 (ddd, *J* = 13.3, 11.5, 3.8 Hz, 1 H, H6), 2.16 – 1.93 (comp, 5 H, H3, H5, H9, H12), 1.87 – 1.75 (comp, 2 H, H5, H10), 1.66 – 1.50 (comp, 2 H, H9, H11), 1.49 – 1.40 (m, 1 H, H11), 1.40 – 1.25 (comp, 2 H, H1, H10), 0.99 (ddd, *J* = 14.1, 11.8, 3.7 Hz, 1 H, H12).^{13}C NMR (126 MHz, $CDCl_3$) δ 157.2 (C13), 145.3 (C4), 141.0 (C16), 110.1 (C15), 108.8 (C7), 106.8 (C14), 55.2 (C2), 46.6 (C3), 46.2 (C8), 41.4 (C6), 36.2 (C5), 31.7 (C12), 26.8 (C9), 25.8 (C10), 20.7 (C11).

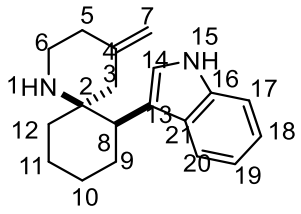

4.45

(6S,7R)-7-(1H-Indol-3-yl)-4-methylene-1-azaspiro[5.5]undecane (4.45) (LTL-IV-282). The title compound was prepared following the general procedure of **4.39**. The crude material was purified by flash column chromatography, eluting with hexanes:EtOAc:Et_3N (75 : 25 : 1) to give 21 mg (75 %) of the title compound as a white solid, mp 178–180 ˚C. ^{1}H NMR (500 MHz, $CDCl_3$) δ 8.17 (s, 1 H), 7.66 (d, *J* = 7.9 Hz, 1 H), 7.40 (d, *J* = 8.1 Hz, 1 H), 7.22 (t, *J* = 7.6 Hz, 1 H), 7.16 (comp, 2 H), 4.68 (s, 1 H), 4.60 (s, 1 H), 2.99 (dd, *J* = 12.6, 3.5 Hz, 1 H), 2.93 (dd, *J* = 13.7, 5.9 Hz, 1 H), 2.72 (td, *J* = 12.9, 3.5 Hz, 1 H), 2.28 – 2.11 (comp, 2 H), 2.11 – 1.94 (comp, 3 H), 1.86 (dt, *J* = 13.0, 3.8 Hz, 1 H), 1.71 – 1.48 (comp, 6 H), 1.42 (qt, *J* = 12.4, 3.8 Hz, 1 H), 1.10 (td, *J* = 13.6, 3.7 Hz, 1 H); ^{13}C NMR (126 MHz, $CDCl_3$) δ 145.6, 135.8, 128.6, 122.1, 122.0, 119.7, 119.4, 117.8, 111.0, 108.5, 55.5, 47.7, 41.5, 36.3, 31.7, 29.0, 27.0, 20.9; HRMS (ESI) *m/z* calcd for $C_{19}H_{24}N_2$ (M+H)+, 281.2012; found 281.2011.

NMR Assignment. ^{1}H NMR (499 MHz, $CDCl_3$) δ 8.17 (s, 1 H, H15), 7.66 (d, *J* = 7.9 Hz, 1 H, H17), 7.40 (d, *J* = 8.1 Hz, 1 H, H20), 7.22 (t, *J* = 7.6 Hz, 1 H, H19), 7.16 (comp, 2 H, H14, H18), 4.68 (s, 1 H, H7), 4.60 (s, 1 H, H7), 2.99 (dd, *J* = 12.6, 3.5 Hz, 1 H, H8), 2.93 (dd, *J* = 13.7, 5.9 Hz, 1 H, H6), 2.72 (td, *J* = 12.9, 3.5 Hz, 1 H, H6), 2.28 – 2.11 (comp, 2 H, H9, H12), 2.11 – 1.94 (comp, 3 H, H5, H3), 1.86 (dt, *J* = 13.0, 3.8 Hz, 1 H, H10), 1.71 – 1.48 (comp, 6 H, H9, H5, H11, H1), 1.42 (qt, *J* = 12.4, 3.8 Hz, 1 H, H10), 1.10 (td, *J* = 13.6, 3.7 Hz, 1 H, H12); ^{13}C NMR (126 MHz, $CDCl_3$) δ 145.6 (C4), 135.8 (C16), 128.6 (C21), 122.1 (C14), 122.0 (C19), 119.7 (C17), 119.4 (C18), 117.8 (C13), 111.0 (C20), 108.5 (C7), 55.5, 47.7 (C3), 43.9 (C8), 41.5 (C6), 36.3 (C5), 31.7 (C12), 29.0 (C9), 27.0 (C10), 20.9 (C11).

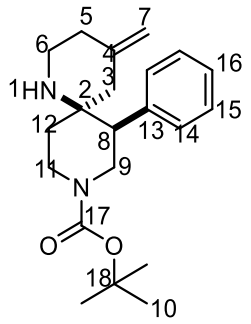

4.46

***Tert*-butyl (6R,7S)-4-methylene-7-phenyl-1,9-diazaspiro[5.5]undecane-9-carboxylate (LTL-V-077).** A stirred solution of **4.18** (28 mg, 0.1 mmol), **4.2** (19 mg, 0.12 mmol), and AcOH (6 mg, 0.1 mmol) in MeOH (1 mL) was heated to 50 ˚C (bath temp.) for 24 h, whereupon the mixture was diluted with aqueous Na_2CO_3 (1.4 M, 20 mL) and extracted with CH_2Cl_2 (3 x 15 mL). The combined organic extracts were dried (Na_2SO_4) and concentrated via rotary evaporation. The crude material was purified by flash column chromatography, eluting with hexanes:EtOAc:Et_3N (90 : 10 : 1) to give 27 mg (79%) of the title compound as an off-white solid. ^{1}H NMR (400 MHz, $CDCl_3$) δ 7.33 (comp, 3 H), 7.20 (comp, 2 H), 4.72 (s, 1 H), 4.62 (s, 1 H), 3.85 (comp, 2 H), 3.63 (br, 1 H), 3.16 (t, *J* = 13.0 Hz, 1 H), 2.91 (dd, *J* = 13.9, 5.9 Hz, 1 H), 2.73 – 2.59 (comp, 2 H), 2.09 (comp, 2 H), 1.93 (s, 2 H), 1.68 (td, *J* = 12.9, 6.0 Hz, 1 H), 1.43 (s, 10 H), 1.18 (s, 1 H); ^{13}C NMR (126 MHz, $CDCl_3$) δ 155.0, 144.5, 138.6, 129.5, 128.4, 127.2, 109.5, 83.7, 79.4, 54.1, 51.9, 50.3, 46.2, 44.0, 43.1, 41.5, 39.9, 38.9, 36.2, 30.7, 28.5, 28.1; HRMS (ESI) *m/z* calcd for $C_{21}H_{30}N_2O_2$ (M+H)+ 343.2380; found 343.2375;

NMR Assignment. ^{1}H NMR (400 MHz, $CDCl_3$) δ 7.33 (comp, 3 H, H13, H15), 7.20 (comp, 2 H, H14), 4.72 (s, 1 H, H7), 4.62 (s, 1 H, H7), 3.85 (comp, 2 H, H9, H10), 3.63 (br, 1 H, H9), 3.16 (t, *J* = 13.0 Hz, 1 H, H10), 2.91 (dd, *J* = 13.9, 5.9 Hz, 1 H, H6), 2.73 – 2.59 (comp, 2 H, H6, H8), 2.09 (comp, 2 H, H5, H11), 1.93 (s, 2 H, H3), 1.68 (td, *J* = 12.9, 6.0 Hz, 1 H, H5), 1.43 (s, 10 H, H1, H18), 1.18 (s, 1 H), H11; ^{13}C NMR (126 MHz, $CDCl_3$) δ 155.0 (C16), 144.5 (C4), 138.6 (C12), 129.5 (C14), 128.4 (C13), 127.2 (C15), 109.5 (C7), 83.7 (C17*), 79.4 (C17), 54.1 (C2), 51.9 (C8), 46.2 (C3), 44.0 (C9), 43.1 (C9), 41.5 (C6), 39.9 (C10), 38.9 (C10), 36.2 (C5), 30.7 (C11), 28.5 (C18), 28.1 (C18).

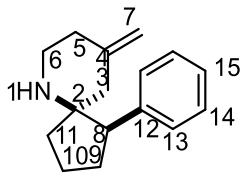

4.47

(1R,5S)-9-Methylene-1-phenyl-6-azaspiro[4.5]decane (4.47) (LTL-V-027). A stirred solution of **4.37** (16 mg, 0.1 mmol), **4.2** (19 mg, 0.12 mmol), and AcOH (6 mg, 0.1 mmol) in MeOH (1 mL) was heated under reflux for 11 h, whereupon the mixture was diluted with aqueous Na_2CO_3 (1.4 M, 15 mL) and extracted with CH_2Cl_2 (3 x 10 mL). The combined organic extracts were dried (Na_2SO_4) and concentrated via rotary evaporation. The crude material was purified by flash column chromatography, eluting with hexanes:Et_3N (100 : 1) to give 12 mg (52%) of the title compound as a clear oil. ^{1}H NMR (500 MHz, $CDCl_3$) δ 7.36 – 7.31 (comp, 2 H), 7.29 – 7.25 (comp, 3 H), 4.68 (s, 1 H), 4.66 (s, 1 H), 2.88 (ddd, *J* = 13.3, 5.6, 2.3 Hz, 1 H), 2.80 (dd, *J* = 10.8, 7.5 Hz, 1 H), 2.68 (ddd, *J* = 13.3, 11.8, 3.6 Hz, 1 H), 2.26 – 2.15 (m, 1 H), 2.13 – 2.05 (comp, 3 H), 2.05 – 1.97 (m, 1 H), 1.92 – 1.82 (comp, 2 H), 1.79 – 1.70 (m, 1 H), 1.70 – 1.62 (m, 1 H), 1.62 – 1.56 (m, 1 H), 1.14 – 0.94 (s, 1 H); ^{13}C NMR (126 MHz, $CDCl_3$) δ 146.2, 139.9, 129.5, 128.2, 126.7, 108.1, 64.6, 56.4, 46.7, 43.0, 36.2, 34.5, 30.3, 22.0; HRMS (ESI) *m/z* calcd for $C_{16}H_{21}N$ (M+H)+, 228.1747; found 228.1745.

NMR Assignment. ^{1}H NMR (500 MHz, $CDCl_3$) δ 7.36 – 7.31 (comp, 2 H, H14), 7.29 – 7.25 (comp, 3 H, H13, H15), 4.68 (s, 1 H, H7), 4.66 (s, 1 H, H7), 2.88 (ddd, *J* = 13.3, 5.6, 2.3 Hz, 1 H, H6), 2.80 (dd, *J* = 10.8, 7.5 Hz, 1 H, H8), 2.68 (ddd, *J* = 13.3, 11.8, 3.6 Hz, 1 H, H6), 2.26 – 2.15 (m, 1 H, H9), 2.13 – 2.05 (comp, 3 H, H5, H3), 2.05 – 1.97 (m, 1 H, H9), 1.92 – 1.82 (comp, 2 H, H10, H11), 1.79 – 1.70 (m, 1 H, H5), 1.70 – 1.62 (m, 1 H, H11), 1.62 – 1.56 (m, 1 H, H10), 1.14 – 0.94 (s, 1 H, H1); ^{13}C NMR (126 MHz, $CDCl_3$) δ 146.2 (C4), 139.9 (C8), 129.5 (C15), 128.2 (C14), 126.7 (C13), 108.1 (C7), 64.6 (C2), 56.4 (C8), 46.7 (C3), 43.0 (C6), 36.2 (C5), 34.5 (C10), 30.3 (C9), 22.0 (C11).

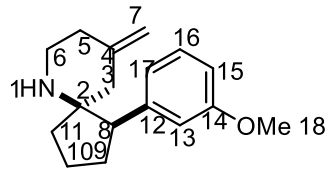

4.48

(1R,5S)-1-(3-Methoxyphenyl)-9-methylene-6-azaspiro[4.5]decane (4.48) (LTL-V-036). The title compound was prepared following the procedure of **4.47**. The crude material was purified by flash column chromatography, eluting with hexanes:Et_3N (100 : 1) to give 76 mg (59%) of the title compound as a yellow oil. ^1H NMR (500 MHz, $CDCl_3$) δ 7.21 (m, 1 H), 6.83 (dt, *J* = 7.6, 1.4 Hz, 1 H), 6.80 – 6.75 (comp, 2 H), 4.64 (s, 1 H), 4.62 (s, 1 H), 3.78 (s, 3 H), 2.86 (ddd, *J* = 13.3, 5.6, 2.4 Hz, 1 H), 2.74 (dd, *J* = 10.8, 7.5 Hz, 1 H), 2.65 (ddd, *J* = 13.3, 11.8, 3.6 Hz, 1 H), 2.16 (dddd, *J* = 17.5, 10.9, 8.7, 3.6 Hz, 1 H), 2.10 – 2.02 (comp, 3 H), 2.01 – 1.92 (m, 1 H), 1.89 – 1.79 (comp, 2 H), 1.77 – 1.68 (m, 1 H), 1.68 – 1.58 (m, 1 H), 1.58 – 1.49 (m, 1 H); ^{13}C NMR (126 MHz, $CDCl_3$) δ 159.4, 146.3, 141.6, 129.1, 122.0, 115.2, 111.9, 108.0, 64.7, 56.5, 55.2, 46.7, 43.0, 36.2, 34.4, 30.3, 21.9; HRMS (ESI) *m/z* calcd for $C_{17}H_{23}NO$ (M+H)+ 258.1852; found 258.1849.

NMR Assignment. ^1H NMR (500 MHz, $CDCl_3$) δ 7.21 (m, 1 H, H16), 6.83 (dt, *J* = 7.6, 1.4 Hz, 1 H, H17), 6.80 – 6.75 (comp, 2 H, H13, H15), 4.64 (s, 1 H, H7), 4.62 (s, 1 H, H7), 3.78 (s, 3 H, H18), 2.86 (ddd, *J* = 13.3, 5.6, 2.4 Hz, 1 H, H6), 2.74 (dd, *J* = 10.8, 7.5 Hz, 1 H, H8), 2.65 (ddd, *J* = 13.3, 11.8, 3.6 Hz, 1 H, H6), 2.16 (dddd, *J* = 17.5, 10.9, 8.7, 3.6 Hz, 1 H, H9), 2.10 – 2.02 (comp, 3 H, H5, H3), 2.01 – 1.92 (m, 1 H, H9), 1.89 – 1.79 (comp, 2 H, H10, H11), 1.77 – 1.68 (m, 1 H, H5), 1.68 – 1.58 (m, 1 H, H11), 1.58 – 1.49 (m, 1 H, H10); ^{13}C NMR (126 MHz, $CDCl_3$) δ 159.4 (C14), 146.3 (C4), 141.6 (C12), 129.1 (C16), 122.0 (C17), 115.2 (C13), 111.9 (C15), 108.0 (C7), 64.7 (C2), 56.5 (C8), 55.2 (C18), 46.7 (C3), 43.0 (C6), 36.2 (C5), 34.4 (C10), 30.3 (C9), 21.9 (C11).

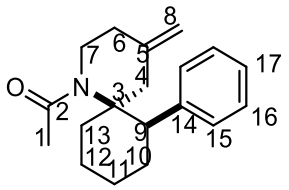

4.51

1-((6S,7R)-4-Methylene-7-phenyl-1-azaspiro[5.5]undecan-1-yl)ethan-1-one (4.51) (LTL-V-060). A solution of **4.39** (241 mg, 1.0 mmol), AcCl (157 mg, 0.14 mmol), and *i*Pr$_2$NEt (387 mg, 3.0 mmol) in THF (10 mL) was stirred at room temperature overnight, whereupon an additional equivalent of AcCl (78 mg, 1.0 mmol) and *i*Pr$_2$NEt (129 mg, 1.0 mmol) was added every 3 h until **4.39** was consumed. The solvent was removed via rotary evaporation, and the resulting solid was resuspended in Et$_2$O and decanted into a separatory funnel. The solid was rinsed with Et$_2$O and decanted an additional two times. The combined organic layer was washed sequentially with aqueous HCl (3M, 20 mL), aqueous NaOH (3M, 20 mL), and brine (20 mL). The organic layer was dried (Na$_2$SO$_4$) and concentrated via rotary evaporation. The crude material was purified by flash column chromatography, eluting with hexanes:EtOAc (85 : 15) to give 247 mg (87 %) of the title compound as a white solid. ^{1}H NMR (500 MHz, CDCl$_3$) δ 7.38 – 7.34 (comp, 2 H), 7.26 – 7.20 (comp, 2 H), 7.18 – 7.13 (m, 1 H), 4.85 (s, 2 H), 3.23 – 3.12 (m, 1 H), 3.11 – 3.01 (m, 1 H), 3.00 – 2.86 (comp, 2 H), 2.53 (s, 1 H), 2.27 – 2.09 (comp, 4 H), 2.03 (dt, *J* = 14.7, 3.9 Hz, 1 H), 1.85 (s, 3 H), 1.80 – 1.71 (m, 1 H), 1.70 – 1.62 (m, 1 H), 1.61 – 1.36 (comp, 3 H); ^{13}C NMR (126 MHz, CDCl$_3$) δ 171.2, 142.6, 142.0, 129.4, 127.9, 126.1, 112.1, 64.1, 47.5, 44.0, 43.4, 32.6, 32.1, 29.1, 25.9, 21.2, 20.7; HRMS (ESI) *m/z* calcd for C$_{19}$H$_{25}$NO 284.2009; found 284.2000;

NMR Assignment. ^{1}H NMR (500 MHz, CDCl$_3$) δ 7.38 – 7.34 (comp, 2 H, H15), 7.26 – 7.20 (comp, 2 H, H16), 7.18 – 7.13 (m, 1 H, H17), 4.85 (s, 2 H, H8), 3.23 – 3.12 (m, 1 H, H13), 3.11 – 3.01 (m, 1 H, H7), 3.00 – 2.86 (comp, 2 H, H9, H6), 2.53 (s, 1 H, H7), 2.27 – 2.09 (comp, 4 H, H6, H10, H4), 2.03 (dt, *J* = 14.7, 3.9 Hz, 1 H, H13), 1.85 (s, 3 H, H1), 1.80 – 1.71 (m, 1 H, H12), 1.70 – 1.62 (m, 1 H, H10), 1.61 – 1.36 (comp, 3 H, H11, H12); ^{13}C NMR (126 MHz,

$CDCl_3$) δ 171.2 (C2), 142.6 (C5), 142.0 (C14), 129.4 (C15), 127.9 (C16), 126.1 (C17), 112.1 (C8), 64.1 (C3), 47.5 (C9), 44.0 (C6), 43.4 (C7), 32.6 (C4), 32.1 (C13), 29.1 (C10), 25.9 (C1), 21.2 (C12), 20.7 (C11).

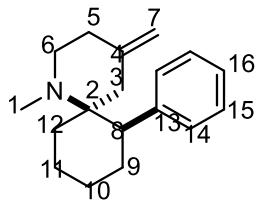

4.52

(6S,7R)-1-Methyl-4-methylene-7-phenyl-1-azaspiro[5.5]undecane (4.52) (LTL-IV-113). A solution of **4.39** (22 mg, 0.09 mmol), 37% aq. CH_2O (73 mg, 0.9 mmol), and $NaBH_3CN$ (11 mg, 0.18 mmol) was stirred for 24 h, whereupon the reaction was diluted with 1M NaOH (20 mL) and extracted with Et_2O (3 x 10 mL). The combined organic extracts were dried (Na_2SO_4) and concentrated via rotary evaporation. The crude material was purified via flash column chromatography, eluting with hexanes:Et_3N (100 : 1) to give 18 mg (78%) of the title compound as a tan solid, mp 55–56 ˚C. ^{1}H NMR (400 MHz, $CDCl_3$) δ 7.48 – 7.43 (comp, 2 H), 7.30 – 7.22 (comp, 2 H), 7.19 – 7.13 (m, 1 H), 4.78 (s, 1 H), 4.69 (s, 1 H), 3.12 (t, *J* = 4.4 Hz, 1 H), 2.84 – 2.65 (comp, 2 H), 2.54 (d, *J* = 13.4 Hz, 1 H), 2.26 (s, 3 H), 2.24 – 2.04 (comp, 4 H), 1.87 (dddd, *J* = 13.7, 10.8, 7.4, 4.7 Hz, 1 H), 1.82 – 1.71 (comp, 2 H), 1.68 – 1.57 (m, 1 H), 1.54 – 1.42 (comp, 2 H), 1.42 – 1.33 (m, 1 H); ^{13}C NMR (101 MHz, $CDCl_3$) δ 145.9, 144.6, 130.3, 127.5, 125.3, 108.3, 59.2, 49.6, 46.0, 37.5, 36.1, 32.3, 30.4, 29.2, 22.1, 20.3; IR (film, NaCl) 3066, 3024, 2937, 2862, 2791, 1648, 1601, 1494, 1454, 1375, 1348, 1289, 1239, 1196, 1155, 1120, 1073, 1056, 1033, 1004 cm^{-1}; HRMS (ESI) *m/z* calcd for $C_{18}H_{25}N$ (M+H)+, 256.2060; found 256.2066.

NMR Assignment. ^{1}H NMR (400 MHz, $CDCl_3$) δ 7.48 – 7.43 (comp, 2 H, H14), 7.30 – 7.22 (comp, 2 H, H15), 7.19 – 7.13 (m, 1 H, H16), 4.78 (s, 1 H, H7), 4.69 (s, 1 H, H7), 3.12 (t, *J* = 4.4 Hz, 1 H, H8), 2.84 – 2.65 (comp, 2 H, H6), 2.54 (d, *J* = 13.4 Hz, 1 H, H3), 2.26 (s, 3 H,

H1), 2.24 – 2.04 (comp, 4 H, H3, H5, H12), 1.87 (dddd, *J* = 13.7, 10.8, 7.4, 4.7 Hz, 1 H, H9), 1.82 – 1.71 (comp, 2 H, H11, H12), 1.68 – 1.57 (m, 1 H, H9), 1.54 – 1.42 (comp, 2 H, H10, H11), 1.42 – 1.33 (m, 1 H, H10); ^{13}C NMR (101 MHz, $CDCl_3$) δ 145.9 (C4), 144.6 (C13), 130.3 (C14), 127.5 (C15), 125.3 (C16), 108.3 (C7), 59.2 (C2), 49.6 (C6), 46.0 (C8), 37.5 (C3), 36.1 (C1), 32.3 (C12), 30.4 (C9), 29.2 (C5), 22.1 (C11), 20.3 (C10).

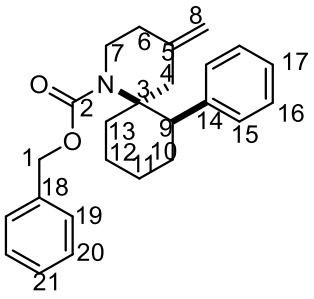

4.53

Benzyl (6S,7R)-4-methylene-7-phenyl-1-azaspiro[5.5]undecane-1-carboxylate (4.53) (LTL-V-095). A solution of **4.39** (12 mg, 0.05 mmol), benzyl chloroformate (26 mg, 0.15 mmol), and K_2CO_3 (28 mg, 0.2 mmol) in THF (0.5 mL) in a 1 dram vial was capped, sealed with Teflon tape, and submerged in an oil bath heated at 60 ˚C for 3 h, whereupon the reaction was cooled to room temperature, diluted with aqueous Na_2CO_3 (1.4 M, 15 mL) and extracted with CH_2Cl_2 (3 x 10 mL). The combined organic extracts dried (Na_2SO_4) and concentrated via rotary evaporation. The crude material was purified by flash column chromatography, eluting with hexanes:EtOAc (100 : 1) to give 13 mg (68%) of the title compound as a white solid. ^{1}H NMR (500 MHz, $CDCl^3$) δ 7.41 – 7.37 (comp, 2 H), 7.35 – 7.27 (comp, 3 H), 7.25 – 7.14 (comp, 5 H), 5.03 (d, *J* = 12.6 Hz, 1 H), 4.92 (d, *J* = 12.6 Hz, 1 H), 4.88 (s, 1 H), 4.85 (s, 1 H), 3.86 (d, *J* = 14.4 Hz, 1 H), 3.29 (s, 2 H), 2.98 (d, *J* = 13.7 Hz, 1 H), 2.58 (s, 1 H), 2.30 – 2.03 (comp, 4 H), 1.99 – 1.89 (m, 1 H), 1.87 – 1.71 (comp, 2 H), 1.56 – 1.40 (comp, 3 H). ^{13}C NMR (126 MHz, $CDCl_3$) δ 155.4, 143.0, 142.6, 137.2, 129.5, 128.4, 127.9, 127.7, 127.6, 125.9, 111.4, 66.3, 62.8, 45.4, 44.2, 41.6, 33.4, 33.2, 29.8, 22.0, 20.2; HRMS (ESI) *m/z* calcd for $C_{25}H_{29}NO_2$ 375.2198; found 375.2198.

NMR Assignment. ^{1}H NMR (500 MHz, CDCl^{3}) δ [7.41 – 7.37 (comp, 2 H), 7.35 – 7.27 (comp, 3 H), 7.25 – 7.14 (comp, 5 H)] [H15, H16, H17, H19, H20, H21], 5.03 (d, *J* = 12.6 Hz, 1 H, H1), 4.92 (d, *J* = 12.6 Hz, 1 H, H1), 4.88 (s, 1 H, H8), 4.85 (s, 1 H, H8), 3.86 (d, *J* = 14.4 Hz, 1 H, H7), 3.29 (comp, 2 H, H9, H13), 2.98 (d, *J* = 13.7 Hz, 1 H, H6), 2.58 (s, 1 H, H7), 2.30 – 2.03 (comp, 4 H, H4, H6, H13), 1.99 – 1.89 (m, 1 H, H10), 1.87 – 1.71 (comp, 2 H, H10, H12), 1.56 – 1.40 (comp, 3 H, H11, H12). ^{13}C NMR (126 MHz, $CDCl_3$) δ 155.4 (C2), 143.0 (C14), 142.6 (C5), 137.2 (C18), [129.5, 128.4, 127.9, 127.7, 127.6, 125.9] [C15, C16, C17, C19, C20, C21], 111.4 (C8), 66.3 (C1), 62.8 (C4), 45.4 (C9), 44.2 (C6), 41.6 (C7), 33.4 (C13), 33.2 (C4), 29.8 (C10), 22.0 (C12), 20.2 (C11).

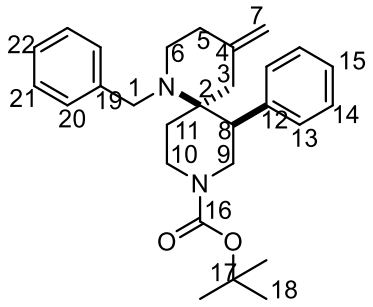

7.10

***tert*-Butyl (6R,7S)-1-benzyl-4-methylene-7-phenyl-1,9-diazaspiro[5.5]undecane-9-carboxylate (7.10) (LTL-V-065).** A solution of **4.46** (100 mg, 0.29 mmol), BnBr (248 mg, 1.45 mmol), and K_2CO_3 (200 mg, 1.45 mmol) in MeCN (3 mL) was heated under reflux for 24 h, whereupon the reaction was cooled to room temperature, diluted with aqueous Na_2CO_3 (1.4 M, 30 mL) and extracted with CH_2Cl_2 (3 x 20 mL). The combined organic extracts were washed with brine (20 mL), dried ($MgSO_4$) and concentrated via rotary evaporation. The crude material was purified by flash column chromatography, eluting with hexanes:Et_3N (100 : 1) to give 105 mg (84%) of the title compound as a white solid. ^{1}H NMR (500 MHz, $CDCl_3$) δ 7.43 – 7.35 (comp, 2 H), 7.22 (comp, 3 H), 7.14 – 7.06 (comp, 3 H), 6.84 (d, *J* = 6.7 Hz, 2 H), 4.85 (s, 1 H), 4.74 (s, 1 H), 4.42 – 3.87 (comp, 2 H), 3.67 (d, *J* = 14.6 Hz, 1 H), 3.37 – 2.88 (comp, 4 H), 2.86 – 2.62 (comp, 2 H), 2.48 (dt, *J* = 13.7, 5.0 Hz, 1 H), 2.43 – 2.31 (m, 1 H), 2.26 (d, *J* = 13.6 Hz, 1

H), 2.13 (comp, 2 H), 1.75 – 1.59 (m, 1 H), 1.42 (s, 3 H), 1.18 (s, 6 H); ^{13}C NMR (126 MHz, $CDCl_3$) δ 154.8, 144.9, 142.3, 141.4, 129.8, 128.6, 128.4, 127.9, 127.8, 126.3, 126.1, 109.6, 79.3, 69.8, 58.8, 50.0, 47.3, 45.1, 44.8, 39.6, 39.3, 31.7, 30.2, 28.2; HRMS (ESI) *m/z* calcd for $C_{28}H_{36}N_2O_2$ (M+H)+ 433.2850; found 433.2847.

NMR Assignment. ^{1}H NMR (500 MHz, $CDCl_3$) δ 7.43 – 7.35 (comp, 2 H, H14), 7.22 (comp, 3 H, H13, H15), 7.14 – 7.06 (comp, 3 H, H21, H22), 6.84 (d, *J* = 6.7 Hz, 2 H, H20), 4.85 (s, 1 H, H7), 4.74 (s, 1 H, H7), 4.42 – 3.87 (comp, 2 H, H6, H9), 3.67 (d, *J* = 14.6 Hz, 1 H, H1), 3.37 – 2.88 (comp, 4 H, H1, H6, H8, H9), 2.86 – 2.62 (comp, 2 H, H10, H11), 2.48 (dt, *J* = 13.7, 5.0 Hz, 1 H, H11), 2.43 – 2.31 (m, 1 H, H5), 2.26 (d, *J* = 13.6 Hz, 1 H, H10), 2.13 (comp, 2 H, H3), 1.75 – 1.59 (m, 1 H, H5), 1.42 (s, 3 H, H18), 1.18 (s, 6 H, H18); ^{13}C NMR (126 MHz, $CDCl_3$) δ 154.8 (C16), 144.9 (C4), 142.3 (C19), 141.4 (C12), (129.8, 128.6, 128.4, 127.9, 127.8, 126.3, 126.1) (C13, C14, C15, C20, C21, C22), 109.6 (C7), 79.3 (C17), 69.8, 58.8 (C2), 50.0 (C1), 47.3 (C9), 45.1 (C8), 44.8 (C11), 39.6 (C10), 39.3 (C6), 31.7 (C5), 30.2 (C3), 28.2 (C18).

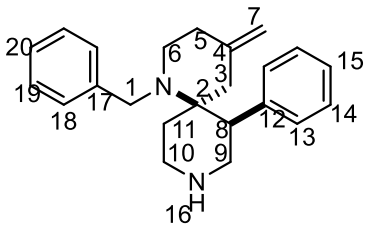

4.54

(6R,7S)-1-Benzyl-4-methylene-7-phenyl-1,9-diazaspiro[5.5]undecane (4.54) (LTL-V-091). A solution of **7.10** (20 mg, 0.046 mmol) in HCl/dioxane (4 M, 0.46 mL) was stirred for 30 min. Saturated aqueous Na_2CO_3 was then added dropwise until the solution reached pH 10 as determined by pH paper. The solution was extracted with EtOAc (3 x 10 mL), and the combined organic extracts were dried ($MgSO_4$) and concentrated via rotary evaporation. The crude material was purified by flash column chromatography, eluting with hexanes:EtOAc:Et_3N (60 : 40 : 1) to give 12 mg (80%) of the title compound as a yellow oil. ^{1}H NMR (400 MHz, $CDCl_3$) δ 7.59 – 7.53 (comp, 2 H), 7.33 – 7.26 (comp, 2 H), 7.24 – 7.20 (m, 1 H), 7.16 – 7.08 (comp, 3 H), 6.87

(d, *J* = 7.0 Hz, 2 H), 4.82 (s, 1 H), 4.73 (s, 1 H), 3.74 (d, *J* = 14.1 Hz, 1 H), 3.52 (d, *J* = 14.1 Hz, 1 H), 3.22 – 3.08 (comp, 3 H), 2.94 – 2.82 (comp, 2 H), 2.71 (d, *J* = 13.4 Hz, 1 H), 2.63 (dt, *J* = 13.5, 6.5 Hz, 1 H), 2.53 – 2.43 (m, 1 H), 2.31 (d, *J* = 13.4 Hz, 1 H), 2.27 – 2.15 (m, 1 H), 2.11 (s, 2 H), 1.75 (d, *J* = 13.5 Hz, 1 H); ^{13}C NMR (126 MHz, $CDCl_3$) δ 145.3, 143.3, 141.4, 130.4, 128.1, 127.9, 127.8, 126.3, 125.9, 109.4, 58.5, 50.3, 48.9, 46.2, 43.7, 43.0, 39.1, 33.3, 29.0; HRMS (ESI) *m/z* calcd for $C_{23}H_{28}N_2$ $C_{23}H_{28}N_2$ (M+H)+ 333.2325; found 333.2319.

NMR Assignment. ^{1}H NMR (400 MHz, $CDCl_3$) δ 7.59 – 7.53 (comp, 2 H, H13), 7.33 – 7.26 (comp, 2 H, H14), 7.24 – 7.20 (m, 1 H, H15), 7.16 – 7.08 (comp, 3 H, H19, H20), 6.87 (d, *J* = 7.0 Hz, 2 H, H18), 4.82 (s, 1 H, H7), 4.73 (s, 1 H, H7), 3.74 (d, *J* = 14.1 Hz, 1 H, H1), 3.52 (d, *J* = 14.1 Hz, 1 H, H1), 3.22 – 3.08 (comp, 3 H, H6, H8, H9), 2.94 – 2.82 (comp, 2 H, H6, H9), 2.71 (d, *J* = 13.4 Hz, 1 H, H10), 2.63 (dt, *J* = 13.5, 6.5 Hz, 1 H, H11), 2.53 – 2.43 (m, 1 H, H11), 2.31 (d, *J* = 13.4 Hz, 1 H, H10), 2.27 – 2.15 (m, 1 H, H5), 2.11 (s, 2 H, H3), 1.75 (d, *J* = 13.5 Hz, 1 H, H5); ^{13}C NMR (126 MHz, $CDCl_3$) δ 145.3 (C17), 143.3 (C4), 141.4 (C12), 130.4 (C13), 128.1 (C19), 127.9 (C18), 127.8 (C14), 126.3 (C20), 125.9 (C15), 109.4 (C7), 58.5 (C2), 50.3 (C9), 48.9 (C1), 46.2 (C8), 43.7 (C11), 43.0 (C6), 39.1 (C10), 33.3 (C5), 29.0 (C3).

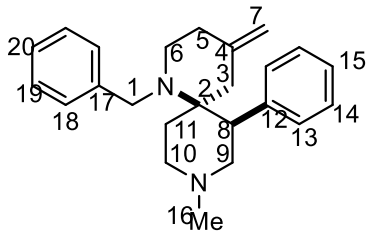

4.55

(6R,7S)-1-Benzyl-9-methyl-4-methylene-7-phenyl-1,9-diazaspiro[5.5]undecane (4.55) (LTL-V-072). A solution of **4.54** (18 mg, 0.054 mmol), aqueous formaldehyde (37%, 40 mg, 0.5 mmol), and $NaBH_3CN$ (6 mg, 0.1 mmol) in MeCN (0.5 mL) was stirred for 20 h, whereupon the reaction was diluted with aqueous Na_2CO_3 (1.4 M, 30 mL) and extracted with CH_2Cl_2 (3 x 20 mL). The combined organic extracts were dried (Na_2SO_4) and concentrated via rotary evaporation. The crude material was purified by flash column chromatography, eluting with

hexanes:EtOAc:Et_3N (95 : 5 : 1) to give 17 mg (89%) of the title compound as a white paste. ^1H NMR (500 MHz, $CDCl_3$) δ 7.74 – 7.69 (comp, 2 H), 7.31 – 7.23 (comp, 3 H), 7.16 – 7.08 (comp, 3 H), 6.90 – 6.85 (comp, 2 H), 4.85 (s, 1 H), 4.75 (s, 1 H), 3.73 (d, *J* = 14.8 Hz, 1 H), 3.24 – 3.11 (comp, 2 H), 2.90 (ddt, *J* = 11.3, 4.8, 2.3 Hz, 1 H), 2.86 – 2.73 (comp, 2 H), 2.70 (dt, *J* = 11.9, 2.1 Hz, 1 H), 2.50 (comp, 3 H), 2.33 – 2.26 (m, 1 H), 2.21 (s, 3 H), 2.14 (comp, 3 H), 1.64 (d, *J* = 13.4 Hz, 1 H); ^{13}C NMR (126 MHz, $CDCl_3$) δ 145.4, 144.0, 141.9, 130.7, 127.9, 127.8, 127.5, 126.2, 125.9, 109.2, 59.1, 58.1, 52.3, 50.3, 46.5, 45.8, 45.3, 40.4, 33.1, 30.8; HRMS (ESI) *m/z* calcd for $C_{24}H_{30}N_2$ 347.2482; found 347.2481.

NMR Assignment. ^1H NMR (500 MHz, $CDCl_3$) δ 7.74 – 7.69 (comp, 2 H, H13), 7.31 – 7.23 (comp, 3 H, H14, H15), 7.16 – 7.08 (comp, 3 H, H19, H20), 6.90 – 6.85 (comp, 2 H, H18), 4.85 (s, 1 H, H7), 4.75 (s, 1 H, H7), 3.73 (d, *J* = 14.8 Hz, 1 H, H1), 3.24 – 3.11 (comp, 2 H, H1, H8), 2.90 (ddt, *J* = 11.3, 4.8, 2.3 Hz, 1 H, H6), 2.86 – 2.73 (comp, 2 H, H10, H11), 2.70 (dt, *J* = 11.9, 2.1 Hz, 1 H, H9), 2.50 (comp, 3 H, H5, H9, H10), 2.33 – 2.26 (m, 1 H, H6), 2.21 (s, 3 H, H16), 2.14 (comp, 3 H, H3, H11), 1.64 (d, *J* = 13.4 Hz, 1 H, H5); ^{13}C NMR (126 MHz, $CDCl_3$) δ 145.4 (C17), 144.0 (C4), 141.9 (C12), 130.7 (C13), 127.9 (C19), 127.8 (C18), 127.5 (C14), 126.2 (C20), 125.9 (C15), 109.2 (C7), 59.1 (C9), 58.1 (C2), 52.3 (C6), 50.3 (C1), 46.5 (C16), 45.8 (C8), 45.3 (C10), 40.4 (C11), 33.1 (C5), 30.8 (C3).

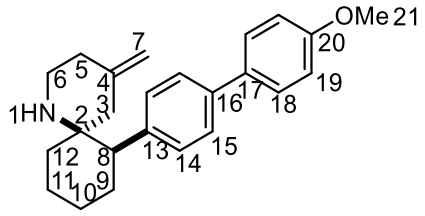

4.60

(6S,7R)-7-(4'-Methoxy-[1,1'-biphenyl]-4-yl)-4-methylene-1-azaspiro[5.5]undecane (4.60) (LTL-V-086). A solution of **4.43** (30 mg, 0.09 mmol), **4.59** (25 mg, 0.18 mmol), SPhos (6 mg, 0.014 mmol), K_3PO_4-$7H_2O$ (61 mg, 0.18 mmol), and $Pd(OAc)_2$ (1 mg, 0.0045 mmol) in THF (0.5 mL) was stirred at rt for 24 h, whereupon the reaction was diluted with Et_2O (10 mL)

and filtered over a 1:1 slurry of celite:SiO_2 (6 mL), eluting with Et_2O. The filtrate was concentrated by rotary evaporation, and the crude material was purified by flash column chromatography, eluting with hexanes:Et_3N (100 : 1) to give 21 mg (70 %) of the title compound as a yellow solid. ^{1}H NMR (500 MHz, $CDCl_3$) δ 7.54 (d, J = 8.7 Hz, 2 H), 7.50 (d, J = 8.1 Hz, 2 H), 7.28 (d, J = 8.1 Hz, 2 H), 6.97 (d, J = 8.7 Hz, 2 H), 4.69 (s, 1 H), 4.59 (s, 1 H), 3.85 (s, 3 H), 2.91 (dd, J = 13.4, 6.1 Hz, 1 H), 2.71 (td, J = 12.9, 3.6 Hz, 1 H), 2.59 (dd, J = 12.8, 3.4 Hz, 1 H), 2.31 – 2.19 (comp, 2 H), 2.08 (d, J = 13.5 Hz, 1 H), 1.99 – 1.82 (comp, 3 H), 1.71 (tt, J = 12.7, 3.2 Hz, 1 H), 1.63 – 1.48 (comp, 3 H), 1.45 – 1.34 (comp, 1 H), 0.97 (ddd, J = 14.3, 13.0, 3.9 Hz, 1 H); HRMS (ESI) *m/z* calcd for $C_{24}H_{29}NO$ (M+H)+ 348.2322; found 348.2321.

NMR Assignment. ^{1}H NMR (500 MHz, $CDCl_3$) δ 7.54 (d, J = 8.7 Hz, 2 H, H18), 7.50 (d, J = 8.1 Hz, 2 H, H15), 7.28 (d, J = 8.1 Hz, 2 H, H14), 6.97 (d, J = 8.7 Hz, 2 H, H19), 4.69 (s, 1 H, H7), 4.59 (s, 1 H, H7), 3.85 (s, 3 H, H21), 2.91 (dd, J = 13.4, 6.1 Hz, 1 H, H6), 2.71 (td, J = 12.9, 3.6 Hz, 1 H, H6), 2.59 (dd, J = 12.8, 3.4 Hz, 1 H, H8), 2.31 – 2.19 (comp, 2 H, H9, H12), 2.08 (d, J = 13.5 Hz, 1 H, H5), 1.99 – 1.82 (comp, 3 H, H3, H10), 1.71 (tt, J = 12.7, 3.2 Hz, 1 H, H5), 1.63 – 1.48 (comp, 3 H, H9, H11), 1.45 – 1.34 (comp, 1 H, H1), 0.97 (ddd, J = 14.3, 13.0, 3.9 Hz, 1 H, H12).

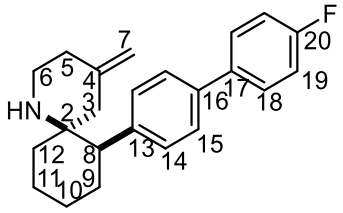

4.65

(6S,7R)-7-(4'-Fluoro-[1,1'-biphenyl]-4-yl)-4-methylene-1-azaspiro[5.5]undecane (4.65) (LTL-V-085). The title compound was prepared following the procedure of **4.60**. The crude material was purified by flash column chromatography, eluting with hexanes:Et_3N (100 : 1) to give 30 mg (100%) of the title compound as a yellow solid. ^{1}H NMR (500 MHz, $CDCl_3$) δ 7.55 (q, J = 5.6, 5.2 Hz, 2 H), 7.49 (d, J = 8.1 Hz, 2 H), 7.31 (d, J = 8.1 Hz, 2 H), 7.12 (t, J = 8.7

Hz, 2 H), 4.69 (s, 1 H), 4.60 (s, 1 H), 2.91 (ddd, *J* = 13.5, 6.1, 1.6 Hz, 1 H), 2.71 (td, *J* = 12.9, 3.6 Hz, 1 H), 2.60 (dd, *J* = 12.9, 3.4 Hz, 1 H), 2.31 – 2.18 (comp, 2 H), 2.09 (d, *J* = 13.3 Hz, 1 H), 1.98 – 1.83 (comp, 3 H), 1.71 (tt, *J* = 13.0, 3.9 Hz, 1 H), 1.65 – 1.48 (comp, 3 H), 1.46 – 1.34 (m, 1 H), 1.23 – 1.14 (br, 1 H), 0.97 (ddd, *J* = 14.4, 13.0, 4.0 Hz, 1 H); ^{13}C NMR (126 MHz, $CDCl_3$) δ 163.3, 161.4, 145.4, 141.4, 138.3, 137.0, 137.0, 130.0, 128.5, 128.4, 126.5, 115.7, 115.5, 108.8, 77.3, 55.3, 53.5, 47.2, 41.3, 36.1, 31.7, 27.8, 26.9, 20.9; HRMS (ESI) *m/z* calcd for $C_{23}H_{26}FN$ 336.2122; found 336.2117.

NMR Assignment. ^{1}H NMR (500 MHz, $CDCl_3$) δ 7.55 (q, J = 5.6, 5.2 Hz, 2 H, H18), 7.49 (d, J = 8.1 Hz, 2 H, H15), 7.31 (d, J = 8.1 Hz, 2 H, H14), 7.12 (t, J = 8.7 Hz, 2 H, H19), 4.69 (s, 1 H, H7), 4.60 (s, 1 H, H7), 2.91 (ddd, *J* = 13.5, 6.1, 1.6 Hz, 1 H, H6), 2.71 (td, *J* = 12.9, 3.6 Hz, 1 H, H6), 2.60 (dd, *J* = 12.9, 3.4 Hz, 1 H, H8), 2.31 – 2.18 (comp, 2 H, H9, H12), 2.09 (d, *J* = 13.3 Hz, 1 H, H5), 1.98 – 1.83 (comp, 3 H, H3, H10), 1.71 (tt, *J* = 13.0, 3.9 Hz, 1 H, H5), 1.65 – 1.48 (comp, 3 H, H9, H11), 1.46 – 1.34 (m, 1 H, H10), 1.23 – 1.14 (br, 1 H, H1), 0.97 (ddd, *J* = 14.4, 13.0, 4.0 Hz, 1 H, H12); ^{13}C NMR (126 MHz, $CDCl_3$) δ 163.3 (C20), 161.4 (C20), 145.4 (C4), 141.4 (C13), 138.3 (C16), 137.0 (C17), 130.0 (C14), 128.5 (C18), 128.4 (C18), 126.5 (C15), 115.7 (C19), 115.5 (C19), 108.8 (C7), 55.3 (C2), 53.5 (C8), 47.2 (C3), 41.3 (C6), 36.1 (C5), 31.7 (C12), 27.8 (C9), 26.9 (C10), 20.9 (C11).

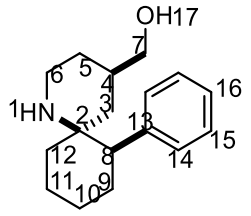

4.66

((4R,6S,7R)-7-Phenyl-1-azaspiro[5.5]undecan-4-yl)methanol (4.66) (LTL-V-071). BH_3·DMS (15 mg, 0.2 mmol), was added dropwise to a solution of **4.39** (24 mg, 0.1 mmol) in THF (2 mL) at -78 ˚C and stirred for 1 h, whereupon the reaction was warmed to room temperature and stirred for an additional 3.5 h. The reaction was cooled to 0 ˚C, and MeOH (0.5

mL), NaOH (3 M aq., 0.5 mmol), and H_2O_2 (11.6 M, 1 mmol) were added, the reaction was warmed to room temperature and stirred for 2.5 h. The mixture was diluted with sat. Na_2CO_3 (15 mL) and extracted with CH_2Cl_2 (3 x 15 mL). The combined organic extracts were dried (Na_2SO_4) and concentrated via rotary evaporation. The crude material was purified by flash column chromatography, eluting with hexanes:EtOAc:Et_3N (80 : 20 : 1) to give 16 mg (62 %) of the title compound as a clear oil. ^{1}H NMR (400 MHz, $CDCl_3$) δ 7.31 – 7.26 (comp, 2 H), 7.24 – 7.18 (comp, 3 H), 3.27 (d, *J* = 6.4 Hz, 2 H), 2.85 (ddd, *J* = 13.6, 5.0, 1.8 Hz, 1 H), 2.72 (ddd, *J* = 13.7, 12.7, 3.1 Hz, 1 H), 2.53 (dd, *J* = 13.0, 3.3 Hz, 1 H), 2.43 – 2.35 (m, 1 H), 2.18 (qd, *J* = 13.1, 3.9 Hz, 1 H), 1.97 – 1.78 (comp, 2 H), 1.70 – 1.58 (m, 1 H), 1.58 – 1.49 (comp, 3 H), 1.41 – 1.30 (comp, 3 H), 1.03 (td, *J* = 13.5, 3.8 Hz, 1 H), 0.78 (t, *J* = 12.6 Hz, 1 H), 0.55 (qd, *J* = 12.6, 5.0 Hz, 1 H); ^{13}C NMR (126 MHz, $CDCl_3$) δ 142.4, 129.6, 127.9, 126.3, 69.0, 54.5, 53.4, 39.9, 39.8, 34.0, 31.8, 30.5, 27.8, 26.9, 21.1; HRMS (ESI) *m/z* calcd for $C_{17}H_{25}NO$ 260.2009; found 260.2008.

NMR Assignment. ^{1}H NMR (400 MHz, $CDCl_3$) δ 7.31 – 7.26 (comp, 2 H), 7.24 – 7.18 (comp, 3 H), 3.27 (d, *J* = 6.4 Hz, 2 H), 2.85 (ddd, *J* = 13.6, 5.0, 1.8 Hz, 1 H), 2.72 (ddd, *J* = 13.7, 12.7, 3.1 Hz, 1 H), 2.53 (dd, *J* = 13.0, 3.3 Hz, 1 H), 2.43 – 2.35 (m, 1 H), 2.18 (qd, *J* = 13.1, 3.9 Hz, 1 H), 1.97 – 1.78 (comp, 2 H), 1.70 – 1.58 (m, 1 H), 1.58 – 1.49 (comp, 3 H), 1.41 – 1.30 (comp, 3 H), 1.03 (td, *J* = 13.5, 3.8 Hz, 1 H), 0.78 (t, *J* = 12.6 Hz, 1 H), 0.55 (qd, *J* = 12.6, 5.0 Hz, 1 H); ^{13}C NMR (126 MHz, $CDCl_3$) δ 142.4, 129.6, 127.9, 126.3, 69.0, 54.5, 53.4, 39.9, 39.8, 34.0, 31.8, 30.5, 27.8, 26.9, 21.1.

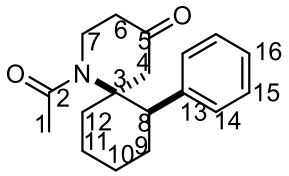

4.69

(6S,7R)-1-Acetyl-7-phenyl-1-azaspiro[5.5]undecan-4-one (4.69) (LTL05076). 4.51 (28 mg, 0.1 mmol) was dissolved in CH_2Cl_2:MeOH (0.9 mL : 0.1 mL) and cooled to –78 ˚C.

O_3/O_2 was bubbled through the solution until a blue color persisted (ca. 3 min). N_2 was then bubbled through the solution for 5 min, and DMS (31 mg, 0.04 mL) was added. The reaction was stirred at -78 ˚C for 1 h, then overnight at room temperature. The solvent was removed via rotary evaporation, and the crude material was purified by flash column chromatography, eluting with hexanes:EtOAc (80 : 20) to give 20 mg (69%) of the title compound as a white solid. ^{1}H NMR (500 MHz, $CDCl_3$) δ 7.26 – 7.21 (comp, 4 H), 7.21 – 7.16 (m, 1 H), 3.30 – 3.18 (m, 1 H), 3.07 (d, *J* = 14.2 Hz, 1 H), 2.95 (t, *J* = 12.6 Hz, 1 H), 2.73 – 2.62 (m, 1 H), 2.61 – 2.43 (comp, 3 H), 2.21 (ddd, *J* = 18.2, 12.3, 5.8 Hz, 1 H), 2.10 (ddd, *J* = 18.2, 3.9, 2.1 Hz, 1 H), 1.92 (s, 3 H), 1.81 – 1.67 (comp, 2 H), 1.59 – 1.39 (comp, 4 H); ^{13}C NMR (126 MHz, $CDCl_3$) δ 208.9, 171.0, 141.4, 129.2, 128.1, 126.8, 64.0, 51.6, 51.6, 43.1, 39.9, 32.1, 27.1, 25.7, 21.4, 19.4; HRMS (ESI) *m/z* calcd for $C_{18}H_{23}NO_2$ (M+H)+ 286.1802; found 286.1794.

NMR Assignment. ^{1}H NMR (500 MHz, $CDCl_3$) δ 7.26 – 7.21 (comp, 4 H, H15, H16), 7.21 – 7.16 (m, 1 H, H17), 3.30 – 3.18 (m, 1 H, H7), 3.07 (d, *J* = 14.2 Hz, 1 H, H4), 2.95 (t, *J* = 12.6 Hz, 1 H, H12), 2.73 – 2.62 (m, 1 H, H9), 2.61 – 2.43 (comp, 3 H, H4, H7, H8), 2.21 (ddd, *J* = 18.2, 12.3, 5.8 Hz, 1 H, H6), 2.10 (ddd, *J* = 18.2, 3.9, 2.1 Hz, 1 H, H6), 1.92 (s, 3 H, H1), 1.81 – 1.67 (comp, 2 H, H10, H11), 1.59 – 1.39 (comp, 4 H, H9, H10, H11, H12); ^{13}C NMR (126 MHz, $CDCl_3$) δ 208.9 (C5), 171.0 (C2), 141.4 (C13), 129.2 (C15), 128.1 (C16), 126.8 (C17), 64.0 (C3), 51.6 (C8), 51.6 (C4), 43.1 (C7), 39.9 (C6), 32.1 (C12), 27.1 (C9), 25.7 (C1), 21.4 (C11), 19.4 (C10).

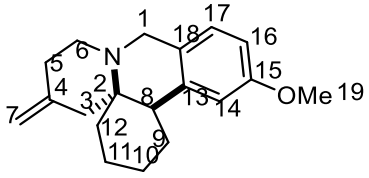

4.71

(4aS,14bR)-13-Methoxy-6-methylene-1,2,3,4,5,6,7,8,10,14b-decahydropyrido[2,1-e]phenanthridine (4.71) (LTL-IV-180). A solution of **4.41** (10 mg, 0.04 mmol) and aq. formaldehyde (37%, 0.03 mL, 0.4 mmol) in EtOH (0.8 mL) was stirred for 2h at rt. AcOH (0.02

mL, 0.4 mmol) was added, and the reaction was heated under reflux for 24 h, whereupon the reaction was cooled to rt and diluted with 1M aq. NaOH (10 mL). The mixture was extracted with CH_2Cl_2 (3 x 10 mL), and the combined organic extracts were dried (Na_2SO_4) and concentrated via rotary evaporation. The crude material was purified via flash column chromatography, eluting with hexanes:Et_3N (100 : 1) to give 8 mg (80%) of the title compound as an off-white solid. ^{1}H NMR (400 MHz, $CDCl_3$) δ 6.95 (d, *J* = 8.4 Hz, 1 H), 6.90 – 6.85 (m, 1 H), 6.71 (ddd, *J* = 8.3, 2.6, 0.8 Hz, 1 H), 4.79 (d, *J* = 2.0 Hz, 1 H), 4.71 (s, 1 H), 3.87 (d, *J* = 16.0 Hz, 1 H), 3.78 (s, 3 H), 3.71 (d, *J* = 16.0 Hz, 1 H), 2.85 – 2.75 (comp, 2 H), 2.75 – 2.63 (comp, 2 H), 2.40 (td, *J* = 11.6, 10.3, 5.3 Hz, 1 H), 2.33 – 2.12 (comp, 4 H), 1.88 (ddt, *J* = 20.3, 15.7, 5.9 Hz, 2 H), 1.55 – 1.37 (m, 6 H), 1.11 (d, *J* = 13.0 Hz, 1 H). HRMS (ESI) *m/z* calcd for $C_{19}H_{25}NO$ (M+H)+, 284.2009; found 284.2007.

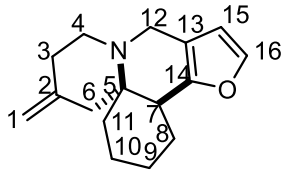

4.72

(4aS,13bS)-6-Methylene-1,2,3,4,5,6,7,8,10,13b-decahydrofuro[3,2-c]pyrido[2,1-j]quinoline (4.72) (LTL-V-096). A solution of **4.44** (46 mg, 0.2 mmol), paraformaldehyde (60 mg, 2 mmol) and AcOH (24 mg, 0.4 mmol) in EtOH (2 mL) was heated under reflux for 7 h, whereupon the mixture was diluted with aqueous Na_2CO_3 (1.4 M, 25 mL) and extracted with CH_2Cl_2 (3 x 15 mL). The combined organic extracts were dried (Na_2SO_4) and concentrated via rotary evaporation. The crude material was purified by flash column chromatography, eluting with hexanes:Et_3N (200 : 1) to give 31 mg (65%) of the title compound as a clear oil. ^{1}H NMR (400 MHz, $CDCl_3$) δ 7.31 – 7.27 (m, 1 H), 6.18 (d, *J* = 1.8 Hz, 1 H), 4.79 (s, 1 H), 4.71 (s, 1 H), 3.66 (dd, *J* = 15.5, 3.0 Hz, 1 H), 3.51 (dd, *J* = 15.5, 1.9 Hz, 1 H), 2.89 (m, 1 H), 2.81 (dt, *J* = 10.9, 5.3 Hz, 1 H), 2.70 (ddd, *J* = 11.5, 8.7, 4.8 Hz, 1 H), 2.60 (d, *J* = 13.2 Hz, 1 H), 2.39 – 2.24 (comp, 4 H), 1.70 (tt, *J* = 13.9, 4.1 Hz, 1 H), 1.56 – 1.45 (comp, 3 H), 1.42 – 1.34 (comp, 2 H),

1.01 – 0.86 (m, 1 H); ^{13}C NMR (126 MHz, $CDCl_3$) δ 150.5, 144.0, 140.8, 113.9, 109.5, 108.3, 57.2, 50.5, 47.8, 42.0, 38.3, 34.6, 23.8, 23.0, 21.9, 21.8; HRMS (ESI) *m/z* calcd for $C_{16}H_{21}NO$ 244.1696; found 244.1690.

NMR Assignment. ^{1}H NMR (400 MHz, $CDCl_3$) δ 7.31 – 7.27 (m, 1 H, H15), 6.18 (d, *J* = 1.8 Hz, 1 H, H16), 4.79 (s, 1 H, H1), 4.71 (s, 1 H, H1), 3.66 (dd, *J* = 15.5, 3.0 Hz, 1 H, H12), 3.51 (dd, *J* = 15.5, 1.9 Hz, 1 H, H12), 2.89 (m, 1 H, H7), 2.81 (dt, *J* = 10.9, 5.3 Hz, 1 H, H4), 2.70 (ddd, *J* = 11.5, 8.7, 4.8 Hz, 1 H, H4), 2.60 (d, *J* = 13.2 Hz, 1 H, H3), 2.39 – 2.24 (comp, 4 H, H3, H6, H8), 1.70 (tt, *J* = 13.9, 4.1 Hz, 1 H, H8), 1.56 – 1.45 (comp, 3 H, H9, H10, H11), 1.42 – 1.34 (comp, 2 H, H10, H11), 1.01 – 0.86 (m, 1 H, H9); ^{13}C NMR (126 MHz, $CDCl_3$) δ 150.5 (C14), 144.0 (C2), 140.8 (C15), 113.9 (C13), 109.5 (C1), 108.3 (C16), 57.2 (C5), 50.5 (C4), 47.8 (C12), 42.0 (C3), 38.3 (C7), 34.6 (C6), 23.8 (C8), 23.0 (C11), 21.9 (C10), 21.8 (C9).

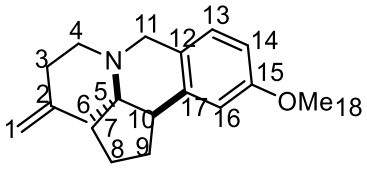

4.73

(3aS,13bR)-12-Methoxy-5-methylene-2,3,4,5,6,7,9,13b-octahydro-1H-cyclopenta[c]pyrido[1,2-b]isoquinoline (4.73) (LTL-V-083). A solution of **4.48** (24 mg, 0.09 mmol) in aqueous formaldehyde (37%, 0.45 mL) and formic acid (0.45 mL) was submerged in an oil bath heated at 55 ˚C and stirred for 1 h, whereupon the mixture was diluted with aqueous Na_2CO_3 (1.4 M, 15 mL) and extracted with CH_2Cl_2 (3 x 15 mL). The combined organic extracts were dried (Na_2SO_4) and concentrated via rotary evaporation. The crude material was purified by flash column chromatography, eluting with hexanes:EtOAc:Et_3N (95 : 5 : 1) to give 22 mg (92%) of the title compound as a yellow oil. ^{1}H NMR (500 MHz, $CDCl_3$) δ 6.97 (d, *J* = 7.9 Hz, 1 H), 6.71 – 6.67 (comp, 2 H), 4.80 (s, 1 H), 4.71 (s, 1 H), 3.79 (s, 3 H), 3.67 (d, *J* = 14.8 Hz, 1 H), 3.58 (d, *J* = 14.9 Hz, 1 H), 2.94 (dd, *J* = 7.9, 4.5 Hz, 1 H), 2.85 (ddd, *J* = 11.3, 5.5, 3.1 Hz, 1 H), 2.59 (td, *J* = 11.4, 3.5 Hz, 1 H), 2.50 – 2.39 (m, 1 H), 2.37 – 2.14 (comp, 4 H), 1.78 – 1.64

(comp, 2 H), 1.63 – 1.45 (comp, 3 H); ^{13}C NMR (126 MHz, $CDCl_3$) δ 158.4, 144.8, 140.3, 126.9, 126.8, 113.0, 111.3, 109.5, 65.7, 55.3, 52.0, 51.2, 48.2, 46.9, 34.2, 33.7, 25.4, 23.0; HRMS (ESI) *m/z* calcd for 270.1852; found 270.1848.

NMR Assignment. ^{1}H NMR (500 MHz, $CDCl_3$) δ 6.97 (d, *J* = 7.9 Hz, 1 H, H13), 6.71 – 6.67 (comp, 2 H, H14, H16), 4.80 (s, 1 H, H1), 4.71 (s, 1 H, H1), 3.79 (s, 3 H, H18), 3.67 (d, *J* = 14.8 Hz, 1 H, H11), 3.58 (d, *J* = 14.9 Hz, 1 H, H11), 2.94 (dd, *J* = 7.9, 4.5 Hz, 1 H, H10), 2.85 (ddd, *J* = 11.3, 5.5, 3.1 Hz, 1 H, H4), 2.59 (td, *J* = 11.4, 3.5 Hz, 1 H, H4), 2.50 – 2.39 (m, 1 H, H5), 2.37 – 2.14 (comp, 4 H, H5, H6, H9), 1.78 – 1.64 (comp, 2 H, H7, H9), 1.63 – 1.45 (comp, 3 H, H7, H8); ^{13}C NMR (126 MHz, $CDCl_3$) δ 158.4 (C15), 144.8 (C2), 140.3 (C17), 126.9 (C13), 126.8 (C12), 113.0 (C16), 111.3 (C14), 109.5 (C1), 65.7 (C5), 55.3 (C18), 52.0 (C4), 51.2 (C11), 48.2 (C10), 46.9 (C6), 34.2 (C9), 33.7 (C5), 25.4 (C7), 23.0 (C8).

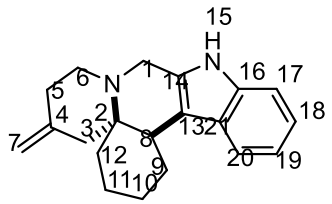

4.75

(4aS,15cR)-6-Methylene-1,3,4,5,6,7,8,10,11,15c-decahydro-2H-indolo[2,3-c]pyrido[2,1-j]quinoline (4.75) (LTL-IV-254). A solution of **4.45** (26 mg, 0.09 mmol) and paraformaldehyde (5 mg, 0.18 mmol) in toluene (1.8 mL) was heated under reflux for 24 h, whereupon the reaction was cooled to rt and diluted with 1.4 M aqueous Na_2CO_3. The mixture was extracted with CH_2Cl_2 (3 x 10 mL), and the combined organic extracts were dried (Na_2SO_4) and concentrated via rotary evaporation. The crude material was purified via flash column chromatography, eluting with EtOAc:hexanes:Et_3N (75 : 25 : 1) to give 31 mg (69%) of the title compound as a pale pink solid, mp 198–202 ˚C. ^{1}H NMR (499 MHz, $CDCl_3$) δ 7.69 (s, 1 H), 7.59 (d, *J* = 7.9 Hz, 1 H), 7.22 (d, *J* = 8.0 Hz, 1 H), 7.04 (t, *J* = 8.0 Hz, 1 H), 6.98 (t, *J* = 7.9 Hz, 1 H), 4.74 (s, 1 H), 4.68 (s, 1 H), 3.95 (d, *J* = 16.1 Hz, 1 H), 3.58 (d, *J* = 16.1 Hz, 1 H), 3.12 (s, 1

H), 2.78 (dt, *J* = 11.6, 5.7 Hz, 1 H), 2.65 (ddd, *J* = 11.6, 7.2, 5.6 Hz, 1 H), 2.62 – 2.54 (m, 1 H), 2.51 (d, *J* = 13.3 Hz, 1 H), 2.40 (d, *J* = 13.3 Hz, 1 H), 2.29 (comp, 2 H), 1.80 (tt, *J* = 13.9, 3.9 Hz, 1 H), 1.56 (m, 1 H), 1.46 – 1.33 (comp, 4 H), 1.01 (m, 1 H). ^{13}C NMR (126 MHz, $CDCl_3$) δ 144.3, 136.5, 131.1, 127.1, 120.9, 119.7, 119.1, 110.7, 109.8, 109.4, 77.3, 77.2, 77.0, 76.8, 57.3, 50.7, 47.8, 42.0, 36.8, 34.6, 25.3, 24.3, 22.0, 21.5. HRMS (ESI) *m/z* calcd for $C_{20}H_{24}N_2$ (M+H)+, 293.2012; found 293.2015.

NMR Assignment. ^{1}H NMR (499 MHz, $CDCl_3$) δ 7.69 (s, 1 H, H15), 7.59 (d, *J* = 7.9 Hz, 1 H, H20), 7.22 (d, *J* = 8.0 Hz, 1 H, H17), 7.04 (t, *J* = 8.0 Hz, 1 H, H18), 6.98 (t, *J* = 7.9 Hz, 1 H, H19), 4.74 (s, 1 H, H7), 4.68 (s, 1 H, H7), 3.95 (d, *J* = 16.1 Hz, 1 H, H1), 3.58 (d, *J* = 16.1 Hz, 1 H, H1), 3.12 (s, 1 H, H8), 2.78 (dt, *J* = 11.6, 5.7 Hz, 1 H, H6), 2.65 (ddd, *J* = 11.6, 7.2, 5.6 Hz, 1 H, H6), 2.62 – 2.54 (m, 1 H, H9), 2.51 (d, *J* = 13.3 Hz, 1 H, H3), 2.40 (d, *J* = 13.3 Hz, 1 H, H3), 2.29 (comp, 2 H, H5), 1.80 (tt, *J* = 13.9, 3.9 Hz, 1 H, H9), 1.56 (m, 1 H, H12), 1.46 – 1.33 (comp, 4 H, H10, H11, H12), 1.01 (m, 1 H, H10). ^{13}C NMR (126 MHz, $CDCl_3$) δ 144.3 (C4), 136.5 (C16), 131.1 (C21), 127.1 (C14), 120.9 (C18), 119.7 (C20), 119.1 (C19), 110.7 (C17), 109.8 (C13), 109.4 (C7), 57.3 (C2), 50.7 (C6), 47.8 (C1), 42.0 (C3), 36.8 (C8), 34.6 (C5), 25.3 (C9), 24.3 (C12), 22.0 (C11), 21.5 (C10).

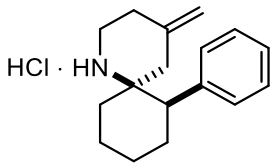

4.39 · HCl

X-ray Experimental for $C_{17}H_{24}N^{1+}Cl^{1-}$ (4.39 · HCl): Crystals grew as clear, colorless prisms by slow evaporation from $CHCl_3$. The data crystal was cut from a larger crystal and had approximate dimensions; 0.16 x 0.14 x 0.12 mm. The data were collected at -150 °C on a Nonius Kappa CCD diffractometer using a Bruker AXS Apex II detector and a graphite monochromator with MoKα radiation (λ = 0.71073Å). Reduced temperatures were maintained

by use of an Oxford Cryosystems 700 low-temperature device. A total of 1322 frames of data were collected using ω and ϕ-scans with a scan range of 0.7° and a counting time of 39 seconds per frame. Details of crystal data, data collection and structure refinement are listed in Table 7.1. Data reduction were performed using SAINT V8.27B. The structure was solved by direct methods using SHELXT and refined by full-matrix least-squares on F^2 with anisotropic displacement parameters for the non-H atoms using SHELXL-2014/7.[250,251] Structure analysis was aided by use of the programs PLATON98 and WinGX.[252] The hydrogen atoms bound to carbon atoms were calculated in idealized positions. The hydrogen atoms on the nitrogen atoms were observed in a ΔF map and constrained in a riding model with Uiso set to 1.5xUeq of the water molecule, O3. While the contents of the unit cell are racemic, the crystal symmetry is chiral. The absolute structure was determined by the method of Flack.[253] The Flack x parameter refined to 0.09(3). The assignment was corroborated by use of the Hooft y-parameter method (y = 0.08(3)).[254]

The function, $\Sigma w(|F_o|^2 - |F_c|^2)^2$, was minimized, where $w = 1/[(\sigma(F_o))^2 + (0.0469*P)^2 + (0.5368*P)]$ and $P = (|F_o|^2 + 2|F_c|^2)/3$. $R_w(F^2)$ refined to 0.106, with R(F) equal to 0.0455 and a goodness of fit, S, = 1.03. Definitions used for calculating R(F), $R_w(F^2)$ and the goodness of fit, S, are as follows: $R_w(F^2) = \{\Sigma w(|F_o|^2 - |F_c|^2)^2/\Sigma w(|F_o|)^4\}^{1/2}$ where w is the weight given each reflection; $R(F) = \Sigma(|F_o| - |F_c|)/\Sigma|F_o|\}$ for reflections with $F_o > 4(\sigma(F_o))$; $S = [\Sigma w(|F_o|^2 - |F_c|^2)^2/(n - p)]^{1/2}$, where n is the number of reflections and p is the number of refined parameters. The data were checked for secondary extinction but no correction was necessary. Neutral atom scattering factors and values used to calculate the linear absorption coefficient are from the International Tables for X-ray Crystallography (1992). All figures were generated using SHELXTL/PC. Tables of positional and thermal parameters, bond lengths and angles, torsion angles and figures are found in Tables 7.1 – 7.7.

Table 7.1. Crystal data and structure refinement for **4.39·HCl**.

Empirical formula	C17 H24 Cl N	
Formula weight	277.82	
Temperature	123(2) K	
Wavelength	0.71073 Å	
Crystal system	orthorhombic	
Space group	P 21 21 2	
Unit cell dimensions	a = 13.5380(10) Å	α= 90°.
	b = 13.8012(10) Å	β= 90°.
	c = 16.2638(11) Å	γ = 90°.
Volume	3038.7(4) $Å^3$	
Z	8	
Density (calculated)	1.215 Mg/m^3	
Absorption coefficient	0.239 mm^{-1}	
F(000)	1200	
Crystal size	0.160 x 0.140 x 0.120 mm^3	
Theta range for data collection	1.252 to 27.558°.	
Index ranges	-17<=h<=17, -17<=k<=17, -21<=l<=13	
Reflections collected	50611	
Independent reflections	7020 [R(int) = 0.0959]	
Completeness to theta = 25.242°	99.9 %	
Absorption correction	Semi-empirical from equivalents	
Max. and min. transmission	1.00 and 0.869	
Refinement method	Full-matrix least-squares on F^2	
Data / restraints / parameters	7020 / 0 / 359	
Goodness-of-fit on F^2	1.034	
Final R indices [I>2sigma(I)]	R1 = 0.0455, wR2 = 0.0979	
R indices (all data)	R1 = 0.0677, wR2 = 0.1064	
Absolute structure parameter	0.09(3)	
Extinction coefficient	n/a	
Largest diff. peak and hole	0.354 and -0.268 $e.Å^{-3}$	

Table 7.2. Atomic coordinates (x 10^4) and equivalent isotropic displacement parameters ($Å^2$x 10^3) for **4.39·HCl**. U(eq) is defined as one third of the trace of the orthogonalized U^{ij} tensor.

	x	y	z	U(eq)
C1	7062(2)	3252(2)	-373(2)	17(1)
C2	8056(2)	3740(3)	-552(2)	20(1)
C3	8148(2)	4040(3)	-1445(2)	22(1)
C4	7313(2)	4659(3)	-1734(2)	20(1)
C5	6315(2)	4234(2)	-1533(2)	18(1)
C6	8903(3)	3785(3)	-1909(2)	34(1)
C7	6961(2)	3024(2)	555(2)	20(1)
C8	6031(3)	2422(2)	751(2)	21(1)
C9	5981(3)	1502(2)	239(2)	26(1)
C10	6028(3)	1746(2)	-676(2)	25(1)
C11	6959(3)	2308(2)	-859(2)	22(1)
C12	7051(2)	3887(2)	1126(2)	18(1)
C13	6277(3)	4528(2)	1253(2)	21(1)
C14	6368(3)	5298(3)	1799(2)	26(1)
C15	7231(3)	5429(3)	2237(2)	28(1)
C16	8013(3)	4787(3)	2122(2)	31(1)
C17	7923(2)	4034(3)	1570(2)	25(1)
C18	6802(2)	3007(2)	4643(2)	16(1)
C19	6320(2)	2021(2)	4463(2)	18(1)
C20	6033(3)	1926(2)	3568(2)	19(1)
C21	5381(2)	2726(2)	3269(2)	19(1)
C22	5800(2)	3718(2)	3473(2)	17(1)
C23	6331(3)	1204(3)	3103(2)	32(1)
C24	7023(2)	3109(2)	5572(2)	18(1)
C25	7613(2)	4035(3)	5769(2)	21(1)
C26	8559(2)	4103(3)	5266(2)	25(1)
C27	8326(2)	4045(3)	4352(2)	24(1)
C28	7771(2)	3117(3)	4165(2)	21(1)

Table 7.2 continued:

C29	6142(2)	3003(2)	6138(2)	18(1)
C30	5995(3)	2145(2)	6569(2)	23(1)
C31	5220(3)	2046(3)	7119(2)	30(1)
C32	4562(3)	2799(3)	7237(2)	27(1)
C33	4687(2)	3651(3)	6803(2)	23(1)
C34	5477(2)	3753(3)	6265(2)	20(1)
N1	6272(2)	3970(2)	-642(2)	15(1)
N2	6067(2)	3768(2)	4365(2)	14(1)
Cl1	4039(1)	3752(1)	-394(1)	22(1)
Cl2	6263(1)	5969(1)	4601(1)	21(1)

Table 7.3. Bond lengths [Å] and angles [°] for **4.39·HCl.**

C1-N1	1.523(4)	C11-H11B	0.99
C1-C11	1.531(4)	C12-C13	1.387(5)
C1-C2	1.532(4)	C12-C17	1.399(4)
C1-C7	1.548(4)	C13-C14	1.390(5)
C2-C3	1.516(4)	C13-H13	0.95
C2-H2A	0.99	C14-C15	1.380(5)
C2-H2B	0.99	C14-H14	0.95
C3-C6	1.318(5)	C15-C16	1.393(5)
C3-C4	1.492(5)	C15-H15	0.95
C4-C5	1.510(4)	C16-C17	1.380(5)
C4-H4A	0.99	C16-H16	0.95
C4-H4B	0.99	C17-H17	0.95
C5-N1	1.495(4)	C18-N2	1.515(4)
C5-H5A	0.99	C18-C28	1.533(4)
C5-H5B	0.99	C18-C19	1.537(4)
C6-H6A	0.95	C18-C24	1.547(4)
C6-H6B	0.95	C19-C20	1.512(4)
C7-C12	1.516(4)	C19-H19A	0.99
C7-C8	1.541(5)	C19-H19B	0.99
C7-H7	1.00	C20-C23	1.315(5)
C8-C9	1.520(5)	C20-C21	1.495(4)
C8-H8A	0.99	C21-C22	1.520(4)
C8-H8B	0.99	C21-H21A	0.99
C9-C10	1.527(5)	C21-H21B	0.99
C9-H9A	0.99	C22-N2	1.495(4)
C9-H9B	0.99	C22-H22A	0.99
C10-C11	1.509(5)	C22-H22B	0.99
C10-H10A	0.99	C23-H23A	0.95
C10-H10B	0.99	C23-H23B	0.95
C11-H11A	0.99	C24-C29	1.514(4)

Table 7.3 continued:

C24-C25	1.540(5)	C29-C30	1.391(4)
C24-H24	1.00	C30-C31	1.384(5)
C25-C26	1.523(4)	C30-H30	0.95
C25-H25A	0.99	C31-C32	1.383(5)
C25-H25B	0.99	C31-H31	0.95
C26-C27	1.521(5)	C32-C33	1.383(5)
C26-H26A	0.99	C32-H32	0.95
C26-H26B	0.99	C33-C34	1.390(5)
C27-C28	1.515(5)	C33-H33	0.95
C27-H27A	0.99	C34-H34	0.95
C27-H27B	0.99	N1-H1NA	0.94(4)
C28-H28A	0.99	N1-H1NB	1.00(4)
C28-H28B	0.99	N2-H2NB	0.89(3)
C29-C34	1.387(5)	N2-H2NA	0.89(3)

N1-C1-C11	110.0(3)	H4A-C4-H4B	107.8
N1-C1-C2	106.1(2)	N1-C5-C4	109.9(3)
C11-C1-C2	110.9(3)	N1-C5-H5A	109.7
N1-C1-C7	110.5(2)	C4-C5-H5A	109.7
C11-C1-C7	108.8(3)	N1-C5-H5B	109.7
C2-C1-C7	110.6(3)	C4-C5-H5B	109.7
C3-C2-C1	112.0(3)	H5A-C5-H5B	108.2
C3-C2-H2A	109.2	C3-C6-H6A	120.0
C1-C2-H2A	109.2	C3-C6-H6B	120.0
C3-C2-H2B	109.2	H6A-C6-H6B	120.0
C1-C2-H2B	109.2	C12-C7-C8	111.2(3)
H2A-C2-H2B	107.9	C12-C7-C1	115.5(3)
C6-C3-C4	124.0(3)	C8-C7-C1	112.5(3)
C6-C3-C2	122.6(3)	C12-C7-H7	105.5
C4-C3-C2	113.3(3)	C8-C7-H7	105.5
C3-C4-C5	112.8(3)	C1-C7-H7	105.5
C3-C4-H4A	109.0	C9-C8-C7	111.9(3)
C5-C4-H4A	109.0	C9-C8-H8A	109.2
C3-C4-H4B	109.0	C7-C8-H8A	109.2
C5-C4-H4B	109.0	C9-C8-H8B	109.2

Table 7.3 continued:

C7-C8-H8B	109.2	C16-C17-C12	121.3(3)
H8A-C8-H8B	107.9	C16-C17-H17	119.3
C8-C9-C10	110.3(3)	C12-C17-H17	119.3
C8-C9-H9A	109.6	N2-C18-C28	110.0(3)
C10-C9-H9A	109.6	N2-C18-C19	106.1(2)
C8-C9-H9B	109.6	C28-C18-C19	110.7(3)
C10-C9-H9B	109.6	N2-C18-C24	110.9(2)
H9A-C9-H9B	108.1	C28-C18-C24	108.7(3)
C11-C10-C9	109.9(3)	C19-C18-C24	110.4(3)
C11-C10-H10A	109.7	C20-C19-C18	111.7(3)
C9-C10-H10A	109.7	C20-C19-H19A	109.3
C11-C10-H10B	109.7	C18-C19-H19A	109.3
C9-C10-H10B	109.7	C20-C19-H19B	109.3
H10A-C10-H10B	108.2	C18-C19-H19B	109.3
C10-C11-C1	114.3(3)	H19A-C19-H19B	107.9
C10-C11-H11A	108.7	C23-C20-C21	123.6(3)
C1-C11-H11A	108.7	C23-C20-C19	122.8(3)
C10-C11-H11B	108.7	C21-C20-C19	113.6(3)
C1-C11-H11B	108.7	C20-C21-C22	111.9(3)
H11A-C11-H11B	107.6	C20-C21-H21A	109.2
C13-C12-C17	117.9(3)	C22-C21-H21A	109.2
C13-C12-C7	122.2(3)	C20-C21-H21B	109.2
C17-C12-C7	119.8(3)	C22-C21-H21B	109.2
C12-C13-C14	121.1(3)	H21A-C21-H21B	107.9
C12-C13-H13	119.4	N2-C22-C21	110.0(3)
C14-C13-H13	119.4	N2-C22-H22A	109.7
C15-C14-C13	120.3(3)	C21-C22-H22A	109.7
C15-C14-H14	119.9	N2-C22-H22B	109.7
C13-C14-H14	119.9	C21-C22-H22B	109.7
C14-C15-C16	119.4(3)	H22A-C22-H22B	108.2
C14-C15-H15	120.3	C20-C23-H23A	120.0
C16-C15-H15	120.3	C20-C23-H23B	120.0
C17-C16-C15	120.0(3)	H23A-C23-H23B	120.0
C17-C16-H16	120.0	C29-C24-C25	111.2(3)
C15-C16-H16	120.0	C29-C24-C18	115.6(3)

Table 7.3 continued:

C25-C24-C18	112.3(3)	C34-C29-C24	122.0(3)
C29-C24-H24	105.6	C30-C29-C24	120.1(3)
C25-C24-H24	105.6	C31-C30-C29	121.2(3)
C18-C24-H24	105.6	C31-C30-H30	119.4
C26-C25-C24	112.0(3)	C29-C30-H30	119.4
C26-C25-H25A	109.2	C32-C31-C30	120.3(3)
C24-C25-H25A	109.2	C32-C31-H31	119.9
C26-C25-H25B	109.2	C30-C31-H31	119.9
C24-C25-H25B	109.2	C33-C32-C31	119.3(3)
H25A-C25-H25B	107.9	C33-C32-H32	120.4
C27-C26-C25	110.4(3)	C31-C32-H32	120.4
C27-C26-H26A	109.6	C32-C33-C34	120.2(3)
C25-C26-H26A	109.6	C32-C33-H33	119.9
C27-C26-H26B	109.6	C34-C33-H33	119.9
C25-C26-H26B	109.6	C29-C34-C33	121.2(3)
H26A-C26-H26B	108.1	C29-C34-H34	119.4
C28-C27-C26	110.1(3)	C33-C34-H34	119.4
C28-C27-H27A	109.6	C5-N1-C1	114.1(2)
C26-C27-H27A	109.6	C5-N1-H1NA	109(2)
C28-C27-H27B	109.6	C1-N1-H1NA	113(2)
C26-C27-H27B	109.6	C5-N1-H1NB	108(2)
H27A-C27-H27B	108.2	C1-N1-H1NB	110(2)
C27-C28-C18	113.9(3)	H1NA-N1-H1NB	102(3)
C27-C28-H28A	108.8	C22-N2-C18	114.6(2)
C18-C28-H28A	108.8	C22-N2-H2NB	104(2)
C27-C28-H28B	108.8	C18-N2-H2NB	111(2)
C18-C28-H28B	108.8	C22-N2-H2NA	109(2)
H28A-C28-H28B	107.7	C18-N2-H2NA	111(2)
C34-C29-C30	117.9(3)	H2NB-N2-H2NA	106(3)

Table 7.4. Anisotropic displacement parameters ($Å^2 x\ 10^3$) for **4.39·HCl**. The anisotropic displacement factor exponent takes the form: $-2\pi^2[\ h^2\ a^{*2}U^{11} + ...\ + 2\ h\ k\ a^*\ b^*\ U^{12}\ ]$

	U^{11}	U^{22}	U^{33}	U^{23}	U^{13}	U^{12}
C1	17(2)	20(2)	14(2)	-1(1)	-1(1)	5(1)
C2	15(1)	28(2)	17(2)	3(1)	1(1)	3(1)
C3	20(2)	26(2)	18(2)	0(2)	1(1)	1(2)
C4	23(2)	23(2)	13(2)	1(1)	1(1)	4(1)
C5	22(2)	20(2)	11(2)	3(1)	-2(1)	3(1)
C6	26(2)	56(3)	19(2)	4(2)	2(2)	13(2)
C7	19(2)	21(2)	18(2)	3(1)	0(1)	4(1)
C8	23(2)	20(2)	18(2)	5(1)	1(1)	2(2)
C9	28(2)	17(2)	32(2)	2(2)	1(2)	2(1)
C10	31(2)	18(2)	25(2)	-4(1)	0(2)	3(2)
C11	26(2)	21(2)	18(2)	0(1)	-1(1)	8(2)
C12	23(2)	22(2)	10(2)	5(1)	0(1)	-4(1)
C13	21(2)	26(2)	15(2)	2(1)	0(1)	-1(1)
C14	35(2)	25(2)	17(2)	0(2)	2(2)	-4(2)
C15	42(2)	27(2)	16(2)	1(2)	-3(2)	-10(2)
C16	34(2)	42(2)	18(2)	7(2)	-10(2)	-18(2)
C17	22(2)	31(2)	20(2)	9(2)	-1(1)	-1(2)
C18	18(2)	16(2)	14(2)	0(1)	-1(1)	5(1)
C19	27(2)	14(2)	13(2)	0(1)	-3(1)	2(1)
C20	26(2)	18(2)	14(2)	-2(1)	-1(1)	2(2)
C21	23(2)	18(2)	15(2)	-4(1)	-3(1)	2(1)
C22	23(2)	18(2)	10(2)	2(1)	-2(1)	5(1)
C23	49(2)	27(2)	20(2)	-3(2)	-6(2)	16(2)
C24	19(2)	16(2)	18(2)	-1(1)	-2(1)	4(1)
C25	20(2)	24(2)	17(2)	-1(2)	-4(1)	0(2)
C26	18(2)	31(2)	28(2)	-4(2)	-2(1)	1(2)
C27	18(2)	31(2)	24(2)	0(2)	4(1)	3(2)

Table 7.4 continued:

C28	19(2)	25(2)	18(2)	-1(1)	1(1)	7(1)
C29	23(2)	21(2)	9(2)	-1(1)	-5(1)	-1(1)
C30	30(2)	20(2)	19(2)	-1(1)	-7(2)	1(2)
C31	46(2)	27(2)	16(2)	7(2)	-6(2)	-16(2)
C32	28(2)	39(2)	15(2)	1(2)	-1(2)	-9(2)
C33	24(2)	30(2)	15(2)	-5(2)	1(1)	-2(2)
C34	26(2)	21(2)	12(2)	0(1)	-1(1)	0(1)
N1	14(1)	17(1)	13(1)	0(1)	0(1)	2(1)
N2	17(1)	13(1)	12(1)	-2(1)	0(1)	1(1)
Cl1	17(1)	20(1)	28(1)	4(1)	1(1)	-1(1)
Cl2	20(1)	15(1)	27(1)	-1(1)	-4(1)	0(1)

Table 7.5. Hydrogen coordinates (x 10^4) and isotropic displacement parameters ($Å^2$x 10^3) for **4.39·HCl**.

	x	y	z	U(eq)
H2A	8126	4319	-197	24
H2B	8597	3286	-414	24
H4A	7366	4745	-2337	24
H4B	7368	5306	-1476	24
H5A	5791	4711	-1660	21
H5B	6199	3650	-1873	21
H6A	8938	3997	-2464	41
H6B	9412	3389	-1688	41
H7	7533	2594	691	23
H8A	6033	2249	1342	25
H8B	5436	2820	643	25
H9A	5358	1154	360	31
H9B	6538	1071	386	31
H10A	6020	1141	-1003	30
H10B	5444	2136	-832	30
H11A	6974	2461	-1454	26
H11B	7535	1890	-738	26
H13	5675	4440	963	25
H14	5834	5737	1870	31
H15	7290	5951	2614	34
H16	8608	4868	2424	38
H17	8464	3606	1489	29
H19A	6787	1497	4608	22
H19B	5724	1946	4810	22
H21A	4720	2659	3524	22
H21B	5300	2669	2666	22
H22A	6395	3841	3134	21

Table 7.5 continued:

H22B	5305	4224	3345	21
H23A	6131	1171	2543	39
H23B	6746	715	3325	39
H24	7473	2558	5710	21
H25A	7196	4609	5655	25
H25B	7781	4041	6362	25
H26A	8897	4723	5386	31
H26B	9008	3567	5420	31
H27A	7920	4610	4188	29
H27B	8947	4062	4032	29
H28A	8203	2559	4293	25
H28B	7624	3096	3569	25
H30	6434	1617	6485	28
H31	5141	1458	7415	36
H32	4029	2731	7613	33
H33	4232	4168	6873	27
H34	5564	4347	5978	24
H1NA	5630(30)	3760(30)	-510(20)	27(10)
H1NB	6330(20)	4580(30)	-310(20)	25(9)
H2NB	5500(20)	3700(20)	4630(20)	13(8)
H2NA	6280(20)	4360(20)	4485(19)	11(8)

Table 7.6. Torsion angles [°] for **4.39·HCl**.

N1-C1-C2-C3	-56.0(3)	C15-C16-C17-C12	-1.0(5)
C11-C1-C2-C3	63.4(4)	C13-C12-C17-C16	0.5(5)
C7-C1-C2-C3	-175.8(3)	C7-C12-C17-C16	-177.1(3)
C1-C2-C3-C6	-127.0(4)	N2-C18-C19-C20	56.1(3)
C1-C2-C3-C4	53.9(4)	C28-C18-C19-C20	-63.2(3)
C6-C3-C4-C5	130.7(4)	C24-C18-C19-C20	176.3(3)
C2-C3-C4-C5	-50.2(4)	C18-C19-C20-C23	125.2(4)
C3-C4-C5-N1	50.9(4)	C18-C19-C20-C21	-55.0(4)
N1-C1-C7-C12	-59.4(3)	C23-C20-C21-C22	-129.1(4)
C11-C1-C7-C12	179.8(3)	C19-C20-C21-C22	51.1(4)
C2-C1-C7-C12	57.8(4)	C20-C21-C22-N2	-50.7(4)
N1-C1-C7-C8	69.8(3)	N2-C18-C24-C29	59.9(4)
C11-C1-C7-C8	-51.0(3)	C28-C18-C24-C29	-179.1(3)
C2-C1-C7-C8	-173.0(3)	C19-C18-C24-C29	-57.4(4)
C12-C7-C8-C9	-174.6(3)	N2-C18-C24-C25	-69.2(3)
C1-C7-C8-C9	54.1(4)	C28-C18-C24-C25	51.8(3)
C7-C8-C9-C10	-56.2(4)	C19-C18-C24-C25	173.5(3)
C8-C9-C10-C11	57.2(4)	C29-C24-C25-C26	174.2(3)
C9-C10-C11-C1	-58.1(4)	C18-C24-C25-C26	-54.4(4)
N1-C1-C11-C10	-66.9(3)	C24-C25-C26-C27	56.1(4)
C2-C1-C11-C10	176.1(3)	C25-C26-C27-C28	-56.9(4)
C7-C1-C11-C10	54.3(4)	C26-C27-C28-C18	58.2(4)
C8-C7-C12-C13	-51.0(4)	N2-C18-C28-C27	66.8(3)
C1-C7-C12-C13	78.9(4)	C19-C18-C28-C27	-176.2(3)
C8-C7-C12-C17	126.5(3)	C24-C18-C28-C27	-54.7(4)
C1-C7-C12-C17	-103.7(3)	C25-C24-C29-C34	50.3(4)
C17-C12-C13-C14	0.6(5)	C18-C24-C29-C34	-79.4(4)
C7-C12-C13-C14	178.1(3)	C25-C24-C29-C30	-127.8(3)
C12-C13-C14-C15	-1.1(5)	C18-C24-C29-C30	102.6(3)
C13-C14-C15-C16	0.6(5)	C34-C29-C30-C31	-1.1(5)
C14-C15-C16-C17	0.4(5)	C24-C29-C30-C31	177.0(3)

Table 7.6 continued:

C29-C30-C31-C32	1.3(5)	C11-C1-N1-C5	-59.9(3)
C30-C31-C32-C33	-0.2(5)	C2-C1-N1-C5	60.1(3)
C31-C32-C33-C34	-1.1(5)	C7-C1-N1-C5	179.9(3)
C30-C29-C34-C33	-0.2(5)	C21-C22-N2-C18	57.7(3)
C24-C29-C34-C33	-178.3(3)	C28-C18-N2-C22	60.3(3)
C32-C33-C34-C29	1.3(5)	C19-C18-N2-C22	-59.6(3)
C4-C5-N1-C1	-58.2(3)	C24-C18-N2-C22	-179.5(3)

Table 7.7. Hydrogen bonds for **4.39·HCl** [Å and °].

D-H...A	d(D-H)	d(H...A)	d(D...A)	<(DHA)
N1-H1NA...Cl1	0.94(4)	2.16(4)	3.065(3)	160(3)
N1-H1NB...Cl1#1	1.00(4)	2.37(4)	3.196(3)	140(3)
N2-H2NB...Cl2#1	0.89(3)	2.43(3)	3.198(3)	146(3)
N2-H2NA...Cl2	0.89(3)	2.22(3)	3.074(3)	159(3)

Symmetry transformations used to generate equivalent atoms:

#1 -x+1,-y+1,z

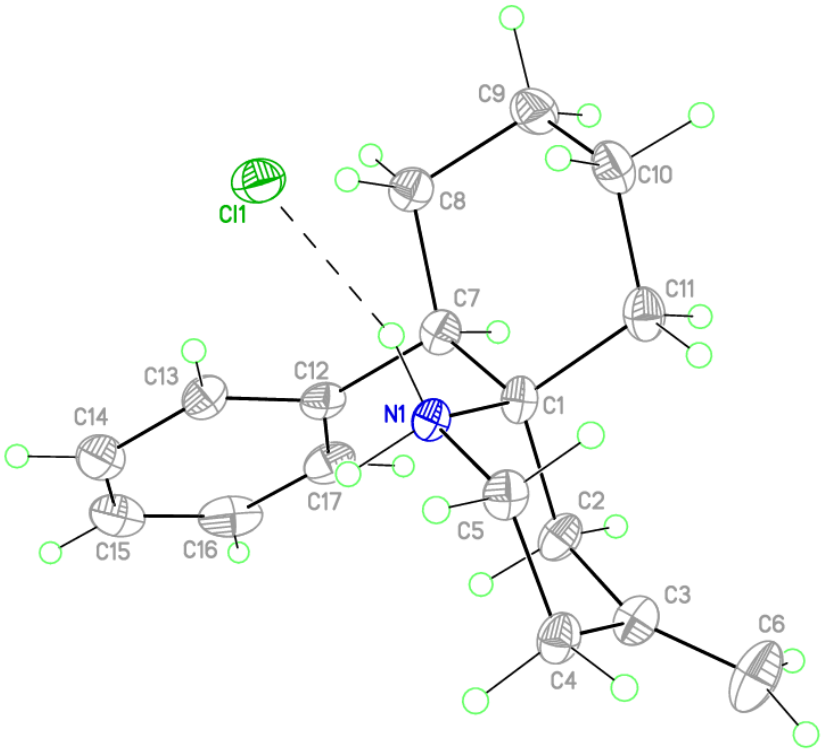

Figure 7.1. View of **4.39·HCl** showing the atom labeling scheme. Displacement ellipsoids are scaled to the 50% probability level.

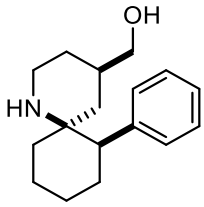

4.66

X-ray Experimental for complex $C_{17}H_{26}NO^{1+}$ - Cl^{1-} - ¼ H_2O (4.66): Crystals grew as clusters of multiply intergrown colorless plates by evaporation from ethyl acetate. The data crystal was cut from a cluster of crystals and had approximate dimensions; 0.13 x 0.08 x 0.07 mm. The data were collected on an Agilent Technologies SuperNova Dual Source diffractometer using a μ-focus Cu Kα radiation source (λ = 1.5418Å) with collimating mirror monochromators. A total of 750 frames of data were collected using ω-scans with a scan range of 1° and a counting time of 15 seconds per frame with a detector offset of 0.0° and 41 seconds per frame with a detector offset of +/- 78.3°. The data were collected at 100 K using an Oxford Cryostream low temperature device. Details of crystal data, data collection and structure refinement are listed in Table 7.8. Data collection, unit cell refinement and data reduction were performed using Agilent Technologies CrysAlisPro V 1.171.38.46. The structure was solved by direct methods using SHELXT[2] and refined by full-matrix least-squares on F^2 with anisotropic displacement parameters for the non-H atoms using SHELXL-2016/6.[255,256] Structure analysis was aided by use of the programs PLATON and WinGX.[252,257] The hydrogen atoms were calculated in ideal positions with isotropic displacement parameters set to 1.2xUeq of the attached atom (1.5xUeq for methyl hydrogen atoms).

The crystal was refined as a 2-component twin. The twin law was determined using CrysAlisPro. The twin was due to a 180º rotation about the [1,0,0] direct axis direction. The twin fraction refined to 0.308(2). There are four ion pairs in the asymmetric unit. The four are clustered around a single water molecule. The hydroxyl groups for all four are directed toward the water molecule and are presumably H-bound to it. The four hydroxyl groups are disordered about two orientations each.

The function, $\Sigma w(|F_o|^2 - |F_c|^2)^2$, was minimized, where $w = 1/[(\sigma(F_o))^2 + (0.0961*P)^2]$ and $P = (|F_o|^2 + 2|F_c|^2)/3$. $R_w(F^2)$ refined to 0.268, with R(F) equal to 0.0972 and a goodness of fit, S, = 1.01. Definitions used for calculating R(F), $R_w(F^2)$ and the goodness of fit, S, are as follows: $R_w(F^2) = \{\Sigma w(|F_o|^2 - |F_c|^2)^2/\Sigma w(|F_o|)^4\}^{1/2}$ where w is the weight given each reflection; $R(F) = \Sigma(|F_o| - |F_c|)/\Sigma|F_o|\}$ for reflections with $F_o > 4(\sigma(F_o))$; $S = [\Sigma w(|F_o|^2 -$

$|F_C|^2)^2/(n - p)]^{1/2}$, where n is the number of reflections and p is the number of refined parameters. The data were checked for secondary extinction effects but no correction was necessary. Neutral atom scattering factors and values used to calculate the linear absorption coefficient are from the International Tables for X-ray Crystallography (1992). All figures were generated using SHELXTL/PC. Tables of positional and thermal parameters, bond lengths and angles, torsion angles and figures are found in Tables 7.8 – 7.14.

Table 7.8. Crystal data and structure refinement for **4.66**.

Empirical formula	C17 H26 Cl N O1.25
Formula weight	299.84
Temperature	100(2) K
Wavelength	1.54184 Å

Crystal system	triclinic	
Space group	P -1	
Unit cell dimensions	a = 12.6755(8) Å	α= 108.860(9)°.
	b = 15.7168(12) Å	β= 98.379(8)°.
	c = 17.551(3) Å	γ = 90.045(6)°.
Volume	3269.1(6) $Å^3$	
Z	8	
Density (calculated)	1.218 Mg/m^3	
Absorption coefficient	2.041 mm^{-1}	
F(000)	1296	
Crystal size	0.130 x 0.080 x 0.070 mm^3	
Theta range for data collection	4.500 to 59.670°.	
Index ranges	-13<=h<=14, -17<=k<=17, -19<=l<=19	
Reflections collected	14543	
Independent reflections	14543 [R(int) = ?]	
Completeness to theta = 59.670°	97.2 %	
Absorption correction	Semi-empirical from equivalents	
Max. and min. transmission	1.00 and 0.607	
Refinement method	Full-matrix least-squares on F^2	
Data / restraints / parameters	14543 / 566 / 761	
Goodness-of-fit on F^2	1.002	
Final R indices [I>2sigma(I)]	R1 = 0.0972, wR2 = 0.2498	
R indices (all data)	R1 = 0.1982, wR2 = 0.2681	
Extinction coefficient	n/a	
Largest diff. peak and hole	0.713 and -0.492 $e.Å^{-3}$	

Table 7.9. Atomic coordinates (x 10^4) and equivalent isotropic displacement parameters ($Å^2$x 10^3) for **4.66**. U(eq) is defined as one third of the trace of the orthogonalized U^{ij} tensor.

	x	y	z	U(eq)
C1	9154(8)	5432(7)	2754(7)	23(3)
C2	8825(8)	4642(7)	3035(7)	25(3)
C3	8941(8)	4934(6)	3996(6)	27(3)
C4	8330(9)	5749(7)	4313(7)	33(3)
C5	8569(9)	6526(8)	4005(7)	39(3)
C6	8987(8)	5113(7)	1796(7)	29(3)
C7	9427(8)	5865(8)	1497(7)	37(3)
C8	10561(9)	6177(8)	1831(8)	48(3)
C9	10755(9)	6462(8)	2773(8)	43(3)
C10	10359(8)	5718(7)	3068(7)	32(3)
C11	7900(8)	4757(7)	1382(6)	24(3)
C12	7065(8)	5330(8)	1277(7)	32(3)
C13	6051(9)	4976(9)	870(7)	40(3)
C14	5845(10)	4062(9)	559(7)	38(3)
C15	6649(10)	3498(8)	682(7)	43(3)
C16	7633(10)	3837(8)	1078(7)	38(3)
C17	8588(9)	4108(8)	4199(8)	54(4)
C18	5766(8)	6202(7)	7182(7)	31(3)
C19	6074(8)	5246(7)	6918(6)	24(3)
C20	6046(8)	4817(6)	6001(6)	29(3)
C21	6735(9)	5372(7)	5697(7)	30(3)
C22	6481(9)	6365(7)	5939(7)	29(3)
C23	5877(8)	6655(7)	8116(6)	24(3)
C24	5515(9)	7624(7)	8365(7)	36(3)
C25	4401(9)	7695(8)	7989(8)	42(3)
C26	4245(10)	7288(7)	7049(7)	37(3)
C27	4588(8)	6321(7)	6797(7)	31(3)
C28	6943(9)	6548(7)	8599(7)	30(3)

Table 7.9 continued:

C29	7057(9)	5884(8)	8942(7)	35(3)
C30	8025(9)	5804(7)	9418(7)	31(3)
C31	8885(10)	6356(8)	9511(8)	43(3)
C32	8801(9)	7048(8)	9160(7)	39(3)
C33	7816(8)	7157(7)	8726(6)	31(3)
C34	6365(9)	3848(7)	5803(6)	44(4)
C35	4954(8)	-1208(7)	2871(7)	22(3)
C36	5363(9)	-222(7)	3132(7)	37(3)
C37	5735(9)	209(6)	4044(7)	39(3)
C38	6609(10)	-376(8)	4298(8)	47(4)
C39	6266(10)	-1347(8)	4048(8)	45(4)
C40	4603(8)	-1606(7)	1934(7)	29(3)
C41	4166(8)	-2588(7)	1663(7)	33(3)
C42	3210(9)	-2651(8)	2092(7)	45(3)
C43	3550(9)	-2235(8)	3045(7)	35(3)
C44	3960(9)	-1303(8)	3245(7)	38(3)
C45	5439(8)	-1499(7)	1418(6)	24(3)
C46	5422(9)	-754(8)	1137(7)	40(3)
C47	6155(10)	-600(9)	693(8)	45(4)
C48	6943(11)	-1204(9)	521(8)	44(3)
C49	6977(10)	-1966(9)	756(8)	47(4)
C50	6227(9)	-2090(8)	1227(7)	41(3)
C51	6083(9)	1169(8)	4232(7)	54(4)
C52	10083(9)	-424(7)	7396(7)	34(3)
C53	9664(9)	354(7)	7100(7)	31(3)
C54	9472(9)	114(7)	6160(7)	37(3)
C55	8671(10)	-692(8)	5801(8)	45(3)
C56	9016(9)	-1477(8)	6079(7)	40(3)
C57	10228(8)	-151(7)	8352(7)	30(3)
C58	10628(8)	-951(7)	8624(7)	33(3)
C59	11663(9)	-1268(8)	8343(8)	45(3)
C60	11546(9)	-1498(8)	7409(8)	46(4)
C61	11153(10)	-755(8)	7128(8)	44(3)
C62	9298(9)	284(8)	8737(7)	30(3)
C63	9257(10)	1226(8)	9048(7)	37(3)

Table 7.9 continued:

C64	8423(11)	1602(9)	9412(8)	52(4)
C65	7542(11)	1088(9)	9476(8)	47(4)
C66	7600(10)	178(9)	9155(8)	43(3)
C67	8411(9)	-229(8)	8796(7)	36(3)
C68	9070(10)	922(9)	5955(8)	65(4)
N1	8451(6)	6205(5)	3093(5)	26(2)
N2	6553(6)	6725(5)	6857(5)	23(2)
N3	5852(7)	-1677(6)	3165(5)	30(2)
N4	9234(6)	-1202(5)	7005(5)	22(2)
O1	9429(8)	3577(6)	4274(7)	44(3)
O1A	8740(20)	4172(14)	4982(10)	46(8)
O2	6352(9)	3393(6)	5004(6)	43(3)
O2A	5496(15)	3243(9)	5521(16)	43(3)
O1W	8520(7)	2448(6)	4984(6)	67(3)
O3	5295(11)	1758(7)	4499(10)	41(4)
O3A	6518(12)	1652(8)	4992(7)	45(4)
O4	9860(12)	1410(10)	5795(11)	67(6)
O4A	8862(12)	871(9)	5174(8)	48(5)
Cl4	9073(2)	-3133(2)	7035(2)	38(1)
Cl3	5971(2)	-3695(2)	3063(2)	40(1)
Cl1	8248(2)	8031(2)	2810(2)	56(1)
Cl2	6723(2)	8719(2)	6972(2)	45(1)

Table 7.10. Bond lengths [Å] and angles [°] for 4.66

C1-N1	1.521(12)	C12-C13	1.395(14)
C1-C2	1.554(14)	C12-H12	0.95
C1-C10	1.559(14)	C13-C14	1.372(15)
C1-C6	1.572(15)	C13-H13	0.95
C2-C3	1.582(14)	C14-C15	1.390(16)
C2-H2A	0.99	C14-H14	0.95
C2-H2B	0.99	C15-C16	1.352(15)
C3-C4	1.488(13)	C15-H15	0.95
C3-C17	1.536(14)	C16-H16	0.95
C3-H3	1.00	C17-O1A	1.330(10)
C4-C5	1.532(15)	C17-O1	1.371(9)
C4-H4A	0.99	C17-H17A	0.96
C4-H4B	0.99	C17-H17B	0.96
C5-N1	1.500(14)	C17-H17C	0.96
C5-H5A	0.99	C17-H17D	0.96
C5-H5B	0.99	C18-C19	1.493(14)
C6-C11	1.478(14)	C18-C23	1.546(14)
C6-C7	1.571(14)	C18-N2	1.570(12)
C6-H6	1.00	C18-C27	1.584(14)
C7-C8	1.490(15)	C19-C20	1.525(14)
C7-H7A	0.99	C19-H19A	0.99
C7-H7B	0.99	C19-H19B	0.99
C8-C9	1.547(16)	C20-C21	1.498(13)
C8-H8A	0.99	C20-C34	1.517(13)
C8-H8B	0.99	C20-H20	1.00
C9-C10	1.533(15)	C21-C22	1.527(14)
C9-H9A	0.99	C21-H21A	0.99
C9-H9B	0.99	C21-H21B	0.99
C10-H10A	0.99	C22-N2	1.513(13)
C10-H10B	0.99	C22-H22A	0.99
C11-C16	1.391(14)	C22-H22B	0.99
C11-C12	1.420(14)	C23-C28	1.527(15)

C23-C24	1.534(14)	C36-H36A	0.99
C23-H23	1.00	C36-H36B	0.99

Table 7.10 continued:

C24-C25	1.489(15)	C37-C51	1.488(14)
C24-H24A	0.99	C37-C38	1.548(14)
C24-H24B	0.99	C37-H37	1.00
C25-C26	1.547(16)	C38-C39	1.491(15)
C25-H25A	0.99	C38-H38A	0.99
C25-H25B	0.99	C38-H38B	0.99
C26-C27	1.523(14)	C39-N3	1.481(14)
C26-H26A	0.99	C39-H39A	0.99
C26-H26B	0.99	C39-H39B	0.99
C27-H27A	0.99	C40-C45	1.532(14)
C27-H27B	0.99	C40-C41	1.536(13)
C28-C29	1.360(15)	C40-H40	1.00
C28-C33	1.408(14)	C41-C42	1.535(15)
C29-C30	1.411(15)	C41-H41A	0.99
C29-H29	0.95	C41-H41B	0.99
C30-C31	1.349(15)	C42-C43	1.579(16)
C30-H30	0.95	C42-H42A	0.99
C31-C32	1.409(16)	C42-H42B	0.99
C31-H31	0.95	C43-C44	1.467(14)
C32-C33	1.406(15)	C43-H43A	0.99
C32-H32	0.95	C43-H43B	0.99
C33-H33	0.95	C44-H44A	0.99
C34-O2	1.350(9)	C44-H44B	0.99
C34-O2A	1.378(10)	C45-C50	1.368(15)
C34-H34A	0.96	C45-C46	1.410(15)
C34-H34B	0.96	C46-C47	1.365(15)
C34-H34C	0.96	C46-H46	0.95
C34-H34D	0.96	C47-C48	1.375(17)
C35-N3	1.476(12)	C47-H47	0.95
C35-C44	1.532(14)	C48-C49	1.387(17)
C35-C36	1.534(14)	C48-H48	0.95
C35-C40	1.554(14)	C49-C50	1.400(16)
C36-C37	1.523(14)	C49-H49	0.95

C50-H50	0.95	C61-H61A	0.99
C51-O3A	1.337(9)		

Table 7.10 continued:

C51-O3	1.390(9)	C61-H61B	0.99
C51-H51A	0.96	C62-C63	1.407(15)
C51-H51B	0.96	C62-C67	1.418(15)
C51-H51C	0.96	C63-C64	1.352(16)
C51-H51D	0.96	C63-H63	0.95
C52-C61	1.536(15)	C64-C65	1.416(17)
C52-N4	1.538(12)	C64-H64	0.95
C52-C53	1.542(15)	C65-C66	1.364(15)
C52-C57	1.574(15)	C65-H65	0.95
C53-C54	1.551(15)	C66-C67	1.339(15)
C53-H53A	0.99	C66-H66	0.95
C53-H53B	0.99	C67-H67	0.95
C54-C68	1.498(15)	C68-O4A	1.332(10)
C54-C55	1.526(15)	C68-O4	1.374(10)
C54-H54	1.00	C68-H68A	0.96
C55-C56	1.510(16)	C68-H68B	0.96
C55-H55A	0.99	C68-H68C	0.96
C55-H55B	0.99	C68-H68D	0.96
C56-N4	1.522(14)	N1-H1A	0.91
C56-H56A	0.99	N1-H1B	0.91
C56-H56B	0.99	N2-H2C	0.91
C57-C62	1.500(15)	N2-H2D	0.91
C57-C58	1.544(15)	N3-H3A	0.91
C57-H57	1.00	N3-H3B	0.91
C58-C59	1.498(14)	N4-H4C	0.91
C58-H58A	0.99	N4-H4D	0.91
C58-H58B	0.99	O1-H1	0.84
C59-C60	1.545(16)	O1A-H17B	0.7835
C59-H59A	0.99	O1A-H1A1	0.84
C59-H59B	0.99	O2-H2	0.84
C60-C61	1.467(16)	O2A-H2A1	0.84
C60-H60A	0.99	O3-H3C	0.84
C60-H60B	0.99	O3A-H3A1	0.84

O4-H4	0.84	O4A-H4A1	0.84

Table 7.10 continued:

		C11-C6-H6	105.6
N1-C1-C2	107.2(8)		
N1-C1-C10	111.0(8)	C7-C6-H6	105.6
C2-C1-C10	110.5(9)	C1-C6-H6	105.6
N1-C1-C6	111.2(8)	C8-C7-C6	115.1(10)
C2-C1-C6	109.1(8)	C8-C7-H7A	108.5
C10-C1-C6	107.8(8)	C6-C7-H7A	108.5
C1-C2-C3	111.4(8)	C8-C7-H7B	108.5
C1-C2-H2A	109.3	C6-C7-H7B	108.5
C3-C2-H2A	109.3	H7A-C7-H7B	107.5
C1-C2-H2B	109.3	C7-C8-C9	111.0(10)
C3-C2-H2B	109.3	C7-C8-H8A	109.4
H2A-C2-H2B	108.0	C9-C8-H8A	109.4
C4-C3-C17	114.7(8)	C7-C8-H8B	109.4
C4-C3-C2	110.2(8)	C9-C8-H8B	109.4
C17-C3-C2	106.6(9)	H8A-C8-H8B	108.0
C4-C3-H3	108.4	C10-C9-C8	111.3(10)
C17-C3-H3	108.4	C10-C9-H9A	109.4
C2-C3-H3	108.4	C8-C9-H9A	109.4
C3-C4-C5	114.5(9)	C10-C9-H9B	109.4
C3-C4-H4A	108.6	C8-C9-H9B	109.4
C5-C4-H4A	108.6	H9A-C9-H9B	108.0
C3-C4-H4B	108.6	C9-C10-C1	113.3(9)
C5-C4-H4B	108.6	C9-C10-H10A	108.9
H4A-C4-H4B	107.6	C1-C10-H10A	108.9
N1-C5-C4	110.6(9)	C9-C10-H10B	108.9
N1-C5-H5A	109.5	C1-C10-H10B	108.9
C4-C5-H5A	109.5	H10A-C10-H10B	107.7
N1-C5-H5B	109.5	C16-C11-C12	116.1(10)
C4-C5-H5B	109.5	C16-C11-C6	121.7(10)
H5A-C5-H5B	108.1	C12-C11-C6	122.2(9)
C11-C6-C7	113.0(9)	C13-C12-C11	121.0(10)
C11-C6-C1	115.8(9)	C13-C12-H12	119.5
C7-C6-C1	110.1(9)	C11-C12-H12	119.5

C14-C13-C12	120.3(11)	N2-C18-C27	107.9(9)
C14-C13-H13	119.9	C18-C19-C20	114.7(9)

Table 7.10 continued:

C12-C13-H13	119.9	C18-C19-H19A	108.6
C13-C14-C15	118.9(11)	C20-C19-H19A	108.6
C13-C14-H14	120.6	C18-C19-H19B	108.6
C15-C14-H14	120.6	C20-C19-H19B	108.6
C16-C15-C14	121.1(11)	H19A-C19-H19B	107.6
C16-C15-H15	119.5	C21-C20-C34	112.7(8)
C14-C15-H15	119.5	C21-C20-C19	110.0(8)
C15-C16-C11	122.6(12)	C34-C20-C19	110.2(9)
C15-C16-H16	118.7	C21-C20-H20	108.0
C11-C16-H16	118.7	C34-C20-H20	108.0
O1A-C17-C3	116.6(12)	C19-C20-H20	108.0
O1-C17-C3	111.1(9)	C20-C21-C22	113.8(9)
O1A-C17-H17A	129.3	C20-C21-H21A	108.8
O1-C17-H17A	108.6	C22-C21-H21A	108.8
C3-C17-H17A	108.7	C20-C21-H21B	108.8
O1A-C17-H17B	35.6	C22-C21-H21B	108.8
O1-C17-H17B	110.1	H21A-C21-H21B	107.7
C3-C17-H17B	110.0	N2-C22-C21	108.1(8)
H17A-C17-H17B	108.2	N2-C22-H22A	110.1
O1A-C17-H17C	106.7	C21-C22-H22A	110.1
C3-C17-H17C	108.5	N2-C22-H22B	110.1
H17A-C17-H17C	77.8	C21-C22-H22B	110.1
H17B-C17-H17C	136.1	H22A-C22-H22B	108.4
O1A-C17-H17D	109.7	C28-C23-C24	113.4(9)
C3-C17-H17D	107.5	C28-C23-C18	115.5(9)
H17A-C17-H17D	31.3	C24-C23-C18	113.1(9)
H17B-C17-H17D	79.9	C28-C23-H23	104.5
H17C-C17-H17D	107.5	C24-C23-H23	104.5
C19-C18-C23	114.4(9)	C18-C23-H23	104.5
C19-C18-N2	105.7(8)	C25-C24-C23	112.8(9)
C23-C18-N2	107.8(8)	C25-C24-H24A	109.0
C19-C18-C27	112.8(9)	C23-C24-H24A	109.0
C23-C18-C27	108.0(9)	C25-C24-H24B	109.0

C23-C24-H24B	109.0	C32-C33-C28	120.3(11)
H24A-C24-H24B	107.8	C32-C33-H33	119.8

Table 7.10 continued:

C24-C25-C26	112.0(10)	C28-C33-H33	119.8
C24-C25-H25A	109.2	O2-C34-C20	115.5(10)
C26-C25-H25A	109.2	O2A-C34-C20	112.4(10)
C24-C25-H25B	109.2	O2-C34-H34A	108.6
C26-C25-H25B	109.2	C20-C34-H34A	108.9
H25A-C25-H25B	107.9	O2-C34-H34B	108.0
C27-C26-C25	109.9(10)	C20-C34-H34B	107.9
C27-C26-H26A	109.7	H34A-C34-H34B	107.7
C25-C26-H26A	109.7	O2A-C34-H34C	109.1
C27-C26-H26B	109.7	C20-C34-H34C	108.4
C25-C26-H26B	109.7	O2A-C34-H34D	109.1
H26A-C26-H26B	108.2	C20-C34-H34D	109.7
C26-C27-C18	114.4(9)	H34C-C34-H34D	108.0
C26-C27-H27A	108.7	N3-C35-C44	111.2(9)
C18-C27-H27A	108.7	N3-C35-C36	104.9(8)
C26-C27-H27B	108.7	C44-C35-C36	111.3(9)
C18-C27-H27B	108.7	N3-C35-C40	112.4(8)
H27A-C27-H27B	107.6	C44-C35-C40	105.4(8)
C29-C28-C33	118.6(11)	C36-C35-C40	111.8(9)
C29-C28-C23	120.8(10)	C37-C36-C35	114.6(9)
C33-C28-C23	120.5(10)	C37-C36-H36A	108.6
C28-C29-C30	121.2(11)	C35-C36-H36A	108.6
C28-C29-H29	119.4	C37-C36-H36B	108.6
C30-C29-H29	119.4	C35-C36-H36B	108.6
C31-C30-C29	120.7(11)	H36A-C36-H36B	107.6
C31-C30-H30	119.6	C51-C37-C36	110.1(10)
C29-C30-H30	119.6	C51-C37-C38	114.4(9)
C30-C31-C32	119.7(12)	C36-C37-C38	107.3(9)
C30-C31-H31	120.2	C51-C37-H37	108.3
C32-C31-H31	120.2	C36-C37-H37	108.3
C33-C32-C31	119.3(11)	C38-C37-H37	108.3
C33-C32-H32	120.4	C39-C38-C37	113.4(10)
C31-C32-H32	120.4	C39-C38-H38A	108.9

C37-C38-H38A	108.9	C43-C44-H44A	108.7
C39-C38-H38B	108.9	C35-C44-H44A	108.7
Table 7.10 continued:			
C37-C38-H38B	108.9	C43-C44-H44B	108.7
H38A-C38-H38B	107.7	C35-C44-H44B	108.7
N3-C39-C38	109.3(10)	H44A-C44-H44B	107.6
N3-C39-H39A	109.8	C50-C45-C46	117.7(11)
C38-C39-H39A	109.8	C50-C45-C40	122.8(10)
N3-C39-H39B	109.8	C46-C45-C40	119.5(10)
C38-C39-H39B	109.8	C47-C46-C45	122.9(12)
H39A-C39-H39B	108.3	C47-C46-H46	118.5
C45-C40-C41	110.9(9)	C45-C46-H46	118.5
C45-C40-C35	115.2(8)	C46-C47-C48	117.7(13)
C41-C40-C35	112.5(9)	C46-C47-H47	121.1
C45-C40-H40	105.8	C48-C47-H47	121.1
C41-C40-H40	105.8	C47-C48-C49	121.9(13)
C35-C40-H40	105.8	C47-C48-H48	119.1
C42-C41-C40	109.9(9)	C49-C48-H48	119.1
C42-C41-H41A	109.7	C48-C49-C50	118.7(12)
C40-C41-H41A	109.7	C48-C49-H49	120.7
C42-C41-H41B	109.7	C50-C49-H49	120.7
C40-C41-H41B	109.7	C45-C50-C49	121.0(12)
H41A-C41-H41B	108.2	C45-C50-H50	119.5
C41-C42-C43	109.7(9)	C49-C50-H50	119.5
C41-C42-H42A	109.7	O3A-C51-C37	119.6(11)
C43-C42-H42A	109.7	O3-C51-C37	112.8(10)
C41-C42-H42B	109.7	O3-C51-H51A	108.7
C43-C42-H42B	109.7	C37-C51-H51A	108.3
H42A-C42-H42B	108.2	O3-C51-H51B	109.1
C44-C43-C42	108.9(10)	C37-C51-H51B	109.8
C44-C43-H43A	109.9	H51A-C51-H51B	108.1
C42-C43-H43A	109.9	O3A-C51-H51C	107.4
C44-C43-H43B	109.9	C37-C51-H51C	108.1
C42-C43-H43B	109.9	O3A-C51-H51D	107.1
H43A-C43-H43B	108.3	C37-C51-H51D	106.8
C43-C44-C35	114.2(10)	H51C-C51-H51D	107.2

C61-C52-N4	108.2(9)	C52-C57-H57	105.5
C61-C52-C53	113.7(10)	C59-C58-C57	112.3(10)

Table 7.10 continued:

N4-C52-C53	105.5(8)	C59-C58-H58A	109.1
C61-C52-C57	107.7(9)	C57-C58-H58A	109.1
N4-C52-C57	110.2(8)	C59-C58-H58B	109.1
C53-C52-C57	111.6(9)	C57-C58-H58B	109.1
C52-C53-C54	113.9(9)	H58A-C58-H58B	107.9
C52-C53-H53A	108.8	C58-C59-C60	109.6(10)
C54-C53-H53A	108.8	C58-C59-H59A	109.7
C52-C53-H53B	108.8	C60-C59-H59A	109.7
C54-C53-H53B	108.8	C58-C59-H59B	109.7
H53A-C53-H53B	107.7	C60-C59-H59B	109.7
C68-C54-C55	112.0(9)	H59A-C59-H59B	108.2
C68-C54-C53	108.5(10)	C61-C60-C59	113.1(11)
C55-C54-C53	108.3(9)	C61-C60-H60A	109.0
C68-C54-H54	109.3	C59-C60-H60A	109.0
C55-C54-H54	109.3	C61-C60-H60B	109.0
C53-C54-H54	109.3	C59-C60-H60B	109.0
C56-C55-C54	112.3(9)	H60A-C60-H60B	107.8
C56-C55-H55A	109.2	C60-C61-C52	113.4(11)
C54-C55-H55A	109.2	C60-C61-H61A	108.9
C56-C55-H55B	109.2	C52-C61-H61A	108.9
C54-C55-H55B	109.2	C60-C61-H61B	108.9
H55A-C55-H55B	107.9	C52-C61-H61B	108.9
C55-C56-N4	111.3(10)	H61A-C61-H61B	107.7
C55-C56-H56A	109.4	C63-C62-C67	116.7(11)
N4-C56-H56A	109.4	C63-C62-C57	121.4(10)
C55-C56-H56B	109.4	C67-C62-C57	121.9(10)
N4-C56-H56B	109.4	C64-C63-C62	120.3(12)
H56A-C56-H56B	108.0	C64-C63-H63	119.9
C62-C57-C58	113.8(10)	C62-C63-H63	119.9
C62-C57-C52	115.5(9)	C63-C64-C65	122.9(13)
C58-C57-C52	110.1(9)	C63-C64-H64	118.5
C62-C57-H57	105.5	C65-C64-H64	118.5
C58-C57-H57	105.5	C66-C65-C64	115.2(13)

C66-C65-H65	122.4	C22-N2-H2C	109.1
C64-C65-H65	122.4		
Table 7.10 continued:		C18-N2-H2C	109.1
C67-C66-C65	124.4(13)	C22-N2-H2D	109.1
C67-C66-H66	117.8	C18-N2-H2D	109.1
C65-C66-H66	117.8	H2C-N2-H2D	107.8
C66-C67-C62	120.6(12)	C35-N3-C39	117.2(9)
C66-C67-H67	119.7	C35-N3-H3A	108.0
C62-C67-H67	119.7	C39-N3-H3A	108.0
O4A-C68-C54	118.8(12)	C35-N3-H3B	108.0
O4-C68-C54	112.9(11)	C39-N3-H3B	108.0
O4-C68-H68A	108.7	H3A-N3-H3B	107.2
C54-C68-H68A	107.9	C56-N4-C52	113.2(8)
O4-C68-H68B	109.5	C56-N4-H4C	108.9
C54-C68-H68B	109.6	C52-N4-H4C	108.9
H68A-C68-H68B	108.1	C56-N4-H4D	108.9
O4A-C68-H68C	106.7	C52-N4-H4D	108.9
C54-C68-H68C	106.5	H4C-N4-H4D	107.8
O4A-C68-H68D	108.3	C17-O1-H1	109.5
C54-C68-H68D	108.6	C17-O1A-H17B	45.5
H68C-C68-H68D	107.4	C17-O1A-H1A1	109.5
C5-N1-C1	113.3(9)	H17B-O1A-H1A1	105.1
C5-N1-H1A	108.9	C34-O2-H2	109.5
C1-N1-H1A	108.9	C34-O2A-H2A1	109.5
C5-N1-H1B	108.9	C51-O3-H3C	109.5
C1-N1-H1B	108.9	C51-O3A-H3A1	109.5
H1A-N1-H1B	107.7	C68-O4-H4	109.5
C22-N2-C18	112.6(8)	C68-O4A-H4A1	109.5

Table 7.11. Anisotropic displacement parameters ($Å^2 x\ 10^3$) for **4.66**. The anisotropic displacement factor exponent takes the form: $-2\pi^2[h^2a^{*2}U^{11} + ... + 2\ h\ k\ a^*\ b^*\ U^{12}]$

	U^{11}	U^{22}	U^{33}	U^{23}	U^{13}	U^{12}
C1	21(5)	24(6)	27(6)	8(5)	9(5)	-3(5)
C2	17(5)	28(6)	32(6)	12(5)	2(5)	1(5)
C3	24(5)	30(6)	30(7)	15(5)	5(5)	6(5)
C4	39(6)	40(7)	23(7)	10(5)	11(5)	-4(5)
C5	29(6)	45(7)	38(7)	9(6)	6(5)	-1(5)
C6	28(6)	32(6)	34(7)	17(5)	9(5)	6(5)
C7	33(6)	50(7)	34(7)	21(6)	6(5)	-5(5)
C8	44(7)	51(7)	56(8)	28(6)	11(6)	0(6)
C9	22(6)	51(7)	49(8)	7(6)	7(6)	-9(5)
C10	32(6)	32(6)	32(7)	13(5)	-1(5)	12(5)
C11	27(6)	31(6)	17(6)	9(5)	8(5)	8(5)
C12	36(6)	33(6)	24(6)	4(5)	6(5)	4(5)
C13	26(6)	58(8)	37(7)	21(6)	-8(5)	13(6)
C14	40(7)	49(7)	18(6)	5(6)	-3(5)	-10(6)
C15	54(7)	34(7)	28(7)	-9(5)	10(6)	-5(6)
C16	52(7)	38(7)	21(6)	8(5)	0(6)	16(6)
C17	42(7)	73(8)	64(9)	42(7)	14(6)	20(6)
C18	28(6)	32(6)	35(7)	14(5)	9(5)	-5(5)
C19	20(5)	29(6)	26(6)	14(5)	3(5)	8(5)
C20	24(6)	25(6)	36(7)	9(5)	1(5)	1(5)
C21	35(6)	21(6)	29(7)	7(5)	-6(5)	-14(5)
C22	35(6)	33(6)	22(6)	14(5)	3(5)	-7(5)
C23	27(6)	28(6)	17(6)	7(5)	5(5)	-3(5)
C24	40(6)	45(7)	26(7)	12(5)	11(5)	2(6)
C25	38(6)	37(7)	51(8)	11(6)	12(6)	6(5)
C26	44(6)	32(6)	35(7)	12(5)	6(6)	-1(5)
C27	37(6)	28(6)	26(6)	9(5)	-5(5)	-9(5)
C28	37(6)	33(6)	17(6)	2(5)	10(5)	1(5)

Table 7.11 continued:

C29	32(6)	44(7)	33(7)	12(6)	13(5)	5(5)
C30	42(6)	34(6)	19(6)	13(5)	0(5)	-2(5)
C31	46(7)	49(7)	33(7)	10(6)	6(6)	6(6)
C32	38(6)	47(7)	30(7)	14(6)	-2(5)	-8(5)
C33	34(6)	34(6)	20(6)	6(5)	-1(5)	-3(5)
C34	44(7)	34(7)	45(8)	-1(6)	9(6)	-6(6)
C35	15(5)	22(6)	28(6)	5(5)	10(5)	9(4)
C36	37(6)	41(7)	34(7)	15(5)	0(5)	21(6)
C37	48(7)	34(7)	24(7)	0(5)	-4(5)	11(6)
C38	56(7)	45(7)	36(7)	15(6)	-5(6)	17(6)
C39	49(7)	48(7)	35(7)	15(6)	-10(6)	4(6)
C40	24(5)	29(6)	35(7)	16(5)	-2(5)	-2(5)
C41	35(6)	28(6)	35(7)	12(5)	2(5)	-2(5)
C42	42(6)	43(7)	50(8)	22(6)	-6(6)	-7(6)
C43	26(6)	47(7)	36(7)	18(6)	8(5)	2(5)
C44	30(6)	51(7)	34(7)	18(6)	3(5)	4(6)
C45	27(6)	26(6)	17(6)	3(5)	5(5)	7(5)
C46	39(6)	45(7)	37(7)	17(6)	6(6)	6(6)
C47	52(7)	48(7)	36(7)	15(6)	10(6)	-11(6)
C48	50(7)	46(7)	32(7)	9(6)	9(6)	-13(6)
C49	50(7)	51(7)	33(7)	1(6)	12(6)	13(6)
C50	41(6)	45(7)	36(7)	14(6)	2(6)	-5(6)
C51	56(7)	33(7)	55(8)	-4(6)	-6(7)	13(6)
C52	31(6)	28(6)	36(7)	4(5)	1(5)	-6(5)
C53	34(6)	28(6)	34(7)	16(5)	-2(5)	-7(5)
C54	33(6)	40(7)	38(7)	11(6)	11(5)	6(5)
C55	44(7)	54(7)	37(7)	18(6)	1(6)	5(6)
C56	25(6)	54(7)	37(7)	10(6)	2(5)	-11(6)
C57	29(6)	27(6)	26(7)	1(5)	-8(5)	-7(5)
C58	28(6)	29(6)	33(7)	1(5)	-3(5)	14(5)
C59	38(6)	37(7)	52(8)	12(6)	-7(6)	0(5)
C60	30(6)	50(7)	54(8)	6(6)	18(6)	5(6)
C61	48(7)	49(7)	35(7)	13(6)	13(6)	18(6)
C62	32(6)	31(6)	26(6)	8(5)	-3(5)	4(5)
C63	41(7)	42(7)	20(6)	1(5)	-2(5)	3(6)

Table 7.11 continued:

C64	68(8)	47(7)	35(7)	12(6)	-5(6)	17(7)
C65	45(7)	56(8)	39(7)	17(6)	2(6)	23(6)
C66	47(7)	46(7)	39(7)	18(6)	8(6)	18(6)
C67	41(6)	39(7)	37(7)	24(6)	10(6)	14(6)
C68	66(8)	78(9)	66(9)	50(7)	0(7)	-17(7)
N1	21(5)	25(5)	31(6)	7(4)	-1(4)	-14(4)
N2	24(5)	16(5)	31(6)	7(4)	10(4)	-9(4)
N3	35(5)	25(5)	28(6)	3(4)	9(4)	3(4)
N4	11(4)	26(5)	25(5)	4(4)	0(4)	8(4)
O1	54(7)	37(7)	59(8)	38(6)	9(6)	22(6)
O1A	51(15)	45(15)	40(16)	10(13)	12(13)	17(13)
O2	67(7)	29(6)	30(7)	7(5)	6(5)	-1(5)
O2A	67(7)	29(6)	30(7)	7(5)	6(5)	-1(5)
O1W	76(6)	77(6)	50(6)	21(5)	17(6)	-15(6)
O3	54(10)	23(8)	53(11)	17(8)	23(9)	4(8)
O3A	61(10)	47(10)	25(10)	14(8)	-5(8)	13(8)
O4	61(11)	77(12)	70(13)	47(10)	-15(10)	-42(10)
O4A	48(10)	48(10)	41(11)	2(8)	9(9)	2(8)
Cl4	28(2)	35(2)	54(2)	17(2)	12(2)	6(1)
Cl3	25(2)	26(2)	71(2)	18(2)	8(2)	1(1)
Cl1	30(2)	44(2)	106(3)	43(2)	2(2)	-4(2)
Cl2	26(2)	36(2)	72(3)	19(2)	1(2)	2(1)

Table 7.12. Hydrogen coordinates (x 10^4) and isotropic displacement parameters (Å^{2}x 10^3) for **4.66**.

	x	y	z	U(eq)
H2A	9281	4131	2836	30
H2B	8075	4438	2794	30
H3	9713	5087	4227	32
H4A	8490	5965	4916	40
H4B	7558	5576	4158	40
H5A	8071	7009	4188	46
H5B	9306	6778	4239	46
H6	9460	4598	1628	35
H7A	9352	5634	895	45
H7B	8976	6390	1647	45
H8A	10744	6694	1661	57
H8B	11033	5686	1607	57
H9A	11527	6596	2975	52
H9B	10377	7016	3000	52
H10A	10476	5932	3671	38
H10B	10788	5185	2883	38
H12	7199	5964	1488	38
H13	5501	5370	808	48
H14	5163	3818	263	46
H15	6506	2865	485	51
H16	8162	3432	1153	45
H17A	8051	3760	3765	65
H17B	8282	4296	4692	65
H17C	8974	3604	3923	65
H17D	7846	3973	3978	65
H19A	5587	4886	7101	29
H19B	6805	5217	7195	29

Table 7.12 continued:

H20	5294	4813	5730	35
H21A	6648	5120	5095	36
H21B	7491	5325	5912	36
H22A	6997	6705	5760	35
H22B	5754	6431	5677	35
H23	5343	6313	8287	29
H24A	5566	7862	8966	43
H24B	6003	8003	8202	43
H25A	4226	8336	8146	50
H25B	3902	7376	8202	50
H26A	3485	7302	6823	44
H26B	4675	7651	6826	44
H27A	4529	6087	6196	38
H27B	4087	5950	6958	38
H29	6475	5467	8858	43
H30	8073	5357	9677	37
H31	9543	6278	9811	52
H32	9403	7435	9216	47
H33	7740	7645	8517	37
H34A	5900	3528	6014	53
H34B	7077	3851	6080	53
H34C	6750	3774	6289	53
H34D	6832	3721	5400	53
H36A	5965	-185	2841	45
H36B	4785	131	2961	45
H37	5118	188	4334	46
H38A	7248	-318	4050	56
H38B	6816	-143	4897	56
H39A	6879	-1698	4168	54
H39B	5703	-1426	4359	54
H40	3988	-1253	1804	34
H41A	3940	-2809	1065	39
H41B	4733	-2971	1800	39
H42A	2962	-3289	1946	54
H42B	2615	-2319	1910	54

Table 7.12 continued:

H43A	2926	-2248	3322	42
H43B	4108	-2593	3234	42
H44A	4132	-1034	3845	45
H44B	3390	-956	3054	45
H46	4876	-340	1262	47
H47	6123	-94	508	53
H48	7479	-1095	232	52
H49	7499	-2396	600	57
H50	6265	-2593	1417	49
H51A	6269	1246	3746	65
H51B	6707	1320	4641	65
H51C	5479	1480	4079	65
H51D	6598	1179	3885	65
H53A	10185	876	7337	37
H53B	8985	538	7307	37
H54	10160	-49	5947	44
H55A	7968	-509	5965	54
H55B	8586	-884	5199	54
H56A	9670	-1712	5856	48
H56B	8449	-1965	5865	48
H57	10829	318	8560	36
H58A	10723	-767	9226	40
H58B	10082	-1455	8403	40
H59A	11863	-1808	8493	54
H59B	12235	-791	8612	54
H60A	12249	-1658	7235	55
H60B	11047	-2031	7144	55
H61A	11069	-956	6526	52
H61B	11693	-246	7342	52
H63	9817	1600	9003	45
H64	8428	2240	9635	62
H65	6953	1358	9723	56
H66	7027	-192	9189	52
H67	8393	-867	8580	43
H68A	8771	1302	6411	77

Table 7.12 continued:

H68B	8512	737	5493	77
H68C	8414	1057	6172	77
H68D	9569	1424	6237	77
H1A	8618	6673	2926	32
H1B	7757	6025	2883	32
H2C	6404	7317	7010	28
H2D	7233	6684	7089	28
H3A	6401	-1646	2892	36
H3B	5642	-2269	3025	36
H4C	9454	-1686	7150	27
H4D	8615	-1034	7204	27
H1	9216	3126	4378	67
H1A1	8523	3690	5030	68
H2	6538	2866	4947	65
H2A1	5705	2717	5420	65
H3C	5522	2289	4591	61
H3A1	7066	1408	5135	67
H4	10341	1584	6204	100
H4A1	8630	1360	5141	72

Table 7.13. Torsion angles [°] for **4.66**.

N1-C1-C2-C3	-57.6(10)	C14-C15-C16-C11	-0.1(19)
C10-C1-C2-C3	63.5(11)	C12-C11-C16-C15	2.1(17)
C6-C1-C2-C3	-178.1(8)	C6-C11-C16-C15	-178.6(11)
C1-C2-C3-C4	54.5(11)	C4-C3-C17-O1A	-65.5(17)
C1-C2-C3-C17	179.6(8)	C2-C3-C17-O1A	172.3(16)
C17-C3-C4-C5	-171.4(9)	C4-C3-C17-O1	-149.4(11)
C2-C3-C4-C5	-51.1(12)	C2-C3-C17-O1	88.3(12)
C3-C4-C5-N1	52.3(13)	C23-C18-C19-C20	-175.7(9)
N1-C1-C6-C11	-61.9(11)	N2-C18-C19-C20	-57.2(11)
C2-C1-C6-C11	56.1(12)	C27-C18-C19-C20	60.4(12)
C10-C1-C6-C11	176.2(9)	C18-C19-C20-C21	55.6(12)
N1-C1-C6-C7	67.9(10)	C18-C19-C20-C34	-179.7(8)
C2-C1-C6-C7	-174.0(8)	C34-C20-C21-C22	-176.0(9)
C10-C1-C6-C7	-54.0(11)	C19-C20-C21-C22	-52.7(12)
C11-C6-C7-C8	-173.8(10)	C20-C21-C22-N2	55.2(11)
C1-C6-C7-C8	54.9(13)	C19-C18-C23-C28	49.3(12)
C6-C7-C8-C9	-52.8(14)	N2-C18-C23-C28	-67.9(11)
C7-C8-C9-C10	52.4(14)	C27-C18-C23-C28	175.7(9)
C8-C9-C10-C1	-57.0(13)	C19-C18-C23-C24	-177.9(8)
N1-C1-C10-C9	-64.4(12)	N2-C18-C23-C24	64.9(11)
C2-C1-C10-C9	176.8(10)	C27-C18-C23-C24	-51.4(11)
C6-C1-C10-C9	57.6(12)	C28-C23-C24-C25	-170.6(10)
C7-C6-C11-C16	134.1(11)	C18-C23-C24-C25	55.5(12)
C1-C6-C11-C16	-97.5(13)	C23-C24-C25-C26	-55.7(13)
C7-C6-C11-C12	-46.6(14)	C24-C25-C26-C27	54.8(13)
C1-C6-C11-C12	81.8(13)	C25-C26-C27-C18	-54.6(12)
C16-C11-C12-C13	-1.9(16)	C19-C18-C27-C26	-179.7(9)
C6-C11-C12-C13	178.8(11)	C23-C18-C27-C26	52.9(12)
C11-C12-C13-C14	-0.3(18)	N2-C18-C27-C26	-63.4(12)
C12-C13-C14-C15	2.3(18)	C24-C23-C28-C29	131.4(11)
C13-C14-C15-C16	-2.2(19)	C18-C23-C28-C29	-95.9(13)

Table 7.13 continued:

C24-C23-C28-C33	-46.2(14)	C40-C35-C44-C43	60.9(12)
C18-C23-C28-C33	86.5(12)	C41-C40-C45-C50	-44.4(14)
C33-C28-C29-C30	0.3(18)	C35-C40-C45-C50	84.8(13)
C23-C28-C29-C30	-177.3(10)	C41-C40-C45-C46	136.9(10)
C28-C29-C30-C31	-3.6(18)	C35-C40-C45-C46	-93.8(12)
C29-C30-C31-C32	3.0(18)	C50-C45-C46-C47	-0.4(17)
C30-C31-C32-C33	0.7(19)	C40-C45-C46-C47	178.3(10)
C31-C32-C33-C28	-4.0(18)	C45-C46-C47-C48	-0.3(18)
C29-C28-C33-C32	3.4(17)	C46-C47-C48-C49	2.7(19)
C23-C28-C33-C32	-178.9(10)	C47-C48-C49-C50	-4.2(19)
C21-C20-C34-O2	-57.9(13)	C46-C45-C50-C49	-1.2(16)
C19-C20-C34-O2	178.9(10)	C40-C45-C50-C49	-179.8(10)
C21-C20-C34-O2A	-136.1(15)	C48-C49-C50-C45	3.4(18)
C19-C20-C34-O2A	100.7(15)	C36-C37-C51-O3A	-174.8(13)
N3-C35-C36-C37	-57.2(12)	C38-C37-C51-O3A	-53.9(17)
C44-C35-C36-C37	63.2(12)	C36-C37-C51-O3	97.6(13)
C40-C35-C36-C37	-179.3(9)	C38-C37-C51-O3	-141.5(12)
C35-C36-C37-C51	-178.4(9)	C61-C52-C53-C54	59.8(12)
C35-C36-C37-C38	56.5(13)	N4-C52-C53-C54	-58.6(11)
C51-C37-C38-C39	-175.8(11)	C57-C52-C53-C54	-178.2(9)
C36-C37-C38-C39	-53.3(14)	C52-C53-C54-C68	-179.9(9)
C37-C38-C39-N3	52.9(14)	C52-C53-C54-C55	58.4(12)
N3-C35-C40-C45	-64.7(11)	C68-C54-C55-C56	-173.8(11)
C44-C35-C40-C45	174.0(9)	C53-C54-C55-C56	-54.2(13)
C36-C35-C40-C45	53.0(12)	C54-C55-C56-N4	54.9(13)
N3-C35-C40-C41	63.7(11)	C61-C52-C57-C62	173.7(9)
C44-C35-C40-C41	-57.6(11)	N4-C52-C57-C62	-68.5(12)
C36-C35-C40-C41	-178.6(9)	C53-C52-C57-C62	48.3(12)
C45-C40-C41-C42	-171.0(9)	C61-C52-C57-C58	-55.7(11)
C35-C40-C41-C42	58.3(12)	N4-C52-C57-C58	62.1(11)
C40-C41-C42-C43	-55.4(12)	C53-C52-C57-C58	179.0(8)
C41-C42-C43-C44	56.9(12)	C62-C57-C58-C59	-170.3(9)
C42-C43-C44-C35	-61.7(12)	C52-C57-C58-C59	58.2(11)
N3-C35-C44-C43	-61.2(12)	C57-C58-C59-C60	-55.2(12)
C36-C35-C44-C43	-177.8(9)	C58-C59-C60-C61	54.0(13)

Table 7.13 continued:

C59-C60-C61-C52	-56.3(14)	C55-C54-C68-O4	-142.1(13)
N4-C52-C61-C60	-62.9(13)	C53-C54-C68-O4	98.4(14)
C53-C52-C61-C60	-179.7(10)	C4-C5-N1-C1	-56.8(11)
C57-C52-C61-C60	56.1(13)	C2-C1-N1-C5	59.9(10)
C58-C57-C62-C63	135.7(11)	C10-C1-N1-C5	-60.8(11)
C52-C57-C62-C63	-95.5(12)	C6-C1-N1-C5	179.1(8)
C58-C57-C62-C67	-45.2(14)	C21-C22-N2-C18	-58.8(11)
C52-C57-C62-C67	83.6(13)	C19-C18-N2-C22	59.7(11)
C67-C62-C63-C64	2.6(16)	C23-C18-N2-C22	-177.6(8)
C57-C62-C63-C64	-178.2(11)	C27-C18-N2-C22	-61.2(11)
C62-C63-C64-C65	-2.3(19)	C44-C35-N3-C39	-63.0(12)
C63-C64-C65-C66	1.2(18)	C36-C35-N3-C39	57.5(12)
C64-C65-C66-C67	-0.5(18)	C40-C35-N3-C39	179.1(9)
C65-C66-C67-C62	0.9(19)	C38-C39-N3-C35	-57.5(13)
C63-C62-C67-C66	-1.9(16)	C55-C56-N4-C52	-57.3(11)
C57-C62-C67-C66	178.9(11)	C61-C52-N4-C56	-64.9(12)
C55-C54-C68-O4A	-61.3(15)	C53-C52-N4-C56	57.0(11)
C53-C54-C68-O4A	179.2(12)	C57-C52-N4-C56	177.6(9)

Table 7.14. Hydrogen bonds for **4.66** [Å and °].

D-H...A	d(D-H)	d(H...A)	d(D...A)	<(DHA)
N1-H1A...Cl1	0.91	2.25	3.072(9)	149.6
N1-H1B...Cl3#1	0.91	2.35	3.141(8)	144.9
N2-H2C...Cl2	0.91	2.26	3.080(8)	149.1
N2-H2D...Cl4#1	0.91	2.37	3.164(8)	146.0
N3-H3A...Cl1#2	0.91	2.41	3.192(9)	144.1
N3-H3B...Cl3	0.91	2.30	3.123(9)	150.2
N4-H4C...Cl4	0.91	2.26	3.060(8)	146.1
N4-H4D...Cl2#2	0.91	2.38	3.176(8)	145.7
O1-H1...O1W	0.84	2.01	2.805(14)	157.1
O1A-H1A1...O1W	0.84	1.93	2.72(2)	158.1
O2-H2...O1W	0.84	2.59	3.125(14)	122.3
O2-H2...O3	0.84	2.21	2.713(15)	118.5
O2A-H2A1...O3A	0.84	1.96	2.77(2)	160.4
O3-H3C...O2	0.84	1.90	2.713(15)	163.3
O3A-H3A1...O4A	0.84	2.43	3.23(2)	159.7
O4-H4...Cl1#3	0.84	2.23	3.068(17)	173.3

Symmetry transformations used to generate equivalent atoms:

#1 x,y+1,z #2 x,y-1,z #3 -x+2,-y+1,-z+1

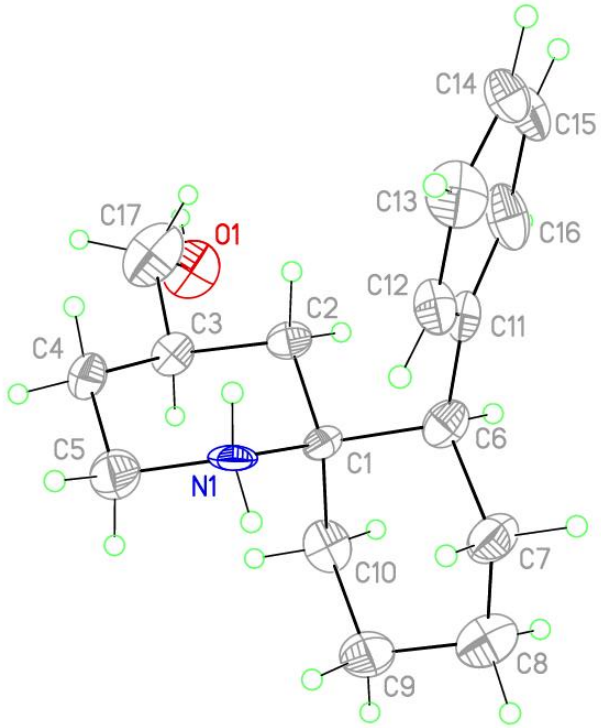

Figure 7.2. View of cation 1 of **4.66** showing the atom labeling scheme. Displacement ellipsoids are scaled to the 50% probability level. The lower occupancy atoms of the disordered hydroxyl group are not shown.

7.3. THE TOTAL SYNTHESIS OF EXOTINES A AND B

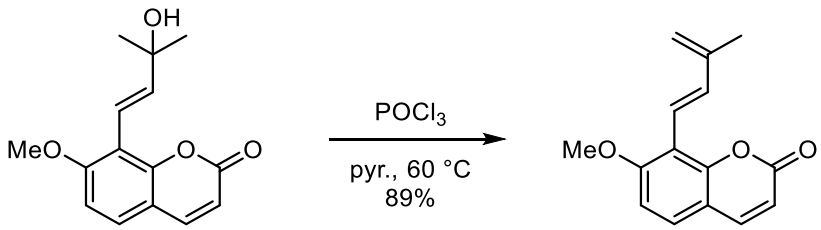

7.11 **6.32**

***trans*-Dehydroosthol (6.32) (LTL-V-211).** To a stirred solution of alcohol **7.11**[243] (1.31 g, 5 mmol) in pyridine (25 mL) was added $POCl_3$ (2.3 mL, 25 mmol). The flask was submerged in an oil bath pre-heated to 60 ˚C and stirred for 1 h, whereupon the reaction was cooled to room temperature and diluted with H_2O (25 mL). The aqueous mixture was extracted with Et_2O (3 x 25 mL), and the combined organic extracts were washed sequentially with sat. $CuSO_4$ (20 mL), 1 M HCl (20 mL), sat. $NaHCO_3$ (20 mL), and brine (20 mL). The organic phase was dried ($MgSO_4$) and concentrated via rotary evaporation to afford **3** (1.08 g, 89%) as a tan solid which was used without further purification. The ^1H NMR spectra of **6.32** thus obtained is consistent with the reported literature spectra.[243]

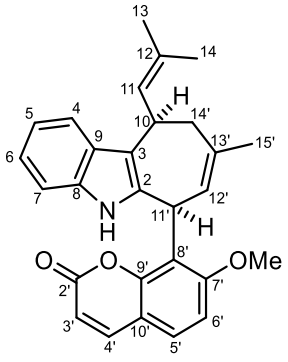

exotine A (**6.1**)

(±)-Exotine A (6.1) (LTL-V-257). Indole (**6.6**, 70 mg, 0.6 mmol), prenal (**10**, 38 mg, 0.45 mmol), and *trans*-dehydroosthol (**6.32**, 36 mg, 0.15 mmol) were dissolved in CH_2Cl_2 (1.5

mL) and cooled to 0 ˚C, whereupon *p*-TsOH (29 mg, 0.15 mmol) was added. The solution was stirred for 24 h, whereupon CH_2Cl_2 (15 mL) was added, and the solution was washed with saturated aq. $NaHCO_3$ (30 mL). The organic layer was separated, and the aqueous layer was extracted with CH_2Cl_2 (2 x 15 mL). The combined organic extracts were dried ($MgSO_4$) and concentrated under reduced pressure. The residue was purified via flash column chromatography, eluting with EtOAc/hexanes (20 : 80) to afford 26 mg (43%) of a mixture of (±)-exotine A (**6.1**) and *trans*-diastereomer **6.42** in a 17 : 1 ratio as an amorphous yellow-orange solid. A sample of pure (±)-exotine A (**6.1**) was obtained via reverse-phase HPLC, eluting with MeCN : H_2O (35 : 65 → 50 : 50, 90 min) and recrystallized (MeOH-$CHCl_3$) to afford pure (±)-exotine A as pale yellow needles, mp 246–247 ˚C (lit.[184] mp 249–250 °C).

^{1}H NMR (500 MHz, $CDCl_3$) δ 7.70 (d, *J* = 9.5 Hz, 1 H), 7.50 (d, *J* = 8.6 Hz, 1 H), 7.37 – 7.34 (m, 1 H), 7.07 – 7.03 (comp, 2 H), 7.02 – 6.99 (comp, 2 H), 6.96 (d, *J* = 8.6 Hz, 1 H), 6.29 (d, *J* = 9.5 Hz, 1 H), 6.00 (s, 1 H), 5.54 – 5.49 (m, 1 H), 5.46 (d, *J* = 10.0 Hz, 1 H), 4.16 – 4.09 (m, 1 H), 3.76 (s, 3 H), 3.16 (d, *J* = 13.1 Hz, 1 H), 2.25 (dd, *J* = 13.2, 5.1 Hz, 1 H), 1.96 (s, 3 H), 1.83 (s, 3 H), 1.74 (s, 3 H); ^{13}C NMR (126 MHz, $CDCl_3$) δ 161.2, 160.6, 153.1, 143.6, 137.5, 133.7, 132.6, 129.6, 129.0, 128.9, 128.3, 126.6, 120.6, 118.8, 118.4, 118.1, 114.8, 113.6, 113.2, 109.9, 108.4, 56.4, 37.7, 33.0, 32.8, 27.4, 25.9, 18.1; IR (neat) ν_{max} 3462, 2932, 1721, 1606, 1460, 1273, 1249, 1121, 1092 cm^{-1}; HRMS (ESI) *m/z* calcd for $C_{28}H_{27}NO_3$ (M+H)+ 426.2064; found, 426.2062.

Table 7.15. Tabulated ^{1}H and ^{13}C NMR data for natural and synthetic **6.1**.[184]

	^{1}H NMR (δ in ppm, multiplicity, *J* in Hz)		^{13}C NMR (δ in ppm)	
Position	**Natural (400 MHz)**	**Synthetic (500 MHz)**	**Natural (100 MHz)**	**Synthetic (126 MHz)**
2			132.5	132.6
3			114.8	114.8
4	7.36 (m)	7.37 - 7.34 (m)	118.1	118.1
5	7.00 (m)	7.02 - 6.99 (comp)	118.8	118.8
6	7.00 (m)	7.02 - 6.99 (comp)	120.6	120.6
7	7.04 (m)	7.07 - 7.03 (comp)	109.9	109.9
8			133.7	133.7
9			129.6	129.6
10	4.12 (m)	4.16 - 4.09 (m)	33.0	33.0
11	5.47 (d, 9.8)	5.46 (d, 10.0)	128.9	128.9
12			129.0	129.0
13	1.74 (s)	1.74 (s)	25.8	25.9
14	1.96 (s)	1.96 (s)	18.1	18.1
2'			160.5	160.6
3'	6.28 (d, 9.5)	6.29 (d, 9.5)	113.6	113.6
4'	7.69 (d, 9.5)	7.70 (d, 9.5)	143.6	143.6
5'	7.49 (d, 8.7)	7.50 (d, 8.6)	128.2	128.3
6'	6.95 (d, 8.7)	6.96 (d, 8.6)	108.4	108.4
7'			161.2	161.2
8'			118.5	118.4
9'			153.1	153.1
10'			113.2	113.2
11'	6.01 (s)	6.00 (s)	32.8	32.8
12'	5.51 (dd, 1.6, 3.2)	5.54 - 5.49 (m)	126.6	126.6
13'			137.4	137.5
14'a	3.16 (d, 13.1)	3.16 (d, 13.1)	37.7	37.7
14'b	2.25 (dd, 4.9, 13.1)	2.25 (dd, 5.1, 13.2)		
15'	1.83 (s)	1.83 (s)	27.3	27.4
7'-OCH_3	3.76 (s)	3.76 (s)	56.3	56.4
N-H	7.01 (br s)	7.07 - 7.03 (comp)		

Basis for assignment of the structure of 6.42 as being 11'-*epi*-6.1:

Although we isolated pure **6.1** via preparative HPLC, attempts to isolate a pure sample of **6.42** have not been successful, and mixtures of **6.1** and **6.42** were invariably obtained. Despite our inability to fully characterize a pure sample of **6.42**, analysis of the ^{1}H NMR and COSY spectra of a mixture (3:1) of **6.1**:**6.42** supports our assignment of **6.42** being the 11'-epimer of **6.1**, not a double bond isomer.

^{1}H NMR spectrum of mixture (3:1) of **6.1** and **6.42**:

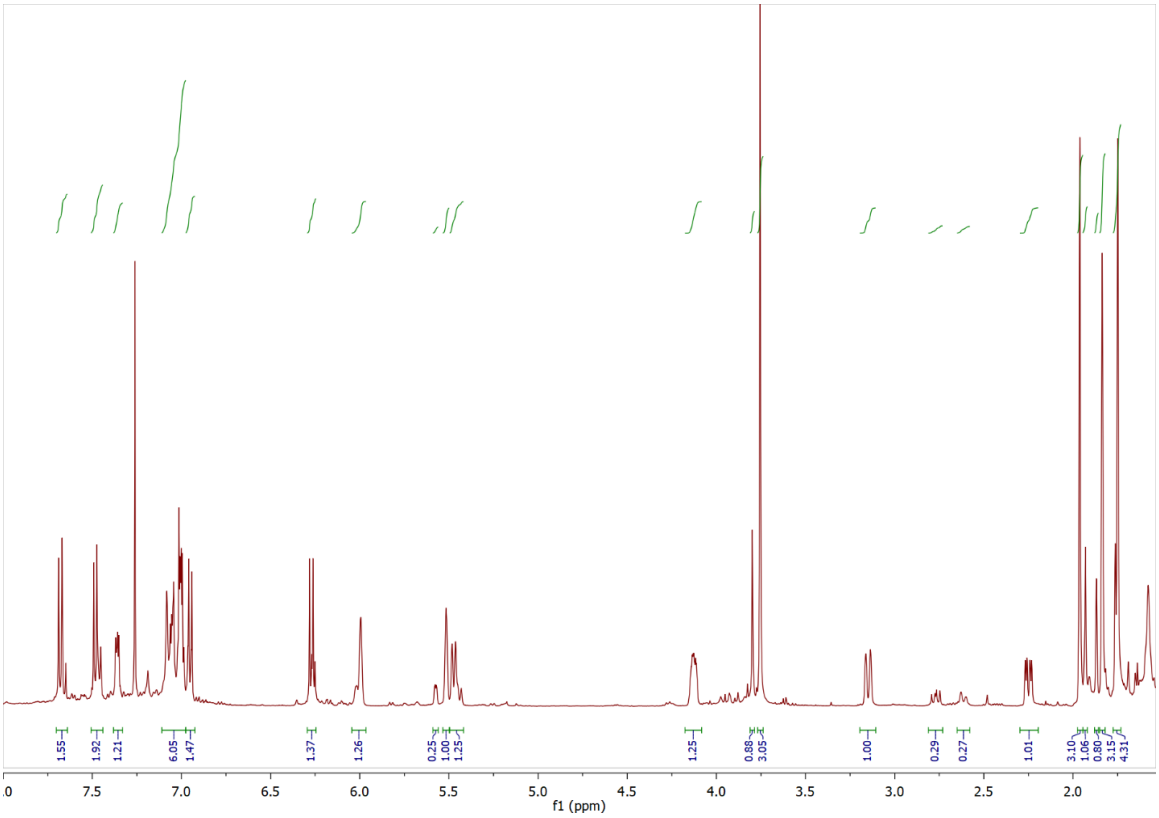

Expanded ^{1}H NMR spectrum with key peak assignments:

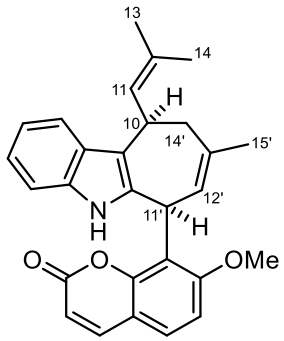

6.1

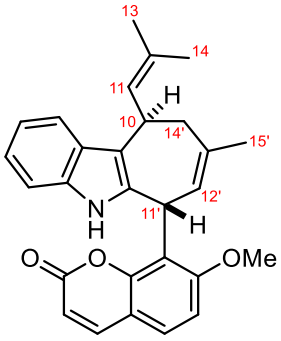

6.42

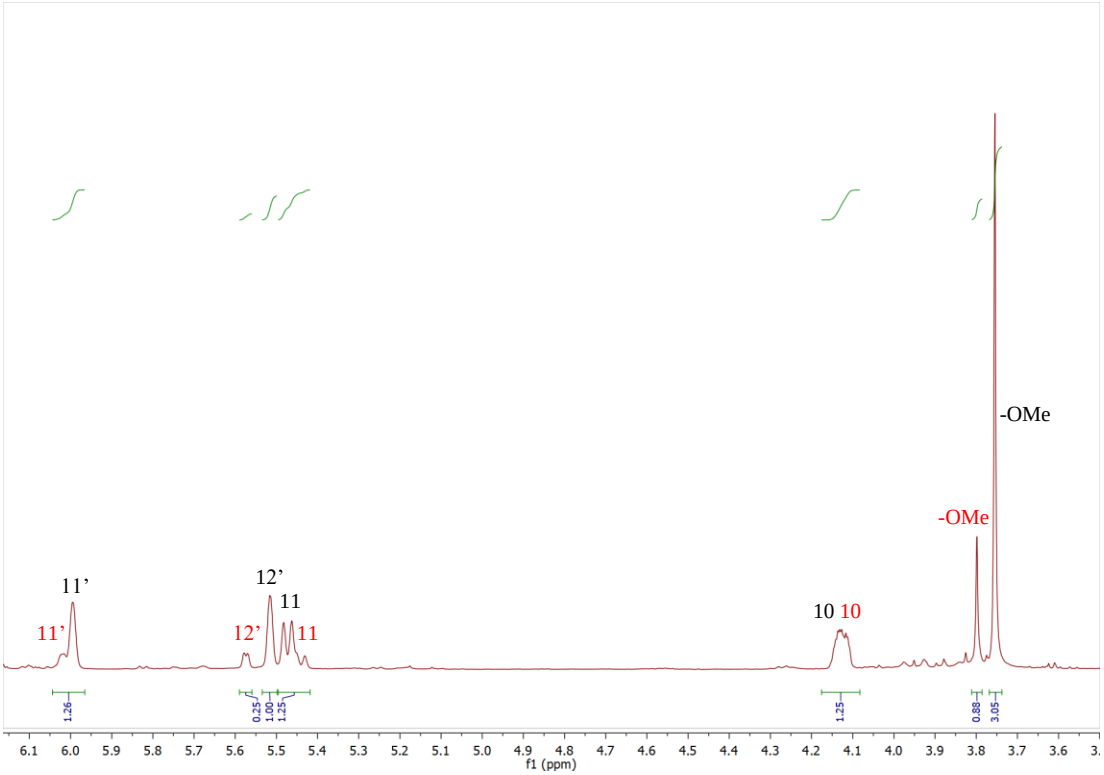

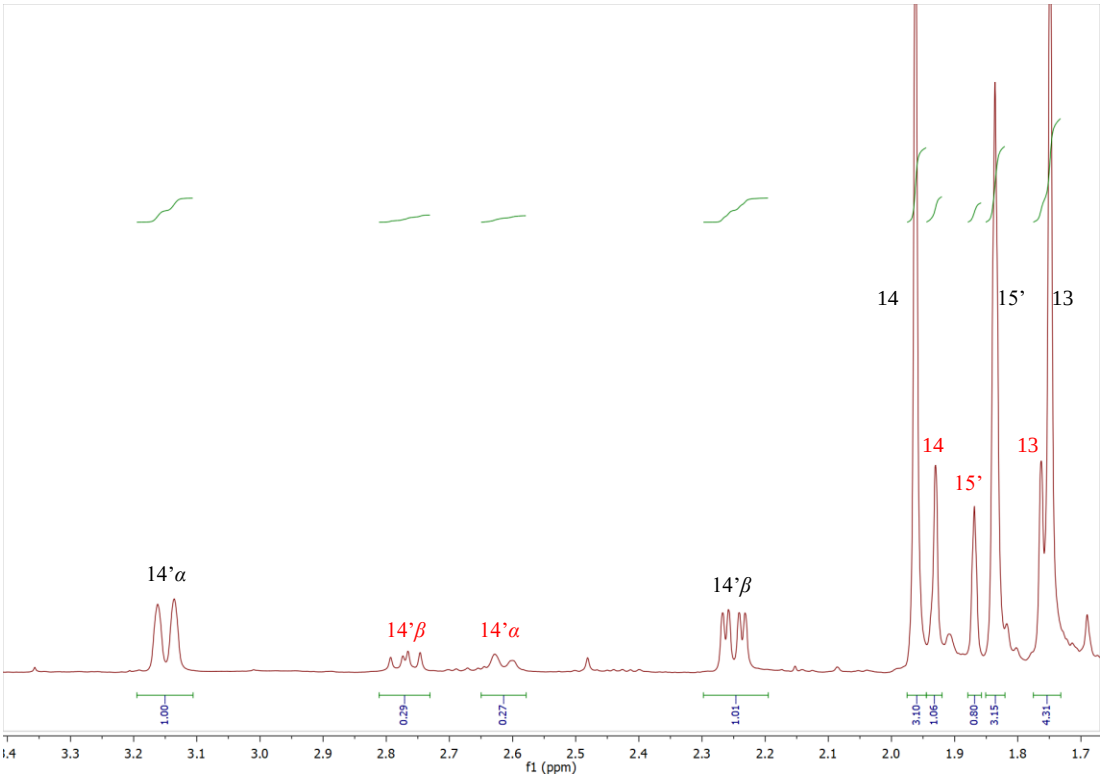

The presence of three methyl singlets belonging to **6.42** in the 1.7 – 2.0 ppm region rules out the possibility of **6.42** being a terminal olefin isomer such as **7.12** or **7.13**, or an isomer that brings either olefin in conjugation with the aromatic moieties such as **7.14** or **7.15**.

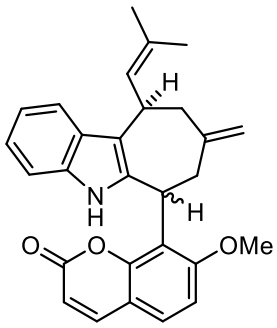

7.12

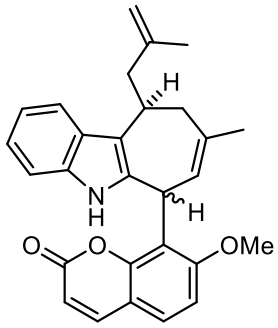

7.13

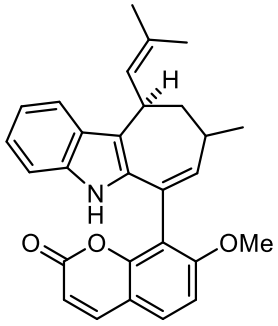

7.14

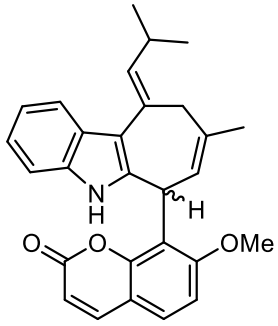

7.15

Table 7.16. Comparison of diagnostic peaks of **6.1** and **6.42**

	^{1}H NMR (d **in ppm, multiplicity, *J* in Hz)**	
Position	**1**	**15**
10	4.16 - 4.09 (m)	4.16 - 4.09 (m)
11	5.46 (d, 10.0)	5.44 (comp)
13	1.74 (s)	1.76 (s)
14	1.96 (s)	1.93 (s)
11'	6.00 (s)	6.02 (s)
12'	5.54 - 5.49 (m)	5.59 - 5.56 (m)
14'a	3.16 (d, 13.1)	2.62 (d, 12.6)
14'b	2.25 (dd, 5.1, 13.2)	2.77 (dd, 9.6, 13.8)
15'	1.83 (s)	1.87 (s)
7'-OCH_3	3.76 (s)	3.80 (s)

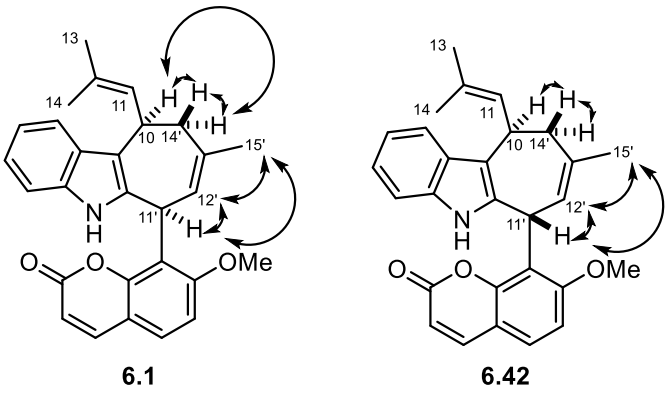

Figure 7.3. Key COSY correlations of **6.1** and **6.42** that support the assignments in Table 7.2.

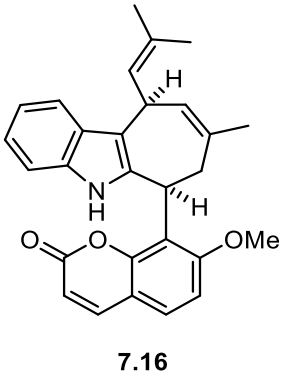

The presence of COSY correlations in both **6.1** and **6.42** between H10 and H14'α/H14'β, and between H11' and H12'/H15' exclude the possibility that **6.42** is isomer **7.16**. Based on these observations, we conclude that the identity of **6.42** is 11'-*epi*-**6.1**.

Deuterium incorporation experiment (LTL-V-275):

A mixture (10:1) of **6.1** and **6.42** (10 mg, 0.02 mmol) was dissolved in CD_2Cl_2 (0.8 mL) at 0 °C, CF_3CO_2D (12 mg, 0.1 mmol) was added, the mixture was stirred briefly and then stored at 0 ˚C for 5 h. CH_2Cl_2 (10 mL) was added, and the resultant solution was washed with saturated $NaHCO_3$ (20 mL). The organic layer was separated, and the aqueous layer was extracted with CH_2Cl_2 (2 x 10 mL). The combined organic extracts were dried ($MgSO_4$) and concentrated under reduced pressure. The residue was purified via flash column chromatography, eluting with EtOAc/hexanes (20 : 80) to afford 5 mg of an epimeric mixture (1.6:1) containing a mixture (1:4,

80% deuterium incorporation at C11') of the isotopomeric pairs **6.1** and **6.42** and **6.1**(11'-d_1) and **6.42**(11'-d_1).

^{1}H NMR spectrum of mixture of **6.1**, **6.42**, **6.1**(11'-d_1) and **6.42**(11'-d_1) in $CDCl_3$ showing residual proton at C11' centered at δ 6.0:

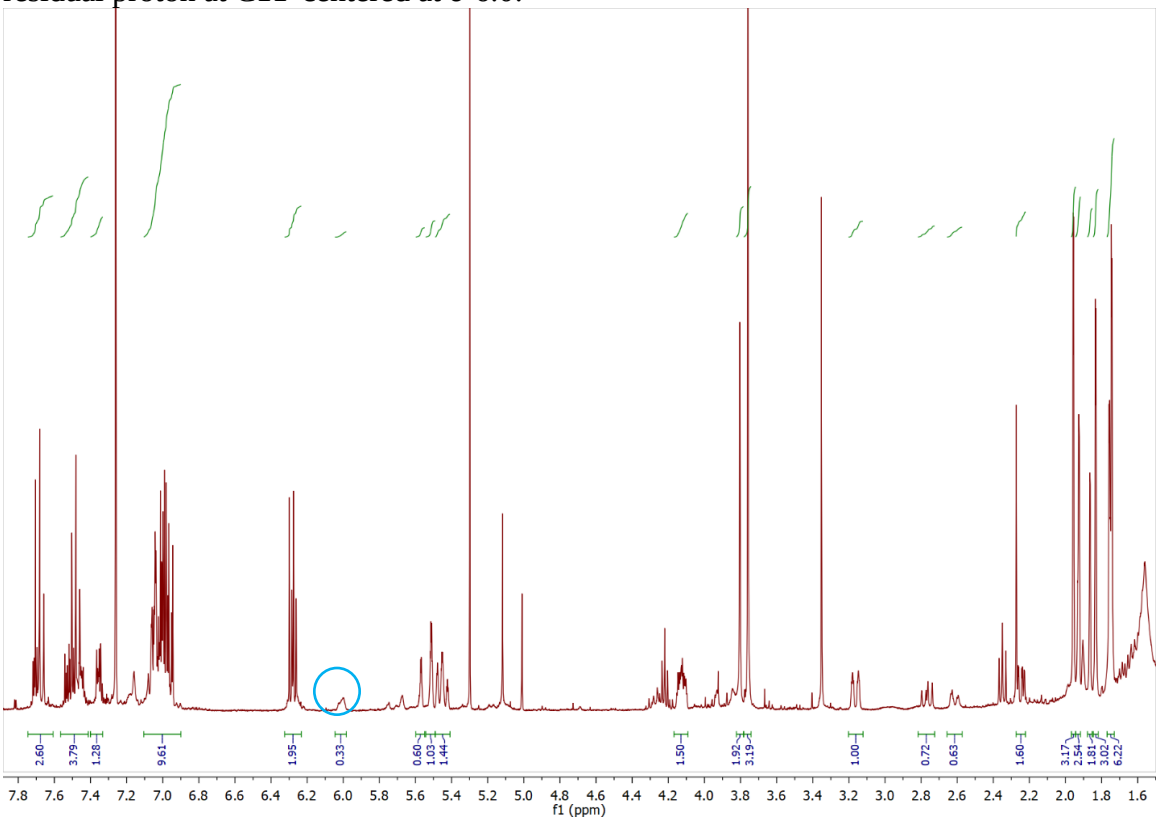

(±)-Exotine B (6.2) (LTL-V-298). Indole (**6.6**, 47 mg, 0.4 mmol), prenal (**6.7**, 25 mg, 0.3 mmol), and gleinadiene (**6.43**, 27 mg, 0.1 mmol) were dissolved in CH_2Cl_2 (1 mL) and cooled to 0 ˚C, whereupon *p*-TsOH·H_2O (19 mg, 0.1 mmol) was added. The solution was stirred for 24 h, whereupon CH_2Cl_2 (15 mL) was added, and the solution was washed with saturated aq. $NaHCO_3$ (30 mL). The organic layer was separated, and the aqueous layer was extracted with CH_2Cl_2 (2 x 15 mL). The combined organic extracts were dried ($MgSO_4$) and concentrated under reduced pressure. The residue was purified via flash column chromatography, eluting with

EtOAc/hexanes (15 : 85) to afford 23 mg (50%) of a mixture (4:1) of (±)-exotine B and *epi*-exotine B as an amorphous pale yellow solid. A sample of pure (±)-exotine B (**6.2**) was obtained via reverse-phase HPLC, eluting with MeCN : H_2O (50 : 50 → 60 : 40, 60 min). ^{1}H NMR (500 MHz, $CDCl_3$) δ 8.06 (d, *J* = 9.6 Hz, 1 H), 7.37 – 7.32 (m, 1 H), 7.09 (s, 1 H), 7.07 – 7.03 (m, 1 H), 7.03 – 6.97 (comp, 2 H), 6.42 (s, 1 H), 6.19 (d, *J* = 9.7 Hz, 1 H), 5.89 (d, *J* = 2.9 Hz, 1 H), 5.51 (dq, *J* = 3.3, 1.6 Hz, 1 H), 5.44 (ddd, *J* = 10.0, 2.8, 1.4 Hz, 1 H), 4.11 (ddt, *J* = 9.9, 5.0, 2.7 Hz, 1 H), 4.00 (s, 3 H), 3.76 (s, 3 H), 3.15 (d, *J* = 13.1 Hz, 1 H), 2.23 (ddd, *J* = 13.2, 4.9, 1.4 Hz, 1 H), 1.95 (d, *J* = 1.4 Hz, 3 H), 1.82 (t, *J* = 1.9 Hz, 3 H), 1.74 (d, *J* = 1.4 Hz, 3 H); ^{13}C NMR (126 MHz, $CDCl_3$) δ 162.1, 160.9, 156.5, 153.9, 138.7, 137.1, 133.6, 133.1, 129.7, 129.0, 128.9, 127.4, 120.5, 118.7, 118.0, 114.5, 111.3, 110.6, 109.8, 103.8, 91.1, 56.3, 56.0, 37.7, 33.1, 32.4, 27.3, 25.8, 18.1; IR (neat) ν_{max} 2923, 1724, 1619, 1599, 1499, 1459, 1434, 1336, 1145, 1118 cm^{-1}; HRMS (ESI) *m/z* calcd for $C_{29}H_{29}NO_4$ (M+Na)+ 478.1989; found, 478.1990.

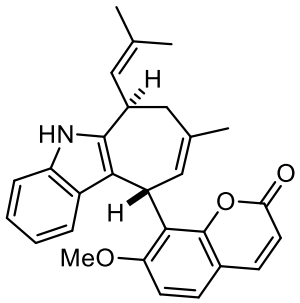

6.49

X-ray Experimental for $C_{28}H_{27}NO_3$ (6.49): Crystals grew as clusters of colorless needles by slow evaporation from methanol. The data crystal had approximate dimensions; 0.14 x 0.065 x 0.042 mm. The data were collected on an Agilent Technologies SuperNova Dual Source diffractometer using a μ-focus Cu Kα radiation source (λ = 1.5418Å) with collimating mirror monochromators. A total of 1020 frames of data were collected using □-scans with a scan range of 1° and a counting time of 15 seconds per frame using a detector offset of +/- 42.7° and a counting time of 38.5 seconds per frame using a detector offset of +/- 111.0°. The data

were collected at 100 K using an Oxford Cryostream low temperature device. Details of crystal data, data collection and structure refinement are listed in Table 7.17. Data collection, unit cell refinement and data reduction were performed using Agilent Technologies CrysAlisPro V 1.171.39.46f.[1] The structure was solved by direct methods using SIR2004 and refined by full-matrix least-squares on F2 with anisotropic displacement parameters for the non-H atoms using SHELXL-2016/6.[250,256] Structure analysis was aided by use of the programs PLATON and WinGX.[252,257] The hydrogen atoms were calculated in ideal positions with isotropic displacement parameters set to 1.2xUeq of the attached atom (1.5xUeq for methyl hydrogen atoms. The hydrogen atoms bound to the nitrogen atoms were observed in a ΔF map and refined with isotropic displacement parameters. A molecule of unknown composition was found to be badly disordered. The contributions to the scattering factors due to this solvent molecule were removed by use of the utility SQUEEZE in PLATON. PLATON was used as incorporated in WinGX.

The function, Σw(|Fo|2 - |Fc|2)2, was minimized, where w = 1/[(□(Fo))2 + (0.0668*P)2] and P = (|Fo|2 + 2|Fc|2)/3. Rw(F2) refined to 0.213, with R(F) equal to 0.0797 and a goodness of fit, S, = 1.00. Definitions used for calculating R(F), Rw(F2) and the goodness of fit, S, are as follows: $R_w(F^2) = \{\Sigma w(|F_o|^2 - |F_c|^2)^2/\Sigma w(|F_o|)^4\}^{1/2}$ where w is the weight given each reflection; $R(F) = \Sigma(|F_o| - |F_c|)/\Sigma|F_o|\}$ for reflections with $F_o > 4(\sigma(F_o))$; $S = [\Sigma w(|F_o|^2 - |F_c|^2)^2/(n - p)]^{1/2}$, where n is the number of reflections and p is the number of refined parameters. The data were checked for secondary extinction effects but no correction was necessary. Neutral atom scattering factors and values used to calculate the linear absorption coefficient are from the International Tables for X-ray Crystallography (1992). All figures were generated using SHELXTL/PC. Tables of positional and thermal parameters, bond lengths and angles, torsion angles and figures are found in Tables 7.17 – 7.22.

Table 7.17. Crystal data and structure refinement for **6.49**.

Empirical formula	C28 H27 N O3	
Formula weight	425.50	
Temperature	100(2) K	
Wavelength	0.71073 Å	
Crystal system	triclinic	
Space group	P -1	
Unit cell dimensions	a = 11.4662(15) Å	α= 82.877(9)°.
	b = 13.068(2) Å	β= 88.111(9)°.
	c = 16.186(2) Å	γ = 79.015(11)°.
Volume	2362.4(6) $Å^3$	
Z	4	
Density (calculated)	1.196 Mg/m^3	
Absorption coefficient	0.077 mm^{-1}	
F(000)	904	
Crystal size	0.140 x 0.065 x 0.042 mm^3	
Theta range for data collection	1.268 to 26.484°.	
Index ranges	-14<=h<=14, -16<=k<=11, -20<=l<=18	
Reflections collected	15116	
Independent reflections	9259 [R(int) = 0.0821]	
Completeness to theta = 25.242°	98.9 %	
Absorption correction	Semi-empirical from equivalents	
Max. and min. transmission	1.00 and 0.739	
Refinement method	Full-matrix least-squares on F^2	
Data / restraints / parameters	9259 / 0 / 593	
Goodness-of-fit on F^2	1.004	
Final R indices [I>2sigma(I)]	R1 = 0.0797, wR2 = 0.1745	
R indices (all data)	R1 = 0.1310, wR2 = 0.2133	
Extinction coefficient	n/a	
Largest diff. peak and hole	0.293 and -0.379 $e.Å^{-3}$	

Table 7.18. Atomic coordinates (x 10^4) and equivalent isotropic displacement parameters ($Å^2$x 10^3) for **6.49**. U(eq) is defined as one third of the trace of the orthogonalized U^{ij} tensor.

	x	y	z	U(eq)
C1	3921(3)	7080(3)	4718(2)	25(1)
C2	3095(3)	7139(3)	4001(2)	28(1)
C3	1868(3)	6925(3)	4325(2)	30(1)
C4	1105(3)	7766(3)	4776(2)	29(1)
C5	1462(3)	8310(3)	5328(2)	28(1)
C6	2642(3)	8232(3)	5735(2)	25(1)
C7	3710(3)	7511(3)	5439(2)	25(1)
C8	4796(3)	7218(3)	5903(2)	26(1)
C9	5148(4)	7407(3)	6684(2)	30(1)
C10	6306(4)	7032(3)	6941(2)	36(1)
C11	7131(4)	6471(3)	6423(3)	38(1)
C12	6811(4)	6254(3)	5657(2)	34(1)
C13	5647(3)	6618(3)	5413(2)	26(1)
C14	3559(3)	6384(3)	3379(2)	30(1)
C15	4161(4)	6566(3)	2679(2)	31(1)
C16	4587(4)	7577(3)	2415(2)	37(1)
C17	4437(4)	5745(3)	2082(2)	36(1)
C18	-186(3)	7948(3)	4549(3)	38(1)
C19	2883(3)	9333(3)	5788(2)	24(1)
C20	2705(3)	9779(3)	6529(2)	24(1)
C21	2062(3)	9515(3)	7965(2)	29(1)
C22	2241(4)	10555(3)	8058(2)	32(1)
C23	2616(3)	11158(3)	7412(2)	31(1)
C24	2876(3)	10785(3)	6621(2)	26(1)
C25	3251(3)	11385(3)	5919(2)	29(1)
C26	3435(3)	10970(3)	5169(2)	28(1)
C27	3250(3)	9967(3)	5102(2)	25(1)
C28	3793(3)	10139(3)	3670(2)	30(1)
C29	8560(3)	8336(3)	9567(2)	24(1)

Table 7.18 continued:

C30	7762(3)	8643(3)	8828(2)	28(1)
C31	6477(4)	9060(3)	9080(3)	38(1)
C32	5808(3)	8274(3)	9555(2)	35(1)
C33	6215(3)	7517(3)	10160(2)	32(1)
C34	7395(3)	7209(3)	10605(2)	28(1)
C35	8407(3)	7737(3)	10310(2)	23(1)
C36	9464(3)	7653(3)	10783(2)	25(1)
C37	9836(4)	7151(3)	11568(2)	29(1)
C38	10953(4)	7209(3)	11835(2)	34(1)
C39	11696(4)	7773(3)	11333(2)	36(1)
C40	11343(4)	8293(3)	10556(2)	32(1)
C41	10226(3)	8220(3)	10292(2)	27(1)
C42	8188(4)	9459(3)	8208(2)	32(1)
C43	8839(3)	9298(3)	7529(2)	31(1)
C44	9305(4)	8246(3)	7256(3)	45(1)
C45	9157(4)	10218(3)	6956(2)	38(1)
C46	4536(4)	8421(4)	9278(3)	50(1)
C47	7769(3)	6005(3)	10702(2)	25(1)
C48	7715(3)	5397(3)	11463(2)	28(1)
C49	7278(4)	5424(3)	12935(2)	32(1)
C50	7460(4)	4306(3)	13024(2)	42(1)
C51	7789(4)	3772(3)	12368(2)	38(1)
C52	7947(4)	4304(3)	11563(2)	32(1)
C53	8303(4)	3791(3)	10860(2)	36(1)
C54	8406(4)	4365(3)	10102(2)	34(1)
C55	8137(3)	5448(3)	10019(2)	27(1)
C56	8635(4)	5534(3)	8584(2)	34(1)
N1	5079(3)	6538(2)	4692(2)	27(1)
N2	9647(3)	8633(2)	9569(2)	24(1)
O1	2335(2)	9155(2)	7208(1)	27(1)
O2	1684(2)	8910(2)	8496(2)	32(1)
O3	3375(2)	9534(2)	4379(1)	28(1)
O4	7406(2)	5930(2)	12150(2)	28(1)
O5	7027(3)	5984(2)	13486(2)	35(1)
O6	8176(2)	6062(2)	9277(1)	28(1)

Table 7.19. Bond lengths [Å] and angles [°] for **6.49**.

C1-C7	1.354(5)	C16-H16B	0.98
C1-N1	1.383(5)	C16-H16C	0.98
C1-C2	1.507(5)	C17-H17A	0.98
C2-C14	1.510(5)	C17-H17B	0.98
C2-C3	1.548(5)	C17-H17C	0.98
C2-H2	1.0000	C18-H18A	0.98
C3-C4	1.515(5)	C18-H18B	0.98
C3-H3A	0.99	C18-H18C	0.98
C3-H3B	0.99	C19-C20	1.390(5)
C4-C5	1.328(5)	C19-C27	1.404(5)
C4-C18	1.505(5)	C20-O1	1.390(4)
C5-C6	1.504(5)	C20-C24	1.391(5)
C5-H5	0.95	C21-O2	1.220(5)
C6-C7	1.500(5)	C21-O1	1.372(4)
C6-C19	1.530(5)	C21-C22	1.439(5)
C6-H6	1.0000	C22-C23	1.340(6)
C7-C8	1.439(5)	C22-H22	0.95
C8-C9	1.405(5)	C23-C24	1.429(5)
C8-C13	1.416(5)	C23-H23	0.95
C9-C10	1.384(6)	C24-C25	1.402(5)
C9-H9	0.95	C25-C26	1.384(5)
C10-C11	1.405(6)	C25-H25	0.95
C10-H10	0.95	C26-C27	1.384(5)
C11-C12	1.380(6)	C26-H26	0.95
C11-H11	0.95	C27-O3	1.354(4)
C12-C13	1.382(6)	C28-O3	1.433(4)
C12-H12	0.95	C28-H28A	0.98
C13-N1	1.380(5)	C28-H28B	0.98
C14-C15	1.328(5)	C28-H28C	0.98
C14-H14	0.95	C29-N2	1.374(4)
C15-C16	1.504(5)	C29-C35	1.377(5)
C15-C17	1.514(5)	C29-C30	1.497(5)
C16-H16A	0.98	C30-C42	1.512(5)

Table 7.19 continued:

C30-C31	1.531(5)	C44-H44C	0.98
C30-H30	1.00	C45-H45A	0.98
C31-C32	1.517(6)	C45-H45B	0.98
C31-H31A	0.99	C45-H45C	0.98
C31-H31B	0.99	C46-H46A	0.98
C32-C33	1.330(6)	C46-H46B	0.98
C32-C46	1.510(6)	C46-H46C	0.98
C33-C34	1.516(5)	C47-C48	1.387(5)
C33-H33	0.95	C47-C55	1.408(5)
C34-C35	1.495(5)	C48-O4	1.385(4)
C34-C47	1.539(5)	C48-C52	1.392(5)
C34-H34	1.00	C49-O5	1.216(4)
C35-C36	1.434(5)	C49-O4	1.375(4)
C36-C37	1.396(5)	C49-C50	1.426(6)
C36-C41	1.414(5)	C50-C51	1.346(5)
C37-C38	1.383(6)	C50-H50	0.95
C37-H37	0.95	C51-C52	1.422(5)
C38-C39	1.404(6)	C51-H51	0.95
C38-H38	0.95	C52-C53	1.403(5)
C39-C40	1.388(6)	C53-C54	1.371(6)
C39-H39	0.95	C53-H53	0.95
C40-C41	1.387(5)	C54-C55	1.381(5)
C40-H40	0.95	C54-H54	0.95
C41-N2	1.364(5)	C55-O6	1.363(4)
C42-C43	1.325(5)	C56-O6	1.424(4)
C42-H42	0.95	C56-H56A	0.98
C43-C44	1.491(5)	C56-H56B	0.98
C43-C45	1.519(5)	C56-H56C	0.98
C44-H44A	0.98	N1-H1N	0.90(3)
C44-H44B	0.98	N2-H2N	0.94(4)

C7-C1-N1	110.2(3)	C1-C2-C3	110.4(3)
C7-C1-C2	129.0(3)	C14-C2-C3	108.4(3)
N1-C1-C2	120.8(3)	C1-C2-H2	108.1
C1-C2-C14	113.7(3)	C14-C2-H2	108.1

Table 7.19 continued:

C3-C2-H2	108.1	C11-C12-H12	121.2
C4-C3-C2	116.7(3)	C13-C12-H12	121.2
C4-C3-H3A	108.1	N1-C13-C12	130.7(3)
C2-C3-H3A	108.1	N1-C13-C8	106.4(3)
C4-C3-H3B	108.1	C12-C13-C8	122.8(3)
C2-C3-H3B	108.1	C15-C14-C2	128.0(4)
H3A-C3-H3B	107.3	C15-C14-H14	116.0
C5-C4-C18	120.0(3)	C2-C14-H14	116.0
C5-C4-C3	127.1(4)	C14-C15-C16	123.6(3)
C18-C4-C3	112.9(3)	C14-C15-C17	120.5(3)
C4-C5-C6	132.1(3)	C16-C15-C17	115.8(3)
C4-C5-H5	113.9	C15-C16-H16A	109.5
C6-C5-H5	113.9	C15-C16-H16B	109.5
C7-C6-C5	119.4(3)	H16A-C16-H16B	109.5
C7-C6-C19	112.2(3)	C15-C16-H16C	109.5
C5-C6-C19	109.7(3)	H16A-C16-H16C	109.5
C7-C6-H6	104.7	H16B-C16-H16C	109.5
C5-C6-H6	104.7	C15-C17-H17A	109.5
C19-C6-H6	104.7	C15-C17-H17B	109.5
C1-C7-C8	106.4(3)	H17A-C17-H17B	109.5
C1-C7-C6	130.9(3)	C15-C17-H17C	109.5
C8-C7-C6	122.5(3)	H17A-C17-H17C	109.5
C9-C8-C13	118.0(3)	H17B-C17-H17C	109.5
C9-C8-C7	134.3(3)	C4-C18-H18A	109.5
C13-C8-C7	107.7(3)	C4-C18-H18B	109.5
C10-C9-C8	119.7(3)	H18A-C18-H18B	109.5
C10-C9-H9	120.2	C4-C18-H18C	109.5
C8-C9-H9	120.2	H18A-C18-H18C	109.5
C9-C10-C11	120.3(4)	H18B-C18-H18C	109.5
C9-C10-H10	119.8	C20-C19-C27	115.9(3)
C11-C10-H10	119.8	C20-C19-C6	120.9(3)
C12-C11-C10	121.6(4)	C27-C19-C6	123.1(3)
C12-C11-H11	119.2	C19-C20-O1	116.0(3)
C10-C11-H11	119.2	C19-C20-C24	124.2(3)
C11-C12-C13	117.5(4)	O1-C20-C24	119.8(3)

Table 7.19 continued:

O2-C21-O1	115.7(3)	C31-C30-H30	108.0
O2-C21-C22	126.5(3)	C32-C31-C30	116.7(3)
O1-C21-C22	117.8(3)	C32-C31-H31A	108.1
C23-C22-C21	120.5(3)	C30-C31-H31A	108.1
C23-C22-H22	119.7	C32-C31-H31B	108.1
C21-C22-H22	119.7	C30-C31-H31B	108.1
C22-C23-C24	121.4(3)	H31A-C31-H31B	107.3
C22-C23-H23	119.3	C33-C32-C46	119.7(4)
C24-C23-H23	119.3	C33-C32-C31	127.7(4)
C20-C24-C25	117.7(3)	C46-C32-C31	112.7(4)
C20-C24-C23	118.3(3)	C32-C33-C34	132.5(4)
C25-C24-C23	124.0(3)	C32-C33-H33	113.7
C26-C25-C24	119.8(3)	C34-C33-H33	113.7
C26-C25-H25	120.1	C35-C34-C33	119.8(3)
C24-C25-H25	120.1	C35-C34-C47	111.6(3)
C25-C26-C27	120.7(3)	C33-C34-C47	108.9(3)
C25-C26-H26	119.6	C35-C34-H34	105.0
C27-C26-H26	119.6	C33-C34-H34	105.0
O3-C27-C26	123.4(3)	C47-C34-H34	105.0
O3-C27-C19	115.1(3)	C29-C35-C36	106.7(3)
C26-C27-C19	121.6(3)	C29-C35-C34	129.7(3)
O3-C28-H28A	109.5	C36-C35-C34	123.5(3)
O3-C28-H28B	109.5	C37-C36-C41	119.2(3)
H28A-C28-H28B	109.5	C37-C36-C35	133.7(3)
O3-C28-H28C	109.5	C41-C36-C35	107.1(3)
H28A-C28-H28C	109.5	C38-C37-C36	118.7(4)
H28B-C28-H28C	109.5	C38-C37-H37	120.6
N2-C29-C35	108.8(3)	C36-C37-H37	120.6
N2-C29-C30	121.2(3)	C37-C38-C39	120.9(4)
C35-C29-C30	129.9(3)	C37-C38-H38	119.6
C29-C30-C42	111.7(3)	C39-C38-H38	119.6
C29-C30-C31	112.0(3)	C40-C39-C38	121.7(4)
C42-C30-C31	109.0(3)	C40-C39-H39	119.1
C29-C30-H30	108.0	C38-C39-H39	119.1
C42-C30-H30	108.0	C41-C40-C39	116.8(4)

Table 7.19 continued:

C41-C40-H40	121.6	O5-C49-O4	116.0(3)
C39-C40-H40	121.6	O5-C49-C50	126.7(4)
N2-C41-C40	130.3(3)	O4-C49-C50	117.3(3)
N2-C41-C36	107.1(3)	C51-C50-C49	120.9(4)
C40-C41-C36	122.6(3)	C51-C50-H50	119.5
C43-C42-C30	127.3(3)	C49-C50-H50	119.5
C43-C42-H42	116.3	C50-C51-C52	121.1(4)
C30-C42-H42	116.3	C50-C51-H51	119.4
C42-C43-C44	124.8(4)	C52-C51-H51	119.4
C42-C43-C45	120.5(4)	C48-C52-C53	118.0(3)
C44-C43-C45	114.7(3)	C48-C52-C51	118.3(3)
C43-C44-H44A	109.5	C53-C52-C51	123.7(4)
C43-C44-H44B	109.5	C54-C53-C52	120.0(4)
H44A-C44-H44B	109.5	C54-C53-H53	120.0
C43-C44-H44C	109.5	C52-C53-H53	120.0
H44A-C44-H44C	109.5	C53-C54-C55	120.5(3)
H44B-C44-H44C	109.5	C53-C54-H54	119.7
C43-C45-H45A	109.5	C55-C54-H54	119.7
C43-C45-H45B	109.5	O6-C55-C54	123.4(3)
H45A-C45-H45B	109.5	O6-C55-C47	114.7(3)
C43-C45-H45C	109.5	C54-C55-C47	121.9(3)
H45A-C45-H45C	109.5	O6-C56-H56A	109.5
H45B-C45-H45C	109.5	O6-C56-H56B	109.5
C32-C46-H46A	109.5	H56A-C56-H56B	109.5
C32-C46-H46B	109.5	O6-C56-H56C	109.5
H46A-C46-H46B	109.5	H56A-C56-H56C	109.5
C32-C46-H46C	109.5	H56B-C56-H56C	109.5
H46A-C46-H46C	109.5	C13-N1-C1	109.2(3)
H46B-C46-H46C	109.5	C13-N1-H1N	128(2)
C48-C47-C55	115.8(3)	C1-N1-H1N	122(2)
C48-C47-C34	122.0(3)	C41-N2-C29	110.2(3)
C55-C47-C34	122.2(3)	C41-N2-H2N	128(2)
O4-C48-C47	116.7(3)	C29-N2-H2N	121(2)
O4-C48-C52	119.6(3)	C21-O1-C20	122.2(3)
C47-C48-C52	123.7(3)	C27-O3-C28	116.8(3)

Table 7.19 continued:

C49-O4-C48	122.7(3)	C55-O6-C56	116.3(3)

Table 7.20. Anisotropic displacement parameters ($Å^2 x\ 10^3$) for **6.49**. The anisotropic displacement factor exponent takes the form: $-2\pi^2[\ h^2\ a^{*2}U^{11} + ...\ + 2\ h\ k\ a^*\ b^*\ U^{12}\ ]$

	U^{11}	U^{22}	U^{33}	U^{23}	U^{13}	U^{12}
C1	31(2)	22(2)	23(2)	1(1)	6(1)	-9(1)
C2	36(2)	29(2)	20(2)	-2(1)	4(1)	-12(2)
C3	34(2)	37(2)	24(2)	-6(1)	7(1)	-17(2)
C4	30(2)	31(2)	29(2)	1(1)	8(1)	-14(2)
C5	29(2)	25(2)	31(2)	-2(1)	12(1)	-11(1)
C6	28(2)	26(2)	21(2)	-3(1)	9(1)	-10(1)
C7	29(2)	25(2)	22(2)	-2(1)	7(1)	-12(1)
C8	34(2)	19(2)	28(2)	0(1)	7(1)	-11(1)
C9	41(2)	26(2)	23(2)	-1(1)	2(2)	-11(2)
C10	52(2)	30(2)	28(2)	3(2)	-6(2)	-16(2)
C11	38(2)	31(2)	42(2)	4(2)	-4(2)	-8(2)
C12	40(2)	27(2)	36(2)	-2(2)	4(2)	-8(2)
C13	31(2)	22(2)	26(2)	1(1)	3(1)	-9(1)
C14	34(2)	31(2)	28(2)	-5(2)	2(1)	-9(2)
C15	38(2)	32(2)	26(2)	-4(2)	4(2)	-13(2)
C16	38(2)	41(2)	32(2)	-3(2)	12(2)	-14(2)
C17	40(2)	41(2)	29(2)	-11(2)	10(2)	-12(2)
C18	29(2)	39(2)	48(2)	-3(2)	4(2)	-14(2)
C19	25(2)	23(2)	25(2)	-1(1)	8(1)	-6(1)
C20	22(2)	27(2)	24(2)	-2(1)	7(1)	-6(1)
C21	28(2)	33(2)	28(2)	-9(2)	7(1)	-6(2)
C22	38(2)	32(2)	27(2)	-10(2)	10(2)	-5(2)
C23	30(2)	28(2)	37(2)	-10(2)	8(2)	-5(2)
C24	22(2)	25(2)	32(2)	-4(1)	6(1)	-7(1)

Table 7.20 continued:

C25	27(2)	26(2)	36(2)	-4(2)	8(1)	-9(1)
C26	24(2)	29(2)	32(2)	-2(1)	5(1)	-6(1)
C27	22(2)	26(2)	27(2)	-3(1)	6(1)	-5(1)
C28	36(2)	33(2)	23(2)	2(1)	7(1)	-13(2)
C29	25(2)	25(2)	21(2)	-5(1)	6(1)	-3(1)
C30	34(2)	24(2)	26(2)	-1(1)	5(1)	-6(1)
C31	39(2)	38(2)	33(2)	2(2)	3(2)	-1(2)
C32	28(2)	39(2)	35(2)	-6(2)	8(2)	-3(2)
C33	26(2)	37(2)	33(2)	-4(2)	9(2)	-6(2)
C34	31(2)	29(2)	23(2)	-5(1)	8(1)	-7(2)
C35	26(2)	22(2)	21(2)	-4(1)	6(1)	-5(1)
C36	30(2)	25(2)	21(2)	-9(1)	10(1)	-3(1)
C37	38(2)	26(2)	23(2)	-5(1)	5(1)	-3(2)
C38	40(2)	38(2)	25(2)	-11(2)	-1(2)	-5(2)
C39	35(2)	39(2)	39(2)	-13(2)	-4(2)	-9(2)
C40	36(2)	29(2)	31(2)	-7(2)	4(2)	-9(2)
C41	27(2)	31(2)	24(2)	-8(1)	6(1)	-10(2)
C42	42(2)	24(2)	29(2)	0(1)	0(2)	-7(2)
C43	34(2)	29(2)	27(2)	3(1)	0(2)	-8(2)
C44	43(2)	47(3)	48(2)	-11(2)	20(2)	-14(2)
C45	40(2)	42(2)	31(2)	4(2)	3(2)	-13(2)
C46	27(2)	68(3)	48(2)	6(2)	2(2)	-1(2)
C47	25(2)	25(2)	26(2)	-6(1)	9(1)	-4(1)
C48	28(2)	32(2)	25(2)	-5(1)	12(1)	-7(2)
C49	39(2)	37(2)	22(2)	-3(2)	13(2)	-10(2)
C50	61(3)	34(2)	28(2)	0(2)	15(2)	-9(2)
C51	52(3)	30(2)	32(2)	1(2)	13(2)	-7(2)
C52	39(2)	26(2)	31(2)	-4(2)	14(2)	-8(2)
C53	46(2)	26(2)	37(2)	-8(2)	13(2)	-6(2)
C54	42(2)	30(2)	29(2)	-7(2)	11(2)	-4(2)
C55	28(2)	27(2)	26(2)	-4(1)	9(1)	-9(1)
C56	50(2)	28(2)	23(2)	-5(1)	8(2)	-9(2)
N1	33(2)	29(2)	22(1)	-5(1)	7(1)	-9(1)
N2	27(2)	24(1)	23(1)	-4(1)	8(1)	-7(1)
O1	32(1)	28(1)	21(1)	-3(1)	9(1)	-10(1)

Table 7.20 continued:

O2	38(2)	34(1)	24(1)	-4(1)	12(1)	-10(1)
O3	36(1)	26(1)	22(1)	-1(1)	7(1)	-12(1)
O4	34(1)	29(1)	22(1)	-4(1)	10(1)	-7(1)
O5	47(2)	35(1)	22(1)	-6(1)	11(1)	-8(1)
O6	36(1)	25(1)	23(1)	-6(1)	11(1)	-7(1)

Table 7.21. Hydrogen coordinates (x 10^4) and isotropic displacement parameters ($Å^2$x 10^3) for **6.49**.

	x	y	z	U(eq)
H2	2977	7868	3702	34
H3A	1414	6813	3844	36
H3B	1999	6261	4706	36
H5	858	8849	5499	33
H6	2521	7940	6326	30
H9	4593	7791	7035	36
H10	6545	7155	7471	43
H11	7928	6235	6603	45
H12	7371	5868	5311	41
H14	3401	5693	3505	36
H16A	4273	8087	2801	55
H16B	4309	7857	1851	55
H16C	5457	7447	2421	55
H17A	4224	5087	2343	54
H17B	5287	5626	1945	54
H17C	3978	5990	1572	54
H18A	-636	8502	4853	57
H18B	-493	7298	4698	57
H18C	-272	8164	3949	57
H22	2093	10815	8582	39
H23	2711	11849	7482	38
H25	3379	12074	5958	35
H26	3691	11378	4695	34
H28A	3250	10816	3561	45
H28B	3827	9757	3183	45
H28C	4589	10258	3782	45
H30	7772	8003	8546	34

Table 7.21 continued:

H31A	6479	9635	9424	46
H31B	6029	9370	8568	46
H33	5658	7086	10350	39
H34	7218	7391	11184	33
H37	9333	6776	11912	35
H38	11221	6864	12365	41
H39	12459	7798	11531	44
H40	11843	8681	10220	38
H42	7963	10168	8318	38
H44A	9164	7697	7696	68
H44B	10160	8174	7144	68
H44C	8898	8178	6748	68
H45A	8845	10872	7191	57
H45B	8808	10244	6407	57
H45C	10023	10130	6899	57
H46A	4133	7919	9621	75
H46B	4522	8301	8693	75
H46C	4127	9138	9340	75
H50	7346	3932	13553	50
H51	7919	3026	12445	46
H53	8474	3046	10910	44
H54	8664	4014	9629	40
H56A	9430	5124	8714	50
H56B	8682	6051	8096	50
H56C	8108	5062	8464	50
H1N	5400(30)	6280(30)	4230(20)	10(8)
H2N	9940(30)	8980(30)	9090(20)	17(9)

Table 7.22. Torsion angles [°] for **6.49**.

C7-C1-C2-C14	-168.4(4)	C9-C8-C13-N1	179.2(3)
N1-C1-C2-C14	12.5(5)	C7-C8-C13-N1	-1.3(4)
C7-C1-C2-C3	-46.3(5)	C9-C8-C13-C12	-2.8(5)
N1-C1-C2-C3	134.6(3)	C7-C8-C13-C12	176.7(3)
C1-C2-C3-C4	70.4(4)	C1-C2-C14-C15	-94.6(5)
C14-C2-C3-C4	-164.5(3)	C3-C2-C14-C15	142.2(4)
C2-C3-C4-C5	-41.8(5)	C2-C14-C15-C16	5.6(7)
C2-C3-C4-C18	139.2(3)	C2-C14-C15-C17	-173.1(4)
C18-C4-C5-C6	173.2(4)	C7-C6-C19-C20	-123.7(3)
C3-C4-C5-C6	-5.8(6)	C5-C6-C19-C20	101.2(4)
C4-C5-C6-C7	8.0(6)	C7-C6-C19-C27	58.7(5)
C4-C5-C6-C19	139.5(4)	C5-C6-C19-C27	-76.5(4)
N1-C1-C7-C8	-0.5(4)	C27-C19-C20-O1	179.6(3)
C2-C1-C7-C8	-179.7(3)	C6-C19-C20-O1	1.8(5)
N1-C1-C7-C6	174.7(3)	C27-C19-C20-C24	-0.5(5)
C2-C1-C7-C6	-4.5(6)	C6-C19-C20-C24	-178.3(3)
C5-C6-C7-C1	19.3(5)	O2-C21-C22-C23	-177.2(4)
C19-C6-C7-C1	-111.1(4)	O1-C21-C22-C23	2.7(6)
C5-C6-C7-C8	-166.1(3)	C21-C22-C23-C24	-1.5(6)
C19-C6-C7-C8	63.5(4)	C19-C20-C24-C25	0.0(6)
C1-C7-C8-C9	-179.5(4)	O1-C20-C24-C25	180.0(3)
C6-C7-C8-C9	4.8(6)	C19-C20-C24-C23	177.6(4)
C1-C7-C8-C13	1.1(4)	O1-C20-C24-C23	-2.4(5)
C6-C7-C8-C13	-174.6(3)	C22-C23-C24-C20	1.4(6)
C13-C8-C9-C10	1.7(5)	C22-C23-C24-C25	178.8(4)
C7-C8-C9-C10	-177.6(4)	C20-C24-C25-C26	0.1(5)
C8-C9-C10-C11	0.4(6)	C23-C24-C25-C26	-177.3(4)
C9-C10-C11-C12	-1.6(6)	C24-C25-C26-C27	0.2(6)
C10-C11-C12-C13	0.6(6)	C25-C26-C27-O3	177.7(3)
C11-C12-C13-N1	179.1(4)	C25-C26-C27-C19	-0.7(6)
C11-C12-C13-C8	1.7(6)	C20-C19-C27-O3	-177.7(3)

Table 7.22 continued:

C6-C19-C27-O3	0.1(5)	C35-C36-C41-N2	0.7(4)
C20-C19-C27-C26	0.8(5)	C37-C36-C41-C40	0.6(5)
C6-C19-C27-C26	178.6(3)	C35-C36-C41-C40	-179.1(3)
N2-C29-C30-C42	-11.4(4)	C29-C30-C42-C43	97.0(5)
C35-C29-C30-C42	170.2(3)	C31-C30-C42-C43	-138.8(4)
N2-C29-C30-C31	-134.0(3)	C30-C42-C43-C44	-1.5(7)
C35-C29-C30-C31	47.7(5)	C30-C42-C43-C45	178.0(4)
C29-C30-C31-C32	-68.3(4)	C35-C34-C47-C48	118.8(4)
C42-C30-C31-C32	167.6(3)	C33-C34-C47-C48	-106.6(4)
C30-C31-C32-C33	40.9(6)	C35-C34-C47-C55	-64.1(4)
C30-C31-C32-C46	-139.4(4)	C33-C34-C47-C55	70.4(4)
C46-C32-C33-C34	-176.0(4)	C55-C47-C48-O4	177.2(3)
C31-C32-C33-C34	3.6(7)	C34-C47-C48-O4	-5.5(5)
C32-C33-C34-C35	-6.9(6)	C55-C47-C48-C52	-3.0(6)
C32-C33-C34-C47	-137.1(4)	C34-C47-C48-C52	174.3(4)
N2-C29-C35-C36	-0.9(4)	O5-C49-C50-C51	-176.9(5)
C30-C29-C35-C36	177.6(3)	O4-C49-C50-C51	2.6(7)
N2-C29-C35-C34	-178.4(3)	C49-C50-C51-C52	-1.1(7)
C30-C29-C35-C34	0.1(6)	O4-C48-C52-C53	-177.5(4)
C33-C34-C35-C29	-15.7(5)	C47-C48-C52-C53	2.7(6)
C47-C34-C35-C29	113.4(4)	O4-C48-C52-C51	3.6(6)
C33-C34-C35-C36	167.1(3)	C47-C48-C52-C51	-176.2(4)
C47-C34-C35-C36	-63.9(4)	C50-C51-C52-C48	-2.0(7)
C29-C35-C36-C37	-179.6(3)	C50-C51-C52-C53	179.2(5)
C34-C35-C36-C37	-1.8(6)	C48-C52-C53-C54	-0.4(6)
C29-C35-C36-C41	0.1(4)	C51-C52-C53-C54	178.4(4)
C34-C35-C36-C41	177.8(3)	C52-C53-C54-C55	-1.4(7)
C41-C36-C37-C38	-1.1(5)	C53-C54-C55-O6	-177.4(4)
C35-C36-C37-C38	178.5(3)	C53-C54-C55-C47	1.0(6)
C36-C37-C38-C39	0.7(5)	C48-C47-C55-O6	179.6(3)
C37-C38-C39-C40	0.2(6)	C34-C47-C55-O6	2.3(5)
C38-C39-C40-C41	-0.8(5)	C48-C47-C55-C54	1.1(6)
C39-C40-C41-N2	-179.5(3)	C34-C47-C55-C54	-176.2(3)
C39-C40-C41-C36	0.4(5)	C12-C13-N1-C1	-176.8(4)
C37-C36-C41-N2	-179.6(3)	C8-C13-N1-C1	1.0(4)

Table 7.22 continued:

C7-C1-N1-C13	-0.3(4)	C24-C20-O1-C21	3.8(5)
C2-C1-N1-C13	179.0(3)	C26-C27-O3-C28	4.0(5)
C40-C41-N2-C29	178.5(4)	C19-C27-O3-C28	-177.6(3)
C36-C41-N2-C29	-1.3(4)	O5-C49-O4-C48	178.6(4)
C35-C29-N2-C41	1.4(4)	C50-C49-O4-C48	-0.9(6)
C30-C29-N2-C41	-177.3(3)	C47-C48-O4-C49	177.6(3)
O2-C21-O1-C20	176.0(3)	C52-C48-O4-C49	-2.2(5)
C22-C21-O1-C20	-3.8(5)	C54-C55-O6-C56	-6.4(5)
C19-C20-O1-C21	-176.3(3)	C47-C55-O6-C56	175.1(3)

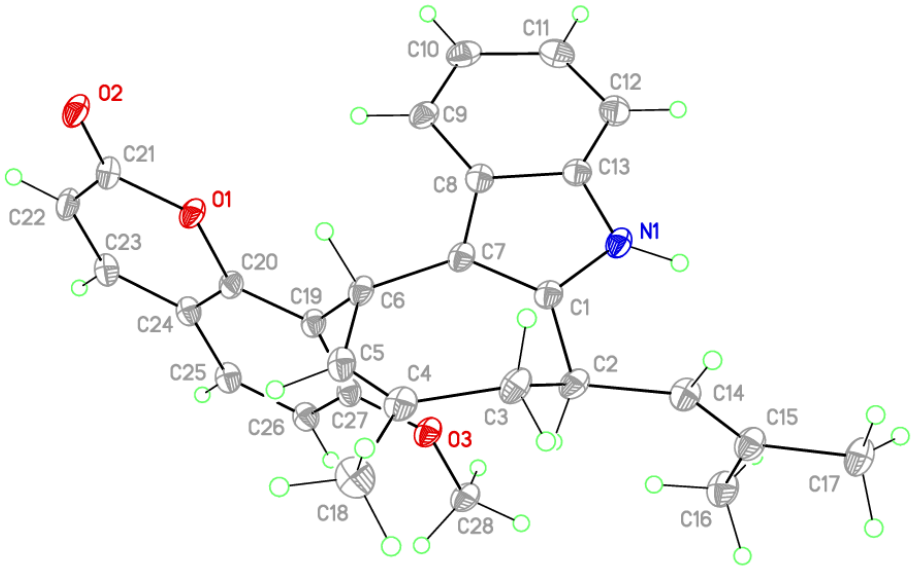

Figure 7.4. View of **6.49** showing the atom labeling scheme. Displacement ellipsoids are scaled to the 30% probability level.

References

(1) Kennedy, P. G. Clinical Features, Diagnosis, and Treatment of Human African Trypanosomiasis (Sleeping Sickness). *The Lancet Neurology* **2013**, *12*, 186–194.

(2) Brun, R.; Blum, J.; Chappuis, F.; Burri, C. Human African Trypanosomiasis. *The Lancet* **2010**, *375*, 148–159.

(3) Hotez, P. J.; Kamath, A. Neglected Tropical Diseases in Sub-Saharan Africa: Review of Their Prevalence, Distribution, and Disease Burden. *PLOS Neglected Tropical Diseases* **2009**, *3*, e412.

(4) World Health Organization. Trypanosomiasis, human African (sleeping sickness) https://www.who.int/news-room/fact-sheets/detail/trypanosomiasis-human-african-(sleeping-sickness) (accessed Feb 22, 2019).

(5) Nagle, A. S.; Khare, S.; Kumar, A. B.; Supek, F.; Buchynskyy, A.; Mathison, C. J. N.; Chennamaneni, N. K.; Pendem, N.; Buckner, F. S.; Gelb, M. H.; et al. Recent Developments in Drug Discovery for Leishmaniasis and Human African Trypanosomiasis. *Chem. Rev.* **2014**, *114*, 11305–11347.

(6) Barrett, M. P.; Boykin, D. W.; Brun, R.; Tidwell, R. R. Human African Trypanosomiasis: Pharmacological Re-Engagement with a Neglected Disease. *British Journal of Pharmacology* **2007**, *152*, 1155–1171.

(7) Greenidge, P. A.; Jenkins, T. C.; Neidle, S. DNA Minor Groove Recognition Properties of Pentamidine and Its Analogs: A Molecular Modeling Study. *Mol Pharmacol* **1993**, *43*, 982–988.

(8) Hentzer, B.; Kobayasi, T. The Ultrastructural Changes of Leishmania Tropica after Treatment with Pentamidine. *Ann Trop Med Parasitol* **1977**, *71*, 157–166.

(9) Yun, O.; Priotto, G.; Tong, J.; Flevaud, L.; Chappuis, F. NECT Is Next: Implementing the New Drug Combination Therapy for Trypanosoma Brucei Gambiense Sleeping Sickness. *PLOS Neglected Tropical Diseases* **2010**, *4*, e720.

(10) Torreele, E.; Trunz, B. B.; Tweats, D.; Kaiser, M.; Brun, R.; Mazué, G.; Bray, M. A.; Pécoul, B. Fexinidazole – A New Oral Nitroimidazole Drug Candidate Entering Clinical Development for the Treatment of Sleeping Sickness. *PLOS Neglected Tropical Diseases* **2010**, *4*, e923.

(11) Kaiser, M.; Bray, M. A.; Cal, M.; Trunz, B. B.; Torreele, E.; Brun, R. Antitrypanosomal Activity of Fexinidazole, a New Oral Nitroimidazole Drug Candidate for Treatment of Sleeping Sickness. *Antimicrobial Agents and Chemotherapy* **2011**, *55*, 5602–5608.

(12) Mesu, V. K. B. K.; Kalonji, W. M.; Bardonneau, C.; Mordt, O. V.; Blesson, S.; Simon, F.; Delhomme, S.; Bernhard, S.; Kuziena, W.; Lubaki, J.-P. F.; et al. Oral Fexinidazole for Late-Stage African Trypanosoma Brucei Gambiense Trypanosomiasis: A Pivotal Multicentre, Randomised, Non-Inferiority Trial. *The Lancet* **2018**, *391*, 144–154.

(13) DNDi. European Medicines Agency recommends fexinidazole, the first all-oral treatment for sleeping sickness https://www.dndi.org/2018/media-centre/press-releases/ema-recommends-fexinidazole-first-all-oral-treatment-sleeping-sickness/ (accessed Mar 1, 2019).
(14) Jacobs, R. T.; Nare, B.; Wring, S. A.; Orr, M. D.; Chen, D.; Sligar, J. M.; Jenks, M. X.; Noe, R. A.; Bowling, T. S.; Mercer, L. T.; et al. SCYX-7158, an Orally-Active Benzoxaborole for the Treatment of Stage 2 Human African Trypanosomiasis. *PLoS Negl Trop Dis* **2011**, *5*, e1151.
(15) Jones, D. C.; Foth, B. J.; Urbaniak, M. D.; Patterson, S.; Ong, H. B.; Berriman, M.; Fairlamb, A. H. Genomic and Proteomic Studies on the Mode of Action of Oxaboroles against the African Trypanosome. *PLOS Neglected Tropical Diseases* **2015**, *9*, e0004299.
(16) Hurdle, J. G.; O'Neill, A. J.; Chopra, I. Prospects for Aminoacyl-TRNA Synthetase Inhibitors as New Antimicrobial Agents. *Antimicrob. Agents Chemother.* **2005**, *49*, 4821–4833.
(17) Pham, J. S.; Dawson, K. L.; Jackson, K. E.; Lim, E. E.; Pasaje, C. F. A.; Turner, K. E. C.; Ralph, S. A. Aminoacyl-TRNA Synthetases as Drug Targets in Eukaryotic Parasites. *International Journal for Parasitology: Drugs and Drug Resistance* **2014**, *4*, 1–13.
(18) Cestari, I.; Stuart, K. Inhibition of Isoleucyl-TRNA Synthetase as a Potential Treatment for Human African Trypanosomiasis. *J. Biol. Chem.* **2013**, *288*, 14256–14263.
(19) Rock, F. L.; Mao, W.; Yaremchuk, A.; Tukalo, M.; Crépin, T.; Zhou, H.; Zhang, Y.-K.; Hernandez, V.; Akama, T.; Baker, S. J.; et al. An Antifungal Agent Inhibits an Aminoacyl-TRNA Synthetase by Trapping TRNA in the Editing Site. *Science* **2007**, *316*, 1759–1761.
(20) Ding, D.; Meng, Q.; Gao, G.; Zhao, Y.; Wang, Q.; Nare, B.; Jacobs, R.; Rock, F.; Alley, M. R. K.; Plattner, J. J.; et al. Design, Synthesis, and Structure−Activity Relationship of Trypanosoma Brucei Leucyl-TRNA Synthetase Inhibitors as Antitrypanosomal Agents. *J. Med. Chem.* **2011**, *54*, 1276–1287.
(21) Zhao, Y.; Wang, Q.; Meng, Q.; Ding, D.; Yang, H.; Gao, G.; Li, D.; Zhu, W.; Zhou, H. Identification of Trypanosoma Brucei Leucyl-TRNA Synthetase Inhibitors by Pharmacophore- and Docking-Based Virtual Screening and Synthesis. *Bioorganic & Medicinal Chemistry* **2012**, *20*, 1240–1250.
(22) Zhang, F.; Du, J.; Wang, Q.; Hu, Q.; Zhang, J.; Ding, D.; Zhao, Y.; Yang, F.; Wang, E.; Zhou, H. Discovery of N-(4-Sulfamoylphenyl)Thioureas as Trypanosoma Brucei Leucyl-TRNA Synthetase Inhibitors. *Org. Biomol. Chem.* **2013**, *11*, 5310–5324.
(23) Shibata, S.; Gillespie, J. R.; Kelley, A. M.; Napuli, A. J.; Zhang, Z.; Kovzun, K. V.; Pefley, R. M.; Lam, J.; Zucker, F. H.; Voorhis, W. C. V.; et al. Selective Inhibitors of Methionyl-TRNA Synthetase Have Potent Activity against

Trypanosoma Brucei Infection in Mice. *Antimicrobial Agents and Chemotherapy* **2011**, *55*, 1982–1989.
(24) Koh, C. Y.; Kim, J. E.; Shibata, S.; Ranade, R. M.; Yu, M.; Liu, J.; Gillespie, J. R.; Buckner, F. S.; Verlinde, C. L. M. J.; Fan, E.; et al. Distinct States of Methionyl-TRNA Synthetase Indicate Inhibitor Binding by Conformational Selection. *Structure* **2012**, *20*, 1681–1691.
(25) Critchley, I. A.; Young, C. L.; Stone, K. C.; Ochsner, U. A.; Guiles, J.; Tarasow, T.; Janjic, N. Antibacterial Activity of REP8839, a New Antibiotic for Topical Use. *Antimicrobial Agents and Chemotherapy* **2005**, *49*, 4247–4252.
(26) Vondenhoff, G. H. M.; Van Aerschot, A. Aminoacyl-TRNA Synthetase Inhibitors as Potential Antibiotics. *European Journal of Medicinal Chemistry* **2011**, *46*, 5227–5236.
(27) Shibata, S.; Gillespie, J. R.; Ranade, R. M.; Koh, C. Y.; Kim, J. E.; Laydbak, J. U.; Zucker, F. H.; Hol, W. G. J.; Verlinde, C. L. M. J.; Buckner, F. S.; et al. Urea-Based Inhibitors of Trypanosoma Brucei Methionyl-TRNA Synthetase: Selectivity and in Vivo Characterization. *J. Med. Chem.* **2012**, *55*, 6342–6351.
(28) Zhang, Z.; Koh, C. Y.; Ranade, R. M.; Shibata, S.; Gillespie, J. R.; Hulverson, M. A.; Huang, W.; Nguyen, J.; Pendem, N.; Gelb, M. H.; et al. 5-Fluoroimidazo[4,5-b]Pyridine Is a Privileged Fragment That Conveys Bioavailability to Potent Trypanosomal Methionyl-TRNA Synthetase Inhibitors. *ACS Infect. Dis.* **2016**, *2*, 399–404.
(29) Koh, C. Y.; Kim, J. E.; Wetzel, A. B.; Schueren, W. J. de van der; Shibata, S.; Ranade, R. M.; Liu, J.; Zhang, Z.; Gillespie, J. R.; Buckner, F. S.; et al. Structures of Trypanosoma Brucei Methionyl-TRNA Synthetase with Urea-Based Inhibitors Provide Guidance for Drug Design against Sleeping Sickness. *PLOS Neglected Tropical Diseases* **2014**, *8*, e2775.
(30) Huang, W.; Zhang, Z.; Barros-Álvarez, X.; Koh, C. Y.; Ranade, R. M.; Gillespie, J. R.; Creason, S. A.; Shibata, S.; Verlinde, C. L. M. J.; Hol, W. G. J.; et al. Structure-Guided Design of Novel Trypanosoma Brucei Methionyl-TRNA Synthetase Inhibitors. *European Journal of Medicinal Chemistry* **2016**, *124*, 1081–1092.
(31) Sahn, J. J.; Granger, B. A.; Martin, S. F. Evolution of a Strategy for Preparing Bioactive Small Molecules by Sequential Multicomponent Assembly Processes, Cyclizations, and Diversification. *Org. Biomol. Chem.* **2014**, *12*, 7659–7672.
(32) Martin, S. F.; Benage, Brigitte.; Hunter, J. E. A Concise Strategy for the Syntheses of Indole Alkaloids of the Heteroyohimboid and Corynantheioid Families. Total Syntheses of (.+-.)-Tetrahydroalstonine, (.+-.)-Cathenamine and (.+-.)-Geissoschizine. *J. Am. Chem. Soc.* **1988**, *110*, 5925–5927.
(33) Martin, S. F. Evolution of the Vinylogous Mannich Reaction as a Key Construction for Alkaloid Synthesis. *Acc. Chem. Res.* **2002**, *35*, 895–904.

(34) Martin, S. F.; Mortimore, M. New Methods for the Synthesis of Oxindole Alkaloids. Total Syntheses of Isopteropodine and Pteropodine. *Tetrahedron Letters* **1990**, *31*, 4557–4560.
(35) Martin, S. F.; Geraci, L. S. Concise Approach to the Aromatic Yohimboid and Protoberberine Alkaloids via Intramolecular Diels-Alder Reactions. *Tetrahedron Letters* **1988**, *29*, 6725–6728.
(36) Ito, M.; Clark, C. W.; Mortimore, M.; Goh, J. B.; Martin, S. F. Biogenetically Inspired Approach to the Strychnos Alkaloids. Concise Syntheses of (±)-Akuammicine and (±)-Strychnine. *J. Am. Chem. Soc.* **2001**, *123*, 8003–8010.
(37) Martin, S. F.; Liras, S. Novel Applications of Vinylogous Mannich Reactions. Total Synthesis of Rugulovasines A and B. *J. Am. Chem. Soc.* **1993**, *115*, 10450–10451.
(38) Liras, S.; Lynch, C. L.; Fryer, A. M.; Vu, B. T.; Martin, S. F. Applications of Vinylogous Mannich Reactions. Total Syntheses of the Ergot Alkaloids Rugulovasines A and B and Setoclavine. *J. Am. Chem. Soc.* **2001**, *123*, 5918–5924.
(39) Martin, S. F.; Bur, S. K. Vinylogous Mannich Reactions. Stereoselective Formal Synthesis of Pumiliotoxin 251D. *Tetrahedron* **1999**, *55*, 8905–8914.
(40) Wang, Z.; Kaneda, K.; Fang, Z.; Martin, S. F. Diversity Oriented Synthesis: Concise Entry to Novel Derivatives of Yohimbine and Corynanthe Alkaloids. *Tetrahedron Letters* **2012**, *53*, 477–479.
(41) Granger, B. A.; Wang, Z.; Kaneda, K.; Fang, Z.; Martin, S. F. Multicomponent Assembly Processes for the Synthesis of Diverse Yohimbine and Corynanthe Alkaloid Analogues. *ACS Comb. Sci.* **2013**, *15*, 379–386.
(42) Austin, C. P.; Brady, L. S.; Insel, T. R.; Collins, F. S. NIH Molecular Libraries Initiative. *Science* **2004**, *306*, 1138–1139.
(43) Zerhouni, E. The NIH Roadmap. *Science* **2003**, *302*, 63–72.
(44) Meis, A. R. Synthesis of Homoaporphine-Type Alkaloids via Intramolecular Phenol Alkylation, Design and Synthesis of a New Class of Trypanosoma Brucei Growth Inhibitors, and Neurons That Matter : Using Light to Tag Neuronal Ensembles Based on Function. Dissertation, The University of Texas at Austin, 2017. https://doi.org/10.15781/T2513VC2B.
(45) Tecle, H.; Bergmeier, S. C.; Wise, L. D.; Hershenson, F. M.; Coughenour, L. L.; Heffner, T. G. Alkyl Substituted 3-PPP Derivatives. Synthesis and Biological Investigation. *Journal of Heterocyclic Chemistry* **1989**, *26*, 1125–1128.
(46) Gálvez, C.; Viladoms, P. Reactivity of 1H-Pyrrolo[2,3-b]Pyridine. II. Synthesis of 3-(β-Haloethyl)-7-Azaindole. *Journal of Heterocyclic Chemistry* **1984**, *21*, 421–423.
(47) Macor, J. E.; Fox, C. B.; Johnson, C.; Koe, B. K.; Lebel, L. A.; Zorn, S. H. 1-(2-Aminoethyl)-3-Methyl-8,9-Dihydropyrano[3,2-e]Indole: A Rotationally Restricted Phenolic Analog of the Neurotransmitter Serotonin and Agonist Selective for Serotonin (5-HT2-Type) Receptors. *J. Med. Chem.* **1992**, *35*, 3625–3632.

(48) Cestari, I.; Stuart, K. A Spectrophotometric Assay for Quantitative Measurement of Aminoacyl-TRNA Synthetase Activity. *J Biomol Screen* **2012**, 1087057112465980.
(49) Baykov, A. A.; Evtushenko, O. A.; Avaeva, S. M. A Malachite Green Procedure for Orthophosphate Determination and Its Use in Alkaline Phosphatase-Based Enzyme Immunoassay. *Anal. Biochem.* **1988**, *171*, 266–270.
(50) Kalliokoski, T.; Kramer, C.; Vulpetti, A.; Gedeck, P. Comparability of Mixed IC50 Data – A Statistical Analysis. *PLOS ONE* **2013**, *8*, e61007.
(51) Niesen, F. H.; Berglund, H.; Vedadi, M. The Use of Differential Scanning Fluorimetry to Detect Ligand Interactions That Promote Protein Stability. *Nat. Protocols* **2007**, *2*, 2212–2221.
(52) Martin, S. F.; Rueger, H.; Williamson, S. A.; Grzejszczak, S. General Strategies for the Synthesis of Indole Alkaloids. Total Synthesis of (.+-.)-Reserpine and (.+-.)-.Alpha.-Yohimbine. *J. Am. Chem. Soc.* **1987**, *109*, 6124–6134.
(53) Spandl, R. J.; Díaz-Gavilán, M.; O'Connell, K. M. G.; Thomas, G. L.; Spring, D. R. Diversity-Oriented Synthesis. *The Chemical Record* **2008**, *8*, 129–142.
(54) Galloway, W. R. J. D.; Isidro-Llobet, A.; Spring, D. R. Diversity-Oriented Synthesis as a Tool for the Discovery of Novel Biologically Active Small Molecules. *Nature Communications* **2010**, *1*, 80.
(55) Schreiber, S. L. Target-Oriented and Diversity-Oriented Organic Synthesis in Drug Discovery. *Science* **2000**, *287* (5460), 1964–1969. https://doi.org/10.1126/science.287.5460.1964.
(56) Lovering, F.; Bikker, J.; Humblet, C. Escape from Flatland: Increasing Saturation as an Approach to Improving Clinical Success. *J. Med. Chem.* **2009**, *52*, 6752–6756.
(57) Lovering, F. Escape from Flatland 2: Complexity and Promiscuity. *Med. Chem. Commun.* **2013**, *4*, 515–519.
(58) Hann, M. M.; Leach, A. R.; Harper, G. Molecular Complexity and Its Impact on the Probability of Finding Leads for Drug Discovery. *J. Chem. Inf. Comput. Sci.* **2001**, *41*, 856–864.
(59) Schuffenhauer, A.; Brown, N.; Selzer, P.; Ertl, P.; Jacoby, E. Relationships between Molecular Complexity, Biological Activity, and Structural Diversity. *J. Chem. Inf. Model.* **2006**, *46*, 525–535.
(60) Warr, W. A. Combinatorial Chemistry and Molecular Diversity. An Overview. *J. Chem. Inf. Comput. Sci.* **1997**, *37*, 134–140.
(61) Burke, M. D.; Schreiber, S. L. A Planning Strategy for Diversity-Oriented Synthesis. *Angewandte Chemie International Edition* **2004**, *43* (1), 46–58. https://doi.org/10.1002/anie.200300626.
(62) Nielsen, T. E.; Schreiber, S. L. Towards the Optimal Screening Collection: A Synthesis Strategy. *Angewandte Chemie International Edition* **2008**, *47*, 48–56.

(63) Bienaymé, H.; Hulme, C.; Oddon, G.; Schmitt, P. Maximizing Synthetic Efficiency: Multi-Component Transformations Lead the Way. *Chemistry – A European Journal* **2000**, *6*, 3321–3329.
(64) Biggs-Houck, J. E.; Younai, A.; Shaw, J. T. Recent Advances in Multicomponent Reactions for Diversity-Oriented Synthesis. *Current Opinion in Chemical Biology* **2010**, *14*, 371–382.
(65) Sunderhaus, J. D.; Dockendorff, C.; Martin, S. F. Applications of Multicomponent Reactions for the Synthesis of Diverse Heterocyclic Scaffolds. *Org. Lett.* **2007**, *9*, 4223–4226.
(66) Sunderhaus, J. D.; Dockendorff, C.; Martin, S. F. Synthesis of Diverse Heterocyclic Scaffolds via Tandem Additions to Imine Derivatives and Ring-Forming Reactions. *Tetrahedron* **2009**, *65*, 6454–6469.
(67) Hardy, S.; Martin, S. F. Multicomponent Assembly and Diversification of Novel Heterocyclic Scaffolds Derived from 2-Arylpiperidines. *Org. Lett.* **2011**, *13*, 3102–3105.
(68) Donald, J. R.; Martin, S. F. Synthesis and Diversification of 1,2,3-Triazole-Fused 1,4-Benzodiazepine Scaffolds. *Org. Lett.* **2011**, *13*, 852–855.
(69) Granger, B. A.; Kaneda, K.; Martin, S. F. Multicomponent Assembly Strategies for the Synthesis of Diverse Tetrahydroisoquinoline Scaffolds. *Org. Lett.* **2011**, *13*, 4542–4545.
(70) Donald, J. R.; Wood, R. R.; Martin, S. F. Application of a Sequential Multicomponent Assembly Process/Huisgen Cycloaddition Strategy to the Preparation of Libraries of 1,2,3-Triazole-Fused 1,4-Benzodiazepines. *ACS Comb. Sci.* **2012**, *14*, 135–143.
(71) Granger, B. A.; Kaneda, K.; Martin, S. F. Libraries of 2,3,4,6,7,11b-Hexahydro-1H-Pyrido[2,1-a]Isoquinolin-2-Amine Derivatives via a Multicomponent Assembly Process/1,3-Dipolar Cycloaddition Strategy. *ACS Comb. Sci.* **2012**, *14*, 75–79.
(72) Stirzaker, C.; Song, J. Z.; Ng, W.; Du, Q.; Armstrong, N. J.; Locke, W. J.; Statham, A. L.; French, H.; Pidsley, R.; Valdes-Mora, F.; et al. Methyl-CpG-Binding Protein MBD2 Plays a Key Role in Maintenance and Spread of DNA Methylation at CpG Islands and Shores in Cancer. *Oncogene* **2017**, *36*, 1328–1338.
(73) Dykhuizen, E. C.; Carmody, L. C.; Tolliday, N.; Crabtree, G. R.; Palmer, M. A. J. Screening for Inhibitors of an Essential Chromatin Remodeler in Mouse Embryonic Stem Cells by Monitoring Transcriptional Regulation. *J Biomol Screen* **2012**, *17*, 1221–1230.
(74) Neumann, M.; Sampathu, D. M.; Kwong, L. K.; Truax, A. C.; Micsenyi, M. C.; Chou, T. T.; Bruce, J.; Schuck, T.; Grossman, M.; Clark, C. M.; et al. Ubiquitinated TDP-43 in Frontotemporal Lobar Degeneration and Amyotrophic Lateral Sclerosis. *Science* **2006**, *314* (5796), 130–133.

(75) Sahn, J. J.; Martin, S. F. Facile Syntheses of Substituted, Conformationally-Constrained Benzoxazocines and Benzazocines via Sequential Multicomponent Assembly and Cyclization. *Tetrahedron Letters* **2011**, *52*, 6855–6858.
(76) Sahn, J. J.; Martin, S. F. Expedient Synthesis of Norbenzomorphan Library via Multicomponent Assembly Process Coupled with Ring-Closing Reactions. *ACS Comb. Sci.* **2012**, *14*, 496–502.
(77) Sahn, J. J.; Su, J. Y.; Martin, S. F. Facile and Unified Approach to Skeletally Diverse, Privileged Scaffolds. *Org. Lett.* **2011**, *13*, 2590–2593.
(78) Sahn, J. J.; Hodges, T. R.; Chan, J. Z.; Martin, S. F. Norbenzomorphan Scaffold: Chemical Tool for Modulating Sigma Receptor-Subtype Selectivity. *ACS Med. Chem. Lett.* **2017**, *8*, 455–460.
(79) Chu, U. B.; Ruoho, A. E. Biochemical Pharmacology of the Sigma-1 Receptor. *Mol Pharmacol* **2016**, *89*, 142–153.
(80) Yi, B.; Sahn, J. J.; Ardestani, P. M.; Evans, A. K.; Scott, L. L.; Chan, J. Z.; Iyer, S.; Crisp, A.; Zuniga, G.; Pierce, J. T.; et al. Small Molecule Modulator of Sigma 2 Receptor Is Neuroprotective and Reduces Cognitive Deficits and Neuroinflammation in Experimental Models of Alzheimer's Disease. *Journal of Neurochemistry* **2017**, *140*, 561–575.
(81) Sahn, J. J.; Mejia, G. L.; Ray, P. R.; Martin, S. F.; Price, T. J. Sigma 2 Receptor/Tmem97 Agonists Produce Long Lasting Antineuropathic Pain Effects in Mice. *ACS Chem. Neurosci.* **2017**, *8*, 1801–1811.
(82) Vázquez-Rosa, E.; Watson, M. R.; Sahn, J. J.; Hodges, T. R.; Schroeder, R. E.; Cintrón-Pérez, C. J.; Shin, M.-K.; Yin, T. C.; Emery, J. L.; Martin, S. F.; et al. Neuroprotective Efficacy of a Sigma 2 Receptor/TMEM97 Modulator (DKR-1677) after Traumatic Brain Injury. *ACS Chem. Neurosci.* **2018**. https://doi.org/10.1021/acschemneuro.8b00543.
(83) Scott, L. L.; Sahn, J. J.; Ferragud, A.; Yen, R. C.; Satarasinghe, P. N.; Wood, M. D.; Hodges, T. R.; Shi, T.; Prakash, B. A.; Friese, K. M.; et al. Small Molecule Modulators of Σ2R/Tmem97 Reduce Alcohol Withdrawal-Induced Behaviors. *Neuropsychopharmacology* **2018**, *43*, 1867.
(84) Linkens, K.; Schmidt, H. R.; Sahn, J. J.; Kruse, A. C.; Martin, S. F. Investigating Isoindoline, Tetrahydroisoquinoline, and Tetrahydrobenzazepine Scaffolds for Their Sigma Receptor Binding Properties. *European Journal of Medicinal Chemistry* **2018**, *151*, 557–567.
(85) Alon, A.; Schmidt, H. R.; Wood, M. D.; Sahn, J. J.; Martin, S. F.; Kruse, A. C. Identification of the Gene That Codes for the Σ2 Receptor. *PNAS* **2017**, *114*, 7160–7165.
(86) Kim, J.; Kim, H.; Park, S. B. Privileged Structures: Efficient Chemical "Navigators" toward Unexplored Biologically Relevant Chemical Spaces. *J. Am. Chem. Soc.* **2014**, *136*, 14629–14638.
(87) Dobson, C. M. Chemical Space and Biology. *Nature* **2004**, *432*, 824–828.

(88) Evans, B. E.; Rittle, K. E.; Bock, M. G.; DiPardo, R. M.; Freidinger, R. M.; Whitter, W. L.; Lundell, G. F.; Veber, D. F.; Anderson, P. S.; Chang, R. S. L.; et al. Methods for Drug Discovery: Development of Potent, Selective, Orally Effective Cholecystokinin Antagonists. *J. Med. Chem.* **1988**, *31*, 2235–2246.
(89) Evans, B. E.; Bock, M. G.; Rittle, K. E.; DiPardo, R. M.; Whitter, W. L.; Veber, D. F.; Anderson, P. S.; Freidinger, R. M. Design of Potent, Orally Effective, Nonpeptidal Antagonists of the Peptide Hormone Cholecystokinin. *PNAS* **1986**, *83*, 4918–4922.
(90) Griffin, C. E.; Kaye, A. M.; Bueno, F. R.; Kaye, A. D. Benzodiazepine Pharmacology and Central Nervous System–Mediated Effects. *Ochsner J* **2013**, *13*, 214–223.
(91) Welsch, M. E.; Snyder, S. A.; Stockwell, B. R. Privileged Scaffolds for Library Design and Drug Discovery. *Current Opinion in Chemical Biology* **2010**, *14*, 347–361.
(92) Barreiro, E. J. Chapter 1:Privileged Scaffolds in Medicinal Chemistry: An Introduction. In *Privileged Scaffolds in Medicinal Chemistry*; 2015; pp 1–15. https://doi.org/10.1039/9781782622246-00001.
(93) Wetzel, S.; Bon, R. S.; Kumar, K.; Waldmann, H. Biology-Oriented Synthesis. *Angew. Chem. Int. Ed.* **2011**, *50*, 10800–10826.
(94) Zhang, X.; Rao, M. N.; Jones, S. R.; Shao, B.; Feibush, P.; McGuigan, M.; Tzodikov, N.; Feibush, B.; Sharkansky, I.; Snyder, B.; et al. Synthesis of Squalamine Utilizing a Readily Accessible Spermidine Equivalent. *J. Org. Chem.* **1998**, *63*, 8599–8603.
(95) Galletti, F.; Gardi, R. Metabolism of 1-Dehydroand Rostanes in Man: I. Metabolism of 17β-Hydroxyandrosta-1, 4-Dien-3-One, 17β-Cyclopent-1'-Enyloxyandrosta-1, 4-Dien-3-One (Quinbolone) and Androsta-1, 4-Diene-3, 17-Dione. *Steroids* **1971**, *18*, 39–50.
(96) Vitaku, E.; Smith, D. T.; Njardarson, J. T. Analysis of the Structural Diversity, Substitution Patterns, and Frequency of Nitrogen Heterocycles among U.S. FDA Approved Pharmaceuticals. *J. Med. Chem.* **2014**, *57*, 10257–10274.
(97) Rao, R. N.; Maiti, B.; Chanda, K. Application of Pictet–Spengler Reaction to Indole-Based Alkaloids Containing Tetrahydro-β-Carboline Scaffold in Combinatorial Chemistry. *ACS Comb. Sci.* **2017**, *19*, 199–228.
(98) Setti-Perdigão, P.; Serrano, M. A. R.; Jr, O. A. F.; Bolzani, V. S.; Guimarães, M. Z. P.; Castro, N. G. Erythrina Mulungu Alkaloids Are Potent Inhibitors of Neuronal Nicotinic Receptor Currents in Mammalian Cells. *PLOS ONE* **2013**, *8*, e82726.
(99) Faggion, S. A.; Cunha, A. O. S.; Fachim, H. A.; Gavin, A. S.; dos Santos, W. F.; Pereira, A. M. S.; Beleboni, R. O. Anticonvulsant Profile of the Alkaloids (+)-Erythravine and (+)-11-α-Hydroxy-Erythravine Isolated from the Flowers of Erythrina Mulungu Mart Ex Benth (Leguminosae–Papilionaceae). *Epilepsy & Behavior* **2011**, *20*, 441–446.

(100) Dyke, S. F.; Quessy, S. N. Chapter 1 Erythrina and Related Alkaloids. In *The Alkaloids: Chemistry and Physiology*; Rodrigo, R. G. A., Ed.; Academic Press, 1981; Vol. 18, pp 1–98. https://doi.org/10.1016/S1876-0813(08)60236-5.
(101) Jenner, P.; Katzenschlager, R. Apomorphine - Pharmacological Properties and Clinical Trials in Parkinson's Disease. *Parkinsonism & Related Disorders* **2016**, *33*, S13–S21. https://doi.org/a.
(102) Auffret, M.; Drapier, S.; Vérin, M. The Many Faces of Apomorphine: Lessons from the Past and Challenges for the Future. *Drugs R D* **2018**, *18*, 91–107.
(103) Reserpine - an overview | ScienceDirect Topics https://www.sciencedirect.com/topics/pharmacology-toxicology-and-pharmaceutical-science/reserpine (accessed Mar 20, 2019).
(104) Nur, S.; Adams, C. E. Chlorpromazine versus Reserpine for Schizophrenia. *Cochrane Database of Systematic Reviews* **2016**, No. 4. https://doi.org/10.1002/14651858.CD012122.pub2.
(105) Forgue, S. T.; Patterson, B. E.; Bedding, A. W.; Payne, C. D.; Phillips, D. L.; Wrishko, R. E.; Mitchell, M. I. Tadalafil Pharmacokinetics in Healthy Subjects. *British Journal of Clinical Pharmacology* **2006**, *61*, 280–288.
(106) Irsfeld, M.; Spadafore, M.; Prüß, B. M. β-Phenylethylamine, a Small Molecule with a Large Impact. *Webmedcentral* **2013**, *4* (9).
(107) Xie, Z.; Miller, G. M. β-Phenylethylamine Alters Monoamine Transporter Function via Trace Amine-Associated Receptor 1: Implication for Modulatory Roles of Trace Amines in Brain. *J Pharmacol Exp Ther* **2008**, *325*, 617–628.
(108) Wilens, T. E.; Adler, L. A.; Adams, J.; Sgambati, S.; Rotrosen, J.; Sawtelle, R.; Utzinger, L.; Fusillo, S. Misuse and Diversion of Stimulants Prescribed for ADHD: A Systematic Review of the Literature. *Journal of the American Academy of Child & Adolescent Psychiatry* **2008**, *47*, 21–31.
(109) Mithoefer, M. C.; Mithoefer, A. T.; Feduccia, A. A.; Jerome, L.; Wagner, M.; Wymer, J.; Holland, J.; Hamilton, S.; Yazar-Klosinski, B.; Emerson, A.; et al. 3,4-Methylenedioxymethamphetamine (MDMA)-Assisted Psychotherapy for Post-Traumatic Stress Disorder in Military Veterans, Firefighters, and Police Officers: A Randomised, Double-Blind, Dose-Response, Phase 2 Clinical Trial. *The Lancet Psychiatry* **2018**, *5*, 486–497.
(110) Shulgin, A. T.; Shulgin, Ann. *PiHKAL: A Chemical Love Story*; Transform Press, 1991.
(111) Bruhn, J. G.; Smet, P. A. D.; El-Seedi, H. R.; Beck, O. Mescaline Use for 5700 Years. *The Lancet* **2002**, *359*, 1866.
(112) McGrath, N. A.; Brichacek, M.; Njardarson, J. T. A Graphical Journey of Innovative Organic Architectures That Have Improved Our Lives. *J. Chem. Educ.* **2010**, *87*, 1348–1349.
(113) Horst, W. D.; Preskorn, S. H. Mechanisms of Action and Clinical Characteristics of Three Atypical Antidepressants: Venlafaxine, Nefazodone, Bupropion. *Journal of Affective Disorders* **1998**, *51*, 237–254.

(114) Ahrens, R. C.; Smith, G. D. Albuterol: An Adrenergic Agent for Use in the Treatment of Asthma Pharmacology, Pharmacokinetics and Clinical Use. *Pharmacotherapy: The Journal of Human Pharmacology and Drug Therapy* **1984**, *4*, 105–120.
(115) Brogden, R. N.; Speight, T. M.; Avery, G. S. Baclofen: A Preliminary Report of Its Pharmacological Properties and Therapeutic Efficacy in Spasticity. *Drugs* **1974**, *8*, 1–14.
(116) Lilja, J. J.; Laitinen, K.; Neuvonen, P. J. Effects of Grapefruit Juice on the Absorption of Levothyroxine. *British Journal of Clinical Pharmacology* **2005**, *60*, 337–341.
(117) Karasik, A.; Aschner, P.; Katzeff, H.; Davies, M. J.; Stein, P. P. Sitagliptin, a DPP-4 Inhibitor for the Treatment of Patients with Type 2 Diabetes: A Review of Recent Clinical Trials. *Current Medical Research and Opinion* **2008**, *24*, 489–496.
(118) Brogden, R. N.; Heel, R. C.; Pakes, G. E.; Speight, T. M.; Avery, G. S. Glipizide: A Review of Its Pharmacological Properties and Therapeutic Use. *Drugs* **1979**, *18*, 329–353.
(119) Marson, C. M. New and Unusual Scaffolds in Medicinal Chemistry. *Chem. Soc. Rev.* **2011**, *40*, 5514–5533.
(120) Müller, G.; Berkenbosch, T.; Benningshof, J. C. J.; Stumpfe, D.; Bajorath, J. Charting Biologically Relevant Spirocyclic Compound Space. *Chem. Eur. J.* **2016**, n/a-n/a.
(121) Zheng, Y.; Tice, C. M.; Singh, S. B. The Use of Spirocyclic Scaffolds in Drug Discovery. *Bioorganic & Medicinal Chemistry Letters* **2014**, *24*, 3673–3682.
(122) Zheng, Y.-J.; Tice, C. M. The Utilization of Spirocyclic Scaffolds in Novel Drug Discovery. *Expert Opinion on Drug Discovery* **2016**, *11*, 831–834.
(123) Martin, S. F.; Clements, J. H. Correlating Structure and Energetics in Protein-Ligand Interactions: Paradigms and Paradoxes. *Annual Review of Biochemistry* **2013**, *82*, 267–293.
(124) Burkhard, J. A.; Wagner, B.; Fischer, H.; Schuler, F.; Müller, K.; Carreira, E. M. Synthesis of Azaspirocycles and Their Evaluation in Drug Discovery. *Angewandte Chemie International Edition* **2010**, *49*, 3524–3527.
(125) Johansson, A.; Löfberg, C.; Antonsson, M.; von Unge, S.; Hayes, M. A.; Judkins, R.; Ploj, K.; Benthem, L.; Lindén, D.; Brodin, P.; et al. Discovery of (3-(4-(2-Oxa-6-Azaspiro[3.3]Heptan-6-Ylmethyl)Phenoxy)Azetidin-1-Yl)(5-(4-Methoxyphenyl)-1,3,4-Oxadiazol-2-Yl)Methanone (AZD1979), a Melanin Concentrating Hormone Receptor 1 (MCHr1) Antagonist with Favorable Physicochemical Properties. *J. Med. Chem.* **2016**, *59*, 2497–2511.
(126) Smith, L. K.; Baxendale, I. R. Total Syntheses of Natural Products Containing Spirocarbocycles. *Org. Biomol. Chem.* **2015**, *13*, 9907–9933.
(127) Bariwal, J.; Voskressensky, L. G.; Van der Eycken, E. V. Recent Advances in Spirocyclization of Indole Derivatives. *Chemical Society Reviews* **2018**, *47*, 3831–3848.

(128) Panda, S. S.; Jones, R. A.; Bachawala, P.; Mohapatra, P. P. Spirooxindoles as Potential Pharmacophores. *Mini reviews in medicinal chemistry* **2017**, *17*, 1515–1536.
(129) Trost, B. M.; Brennan, M. K. Asymmetric Syntheses of Oxindole and Indole Spirocyclic Alkaloid Natural Products. *Synthesis* **2009**, *2009*, 3003–3025.
(130) James, M. J.; O'Brien, P.; Taylor, R. J. K.; Unsworth, W. P. Synthesis of Spirocyclic Indolenines. *Chemistry – A European Journal* **2016**, *22*, 2856–2881.
(131) Liddon, J. T. R.; Rossi-Ashton, J. A.; Taylor, R. J. K.; Unsworth, W. P. Dearomatizing Spiroannulation Reagents: Direct Access to Spirocycles from Indoles and Dihalides. *Org. Lett.* **2018**, *20*, 3349–3353.
(132) Sinclair, A.; Stockman, R. A. Thirty-Five Years of Synthetic Studies Directed towards the Histrionicotoxin Family of Alkaloids. *Nat. Prod. Rep.* **2007**, *24*, 298–326.
(133) Ma, X.; Gang, D. R. The Lycopodium Alkaloids. *Nat. Prod. Rep.* **2004**, *21*, 752–772.
(134) Mandal, S. K.; Biswas, R.; Bhattacharyya, S. S.; Paul, S.; Dutta, S.; Pathak, S.; Khuda-Bukhsh, A. R. Lycopodine from Lycopodium Clavatum Extract Inhibits Proliferation of HeLa Cells through Induction of Apoptosis via Caspase-3 Activation. *European Journal of Pharmacology* **2010**, *626*, 115–122.
(135) Blasko, G.; Murugesan, N.; Freyer, A. J.; Shamma, M.; Ansari, A. A.; Atta-ur-Rahman. Karachine: An Unusual Protoberberine Alkaloid. *J. Am. Chem. Soc.* **1982**, *104*, 2039–2041.
(136) V. Stevens, R.; R. Pruitt, J. On the Annulation of Δ 2 -Tetrahydropyridines. An Expeditious Total Synthesis of the Protoberberine Alkaloid Karachine. *Journal of the Chemical Society, Chemical Communications* **1983**, *0*, 1425–1425.
(137) Heathcock, C. H.; Davidsen, S. K.; Mills, Sander.; Sanner, M. A. Total Synthesis of (.+-.)-Methyl Homodaphniphyllate. *J. Am. Chem. Soc.* **1986**, *108*, 5650–5651.
(138) Chattopadhyay, A. K.; Hanessian, S. Recent Progress in the Chemistry of Daphniphyllum Alkaloids. *Chem. Rev.* **2017**, *117*, 4104–4146.
(139) Hardardottir, I.; Olafsdottir, E. S.; Freysdottir, J. Dendritic Cells Matured in the Presence of the Lycopodium Alkaloid Annotine Direct T Cell Responses toward a Th2/Treg Phenotype. *Phytomedicine* **2015**, *22*, 277–282.
(140) Fukumoto, H.; Esumi, T.; Ishihara, J.; Hatakeyama, S. Total Synthesis of (±)-Erythravine Based on Ring Closing Dienyne Metathesis. *Tetrahedron Letters* **2003**, *44*, 8047–8049.
(141) Adachi, Y.; Kamei, N.; Yokoshima, S.; Fukuyama, T. Total Synthesis of (−)-Histrionicotoxin. *Org. Lett.* **2011**, *13*, 4446–4449.
(142) Ayer, W. A.; Bowman, W. R.; Joseph, T. C.; Smith, P. Synthesis of Dl-Lycopodine. *J. Am. Chem. Soc.* **1968**, *90*, 1648–1650.
(143) Stork, G.; Kretchmer, R. A.; Schlessinger, R. H. The Sterospecific Total Synthesis of Dl-Lycopodine. *J. Am. Chem. Soc.* **1968**, *90* (6), 1647–1648. https://doi.org/10.1021/ja01008a042.

(144) Heathcock, C. H.; Kleinman, E. F.; Binkley, E. S. Total Synthesis of Lycopodium Alkaloids: (.+-.)-Lycopodine, (.+-.)-Lycodine, and (.+-.)-Lycodoline. *J. Am. Chem. Soc.* **1982**, *104*, 1054–1068.
(145) Yang, H.; Carter, R. G.; Zakharov, L. N. Enantioselective Total Synthesis of Lycopodine. *J. Am. Chem. Soc.* **2008**, *130* (29), 9238–9239. https://doi.org/10.1021/ja803613w.
(146) Ruggeri, R. B.; Heathcock, C. H. Daphniphyllum Alkaloids. Part 7. Biomimetic Total Synthesis of (.+-.)-Methyl Homodaphniphyllate. *The Journal of Organic Chemistry* **1990**, *55*, 3714–3715.
(147) Heathcock, C. H.; Ruggeri, R. B.; McClure, K. F. Daphniphyllum Alkaloids. 15. Total Syntheses of (.+-.)-Methyl Homodaphniphyllate and (.+-.)-Daphnilactone A. *The Journal of Organic Chemistry* **1992**, *57*, 2585–2594.
(148) Heathcock, C. H.; Davidsen, S. K.; Mills, S. G.; Sanner, M. A. Daphniphyllum Alkaloids. 10. Classical Total Synthesis of Methyl Homodaphniphyllate. *The Journal of Organic Chemistry* **1992**, *57*, 2531–2544.
(149) Hosomi, A.; Sakurai, H. Syntheses of γ,δ-Unsaturated Alcohols from Allylsilanes and Carbonyl Compounds in the Presence of Titanium Tetrachloride. *Tetrahedron Letters* **1976**, *17*, 1295–1298.
(150) Hosomi, A. Characteristics in the Reactions of Allylsilanes and Their Applications to Versatile Synthetic Equivalents. *Acc. Chem. Res.* **1988**, *21*, 200–206.
(151) Hosomi, A.; Sakurai, H. Chemistry of Organosilicon Compounds. 99. Conjugate Addition of Allylsilanes to .Alpha.,.Beta.-Enones. A New Method of Stereoselective Introduction of the Angular Allyl Group in Fused Cyclic .Alpha.,.Beta.-Enones. *J. Am. Chem. Soc.* **1977**, *99*, 1673–1675.
(152) Hosomi, A.; Endo, M.; Sakurai, H. Allylsilanes as Synthetic Intermediates. Ii. Syntheses of Homoallyl Ethers from Allylsilanes and Acetals Promoted by Titanium Tetrachloride. *Chem. Lett.* **1976**, *5*, 941–942.
(153) Hosomi, A.; Imai, T.; Endo, M.; Sakurai, H. Chemistry of Organosilicon Compounds: CC. Allyl Coupling Reactions of Allylsilanes and Allylstannanes with Allylic Halides, Ethers and Acetates Promoted by a Lewis Acid. *Journal of Organometallic Chemistry* **1985**, *285*, 95–107.
(154) Fleming, I.; Paterson, I. Allylsilanes in Organic Synthesis: A Method for the Introduction of Two Carbon Substituents in Place of Carbonyl Oxygen. *Synthesis* **1979**, *1979*, 446–448.
(155) Kozikowski, A. P.; Park, P. U. Synthesis of 2-Substituted .DELTA.3-Piperidines: The Nitrogen Analog of the Ferrier Rearrangement. An Approach to Streptazolin. *The Journal of Organic Chemistry* **1984**, *49*, 1674–1676.
(156) Pillot, J.-P.; Dunogues, J.; Calas, R. Synthese Originale et Pratique de l'artemisia Cetone. *Tetrahedron Letters* **1976**, *17*, 1871–1872.
(157) Grieco, P. A.; Fobare, W. F. Intramolecular Variants of Aminomethano Desilylation: Reactions of in Situ Generated Immonium Ions with Allylsilanes. *Tetrahedron Letters* **1986**, *27*, 5067–5070.

(158) Larsen, S. D.; Grieco, P. A.; Fobare, W. F. Reactions of Allylsilanes with Simple Iminium Salts in Water: A Facile Route to Piperidines via a Aminomethano Desilylation-Cyclization Process. *J. Am. Chem. Soc.* **1986**, *108*, 3512–3513.
(159) Guiles, J. W.; Meyers, A. I. Asymmetric Synthesis of Benzoquinolizidines: A Formal Synthesis of (-)-Emetine. *J. Org. Chem.* **1991**, *56*, 6873–6878.
(160) Hong, C. Y.; Kado, N.; Overman, L. E. Asymmetric Synthesis of Either Enantiomer of Opium Alkaloids and Morphinans. Total Synthesis of (-)- and (+)-Dihydrocodeinone and (-)- and (+)-Morphine. *J. Am. Chem. Soc.* **1993**, *115*, 11028–11029.
(161) Son, Y. W.; Kwon, T. H.; Lee, J. K.; Pae, A. N.; Lee, J. Y.; Cho, Y. S.; Min, S.-J. A Concise Synthesis of Tetrabenazine: An Intramolecular Aza-Prins-Type Cyclization via Oxidative C–H Activation. *Org. Lett.* **2011**, *13*, 6500–6503.
(162) Benimana, S. E.; Cromwell, N. E.; Meer, H. N.; Marvin, C. C. Visible Light Photoredox and Polonovski-Potier Cyclizations for the Synthesis of (±)-5-Epi-Cermizine C and (±)-Epimyrtine. *Tetrahedron Letters* **2016**, *57*, 5062–5064.
(163) Rubiralta, M.; Diez, A.; Miguel, D.; Remuson, R.; Gelas-mialhe, Y. Synthesis of 2-(3-Indolyl)-4-Methylenepiperidines VIA Intramolecular Cyclization of Allylsilanes. *Synthetic Communications* **1992**, *22*, 359–367.
(164) Heerding, D. A.; Hong, C. Y.; Kado, N.; Look, G. C.; Overman, L. E. Simple Method for Controlling Stereoselection in Mannich Cyclization Reactions of Aldehydes. *J. Org. Chem.* **1993**, *58*, 6947–6948.
(165) Agami, C.; Comesse, S.; Kadouri-Puchot, C.; Lusinchi, M. Efficient 1,3-Asymmetric Inductions during Nucleophilic Additions to Imine and Iminium Ion Derivatives. *Synlett* **1999**, *1999*, 1094–1096. https://doi.org/10.1055/s-1999-2756.
(166) Furman, B.; Dziedzic, M. An Efficient Route to 4-(Substituted Benzyl)Piperidines. *Tetrahedron Letters* **2003**, *44*, 8249–8252.
(167) Yang, D.; Micalizio, G. C. A Convergent Stereoselective Synthesis of Quinolizidines and Indolizidines: Chemoselective Coupling of 2-Hydroxymethyl-Substituted Allylic Silanes with Imines. *J. Am. Chem. Soc.* **2009**, *131*, 17548–17549.
(168) Amorde, S. M.; Judd, A. S.; Martin, S. F. Cascade Iminium Ion Reactions for the Facile Synthesis of Quinolizidines. Concise Syntheses of (±)-Epilupinine and (−)-Epimyrtine. *Org. Lett.* **2005**, *7*, 2031–2033. https://doi.org/10.1021/ol050544b.
(169) Amorde, S. M.; Jewett, I. T.; Martin, S. F. Iminium Ion Cascade Reactions: Stereoselective Synthesis of Quinolizidines and Indolizidines. *Tetrahedron* **2009**, *65*, 3222–3231.
(170) Kawatsura, M.; Hartwig, J. F. Simple, Highly Active Palladium Catalysts for Ketone and Malonate Arylation: Dissecting the Importance of Chelation and Steric Hindrance. *J. Am. Chem. Soc.* **1999**, *121*, 1473–1478.
(171) Yang, X.; Phipps, R. J.; Toste, F. D. Asymmetric Fluorination of α-Branched Cyclohexanones Enabled by a Combination of Chiral Anion Phase-Transfer

Catalysis and Enamine Catalysis Using Protected Amino Acids. *J. Am. Chem. Soc.* **2014**, *136*, 5225–5228.
(172) Eis, M. J.; Wrobel, J. E.; Ganem, B. Mechanism and Synthetic Utility of Boron Trifluoride Etherate-Promoted Organolithium Additions. *J. Am. Chem. Soc.* **1984**, *106*, 3693–3694.
(173) Ghosh, A.; Wang, W.; Freeman, J. P.; Althaust, J. S.; VonVoigtlander, P. F.; Scahill, T. A.; Mizsak, S. A.; Szmuszkovicz, J. Stereocontrolled Syntheses of Some Conformationally Restricted Analogs of Serotonin. *Tetrahedron* **1991**, *47*, 8653–8662.
(174) Bartlett, S. L.; Keiter, K. M.; Johnson, J. S. Synthesis of Complex Tertiary Glycolates by Enantioconvergent Arylation of Stereochemically Labile α-Keto Esters. *J. Am. Chem. Soc.* **2017**, *139*, 3911–3916.
(175) Brown, H. C.; Ichikawa, K. Chemical Effects of Steric Strains—XIV: The Effect of Ring Size on the Rate of Reaction of the Cyclanones with Sodium Borohydride. *Tetrahedron* **1957**, *1*, 221–230.
(176) Trost, B. M.; Brindle, C. S. The Direct Catalytic Asymmetric Aldol Reaction. *Chem. Soc. Rev.* **2010**, *39*, 1600–1632.
(177) Coleman, R. S.; Shah, J. A. Chemoselective Cleavage of Benzyl Ethers, Esters, and Carbamates in the Presence of Other Easily Reducible Groups. *Synthesis* **1999**, *1999* (Sup. 1), 1399–1400.
(178) Barder, T. E.; Walker, S. D.; Martinelli, J. R.; Buchwald, S. L. Catalysts for Suzuki−Miyaura Coupling Processes: Scope and Studies of the Effect of Ligand Structure. *J. Am. Chem. Soc.* **2005**, *127*, 4685–4696.
(179) Caron, G.; Ermondi, G. Molecular Descriptors for Polarity: The Need for Going beyond Polar Surface Area. *Future Medicinal Chemistry* **2016**, *8*, 2013–2016.
(180) Rejzek, M.; Stockman, R. A.; Hughes, D. L. Combining Two-Directional Synthesis and Tandem Reactions: An Efficient Strategy for the Total Syntheses of (±)-Hippodamine and (±)-Epi-Hippodamine. *Org. Biomol. Chem.* **2005**, *3*, 73–83.
(181) Pan, X.; Liu, Z. The Preparation of Novel Chiral Auxiliaries SAMIQ/RAMIQ and Their Application in the Asymmetric Michael Addition. *Tetrahedron* **2014**, *70*, 4602–4610.
(182) Cox, E. D.; Cook, J. M. The Pictet-Spengler Condensation: A New Direction for an Old Reaction. *Chem. Rev.* **1995**, *95*, 1797–1842.
(183) Almodovar, I.; Rezende, M. C.; Cassels, B. K.; García-Arriagada, M. Theoretical Insights into the Regioselectivity of a Pictet-Spengler Reaction: Transition State Structures Leading to Salsolinol and Isosalsolinol. *Journal of Physical Organic Chemistry* **2017**, *30* (8). https://doi.org/10.1002/poc.3666.
(184) Liu, B.-Y.; Zhang, C.; Zeng, K.-W.; Li, J.; Guo, X.-Y.; Zhao, M.-B.; Tu, P.-F.; Jiang, Y. Exotines A and B, Two Heterodimers of Isopentenyl-Substituted Indole and Coumarin Derivatives from Murraya Exotica. *Org. Lett.* **2015**, *17*, 4380–4383.
(185) Stempel, E.; Gaich, T. Cyclohepta[b]Indoles: A Privileged Structure Motif in Natural Products and Drug Design. *Acc. Chem. Res.* **2016**, *49*, 2390–2402.

(186) Liu, B.-Y.; Zhang, C.; Zeng, K.-W.; Li, J.; Guo, X.-Y.; Zhao, M.-B.; Tu, P.-F.; Jiang, Y. Anti-Inflammatory Prenylated Phenylpropenols and Coumarin Derivatives from Murraya Exotica. *J. Nat. Prod.* **2018**, *81*, 22–33.
(187) Ito, C.; Furukawa, H. Two New Coumarins from Murraya Plants. *Chem. Pharm. Bull.* **1989**, *37*, 819–820.
(188) Patel, O. P. S.; Mishra, A.; Maurya, R.; Saini, D.; Pandey, J.; Taneja, I.; Raju, K. S. R.; Kanojiya, S.; Shukla, S. K.; Srivastava, M. N.; et al. Naturally Occurring Carbazole Alkaloids from Murraya Koenigii as Potential Antidiabetic Agents. *J. Nat. Prod.* **2016**, *79*, 1276–1284.
(189) Meragelman, K. M.; McKee, T. C.; Boyd, M. R. Siamenol, a New Carbazole Alkaloid from Murraya Siamensis. *J. Nat. Prod.* **2000**, *63*, 427–428.
(190) Ganguly, S. N.; Sarkar, A. Exozoline, a New Carbazole Alkaloid from the Leaves of Murraya Exotica. *Phytochemistry* **1978**, *17*, 1816–1817.
(191) Desai, S. N.; Patel, D. K.; Devkar, R. V.; Patel, P. V.; Ramachandran, A. V. Hepatoprotective Potential of Polyphenol Rich Extract of Murraya Koenigii L.: An in Vivo Study. *Food and Chemical Toxicology* **2012**, *50*, 310–314.
(192) Wu, L.; Li, P.; Wang, X.; Zhuang, Z.; Farzaneh, F.; Xu, R. Evaluation of Anti-Inflammatory and Antinociceptive Activities of Murraya Exotica. *Pharmaceutical Biology* **2010**, *48* (12), 1344–1353. https://doi.org/10.3109/13880201003793723.
(193) Menezes, I. R. A.; Santana, T. I.; Varela, V. J. C.; Saraiva, R. A.; Matias, E. F. F.; Boligon, A. A.; Athayde, M. L.; Coutinho, H. D. M.; Costa, J. G. M.; Rocha, J. B. T. Chemical Composition and Evaluation of Acute Toxicological, Antimicrobial and Modulatory Resistance of the Extract of Murraya Paniculata. *Pharmaceutical Biology* **2015**, *53*, 185–191.
(194) El-Sakhawy, F. S.; El-Tantawy, M. E.; Ross, S. A.; El-Sohly, M. A. Composition and Antimicrobial Activity of the Essential Oil of Murraya Exotica L. *Flavour and Fragrance Journal* **1998**, *13*, 59–62.
(195) Wong, V. (Wai C.; Lerner, E. Nitric Oxide Inhibition Strategies. *Future Science OA* **2015**, *1*, FSO35. https://doi.org/10.4155/fso.15.35.
(196) Pradhan, A. A.; Bertels, Z.; Akerman, S. Targeted Nitric Oxide Synthase Inhibitors for Migraine. *Neurotherapeutics* **2018**, *15*, 391–401.
(197) Alderton, W. K.; Cooper, C. E.; Knowles, R. G. Nitric Oxide Synthases: Structure, Function and Inhibition. *Biochemical Journal* **2001**, *357* (3), 593–615. https://doi.org/10.1042/bj3570593.
(198) Wu, T.-S.; Liou, M.-J.; Lee, C.-J.; Jong, T.-T.; McPhail, A. T.; McPhail, D. R.; Lee, K.-H. Structure and Synthesis of Murrapanine, a Novel Skeletal Indole-Naphthoquinone Alkaloid and Cytotoxic Principal from Murraya Paniculata Var. Omphalocarpa. *Tetrahedron Letters* **1989**, *30*, 6649–6652.
(199) Kong, Y.-C.; Cheng, K.-F.; Cambie, R. C.; Waterman, P. G. Yuehchukene: A Novel Indole Alkaloid with Anti-Implantation Activity. *J. Chem. Soc., Chem. Commun.* **1985**, *0*, 47–48.

(200) Cheng, K.-F.; Kong, Y.-C.; Chan, T.-Y. Biomimetic Synthesis of Yeuhchukene. *J. Chem. Soc., Chem. Commun.* **1985**, *0*, 48–49.
(201) Wenkert, E.; Moeller, P. D. R.; Piettre, S. R.; McPhail, A. T. Yuehchukene Analogs. *J. Org. Chem.* **1988**, *53*, 3170–3178.
(202) Wenkert, E.; Angell, E. C.; Ferreira, V. F.; Michelotti, E. L.; Piettre, S. R.; Sheu, J. H.; Swindell, C. S. Synthesis of Prenylated Indoles. *J. Org. Chem.* **1986**, *51*, 2343–2351.
(203) Sheu, J. H.; Chen, Y. K.; Hong, Y. L. V. Efficient Syntheses of Yuehchukene and .Beta.-(Dehydroprenyl)Indole. *J. Org. Chem.* **1993**, *58*, 5784–5787.
(204) Sheu, J.-H.; Chen, Y.-K.; Chung, H.-F.; Lin, S.-F.; Sung, P.-J. Further Study on the Transformation of β-(1-Hydroxybut-3-Enyl)Indoles into 1-β-(Indolyl)Buta-1,3-Diene, Yuehchukene, Murrapanine and Analogues. *J. Chem. Soc., Perkin Trans. 1* **1998**, *0*, 1959–1966.
(205) Cheng, B.; Volpin, G.; Morstein, J.; Trauner, D. Total Synthesis of (±)–Exotine B. *Org. Lett.* **2018**, *20*, 4358–4361.
(206) Reisch, J.; Wickramasinghe, A.; Wickremaratne, D. B. M. Natural Product Chemistry, 134. Syntheses of the Natural Coumarins Gleinene and Gleinadiene. *Liebigs Annalen der Chemie* **1990**, *1990*, 209–210.
(207) Han, X.; Li, H.; Hughes, R. P.; Wu, J. Gallium(III)-Catalyzed Three-Component (4+3) Cycloaddition Reactions. *Angew. Chem. Int. Ed.* **2012**, *51*, 10390–10393.
(208) Martin, C. L.; Overman, L. E.; Rohde, J. M. Total Synthesis of (±)- and (−)-Actinophyllic Acid. *J. Am. Chem. Soc.* **2010**, *132*, 4894–4906.
(209) Granger, B. A.; Jewett, I. T.; Butler, J. D.; Hua, B.; Knezevic, C. E.; Parkinson, E. I.; Hergenrother, P. J.; Martin, S. F. Synthesis of (±)-Actinophyllic Acid and Analogs: Applications of Cascade Reactions and Diverted Total Synthesis. *J. Am. Chem. Soc.* **2013**, *135*, 12984–12986.
(210) Smitka, T. A.; Bonjouklian, R.; Doolin, L.; Jones, N. D.; Deeter, J. B.; Yoshida, W. Y.; Prinsep, M. R.; Moore, R. E.; Patterson, G. M. L. Ambiguine Isonitriles, Fungicidal Hapalindole-Type Alkaloids from Three Genera of Blue-Green Algae Belonging to the Stigonemataceae. *J. Org. Chem.* **1992**, *57*, 857–861.
(211) Johnson, R. E.; Ree, H.; Hartmann, M.; Lang, L.; Sawano, S.; Sarpong, R. Total Synthesis of Pentacyclic (−)-Ambiguine P Using Sequential Indole Functionalizations. *J. Am. Chem. Soc.* **2019**, *141*, 2233–2237.
(212) Zhang, D.-B.; Yu, D.-G.; Sun, M.; Zhu, X.-X.; Yao, X.-J.; Zhou, S.-Y.; Chen, J.-J.; Gao, K. Ervatamines A–I, Anti-Inflammatory Monoterpenoid Indole Alkaloids with Diverse Skeletons from Ervatamia Hainanensis. *J. Nat. Prod.* **2015**, *78* (6), 1253–1261. https://doi.org/10.1021/acs.jnatprod.5b00051.
(213) Bennasar, M.-L.; Vidal, B.; Bosch, J. Total Synthesis of Indole Alkaloids of the Ervatamine Group. A Biomimetic Approach. *J. Org. Chem.* **1996**, *61*, 1916–1917.
(214) Amat, M.; Llor, N.; Checa, B.; Molins, E.; Bosch, J. A Synthetic Approach to Ervatamine-Silicine Alkaloids. Enantioselective Total Synthesis of (−)-16-Episilicine. *J. Org. Chem.* **2010**, *75*, 178–189.

(215) Napper, A. D.; Hixon, J.; McDonagh, T.; Keavey, K.; Pons, J.-F.; Barker, J.; Yau, W. T.; Amouzegh, P.; Flegg, A.; Hamelin, E.; et al. Discovery of Indoles as Potent and Selective Inhibitors of the Deacetylase SIRT1. *J. Med. Chem.* **2005**, *48*, 8045–8054.
(216) Eckschlager, T.; Plch, J.; Stiborova, M.; Hrabeta, J. Histone Deacetylase Inhibitors as Anticancer Drugs. *Int J Mol Sci* **2017**, *18*.
(217) Ishikawa, K.; Mochizuki, Y.; Hirayama, S.; Nemoto, T.; Nagai, K.; Itoh, K.; Fujii, H. Synthesis and Evaluation of Novel Opioid Ligands with a C-Homomorphinan Skeleton. *Bioorganic & Medicinal Chemistry* **2016**, *24*, 2199–2205.
(218) Shu, D.; Song, W.; Li, X.; Tang, W. Rhodium- and Platinum-Catalyzed [4+3] Cycloaddition with Concomitant Indole Annulation: Synthesis of Cyclohepta[b]Indoles. *Angew. Chem. Int. Ed.* **2013**, *52*, 3237–3240.
(219) Kusama, H.; Sogo, H.; Saito, K.; Suga, T.; Iwasawa, N. Construction of Cyclohepta[b]Indoles via Platinum-Catalyzed Intermolecular Formal [4+3]-Cycloaddition Reaction of α,β-Unsaturated Carbene Complex Intermediates with Siloxydienes. *Synlett* **2013**, *24*, 1364–1370.
(220) Zhang, J.; Shao, J.; Xue, J.; Wang, Y.; Li, Y. One Pot Hydroamination/[4 + 3] Cycloaddition: Synthesis towards the Cyclohepta[b]Indole Core of Silicine and Ervatamine. *RSC Adv.* **2014**, *4*, 63850–63854.
(221) He, S.; Hsung, R. P.; Presser, W. R.; Ma, Z.-X.; Haugen, B. J. An Approach to Cyclohepta[b]Indoles through an Allenamide (4 + 3) Cycloaddition–Grignard Cyclization–Chugaev Elimination Sequence. *Org. Lett.* **2014**, *16*, 2180–2183.
(222) Lohse, A. G.; Hsung, R. P.; Leider, M. D.; Ghosh, S. K. Developing a Diastereoselective Intramolecular [4 + 3] Cycloaddition of Nitrogen-Stabilized Oxyallyl Cations Derived from N-Sulfonyl-Substituted Allenamides. *J. Org. Chem.* **2011**, *76*, 3246–3257.
(223) Xiong, H.; Huang, J.; Ghosh, S. K.; Hsung, R. P. Stereoselective Intramolecular [4 + 3] Cycloadditions of Nitrogen-Stabilized Chiral Oxyallyl Cations via Epoxidation of N-Tethered Allenamides. *J. Am. Chem. Soc.* **2003**, *125*, 12694–12695.
(224) Lohse, A. G.; Hsung, R. P. (4+3) Cycloaddition Reactions of Nitrogen-Stabilized Oxyallyl Cations. *Chemistry – A European Journal* **2011**, *17*, 3812–3822.
(225) Pattenden, G.; Winne, J. M. An Intramolecular [4+3]-Cycloaddition Approach to Rameswaralide Inspired by Biosynthesis Speculation. *Tetrahedron Letters* **2009**, *50*, 7310–7313.
(226) Winne, J. M.; Catak, S.; Waroquier, M.; Van Speybroeck, V. Scope and Mechanism of the (4+3) Cycloaddition Reaction of Furfuryl Cations. *Angewandte Chemie International Edition* **2011**, *50*, 11990–11993.
(227) Granger, B. A.; Jewett, I. T.; Butler, J. D.; Martin, S. F. Concise Total Synthesis of (±)-Actinophyllic Acid. *Tetrahedron* **2014**, *70*, 4094–4104.
(228) Fu, T.; McElroy, W. T.; Shamszad, M.; Martin, S. F. Formal Syntheses of Naturally Occurring Welwitindolinones. *Org. Lett.* **2012**, *14*, 3834–3837.

(229) Fu, T.; McElroy, W. T.; Shamszad, M.; Heidebrecht, R. W.; Gulledge, B.; Martin, S. F. Studies toward Welwitindolinones: Formal Syntheses of N-Methylwelwitindolinone C Isothiocyanate and Related Natural Products. *Tetrahedron* **2013**, *69*, 5588–5603.
(230) Fu, T.; Bonaparte, A.; Martin, S. F. Synthesis of β-Heteroaryl Propionates via Trapping of Carbocations with π-Nucleophiles. *Tetrahedron Letters* **2009**, *50*, 3253–3257.
(231) Schmidt, B.; Krehl, S.; Kelling, A.; Schilde, U. Synthesis of 8-Aryl-Substituted Coumarins Based on Ring-Closing Metathesis and Suzuki–Miyaura Coupling: Synthesis of a Furyl Coumarin Natural Product from Galipea Panamensis. *J. Org. Chem.* **2012**, *77*, 2360–2367.
(232) Trost, B. M.; Van Vranken, D. L. Asymmetric Transition Metal-Catalyzed Allylic Alkylations. *Chem. Rev.* **1996**, *96*, 395–422.
(233) Trost, B. M.; Crawley, M. L. Asymmetric Transition-Metal-Catalyzed Allylic Alkylations: Applications in Total Synthesis. *Chem. Rev.* **2003**, *103*, 2921–2944.
(234) Chausset-Boissarie Laetitia; Ghozati Kazem; LaBine Emily; Chen Jack L.-Y.; Aggarwal Varinder K.; Crudden Cathleen M. Enantiospecific, Regioselective Cross-Coupling Reactions of Secondary Allylic Boronic Esters. *Chemistry – A European Journal* **2013**, *19*, 17698–17701.
(235) Böse, D.; Frey, W.; Pietruszka, J. The 'Mikami'-Catalyst in Enantioselective Diels–Alder Reactions of Juglone-Based Dienophiles with Different 1-Oxygenated Dienes: An Investigation on the Substitution Pattern Dependent Regioselectivity. *Synthesis* **2014**, *46*, 2524–2532.
(236) Iovine, V.; Benni, I.; Sabia, R.; D'Acquarica, I.; Fabrizi, G.; Botta, B.; Calcaterra, A. Total Synthesis of (±)-Kuwanol E. *J. Nat. Prod.* **2016**, *79*, 2495–2503.
(237) Wada, E.; Pei, W.; Yasuoka, H.; Chin, U.; Kanemasa, S. Exclusively Endo-Selective Lewis Acid-Vatalyzed Hetero Diels-Alder Reactions of (E)-1-Phenylsuifonyl-3-Alken-2-Ones with Vinyl Ethers. *Tetrahedron* **1996**, *52*, 1205–1220.
(238) Hwang, S. H.; Kurth, M. J. 1,3-Dipolar Cycloaddition of Nitrile Oxides to 1-Phenylsulfonyl-1,3-Butadienes: Synthesis of 3-(4,5-Dihydroisoxazol-5-Yl)Pyrroles. *Tetrahedron Letters* **2002**, *43*, 53–56.
(239) J. Lennox, A. J.; C. Lloyd-Jones, G. Selection of Boron Reagents for Suzuki–Miyaura Coupling. *Chemical Society Reviews* **2014**, *43*, 412–443.
(240) Kimura, M.; Ezoe, A.; Mori, M.; Iwata, K.; Tamaru, Y. Regio- and Stereoselective Nickel-Catalyzed Homoallylation of Aldehydes with 1,3-Dienes. *J. Am. Chem. Soc.* **2006**, *128*, 8559–8568.
(241) Al-Jawaheri, Y.; Kimber, M. C. Synthesis of 1,3-Dienes via a Sequential Suzuki–Miyaura Coupling/Palladium-Mediated Allene Isomerization Sequence. *Org. Lett.* **2016**, *18*, 3502–3505.
(242) Gillmore, A.; Lauret, C.; Roberts, S. M. A Route to the Structure Proposed for Puetuberosanol and Approaches to the Natural Products Marshrin and Phebalosin.

Tetrahedron **2003**, *59* (24), 4363–4375. https://doi.org/10.1016/S0040-4020(03)00624-0.
(243) Murray, R. D. H.; Zeghdi, S. Synthesis of the Natural Coumarins, Murraol (CM-C2), Trans-Dehydroosthol and Swietenocoumarin G. *Phytochemistry* **1989**, *28*, 227–230.
(244) Reisch Johannes; Bathe Andreas. Naturstoffchemie, 1181) Synthese Der Cumarine 6- Und 8-Naphthoherniarin, Dehydrogeijerin Und Murraol. *Liebigs Annalen der Chemie* **1988**, 543–547. https://doi.org/10.1002/jlac.198819880609.
(245) Mendoza, O.; Rossey, G.; Ghosez, L. Trialkylsilyl Triflimides as Easily Tunable Organocatalysts for Allylation and Benzylation of Silyl Carbon Nucleophiles with Non-Genotoxic Reagents. *Tetrahedron Letters* **2010**, *51*, 2571–2575.
(246) Woodward, R. B.; Bader, F. E.; Bickel, H.; Frey, A. J.; Kierstead, R. W. THE TOTAL SYNTHESIS OF RESERPINE. *J. Am. Chem. Soc.* **1956**, *78*, 2023–2025.
(247) Park, H. B.; Kim, Y.-J.; Lee, J. K.; Lee, K. R.; Kwon, H. C. Spirobacillenes A and B, Unusual Spiro-Cyclopentenones from Lysinibacillus Fusiformis KMC003. *Org. Lett.* **2012**, *14*, 5002–5005.
(248) Hai, M. A.; Preston, N. W.; Hussont, H.-P.; Kan-Fan, C.; Bick, R. C. Aristoserratenine and Tasmanine: Structures and Absolute Configurations. *Tetrahedron* **1984**, *40*, 4359–4361.
(249) Still, W. C.; Kahn, M.; Mitra, A. Rapid Chromatographic Technique for Preparative Separations with Moderate Resolution. *J. Org. Chem.* **1978**, *43*, 2923–2925.
(250) Sheldrick, G. M. SHELXT – Integrated Space-Group and Crystal-Structure Determination. *Acta Cryst A* **2015**, *71*, 3–8.
(251) Sheldrick, G. M. Crystal Structure Refinement with SHELXL. *Acta Cryst C* **2015**, *71*, 3–8.
(252) Farrugia, L. J. WinGX Suite for Small-Molecule Single-Crystal Crystallography. *J Appl Cryst* **1999**, *32*, 837–838.
(253) Flack, H. D. On Enantiomorph-polarity Estimation. *Acta Crystallographica Section A* **1983**, *39*, 876–881.
(254) Hooft, R. W. W.; Straver, L. H.; Spek, A. L. Determination of Absolute Structure Using Bayesian Statistics on Bijvoet Differences. *J Appl Cryst* **2008**, *41*, 96–103.
(255) Burla, M. C.; Caliandro, R.; Camalli, M.; Carrozzini, B.; Cascarano, G. L.; Caro, L. D.; Giacovazzo, C.; Polidori, G.; Spagna, R. SIR2004: An Improved Tool for Crystal Structure Determination and Refinement. *Journal of Applied Crystallography* **2005**, *38*, 381–388.
(256) Spek, A. L. PLATON SQUEEZE: A Tool for the Calculation of the Disordered Solvent Contribution to the Calculated Structure Factors. *Acta Cryst C* **2015**, *71*, 9–18.
(257) Spek, A. L. Structure Validation in Chemical Crystallography. *Acta Cryst D* **2009**, *65*, 148–155.